Mechanisms of DNA Repair and DNA Damage Dependent Cell Cycle Control in *Bacillus subtilis*

by

Peter Edward Burby

A dissertation submitted in partial fulfillment
of the requirements for the degree of
Doctor of Philosophy
(Molecular, Cellular, and Developmental Biology)
in the University of Michigan
2019

Doctoral Committee:

Associate Professor Lyle A. Simmons, Chair
Professor Matthew R. Chapman
Assistant Professor Jayakrishnan Nandakumar
Professor Michele S. Swanson

Peter Edward Burby

pburby@umich.edu

ORCID iD: 0000-0002-0928-9694

DEDICATION

To Lennon E. Burby and Heather M. Burby

ACKNOWLEDGEMENTS

I would like to thank the following people for mentorship throughout my graduate research:

Dr. Ken M. Cadigan
Dr. Matthew R. Chapman
Dr. Justin S. Lenhart
Dr. Jayakrishnan Nandakumar
Dr. Jeremy W. Schroeder
Dr. Kimberley D. Seed
Dr. Lyle A. Simmons
Zackary W. Simmons
Dr. Michele S. Swanson
Dr. Valerie M. Tesmer
Dr. Brian W. Walsh
Dr. Chen U. Zhang

This work was supported by a Graduate Research Fellowship from the National Science Foundation.

TABLE OF CONTENTS

LIST OF FIGURES

Figures

LIST OF TABLES

Tables

ABSTRACT

The DNA damage response is a conserved process found in all domains of life that serves to protect the genetic material of living organisms. When an organism encounters DNA modifications or 'DNA damage,' a response is elicited resulting in increased levels of DNA repair proteins and activation of a cell cycle checkpoint. In bacteria the DNA damage response has been studied extensively in *Escherichia coli*. Although the activation of the DNA damage response is conserved in many bacteria, the downstream steps of DNA repair and cell cycle regulation diverge significantly. Therefore, exactly how bacteria respond to DNA damage is still not clear. I used forward genetics in the model organism *Bacillus subtilis* to screen for non-essential genes that are required for mitigating the toxicity of three distinct classes of DNA damage inducing drugs. I identified two proteases that function in the DNA damage checkpoint. Through studies employing genetics, cell biology, and biochemical approaches, I present that these two proteases degrade the cell division inhibitor that is expressed as part of the DNA damage response. Thus, these two proteases aid in establishing the level of cell division inhibitor required for checkpoint activation, while also serving to clear excess inhibitor preventing further checkpoint activation. Additionally, a detailed investigation using genetics and cell biology uncovered a DNA damage checkpoint antagonist that functions by preventing the cell division inhibitor from activating the checkpoint. Therefore, the checkpoint antagonist aids in establishing the threshold for checkpoint activation along with the checkpoint proteases. The genetic screens also revealed a putative DNA repair pathway. Two genes in a putative operon encoding a helicase and an exonuclease were important for DNA damage caused by a single DNA damaging agent. Genetic analyses indicate that these genes operate as part of a novel nucleotide excision repair pathway that appears to be specific to a natural antibiotic. Finally, I studied a protein that is annotated as a potential mismatch repair protein, yet had no detectable mismatch repair phenotype. My investigation demonstrated that this protein functions by promoting homologous recombination, likely by acting as a secondary Holliday junction endonuclease. Together, my studies have uncovered new pathways of DNA repair and cell cycle

regulation in the DNA damage response in bacteria. Further, in each of my investigations I identified at least two ways of performing a single function in the DNA damage response, uncovering a more general strategy of favoring a robust DNA damage response in *B. subtilis*.

CHAPTER I

The bacterial DNA damage response

Introduction

Living organisms are defined by features that distinguish them from non-living matter, and one of the most fundamental aspects of living organisms is the ability to reproduce. The storage and passage of information allows this process to occur. Information in biological systems is stored in deoxyribonucleic acids (DNA). The identification of DNA as the genetic material (1, 2) and determination of DNA structure (3) provided the key background knowledge required to understand how cells replicate and protect their genetic material. Intriguingly, scientists had already started to recognize that DNA could be modified and repaired prior to fully understanding that DNA serves as the genetic material (4). Still, after understanding the structure and major function of DNA, scientists could begin to fully appreciate the complex assortment of cellular functions critical for DNA replication. DNA can be modified by light, ionizing radiation, and a plethora of chemicals, and such modifications impair the process of DNA replication. In response, cells have evolved numerous DNA repair mechanisms to cope with these environmental stresses. In addition, the cell must coordinate DNA replication with the process of cell growth and division and vice versa. Through coordinating DNA replication with cell division, cells ensure that each daughter cell will receive a complete set of genetic material. Given the importance of the genetic material, it is no surprise that cells have numerous mechanisms to repair and protect their DNA.

DNA damage prevents accurate DNA replication

Although DNA is considered a stable medium for storing information, there are many ways that DNA can be modified (5, 6). The result of many DNA modifications is referred to as DNA damage. Sources of DNA damage include endogenous metabolic intermediates such as

reactive oxygen species as well as exogenous sources of radiation and chemicals that react directly with DNA (6-8). In addition, there are many antibiotics produced by plants and bacteria that cause DNA damage (9). Thus, DNA damage is a prevalent obstacle encountered by all organisms in nature.

DNA damage prevents accurate DNA replication, though the exact mechanism differs depending on the type of DNA damage encountered during DNA replication. For example, treatment with UV results in a very rapid decrease in DNA replication due to the production of thymine-thymine dimers (10, 11). Replicative DNA polymerases cannot utilize thymine dimers as a template because the active site only allows for a single templating base during catalysis (12-15). Similarly, alkylating agents, such as methyl methanesulfonate, can methylate DNA bases, preventing accurate base pairing during DNA synthesis (16). A distinct type of alkylating agents, bi-functional alkylating agents such as mitomycin C, can react with complementary DNA strands resulting in an interstrand cross-link (17). Interstrand DNA cross-links are particularly toxic because the two strands cannot be separated, thus preventing replication and transcription of DNA (18, 19). Yet another type of DNA damage is a break in the phosphodiester backbone of DNA caused by agents such as ionizing radiation and the naturally produced peptides bleomycin and phleomycin (6). A break is toxic to cells because the replication machinery depends on the integrity of the template for synthesis of the nascent DNA strand (20, 21). Therefore, although there are diverse types of DNA damage, the major impediment is the inability to access and replicate the information stored within DNA.

DNA damage activates the SOS response in bacteria

The SOS response is a highly conserved stress response pathway that is activated when bacteria encounter DNA damage (22-25). Activation of the SOS response results in increased transcription of genes important for DNA repair, DNA damage tolerance, and cell cycle regulation (26-28). The collection of genes controlled by the SOS regulatory cascade is referred to as the SOS regulon. Proximal to the promoters of genes in the SOS regulon are DNA binding sites for the transcriptional repressor LexA (29-32). When bound to LexA binding sites, LexA prevents transcription of the SOS regulon (33-36). Thus, activation of the SOS response requires inactivation of LexA, resulting in activated gene transcription **(Fig 1.1)**.

How is the signal of DNA damage transduced to inactivate LexA? Early genetic studies demonstrated that RecA is required for SOS activation (37). RecA catalyzes the pairing of ssDNA to the complementary sequence in dsDNA resulting in synapsis (38, 39). RecA was also shown to be required for LexA inactivation *in vitro*, which led to the suggestion that RecA was a protease that was responsible for cleaving LexA (40). Further study demonstrated that RecA acted as a co-factor when bound to ssDNA that stimulated the auto-proteolytic activity of LexA (41). Thus, LexA is a transcriptional repressor that undergoes auto-digestion stimulated by the RecA/ssDNA nucleoprotein filament **(Fig 1.1)**. A unique feature of the SOS regulatory cascade is that many different DNA damaging treatments result in activation of the pathway. A diverse set of DNA lesions can cause activation of the SOS response because the signal that relays DNA damage to the SOS response is generation of a RecA/ssDNA nucleoprotein filament that can be formed through DNA repair or replication of damaged template DNA.

How does DNA damage lead to the accumulation of ssDNA *in vivo*? Treatment with double strand break inducing agents such as bleomycins or ionizing radiation leads to induction of the SOS response (42-44). Repair of double stranded breaks occurs through homologous recombination (38, 45, 46), during which ssDNA is generated by the helicase/nuclease complex RecBCD in *E. coli* (20), or AddAB in *B. subtilis* (47). RecBCD and AddAB bind to double strand DNA breaks (47, 48) and generate a free 3′ end onto which RecA is loaded (49-53). Thus, double strand breaks result in the generation of a RecA/ssDNA nucleoprotein filament that can activate the SOS response. In *B. subtilis*, replication is required for formation of a RecA-GFP focus and DNA damage is not sufficient, though it is still not clear whether replication is required for SOS activation (54). In *E. coli*, replication is not required to stimulate LexA cleavage following treatment with bleomycin (43). The generation of ssDNA following treatments that cause other types of DNA lesions such as pyrimidine dimers from UV light is less clear, though the process depends on DNA replication (43). One idea is that the stalling of DNA polymerase results in uncoupling of the replicative helicase from the replisome generating excess ssDNA (55). A second model is that the replication machinery stalls at lesions such as pyrimidine dimers and will skip ahead, leaving a gap of ssDNA that was not replicated (55). A primer generated from an RNA transcript (56) or by primase (57) can allow DNA polymerase to advance beyond a DNA lesion on the leading strand. The resulting ssDNA gap generated by DNA polymerase skipping ahead on the leading strand can be used as a substrate for loading

RecA by the RecFOR complex (58). Indeed, activation of the SOS response following UV exposure is also dependent on the RecFOR proteins (59). Thus, when cells encounter DNA damage, the general distress signal is a RecA/ssDNA nucleoprotein filament, which is the initial step in the DNA repair pathway homologous recombination. Therefore, bacteria make use of a DNA repair intermediate generated early in the repair process to activate expression of the genes important for mitigating the stress induced by DNA damage **(Fig 1.1)**.

Homologous recombination in bacteria

DNA damage is a ubiquitous stressor encountered by all organisms. Thus, to ensure the integrity of the genetic material, cells possess repair pathways as diverse as the DNA lesions encountered in the environment (6). Homologous recombination is a highly conserved pathway that functions in several DNA exchange reactions in bacteria (60). Homologous recombination participates in the repair of several types of DNA damage including lesions caused by DNA methylation, alkylation, cross-links, and double strand DNA breaks (18, 19, 61). In all cases, the purpose of homologous recombination as a DNA repair pathway is to restore lost sequence information using a second copy of the chromosome. For simplicity, the model for homologous recombination will be explained using the process of double strand break repair **(Fig 1.2)**.

Repair of double strand DNA breaks begins when a helicase nuclease complex recognizes the broken end of the chromosome (20). In *E. coli*, the RecBCD complex can bind to a dsDNA end, whereas the AddAB complex performs this function in *B. subtilis* (62). The end processing enzymes RecBCD or AddAB then generate a free 3′ overhang (20, 62). RecA is loaded onto the ssDNA by RecBCD or the RecFOR complex (50, 51, 58). RecA performs a homology search to find and pair the broken chromosome with the intact sister chromosome (38, 46). The process continues with the branch migration enzymes RuvAB, which function as a helicase to separate the strands of the sister chromosome providing the template for DNA polymerase to synthesize the sequence information lost at the site of the DNA break (63). The resulting Holliday junction is resolved by the Holliday junction endonuclease RuvC in *E. coli* or RecU in *B. subtilis* resulting in two intact chromosomes (63-65). Although homologous recombination is a well-studied process in bacteria, there remain several genes present in bacterial genomes with phenotypes similar to genes involved in homologous recombination, yet

no clear role in the pathway (45). I present a reverse genetic analysis of the gene *mutS2* in Chapter V, which suggests that MutS2 functions as a back-up to RecU in *B. subtilis*.

Nucleotide excision repair in bacteria

Nucleotide excision repair (NER) is a major DNA repair pathway present in both prokaryotes and eukaryotes (66). The NER machinery is capable of removing many types of DNA lesions that result in bulky adducts or other helix distorting lesions (67). In bacteria, the mechanism of NER was elucidated through studies in the model organism *E. coli* (68-70). The genes *uvrA*, *uvrB*, and *uvrC* were identified by mapping several mutants that were sensitive to UV light to three distinct loci in the *E. coli* genome (71). These three genes encode the nucleotide excision repair machinery UvrABC, which recognizes and initiates the removal of damaged DNA **(Fig 1.3)**.

The process of nucleotide excision repair begins by recognition of a DNA lesion. Purified UvrA binds to UV irradiated DNA with greater affinity than untreated DNA, and ATP is required for preferential binding (72). The ATPase domains of UvrA are also required for recognizing damaged DNA preferentially (73). Based on studies *in vitro* with purified components, it was long thought that a UvrA dimer complexed with one or two UvrB molecules performed genome surveillance and DNA damage recognition (68, 69, 74). Recent work using single molecule microscopy in live cells demonstrated that UvrA can bind to damaged DNA *in vivo* in the absence of UvrB (75). Further, recruitment of UvrB stimulates the release of UvrA from DNA, and UvrA ATPase activity is required for UvrA release (75). UvrB is hypothesized to verify the presence of a DNA lesion by using its helicase activity to unwind the DNA (76, 77). Following lesion verification, UvrB recruits UvrC (78, 79). Successful recruitment of UvrC ultimately leads to incisions occurring on either side of the DNA lesion at approximate 7-8 nucleotides 5′ to the lesion and 3-4 nucleotide 3′ to the lesion (80-82). The subsequent steps of repair are carried out by the helicase UvrD, the DNA polymerase Pol I, and DNA ligase in *E. coli* (69, 70). Repair synthesis by Pol I required the action of UvrD to stimulate the disassociation of UvrC and removal of the excised DNA (83, 84). The resulting product generated by Pol I is a substrate for DNA ligase (83, 84), thus completing the repair process.

Although nucleotide excision repair is well studied in *E. coli*, the process in *B. subtilis* has not been studied in detail. Although *uvrABC* and *polA* (gene coding for Pol I) are conserved, *cho* and *uvrD* are not. There is evidence to suggest that the helicase PcrA in *B. subtilis* can function in place of UvrD (85), though how the excision repair process occurs *in vivo* remains unclear. Further, there is evidence in *E. coli* that multiple NER pathways exist (86, 87), and it is unclear whether other pathways exist in other bacteria. In Chapter IV, I describe the discovery of a novel nucleotide excision repair pathway specific to DNA damage caused by the antibiotic mitomycin C.

DNA damage-dependent cell cycle regulation in bacteria

DNA replication and cell division are essential processes that must be coordinated to ensure that subsequent generations receive an accurate and complete set of genetic material. Under normal conditions DNA replication and cell division occur at rates that allow DNA replication and segregation of a complete chromosome to each daughter cell. When a cell encounters DNA damage, however, DNA replication is blocked, which requires cell division to be delayed to provide enough time for DNA repair and completion of DNA replication. Bacteria make use of multiple mechanisms to ensure that cell division occurs after DNA replication and segregation of the chromosomes including nucleoid occlusion, SOS-independent regulation of the divisome, and an SOS-dependent DNA damage checkpoint. Below, I discuss each of these mechanisms that regulate cytokinesis in bacteria.

Nucleoid Occlusion

A straightforward mechanism of preventing cell division prior to completion of DNA replication is nucleoid occlusion. Nucleoid occlusion prevents the cell division machinery from operating in the same location as the nucleoid. Thus, the nucleoid occludes the cell division machinery. In *E. coli* nucleoid occlusion is carried out by a protein called SlmA (88, 89). SlmA was identified using a genetic screen searching for genes that were important for cell division in the absence of the Min system (90). The Min system, composed of MinCDE, prevents cell division from occurring at the cell poles (91). Therefore, the logic was that mutants defective in both pathways responsible for selection of the site of cell division would not survive. Indeed,

mutants in *slmA* were isolated (90). Intriguingly, deletion of *slmA* alone did not change the frequency of cell division septum formation over the nucleoid, however, deletion of both *slmA* and *minCDE* resulted in a drastic increase in septa forming over the nucleoid region (90). Importantly, when the researchers blocked DNA replication, deletion of *slmA* caused a marked increase in septum formation over nucleoids (90). Therefore, SlmA is required to prevent cell division from occurring at the same location as the nucleoid, thereby providing feedback inhibition to the cell division machinery based on DNA replication.

How does SlmA prevent cell division from occurring over the nucleoid? GFP-SlmA localizes to the nucleoid, and if the helix-turn-helix domain is removed GFP-SlmA becomes diffusely cytosolic (90). The helix-turn-helix domain of SlmA is similar to the sequence specific DNA binding domains of the TetR family of bacterial transcriptional repressors (90). Indeed, SlmA was found to be a sequence specific DNA binding protein that interacts with several distinct sites on the *E. coli* chromosome (92, 93). In addition to DNA binding activity, SlmA can also inhibit FtsZ filament formation (93). FtsZ is a tubulin-like protein that forms a ring structure composed of several filaments at the site of cell division (94). Although SlmA can inhibit FtsZ filament formation, SlmA bound to its DNA binding site inhibits FtsZ far more efficiently (93). Therefore, SlmA localizes to the nucleoid by binding at distinct chromosomal loci and prevents cell division by inhibiting FtsZ ring formation, thereby providing a mechanism to delay cell division if replication and segregation of the chromosome has not completed.

The model bacterium *B. subtilis* also uses nucleoid occlusion to inhibit cell division, though the mechanism differs from the system discovered in *E. coli*. The nucleoid occlusion gene *noc* was identified as a gene that was required in the absence of the Min system (95). When both Noc and the Min system were absent, FtsZ failed to form a distinct band at mid-cell (95). Further, when DNA replication was blocked in cells without Noc, division septa formed over the nucleoids, providing evidence that Noc prevents cell division over the nucleoid (95). Noc is a sequence specific DNA binding protein that binds to several distinct chromosomal loci (96). The N-terminus of Noc is an amphipathic helix that interacts with the cell membrane (97). Thus, Noc is thought to bind to the *B. subtilis* chromosome and localize to the inner leaflet of the cell membrane, which in turn prevents assembly of a complex of proteins necessary for cell division called the divisome (97), providing a mechanism by which the nucleoid can delay cell division to

allow for DNA replication to complete. In addition, a Noc-independent form of nucleoid occlusion following arrest of DNA replication has been observed in *B. subtilis*, though the mechanism and cellular factors responsible for this phenomenon are not clear (98).

SOS-independent regulation of the divisome

In addition to the nucleoid regulating cell division directly, the status of DNA replication provides feedback inhibition to the cell division machinery. Transcriptomic studies of the SOS response in *B. subtilis* revealed that many genes were regulated by DNA damage independently of the SOS activating protein RecA (99). Further analysis showed that several operons were regulated by the essential replication initiator protein DnaA and had binding sites for DnaA in their promoters (99). One of the genes that is repressed following inhibition of DNA replication is *ftsL* (99). FtsL is one of the essential protein components of the cell division machinery, and previous studies had shown that FtsL is a highly unstable protein (100-102). Inhibition of DNA replication caused an increase in cell length independent of the SOS-dependent cell division inhibitor (see below); however, overexpression of FtsL resulted in shorter cells on average, indicating that a decrease in FtsL is responsible for delaying cell division in response to a block in DNA replication (99). Thus, it appears that DnaA relays a block in DNA replication to the cell division machinery by repressing expression of the unstable divisome protein FtsL.

SOS-dependent DNA damage checkpoint

Although the above mechanisms contribute to the regulation of cell division in response to DNA replication status, the most well understood mechanism of control in bacteria is the SOS-dependent cell cycle checkpoint. The bacterial DNA damage checkpoint was originally discovered in *E. coli*. Long before the effects of treatment with UV light on DNA synthesis were understood (11, 103), *E. coli* cells were found to elongate and grow into long filaments following exposure to UV light (104). More than three decades later, the existence of a specific cell division inhibitor was hypothesized (105). The hypothesis was that the gene encoding the cell division inhibitor was regularly repressed, and inhibition of DNA replication would result in de-repression and therefore accumulation of a protein that could prevent cell division (105). Remarkably, this hypothesis was upheld over the course of several years of subsequent investigation of the DNA damage checkpoint in bacteria.

Mutants lacking the ability to elongate or filament in response to DNA damage were isolated and originally called *sfiA* because the mutations suppressed filamentation (106). A subsequent study determined that *sfiA* mutations were in the same gene as *sulA* mutations, which were so named because they suppressed DNA damage sensitivity of *lon* mutants (107, 108). To test whether *sulA* was controlled by exogenous DNA damage treatments, a LacZ reporter at the *sulA* locus was monitored following several types of DNA damage treatment, which verified that *sulA* expression was inducible by DNA damage (109). The promoter of *sulA* contains a binding site for the repressor LexA (110), and binding of LexA at the promoter of *sulA* repressed transcription (111). Thus, activation of the SOS-response, and therefore inactivation of LexA, results in high levels of *sulA* expression.

Other methods of increasing SulA protein levels, including over-expression in the absence of DNA damage or deletion of *lon* leads to filamentation (112-114). One of the first steps in cell division is the assembly of the FtsZ ring at the future division site (94). Over-expression of SulA prevents formation of the FtsZ ring *in vivo* (115). One of the original mutations that suppressed DNA damage-induced filamentation, *sfiB*, mapped to the *ftsZ* locus. Further studies demonstrated that mutations in *ftsZ* could suppress filamentation resulting from SulA accumulation, suggesting that FtsZ could be the direct target of SulA (116, 117). In addition, over-expression of FtsZ rescued inhibition of cell division following UV treatment in *lon* mutants, further establishing a link between SulA function and FtsZ (118). An interaction between SulA and FtsZ was detected using a yeast two-hybrid assay. Moreover, several mutations in SulA that abolished its ability to inhibit cell division also abolished the interaction with FtsZ, and mutations in FtsZ that are not susceptible to SulA over-expression also abolished the interaction (119). Experiments using an FtsZ polymerization assay *in vitro* demonstrated that SulA could directly inhibit FtsZ polymerization (117, 120). Mutations in SulA that cannot block cell division failed to inhibit FtsZ polymerization, whereas mutations in FtsZ that are refractory to SulA accumulation were insensitive to SulA (117, 120). A detailed kinetic analysis of SulA inhibition of FtsZ polymerization revealed that SulA increased the concentration of FtsZ required for polymerization, and that SulA interaction with FtsZ functions by sequestering FtsZ monomers (121). Therefore, increased SulA production that results from SOS activation results in temporary inhibition of FtsZ ring assembly, thereby delaying cell division until the SOS response is turned off and SulA is degraded **(Fig 1.4)**.

The accumulation of SulA is reversed by Lon protease activity. As mentioned above, *sulA* was originally identified by isolation of a mutation that suppressed DNA damage sensitivity in a *lon* mutant (107, 108). The Lon protein was later determined to be an ATP-dependent protease (122), leading to the hypothesis that SulA could be a substrate of Lon. Indeed, SulA was found to be highly unstable in Lon^+ cells; however, in a *lon* mutant SulA was stabilized, indicating that SulA stability is regulated by Lon protease (113). Intriguingly, despite a significant increase in SulA stability in *lon* mutants, pulse-chase labeling experiments demonstrated that SulA was still susceptible to proteolysis *in vivo* (113). Subsequent studies identified a second ATP-dependent protease, ClpYQ, that affects the stability of SulA *in vivo* and degrades SulA *in vitro* (123-125). Although the evidence that Lon protease activity regulated SulA stability *in vivo* was convincing, it was not clear that SulA was a direct substrate of Lon protease. Studies using purified Lon protease demonstrated that SulA was indeed a direct substrate (126). Thus, Lon protease provides recovery from the DNA damage cell cycle checkpoint imposed by SulA, thereby allowing for cell division to proceed **(Fig 1.4)**.

The identification of a DNA damage checkpoint in bacteria was an important conceptual advance; however, extrapolation of the mechanism beyond *E. coli* has proven challenging. The cell division inhibitor SulA is not well conserved in bacteria. Nonetheless, treatment with DNA damaging agents does lead to cell filamentation in *B. subtilis* (127). The SOS response is conserved in *B. subtilis*, however *sulA* is not conserved (128). Thus, it was not clear what gene product acted as the inhibitor in *B. subtilis*. To identify the gene coding for the cell division inhibitor, a micro-array experiment was performed using wild-type and *lexA* mutant cells, reasoning that if there is an SOS-dependent cell division inhibitor it will be highly transcribed in cells lacking the LexA repressor (129). One of the highly transcribed genes in the *lexA* mutant was *yneA*, and a Northern blot analysis confirmed that the *yneA* operon was induced in the absence of functional LexA (129). The *yneA* operon is located adjacent to *lexA* in the *B. subtilis* genome, and inspection of the promoter region of *yneA* revealed two binding sites for LexA, providing evidence that LexA regulates *yneA* expression directly (129). Indeed, purified LexA can bind to the promoter region of *yneA* (31).

Examination of *lexA* mutant cells showed that they were significantly longer relative to the wild-type strain, indicating that cell division is inhibited in the *lexA* mutant (129). Deletion of

the *yneA* operon returned cell length to normal in the *lexA* mutant strain, suggesting that *yneA* is necessary for inhibiting cell division (129). To test if expression of *yneA* is sufficient for increased cell length, *yneA* was placed under the control of an IPTG inducible promoter, and cells were found to increase in length following addition of IPTG (129). Cell elongation following treatment with DNA damage was also mostly dependent on *yneA*, strongly suggesting that YneA is the SOS induced cell division inhibitor (129). Thus, *yneA* expression is induced by DNA damage, and inhibition of cell division is dependent on *yneA* **(Fig 1.5)**.

The mechanism of YneA-dependent inhibition of cell division is still not understood. Given that SulA prevents FtsZ ring assembly (115), it was hypothesized that YneA could also inhibit FtsZ (129). Visualization of FtsZ following YneA expression showed that FtsZ rings still form at mid-cell, suggesting that YneA inhibits a different cellular target (130). YneA is a small protein containing an N-terminal transmembrane domain and a C-terminal LysM domain (129, 130). LysM domains in proteins often interact with the peptidoglycan cell wall (131). Expression of YneA causes increased cell length; however, following a shift to medium that does not induce YneA expression, the cells begin to divide and YneA is rapidly degraded (130). These experiments suggest that YneA reversibly inhibits cell division. An alanine scanning mutagenesis analysis of the transmembrane domain demonstrated that several residues that clustered to a single face of the alpha helix were critical for YneA function *in vivo*, suggesting that YneA may interact with one of the proteins with a transmembrane domain that functions as part of the divisome (130). The transmembrane domain is necessary, though not sufficient for YneA to inhibit cell division (130). Interestingly, Mo and Burkholder found that YneA is cleaved, releasing the YneA C-terminus from the transmembrane domain and into the medium (130). Mutation of the putative signal peptide cleavage site did not appreciably decrease YneA processing, though mutation to a canonical signal peptide cleavage site resulted in increased YneA processing (130). Further, a mutation at the C-terminus of YneA was found to increase YneA stability (130). An analysis of cell elongation using these YneA variants demonstrated that YneA was processed more quickly resulting in shorter cells, whereas the stabilizing mutation resulted in increased cell length, suggesting that full-length YneA is the active form of the protein (130). Together, these studies lead to a model wherein YneA is the SOS-dependent cell division inhibitor that establishes the DNA damage checkpoint, and degradation of YneA by an unknown protease results in cell cycle progression **(Fig 1.5)**.

As several studies continued the search for DNA damage cell cycle checkpoints in other bacteria, it became clear that the mechanism discovered in *E. coli* was not representative of other species (132-136). In fact, the use of a small membrane bound protein similar to YneA in *B. subtilis* appears to be the more wide-spread mechanism. Identification of additional cell division inhibitors has proved challenging as homology searches have failed to identify homologs in distantly related bacterial species, requiring empirical identification. The differences in DNA damage checkpoint mechanisms likely reflect the diversity of bacterial life styles, given that the need to delay cell division in response to DNA damage will depend on growth rate, the frequency and severity of DNA damage encountered in the environment, and DNA repair capability of each organism.

Following the discovery of YneA in *B. subtilis*, the next cell division inhibitor was identified in *Mycobacterium tuberculosis*. The cell division inhibitor Rv2719c was identified by a micro-array experiment as an SOS induced gene (137, 138); and it is located adjacent to LexA similar to YneA (139). Intriguingly, many of the DNA damage inducible genes in *M. tuberculosis* are induced independent of RecA (137). Rv2719c is DNA damage inducible, and its regulation is not dependent on RecA (138). A mutational analysis of the promoter of Rv2719c demonstrated that mutation of LexA binding sites resulted in high levels of reporter expression regardless of DNA damage treatment, suggesting that Rv2719c is regulated by LexA but not RecA (139). Further analysis of Rv2719c expression and cell length demonstrated that increased expression is correlated with increased cell length, and specific over-expression of Rv2719c is sufficient to cause an increase in cell length (132). Increased expression of Rv2719c does not appear to affect FtsZ as is the case for SulA (132). Rv2719c is a protein containing a transmembrane domain and a LysM domain similar to YneA. Purified Rv2719c was found to possess cell wall hydrolase activity *in vitro*, and expression of a GFP-Rv2719c fusion had a localization pattern similar to nascent peptidoglycan synthesis, suggesting that inhibitor activity may be exerted on the cell wall by Rv2719c (132). Overall, Rv2719c is an SOS-inducible cell division inhibitor regulated by LexA independent of RecA, that may act on the cell wall or cell wall synthesis machinery to establish a DNA damage-dependent cell cycle checkpoint.

The observation that *yneA* and *rv2719c* are adjacent to *lexA* in the genomes of their respective organisms and that they are transcribed divergently led to the discovery of the DNA

damage inducible cell division inhibitor in *Corynebacterium glutamicum* and *S. aureus* (133, 136). The *divS* gene in *C. glutamicum* is located adjacent to *lexA* and its expression is dependent on RecA (133). Cell elongation following treatment with DNA damaging agents is dependent on *recA* and *divS* (133). An analysis of the promoter uncovered LexA binding sites, and LexA binds to the promoter region *in vitro* (140). Over-expression of DivS resulted in increased cell length, indicating that increased DivS expression is sufficient to inhibit cell division (133). The DivS protein has three domains: an N-terminal domain, a transmembrane domain, and a C-terminal domain. The N-terminus was found to be dispensable for cell division inhibition, whereas nine amino acids at the C-terminus were required (133). The sites of nascent peptidoglycan synthesis and formation of FtsZ rings were found to be decreased following treatment with DNA damage, which required DivS (133). Over-expression of DivS also resulted in decreased sites of nascent peptidoglycan synthesis (133). The authors hypothesized that disruption of septal peptidoglycan synthesis by DivS was a result of blocking FtsZ ring formation (133), though the exact mechanism by which DivS activates the DNA damage checkpoint and prevents cell division is not clear. The cell division inhibitor SosA in *S. aureus* is also located adjacent to *lexA* in the genome (136). Investigation of SosA function revealed a direct interaction with PBP1 (136), which is crucial for peptidoglycan synthesis at the division septum (141, 142). Although SosA appears to interact with PBP1, exactly how SosA inhibits cell division remains unclear.

The discovery of the SOS inducible cell division inhibitor in *Caulobacter crescentus* required the use of micro-arrays because the inhibitor is not located near *lexA* in the genome. Expression of the gene encoding the cell division inhibitor *sidA* increased rapidly following treatment with MMC or UV light, and inspection of the promoter revealed putative LexA binding sites (134). Deletion of *lexA* resulted in severe cell elongation that could be rescued by deletion of *sidA*, and over-expression of *sidA* resulted in significant cell elongation (134), demonstrating that SidA over-expression is sufficient to inhibit cell division (134). SidA is a small protein that contains a transmembrane domain. A genetic suppressor screen identified mutations in *ftsW* and *ftsI*, genes encoding two essential components of the divisome involved in peptidoglycan synthesis at the division septum, that could suppress cell division inhibition from over-expressing SidA (134). SidA was found to interact with FtsW in a bacterial two-hybrid assay, and when an untagged FtsW was produced with tagged SidA and FtsI a slight interaction was observed (134). SidA did not alter the localization or recruitment of these divisome proteins

to the site of division, and experiments using fluorescently labeled vancomycin did not find a defect in septal peptidoglycan synthesis following SidA over-expression (134). Together, these data support a model wherein SidA is an SOS-induced cell division inhibitor that inhibits the activity of the divisome through an undetermined mechanism to establish the DNA damage checkpoint.

SOS-independent DNA damage checkpoint

A subsequent study in *C. crescentus* identified a second, SOS-independent cell division inhibitor, DidA, whose expression is still DNA damage inducible and that acts by inhibiting the divisome (135). DidA is also a small protein containing a transmembrane domain. The authors identified a new transcription factor, DriD, that positively regulates *didA* expression. Interestingly, DriD is activated via a DNA damage-dependent mechanism, though it is still unclear how DNA damage activates DriD (135). Therefore, in *C. crescentus* there are two cell division inhibitors that interact with the divisome to prevent cell division following DNA damage, thus establishing the cell cycle checkpoint. The mechanism of relieving the checkpoint remains unknown.

Conclusion

The bacterial DNA damage response has been studied for decades. Although significant progress has been made using the model organism *E. coli*, it is becoming clear that the mechanisms of DNA damage-dependent cell division regulation in other bacteria differ significantly. Instead of the small cytoplasmic inhibitor of FtsZ, SulA, the cell division inhibitors in other bacteria are small membrane bound proteins that in some cases have been found to interact with other components of the cell division machinery (134-136). Still, the mechanism of establishing the DNA damage cell cycle checkpoint by membrane bound cell division inhibitors has remained unclear, and the mechanism of recovery has not been determined in any organism. In the highly tractable model organism *B. subtilis,* the cell division inhibitor has been identified; however, the mechanism of action remains to be elucidated. Although YneA is rapidly degraded (130), it was not clear what proteases were responsible for degrading YneA and how they are regulated. In Chapter II, I demonstrate that YneA is degraded by two previously uncharacterized

proteases. Further, in Chapter III I identify another previously uncharacterized gene that negatively regulates YneA, thereby helping to set the threshold for checkpoint activation. Thus, a major thrust of this dissertation is illuminating how the DNA damage checkpoint is established and relieved in *B. subtilis*.

Figures

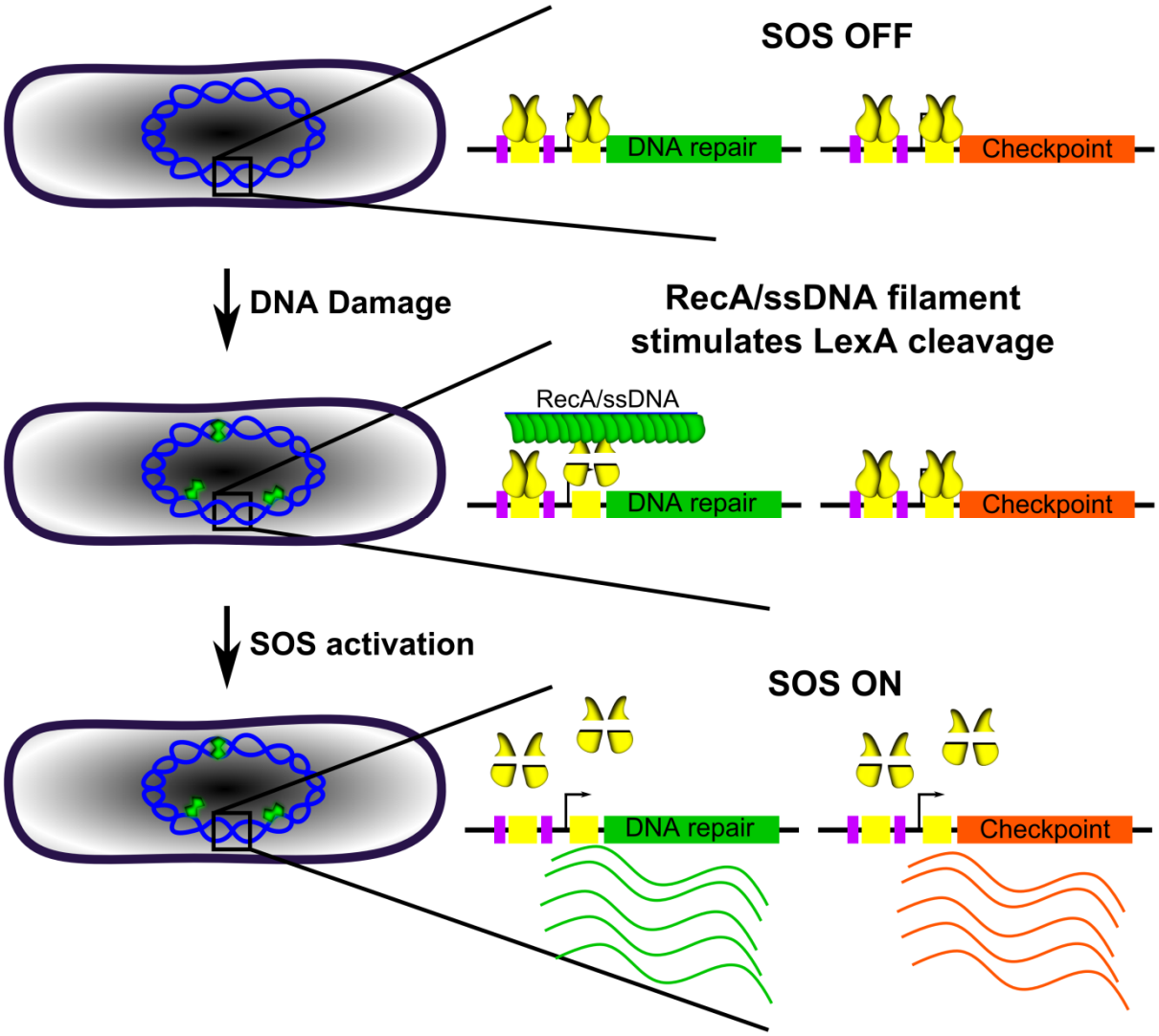

Figure 1.1 A model for activation of the bacterial SOS response. Activation of the SOS response begins with accumulation of ssDNA that occurs when high levels of DNA damage are present (green polygons). The ssDNA is subsequently coated with the protein RecA. The resulting RecA/ssDNA nucleoprotein filament stimulates the protease activity of the transcriptional repressor LexA (yellow protein). LexA undergoes auto-cleavage, which results in de-repression of the LexA regulon. Many of the genes in the LexA regulon are involved in DNA repair, DNA damage tolerance, and regulation of cell division a process known as a cell cycle checkpoint. Yellow boxes represent LexA binding sites, and purple boxes represent -35 and -10 promoter sequences.

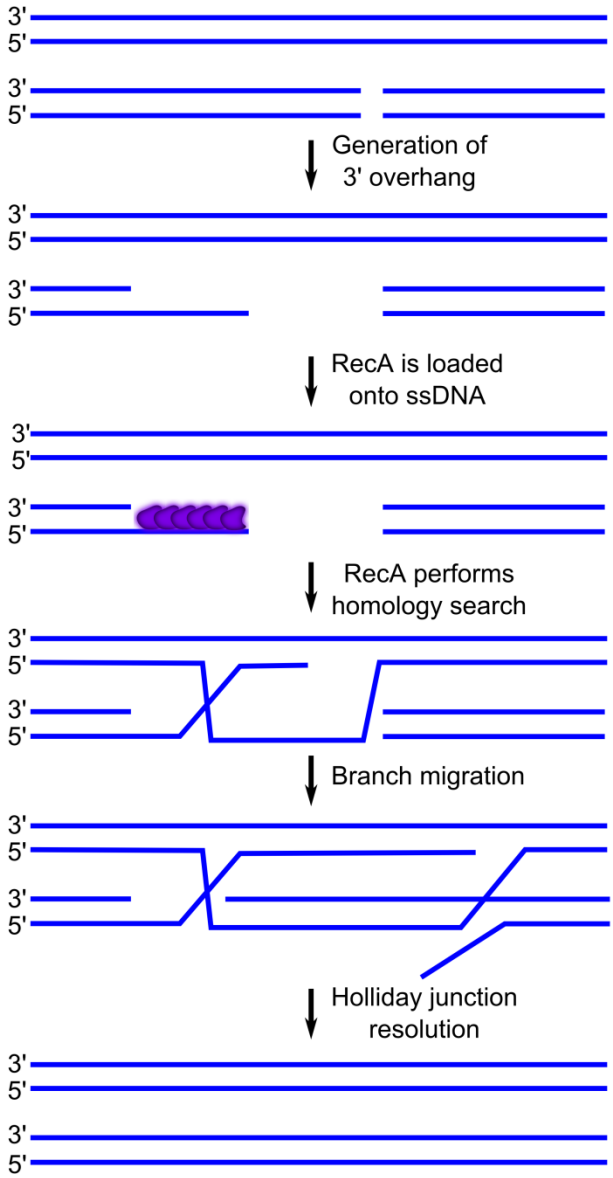

Figure 1.2 Double strand break repair via homologous recombination in bacteria. A double strand break is recognized by the end processing machinery, which generates a free 3′ end. RecA is loaded onto ssDNA and performs a homology search. After synthesis of the sequence information lost at the site of the break, the resulting Holliday junction is resolved, yielding two intact chromosomes.

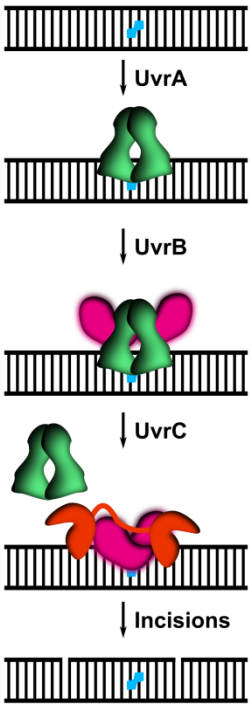

Figure 1.3 Nucleotide excision repair in bacteria. A bulky adduct or thymine dimer is recognized by UvrA. After lesion recognition, UvrB is recruited and lesion verification is performed. Subsequent recruitment of the nuclease UvrC results in two incisions, one on either side of the lesion.

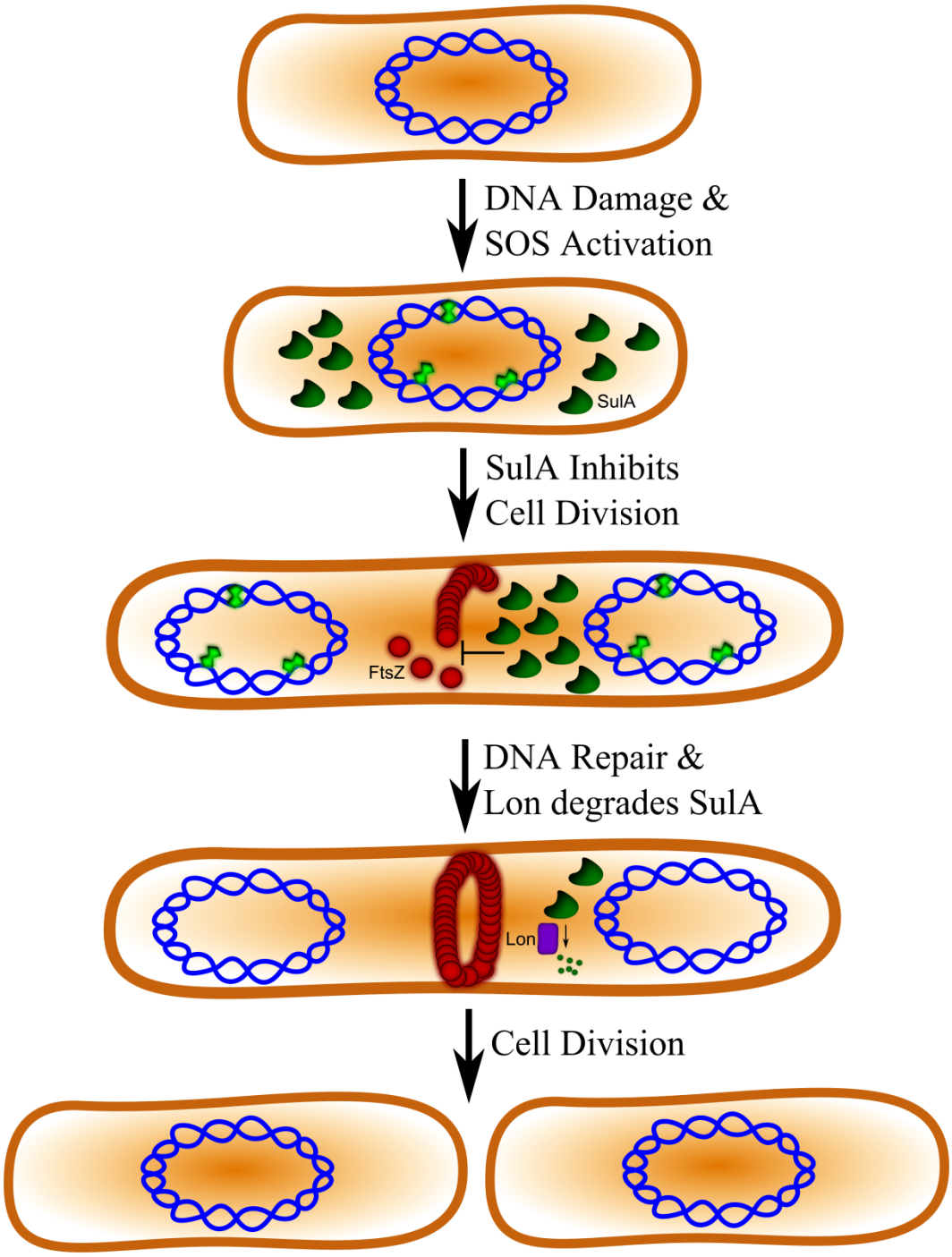

Figure 1.4 DNA damage-dependent cell cycle checkpoint in *E coli*. When *E. coli* cells encounter DNA damage (green polygons), the SOS response is activated and the cell division inhibitor SulA is over-expressed. SulA prevents cell division by inhibiting assembly of the FtsZ ring. Following DNA repair and SOS termination, SulA is degraded by Lon protease, allowing cell division to proceed.

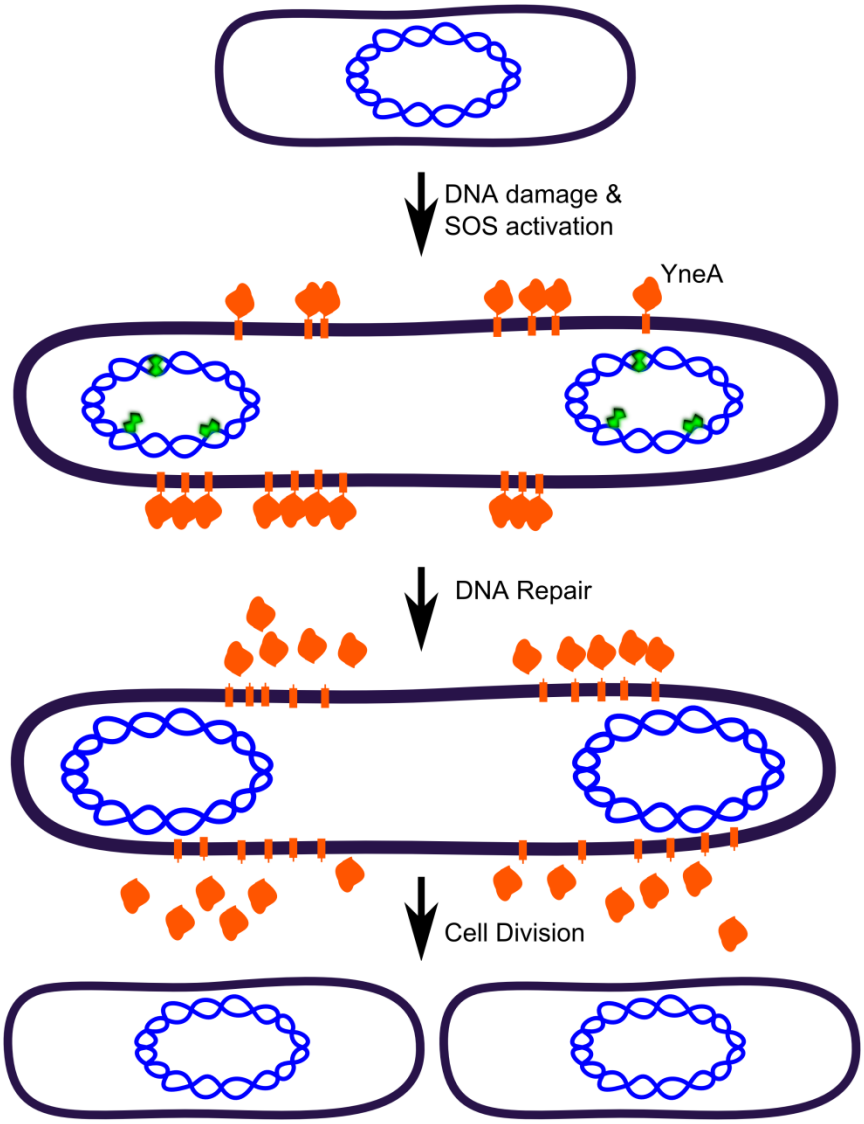

Figure 1.5 DNA damage-dependent cell cycle checkpoint in *B. subtilis*. When *B. subtilis* cells encounter DNA damage (green polygons), the SOS response is activated and the cell division inhibitor YneA is over-expressed. YneA inhibits cell division through an unknown mechanism and subsequent to DNA repair is degraded by unknown proteases, which allows cell division to proceed.

References

1. **Avery OT, MacLeod CM, McCarty M.** 1944. Studies on the chemical nature of the substance inducing transformation of pneumococcal types induction of transformation by a desoxyribonucleic acid fraction isolated from pneumococcus type III. Journal of Experimental Medicine **79:**137-158.
2. **Hershey AD, Chase M.** 1952. Independent functions of viral protein and nucleic acid in growth of bacteriophage. J Gen Physiol **36:**39-56.
3. **Watson JD, Crick FH.** 1953. Molecular structure of nucleic acids; a structure for deoxyribose nucleic acid. Nature **171:**737-738.
4. **Friedberg EC.** 2015. A history of the DNA repair and mutagenesis field I. The discovery of enzymatic photoreactivation. DNA Repair **33:**35-42.
5. **Friedberg EC, Walker GC, Siede W, Wood RD, Schultz RA, Ellenberger T.** 2006. DNA Repair and Mutagenesis, 2nd ed. ASM Press, Washington, D.C.
6. **Chatterjee N, Walker GC.** 2017. Mechanisms of DNA damage, repair, and mutagenesis. Environ Mol Mutagen **58:**235-263.
7. **Ciccia A, Elledge SJ.** 2010. The DNA damage response: making it safe to play with knives. Mol Cell **40:**179-204.
8. **Blanpain C, Mohrin M, Sotiropoulou PA, Passegue E.** 2011. DNA-damage response in tissue-specific and cancer stem cells. Cell Stem Cell **8:**16-29.
9. **Demain AL, Vaishnav P.** 2011. Natural products for cancer chemotherapy. Microb Biotechnol **4:**687-699.
10. **Beukers R, Berends W.** 1960. Isolation and identification of the irradiation product of thymine. Biochim Biophys Acta **41:**550-551.
11. **Setlow RB, Swenson PA, Carrier WL.** 1963. THYMINE DIMERS AND INHIBITION OF DNA SYNTHESIS BY ULTRAVIOLET IRRADIATION OF CELLS. Science **142:**1464-1466.
12. **Ling H, Boudsocq F, Plosky BS, Woodgate R, Yang W.** 2003. Replication of a cis-syn thymine dimer at atomic resolution. Nature **424:**1083-1087.
13. **Doublie S, Tabor S, Long AM, Richardson CC, Ellenberger T.** 1998. Crystal structure of a bacteriophage T7 DNA replication complex at 2.2 A resolution. Nature **391:**251-258.
14. **Kiefer JR, Mao C, Braman JC, Beese LS.** 1998. Visualizing DNA replication in a catalytically active Bacillus DNA polymerase crystal. Nature **391:**304-307.
15. **Johnson RE, Prakash L, Prakash S.** 2005. Distinct mechanisms of cis-syn thymine dimer bypass by Dpo4 and DNA polymerase eta. Proc Natl Acad Sci U S A **102:**12359-12364.
16. **Sedgwick B.** 2004. Repairing DNA-methylation damage. Nat Rev Mol Cell Biol **5:**148-157.
17. **Iyer VN, Szybalski W.** 1963. A molecular mechanism of mitomycin action: Linking of complementary DNA strands. Proc Natl Acad Sci U S A **50:**355-362.
18. **Noll DM, Mason TM, Miller PS.** 2006. Formation and repair of interstrand cross-links in DNA. Chem Rev **106:**277-301.
19. **Dronkert ML, Kanaar R.** 2001. Repair of DNA interstrand cross-links. Mutat Res **486:**217-247.
20. **Dillingham MS, Kowalczykowski SC.** 2008. RecBCD enzyme and the repair of double-stranded DNA breaks. Microbiol Mol Biol Rev **72:**642-671, Table of Contents.

21. **Michel B, Sinha AK, Leach DRF.** 2018. Replication Fork Breakage and Restart in Escherichia coli. Microbiol Mol Biol Rev **82**.
22. **Erill I, Campoy S, Barbe J.** 2007. Aeons of distress: an evolutionary perspective on the bacterial SOS response. FEMS Microbiol Rev **31:**637-656.
23. **Kreuzer KN.** 2013. DNA damage responses in prokaryotes: regulating gene expression, modulating growth patterns, and manipulating replication forks. Cold Spring Harb Perspect Biol **5:**a012674.
24. **Little JW, Mount DW.** 1982. The SOS regulatory system of Escherichia coli. Cell **29:**11-22.
25. **Simmons LA, Foti JJ, Cohen SE, Walker GC.** 2008. The SOS Regulatory Network. EcoSal Plus **2008**.
26. **Kenyon CJ, Walker GC.** 1980. DNA-damaging agents stimulate gene expression at specific loci in Escherichia coli. Proc Natl Acad Sci U S A **77:**2819-2823.
27. **Kenyon CJ, Walker GC.** 1981. Expression of the E. coli uvrA gene is inducible. Nature **289:**808-810.
28. **Courcelle J, Khodursky A, Peter B, Brown PO, Hanawalt PC.** 2001. Comparative gene expression profiles following UV exposure in wild-type and SOS-deficient Escherichia coli. Genetics **158:**41-64.
29. **Schnarr M, Oertel-Buchheit P, Kazmaier M, Granger-Schnarr M.** 1991. DNA binding properties of the LexA repressor. Biochimie **73:**423-431.
30. **Wade JT, Reppas NB, Church GM, Struhl K.** 2005. Genomic analysis of LexA binding reveals the permissive nature of the Escherichia coli genome and identifies unconventional target sites. Genes Dev **19:**2619-2630.
31. **Au N, Kuester-Schoeck E, Mandava V, Bothwell LE, Canny SP, Chachu K, Colavito SA, Fuller SN, Groban ES, Hensley LA, O'Brien TC, Shah A, Tierney JT, Tomm LL, O'Gara TM, Goranov AI, Grossman AD, Lovett CM.** 2005. Genetic composition of the Bacillus subtilis SOS system. Journal of Bacteriology **187:**7655-7666.
32. **Lewis LK, Harlow GR, Gregg-Jolly LA, Mount DW.** 1994. Identification of high affinity binding sites for LexA which define new DNA damage-inducible genes in Escherichia coli. J Mol Biol **241:**507-523.
33. **Brent R, Ptashne M.** 1981. Mechanism of action of the lexA gene product. Proc Natl Acad Sci U S A **78:**4204-4208.
34. **Brent R, Ptashne M.** 1980. The lexA gene product represses its own promoter. Proc Natl Acad Sci U S A **77:**1932-1936.
35. **Little JW, Mount DW, Yanisch-Perron CR.** 1981. Purified lexA protein is a repressor of the recA and lexA genes. Proc Natl Acad Sci U S A **78:**4199-4203.
36. **Sancar A, Sancar GB, Rupp WD, Little JW, Mount DW.** 1982. LexA protein inhibits transcription of the E. coli uvrA gene in vitro. Nature **298:**96-98.
37. **Witkin EM.** 1991. RecA protein in the SOS response: milestones and mysteries. Biochimie **73:**133-141.
38. **Bell JC, Kowalczykowski SC.** 2016. RecA: Regulation and Mechanism of a Molecular Search Engine. Trends Biochem Sci **41:**491-507.
39. **Moreau PL.** 1985. Role of Escherichia coli RecA protein in SOS induction and post-replication repair. Biochimie **67:**353-356.
40. **Little JW, Edmiston SH, Pacelli LZ, Mount DW.** 1980. Cleavage of the Escherichia coli lexA protein by the recA protease. Proc Natl Acad Sci U S A **77:**3225-3229.

41. **Little JW.** 1984. Autodigestion of lexA and phage lambda repressors. Proc Natl Acad Sci U S A **81:**1375-1379.
42. **Simmons LA, Goranov AI, Kobayashi H, Davies BW, Yuan DS, Grossman AD, Walker GC.** 2009. Comparison of responses to double-strand breaks between Escherichia coli and Bacillus subtilis reveals different requirements for SOS induction. J Bacteriol **191:**1152-1161.
43. **Sassanfar M, Roberts JW.** 1990. Nature of the SOS-inducing signal in Escherichia coli. The involvement of DNA replication. J Mol Biol **212:**79-96.
44. **Goranov AI, Kuester-Schoeck E, Wang JD, Grossman AD.** 2006. Characterization of the global transcriptional responses to different types of DNA damage and disruption of replication in Bacillus subtilis. Journal of Bacteriology **188:**5595-5605.
45. **Ayora S, Carrasco B, Cardenas PP, Cesar CE, Canas C, Yadav T, Marchisone C, Alonso JC.** 2011. Double-strand break repair in bacteria: a view from Bacillus subtilis. FEMS Microbiol Rev **35:**1055-1081.
46. **Bell JC, Kowalczykowski SC.** 2016. Mechanics and Single-Molecule Interrogation of DNA Recombination. Annu Rev Biochem **85:**193-226.
47. **Chedin F, Ehrlich SD, Kowalczykowski SC.** 2000. The Bacillus subtilis AddAB helicase/nuclease is regulated by its cognate Chi sequence in vitro. J Mol Biol **298:**7-20.
48. **Taylor AF, Smith GR.** 1985. Substrate specificity of the DNA unwinding activity of the RecBC enzyme of Escherichia coli. J Mol Biol **185:**431-443.
49. **Anderson DG, Kowalczykowski SC.** 1997. The translocating RecBCD enzyme stimulates recombination by directing RecA protein onto ssDNA in a chi-regulated manner. Cell **90:**77-86.
50. **Churchill JJ, Anderson DG, Kowalczykowski SC.** 1999. The RecBC enzyme loads RecA protein onto ssDNA asymmetrically and independently of chi, resulting in constitutive recombination activation. Genes Dev **13:**901-911.
51. **Churchill JJ, Kowalczykowski SC.** 2000. Identification of the RecA protein-loading domain of RecBCD enzyme. J Mol Biol **297:**537-542.
52. **Dixon DA, Kowalczykowski SC.** 1993. The recombination hotspot chi is a regulatory sequence that acts by attenuating the nuclease activity of the E. coli RecBCD enzyme. Cell **73:**87-96.
53. **Taylor AF, Schultz DW, Ponticelli AS, Smith GR.** 1985. RecBC enzyme nicking at Chi sites during DNA unwinding: location and orientation-dependence of the cutting. Cell **41:**153-163.
54. **Simmons LA, Grossman AD, Walker GC.** 2007. Replication is required for the RecA localization response to DNA damage in Bacillus subtilis. Proc Natl Acad Sci U S A **104:**1360-1365.
55. **Indiani C, O'Donnell M.** 2013. A proposal: Source of single strand DNA that elicits the SOS response. Front Biosci (Landmark Ed) **18:**312-323.
56. **Pomerantz RT, O'Donnell M.** 2008. The replisome uses mRNA as a primer after colliding with RNA polymerase. Nature **456:**762-766.
57. **Heller RC, Marians KJ.** 2006. Replication fork reactivation downstream of a blocked nascent leading strand. Nature **439:**557-562.
58. **Morimatsu K, Kowalczykowski SC.** 2003. RecFOR proteins load RecA protein onto gapped DNA to accelerate DNA strand exchange: a universal step of recombinational repair. Mol Cell **11:**1337-1347.

59. **Ivancic-Bace I, Vlasic I, Salaj-Smic E, Brcic-Kostic K.** 2006. Genetic evidence for the requirement of RecA loading activity in SOS induction after UV irradiation in Escherichia coli. J Bacteriol **188:**5024-5032.
60. **Rocha EP, Cornet E, Michel B.** 2005. Comparative and evolutionary analysis of the bacterial homologous recombination systems. PLoS Genet **1:**e15.
61. **Kowalczykowski SC.** 2015. An Overview of the Molecular Mechanisms of Recombinational DNA Repair. Cold Spring Harb Perspect Biol **7**.
62. **Yeeles JT, Dillingham MS.** 2010. The processing of double-stranded DNA breaks for recombinational repair by helicase-nuclease complexes. DNA Repair (Amst) **9:**276-285.
63. **West SC.** 1997. Processing of recombination intermediates by the RuvABC proteins. Annu Rev Genet **31:**213-244.
64. **McGregor N, Ayora S, Sedelnikova S, Carrasco B, Alonso JC, Thaw P, Rafferty J.** 2005. The structure of Bacillus subtilis RecU Holliday junction resolvase and its role in substrate selection and sequence-specific cleavage. Structure **13:**1341-1351.
65. **Sanchez H, Kidane D, Reed P, Curtis FA, Cozar MC, Graumann PL, Sharples GJ, Alonso JC.** 2005. The RuvAB branch migration translocase and RecU Holliday junction resolvase are required for double-stranded DNA break repair in Bacillus subtilis. Genetics **171:**873-883.
66. **Petit C, Sancar A.** 1999. Nucleotide excision repair: from E. coli to man. Biochimie **81:**15-25.
67. **Sancar A.** 1996. DNA excision repair. Annu Rev Biochem **65:**43-81.
68. **Van Houten B.** 1990. Nucleotide excision repair in escherichia-coli. Microbiological Reviews **54:**18-51.
69. **Kisker C, Kuper J, Van Houten B.** 2013. Prokaryotic Nucleotide Excision Repair. Cold Spring Harbor Perspectives in Biology **5:**18.
70. **Truglio JJ, Croteau DL, Van Houten B, Kisker C.** 2006. Prokaryotic nucleotide excision repair: the UvrABC system. Chem Rev **106:**233-252.
71. **Howard-Flanders P, Boyce RP, Theriot L.** 1966. Three loci in Escherichia coli K-12 that control the excision of pyrimidine dimers and certain other mutagen products from DNA. Genetics **53:**1119-1136.
72. **Seeberg E, Steinum AL.** 1982. Purification and properties of the uvrA protein from Escherichia coli. Proc Natl Acad Sci U S A **79:**988-992.
73. **Thiagalingam S, Grossman L.** 1991. Both ATPase sites of Escherichia coli UvrA have functional roles in nucleotide excision repair. J Biol Chem **266:**11395-11403.
74. **Van Houten B, Croteau DL, DellaVecchia MJ, Wang H, Kisker C.** 2005. 'Close-fitting sleeves': DNA damage recognition by the UvrABC nuclease system. Mutat Res **577:**92-117.
75. **Stracy M, Jaciuk M, Uphoff S, Kapanidis AN, Nowotny M, Sherratt DJ, Zawadzki P.** 2016. Single-molecule imaging of UvrA and UvrB recruitment to DNA lesions in living Escherichia coli. Nat Commun **7:**12568.
76. **Seeley TW, Grossman L.** 1990. The role of Escherichia coli UvrB in nucleotide excision repair. J Biol Chem **265:**7158-7165.
77. **Theis K, Chen PJ, Skorvaga M, Van Houten B, Kisker C.** 1999. Crystal structure of UvrB, a DNA helicase adapted for nucleotide excision repair. Embo j **18:**6899-6907.

78. **Orren DK, Sancar A.** 1989. The (A)BC excinuclease of Escherichia coli has only the UvrB and UvrC subunits in the incision complex. Proc Natl Acad Sci U S A **86:**5237-5241.
79. **Moolenaar GF, Franken KL, Dijkstra DM, Thomas-Oates JE, Visse R, van de Putte P, Goosen N.** 1995. The C-terminal region of the UvrB protein of Escherichia coli contains an important determinant for UvrC binding to the preincision complex but not the catalytic site for 3'-incision. J Biol Chem **270:**30508-30515.
80. **Van Houten B, Gamper H, Holbrook SR, Hearst JE, Sancar A.** 1986. Action mechanism of ABC excision nuclease on a DNA substrate containing a psoralen crosslink at a defined position. Proc Natl Acad Sci U S A **83:**8077-8081.
81. **Yeung AT, Mattes WB, Oh EY, Grossman L.** 1983. Enzymatic properties of purified Escherichia coli uvrABC proteins. Proc Natl Acad Sci U S A **80:**6157-6161.
82. **Sancar A, Rupp WD.** 1983. A novel repair enzyme: UVRABC excision nuclease of Escherichia coli cuts a DNA strand on both sides of the damaged region. Cell **33:**249-260.
83. **Caron PR, Kushner SR, Grossman L.** 1985. Involvement of helicase II (uvrD gene product) and DNA polymerase I in excision mediated by the uvrABC protein complex. Proceedings of the National Academy of Sciences **82:**4925-4929.
84. **Van Houten B, Gamper H, Hearst JE, Sancar A.** 1988. Analysis of sequential steps of nucleotide excision repair in Escherichia coli using synthetic substrates containing single psoralen adducts. J Biol Chem **263:**16553-16560.
85. **Manelyte L, Guy CP, Smith RM, Dillingham MS, McGlynn P, Savery NJ.** 2009. The unstructured C-terminal extension of UvrD interacts with UvrB, but is dispensable for nucleotide excision repair. DNA Repair (Amst) **8:**1300-1310.
86. **Lage C, Goncalves SR, Souza LL, de Padula M, Leitao AC.** 2010. Differential survival of Escherichia coli uvrA, uvrB, and uvrC mutants to psoralen plus UV-A (PUVA): Evidence for uncoupled action of nucleotide excision repair to process DNA adducts. J Photochem Photobiol B **98:**40-47.
87. **Weng MW, Zheng Y, Jasti VP, Champeil E, Tomasz M, Wang YS, Basu AK, Tang MS.** 2010. Repair of mitomycin C mono- and interstrand cross-linked DNA adducts by UvrABC: a new model. Nucleic Acids Research **38:**6976-6984.
88. **Adams DW, Wu LJ, Errington J.** 2014. Cell cycle regulation by the bacterial nucleoid. Curr Opin Microbiol **22:**94-101.
89. **Wu LJ, Errington J.** 2011. Nucleoid occlusion and bacterial cell division. Nat Rev Microbiol **10:**8-12.
90. **Bernhardt TG, de Boer PA.** 2005. SlmA, a nucleoid-associated, FtsZ binding protein required for blocking septal ring assembly over Chromosomes in E. coli. Mol Cell **18:**555-564.
91. **Rowlett VW, Margolin W.** 2013. The bacterial Min system. Curr Biol **23:**R553-556.
92. **Tonthat NK, Arold ST, Pickering BF, Van Dyke MW, Liang S, Lu Y, Beuria TK, Margolin W, Schumacher MA.** 2011. Molecular mechanism by which the nucleoid occlusion factor, SlmA, keeps cytokinesis in check. Embo j **30:**154-164.
93. **Cho H, McManus HR, Dove SL, Bernhardt TG.** 2011. Nucleoid occlusion factor SlmA is a DNA-activated FtsZ polymerization antagonist. Proc Natl Acad Sci U S A **108:**3773-3778.

94. **Adams DW, Errington J.** 2009. Bacterial cell division: assembly, maintenance and disassembly of the Z ring. Nat Rev Microbiol **7:**642-653.
95. **Wu LJ, Errington J.** 2004. Coordination of cell division and chromosome segregation by a nucleoid occlusion protein in Bacillus subtilis. Cell **117:**915-925.
96. **Wu LJ, Ishikawa S, Kawai Y, Oshima T, Ogasawara N, Errington J.** 2009. Noc protein binds to specific DNA sequences to coordinate cell division with chromosome segregation. Embo j **28:**1940-1952.
97. **Adams DW, Wu LJ, Errington J.** 2015. Nucleoid occlusion protein Noc recruits DNA to the bacterial cell membrane. Embo j **34:**491-501.
98. **Bernard R, Marquis KA, Rudner DZ.** 2010. Nucleoid occlusion prevents cell division during replication fork arrest in Bacillus subtilis. Mol Microbiol **78:**866-882.
99. **Goranov AI, Katz L, Breier AM, Burge CB, Grossman AD.** 2005. A transcriptional response to replication status mediated by the conserved bacterial replication protein DnaA. Proc Natl Acad Sci U S A **102:**12932-12937.
100. **Robson SA, Michie KA, Mackay JP, Harry E, King GF.** 2002. The Bacillus subtilis cell division proteins FtsL and DivIC are intrinsically unstable and do not interact with one another in the absence of other septasomal components. Mol Microbiol **44:**663-674.
101. **Daniel RA, Errington J.** 2000. Intrinsic instability of the essential cell division protein FtsL of Bacillus subtilis and a role for DivIB protein in FtsL turnover. Mol Microbiol **36:**278-289.
102. **Bramkamp M, Weston L, Daniel RA, Errington J.** 2006. Regulated intramembrane proteolysis of FtsL protein and the control of cell division in Bacillus subtilis. Mol Microbiol **62:**580-591.
103. **Hanawalt P, Setlow R.** 1960. Effect of monochromatic ultraviolet light on macromolecular synthesis in Escherichia coli. Biochim Biophys Acta **41:**283-294.
104. **Gates FL.** 1933. THE REACTION OF INDIVIDUAL BACTERIA TO IRRADIATION WITH ULTRAVIOLET LIGHT. Science **77:**350.
105. **Witkin EM.** 1967. The radiation sensitivity of Escherichia coli B: a hypothesis relating filament formation and prophage induction. Proc Natl Acad Sci U S A **57:**1275-1279.
106. **George J, Castellazzi M, Buttin G.** 1975. Prophage induction and cell division in E. coli. III. Mutations sfiA and sfiB restore division in tif and lon strains and permit the expression of mutator properties of tif. Mol Gen Genet **140:**309-332.
107. **Gayda RC, Yamamoto LT, Markovitz A.** 1976. Second-site mutations in capR (lon) strains of Escherichia coli K-12 that prevent radiation sensitivity and allow bacteriophage lambda to lysogenize. J Bacteriol **127:**1208-1216.
108. **Huisman O, D'Ari R, George J.** 1980. Further characterization of sfiA and sfiB mutations in Escherichia coli. J Bacteriol **144:**185-191.
109. **Huisman O, D'Ari R.** 1981. An inducible DNA replication-cell division coupling mechanism in E. coli. Nature **290:**797-799.
110. **Cole ST.** 1983. Characterisation of the promoter for the LexA regulated sulA gene of Escherichia coli. Mol Gen Genet **189:**400-404.
111. **Mizusawa S, Court D, Gottesman S.** 1983. Transcription of the sulA gene and repression by LexA. J Mol Biol **171:**337-343.
112. **Huisman O, D'Ari R, Gottesman S.** 1984. Cell-division control in Escherichia coli: specific induction of the SOS function SfiA protein is sufficient to block septation. Proc Natl Acad Sci U S A **81:**4490-4494.

113. **Mizusawa S, Gottesman S.** 1983. Protein degradation in Escherichia coli: the lon gene controls the stability of sulA protein. Proc Natl Acad Sci U S A **80:**358-362.
114. **Schoemaker JM, Gayda RC, Markovitz A.** 1984. Regulation of cell division in Escherichia coli: SOS induction and cellular location of the sulA protein, a key to lon-associated filamentation and death. J Bacteriol **158:**551-561.
115. **Bi E, Lutkenhaus J.** 1993. Cell division inhibitors SulA and MinCD prevent formation of the FtsZ ring. J Bacteriol **175:**1118-1125.
116. **Bi E, Lutkenhaus J.** 1990. Analysis of ftsZ mutations that confer resistance to the cell division inhibitor SulA (SfiA). J Bacteriol **172:**5602-5609.
117. **Mukherjee A, Cao C, Lutkenhaus J.** 1998. Inhibition of FtsZ polymerization by SulA, an inhibitor of septation in Escherichia coli. Proc Natl Acad Sci U S A **95:**2885-2890.
118. **Lutkenhaus J, Sanjanwala B, Lowe M.** 1986. Overproduction of FtsZ suppresses sensitivity of lon mutants to division inhibition. J Bacteriol **166:**756-762.
119. **Huang J, Cao C, Lutkenhaus J.** 1996. Interaction between FtsZ and inhibitors of cell division. J Bacteriol **178:**5080-5085.
120. **Trusca D, Scott S, Thompson C, Bramhill D.** 1998. Bacterial SOS checkpoint protein SulA inhibits polymerization of purified FtsZ cell division protein. J Bacteriol **180:**3946-3953.
121. **Chen Y, Milam SL, Erickson HP.** 2012. SulA inhibits assembly of FtsZ by a simple sequestration mechanism. Biochemistry **51:**3100-3109.
122. **Chung CH, Goldberg AL.** 1981. The product of the lon (capR) gene in Escherichia coli is the ATP-dependent protease, protease La. Proc Natl Acad Sci U S A **78:**4931-4935.
123. **Kanemori M, Yanagi H, Yura T.** 1999. The ATP-dependent HslVU/ClpQY protease participates in turnover of cell division inhibitor SulA in Escherichia coli. J Bacteriol **181:**3674-3680.
124. **Wu WF, Zhou Y, Gottesman S.** 1999. Redundant in vivo proteolytic activities of Escherichia coli Lon and the ClpYQ (HslUV) protease. J Bacteriol **181:**3681-3687.
125. **Seong IS, Oh JY, Yoo SJ, Seol JH, Chung CH.** 1999. ATP-dependent degradation of SulA, a cell division inhibitor, by the HslVU protease in Escherichia coli. FEBS Lett **456:**211-214.
126. **Sonezaki S, Ishii Y, Okita K, Sugino T, Kondo A, Kato Y.** 1995. Overproduction and purification of SulA fusion protein in Escherichia coli and its degradation by Lon protease in vitro. Appl Microbiol Biotechnol **43:**304-309.
127. **Love PE, Yasbin RE.** 1984. Genetic characterization of the inducible SOS-like system of Bacillus subtilis. J Bacteriol **160:**910-920.
128. **Yasbin RE, Cheo D, Bayles KW.** 1991. The SOB system of Bacillus subtilis: a global regulon involved in DNA repair and differentiation. Res Microbiol **142:**885-892.
129. **Kawai Y, Moriya S, Ogasawara N.** 2003. Identification of a protein, YneA, responsible for cell division suppression during the SOS response in Bacillus subtilis. Mol Microbiol **47:**1113-1122.
130. **Mo AH, Burkholder WF.** 2010. YneA, an SOS-induced inhibitor of cell division in Bacillus subtilis, is regulated posttranslationally and requires the transmembrane region for activity. J Bacteriol **192:**3159-3173.
131. **Buist G, Steen A, Kok J, Kuipers OP.** 2008. LysM, a widely distributed protein motif for binding to (peptido)glycans. Mol Microbiol **68:**838-847.

132. **Chauhan A, Lofton H, Maloney E, Moore J, Fol M, Madiraju MV, Rajagopalan M.** 2006. Interference of Mycobacterium tuberculosis cell division by Rv2719c, a cell wall hydrolase. Mol Microbiol **62:**132-147.
133. **Ogino H, Teramoto H, Inui M, Yukawa H.** 2008. DivS, a novel SOS-inducible cell-division suppressor in Corynebacterium glutamicum. Mol Microbiol **67:**597-608.
134. **Modell JW, Hopkins AC, Laub MT.** 2011. A DNA damage checkpoint in Caulobacter crescentus inhibits cell division through a direct interaction with FtsW. Genes Dev **25:**1328-1343.
135. **Modell JW, Kambara TK, Perchuk BS, Laub MT.** 2014. A DNA damage-induced, SOS-independent checkpoint regulates cell division in Caulobacter crescentus. PLoS Biol **12:**e1001977.
136. **Bojer MS, Wacnik K, Kjelgaard P, Gallay C, Bottomley AL, Cohn MT, Lindahl G, Frees D, Veening J-W, Foster SJ, Ingmer H.** 2018. SosA inhibits cell division in Staphylococcus aureus in response to DNA damage. bioRxiv doi:10.1101/364299.
137. **Rand L, Hinds J, Springer B, Sander P, Buxton RS, Davis EO.** 2003. The majority of inducible DNA repair genes in Mycobacterium tuberculosis are induced independently of RecA. Mol Microbiol **50:**1031-1042.
138. **Brooks PC, Dawson LF, Rand L, Davis EO.** 2006. The mycobacterium-specific gene Rv2719c is DNA damage inducible independently of RecA. J Bacteriol **188:**6034-6038.
139. **Dullaghan EM, Brooks PC, Davis EO.** 2002. The role of multiple SOS boxes upstream of the Mycobacterium tuberculosis lexA gene--identification of a novel DNA-damage-inducible gene. Microbiology **148:**3609-3615.
140. **Jochmann N, Kurze AK, Czaja LF, Brinkrolf K, Brune I, Huser AT, Hansmeier N, Puhler A, Borovok I, Tauch A.** 2009. Genetic makeup of the Corynebacterium glutamicum LexA regulon deduced from comparative transcriptomics and in vitro DNA band shift assays. Microbiology **155:**1459-1477.
141. **Claessen D, Emmins R, Hamoen LW, Daniel RA, Errington J, Edwards DH.** 2008. Control of the cell elongation-division cycle by shuttling of PBP1 protein in Bacillus subtilis. Mol Microbiol **68:**1029-1046.
142. **Scheffers DJ, Errington J.** 2004. PBP1 is a component of the Bacillus subtilis cell division machinery. J Bacteriol **186:**5153-5156.

CHAPTER II

Discovery of a dual protease mechanism that promotes DNA damage checkpoint recovery

Abstract

The DNA damage response is a signaling pathway found throughout biology. In many bacteria the DNA damage checkpoint is enforced by inducing expression of a small, membrane bound inhibitor that delays cell division providing time to repair damaged chromosomes. How cells promote checkpoint recovery after sensing successful repair is unknown. By using a high-throughput, forward genetic screen, we identified two unrelated proteases, YlbL and CtpA, that promote DNA damage checkpoint recovery in *Bacillus subtilis*. Deletion of both proteases leads to accumulation of the checkpoint protein YneA. We show that DNA damage sensitivity and increased cell elongation in protease mutants depends on *yneA*. Further, expression of YneA in protease mutants was sufficient to inhibit cell proliferation. Finally, we show that both proteases interact with YneA and that one of the two proteases, CtpA, directly cleaves YneA *in vitro*. With these results, we report the mechanism for DNA damage checkpoint recovery in bacteria that use membrane bound cell division inhibitors.

Author summary

Prokaryotes and eukaryotes coordinate cell division to genome integrity using DNA damage checkpoints. Many bacteria express a small, membrane binding protein to slow cell division when obstacles to DNA replication are encountered. Cell division inhibitors of this class have been identified in several bacterial species, yet the mechanism used to alleviate inhibition

The contents of this chapter were published in *PLoS Genetics* by Peter E. Burby, Zackary W. Simmons, Jeremy W. Schroeder, and Lyle A. Simmons. I designed and performed experiments, and analyzed the data. ZWS helped with data collection and data analysis for microscopy experiments in Figures 2.7 and 2.11. JWS helped with next generation sequence data alignment and analysis. Sample processing and data analysis for the proteomics experiment were performed by MSBioworks. LAS and I wrote the manuscript.

has remained unknown. Using forward genetics, we identified two unstudied genes, coding for the proteases YlbL and CtpA, that when deleted result in sensitivity to drugs that directly damage DNA. We show that sensitivity to DNA damage in protease mutants is a result of accumulation of the cell division inhibitor. Further, we show that YlbL and CtpA are responsible for degrading the cell division inhibitor allowing for cell division to resume. Importantly, these two proteases are not homologs, demonstrating a striking example of a bacterium using non-homologous enzymes to degrade a single substrate. Our investigation uncovers the previously unknown mechanism used to remove a cell division inhibitor, while also illuminating a potential strategy that bacteria can use to regulate signaling pathways. The use of multiple, unrelated proteins to perform a single function may represent a strategy employed throughout biological systems.

Introduction

The DNA damage response (DDR, SOS response in bacteria) is an important pathway for maintaining genome integrity in all domains of life. Misregulation of the DDR in humans can result in various disease conditions (1, 2), and in bacteria the SOS response has been found to be important for survival under many stressors (3-5). The DNA damage response in all organisms results in three principle outcomes: a transcriptional response, which can vary depending on the type of DNA damage incurred, DNA repair, and activation of a DNA damage checkpoint (6-9). In eukaryotes, the G1/S and G2/M checkpoints are established by checkpoint kinases, which transduce the signal of DNA damage through inactivation of the phosphatase Cdc25 (7). Checkpoint kinase dependent inhibition of Cdc25 leads to accumulation of phosphorylated cyclin dependent kinases, which prevents cell cycle progression (7). In bacteria, the SOS-dependent DNA damage checkpoint relies on expression of a cell division inhibitor, though the type of inhibitor varies between bacterial species.

In *Escherichia coli*, the SOS-dependent DNA damage checkpoint is the best understood bacterial checkpoint (6). Upon activation of the SOS response, the cytoplasmic cell division inhibitor SulA is expressed (10). SulA accumulation leads to a block in septum formation by preventing the assembly of the cytokinetic ring by FtsZ, a homolog of eukaryotic tubulin (11, 12). SulA binds directly to FtsZ (13) and inhibits FtsZ polymerization (14, 15). Recovery from the SulA-induced checkpoint occurs through proteolysis of SulA. Lon is the primary protease responsible

for clearing SulA (16-18), although ClpYQ (HslUV) were found to contribute to SulA degradation in the absence of Lon (19-21). Thus, the mechanisms of DNA damage checkpoint activation by the cytoplasmic protein SulA and subsequent recovery are well understood in *E. coli*. The SulA-dependent checkpoint, however, is restricted to *E. coli* and a subset of closely related bacteria. It is becoming increasingly clear that most other bacteria use a DNA damage checkpoint with an entirely different mechanism of enforcement and recovery.

An evolutionarily broad group of bacterial organisms have been shown to use a notably different DNA damage checkpoint mechanism (22-25). In these Gram-positive and Gram-negative organisms, a small protein with a transmembrane domain is expressed that inhibits cell division without targeting FtsZ. One example is in the Gram-negative bacterium *Caulobacter crescentus*, where the SidA and DidA proteins bind to the essential membrane bound divisome components, FtsW/N, that contribute to peptidoglycan remodeling (22, 26). Another example is the Gram-positive bacterium *Bacillus subtilis* in which the SOS-dependent cell division inhibitor is YneA (23). YneA contains an N-terminal transmembrane domain with the majority of the protein found in the extracellular space (27). Upon SOS activation, LexA-dependent repression of *yneA* is relieved and *yneA* is expressed (23). Increased expression of *yneA* results in cell elongation, though FtsZ ring formation still occurs (27), suggesting YneA inhibits cell division through a mechanism distinct from that of SulA. Further investigation found that overexpressed YneA is released into the medium, and that full length YneA is likely the active form of the protein (27). The mechanism(s) responsible for YneA inactivation is unknown. Therefore, although the use of a small, membrane bound cell division inhibitor is wide-spread among bacteria, in all cases studied the mechanism of checkpoint recovery remains unknown (22-26).

We report a set of forward genetic screens to three different classes of DNA damaging agents using transposon mutagenesis followed by deep sequencing (Tn-seq). Our screen identified two proteases, YlbL and CtpA, that are important for growth in the presence of DNA damage. Mechanistic investigation demonstrates that YlbL and CtpA have overlapping functions, and in the absence of these two proteases, DNA damage-dependent cell elongation is increased and checkpoint recovery is slowed. A proteomic analysis identified accumulation of YneA in the double protease mutant. We also found that DNA damage sensitivity of protease mutants depends solely on *yneA*. Further, we show that both proteases interact with full length

YneA in a bacterial two-hybrid assay, and that CtpA is able to digest YneA in a purified system. With these results, we present a model of DNA damage checkpoint recovery for bacteria that use the more wide-spread mechanism employing a small, membrane bound cell division inhibitor.

Results

Forward genetic screen rationale and analysis

In order to better understand the DNA damage response in bacteria, we performed three forward genetic screens using *B. subtilis*. We generated a transposon insertion library consisting of more than 120,000 distinct insertions **(Table 2.1)**. The coverage of each transposon mutant in the library was plotted against the genome coordinates, which showed that the distribution of insertions was approximately uniform across the chromosome in the population of mutants **(Fig 2.1A)**. Two small exceptions were detected where coverage decreased. Decreased coverage corresponds to regions where many essential genes are clustered **(Fig 2.1A, arrow heads)**. With the goal of identifying mutants important for the DNA damage response, we grew parallel cultures of either control or DNA damage treatment over three growth periods, modelling our experimental design after a previous report **(Fig 2.1B)** (28). Mitomycin C (MMC), methyl methane sulfonate (MMS), and phleomycin (Phleo) were chosen for screening because these agents represent three different classes of antibiotics that damage DNA directly. MMC causes inter- and intra-strand crosslinks and larger adducts (29, 30), MMS causes smaller adducts consisting of DNA methylation (31), and Phleo results in single and double stranded breaks (32, 33). As a result, we reasoned that the combined data would provide a collection of genes that are generally important for the DNA damage response.

After sequencing, we performed quality control analysis. First, given that sequencing data are count data, the distribution of the coverage should be log-normal (34). Indeed, the distribution of each replicate for the initial library and starter culture samples is approximately log-normal **(Fig 2.2A)**. We also found that the distributions for the remaining time points of the pooled replicates followed an approximate log-normal distribution **(Fig 2.2B)**. The sequencing data and viable cell count data **(Table 2.1)** were used to calculate the fitness of each insertion mutant in each condition **(Fig 2.1C)** (35, 36). The relative fitness of each insertion was calculated by taking the ratio of treatment to control **(Fig 2.1C)**, thereby isolating fitness effects

of the treatments. The relative fitness of each gene was determined by averaging the relative fitness calculated for each insertion within a gene **(Fig 2.1C)**. To verify that a t-test would be appropriate for determining relative fitness deviating significantly from one, we plotted the distribution of insertion relative fitness. All the distributions were normal with a mean close to one **(Fig 2.2C)**. We determined the relative fitness for every gene with sufficient data (see supplemental methods), and report the relative fitness values and the adjusted p-values for genes with the lowest 200 relative fitness values in each growth period (37) **(Table 2.3)**.

Tn-seq identified genes involved in DNA repair and genes of unknown function

Initial inspection found that transposon insertion in several genes known to be involved in DNA repair (*recA*, *ruvAB*, *recN*, and *recOR* (38)) resulted in decreased relative fitness in growth period one of all experiments **(Table 2.2)**. A closer analysis of *recN*, *addA*, and *polA*, three genes that are found toward the top of the lists in all treatments, showed that relative fitness is less than one in most cases, though in the Phleo experiment, it appears that the cultures were adapting to the treatment by growth period three **(Fig 2.1D)**. For comparison, we also plotted the relative fitness of *thrC*, a gene involved in threonine biosynthesis, and found the relative fitness to be about one in all conditions examined **(Fig 2.1D)**. Importantly, insertion in *uvrA*, a component of the nucleotide excision repair machinery (38, 39) which helps repair MMC adducts but not MMS or Phleo related damage (40, 41), decreased relative fitness in growth periods 2 and 3 with MMC, but did not significantly decrease relative fitness in MMS or Phleo **(Fig 2.1D and Table 2.2)**. Taken together, these results validate the approach by demonstrating that we were able to identify genes known to be involved in DNA repair.

We also wondered whether our results contained false positives. To test this, we decided to experimentally validate the genes with the forty lowest relative fitness values from growth period two in the MMC experiment. We found that eight of the forty gene deletions were not sensitive to MMC in a spot titer assay **(Table 2.3)**. Several genes that were false positives are located in the genome near genes with validated phenotypes, suggesting that polar effects explain some of the false positives **(Table 2.3; see supplemental results for detailed analysis)**. To identify genes required generally as part of the DNA damage response, we examined the 200 genes from growth period two with the lowest relative fitness and an adjusted p-value less than 0.01 from all three experiments **(Table 2.4)**. We found that 21 genes overlapped for all three

experiments **(Fig 2.1E)**, some of which are known to be involved in DNA repair (*recN*, *addB*, *polA*, *radA*), while several genes have no known function (*e.g.*, *ylbL* and *ctpA*) **(Table 2.4)**.

YlbL and CtpA require putative catalytic residues for function

Among the genes important for growth in the presence of DNA damage, we focused on two putative proteases YlbL and CtpA. YlbL is predicted to have three domains: a transmembrane domain, a Lon protease domain, and a PDZ domain **(Fig 2.3A)**. CtpA is predicted to have four domains: a transmembrane domain, a S41 peptidase domain, a PDZ domain, and a C-terminal peptidoglycan (PG) binding domain **(Fig 2.3A)**. In all three Tn-seq experiments, the relative fitness of insertions in either *ylbL* or *ctpA* was significantly less than one in the second and third growth periods **(Fig 2.3B)**, suggesting that absence of either protease results in sensitivity to DNA damage. In contrast, a control gene *amyE*, which is involved in starch utilization, had a relative fitness of approximately one in all conditions examined **(Fig 2.3B)**. To verify the Tn-seq results, we constructed clean deletions of *ylbL* and *ctpA* and found both mutants to be sensitive to DNA damage in a spot titer assay **(Fig 2.3C)**. Each phenotype was also complemented by ectopic expression of each protease in its respective mutant background **(Fig 2.3C)**. To identify putative catalytic residues, we aligned the protease domain of YlbL to LonA and LonB from *B. subtilis* and Lon from *E. coli*. The sequence alignment revealed that YlbL contains a putative catalytic dyad consisting of a serine (S234) and a lysine (K279) **(Fig 2.4A)**. Similarly, we aligned CtpA to its homologs CtpB from *B. subtilis* and Prc from *E. coli*, which identified a putative catalytic triad consisting of a serine (S297), a lysine (K322), and a glutamine (Q326) **(Fig 2.4B)**. To test whether these putative catalytic residues were required for function, we attempted to complement the DNA damage sensitivity phenotype via ectopic expression of serine and lysine mutants. Both the serine and lysine mutants of YlbL and CtpA failed to complement the deletion phenotypes **(Fig 2.3C)**. The variants and the wild-type proteases were ectopically expressed to the same level *in vivo* **(Fig 2.3D)**, suggesting that the lack of complementation is not due to instability caused by the amino acid changes. With these results, we conclude that protease activity is required for YlbL and CtpA to function in response to DNA damage.

YlbL and CtpA have overlapping functions

The similarity in phenotypes led us to hypothesize that YlbL and CtpA have overlapping functions. To test this, we performed a cross-complementation experiment using spot titer assays for MMC sensitivity. Over-expression of YlbL, but not YlbL-S234A, complemented a *ctpA* deletion **(Fig 2.5A & B)**. Similarly, over-expression of CtpA, but not CtpA-S297A, complemented a *ylbL* deletion **(Fig 2.5A & B)**. In addition, deletion of both proteases rendered *B. subtilis* hypersensitive to MMC, even more so than loss of *uvrA*, which codes for the protein responsible for recognizing MMC adducts as part of nucleotide excision repair **(Fig 2.5C)** (38, 39). To further test the hypothesis that YlbL and CtpA have overlapping functions, we over-expressed each of the proteases separately in the double protease mutant background and observed a complete rescue of MMC sensitivity upon expression of the wild type (WT), but not the serine variants **(Fig 2.5D & E)**.

DNA damage-dependent cell division delay is increased in protease deletions

The experiments performed thus far cannot distinguish between sensitivity to MMC resulting from cell death, growth inhibition or both. To determine whether sensitivity arises from cell death, we performed a survival assay using an acute treatment of MMC. We detected a slight decrease in percent survival as MMC concentration increased in the Δ*ylbL* and the double mutant strain **(Fig 2.6A)**. We compared the decrease in percent survival in single and double protease mutants to a Δ*uvrA* strain, which has been shown previously to be acutely sensitive to MMC (40). The strain lacking *uvrA* was very sensitive to an acute treatment of MMC **(Fig 2.6A)**, whereas, the double protease deletion strain was significantly less sensitive to acute exposure compared with Δ*uvrA* **(compare Fig 2.5C & 2.6A)**. Taken together, we conclude that MMC sensitivity of the protease mutants observed in spot titer assays is primarily caused by growth inhibition.

We hypothesized that sensitivity to DNA damage resulting from growth inhibition could also be explained by inhibiting cell proliferation, or by inhibiting cell division rather than cell growth. To distinguish between these two possibilities, we measured cell length, because inhibition of proliferation should be observed as an increase in cell length, consistent with a failure in checkpoint recovery. Thus, we designed a MMC recovery assay, reasoning that

following treatment with MMC, cells lacking YlbL, CtpA, or both, would remain elongated showing slower checkpoint recovery relative to the WT strain. We grew cultures either in a vehicle control or in the presence of MMC. After a two-hour treatment, the MMC containing media was removed and cells were washed. Cells were then transferred to fresh media without MMC and allowed to continue growth to assay for checkpoint recovery. Although cells appeared to be elongated in the Δ*ylbL* and double mutant strains, there was heterogeneity in the population **(Fig 2.7A)**. As a result, we measured the cell length of at least 900 cells for each genotype and each condition and plotted the cell length distributions as histograms **(Fig 2.7B)**. There was no difference in the vehicle control cell length distributions **(Fig 2.7B)**. The MMC treatment of all strains resulted in a rightward shift in the distribution for all strains **(Fig 2.7B, compare upper panels)**. When comparing the protease deletions to the WT, the difference in distribution could be visualized by considering the percentage of cells greater than 6.75 μm in length, which is about three cell lengths of 2.25 μm each. We found that deletion of *ylbL* resulted in an increase in the percentage of cells longer than 6.75 μm in MMC treated cultures and after both two hours and four hours of recovery **(Fig 2.7C)**. Deletion of *ctpA*, however, resulted in a very slight, though significant (p-value = 0.0142 for one-tailed Z-test), increased percentage of cells longer than 6.75 μm after 4 hours of recovery **(Fig 2.7C)**. The double mutant resulted in a percentage of cells slightly greater than Δ*ylbL* alone after both two hours (p-value = 0.0001 for one-tailed Z-test) and four hours (p-value = 0.0088 for one-tailed Z-test) of recovery **(Fig 2.7C)**.

Taken together, we conclude that YlbL is the primary protease under these conditions, with CtpA also contributing. We also conclude that cells lacking YlbL or both YlbL and CtpA take longer to divide following exposure to MMC, which is consistent with DNA damage sensitivity resulting from inhibition of cell proliferation. Further, the observation of inhibition of cell proliferation suggests that YlbL and CtpA proteases could be important for DNA damage checkpoint recovery (see below).

YlbL and CtpA levels are not regulated by DNA damage

A potential model to regulate YlbL and CtpA in response to DNA damage is to increase protein levels following exposure to DNA damage. Increased protease levels in response to DNA damage could promote the DNA damage checkpoint recovery when needed. To test this model, we monitored YlbL and CtpA protein levels via Western blotting over the course of the MMC

recovery assay. YlbL and CtpA protein levels did not change relative to the loading control DnaN throughout the course of the experiment **(Fig 2.6B & C)**. As a positive control, we performed the same experiment and monitored RecA protein levels and found that, indeed, RecA protein levels increased **(Fig 2.6B & C)**, as expected because *recA* is induced as part of the SOS response (42, 43). We conclude that YlbL and CtpA protein levels are not regulated by DNA damage.

The cell division inhibitor YneA accumulates in protease mutants

The data presented thus far led us to hypothesize that in the absence of YlbL and CtpA, a protein accumulates which results in inhibition of cell division **(Fig 2.8A)**. To identify the accumulating protein, we performed an analysis of the entire proteome of WT and double protease mutant cell extracts. We chose to analyze the proteomes of cells after two hours of recovery, because the cell length distributions differed most between WT and the double protease mutant **(Fig 2.7B)**. We found that the normalized spectral count data had similar distributions for both WT and the double mutant, which were approximately log normal **(Fig 2.9A)**. We verified that the distribution of the test statistic (the difference in double mutant average and WT average) was normally distributed **(Fig 2.9B)**, thus allowing a t-test to be used. We also performed a principle component analysis and found that WT replicates and double mutant replicates each clustered together **(Fig 2.9C)**.

In total, 2329 proteins were detected, and 183 proteins were found to be differentially represented (p-value < 0.05) in the double mutant relative to WT **(Table 2.5)**. Of the proteins differentially represented in the double mutant, 104 had a fold change greater than one **(Fig 2.8B, red points)**. There are three major mechanisms that have been reported in *B. subtilis* to inhibit cell division: 1) Noc dependent nucleoid occlusion (44), 2) FtsL depletion (45, 46), and 3) expression of YneA (23). One possibility was that Noc protein levels were higher in the double mutant, but we observed no difference in Noc levels **(Fig 2.9D)**. Another possibility was that FtsL or the protease RasP, which degrades FtsL, was affected in the protease mutant background (46). We found no difference in relative protein abundance of FtsL or RasP **(Fig 2.9D)**, ruling out the FtsL/RasP pathway. Among the top 10 proteins that were more abundant in the double mutant was YneA, the SOS-dependent cell division inhibitor **(Table 2.5)**. We asked if the enrichment of YneA was simply because it is SOS induced. We analyzed the relative abundance

of several other proteins that are known to be SOS induced, including RecA, UvrA, UvrB, DinB, and YneB (42), which is encoded in an operon with YneA (23). We found that none of these other proteins were enriched in the double mutant **(Fig 2.9E)**. These results suggest that YneA accumulation is not a result of increased SOS activation, and regulation of YneA accumulation is likely to be post translational, because the protein levels of another member of the operon, YneB were unchanged. Taken together, our proteomics data suggest that YlbL and CtpA promote DNA damage checkpoint recovery through regulating YneA protein abundance.

We directly tested for YneA accumulation in protease mutants throughout the MMC recovery assay using Western blotting. YneA accumulated in all protease deletion strains after 2 hours and 4 hours of recovery, though YneA accumulation in Δ*ctpA* was slight **(Fig 2.8C)**. In the double mutant, YneA accumulated in the MMC treatment condition in addition to both recovery time points **(Fig 2.8C)**. In the double mutant we observed multiple YneA species, which we hypothesize to be the result of unnaturally high YneA protein levels resulting in non-specific cleavage by other proteases. With these results, we suggest that YneA is a substrate of YlbL and CtpA, both of which degrade YneA allowing for checkpoint recovery.

yneA is required for DNA damage sensitivity and cell elongation phenotypes

Although accumulation of YneA fit our data well, we considered that the other proteins enriched greater than five-fold in the double mutant may have contributed to the DNA damage sensitivity phenotype. To test this, we constructed deletions of each gene in WT and the double mutant and tested for MMC sensitivity. We found that no single deletion of each of the 10 genes resulted in sensitivity to MMC **(Fig 2.10A)**. In the double mutant, only deletion of *yneA* was able to rescue the sensitivity to MMC **(Fig 2.10A)**. We verified that deletion of *yneA* could rescue MMC sensitivity in all protease mutant backgrounds **(Fig 2.11A)**. We examined cell length in the DNA damage recovery assay. As expected, deletion of *yneA* resulted in less severe cell elongation relative to WT **(compare WT in Fig 2.7B and Δ*yneA::loxP* in Fig 2.11B)**. In addition, deletion of *ylbL*, *ctpA*, or both no longer changed the cell length distribution in the absence of *yneA* at the two-hour recovery time point **(Fig 2.11B, 2.11C, and 2.10B)**. In the MMC treatment, we did observe a slight increase (p-value = 0.0004 for one-tailed Z-test) in the percentage of cells greater than 6.75 μm in the double protease deletion strain compared to WT **(Fig 2.11C)**. Given that MMC sensitivity and most cell elongation in protease mutants depends

on *yneA*, we hypothesized that expression of YneA alone would be sufficient to inhibit growth to a greater extent in the protease mutants. Indeed, strains lacking YlbL, CtpA or both were more sensitive to over-expression of *yneA* from an IPTG inducible promoter than WT **(Fig 2.11D)**. Further, we show that YneA accumulated in the protease mutant strains following *yneA* ectopic expression **(Fig 2.11E)**. We conclude that YneA accumulation results in severe growth inhibition in cells lacking YlbL and CtpA.

CtpA specifically digests YneA *in vitro*

To test the hypothesis that YneA is a direct substrate of the proteases we purified YneA (a.a. 28-103), CtpA (a.a 38-466), and YlbL (a.a 36-341) lacking their N-terminal transmembrane domains to allow for isolation. We were unable to detect protease activity from YlbL using YneA, lysozyme, or casein as substrates **(Figure 2.12; see discussion)**. When purified CtpA was incubated with YneA, we observed digestion of YneA over time, but no digestion was observed using CtpA-S297A **(Fig 2.13A)**. To test if CtpA activity against YneA was specific we completed the same reaction using lysozyme as a substrate and detected no activity **(Fig 2.13B)**. We conclude that YneA is a direct and specific substrate of CtpA.

YlbL-S234A and CtpA-S297A interact with YneA

Although we could not detect YlbL protease activity *in vitro* we asked if YlbL could interact with YneA. To test this, we used a bacterial two-hybrid assay (47, 48). We used this assay because it is effective at detecting interactions between membrane proteins (22, 26, 49). We tested YlbL-S234A and CtpA-S297A to prevent digestion of YneA, and assayed for interaction with full length YneA or YneA without its transmembrane domain (YneAΔN) as a control. We found that YlbL and CtpA both interacted with full length YneA **(Fig 2.13C)**, but no interaction was detected with YneAΔN **(Fig 2.13C)**, likely due to YneA failing to localize to the membrane. Given that YlbL did not have activity *in vitro* and we detected an interaction with YneA in the bacterial two-hybrid assay, we suggest that YneA is a direct substrate of YlbL and that YlbL requires full length YneA for interaction.

Discussion

How do YlbL and CtpA recognize YneA as a substrate? An intriguing facet of this checkpoint recovery mechanism is the use of unrelated proteases. YlbL and CtpA both have transmembrane domains and PDZ domains, but the peptidase domains are very different. CtpA has a S41 peptidase domain and is homologous to Tail-specific protease or Tsp (also Prc), which recognizes the C-terminus of its substrate through its PDZ domain (50, 51). We suggest that CtpA also recognizes YneA through the PDZ domain and that this mechanism explains how CtpA recognizes its other cognate substrates. In fact, the study by Mo and Burkholder identified a residue at the C-terminus of YneA (D97) which when mutated to alanine stabilizes YneA (27). It is tempting to speculate that D97 in YneA is important for CtpA to recognize YneA. The mechanism by which YlbL recognizes YneA is less clear. YlbL has a unique domain organization not found in other studied proteases. YlbL does not have the AAA+ ATPase domain common in other Lon proteases, which is logical given that YlbL likely resides extracellularly in order to degrade YneA. Instead of an ATPase domain, YlbL has a PDZ domain, which could act as a substrate recognition domain or as an inhibitory domain similar to the PDZ domain of DegS (52-54). The bacterial two hybrid assay suggests that YlbL does recognize YneA directly **(Fig 2.13C)**, though we cannot rule out the possibility that there is an adaptor protein that recognizes YneA when these proteins are tethered to the membrane. We also did not identify a potential adaptor in the Tn-seq data further suggesting a direct interaction does occur between YlbL and YneA. A final possibility is that YlbL recognizes YneA through the transmembrane domain, which then activates the Lon peptidase domain to degrade or cleave YneA. This would also explain the reason we were unable to detect activity using YlbL lacking its transmembrane domain. In any case, further experiments are necessary to elucidate the mechanism by which YlbL recognizes YneA.

All organisms control cellular processes through regulated signaling. To regulate a cellular process a signaling pathway must have mechanisms of activation and inactivation. Many bacteria use a small membrane protein as an SOS-induced DNA damage checkpoint protein (22-25). The mechanism of checkpoint recovery, however, for organisms using membrane protein checkpoints has remained unclear. Our comprehensive study identified a dual protease mechanism of DNA damage checkpoint recovery **(Fig 2.13D)**. Proteases YlbL and CtpA are constitutively present in the plasma membrane of cells even in the absence of DNA damage.

After encountering DNA damage, YneA expression is induced. We hypothesize that YlbL and CtpA activities become saturated by increased YneA expression, which results in a delay of cell division. Following DNA repair, expression of YneA decreases and YlbL and CtpA clear any remaining YneA allowing cell division to resume.

DNA damage checkpoints are of fundamental importance to biology, and we have discovered the pathway responsible for checkpoint inactivation and cell cycle re-entry in *B. subtilis*. These findings represent an important advance in identifying how checkpoint recovery occurs in bacteria. The membrane bound cell division inhibitors identified to date (22-25) are not homologs of YneA, and in fact the only unifying feature is that they are small membrane bound proteins (22-25). This poses a great challenge because the components of checkpoint enforcement and recovery need to be experimentally identified. Our study serves as a model to identify the checkpoint recovery proteases through forward genetics, which in turn could be used to identify the enforcement protein through proteomics. The critical feature of our approach was the use of several growth periods in Tn-seq, which allowed us to identify both proteases. Thus, we propose a strategy using the combined approaches of forward genetics and targeted proteomics to identify the DNA damage checkpoint pathways in genetically tractable bacterial pathogens.

Recovery from a DNA damage checkpoint is a critical process for all organisms. One theme found throughout biology is the use of multiple proteins with overlapping functions. In eukaryotes, the phosphorylation events that establish the checkpoint are removed by multiple phosphatases (55, 56). In *E. coli*, there are two cytoplasmic proteases, Lon and ClpYQ, that have been found to degrade the cell division inhibitor SulA (16, 18-20). Our study further extends the use of multiple factors in regulating checkpoint recovery to *B. subtilis* by describing a mechanism using two proteases. In eukaryotes, multiple proteins with overlapping functions often exist due to spatial or temporal restrictions, which appears to at least partially explain the use of multiple factors in checkpoint recovery (55, 56). In *E. coli*, ClpYQ was found to be important at higher temperatures in the absence of Lon (19), again suggesting that each protease functions under specific conditions. In the case of YlbL and CtpA, however, there appears to be a shared responsibility in rich media. Deletion of each protease results in DNA damage sensitivity and the double mutant has a more severe sensitivity. In contrast, during growth in

minimal media, YlbL appears to be the primary protease, as the cell elongation phenotype is more pronounced in cells lacking *ylbL*. Still it is unclear how or when each protease functions. Why isn't one protease sufficient to degrade YneA? Do the proteases occupy distinct loci in the cell, requiring that each protease degrades a specific YneA pool? Another possibility is that protease levels are constrained by another evolutionary pressure, such as substrates unique to each protease. Thus, the cell cannot maintain the individual proteases at levels required to titrate YneA as part of the DDR, because the levels of another substrate would be too low. Another explanation is that using multiple factors is an evolutionary strategy that increases the fitness of an organism. It is clear that checkpoint recovery is crucial, because the fitness of cells lacking *ylbL* or *ctpA* is significantly decreased in the presence of DNA damage **(Table 2.2)**.

Although the dual protease mechanism described here resolves an important step in the DDR, our data also reveal the complexity of the system. After we exposed cells to MMC the cells elongated. We noticed, however, that not all elongation depended on *yneA* **(Fig 2.11B)**, suggesting another mechanism for cell cycle control. In *B. subtilis*, there have been reports of *yneA*-independent control of cell division following replication stress (45, 57, 58). The essential cell division component FtsL has been reported to be unstable, and depletion leads to inhibition of cell division (58). Further, *ftsL* transcript levels were reported to decrease following replication stress independent of the SOS response (45), thus linking depletion of the unstable FtsL protein to cell division control following replication stress. A study using a replication block, consisting of the Tet-repressor bound to a Tet-operator array, observed cell division inhibition independent of *yneA*, *noc*, and FtsL (57). Interestingly, recent studies of *Caulobacter crescentus* uncovered two cell division inhibitors that are expressed in response to DNA damage, with one inhibitor SOS-dependent and the other SOS-independent (22, 26). In *B. megaterium*, a recent study found that the transcript of *yneA* is unstable following exposure to DNA damage (59), suggesting yet another layer of regulation. No factor was identified to regulate *yneA* transcripts in the previous study, though it is possible that one of the genes of unknown function identified in our screens could regulate *yneA* mRNA. Together, these studies highlight the complexity of regulating the DNA damage checkpoint in bacteria.

Materials and Methods

Bacteriological methods and chemicals

Bacterial strains, plasmids, and oligonucleotides used in this study are listed in **Tables 2.6, 2.7, and 2.8** and the construction of strains and plasmids is detailed in the supplemental methods. All *Bacillus subtilis* strains are isogenic derivatives of PY79 (60). *Bacillus subtilis* strains were grown in LB (10 g/L NaCl, 10 g/L tryptone, and 5 g/L yeast extract) or $S7_{50}$ minimal media with 2% glucose (1x $S7_{50}$ salts (diluted from 10x $S7_{50}$ salts: 104.7g/L MOPS, 13.2 g/L, ammonium sulfate, 6.8 g/L monobasic potassium phosphate, pH 7.0 adjusted with potassium hydroxide), 1x metals (diluted from 100x metals: 0.2 M $MgCl_2$, 70 mM $CaCl_2$, 5 mM $MnCl_2$, 0.1 mM $ZnCl_2$, 100 μg/mL thiamine-HCl, 2 mM HCl, 0.5 mM $FeCl_3$), 0.1% potassium glutamate, 2% glucose, 40 μg/mL phenylalanine, 40 μg/mL tryptophan) at 30°C with shaking (200 rpm). Mitomycin C (MMC), methyl methane sulfonate (MMS), and phleomycin were used at the concentrations indicated in the figures. The following antibiotics were used for selection in *B. subtilis* as indicated in the method details: spectinomycin (100 μg/mL), chloramphenicol (5 μg/mL), and erythromycin (0.5 μg/mL). Selection of *Escherichia coli* (MC1061 or TOP10 cells for cloning or BL21 for protein expression) transformants was performed using the following antibiotics: spectinomycin (100 μg/mL) or kanamycin (50 μg/mL).

Tn-seq

A transposon insertion library was constructed similar to (61) with modifications described in the supplemental methods. Tn-seq experiments were designed with multiple growth periods similar to a prior description (28), with a detailed description in the supplemental methods. Sequencing library construction and data analysis were performed as described previously (35, 61) with modifications described in the supplemental methods. Sequencing data were deposited into the GEO database with accession number GSE109366.

Spot titer assays

B. subtilis strains were struck out on LB agar and incubated at 30°C overnight. The next day, a single colony was used to inoculate a 2 mL LB culture in a 14 mL round bottom culture tube, which was incubated at 37°C on a rolling rack until OD_{600} was 0.5-1. Cultures were normalized to OD_{600} = 0.5 and serial diluted. The serial dilutions were spotted (4 μL) on the agar

media indicated in the figures and the plates were incubated at 30°C overnight (16-20 hours). All spot titer assays were performed at least twice.

Survival assays

Survival assays using an acute treatment of mitomycin C were performed as previously described (62). Cultures were grown to an OD_{600} of about 1, and triplicate samples of 0.6 mL of an OD_{600} = 1 equivalent were taken and cells were pelleted via centrifugation: 10,000 *g* for 5 minutes at room temperature (all subsequent centrifugation steps were identical). Cells were washed with 0.6 mL 0.85% NaCl (saline) and pelleted via centrifugation. Cell pellets were re-suspended in 0.6 mL saline, and 100 µL aliquots were distributed for each MMC concentration. MMC was added to each tube to yield the final concentration stated in the figure in a total volume of 200 µL, and cells were incubated at 37°C for 30 minutes. Cells were pelleted via centrifugation to remove MMC, re-suspended in saline, and a serial dilution yielding a scorable number of cells (about 30-300) was plated on LB agar to determine the surviving fraction of cells. Each experiment was performed three times in triplicate for each strain.

Antiserum production

Purified proteins (see supplemental methods for purification protocols) were submitted to Covance for antibody production using rabbits. Two rabbits were used in the 77 day protocol, and the serum with the least background was used for Western blots.

Western blotting

For YlbL, CtpA, RecA, and DnaN Western blots, a cell pellet equivalent of 1 mL OD_{600} = 1 was re-suspended in 100 µL 1x SMM buffer (0.5 M sucrose, 0.02 M maleic acid, 0.02 M $MgCl_2$, adjusted to pH 6.5) containing 1 mg/mL lysozyme and 2x Roche protease inhibitors at room temperature for 1 or 2 hours. Samples were then lysed by addition of 6x SDS loading dye (0.35 M Tris, pH 6.8, 30% glycerol, 10% SDS, 0.6 M DTT, and 0.012% bromophenol blue) to 1x. Samples (12 µL) were separated via 10% SDS-PAGE, and transferred to nitrocellulose using a Trans-Blot Turbo (BioRad) according to the manufacturer's directions. Membranes were blocked in 5% milk in TBST (25 mM Tris, pH 7.5, 150 mM NaCl, and 0.1% Tween 20) at room temperature for 1 hour or at 4°C overnight. Blocking buffer was removed, and primary

antibodies were added in 2% milk in TBST (αYlbL, 1:5000 or 1:8000; αCtpA, 1:5000; αRecA, 1:4000; αDnaN, 1:4000). Primary antibody incubation was performed at room temperature for 1 hour or overnight at 4°C. Primary antibodies were removed and membranes were washed three times with TBST for 5 minutes at room temperature. Secondary antibodies (Licor; 1:15000) were added in 2% milk in TBST and incubated at room temperature for 1 hour. Membranes were washed three times as above and imaged using the Li-COR Odyssey imaging system. All Western blot experiments were performed at least twice with independent samples. Molecular weight markers were used in the YlbL and CtpA blots. YlbL migrates to a location between the 30 and 40 kDa markers, consistent with its predicted molecular weight of 37.6 kDa. CtpA migrated to a location between the 40 and 80 kDa markers consistent with its molecular weight of 51.1 kDa.

For YneA Western blots, cell pellets, 10 mL OD_{600} = 1 for MMC recovery assay and 25 mL OD_{600} = 1 for over-expression, were re-suspended in 400 or 500 µL, respectively, of sonication buffer (50 mM Tris, pH 8.0, 10 mM EDTA, 20% glycerol, 2x Roche protease inhibitors, and 5 mM PMSF), and lysed via sonication. SDS loading dye was added to 2x and samples were incubated at 100°C for 7 minutes. Samples (10 µL) were separated using 16.5% Tris-Tricine-SDS-PAGE (BioRad) and transferred to a nitrocellulose membrane using a Trans-blot Turbo (BioRad) according to the manufacturer's directions. All subsequent steps were performed as above with a 1:3000 primary antibody dilution.

Mitomycin C recovery assay

An LB agar plate grown at 30°C overnight was washed with pre-warmed $S7_{50}$ minimal media and used to inoculate a culture of $S7_{50}$ minimal media at an OD_{600} = 0.1. The cultures were incubated at 30°C until an OD_{600} of about 0.2 (2- 2.5 hours). MMC was added to 100 ng/mL and cultures were incubated at 30°C for 2 hours. Cells were pelleted via centrifugation (4,696 *g* for 7 minutes) and the media was removed. Cell pellets were washed in an equal volume of 1x PBS, pH 7.4, and pelleted again via centrifugation as above. Cell pellets were re-suspended in an equal volume of pre-warmed $S7_{50}$ minimal media and incubated at 30°C for four hours. Samples for microscopy and Western blot analysis were taken after the two hour MMC treatment and at two and four hours following recovery, as indicated in the figures. The vehicle

control samples were treated for 2 hours with an equivalent volume of the vehicle in which MMC was suspended (25% (v/v) DMSO).

Microscopy

A 500 µL sample from the MMC recovery assay above was taken and FM4-64 was added to 2 µg/mL and incubated at room temperature for 5 minutes. Samples were then transferred to 1% agarose pads made of 1x Spizizen's salts. Images were captured using an Olympus BX61 microscope.

Cell length analysis

Cells were scored for cell length using the measuring tool in ImageJ software. For each image scored, all cells that were in focus were measured. The number of cells scored for each strain/condition is stated in the figures (n=cells measured). The histograms were generated using ggplot2 in R. All scoring was done using unadjusted images. Representative images shown in the figures were modified in ImageJ by subtracting the background (rolling ball radius method) and adjusting the brightness and contrast. Any adjustments made were applied to the entire image.

Proteomics experimental details

Samples (5 mL OD_{600} = 1) were harvested from cultures grown as described in the MMC recovery assay section at 2 hours recovery via centrifugation: 4,696 *g* at room temperature for 10 minutes. Samples were washed twice with 500 µL 1x PBS, pH 7.4 and pelleted via centrifugation: 10,000 *g* at room temperature for 5 minutes. Samples were frozen in liquid nitrogen and stored at -80°C. Samples were submitted for mass-spectrometry analysis to MS Bioworks. Further sample processing and data analysis was performed by MS Bioworks as described in the supplemental methods. The raw data files are available upon request and the processed data table is provided **(Table 2.5)**.

YneA and lysozyme digestion assays

YneA digestion reactions were prepared as a 20 µL reaction in 20 mM Tris pH 7.5, 20 mM NaCl, and 20% glycerol containing 150 µM YneA, and 2 µM CtpA. Reactions were incubated at 30°C for the time indicated in the figure. Reactions were stopped by addition of 6x

SDS-dye to 1x and incubating at 100°C for 5 minutes. Reaction products were separated via 16.5% Tris-Tricine SDS-PAGE. Proteins were detected by staining with coomassie blue. Lysozyme digestion assays were performed as for YneA using 2 mg/mL lysozyme and reactions were incubated at 30°C for 3 hours.

Bacterial two-hybrid assays

Bacterial two hybrid assays were performed as previously described (47, 48, 63). Briefly, T18 and T25 fusion plasmids were co-transformed into BTH101 cells and co-transformants were selected on LB agar + 100 μg/mL ampicillin + 50 μg/mL kanamycin at 37°C overnight. Cultures of LB + 100 μg/mL ampicillin + 50 μg/mL kanamycin were inoculated using several colonies and incubated at 37°C for 90 minutes. Cultures were diluted 250-fold and 4 μL were spotted on LB agar + 100 μg/mL ampicillin + 50 μg/mL kanamycin + 0.5 mM IPTG + 40 μg/mL X-gal and incubated at 30°C for 48 hours, then at room temperature for 24 hours. The brightness and contrast of the images were adjusted using Adobe Photoshop with changes applied to the entire image. All bacterial two-hybrid assays were performed at least twice.

Figures and Tables

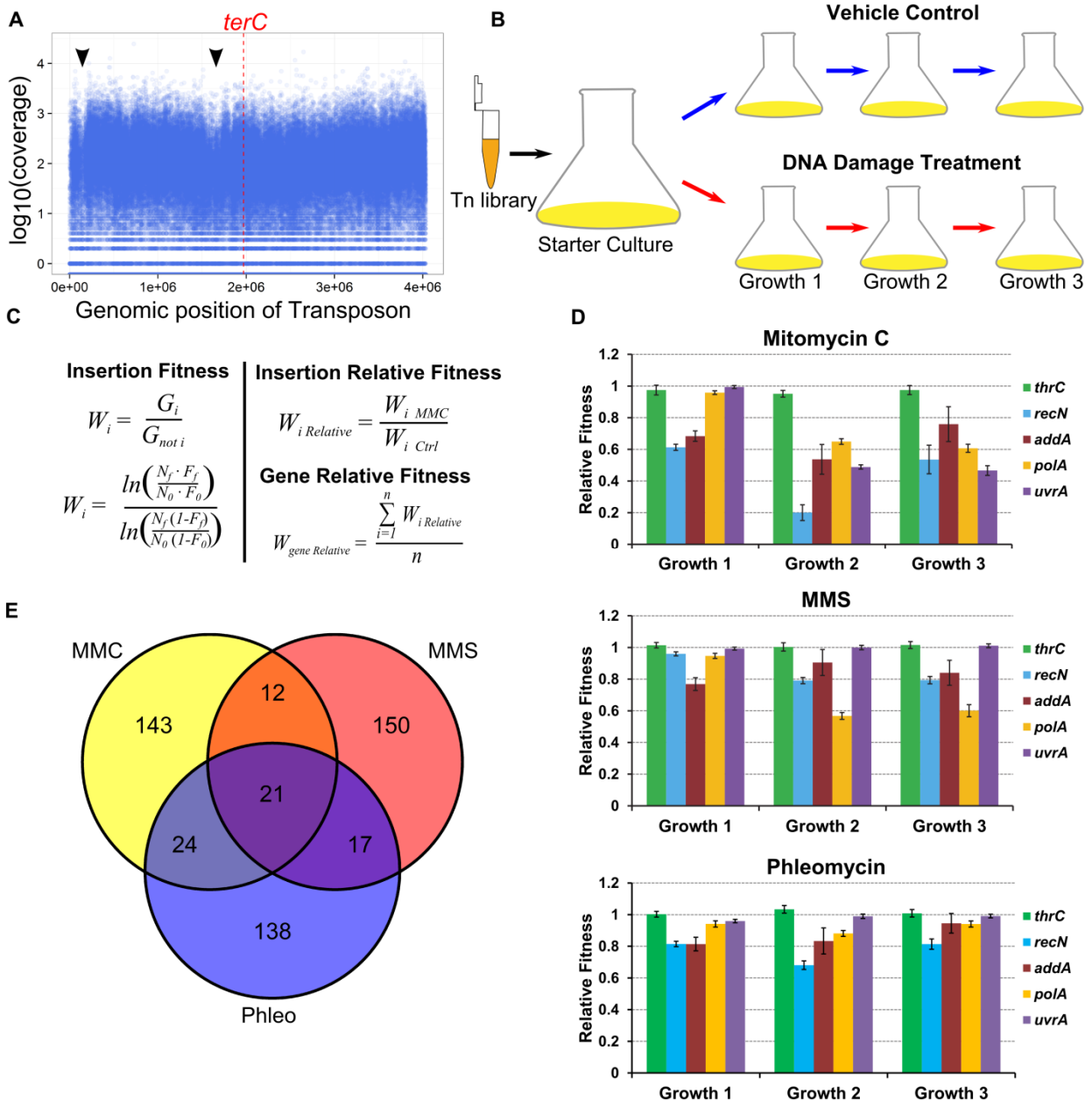

Figure 2.1 Forward genetic screen experimental design and data analysis. **(A)** A plot of the $\log_{10}$ of insertion coverage on the y-axis and genomic position in nucleotides on the x-axis. **(B)** Experimental design for Tn-seq experiments. The transposon library was used to inoculate starter cultures to allow cultures to reach exponential phase. Cultures were split into control and treatment and grown for three growth periods. **(C)** Equations used to calculate relative fitness (W, fitness; G, generations, N, number of cells at the start (N_0) or end (N_f) of growth period; F, insertion frequency at the start (F_0) or end (F_f) of growth period; n, number of insertions used to calculate average). **(D)** The mean gene relative fitness is plotted as a bar graph for the genes indicated for all three Tn-seq experiments, error bars represent the 95% confidence interval. **(E)**

A Venn diagram depicting overlaps of the 200 genes with the lowest fitness and an adjusted p-value less than 0.01 for all three Tn-seq experiments in growth period two.

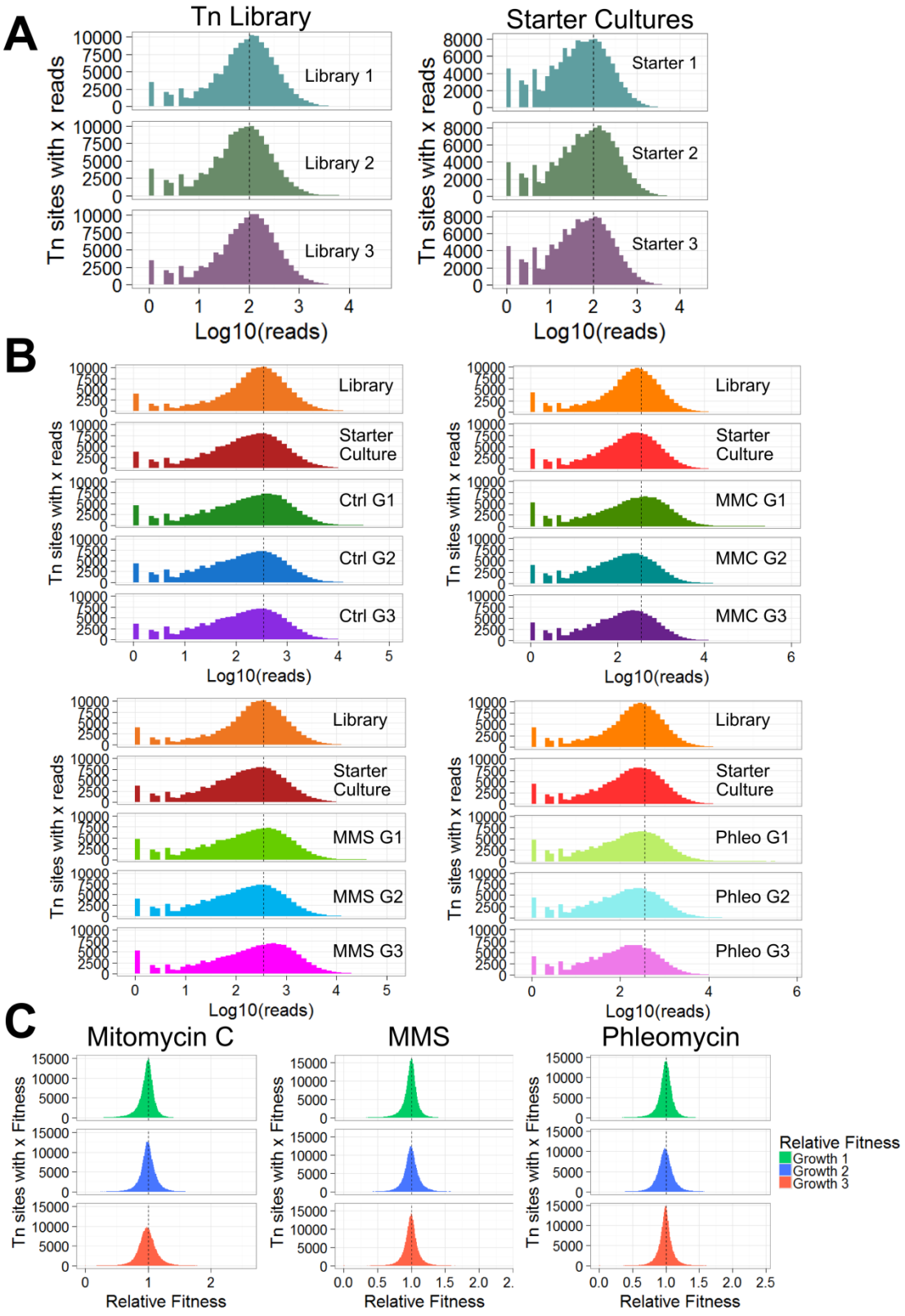

Figure 2.2 Tn-seq data analysis. (A) Sequencing read distributions for transposon (Tn) insertion locations containing greater than 0 reads for each replicate of the library samples (left) or the starter culture samples (right) from the MMC experiment. The y-axis is the frequency of Tn sites, and the x-axis is the $\log_{10}$ of sequencing reads. The dotted vertical line is drawn at $\log_{10}(100)$. **(B)** Sequencing read distributions are plotted for the indicated samples as in panel A, except the replicates were summed prior to plotting. The library and starter cultures are the same in the Ctrl and MMC plots; the library and starter cultures are the same in the MMS and Phleo plots, which are shown twice in each case to allow direct comparison. The dotted vertical line is drawn at $\log_{10}(350)$. **(C)** Relative fitness distributions are plotted for Tn insertions with more than 10 sequencing reads in the control samples. The y-axis is the frequency of Tn sites and the x-axis is the relative fitness. The dotted vertical line is drawn at 1.0. All three growth periods are plotted for the indicated experiments.

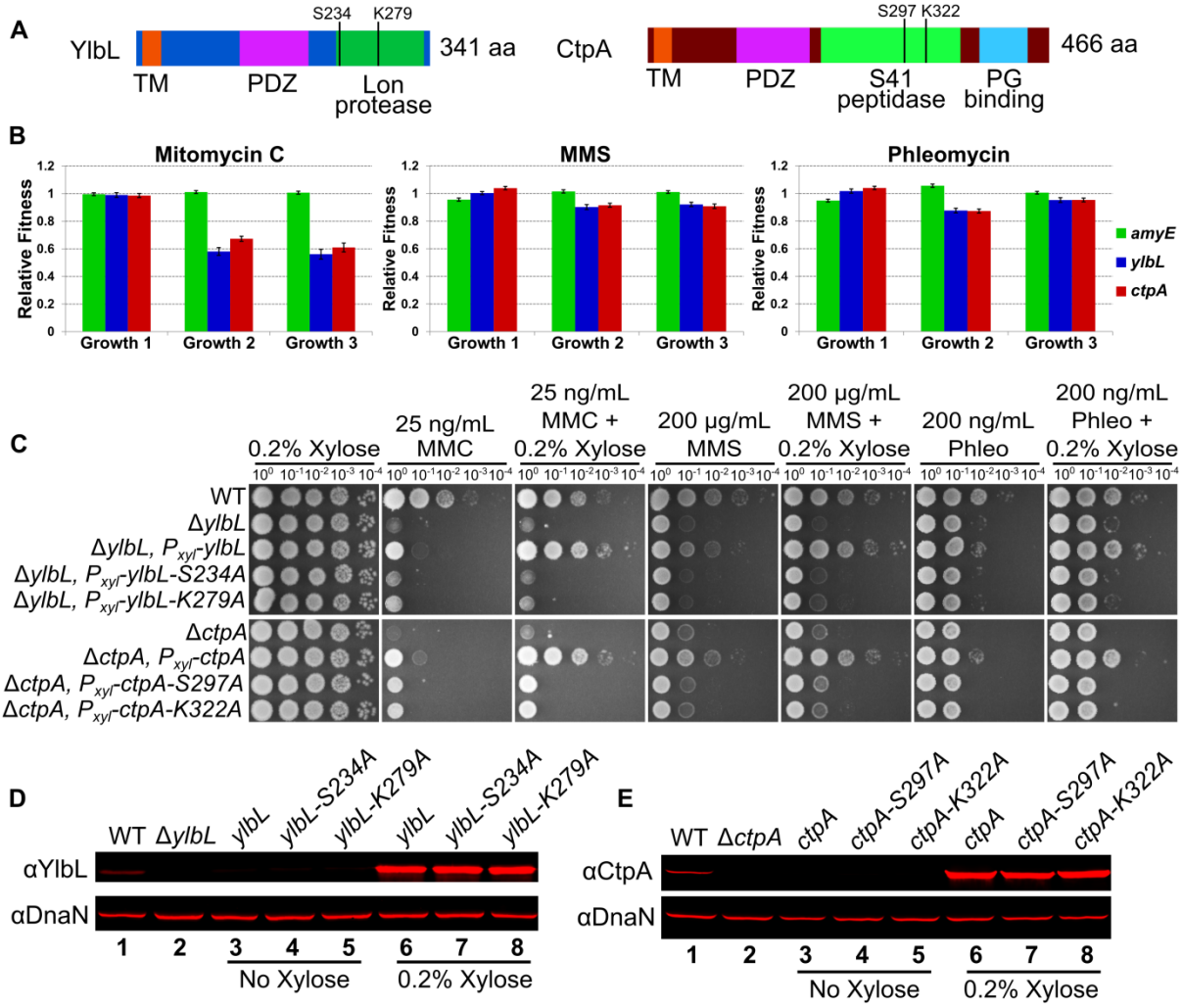

Figure 2.3 YlbL and CtpA require putative catalytic residues for function. (A) Schematics of YlbL and CtpA proteins depicting the domain organization. **(B)** The mean gene relative fitness is plotted as a bar graph for *amyE*, *ylbL*, and *ctpA* for all three Tn-seq experiments, error bars represent the 95% confidence interval. **(C)** Spot titer assays using the genotypes indicated and plated on LB agar media containing the indicated drugs. **(D)** Western blot analysis of cell

lysates from the indicated genotypes grown with or without xylose using antiserum against YlbL (upper panel) and DnaN (lower panel). **(E)** Western blot analysis of cell lysates from the indicated genotypes grown with or without xylose using antiserum against CtpA (upper panel) and DnaN (lower panel).

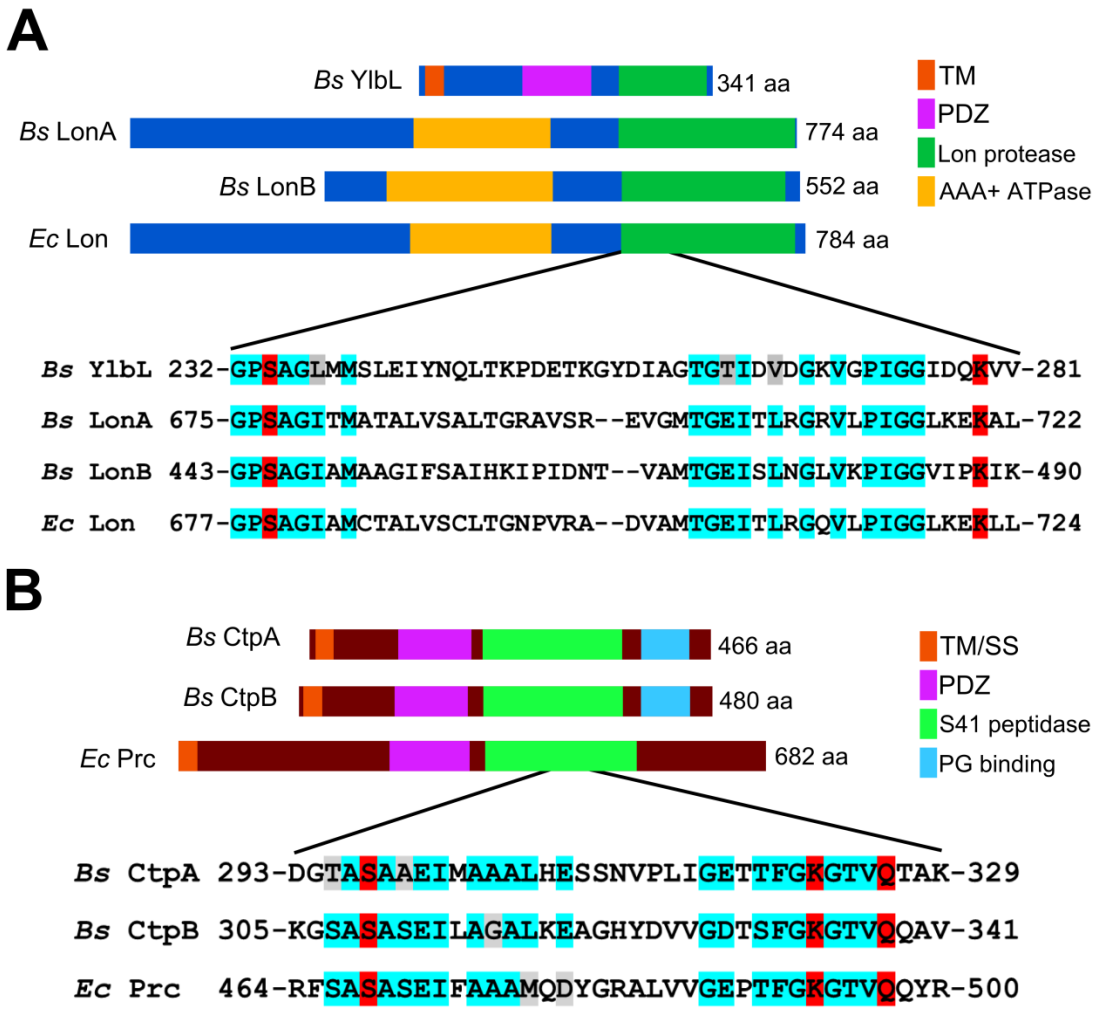

Figure 2.4 YlbL and CtpA catalytic residue identification. (A) The Lon protease domain of YlbL was aligned to LonA and LonB from *B. subtilis* and Lon from *E. coli*. The alignments show that YlbL contains the conserved catalytic dyad of Lon proteases consisting of serine 234 and lysine 279. **(B)** The S41 protease domain of CtpA was aligned to CtpB from *B. subtilis* and Prc from *E. coli*. The alignments showed that CtpA contains a conserved catalytic triad consisting of serine 297, lysine 322, and glutamine 326.

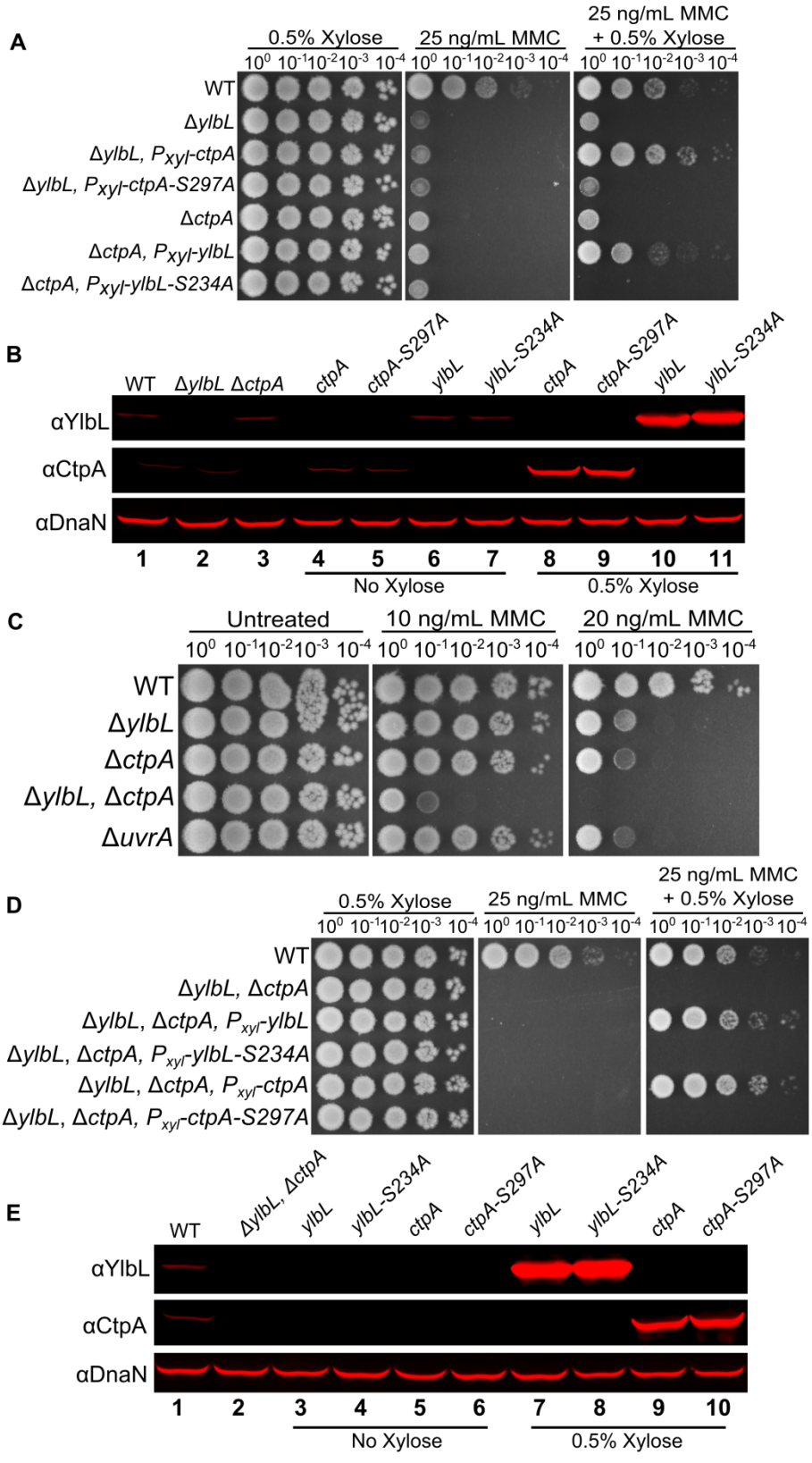
A
0.5% Xylose
25 ng/mL MMC
25 ng/mL MMC + 0.5% Xylose
10^0 10^-1 10^-2 10^-3 10^-4
WT
ΔylbL
ΔylbL, P_xyl-ctpA
ΔylbL, P_xyl-ctpA-S297A
ΔctpA
ΔctpA, P_xyl-ylbL
ΔctpA, P_xyl-ylbL-S234A
B
WT
ΔylbL
ΔctpA
ctpA
ctpA-S297A
ylbL
ylbL-S234A
ctpA
ctpA-S297A
ylbL
ylbL-S234A
αYlbL
αCtpA
αDnaN
1 2 3 4 5 6 7 8 9 10 11
No Xylose
0.5% Xylose
C
Untreated
10 ng/mL MMC
20 ng/mL MMC
10^0 10^-1 10^-2 10^-3 10^-4
WT
ΔylbL
ΔctpA
ΔylbL, ΔctpA
ΔuvrA
D
0.5% Xylose
25 ng/mL MMC
25 ng/mL MMC + 0.5% Xylose
10^0 10^-1 10^-2 10^-3 10^-4
WT
ΔylbL, ΔctpA
ΔylbL, ΔctpA, P_xyl-ylbL
ΔylbL, ΔctpA, P_xyl-ylbL-S234A
ΔylbL, ΔctpA, P_xyl-ctpA
ΔylbL, ΔctpA, P_xyl-ctpA-S297A
E
WT
ΔylbL, ΔctpA
ylbL
ylbL-S234A
ctpA
ctpA-S297A
ylbL
ylbL-S234A
ctpA
ctpA-S297A
αYlbL
αCtpA
αDnaN
1 2 3 4 5 6 7 8 9 10
No Xylose
0.5% Xylose

Figure 2.5 YlbL and CtpA have overlapping functions. (A) Spot titer assay using the indicated genotypes and media. **(B)** Western blot analysis of cell lysates from the genotypes in panel A, using the indicated antiserum. **(C & D)** Spot titer assay using the indicated genotypes and media. **(E)** Western blot analysis of cell lysates from the genotypes indicated in panel D, using the indicated antiserum.

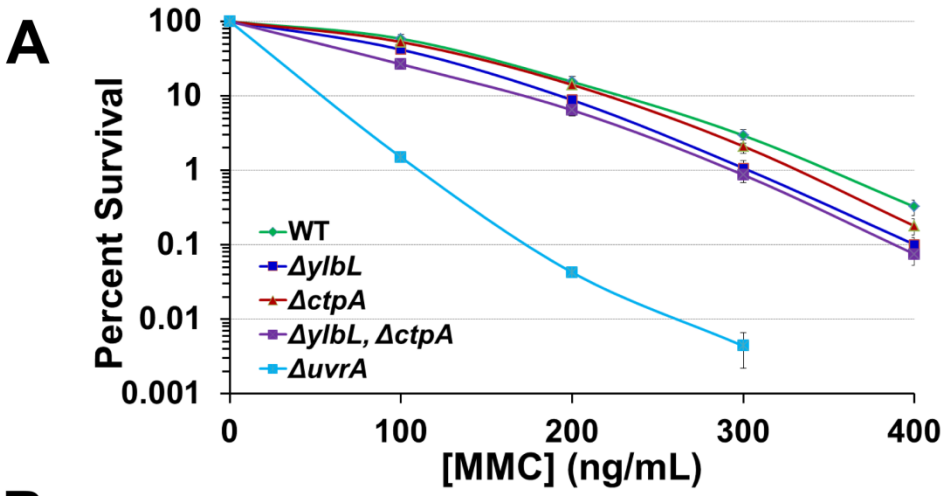
A
100
10
1
0.1
0.01
0.001
Percent Survival
WT
ΔylbL
ΔctpA
ΔylbL, ΔctpA
ΔuvrA
0
100
200
300
400
[MMC] (ng/mL)

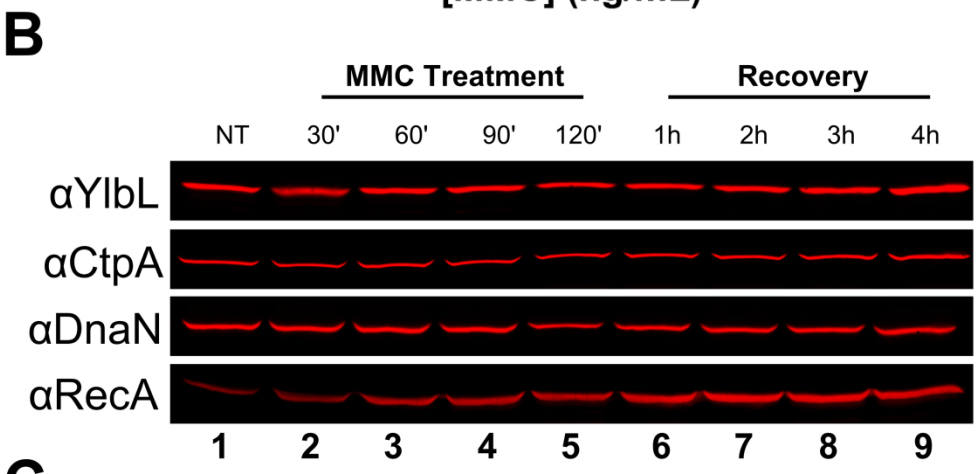
B
MMC Treatment
Recovery
NT
30'
60'
90'
120'
1h
2h
3h
4h
αYlbL
αCtpA
αDnaN
αRecA
1
2
3
4
5
6
7
8
9

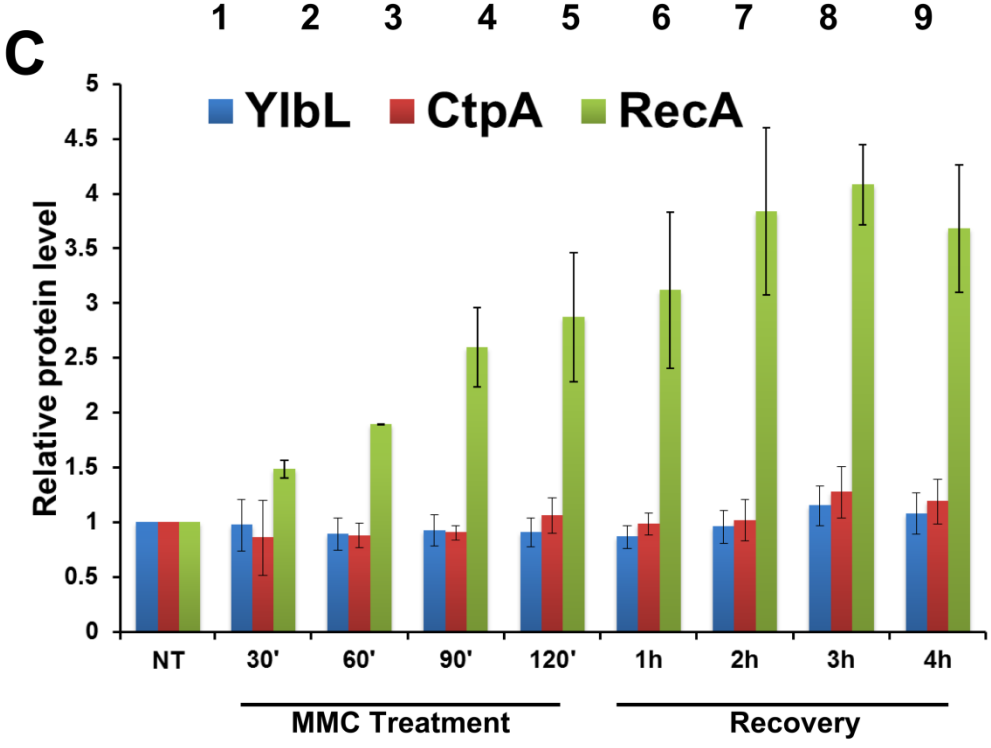
C
YlbL
CtpA
RecA
Relative protein level
5
4.5
4
3.5
3
2.5
2
1.5
1
0.5
0
NT
30'
60'
90'
120'
1h
2h
3h
4h
MMC Treatment
Recovery

Figure 2.6 YlbL and CtpA levels are not regulated by DNA damage. (A) MMC survival assay using strains with the indicated genotypes to test if MMC sensitivity is caused by cell death. The concentration of MMC used during a 30 minute incubation is listed on the x-axis, and the y-axis is the percent of cells surviving the treatment relative to the no treatment (0 ng/mL) condition. Each point is the average of three technical replicates from three individual experiments (n=9), and the error bars represent the standard error of the mean. **(B)** Representative Western blot analysis of cell lysates throughout the MMC recovery assay using YlbL, CtpA, DnaN, or RecA antiserum. **(C)** Quantification of Western blot data plotted as a bar graph. The bars represent the average from three experiments (YlbL, CtpA, and DnaN) or two experiments (RecA), and the error bars are the standard deviation (YlbL and CtpA) or the range (RecA) of the measurements. The y-axis is the relative protein levels, which is the indicated protein level normalized to the loading control, DnaN, and the no treatment measurement.

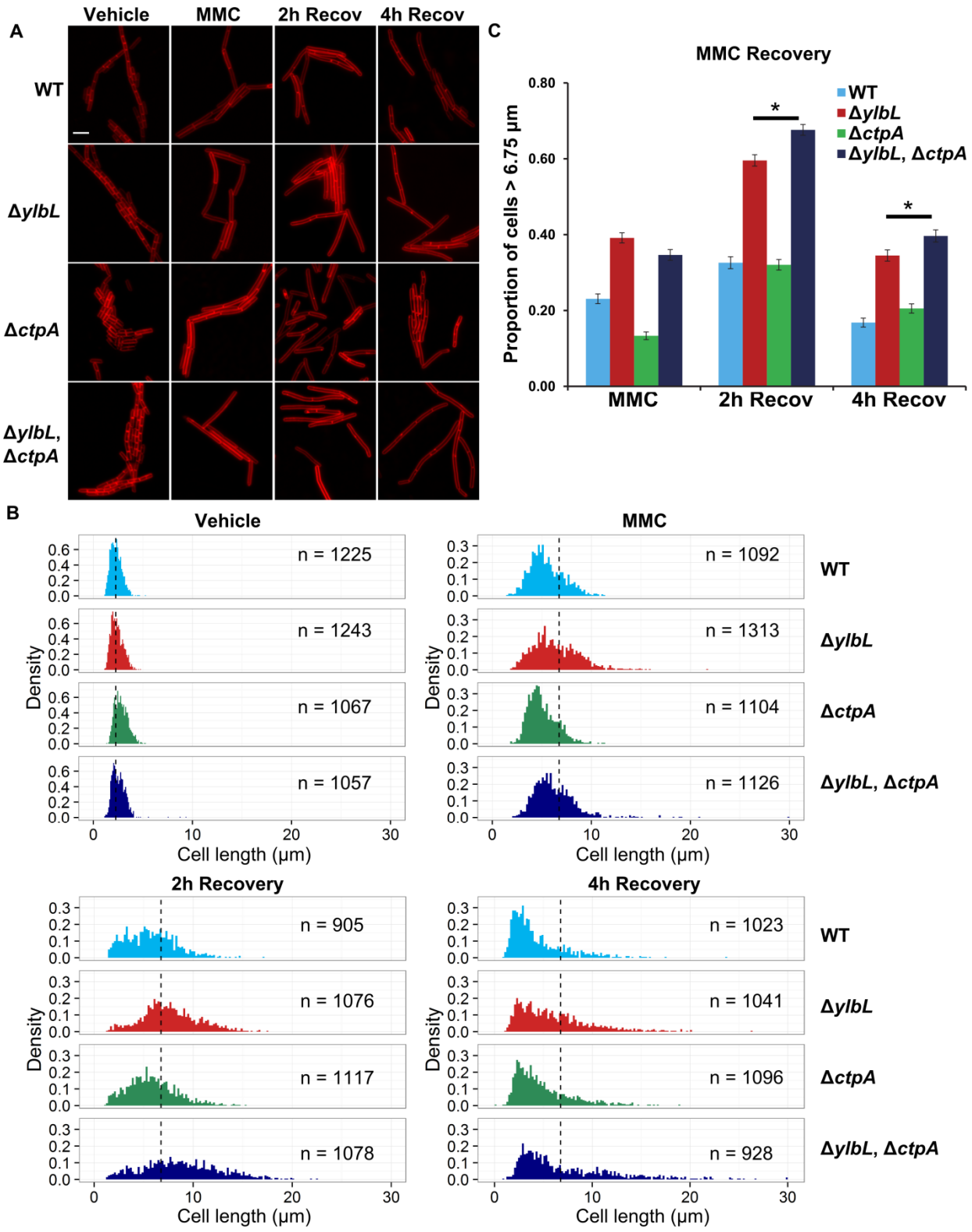

Figure 2.7 DNA damage delays cytokinesis in cells with protease deletions. (A) Representative micrographs of cells with the indicated genotypes at the indicated time points. Membranes were stained with FM4-64. Scale bar is 5 µm. **(B)** Cell length distributions plotted as

histograms. The y-axis in all graphs is normalized by the sample size yielding the density, and the x-axis is the cell length in µm. The number of cells scored in each distribution is indicated as "n=" and the genotype of each strain is indicated. The dotted vertical line in the "Vehicle" distributions is plotted at 2.25 µm, the approximate mean for all strains. The dotted vertical line in the remaining distributions is at 6.75 µm, which is three times the average length of untreated cells. **(C)** The proportion of cells represented by the histograms in panel B with length greater than 6.75 µm is plotted as a bar graph. The error bars represent the standard deviation, $\sqrt{\frac{p(1-p)}{n}}$, where p represents the proportion and n is the sample size. The asterisk indicates a p-value less than 0.05.

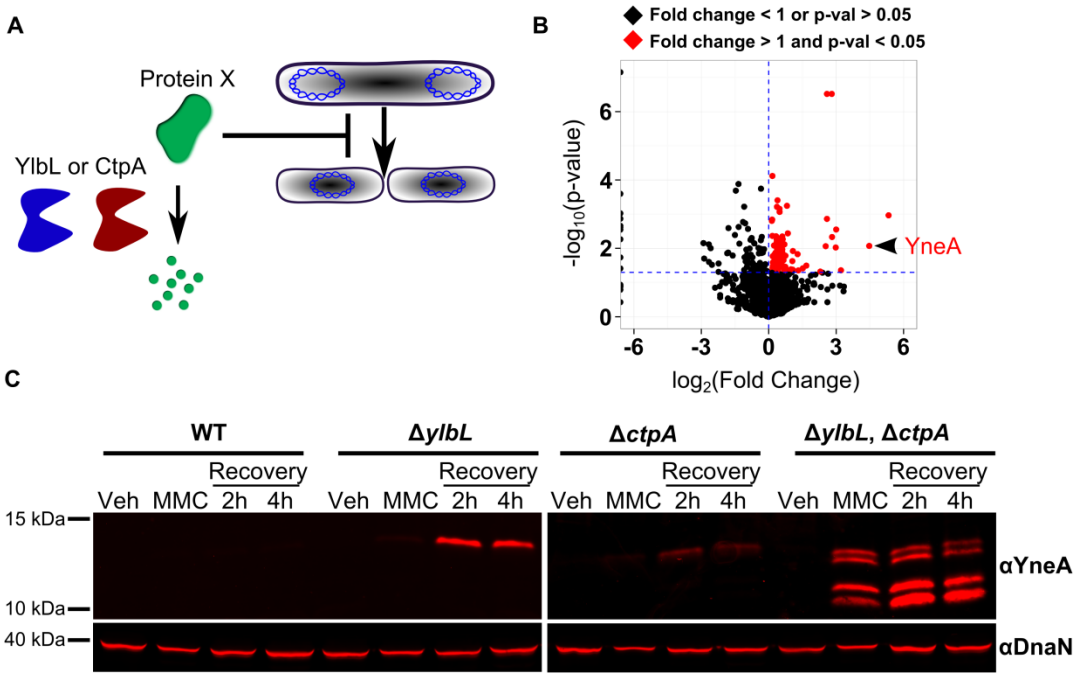

Figure 2.8 YneA accumulates in protease mutants. (A) A model for the function of YlbL and CtpA in regulating cell division. **(B)** Proteomics data plotted as fold change (Double Mutant/WT) vs. the p-value. Points plotted in black have a fold change less than one or a p-value greater than or equal to 0.05, and points plotted in red have a fold change greater than one and a p-value less than 0.05. **(C)** Western blot analysis of cell lysates from strains with the indicated genotypes at the indicated time points from the MMC recovery assay (see methods), using YneA or DnaN antiserum.

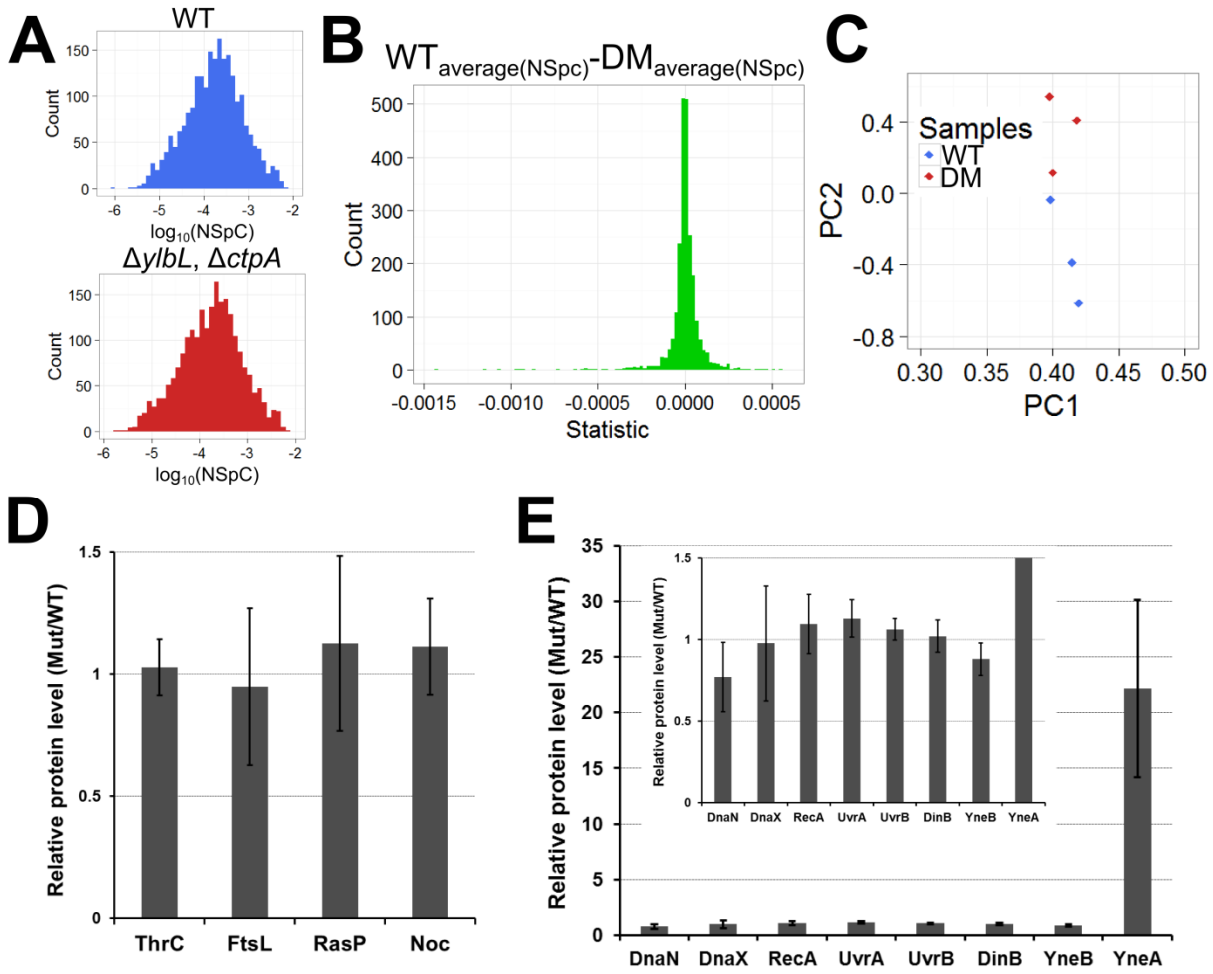

Figure 2.9 YneA accumulates in protease mutants. (A) The averages of the normalized spectral counts are plotted as histograms for WT (blue) and Δ*ylbL*, Δ*ctpA* double mutant (DM; red). The y-axis is the count and the x-axis is the $\log_{10}$(normalized spectral counts for the average of three replicates). **(B)** The distribution of the test statistic (WT average – DM average) is plotted as a histogram. **(C)** A principle component analysis was performed using the normalized spectral counts from WT (blue) and DM (red) samples using the "prcomp" function in R. The first two coordinates are plotted as the x- and y-axes, respectively. **(D & E)** The average relative protein levels (WT/DM) from the proteomics dataset are plotted for the indicated proteins, and the error bars represent the standard deviation. The inset in panel E shows a closer look around one for clarity.

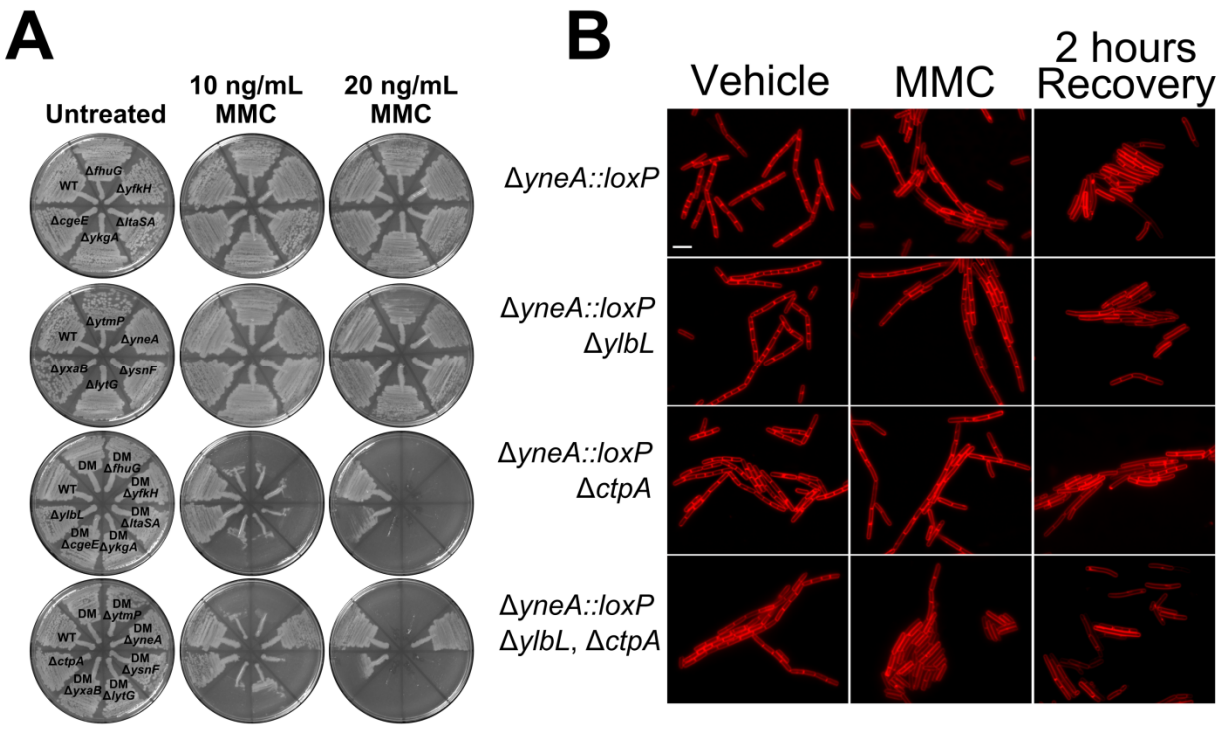

Figure 2.10 *yneA* is required for DNA damage sensitivity and cell elongation phenotypes. **(A)** Strains with the indicated genotypes (plates at left) were struck onto the indicated media (column labels) and incubated at 30°C overnight. Deletion of *yneA* suppresses the Δ*ylbL*, Δ*ctpA* double mutant (DM) MMC sensitivity phenotype. **(B)** Representative micrographs of cells stained with FM4-64 from the indicated genotypes at the indicated time points in the MMC recovery assay. The scale bar is 5 μm.

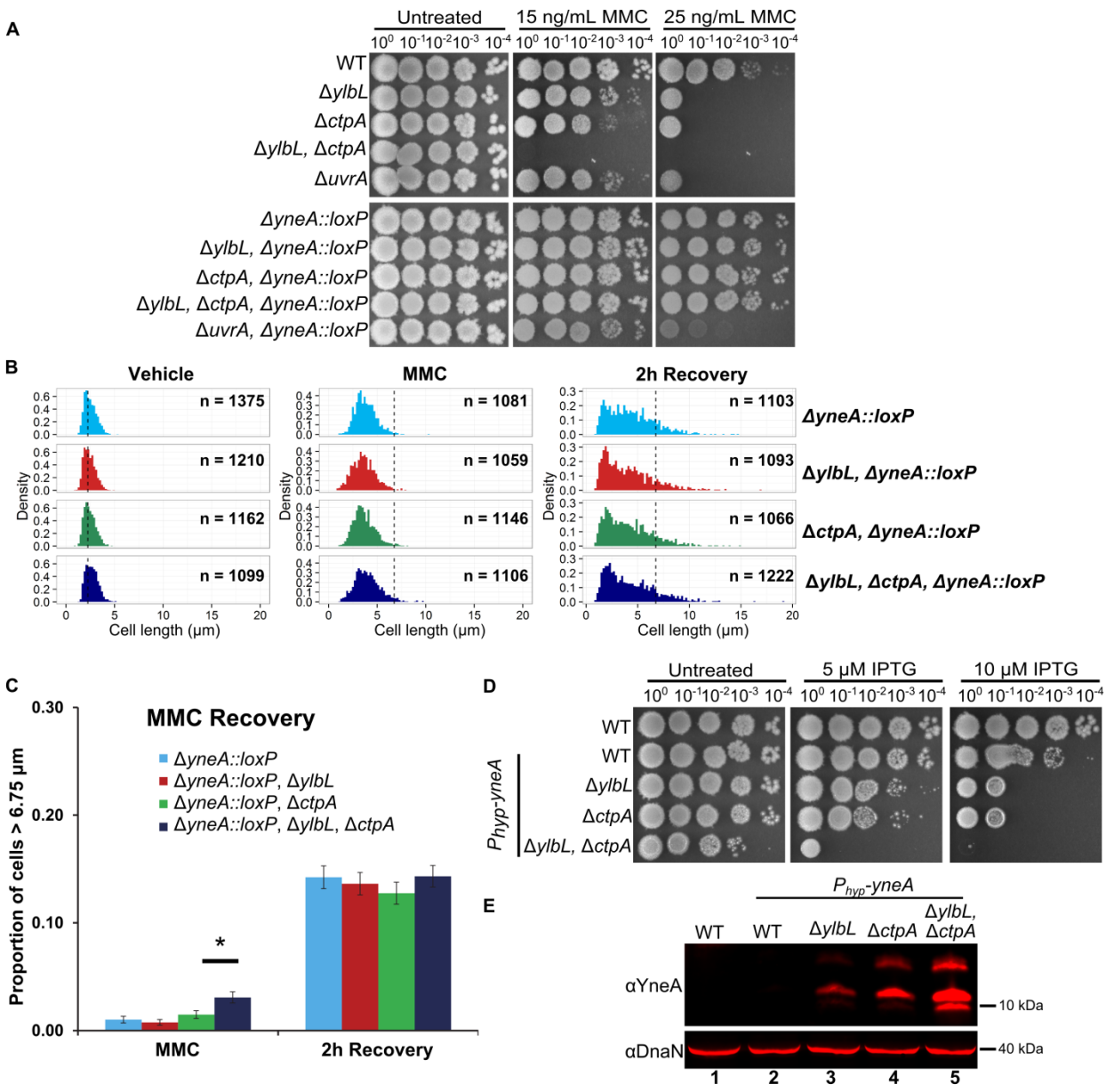

Figure 2.11 *yneA* is required for DNA damage sensitivity and cell elongation phenotypes. **(A)** Spot titer assay using the indicated genotypes and media. **(B)** Cell length distributions plotted as histograms. The number of cells scored in each distribution is indicated as "n=" and the genotype of each strain is indicated above the distributions. The dotted vertical line in the "Vehicle" distributions is at the approximate mean of 2.25 μm. The dotted vertical line in the remaining distributions is at 6.75 μm. The y-axis in all graphs is normalized by the sample size yielding the density, and the x-axis is the cell length in μm. **(C)** The proportion of cells greater than 6.75 μm from the distributions in panel B is plotted as a bar graph. The error bars represent the standard deviation, $\sqrt{\frac{p(1-p)}{n}}$, where p represents the proportion and n is the sample size. The asterisk indicates a p-value less than 0.05. **(D)** Spot titer assay testing the effect of over production of YneA using the indicated concentration of the inducer IPTG. **(E)** Western blot

analysis of cell lysates using 100 μM IPTG for YneA expression with the indicated genotypes, using the indicated antiserum.

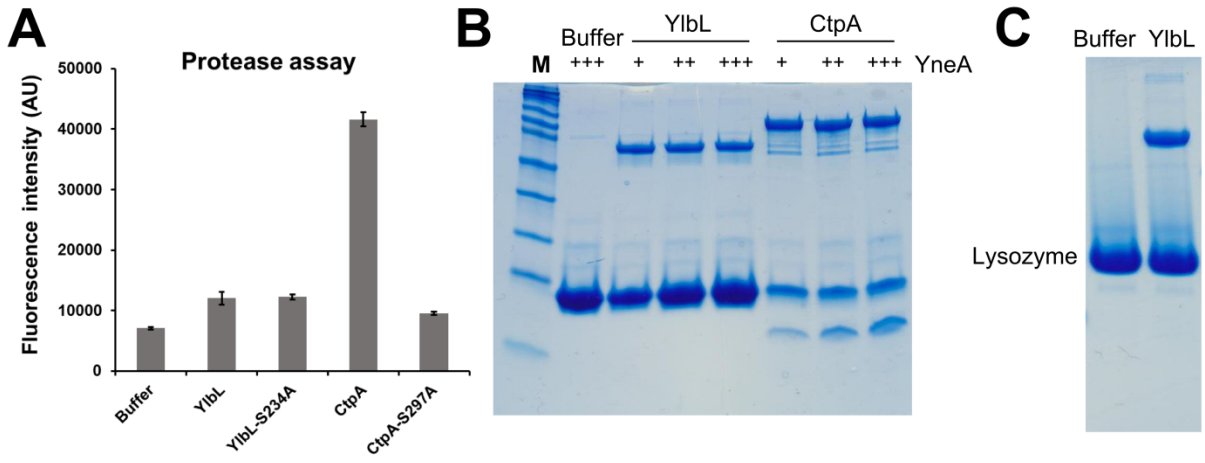

Figure 2.12 Purified YlbL lacking its N-terminal transmembrane shows no protease activity *in vitro*. (A) Protease assay using fluorescently labeled casein. YlbL, YlbL-S234A, CtpA, and CtpA-S297A, all lacking their N-terminal transmembrane domains were incubated with casein. The casein was fluorescently labeled such that the signal was quenched until digested by a protease. **(B)** YneA digestion assay. YlbL and CtpA were incubated with increasing concentrations of YneA. The first lane is a molecular weight marker (M). **(C)** Lysozyme digestion assay. YlbL was incubated with lysozyme.

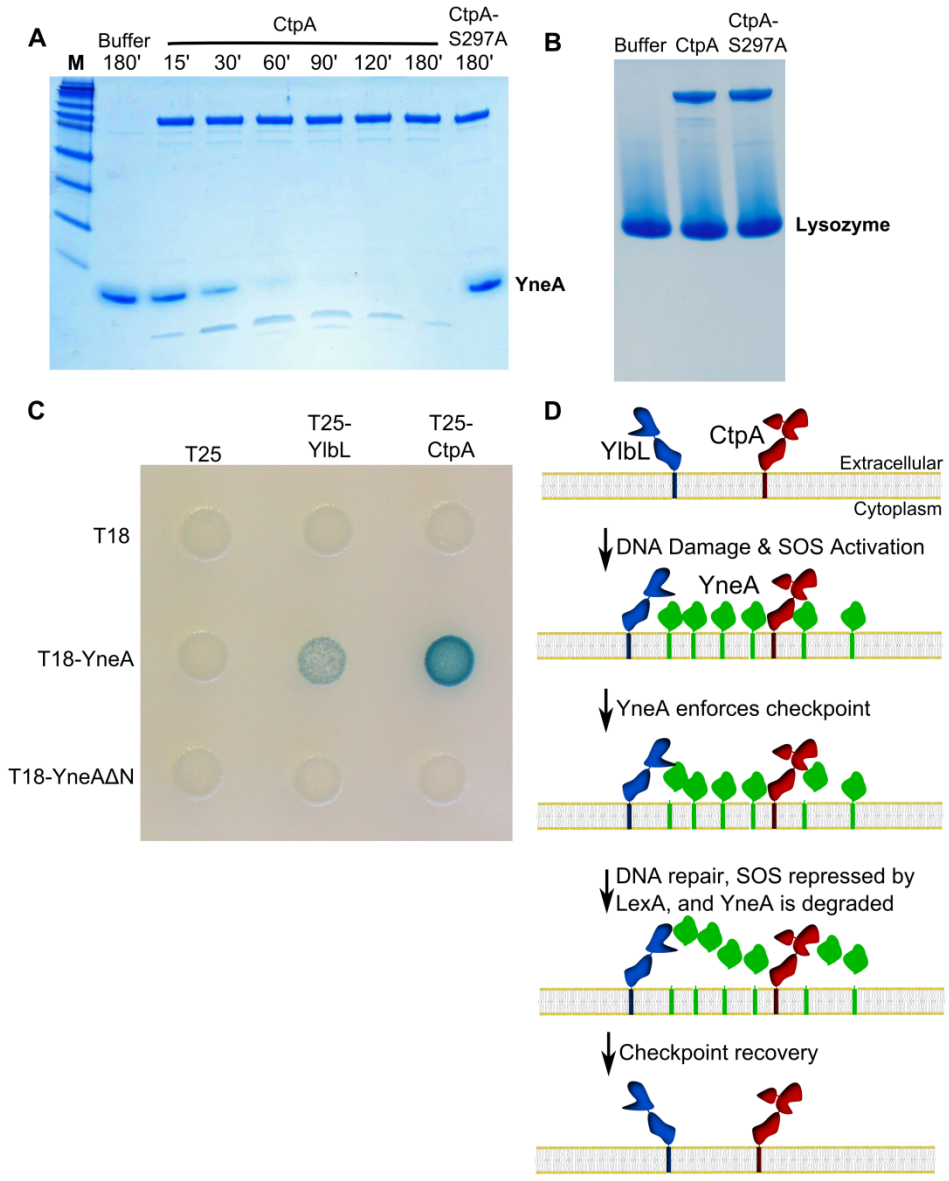

Figure 2.13 DNA damage checkpoint recovery in *Bacillus subtilis*. (A) Protease assay incubating purified CtpA or CtpA-S297A with purified YneA for the indicated time followed by SDS-PAGE and staining with coomassie blue. **(B)** Protease assay incubating purified CtpA or CtpA-S297A with commercially available lysozyme for 3 hours followed by SDS-PAGE and staining with coomassie blue. **(C)** Bacterial two hybrid assay using T18 fusions (rows) and T25 fusions (columns) co-transformed into *E. coli*. The T25 plasmids are: the empty vector (T25), T25-YlbL-S234A (T25-YlbL), and T25-CtpA-S297A (T25-CtpA). The T18 plasmids are: the empty vector (T18), T18-YneA, and T18-YneAΔN (which lacks the transmembrane domain). **(D)** A model for YlbL- and CtpA-dependent DNA damage checkpoint recovery. YlbL and CtpA are present as membrane proteases, and when high amounts of DNA damage are present, YneA production overwhelms both proteases resulting in delayed cell division. After DNA repair is complete and YneA expression decreases, YneA is cleared and cell division proceeds.

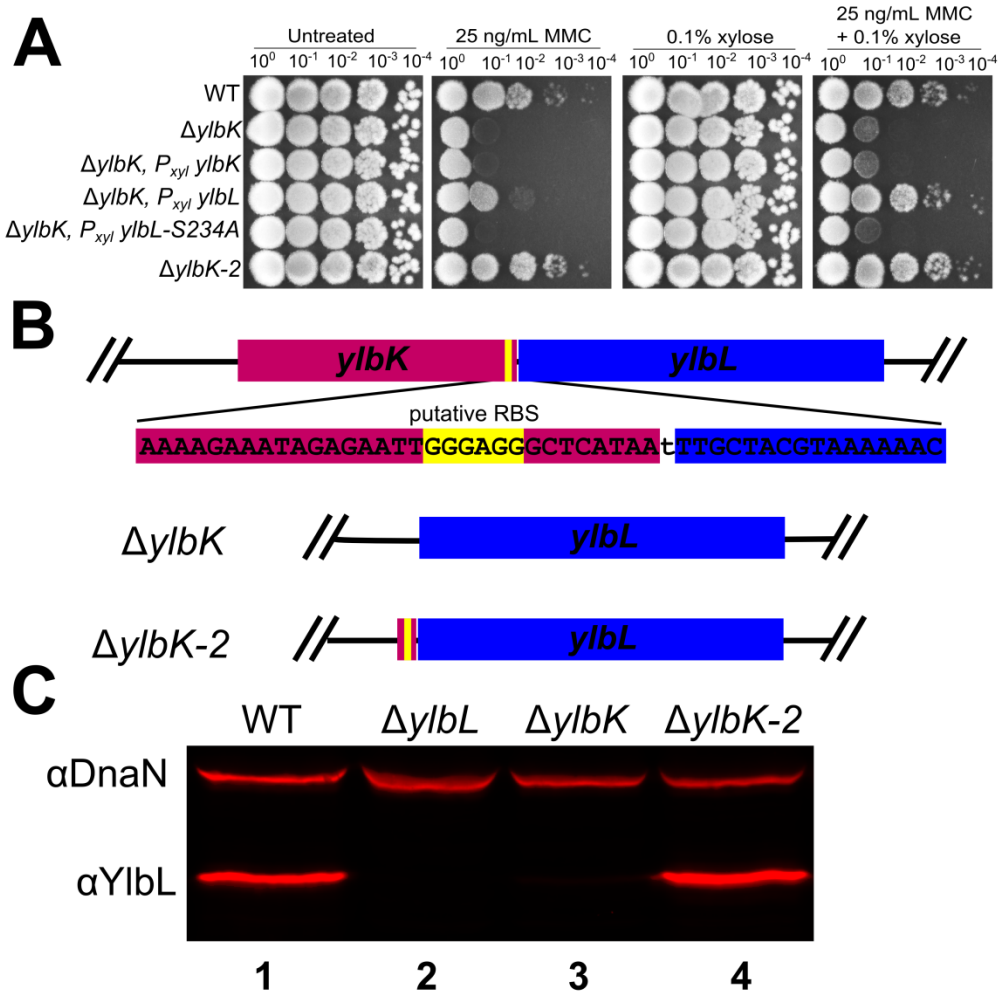

Figure 2.14 Disruption of *ylbK* results in a polar effect on *ylbL*. (A) Spot titer assay using the indicated genotypes and media. **(B)** Schematic of *ylbK* and *ylbL* loci, with the putative ribosome binding site, proposed to control *ylbL* translation, labeled in yellow. **(C)** Western blot analysis of cell lysates of the indicated genotypes using YlbL or DnaN antiserum.

							Viable cell counts per 0.1 mL			
Experiment	**Sample**	**Aliquot**	**Treatment**	**OD600 after outgrowth**	**Time (h)**	**Volume for back dilution (mL)**	**1**	**2**	**3**	**Average**
Mitomycin C	1	A	Library	N/A initial library	N/A	0.27	40	51	18	36.3
	2	B	Library	N/A initial library	N/A	0.27	46	57	67	56.7
	3	C	Library	N/A initial library	N/A	0.27	31	128	57	72.0
	4	A	Starter Culture	0.801	4.5	1.561	54	37	37	42.7
	5	B	Starter Culture	0.795	4.5	1.572	70	53	57	60.0
	6	C	Starter Culture	0.923	4.5	1.354	31	60	83	58.0
	7	A	Vehicle	1.91	3	0.654	243	168	209	206.7
	8	B		1.84	3	0.679	183	185	231	199.7
	9	C		1.97	3	0.635	258	254	252	254.7
	10	A	15 ng/mL MMC	1.52	3	0.822	47	41	55	47.7
	11	B		1.57	3	0.796	41	57	47	48.3
	12	C		1.63	3	0.767	66	52	55	57.7
	13	A	Vehicle	1.5	3	0.833	163	171	189	174.3
	14	B		1.45	3	0.862	173	151	154	159.3
	15	C		1.32	3	0.947	133	154	174	153.7
	16	A	15 ng/mL MMC	1.45	4.75	0.862	36	42	41	39.7
	17	B		1.46	4.75	0.856	46	42	47	45.0
	18	C		1.37	4.75	0.912	63	52	30	48.3
	19	A	Vehicle	1.94	3	N/A	173	214	223	203.3
	20	B		1.55	3	N/A	219	185	202	202.0
	21	C		1.86	3	N/A	250	251	228	243.0
	22	A	15 ng/mL MMC	1.53	5.25	N/A	42	48	36	42.0
	23	B		1.53	5.25	N/A	66	39	67	57.3
	24	C		1.6	5.25	N/A	63	82	82	75.7

Std Dev	Dilution factor	cells/mL	Number of cells in inoculum	Number of cells after growth	Reads mapped	Tnsites with >= 10 reads
16.8	1.0E-07	3.63E+09	N/A	N/A	25,717,552	124,742
10.5	1.0E-07	5.67E+09	N/A	N/A	20,998,165	122,781
50.2	1.0E-07	7.20E+09	N/A	N/A	27,266,350	125,359
9.8	1.0E-05	4.27E+07	9.81E+08	2.14E+09	18,068,418	112,657
8.9	1.0E-05	6.00E+07	1.53E+09	3.02E+09	26,157,733	117,909
26.1	1.0E-05	5.80E+07	1.94E+09	2.92E+09	20,234,204	113,777
37.6	1.0E-05	2.07E+08	6.66E+07	5.49E+09	26,868,722	110,169
27.2	1.0E-05	2.00E+08	9.43E+07	5.31E+09	20,347,670	106,578
3.1	1.0E-05	2.55E+08	7.85E+07	6.71E+09	26,068,577	109,800
7.0	1.0E-05	4.77E+07	6.66E+07	1.27E+09	18,355,525	104,348
8.1	1.0E-05	4.83E+07	9.43E+07	1.28E+09	21,188,844	107,052
7.4	1.0E-05	5.77E+07	7.85E+07	1.52E+09	34,690,534	112,553
13.3	1.0E-05	1.74E+08	1.35E+08	4.47E+09	15,422,397	100,441
11.9	1.0E-05	1.59E+08	1.36E+08	4.09E+09	23,506,462	107,195
20.5	1.0E-05	1.54E+08	1.62E+08	3.94E+09	16,657,662	101,421
3.2	1.0E-05	3.97E+07	3.92E+07	1.02E+09	18,050,792	102,356
2.6	1.0E-05	4.50E+07	3.85E+07	1.16E+09	21,321,795	105,193
16.8	1.0E-05	4.83E+07	4.42E+07	1.25E+09	16,814,156	101,041
26.7	1.0E-05	2.03E+08	1.45E+08	5.25E+09	17,323,113	99,837
17.0	1.0E-05	2.02E+08	1.37E+08	5.22E+09	18,945,785	103,569
13.0	1.0E-05	2.43E+08	1.46E+08	6.31E+09	19,070,938	102,109
6.0	1.0E-05	4.20E+07	3.42E+07	1.09E+09	22,090,553	102,536
15.9	1.0E-05	5.73E+07	3.85E+07	1.48E+09	33,129,406	108,112
11.0	1.0E-05	7.57E+07	4.41E+07	1.96E+09	43,808,521	110,543

Experiment	Sample	Aliquot	Treatment	OD600 after outgrowth	Time (h)	Volume for back dilution (mL)	1	2	3	Average
MMS & Pheomycin	1	A	N/A	N/A initial library	N/A	0.5	ND	ND	ND	ND
	2	B	N/A	N/A initial library	N/A	0.5	ND	ND	ND	ND
	3	C	N/A	N/A initial library	N/A	0.5	ND	ND	ND	ND
	4	A	N/A	0.82	9.5	1.52	97	72	75	81.3
	5	B	N/A	0.879	9.5	1.42	71	81	82	78.0
	6	C	N/A	0.781	9.5	1.6	56	46	63	55.0
	7	A	Vehicle	1.496	3	0.836	372	220	188	260.0
	8	B		1.512	3	0.827	264	192	198	218.0
	9	C		1.5	3	0.834	244	155	185	194.7
	10	A	50 µg/mL MMS	1.51	3.25	0.828	82	102	109	97.7
	11	B		1.508	3.25	0.829	139	146	167	150.7
	12	C		1.466	3.25	0.853	128	121	129	126.0
	13	A	25 ng/mL Phleomycin	1.482	3.25	0.844	140	143	151	144.7
	14	B		1.534	3.25	0.815	129	156	155	146.7
	15	C		1.494	3.25	0.837	140	141	123	134.7
	16	A	Vehicle	1.404	3	0.891	150	133	145	142.7
	17	B		1.432	3	0.873	125	129	187	147.0
	18	C		1.404	3	0.891	110	157	135	134.0
	19	A	50 µg/mL MMS	1.484	3.75	0.843	142	185	138	155.0
	20	B		1.45	3.75	0.862	119	120	113	117.3
	21	C		1.424	3.75	0.878	139	113	136	129.3
	22	A	25 ng/mL Phleomycin	1.478	4	0.846	173	131	176	160.0
	23	B		1.578	4	0.793	162	154	244	186.7
	24	C		1.404	4	0.891	158	149	209	172.0
	25	A	Vehicle	1.546	3	N/A	146	118	204	156.0
	26	B		1.38	3	N/A	194	141	114	149.7
	27	C		1.392	3	N/A	137	172	147	152.0
	28	A	50 µg/mL MMS	1.768	4	N/A	166	165	213	181.3

	29	B		1.784	4	N/A	173	170	236	193.0
	30	C		1.892	4	N/A	178	166	181	175.0
	31	A		1.882	4	N/A	288	400	320	336.0
	32	B	25 ng/mL Phleomycin	1.718	4	N/A	220	211	213	214.7
	33	C		1.716	4	N/A	362	213	322	299.0

Std Dev	Dilution factor	cells/mL	Number of cells in inoculum	Number of cells after growth	Reads mapped	Tnsites with >= 10 reads
ND	ND	ND	N/A	N/A	35,843,091	126,497
ND	ND	ND	N/A	N/A	16,541,861	118,456
ND	ND	ND	N/A	N/A	15,754,152	117,697
13.7	1.0E-05	8.13E+07	ND	4.11E+09	27,956,965	115,134
6.1	1.0E-05	7.80E+07	ND	3.94E+09	25,538,172	114,266
8.5	1.0E-05	5.50E+07	ND	2.78E+09	23,836,182	113,304
98.3	1.0E-05	2.60E+08	1.24E+08	6.90E+09	22,106,601	96,669
39.9	1.0E-05	2.18E+08	1.11E+08	5.76E+09	20,265,859	95,577
45.3	1.0E-05	1.95E+08	8.80E+07	5.18E+09	44,365,650	103,508
14.0	1.0E-05	9.77E+07	1.24E+08	2.59E+09	60,006,387	106,978
14.6	1.0E-05	1.51E+08	1.11E+08	3.98E+09	11,507,552	85,925
4.4	1.0E-05	1.26E+08	8.80E+07	3.35E+09	41,343,336	103,165
5.7	1.0E-05	1.45E+08	1.24E+08	3.84E+09	48,823,094	105,073
15.3	1.0E-05	1.47E+08	1.11E+08	3.87E+09	13,240,328	88,983
10.1	1.0E-05	1.35E+08	8.80E+07	3.58E+09	14,655,221	89,930
8.7	1.0E-05	1.43E+08	2.17E+08	3.69E+09	15,374,897	90,181
34.7	1.0E-05	1.47E+08	1.80E+08	3.80E+09	19,755,901	94,282
23.5	1.0E-05	1.34E+08	1.62E+08	3.46E+09	14,092,828	88,014
26.1	1.0E-05	1.55E+08	8.09E+07	4.00E+09	20,493,595	94,277
3.8	1.0E-05	1.17E+08	1.25E+08	3.03E+09	19,078,748	93,789

14.2	1.0E-05	1.29E+08	1.07E+08	3.34E+09	17,204,870	92,051
25.2	1.0E-05	1.60E+08	1.22E+08	4.14E+09	15,834,903	90,135
49.8	1.0E-05	1.87E+08	1.20E+08	4.82E+09	11,148,113	84,358
32.4	1.0E-05	1.72E+08	1.13E+08	4.44E+09	37,289,108	100,198
43.9	1.0E-05	1.56E+08	1.27E+08	4.04E+09	15,933,177	90,922
40.7	1.0E-05	1.50E+08	1.28E+08	3.87E+09	15,080,780	89,795
18.0	1.0E-05	1.52E+08	1.19E+08	3.94E+09	22,500,677	95,409
27.4	1.0E-05	1.81E+08	1.31E+08	4.69E+09	20,224,601	94,064
37.3	1.0E-05	1.93E+08	1.01E+08	4.99E+09	19,106,876	92,938
7.9	1.0E-05	1.75E+08	1.14E+08	4.53E+09	19,327,030	93,310
57.7	1.0E-05	3.36E+08	1.35E+08	8.68E+09	15,917,971	89,971
4.7	1.0E-05	2.15E+08	1.48E+08	5.54E+09	18,353,865	92,047
77.1	1.0E-05	2.99E+08	1.53E+08	7.74E+09	18,317,223	91,222

Table 2.1 Tn-seq data collected. OD_{600} measurements, incubation times, viable cell counts, growth rates estimated based on viable cell counts, number of generations estimated based on viable cell counts and incubation times, sequencing sample IDs, sequencing reads, reads mapped, and the number of Tn insertions with more than 10 reads for each sample are presented.

Mitomycin C Growth period 1			Mitomycin C Growth period 2			Mitomycin C Growth period 3		
Feature/gene	**Mean Relative fitness**	**Adjusted p-value**	**Feature/gene**	**Mean Relative fitness**	**Adjusted p-value**	**Feature/gene**	**Mean Relative fitness**	**Adjusted p-value**
ktrC	0.580	7.3E-04	***recN***	0.200	1.2E-16	***uvrB***	0.423	1.7E-40
recN	0.613	1.3E-54	***sepF***	0.400	8.0E-06	***uvrA***	0.466	1.2E-67
mntB	0.634	4.2E-10	***uvrB***	0.409	7.2E-68	***uvrC***	0.478	4.0E-33
mntC	0.638	1.8E-19	***uvrC***	0.484	1.6E-56	***recN***	0.536	2.0E-07
mntA	0.641	2.6E-13	***uvrA***	0.489	1.7E-135	***U712_09520***	0.553	5.1E-07
ponA	0.660	2.6E-85	***addA***	0.537	2.0E-10	***ylbL***	0.561	5.8E-36
recA	0.666	8.1E-03	***rnhC***	0.544	3.6E-07	***rnhC***	0.564	2.9E-04
mntD	0.671	4.9E-20	***crh***	0.565	3.0E-03	***yprA***	0.587	1.3E-106
recG	0.679	1.4E-17	***ruvB***	0.568	1.5E-03	***yprB***	0.589	3.6E-35
addA	0.684	3.3E-33	***ylbL***	0.581	1.6E-45	***polA***	0.607	2.5E-54
addB	0.689	6.4E-26	***ponA***	0.587	3.5E-14	***lgt***	0.608	5.8E-06
recU	0.708	8.2E-06	***bcrC***	0.595	4.6E-10	***ctpA***	0.610	6.5E-38
gtaB	0.711	4.4E-03	***ecsA***	0.603	1.7E-04	***cymR***	0.621	2.2E-11
codV	0.720	5.6E-06	***recR***	0.606	2.2E-03	***ysoA***	0.630	5.4E-20
clpY	0.723	8.8E-08	***queA***	0.612	5.3E-06	***ylbK***	0.635	5.2E-16
pgcA	0.728	2.7E-06	***addB***	0.622	4.0E-09	***ig1981***	0.651	5.2E-03
codY	0.739	1.1E-06	***ig3151***	0.627	5.2E-09	***ig1437***	0.660	8.7E-07
ig1685	0.739	5.5E-06	***ecsB***	0.627	4.5E-16	***dnaH***	0.664	2.5E-07
ruvB	0.744	6.4E-15	***polA***	0.649	1.6E-68	***ig2***	0.665	3.7E-08
ahrC	0.746	7.2E-03	***ylmG***	0.656	5.4E-12	***ylmG***	0.667	3.3E-09
odhA	0.755	5.9E-04	***lgt***	0.661	1.2E-13	***recD2***	0.672	3.2E-57
ftsH	0.761	5.4E-03	***ctpA***	0.673	1.9E-52	***bcrC***	0.673	5.3E-05
yaaO	0.774	5.8E-04	***ripX***	0.674	3.4E-04	***ecsB***	0.673	2.6E-08
recO	0.783	5.4E-02	***ytmP***	0.690	2.5E-23	***ig2807***	0.683	1.0E-11
ig3172	0.785	1.8E-03	***recG***	0.695	3.4E-03	***ig3151***	0.684	1.2E-04
ruvA	0.785	8.1E-12	***ig3116***	0.700	9.3E-07	***radA***	0.690	3.3E-34
ig2955	0.792	1.6E-04	***dnaN***	0.702	2.5E-03	***ig100***	0.705	3.1E-11
ymdB	0.794	1.3E-12	***ig1437***	0.705	3.5E-04	***ig2610***	0.706	4.1E-06
metN	0.805	1.3E-08	***ig1200***	0.714	4.5E-04	***ig2551***	0.712	2.1E-09
whiA	0.807	1.9E-03	***ydzU***	0.714	3.1E-06	***yneB***	0.712	1.4E-14
yjbH	0.808	1.1E-06	***walH***	0.715	3.2E-17	***spoIIIE***	0.713	1.7E-59
glpD	0.810	5.2E-09	***tagO***	0.717	3.5E-03	***ylmE***	0.714	8.9E-09
pnpA	0.811	6.4E-04	***ylmE***	0.718	1.6E-08	***ig1935***	0.714	5.3E-05
ig37	0.813	3.2E-03	***sdaAB***	0.724	5.5E-12	***yycI***	0.715	1.1E-07
metQ	0.816	5.8E-07	***ysoA***	0.725	1.2E-22	***ig1717***	0.715	2.9E-10
ccpA	0.824	6.9E-11	***ig2551***	0.726	1.0E-11	***yrrB***	0.719	1.7E-15
ripX	0.824	1.4E-09	***recX***	0.729	5.2E-02	***sdaAB***	0.730	8.5E-08
sdhB	0.824	3.2E-03	***walJ***	0.729	4.1E-18	***ig1921***	0.732	3.2E-06
ig1503	0.828	6.3E-02	***recD2***	0.731	6.4E-68	***ig2801***	0.744	5.7E-09

bcd	0.829	1.1E-06	***ig812***	0.741	1.2E-03	***nrdR***	0.748	6.6E-06
ig1525	0.829	5.0E-02	***ig2801***	0.742	3.8E-14	***recJ***	0.751	1.0E-35
minJ	0.829	2.9E-05	***radA***	0.742	5.4E-30	***ctsR***	0.758	2.3E-04
yneA	0.831	1.7E-07	***ylbK***	0.746	2.2E-11	***recG***	0.759	6.7E-05
walH	0.835	1.1E-10	***U712_09520***	0.752	2.7E-05	***ig2774***	0.759	3.8E-11
braB	0.836	5.7E-15	***ig3234***	0.755	4.7E-07	***addA***	0.759	5.1E-04
ig1977	0.838	6.6E-03	***sodA***	0.763	5.1E-04	***yjzG***	0.761	3.4E-05
sodA	0.839	1.7E-06	***cymR***	0.770	1.5E-11	***ig3623***	0.761	2.0E-05
ctaB	0.843	6.2E-12	***yprA***	0.773	3.6E-92	***ig3404***	0.762	1.3E-13
ytxG	0.844	5.7E-03	***yprB***	0.777	7.7E-32	***ig2409***	0.764	5.8E-09
rnc	0.846	7.1E-03	***ig199***	0.777	9.2E-08	***ig3234***	0.765	2.9E-05
buk	0.848	7.8E-14	***ywrC***	0.785	4.1E-03	***ig199***	0.766	5.2E-07
yvrJ	0.849	1.2E-02	***ig2940***	0.788	2.5E-03	***atpI***	0.769	5.5E-11
queA	0.850	9.0E-11	***yvcI***	0.790	3.9E-15	***ig3558***	0.775	9.7E-22
rnhC	0.851	3.0E-09	***ig2409***	0.790	1.5E-09	***ig1983***	0.778	5.1E-07
metP	0.851	7.0E-09	***ig2807***	0.792	7.8E-09	***U712_00035***	0.783	2.2E-02
czrA	0.852	1.9E-03	***ig3518***	0.792	6.5E-04	***walH***	0.784	1.3E-07
ig1623	0.853	2.3E-04	***yhcF***	0.795	3.0E-10	***ig1925***	0.784	5.0E-11
ssrSA	0.853	2.2E-02	***ylmH***	0.796	4.2E-13	***rnjB***	0.788	4.7E-44
menH	0.854	1.0E-07	***ig589***	0.800	2.7E-24	***ctaB***	0.788	1.0E-05
asnS	0.856	1.8E-08	***yufK***	0.804	3.1E-17	***ponA***	0.792	7.4E-06
minC	0.856	3.4E-03	***yfhH***	0.804	1.3E-04	***atpD***	0.792	1.3E-04
ig2118	0.857	1.1E-04	***yrrB***	0.805	5.0E-11	***ig3116***	0.792	5.4E-03
yvcJ	0.857	1.0E-02	***atpI***	0.805	2.0E-10	***pcrA***	0.793	8.6E-06
yneB	0.857	1.7E-09	***spxA***	0.805	2.9E-05	***ylmD***	0.795	2.9E-10
aroB	0.859	1.2E-05	***ylmD***	0.809	4.8E-07	***abh***	0.796	3.6E-08
yozB	0.862	2.6E-04	***recJ***	0.809	3.7E-34	***ig1505***	0.797	3.7E-11
ptsI	0.862	2.4E-09	***pcrA***	0.810	2.1E-04	***ig110***	0.798	3.1E-06
mswH	0.862	1.2E-04	***pbpD***	0.812	4.1E-42	***abrB***	0.798	2.1E-04
ugtP	0.863	2.2E-06	***ig2610***	0.813	7.2E-09	***lytA***	0.799	2.6E-09
yozO	0.864	1.3E-03	***ig2683***	0.815	2.9E-14	***ig1456***	0.806	1.5E-02
ig1843	0.866	9.8E-03	***abrB***	0.818	2.6E-08	***bsuMB***	0.813	1.4E-03
ig1836	0.866	2.3E-05	***BSU30466***	0.818	2.7E-04	***ig1602***	0.814	2.9E-06
fliQ	0.867	3.0E-03	***U712_17635***	0.819	8.2E-04	***tig***	0.814	3.0E-11
ig1596	0.867	1.8E-05	***ig100***	0.819	1.0E-09	***ig1515***	0.816	4.5E-05
nagBB	0.867	1.2E-05	***ig1983***	0.821	1.1E-10	***yvrJ***	0.817	1.7E-03
ig50	0.867	2.8E-02	***ig2628***	0.823	1.1E-02	***ig3123***	0.818	3.4E-06
ig1907	0.868	3.2E-06	***rpmGB***	0.823	7.1E-04	***ig1708***	0.819	5.5E-04
cshB	0.868	3.1E-07	***ig3131***	0.825	8.0E-06	***ig1601***	0.821	1.5E-11
spoVE	0.868	5.0E-04	***yaaT***	0.835	2.4E-05	***yaaT***	0.821	3.3E-04
yppC	0.868	4.4E-04	***yvsG***	0.837	1.9E-17	***yyaN***	0.822	1.1E-09
ig1515	0.870	3.4E-03	***ltaSB***	0.838	5.7E-02	***ccpA***	0.822	1.1E-07
aroF	0.870	1.4E-01	***U712_17630***	0.839	5.0E-03	***ig99***	0.824	6.8E-04

ig1859	0.871	5.4E-04	***yitW***	0.842	5.6E-05	***bcd***	0.824	1.5E-02
ezrA	0.871	1.0E-03	***ig1717***	0.843	3.0E-05	***bkdAB***	0.824	9.5E-08
sigH	0.872	2.8E-06	***tagF***	0.843	9.5E-04	***ig1266***	0.825	2.3E-06
rttM	0.872	1.2E-01	***ytzH***	0.844	3.3E-04	***ig1418***	0.826	9.9E-05
ig1928	0.872	6.5E-05	***ig3404***	0.844	5.7E-11	***ig248***	0.827	5.5E-09
ig3659	0.872	3.5E-04	***ig2365***	0.845	3.9E-06	***ig286***	0.827	4.2E-12
ndoA	0.872	8.5E-03	***ydjO***	0.846	2.6E-05	***menA***	0.831	9.6E-03
polC	0.873	3.9E-02	***ig1161***	0.848	3.9E-03	***spoVE***	0.832	4.0E-07
ig1633	0.874	1.0E-05	***yhaJ***	0.848	1.0E-20	***rsiV***	0.832	1.0E-12
ig2418	0.874	2.3E-02	***ig2961***	0.850	4.6E-05	***spxA***	0.832	6.6E-04
qoxC	0.875	2.2E-03	***sftA***	0.850	4.6E-38	***cdnD***	0.833	1.2E-60
ypuC	0.875	1.9E-02	***ydeS***	0.851	1.9E-14	***ndoA***	0.834	3.8E-03
ptb	0.875	2.0E-06	***gtaB***	0.852	6.4E-02	***tagA***	0.834	1.8E-02
recR	0.876	3.4E-04	***ig1981***	0.856	1.1E-01	***pbpA***	0.835	1.3E-28
rex	0.876	4.8E-09	***ig587***	0.856	4.9E-13	***ig1281***	0.835	1.7E-03
ymcA	0.877	2.2E-02	***ig644***	0.856	2.3E-05	***rpmGB***	0.835	5.3E-03
ig1580	0.878	7.6E-03	***ig2502***	0.858	1.7E-09	***qoxA***	0.835	8.9E-03
pgi	0.878	1.3E-05	***ig2650***	0.858	3.1E-03	***ig2365***	0.836	5.2E-09
yxeJ	0.878	1.4E-01	***ig590***	0.858	4.8E-12	***bsuMA***	0.836	4.8E-03
ig1602	0.879	4.7E-04	***U712_00035***	0.858	2.6E-03	***yneT***	0.837	1.2E-12
mraW	0.879	5.5E-06	***ig3206***	0.859	2.2E-04	***ig2420***	0.838	5.1E-06
U712_00035	0.880	5.8E-04	***ywzH***	0.859	1.1E-08	***ylbF***	0.838	1.5E-04
qoxA	0.880	3.3E-09	***rex***	0.859	1.1E-04	***yufK***	0.838	7.1E-13
yprA	0.881	2.3E-55	***ig2756***	0.860	1.5E-05	***pgl***	0.838	4.4E-06
comGC	0.881	4.7E-02	***mrpA***	0.861	7.3E-03	***ig3639***	0.839	3.3E-19
fliL	0.881	2.8E-06	***sigV***	0.861	1.2E-07	***ig3614***	0.839	8.7E-12
miaA	0.882	3.7E-02	***pheT***	0.862	2.2E-01	***ig374***	0.840	3.9E-03
ig2391	0.882	7.3E-03	***ig588***	0.863	1.4E-03	***ig1689***	0.841	5.7E-04
ig35	0.882	3.5E-03	***ig7***	0.864	1.1E-01	***yocH***	0.843	1.1E-17
fin	0.883	7.3E-03	***hemL***	0.864	4.4E-08	***sigV***	0.843	7.6E-11
dnaK	0.884	9.8E-06	***accA***	0.865	2.1E-01	***fapR***	0.843	1.4E-04
yfmN	0.884	1.1E-01	***mutM***	0.865	5.2E-06	***ydeS***	0.844	5.3E-13
aroD	0.884	4.7E-02	***ig3118***	0.866	5.6E-07	***ig1429***	0.844	1.5E-04
yoyC	0.884	5.3E-02	***ig3011***	0.867	5.5E-05	***ig2114***	0.844	4.0E-04
ig2293	0.884	5.7E-04	***ig3623***	0.867	2.4E-03	***gpsB***	0.845	1.5E-02
pyk	0.884	2.1E-03	***sdpR***	0.867	2.9E-14	***ig2558***	0.845	7.1E-06
rnpZA	0.885	1.0E-04	***ytnI***	0.868	6.3E-04	***bkdAA***	0.845	1.5E-08
spoIIAB	0.885	3.1E-04	***ig3558***	0.869	1.2E-14	***ig3099***	0.846	7.7E-05
yqaH	0.886	3.4E-02	***ytrB***	0.869	1.1E-15	***ig1582***	0.846	5.0E-03
ig112	0.886	2.1E-02	***ig2513***	0.869	6.7E-04	***metQ***	0.847	4.2E-03
ylbF	0.886	1.2E-06	***ig3279***	0.870	7.7E-12	***ypoC***	0.847	1.0E-06
ig1479	0.886	2.1E-02	***ig3556***	0.870	3.1E-07	***ig55***	0.847	2.2E-06
ig2117	0.887	3.8E-05	***U712_13350***	0.871	4.7E-03	***spoVAB***	0.847	3.9E-07

yxlC	0.887	5.4E-02	***yufS***	0.872	2.4E-02	***ig1369***	0.848	2.0E-04
yndH	0.887	7.4E-08	***ig3123***	0.872	4.8E-02	***yobS***	0.848	2.4E-08
yuxK	0.888	5.1E-03	***ig633***	0.872	4.1E-03	***ig3161***	0.848	1.5E-05
ig1381	0.888	2.2E-03	***rsh***	0.874	1.3E-03	***yufS***	0.848	1.5E-03
ksgA	0.889	5.7E-04	***ig2798***	0.875	9.7E-03	***ig1108***	0.848	3.9E-08
ig1981	0.889	1.1E-01	***ig3155***	0.877	1.9E-03	***ig1479***	0.848	4.4E-02
ig2479	0.890	4.8E-02	***cotT***	0.877	2.4E-04	***ig3423***	0.848	4.7E-06
ypoP	0.890	9.1E-03	***ig2639***	0.877	1.4E-03	***U712_09140***	0.848	1.1E-06
cheB	0.891	2.1E-07	***lmrB***	0.877	5.2E-31	***ylbJ***	0.849	1.9E-10
atpH	0.891	3.4E-03	***ytrC***	0.878	4.4E-35	***ig2955***	0.849	1.7E-03
U712_10355	0.892	7.0E-02	***ytrA***	0.879	2.3E-05	***ig1898***	0.849	4.5E-03
ig2492	0.893	6.4E-03	***ygaB***	0.879	1.8E-03	***ig1381***	0.850	9.5E-07
aroC	0.893	1.2E-07	***ig3113***	0.879	2.9E-04	***U712_02515***	0.851	3.5E-08
ig3099	0.893	1.1E-02	***yneB***	0.880	1.3E-05	***yyaB***	0.851	2.4E-13
ytrA	0.894	1.5E-06	***ktrC***	0.880	6.5E-02	***U712_06030***	0.852	3.9E-05
ig1906	0.894	4.6E-09	***tagA***	0.881	2.2E-03	***ig480***	0.852	1.4E-10
yqkE	0.894	1.3E-02	***ig3114***	0.881	2.5E-03	***addB***	0.852	1.1E-04
rnr	0.894	2.2E-11	***ig499***	0.882	7.0E-07	***ig1692***	0.852	1.7E-11
yqzD	0.894	8.4E-05	***ig987***	0.883	9.9E-08	***ig489***	0.852	1.1E-04
ylyA	0.894	4.9E-03	***U712_14410***	0.883	2.3E-02	***ig1332***	0.853	8.8E-06
ig125	0.895	1.6E-02	***ktrA***	0.884	1.3E-09	***ig987***	0.853	1.9E-13
bsrI	0.896	1.7E-01	***yxaD***	0.884	3.0E-05	***ig2103***	0.854	2.7E-04
mgtE	0.896	2.2E-03	***ig3120***	0.885	2.7E-04	***ig963***	0.854	4.6E-04
yobD	0.896	7.7E-05	***gerAA***	0.885	9.2E-19	***ktrD***	0.855	1.3E-24
ig2397	0.896	2.1E-01	***ytrD***	0.885	5.4E-30	***ig3279***	0.855	7.6E-13
yncF	0.897	8.5E-05	***ydzF***	0.885	2.4E-09	***ltaSB***	0.855	8.4E-03
ig3244	0.897	1.1E-01	***ig2774***	0.885	6.3E-04	***ynzD***	0.855	2.9E-04
ig2205	0.897	2.1E-03	***yrhO***	0.886	8.6E-16	***ig2502***	0.855	5.9E-09
ftsE	0.897	3.1E-06	***ig3219***	0.887	9.5E-04	***ig1478***	0.855	1.3E-03
U712_13765	0.897	2.2E-02	***csbA***	0.887	3.3E-08	***ig2047***	0.855	7.4E-05
pupG	0.897	7.0E-06	***U712_04285***	0.887	2.5E-10	***ig415***	0.856	3.7E-07
ig2013	0.898	1.1E-04	***yuxG***	0.888	1.0E-27	***ig7***	0.856	5.9E-02
trmF	0.898	2.3E-03	***xpaC***	0.889	4.6E-02	***ig3487***	0.857	1.2E-08
dnaJ	0.898	2.4E-05	***yteS***	0.890	7.0E-03	***ig1089***	0.857	3.7E-04
ig2030	0.898	3.8E-02	***ig2713***	0.890	1.6E-06	***ig1078***	0.857	1.0E-03
rhaU	0.898	8.3E-02	***ig3161***	0.891	1.5E-03	***ig1941***	0.858	3.4E-03
ig3299	0.899	6.8E-02	***ig3244***	0.891	3.2E-02	***hemL***	0.858	1.3E-05
hfq	0.899	2.3E-02	***capB***	0.891	3.1E-16	***ig2065***	0.858	1.0E-04
ig1452	0.899	1.1E-02	***yyaN***	0.892	3.4E-04	***ig2650***	0.858	1.3E-03
lpdV	0.899	1.0E-08	***yqzI***	0.893	2.6E-02	***ig256***	0.859	6.3E-08
ig2020	0.899	1.4E-03	***nrnA***	0.893	6.2E-03	***ig1857***	0.860	9.8E-22
ig1782	0.899	2.9E-04	***spoIIIE***	0.893	3.9E-19	***U712_18390***	0.860	8.7E-04
ig1649	0.899	2.4E-04	***rsiV***	0.893	1.1E-06	***dnaE***	0.860	2.1E-04

cymR	0.899	2.8E-04	***U712_15675***	0.894	3.1E-04	***ig1827***	0.861	2.0E-10
ig1804	0.900	1.4E-04	***yyaB***	0.894	5.0E-07	***ig1845***	0.861	8.1E-06
ig1978	0.900	2.9E-02	***apt***	0.895	7.2E-05	***ptsI***	0.861	9.8E-03
speE	0.901	5.5E-06	***abh***	0.895	9.1E-05	***yxaD***	0.861	1.6E-08
ynzG	0.901	5.5E-03	***ig2690***	0.895	1.2E-10	***ig3638***	0.862	3.2E-16
yozI	0.901	9.4E-05	***copZ***	0.896	1.1E-01	***ig617***	0.862	3.0E-03
sdaAA	0.901	6.5E-06	***yhaH***	0.896	1.8E-04	***ylmH***	0.862	1.4E-05
ig1451	0.901	1.8E-01	***csoR***	0.896	5.7E-07	***ig1371***	0.862	2.8E-09
yodL	0.902	8.0E-03	***manA***	0.896	1.2E-08	***ig1963***	0.862	7.3E-07
metA	0.902	4.6E-13	***ig1283***	0.897	1.1E-04	***rplI***	0.863	3.9E-13
ig2079	0.902	4.5E-03	***mutS2***	0.897	2.6E-14	***sbp***	0.863	5.1E-06
cwlC	0.903	2.0E-06	***bsuMA***	0.897	3.8E-02	***ig3617***	0.863	1.6E-07
cheD	0.904	1.0E-03	***ig925***	0.897	3.3E-04	***mutM***	0.863	2.1E-05
ig1773	0.904	5.6E-04	***ygaF***	0.897	7.4E-06	***ig2963***	0.863	1.5E-05
ftsX	0.904	1.5E-04	***ig3659***	0.897	5.2E-02	***nth***	0.863	1.4E-03
cdd	0.904	2.5E-02	***sdhB***	0.897	3.8E-02	***metP***	0.863	5.1E-03
accA	0.904	3.8E-02	***ig3181***	0.898	1.2E-06	***ig1938***	0.864	1.6E-08
yodC	0.904	8.3E-09	***yfkF***	0.898	4.1E-11	***ig212***	0.864	1.5E-05
mnmA	0.905	5.2E-02	***yhcG***	0.898	9.4E-07	***ig1228***	0.864	2.0E-06
rimP	0.905	7.9E-02	***yvzB***	0.898	9.3E-03	***ig2513***	0.864	1.7E-02
ylqD	0.905	4.7E-05	***ylbF***	0.898	1.4E-03	***ig2475***	0.864	3.2E-14
rsmB	0.905	9.9E-06	***ig508***	0.899	1.7E-03	***ig988***	0.865	6.6E-08
cheY	0.905	4.8E-06	***yfhO***	0.900	1.4E-48	***ig2476***	0.865	2.2E-07
ig2136	0.905	6.8E-02	***ig502***	0.900	1.7E-03	***ig261***	0.865	8.5E-05
fur	0.905	1.2E-07	***ig958***	0.900	5.5E-05	***yyaH***	0.866	2.2E-06
menA	0.906	6.3E-03	***ig1162***	0.900	4.9E-06	***walJ***	0.866	1.3E-05
yocB	0.906	1.3E-04	***ig3018***	0.900	8.9E-07	***ig2355***	0.866	1.4E-03
ig2308	0.906	1.3E-04	***ywrB***	0.901	4.8E-05	***ig1503***	0.867	1.7E-02
bkdAA	0.906	1.5E-09	***yusO***	0.901	1.8E-05	***ytnI***	0.867	3.9E-03
nrdR	0.906	1.5E-02	***yhcD***	0.901	2.0E-05	***ig1920***	0.867	8.7E-12
sdaAB	0.906	4.1E-06	***ktrD***	0.901	1.2E-17	***rsiX***	0.867	5.6E-20
ymaC	0.906	9.7E-03	***ig1101***	0.901	4.5E-03	***ig1344***	0.867	2.6E-09

MMS Growth period 1			**MMS Growth period 2**			**MMS Growth period 3**		
Feature/gene	**Mean Relative fitness**	**Adjusted p-value**	**Feature/gene**	**Mean Relative fitness**	**Adjusted p-value**	**Feature/gene**	**Mean Relative fitness**	**Adjusted p-value**
ruvA	0.586	2.5E-06	***polA***	0.589	1.0E-54	***polA***	0.601	1.3E-28
ruvB	0.621	2.5E-07	***hemL***	0.650	9.7E-05	***walJ***	0.705	2.0E-03
pgcA	0.631	6.4E-05	***ezrA***	0.673	1.1E-17	***ezrA***	0.712	3.0E-09
atpD	0.684	2.7E-03	***walJ***	0.743	1.9E-05	***recN***	0.793	1.2E-24

recR	0.695	5.2E-06	***mntD***	0.769	4.5E-02	***cymR***	0.798	3.5E-05
rho	0.718	2.0E-06	***sdaAB***	0.782	2.1E-09	***sdaAB***	0.805	5.8E-08
ponA	0.721	3.9E-04	***radA***	0.782	1.3E-33	***yycI***	0.820	1.6E-01
hemL	0.750	1.4E-10	***resE***	0.783	3.9E-04	***recD2***	0.837	5.4E-23
ytpQ	0.761	5.7E-04	***recN***	0.791	8.3E-30	***radA***	0.840	2.1E-26
addA	0.769	2.9E-15	***ig2551***	0.808	4.8E-03	***addA***	0.840	1.1E-02
addB	0.769	3.2E-14	***yycI***	0.823	2.5E-02	***ig100***	0.854	7.6E-05
recG	0.782	8.0E-03	***ylmE***	0.827	4.8E-03	***ig3623***	0.858	3.1E-03
ccpA	0.803	1.7E-02	***cymR***	0.827	1.1E-05	***ig1200***	0.858	3.2E-02
ugtP	0.806	5.3E-03	***recD2***	0.829	1.8E-34	***sodA***	0.868	9.1E-02
ig3284	0.808	3.2E-05	***ig2204***	0.833	3.2E-02	***ig1717***	0.876	1.1E-04
ybbR	0.817	1.4E-03	***ig1200***	0.834	5.6E-03	***yozN***	0.877	8.5E-04
yitW	0.818	1.1E-01	***ig3219***	0.846	6.7E-02	***ig2409***	0.879	1.3E-02
spoIIP	0.818	6.0E-04	***addB***	0.853	2.9E-04	***ig3590***	0.885	3.1E-02
pabC	0.821	1.9E-03	***ig1503***	0.854	1.6E-03	***ysoA***	0.887	6.6E-10
atpA	0.825	7.0E-03	***yfhH***	0.856	1.5E-02	***ylmD***	0.893	1.3E-01
mcsA	0.827	6.4E-06	***parB***	0.861	1.0E-04	***spoIIIE***	0.893	2.3E-02
pabA	0.829	7.8E-03	***ig100***	0.862	1.2E-06	***ig1503***	0.894	4.7E-02
walJ	0.833	1.8E-03	***ylmG***	0.863	1.4E-02	***yrrB***	0.894	1.0E-07
ig2118	0.835	1.7E-02	***spxA***	0.864	3.3E-06	***ponA***	0.895	1.5E-01
aroC	0.836	4.0E-03	***yrrB***	0.865	2.0E-12	***ylmE***	0.896	2.2E-04
spoIIIE	0.838	1.4E-05	***ytxG***	0.868	2.8E-02	***spxA***	0.896	5.2E-03
pgi	0.839	2.4E-04	***recJ***	0.875	8.7E-22	***ig3284***	0.899	1.5E-02
mntD	0.844	2.2E-07	***ig2409***	0.881	1.0E-03	***recJ***	0.900	2.3E-21
clpC	0.848	4.6E-07	***ponA***	0.882	9.0E-03	***gpsB***	0.900	3.0E-02
yhdK	0.848	2.3E-04	***rsfS***	0.883	4.4E-02	***pyrB***	0.900	1.4E-01
kinC	0.848	9.4E-06	***ylbK***	0.887	5.2E-10	***yppC***	0.901	9.8E-03
queA	0.850	8.1E-03	***ysoA***	0.888	2.2E-09	***addB***	0.903	4.4E-03
yycI	0.850	5.3E-03	***ytxM***	0.892	1.5E-01	***ig2688***	0.906	5.0E-02
sigG	0.850	1.2E-03	***yqaG***	0.894	2.7E-04	***bsuMA***	0.907	3.7E-01
ig112	0.853	1.5E-02	***ig812***	0.894	1.3E-01	***ctpA***	0.907	2.0E-16
znuB	0.854	1.9E-13	***abrB***	0.897	5.9E-02	***yshA***	0.908	2.9E-03
znuC	0.856	2.1E-05	***ig2205***	0.900	6.5E-03	***ig2639***	0.908	1.9E-02
rnhC	0.857	2.8E-04	***efp***	0.901	1.0E-02	***ygaF***	0.909	4.0E-03
nagBB	0.857	5.9E-04	***ylbL***	0.902	3.1E-15	***ig1835***	0.911	4.0E-02
sigE	0.857	5.7E-03	***spoIIB***	0.904	2.9E-02	***rnpZA***	0.912	8.5E-02
ywlE	0.857	1.3E-07	***phrE***	0.904	4.1E-03	***yqxD***	0.912	6.1E-02
cshB	0.859	8.0E-02	***addA***	0.905	8.7E-02	***ppiB***	0.915	5.3E-04
dltC	0.860	1.2E-03	***xseA***	0.907	8.3E-04	***U712_12375***	0.915	5.7E-02
ybbP	0.860	2.7E-03	***ig159***	0.908	1.0E-02	***ig1611***	0.916	2.4E-01
rocG	0.861	5.0E-06	***ig2269***	0.909	4.4E-02	***ig3118***	0.918	5.7E-02
mcsB	0.861	1.4E-06	***ypuI***	0.909	8.3E-04	***pgl***	0.919	4.4E-02
mntA	0.862	6.0E-03	***ylmH***	0.909	3.4E-03	***ig2551***	0.919	2.7E-01

asnO	0.862	5.1E-07	***ywzG***	0.910	4.1E-03	***ig588***	0.919	1.2E-01
spoVT	0.862	1.8E-05	***ykuD***	0.910	3.6E-03	***ig1814***	0.920	1.7E-01
fabHA	0.862	2.2E-02	***speE***	0.910	1.2E-01	***ig1773***	0.920	4.8E-03
speA	0.863	9.6E-03	***disA***	0.911	4.2E-19	***alkA***	0.920	2.6E-15
yjbI	0.865	7.8E-02	***ig2280***	0.911	1.9E-04	***ylbL***	0.921	2.0E-13
mntB	0.865	2.9E-03	***abh***	0.912	4.8E-03	***U712_07230***	0.921	8.9E-02
menA	0.866	5.1E-02	***leuD***	0.912	1.1E-02	***xseA***	0.922	7.0E-03
ig1388	0.866	8.1E-03	***ig993***	0.912	9.0E-02	***ig3006***	0.923	1.8E-02
lgt	0.867	3.3E-04	***sigV***	0.912	1.5E-04	***ig991***	0.924	1.1E-02
pdaA	0.867	1.7E-02	***yrkL***	0.913	9.6E-10	***asnS***	0.924	3.3E-01
pbpA	0.868	2.5E-03	***tgt***	0.915	2.0E-02	***ig112***	0.924	3.5E-01
ig375	0.869	3.0E-04	***ctpA***	0.915	1.3E-17	***ig1745***	0.924	1.2E-01
ig3518	0.869	7.9E-02	***ig2248***	0.915	8.5E-04	***ig624***	0.925	1.5E-01
znuA	0.869	3.8E-21	***ig2195***	0.916	2.3E-02	***ig2722***	0.925	9.8E-04
ig3006	0.871	1.8E-03	***apt***	0.917	8.3E-04	***ig1582***	0.925	4.9E-02
cysK	0.871	4.1E-07	***yjlB***	0.917	7.7E-02	***mecA***	0.926	8.5E-02
ig1071	0.871	1.1E-03	***yycD***	0.918	1.5E-03	***ig1283***	0.926	9.5E-02
cwlD	0.872	3.7E-02	***spoIVA***	0.918	6.1E-03	***yyaB***	0.926	1.4E-05
ig2955	0.872	1.3E-01	***htpX***	0.918	3.4E-04	***ig2183***	0.926	2.5E-02
metP	0.874	8.9E-03	***pycA***	0.918	7.6E-23	***ig3106***	0.928	3.9E-01
U712_14655	0.875	7.1E-02	***ecfA***	0.919	1.8E-01	***yebD***	0.929	1.2E-01
rsiW	0.876	2.5E-04	***yqfT***	0.919	5.4E-02	***ig694***	0.929	6.6E-03
parB	0.876	5.1E-03	***rpsT***	0.920	9.8E-02	***ig644***	0.929	2.0E-01
spoIIIAH	0.879	5.6E-02	***nth***	0.921	8.6E-02	***znuC***	0.929	2.0E-01
ywrC	0.880	3.6E-02	***ig2560***	0.921	1.0E-03	***pbpA***	0.929	1.1E-01
ig331	0.880	1.4E-02	***ypoC***	0.921	1.0E-02	***aroH***	0.930	5.6E-02
walH	0.881	8.2E-02	***prkC***	0.921	1.7E-04	***ig680***	0.930	1.3E-01
ig2204	0.881	7.8E-02	***ytbD***	0.921	1.6E-03	***yqfC***	0.930	2.4E-01
spoIIR	0.882	6.0E-05	***ytpP***	0.922	7.4E-02	***cspD***	0.930	1.2E-01
ig46	0.882	4.4E-06	***yqfA***	0.923	4.7E-04	***yoyD***	0.930	3.0E-01
ig3423	0.882	1.9E-03	***pabC***	0.923	1.3E-01	***walH***	0.931	4.8E-01
ywzH	0.883	1.1E-02	***ig1429***	0.923	2.6E-03	***yycD***	0.931	5.5E-03
spoIVCA	0.883	1.8E-03	***ig2235***	0.924	4.1E-02	***ig2774***	0.931	1.3E-01
ig3250	0.883	8.3E-03	***ig1129***	0.924	5.4E-04	***ig2560***	0.931	3.1E-03
mntC	0.885	1.9E-04	***U712_07190***	0.924	4.9E-03	***ig3607***	0.931	6.3E-03
ig166	0.885	6.9E-03	***ig2348***	0.924	3.0E-02	***ig3151***	0.931	2.4E-01
relP	0.885	1.1E-03	***comER***	0.924	2.8E-06	***ig444***	0.931	1.8E-01
yqfD	0.886	1.3E-02	***yojB***	0.924	4.2E-02	***ig3502***	0.932	7.9E-03
rnpZA	0.886	3.8E-02	***ylzJ***	0.926	5.4E-02	***ig3385***	0.934	2.9E-01
gpr	0.886	8.1E-02	***ylqD***	0.926	3.5E-03	***ig2755***	0.934	5.4E-02
ig159	0.887	6.2E-02	***yshE***	0.926	3.6E-03	***ig1682***	0.934	2.6E-02
ig1465	0.887	6.3E-03	***yjcD***	0.927	1.9E-14	***ywzH***	0.934	2.5E-01
ig1482	0.888	5.2E-02	***rsiV***	0.927	3.0E-03	***fin***	0.934	2.8E-01

ig298	0.889	1.7E-06	***sspB***	0.927	2.2E-02	***ig1963***	0.934	1.7E-02
purR	0.889	1.9E-06	***splA***	0.927	6.4E-03	***disA***	0.934	1.4E-14
dacB	0.889	2.0E-06	***walH***	0.928	4.4E-01	***yoyE***	0.935	2.2E-01
glpD	0.890	3.6E-06	***ig3155***	0.928	1.8E-02	***U712_14285***	0.935	7.7E-02
ig3474	0.890	5.7E-04	***spoVID***	0.928	5.4E-04	***ig1308***	0.935	1.5E-01
ig98	0.890	3.4E-04	***mhqR***	0.929	1.1E-01	***ig2420***	0.935	1.4E-02
U712_02515	0.891	1.7E-02	***gntZ***	0.929	2.2E-04	***ig2019***	0.935	2.0E-01
albA	0.891	3.1E-09	***ig2264***	0.929	8.0E-04	***aroB***	0.936	2.9E-01
ig62	0.892	2.2E-03	***mifM***	0.929	4.1E-03	***ypoC***	0.936	1.6E-01
gltT	0.893	2.9E-05	***ig727***	0.929	2.1E-01	***yneB***	0.936	1.9E-05
truA	0.893	7.8E-07	***mgtE***	0.930	3.6E-02	***ig1671***	0.936	9.8E-04
pgl	0.894	1.4E-05	***yvzF***	0.931	8.6E-03	***ig1818***	0.936	1.8E-03
ig3184	0.895	2.5E-02	***kinC***	0.931	9.9E-03	***ig1141***	0.936	5.9E-05
ig1226	0.895	1.1E-03	***yqzI***	0.931	1.3E-01	***ig1906***	0.936	1.1E-03
dltB	0.896	9.2E-10	***yqeM***	0.931	8.1E-04	***spoVD***	0.936	1.2E-01
efeM	0.896	1.4E-10	***ig1307***	0.931	1.9E-02	***parB***	0.937	7.2E-02
ig3356	0.896	1.1E-09	***dgkA***	0.931	1.3E-05	***U712_16090***	0.937	3.0E-01
spoIIIAA	0.897	4.1E-02	***ykzD***	0.931	3.0E-02	***ykzM***	0.937	3.9E-02
yunB	0.897	7.7E-04	***ylmD***	0.931	2.9E-01	***ig1071***	0.937	1.6E-01
ecfAB	0.897	5.1E-02	***fabHA***	0.932	1.3E-01	***ig1885***	0.937	9.8E-04
oxaAA	0.897	3.8E-04	***mcsA***	0.932	2.2E-01	***yoaF***	0.938	1.0E-04
ig3247	0.898	2.3E-03	***drm***	0.932	1.6E-04	***gntZ***	0.938	8.6E-03
ig2120	0.898	7.7E-02	***spoIIM***	0.932	5.5E-02	***ig3194***	0.938	2.5E-01
atpI	0.899	1.0E-04	***ig2241***	0.933	2.2E-04	***ylbK***	0.938	5.9E-04
ig3276	0.899	7.2E-03	***nfo***	0.933	5.9E-05	***ymaB***	0.938	1.4E-01
yaaL	0.900	1.6E-02	***ig2365***	0.933	8.5E-04	***ig1341***	0.938	3.5E-02
ig34	0.900	6.2E-04	***yrpD***	0.933	1.5E-08	***yobD***	0.938	1.0E-02
ywpF	0.900	2.2E-03	***ecsB***	0.934	2.2E-02	***yyzH***	0.938	3.4E-02
resE	0.900	1.2E-01	***htrC***	0.934	1.1E-05	***ugtP***	0.939	2.6E-01
ig3235	0.900	2.7E-03	***mutS2***	0.934	4.9E-06	***ig1405***	0.939	2.6E-02
ig1633	0.900	5.5E-04	***yqfQ***	0.934	2.1E-04	***ig3009***	0.939	5.6E-02
ig1154	0.900	2.4E-03	***ig2349***	0.934	6.4E-03	***yczN***	0.939	5.1E-02
spoIID	0.900	2.3E-04	***U712_13115***	0.935	7.0E-02	***ig653***	0.939	3.7E-02
ig1325	0.901	7.3E-02	***ig3593***	0.935	2.4E-02	***ig2617***	0.939	1.3E-01
ig3303	0.901	1.4E-04	***sufA***	0.935	3.3E-01	***ig1976***	0.940	4.6E-01
mscL	0.902	3.0E-03	***pyrAB***	0.935	8.6E-05	***U712_03800***	0.940	1.4E-03
pit	0.902	1.6E-04	***yvgO***	0.935	5.5E-02	***ig3105***	0.940	2.5E-02
yvrJ	0.902	2.0E-01	***yqfD***	0.935	8.3E-02	***ig490***	0.940	5.9E-02
speE	0.902	4.5E-02	***argI***	0.936	1.3E-02	***ig1752***	0.940	1.9E-04
albB	0.902	4.0E-03	***ig2368***	0.936	4.1E-03	***ig688***	0.940	1.3E-01
fliL	0.902	1.8E-04	***yrhD***	0.936	2.9E-01	***U712_18660***	0.940	7.9E-03
ig1281	0.903	1.6E-02	***ytrH***	0.936	2.8E-06	***ig3334***	0.940	1.1E-01
ig3264	0.903	8.4E-03	***ig2074***	0.936	2.0E-03	***yocN***	0.941	3.7E-01

ig1921	0.903	2.6E-01	***ig1434***	0.936	2.6E-05	***ig1101***	0.941	6.2E-02
spoVD	0.903	5.8E-03	***yqbI***	0.937	8.3E-03	***ig2234***	0.941	7.0E-02
ig3428	0.904	1.7E-06	***rsmE***	0.937	1.3E-03	***ig2756***	0.941	2.1E-02
qoxB	0.904	1.4E-04	***ig1070***	0.937	2.3E-01	***ykuJ***	0.942	1.7E-02
ig2397	0.905	1.3E-01	***sigG***	0.937	1.4E-01	***ctsR***	0.942	6.5E-01
ig3590	0.905	2.1E-03	***ig807***	0.937	2.7E-01	***ig1708***	0.942	1.5E-01
ig321	0.905	2.0E-02	***ig1142***	0.937	7.4E-02	***yfmL***	0.942	2.7E-01
ig2396	0.906	2.8E-02	***ig2225***	0.937	8.6E-02	***ykuK***	0.942	5.9E-05
ig3411	0.906	1.4E-05	***yrhO***	0.937	1.2E-04	***cotT***	0.942	2.1E-02
ig3279	0.906	2.9E-08	***yizB***	0.937	8.8E-02	***ig1349***	0.942	1.6E-01
U712_17630	0.906	2.6E-02	***pyrK***	0.938	4.1E-04	***ig3505***	0.942	1.2E-01
ig3391	0.906	4.2E-06	***yppC***	0.938	7.7E-02	***ig1110***	0.943	1.6E-01
ig2805	0.907	5.5E-02	***ig2338***	0.938	1.8E-01	***ig658***	0.943	5.7E-02
ecsC	0.907	5.9E-03	***U712_11340***	0.938	1.0E-01	***ig78***	0.943	7.8E-02
ig1240	0.907	3.2E-03	***thiG***	0.938	3.0E-02	***tapA***	0.943	1.4E-02
spoIVFB	0.907	1.7E-02	***yqeC***	0.938	2.4E-03	***ig1915***	0.943	4.4E-02
dltA	0.908	1.3E-08	***yphF***	0.938	5.6E-04	***ig1829***	0.943	4.8E-04
whiA	0.908	8.3E-02	***yrzE***	0.939	9.3E-03	***apt***	0.944	1.3E-01
ycgE	0.909	9.8E-02	***ybbP***	0.939	3.3E-01	***ig660***	0.944	9.8E-02
ig2723	0.909	5.5E-02	***yrrO***	0.939	3.5E-03	***ywlE***	0.944	1.2E-01
recX	0.909	7.1E-02	***ytoI***	0.939	1.7E-05	***ig2598***	0.944	3.9E-02
yczE	0.909	3.5E-04	***ig1201***	0.939	5.7E-02	***ig3117***	0.944	2.0E-02
walK	0.909	1.2E-01	***yqfZ***	0.939	2.0E-01	***treA***	0.944	3.4E-03
ig220	0.910	8.2E-03	***yrdN***	0.939	1.8E-02	***yusD***	0.944	3.1E-01
U712_05070	0.910	6.7E-03	***ypoP***	0.940	4.4E-02	***ig1806***	0.945	3.5E-02
ig644	0.910	4.2E-02	***tsaD***	0.940	3.9E-01	***yozG***	0.945	8.4E-03
ig360	0.911	6.2E-03	***yoyG***	0.941	3.4E-02	***ig1680***	0.945	1.3E-02
ygaF	0.911	1.3E-02	***ig1430***	0.941	7.7E-02	***U712_09520***	0.945	3.3E-01
psd	0.911	1.1E-03	***yrdC***	0.941	2.3E-08	***ig1233***	0.945	2.9E-03
ig2684	0.911	2.0E-01	***yqjX***	0.941	1.2E-02	***ig2092***	0.946	1.6E-01
ig222	0.911	8.9E-06	***ytxO***	0.941	1.7E-02	***yuzH***	0.946	1.6E-01
ig3564	0.911	3.0E-12	***polYB***	0.941	2.6E-06	***ig2773***	0.946	6.5E-03
U712_02080	0.911	4.3E-02	***ig1461***	0.941	4.8E-02	***ig1201***	0.946	4.2E-02
ig3219	0.911	1.9E-02	***yqbO***	0.941	1.5E-27	***yyaN***	0.946	1.0E-01
ig455	0.911	4.1E-03	***spoVB***	0.941	5.0E-03	***ig1589***	0.946	3.5E-01
ig3292	0.912	1.7E-01	***sftA***	0.941	2.0E-13	***ig2845***	0.946	1.0E-02
opuAB	0.912	2.0E-08	***ig1264***	0.941	3.9E-04	***ig917***	0.946	1.6E-01
ecfT	0.912	5.7E-02	***yraJ***	0.941	2.2E-04	***ecsB***	0.946	1.6E-01
cdnD	0.912	6.6E-09	***yqzE***	0.942	2.4E-03	***U712_09540***	0.946	9.0E-02
U712_01385	0.912	5.6E-03	***comZ***	0.942	1.8E-02	***U712_17570***	0.947	2.2E-01
yqfC	0.913	4.0E-02	***dck***	0.942	6.0E-03	***sigG***	0.947	5.9E-01
ig870	0.913	2.9E-01	***ykzQ***	0.942	7.6E-04	***ig102***	0.947	4.3E-02
ig1611	0.913	5.3E-02	***ig969***	0.942	9.3E-02	***yobR***	0.947	1.9E-02

rttM	0.913	1.0E-02	***yqxD***	0.942	1.9E-01	***yozK***	0.947	1.7E-01
dnaE	0.913	1.0E-01	***proB***	0.942	4.6E-03	***ig1887***	0.947	9.7E-03
U712_16090	0.913	1.6E-01	***slp***	0.942	8.7E-03	***gerT***	0.947	4.8E-03
ig125	0.913	8.6E-03	***fruA***	0.942	6.9E-07	***ig3470***	0.947	8.7E-04
ig118	0.914	3.3E-04	***ktrC***	0.942	8.4E-03	***ig1652***	0.947	3.1E-01
ig2610	0.914	2.4E-01	***ig2420***	0.942	3.7E-02	***ig3610***	0.947	4.4E-02
ig199	0.914	2.2E-02	***pstC***	0.942	6.8E-04	***ig203***	0.947	5.3E-05
dltE	0.914	2.2E-03	***yqaS***	0.942	1.0E-04	***yobU***	0.947	1.8E-02
U712_14500	0.914	4.7E-03	***sigZ***	0.943	4.3E-03	***ig2718***	0.947	3.7E-02
tatCy	0.914	1.1E-02	***comGF***	0.943	8.3E-02	***ig1250***	0.948	2.7E-01
ig3306	0.915	5.7E-03	***yqcB***	0.943	1.4E-02	***ig1879***	0.948	1.4E-01
ig88	0.915	1.7E-02	***ig2515***	0.943	4.7E-02	***ig1742***	0.948	5.9E-04
yrzS	0.915	1.8E-02	***adhA***	0.943	1.8E-06	***ig833***	0.948	2.6E-02
ig342	0.916	4.5E-05	***moeA***	0.943	1.3E-06	***BSU30466***	0.948	9.0E-02
dtd	0.916	6.1E-02	***ig2038***	0.943	2.3E-02	***ig633***	0.948	2.6E-01
U712_08775	0.916	1.9E-02	***yqxK***	0.943	9.3E-06	***ig2611***	0.948	1.9E-01
ig612	0.916	3.2E-04	***yqaM***	0.943	3.1E-03	***ig3656***	0.948	1.9E-01
bacA	0.916	8.0E-03	***yqeF***	0.944	5.1E-06	***ig580***	0.948	1.3E-02
ig3502	0.916	9.5E-03	***glpG***	0.944	4.7E-07	***yrzL***	0.948	2.1E-01
speB	0.916	2.4E-05	***ohrB***	0.944	2.4E-02	***ig1184***	0.948	1.7E-01
spoIIIAE	0.916	8.6E-02	***qcrB***	0.944	2.1E-03	***ig2492***	0.949	2.0E-01
ig78	0.916	3.5E-04	***bacA***	0.944	2.2E-01	***U712_14500***	0.949	1.6E-01
ygzB	0.916	1.4E-01	***relP***	0.944	8.2E-02	***spoIVB***	0.949	8.2E-02
U712_09520	0.917	3.1E-02	***ypbG***	0.945	6.4E-03	***yfhF***	0.949	6.4E-02

Phleomycin Growth period 1			**Phleomycin Growth period 2**			**Phleomycin Growth period 2**		
Feature/gene	**Mean Relative fitness**	**Adjusted p-value**	**Feature/gene**	**Mean Relative fitness**	**Adjusted p-value**	**Feature/gene**	**Mean Relative fitness**	**Adjusted p-value**
atpA	0.566	7.8E-04	***ezrA***	0.617	1.2E-16	***ezrA***	0.696	1.1E-04
ruvA	0.624	1.9E-06	***ig1200***	0.649	1.5E-05	***U712_09520***	0.751	1.6E-02
oxaAA	0.652	7.6E-15	***tig***	0.652	2.3E-11	***bkdAB***	0.781	2.0E-02
ig2955	0.672	1.0E-02	***bkdAA***	0.652	2.5E-16	***tig***	0.787	5.0E-06
recA	0.680	1.4E-04	***oxaAA***	0.655	3.8E-13	***yrbF***	0.791	6.5E-02
ruvB	0.702	6.3E-06	***ig1556***	0.671	1.2E-04	***bkdB***	0.795	4.1E-05
ytpQ	0.708	2.5E-03	***recN***	0.681	4.9E-33	***dltB***	0.797	1.2E-15
U712_06030	0.740	4.7E-02	***dltD***	0.696	5.3E-13	***spxA***	0.797	3.7E-05
pgcA	0.764	8.6E-03	***ig3276***	0.697	8.0E-04	***dltA***	0.801	1.1E-07
ywzH	0.764	4.7E-08	***dltC***	0.708	1.8E-03	***dnaK***	0.802	1.9E-35
addB	0.776	5.6E-11	***ig2807***	0.720	3.5E-08	***ig2807***	0.806	1.2E-04
rho	0.789	2.2E-05	***bkdB***	0.722	2.5E-13	***ugtP***	0.809	2.8E-03

ig2118	0.791	3.8E-03	***dltA***	0.722	2.9E-16	***bkdAA***	0.810	2.3E-03
yqeY	0.794	1.7E-02	***fabHA***	0.728	9.1E-05	***recN***	0.814	5.4E-15
recR	0.804	7.7E-04	***ylmG***	0.735	1.9E-03	***ig248***	0.821	1.1E-03
yabP	0.809	4.2E-02	***ig1503***	0.742	7.7E-06	***ytmP***	0.824	1.6E-08
dltC	0.810	3.5E-04	***bkdAB***	0.743	6.1E-09	***ig100***	0.824	6.8E-05
yaaB	0.810	2.3E-03	***dltB***	0.748	3.7E-17	***ykzP***	0.825	5.0E-06
walH	0.813	1.9E-04	***U712_09520***	0.748	1.1E-03	***oxaAA***	0.829	5.2E-03
addA	0.814	5.4E-11	***cymR***	0.758	5.4E-06	***sdaAB***	0.834	2.6E-06
recN	0.815	1.5E-33	***yhgE***	0.762	4.6E-37	***ktrD***	0.837	5.7E-24
spoIIQ	0.816	2.9E-03	***ig2551***	0.763	8.4E-05	***yugI***	0.838	1.7E-06
ig3219	0.817	4.6E-02	***ykzP***	0.779	1.9E-06	***ig199***	0.840	1.6E-03
pbpA	0.818	8.1E-06	***yrbF***	0.780	1.8E-04	***spoIIIE***	0.844	3.9E-05
recX	0.818	6.8E-03	***ig2476***	0.781	2.0E-15	***ig1437***	0.845	2.6E-04
mntA	0.819	1.5E-04	***ktrD***	0.783	2.1E-34	***flgD***	0.845	7.7E-05
walJ	0.822	1.8E-04	***spxA***	0.784	7.2E-06	***kinC***	0.847	5.7E-05
sigG	0.828	2.2E-02	***sdaAB***	0.785	9.6E-09	***yqxD***	0.851	9.0E-04
ponA	0.828	3.0E-03	***pit***	0.786	1.3E-08	***ig3623***	0.854	6.2E-03
dltB	0.830	3.1E-27	***buk***	0.787	4.1E-04	***ig1589***	0.855	5.3E-02
spoIID	0.832	5.6E-07	***ig1437***	0.793	1.0E-04	***defB***	0.857	1.8E-13
dltD	0.834	5.4E-10	***ktrC***	0.800	2.7E-14	***ponA***	0.858	9.4E-03
rnhC	0.835	4.3E-04	***yrrB***	0.801	1.8E-18	***yhaJ***	0.864	4.2E-21
recG	0.837	1.2E-02	***ecfAB***	0.801	1.2E-03	***pit***	0.864	3.4E-05
dltA	0.838	2.0E-13	***ig2133***	0.802	5.0E-05	***U712_05070***	0.867	1.6E-04
queA	0.843	7.0E-03	***ig890***	0.802	1.7E-07	***dnaJ***	0.869	2.3E-13
clpC	0.846	4.4E-07	***ig2204***	0.804	7.6E-04	***ig1071***	0.871	3.9E-02
ecfA	0.846	1.0E-01	***yjlB***	0.804	1.4E-02	***walJ***	0.873	6.4E-03
pabC	0.849	1.1E-02	***ig1108***	0.804	2.7E-08	***yhgE***	0.877	1.4E-15
U712_17630	0.853	6.4E-03	***yqxD***	0.808	5.1E-04	***ig588***	0.878	5.4E-03
ig110	0.853	2.1E-03	***queA***	0.808	2.2E-02	***ywhA***	0.879	1.9E-08
ywrC	0.856	5.9E-02	***ysoA***	0.809	5.8E-18	***ecsB***	0.880	4.6E-03
U712_17635	0.856	2.6E-03	***lpdV***	0.811	4.7E-09	***minD***	0.880	2.8E-05
cymR	0.857	1.1E-03	***ptsG***	0.813	4.6E-26	***ig3151***	0.881	1.7E-01
walK	0.858	5.2E-03	***yhaJ***	0.813	4.7E-25	***cysK***	0.881	2.6E-03
cysK	0.861	5.0E-08	***rppG***	0.814	5.6E-06	***yppC***	0.881	3.2E-04
dltE	0.861	1.1E-05	***ig1589***	0.815	3.5E-03	***fliF***	0.883	4.0E-15
spoIIIAA	0.864	4.1E-04	***kinC***	0.816	1.7E-08	***ktrC***	0.884	1.7E-06
mntC	0.865	6.4E-06	***ig2127***	0.816	2.0E-05	***yjzD***	0.884	1.6E-04
pgi	0.865	9.9E-03	***tgt***	0.816	1.2E-11	***ywzD***	0.886	3.4E-03
cwlD	0.867	1.3E-03	***ylmH***	0.817	1.9E-06	***ig2140***	0.886	3.8E-07
ygzB	0.868	5.2E-02	***yjzD***	0.817	6.6E-09	***mcsB***	0.886	3.9E-05
ig3006	0.869	9.0E-04	***recD2***	0.818	1.5E-29	***yhcF***	0.888	3.6E-02
ig62	0.870	8.0E-04	***ylmE***	0.819	2.6E-03	***dltD***	0.889	1.2E-01
ig367	0.871	7.6E-03	***ylbK***	0.823	7.2E-17	***ig2042***	0.889	3.0E-06

sigE	0.871	9.5E-02	***addB***	0.823	3.6E-03	***ybbP***	0.890	4.1E-03
ig3276	0.871	8.0E-04	***ypoP***	0.823	1.5E-04	***treA***	0.891	7.3E-07
ecfT	0.875	1.5E-01	***ig2365***	0.824	2.3E-06	***yrrB***	0.891	8.5E-07
pabA	0.876	5.9E-02	***ig1887***	0.825	3.3E-10	***yvyC***	0.891	2.8E-04
ig212	0.877	5.6E-05	***ygaC***	0.831	4.8E-10	***fabHA***	0.891	1.1E-01
ydzH	0.877	2.2E-03	***ig248***	0.833	2.2E-03	***ig1390***	0.892	1.5E-05
ywbE	0.877	5.1E-02	***addA***	0.834	1.8E-03	***ig2756***	0.893	9.3E-05
spoIVCA	0.878	2.8E-05	***veg***	0.835	2.3E-03	***yycI***	0.894	1.7E-01
ig199	0.879	5.5E-03	***ig2116***	0.836	2.9E-10	***motB***	0.894	2.4E-08
mscL	0.880	7.9E-05	***ktrA***	0.840	3.9E-11	***bsuMA***	0.895	1.6E-01
spoVFB	0.881	5.9E-02	***ecsB***	0.841	1.1E-06	***fliG***	0.896	2.3E-07
ig474	0.883	2.9E-04	***ybbP***	0.842	6.2E-03	***ig2133***	0.896	3.1E-02
ig3171	0.884	1.6E-02	***rnpZA***	0.846	8.6E-03	***ypoP***	0.896	2.0E-02
speE	0.884	2.5E-02	***flgD***	0.846	2.8E-05	***yozO***	0.897	2.0E-02
ugtP	0.885	2.7E-01	***ig2269***	0.852	5.6E-04	***ig1299***	0.897	3.9E-02
ig2801	0.885	1.8E-03	***defB***	0.852	1.0E-15	***yjbK***	0.898	5.6E-08
purR	0.886	7.4E-07	***ig3234***	0.854	9.6E-04	***sigW***	0.898	4.4E-06
pit	0.886	9.2E-08	***gpsB***	0.855	5.5E-03	***ytoI***	0.898	2.7E-12
ig3279	0.886	4.8E-07	***ig1101***	0.856	4.3E-05	***glcT***	0.898	1.2E-05
gerR	0.887	1.1E-01	***yfhH***	0.856	2.6E-03	***yozN***	0.899	1.6E-02
ig3427	0.887	2.6E-03	***ytgP***	0.857	2.0E-17	***ig1556***	0.900	1.2E-01
ig3428	0.888	1.1E-06	***ig969***	0.857	4.8E-06	***spoVAA***	0.900	4.6E-09
whiA	0.888	1.3E-01	***xseA***	0.858	7.1E-07	***ig680***	0.900	8.4E-02
nagBB	0.889	3.5E-04	***ig1283***	0.858	1.3E-02	***flgE***	0.900	2.4E-09
ywcI	0.890	2.6E-06	***ig2140***	0.860	4.4E-09	***fliZ***	0.903	3.8E-03
ig248	0.890	4.8E-05	***yozO***	0.860	1.9E-04	***ig2220***	0.904	1.7E-03
ig125	0.890	8.1E-04	***ig514***	0.862	6.0E-03	***ig1380***	0.905	1.9E-06
yvrJ	0.890	4.7E-02	***glcT***	0.862	5.9E-14	***ylbK***	0.905	4.7E-07
ig1685	0.891	4.1E-02	***ig3131***	0.862	2.1E-02	***rpfA***	0.905	1.5E-01
ig295	0.891	9.8E-04	***ig1461***	0.863	3.9E-04	***ig1108***	0.905	2.0E-03
clsA	0.891	7.5E-11	***yhcH***	0.863	4.4E-06	***secDF***	0.906	8.4E-62
spoIIIAH	0.892	3.5E-02	***ig1226***	0.864	1.6E-03	***pepF***	0.906	5.7E-24
ig3230	0.892	3.6E-06	***mntD***	0.864	4.9E-02	***fliS***	0.906	2.1E-09
yunB	0.892	8.4E-05	***ymfM***	0.864	1.8E-05	***ig2116***	0.907	2.1E-06
ig3518	0.893	2.5E-02	***ig1095***	0.865	1.0E-03	***ig382***	0.907	7.1E-02
mcsB	0.894	2.2E-06	***motA***	0.866	4.4E-15	***U712_12375***	0.908	1.3E-02
ig3086	0.895	6.5E-03	***ig1717***	0.866	2.1E-07	***ig1110***	0.908	5.8E-03
albA	0.895	3.9E-07	***ig2042***	0.867	6.9E-07	***spoIIIAH***	0.909	4.1E-03
mntD	0.895	1.4E-04	***sftA***	0.867	4.6E-37	***ftsE***	0.909	1.3E-14
ig3292	0.897	6.0E-02	***levD***	0.868	1.5E-05	***mhqR***	0.909	6.8E-02
U712_02515	0.898	6.0E-02	***ig2087***	0.869	3.9E-03	***lspA***	0.910	5.2E-04
ywqB	0.898	3.1E-14	***ig2338***	0.869	2.6E-02	***recD2***	0.910	3.3E-14
ig3206	0.898	1.4E-03	***ig1071***	0.869	7.9E-03	***fliK***	0.910	4.0E-06

ig3502	0.899	2.9E-02	***yfkF***	0.870	2.5E-06	***lipM***	0.911	2.0E-05
ig3235	0.899	5.0E-03	***yppC***	0.870	5.8E-04	***mtnD***	0.911	3.5E-03
asnO	0.899	5.9E-04	***ig2220***	0.871	1.1E-04	***ygaB***	0.911	1.5E-02
yycI	0.899	5.2E-03	***ytmP***	0.871	9.4E-08	***ig2424***	0.912	3.9E-03
abrB	0.900	1.9E-02	***ecfA***	0.871	5.3E-02	***ydeS***	0.913	1.4E-06
ig581	0.900	6.4E-03	***spoVAB***	0.871	1.7E-04	***ig1325***	0.914	2.4E-02
rocG	0.901	2.4E-06	***yknV***	0.872	6.9E-33	***lpdV***	0.915	3.2E-02
ybaN	0.901	2.8E-05	***ig2647***	0.872	3.5E-13	***ptsG***	0.915	1.0E-03
ig1388	0.901	6.3E-03	***ig719***	0.872	4.6E-07	***sigD***	0.915	1.1E-08
lgt	0.901	1.1E-04	***ctpA***	0.873	1.1E-27	***ylmE***	0.915	4.1E-03
ig159	0.901	6.0E-02	***ylmD***	0.873	7.5E-02	***yneB***	0.915	1.1E-07
ycnL	0.901	2.0E-06	***yhfA***	0.874	9.2E-12	***ig1717***	0.915	4.2E-06
ig439	0.902	5.8E-02	***ywnF***	0.874	1.4E-03	***motA***	0.916	1.1E-07
ig3184	0.902	1.2E-02	***ig2205***	0.875	1.2E-02	***ig907***	0.916	3.9E-02
ig46	0.902	7.0E-05	***ylbL***	0.876	1.2E-22	***ymfK***	0.916	2.2E-02
ig375	0.903	5.7E-04	***ig1178***	0.876	1.9E-03	***yqzD***	0.917	1.4E-04
glcR	0.903	4.2E-04	***ponA***	0.876	2.0E-02	***gltC***	0.917	3.4E-05
mntB	0.903	7.1E-03	***ig1390***	0.876	1.6E-04	***cymR***	0.917	1.7E-02
U712_17570	0.903	8.5E-02	***sigV***	0.877	7.4E-05	***ykqA***	0.917	1.7E-06
ecfAB	0.904	8.1E-02	***ig2019***	0.877	6.2E-03	***ppiB***	0.917	6.3E-05
csbA	0.904	2.0E-05	***sigO***	0.877	7.6E-06	***ygaF***	0.918	3.4E-04
ig3423	0.904	1.2E-02	***mhqR***	0.878	1.3E-02	***addB***	0.918	9.4E-02
ig3264	0.905	6.6E-04	***spoVAA***	0.878	1.1E-08	***pbpA***	0.918	4.7E-02
ig3337	0.905	3.9E-04	***ykqA***	0.878	7.8E-11	***yrzL***	0.918	5.2E-02
ig520	0.906	3.3E-03	***fliG***	0.878	2.7E-12	***ig581***	0.918	1.1E-02
ywzD	0.906	3.2E-04	***ygaB***	0.878	1.9E-05	***ig1503***	0.918	3.4E-02
ig387	0.906	3.7E-02	***yhcF***	0.878	1.5E-04	***ylxF***	0.918	7.5E-04
atpI	0.906	3.9E-02	***yhgD***	0.879	4.5E-04	***mecA***	0.919	9.3E-02
ig98	0.907	1.1E-04	***ig2648***	0.880	4.9E-04	***ig3105***	0.919	6.1E-03
rpfA	0.907	1.1E-01	***skfF***	0.880	3.6E-51	***yhdK***	0.919	1.3E-01
ccpA	0.908	3.1E-01	***ig1384***	0.880	3.5E-08	***ykrP***	0.920	1.2E-05
yvcI	0.908	9.4E-02	***ig2475***	0.880	3.5E-12	***spoIIQ***	0.920	2.2E-01
ig3310	0.908	1.3E-05	***yknU***	0.880	2.6E-46	***moaC***	0.921	5.2E-03
ig3468	0.909	2.3E-04	***cysK***	0.880	2.7E-04	***ig633***	0.921	5.9E-02
mcsA	0.909	5.4E-04	***dnaK***	0.881	1.3E-24	***ig2476***	0.921	4.5E-06
yczE	0.909	1.6E-03	***polA***	0.881	1.8E-20	***levD***	0.921	1.4E-02
ydiK	0.909	1.0E-04	***ig3151***	0.883	1.4E-02	***ig1103***	0.921	5.7E-08
ig329	0.910	2.6E-03	***yqjX***	0.883	4.6E-04	***yfiY***	0.922	7.9E-03
sdhB	0.910	3.7E-02	***ymfK***	0.883	6.5E-04	***ysoA***	0.922	7.8E-05
ig7	0.910	7.5E-02	***yjbI***	0.884	3.5E-03	***spoVG***	0.922	4.0E-07
ig70	0.910	4.3E-03	***ig100***	0.884	3.2E-04	***ecfAB***	0.922	2.5E-01
ig3247	0.911	1.2E-02	***cysH***	0.884	4.6E-07	***yplP***	0.922	1.9E-05
ig226	0.911	5.2E-04	***spoIIIE***	0.884	1.3E-02	***fliT***	0.922	3.1E-10

ig34	0.912	1.3E-03	***ig1299***	0.885	1.0E-02	***yhgD***	0.922	2.1E-02
metP	0.912	2.0E-01	***ig2035***	0.885	7.7E-05	***ig2533***	0.923	2.4E-02
ig78	0.912	9.6E-03	***skfE***	0.886	9.5E-23	***ig993***	0.923	3.7E-02
yqfC	0.912	2.1E-01	***yutC***	0.886	2.7E-05	***yloV***	0.924	5.0E-05
cspD	0.912	1.2E-01	***ig3206***	0.886	2.3E-01	***fliD***	0.924	1.9E-23
speA	0.913	3.7E-02	***ig1505***	0.886	2.6E-02	***ig1101***	0.924	4.0E-02
spoVT	0.913	2.5E-04	***ig1201***	0.887	1.4E-04	***relP***	0.924	1.5E-01
opuAC	0.913	7.9E-06	***ig2050***	0.887	4.9E-04	***flhF***	0.925	4.7E-15
ig463	0.913	8.5E-04	***ig2317***	0.887	3.0E-02	***ig2639***	0.925	1.4E-01
spoVD	0.913	1.1E-02	***ylzJ***	0.887	8.0E-03	***ig2317***	0.925	4.0E-02
ig3106	0.913	5.3E-02	***fliI***	0.888	8.3E-10	***cggR***	0.926	8.9E-03
ybbR	0.914	1.0E-02	***ig1107***	0.888	1.9E-04	***ftsX***	0.926	2.7E-09
rttO	0.914	3.3E-02	***ig1328***	0.888	7.0E-03	***ytgP***	0.926	7.1E-07
jag	0.914	9.9E-05	***ylxM***	0.889	4.8E-04	***ig1362***	0.926	3.1E-09
ig407	0.914	9.8E-04	***cotV***	0.889	4.3E-07	***flgB***	0.926	2.7E-05
spoIIP	0.914	3.9E-02	***ytoI***	0.889	6.7E-16	***hag***	0.926	3.3E-06
spoIIR	0.914	1.1E-03	***yqeM***	0.889	3.3E-08	***ig3596***	0.927	5.5E-04
ydzU	0.914	3.1E-03	***ig1287***	0.889	1.8E-05	***ig1349***	0.927	1.0E-02
ig324	0.915	3.8E-03	***ig3301***	0.891	1.7E-01	***ylmH***	0.927	4.2E-02
ig3306	0.915	1.3E-04	***slp***	0.891	1.6E-04	***yhcG***	0.927	1.8E-04
ig3151	0.915	1.0E-01	***ig1123***	0.892	1.9E-05	***spoVAEA***	0.927	8.2E-04
ig100	0.915	1.5E-05	***ig907***	0.892	1.1E-02	***ig2019***	0.928	1.7E-01
ig1556	0.915	2.3E-02	***htpX***	0.892	7.9E-08	***flgC***	0.928	3.1E-03
spoVB	0.915	4.8E-03	***parB***	0.893	2.5E-03	***yqhL***	0.928	1.2E-02
ywpF	0.915	3.7E-03	***ig1418***	0.894	4.6E-04	***rsmD***	0.928	2.8E-02
ig512	0.916	1.7E-04	***pbpA***	0.894	2.8E-04	***cheD***	0.928	2.3E-07
lutC	0.916	2.0E-04	***yneB***	0.894	5.8E-13	***U712_19710***	0.929	4.6E-02
ig292	0.916	4.4E-06	***mecA***	0.894	1.3E-02	***tgt***	0.929	1.2E-02
ftsX	0.916	8.3E-12	***comER***	0.895	3.4E-09	***ytzH***	0.929	2.9E-02
ywlE	0.916	1.3E-04	***yhaL***	0.895	2.6E-04	***yutC***	0.929	7.4E-04
U712_18660	0.917	8.4E-04	***ykhA***	0.895	1.9E-06	***BSU27786***	0.929	1.1E-01
ig179	0.917	4.3E-07	***cheY***	0.895	1.7E-02	***ig726***	0.929	1.6E-03
ig3161	0.917	4.0E-04	***ypoC***	0.895	1.1E-02	***yqzC***	0.930	5.2E-04
cdnD	0.917	3.5E-09	***yhgB***	0.895	3.2E-03	***ig2409***	0.930	3.0E-02
ig3391	0.917	5.9E-04	***ig1302***	0.896	3.0E-11	***ig1769***	0.930	1.2E-05
ykaA	0.918	3.1E-01	***ig1895***	0.896	5.0E-06	***cheA***	0.931	8.5E-22
ftsE	0.918	1.1E-11	***radA***	0.896	5.7E-23	***fliI***	0.931	1.5E-04
ywmB	0.918	3.1E-10	***spoIIIAF***	0.896	1.4E-01	***fliM***	0.931	2.8E-05
ig19	0.918	4.1E-02	***minD***	0.897	2.6E-04	***ydfH***	0.932	6.9E-03
ywdI	0.918	3.3E-03	***ig1241***	0.897	3.6E-06	***ig380***	0.932	2.3E-07
bacA	0.918	1.9E-02	***ig2033***	0.897	1.2E-03	***yycP***	0.932	1.7E-11
U712_01385	0.918	3.1E-03	***yplP***	0.897	3.4E-09	***ig2013***	0.932	8.0E-02
ctsR	0.918	4.1E-02	***yhcG***	0.898	1.0E-03	***yyaN***	0.932	6.5E-02

ig406	0.919	2.9E-06	***U712_06080***	0.898	2.4E-05	***ig2961***	0.932	5.5E-01
ig478	0.919	1.2E-04	***pstS***	0.898	2.9E-05	***U712_14285***	0.933	1.0E-01
yrbF	0.919	1.1E-02	***ecfT***	0.898	6.1E-02	***ykuK***	0.933	1.1E-07
U712_00035	0.919	1.5E-02	***ydeS***	0.898	2.1E-08	***pgl***	0.933	6.8E-02
yxeE	0.919	3.9E-07	***ykzQ***	0.898	1.6E-06	***ywnH***	0.933	3.8E-03
bsdC	0.919	2.5E-08	***fruR***	0.898	1.6E-05	***ig3136***	0.933	2.3E-04
ig2961	0.919	8.1E-02	***yabP***	0.898	5.4E-02	***ig3423***	0.933	9.4E-03
veg	0.919	2.6E-02	***ig1070***	0.898	2.5E-04	***fliY***	0.933	5.7E-08
yyaB	0.919	3.6E-05	***ig2628***	0.899	6.2E-02	***dltE***	0.933	6.0E-02
U712_01115	0.919	1.1E-01	***ygaE***	0.899	3.8E-09	***ig3117***	0.933	2.8E-02
ig3181	0.919	2.5E-06	***sdaAA***	0.900	1.6E-06	***ig2628***	0.934	5.1E-01
yczH	0.919	1.0E-06	***ampS***	0.900	2.8E-14	***ig807***	0.934	3.7E-01
ig488	0.919	2.8E-04	***kduI***	0.900	1.2E-08	***flgL***	0.934	5.2E-10
tdk	0.919	3.9E-03	***yhcK***	0.900	2.6E-13	***ig1845***	0.934	8.9E-02
yqfD	0.919	4.5E-02	***ig1392***	0.900	1.2E-11	***pyrC***	0.934	1.2E-01
ig3558	0.920	1.7E-07	***ig977***	0.901	4.2E-04	***rbsD***	0.935	7.7E-02

Table 2.2 Tn-seq relative fitness lists. The relative fitness values for genes with the lowest 200 relative fitness for each growth period for all three Tn-seq experiments are presented along with the adjusted p-value (BH method; see materials and methods). The gene names or locus tags are listed, and intergenic regions are annotated as "ig" with a number.

Gene	Mean Fitness	Annotated function	Validation	Proximal gene
recN	0.200	Homologous Recombination	(64); this study	
sepF	0.400	Cell Division	This study	
uvrB	0.409	Nucleotide excision repair	This study	
uvrC	0.484	Nucleotide excision repair	This study	
uvrA	0.489	Nucleotide excision repair	(40); this study	
addA	0.537	Homologous Recombination	(65)	
rnhC	0.544	RNase HIII	This study	
crh	0.565	regulation of carbon metabolism	This study	
ruvB	0.568	Homologous Recombination	(66); this study	
ylbL	0.581	putative lon-like protease	This study	
ponA	0.587	Peptidoglycan glycosyl transferase	This study	
bcrC	0.595	UPP phosphatase	This study	
ecsA	0.603	ABC transporter	This study	
recR	0.606	Homologous Recombination	(67); this study	
queA	0.612	S-adenosylmethionine tRNA ribosyltransferase-isomerase	Not Sensitive	downstream of *ruvAB*
addB	0.622	Homologous Recombination	(68)	

ecsB	0.627	ABC transporter	This study	
polA	0.649	DNA polymerase I	(40)	
ylmG	0.656	hypothetical protein	Not sensitive	downstream of *sepF*
lgt	0.661	lipomodification of lipoproteins	Not sensitive	
ctpA	0.673	c-terminal processing protease	This study	
ripX	0.674	Homologous Recombination	(69); this study	
ytmP	0.690	putative kinase/phosphotransferase	This study	
recG	0.695	Homologous Recombination	(69); this study	
ydzU	0.714	unknown	This study	
walH	0.715	Regulation of cell wall metabolism	This study	
ylmE	0.718	hypothetical protein	Not sensitive	upstream of *sepF*
sdaAB	0.724	L-serine dehydratase	Not sensitive	upstream of *recG*
ysoA	0.725	putative hydrolase	This study	
recX	0.729	Homologous Recombination	(70)	
walJ	0.729	Regulation of cell wall metabolism	This study	
recD2	0.731	Homologous Recombination	(41)	
radA	0.742	Homologous Recombination	This study	
ylbK	0.746	putative phospholipase	Not sensitive	upstream of *ylbL*
sodA	0.763	super-oxide dismutase	This study	
cymR	0.770	regulation of sulfur metabolism	Not sensitive	upstream of *recD2*
yprA	0.773	putative helicase	This study	
yprB	0.777	putative DnaQ-like exonuclease	This study	
ywrC	0.785	regulation of chromate export	Not sensitive	
yycI	0.790	Regulation of cell wall metabolism	This study	

Table 2.3 Tn-seq yields many false positive results. The forty genes with the lowest relative fitness in the second growth period of MMC Tn-seq experiment are listed. Each gene was deleted and the deletion mutants were tested for sensitivity to MMC using a spot titer assay and a range of MMC concentrations. Genes labeled as not sensitive had no difference in growth relative to the WT strain on MMC containing media, with the exception of *ylbK*, which resulted in a polar effect on *ylbL* **(see Figure 2.14)**.

MMC, MMS, & Phleomycin	MMC & Phleomycin	MMC & MMS	MMS & Phleomycin
recN	addA	uvrC	ezrA
ylbL	ecsB	ponA	ig1503
addB	ylmG	walJ	parB
polA	ytmP	ig2409	xseA
ctpA	ig1437	recJ	htpX
ig1200	U712_09520	hemL	comER
ylmE	ig3234	yrhO	ylqD
sdaAB	ig2807	rsiV	kinC
ysoA	yhcF	apt	yqeM
ig2551	yfhH	abh	ytoI
recD2	ig1717	yhaH	ykzQ
radA	yhaJ	mutS2	slp
ylbK	ydeS		ktrC
cymR	ygaB		ptsG
ylmH	yneB		ykzP
yrrB	ktrA		yknV
spxA	yfkF		yhgE
ig100	yhcG		
ig2365	ktrD		
sftA	ig1101		
sigV	ytgP		
	ig719		
	sigO		
	ig2476		

Table 2.4 Tn-seq list overlaps. The genes with the lowest relative fitness with an adjusted p-value less than 0.01 are listed for each experiment.

Identified Proteins (183)
Iron(3+)-hydroxamate import system permease protein FhuG OS=Bacillus subtilis (strain 168) GN=fhuG PE=3 SV=1
Putative ribonuclease-like protein YfkH OS=Bacillus subtilis (strain 168) GN=yfkH PE=4 SV=1
Lipoteichoic acid synthase 1 OS=Bacillus subtilis (strain 168) GN=ltaS1 PE=1 SV=1 (aka ltaSA)
Uncharacterized protein YkgA OS=Bacillus subtilis (strain 168) GN=ykgA PE=3 SV=2
Uncharacterized N-acetyltransferase CgeE OS=Bacillus subtilis (strain 168) GN=cgeE PE=4 SV=2
Putative phosphotransferase YtmP OS=Bacillus subtilis (strain 168) GN=ytmP PE=3 SV=1
Cell division suppressor protein YneA OS=Bacillus subtilis (strain 168) GN=yneA PE=1 SV=1
Stress response protein YsnF OS=Bacillus subtilis (strain 168) GN=ysnF PE=2 SV=3
Exo-glucosaminidase LytG OS=Bacillus subtilis (strain 168) GN=lytG PE=1 SV=1
General stress protein 30 OS=Bacillus subtilis (strain 168) GN=yxaB PE=1 SV=5
Putative S-adenosyl-L-methionine-dependent methyltransferase YktD OS=Bacillus subtilis (strain 168) GN=yktD PE=3 SV=1
Uncharacterized oxidoreductase YhxD OS=Bacillus subtilis (strain 168) GN=yhxD PE=3 SV=2
Uncharacterized protein YqgF OS=Bacillus subtilis (strain 168) GN=yqgF PE=3 SV=1
1-phosphofructokinase OS=Bacillus subtilis (strain 168) GN=fruK PE=3 SV=1
Uncharacterized protein YvyC OS=Bacillus subtilis (strain 168) GN=yvyC PE=1 SV=1
Two-component system WalR/WalK regulatory protein YycI OS=Bacillus subtilis (strain 168) GN=yycI PE=1 SV=1
Putative ATP-dependent DNA helicase YjcD OS=Bacillus subtilis (strain 168) GN=yjcD PE=1 SV=1
General stress protein 39 OS=Bacillus subtilis (strain 168) GN=ydaD PE=1 SV=3
Adapter protein MecA 2 OS=Bacillus subtilis (strain 168) GN=mecB PE=1 SV=1
Anti-sigma-W factor RsiW OS=Bacillus subtilis (strain 168) GN=rsiW PE=1 SV=2
Probable manganese catalase OS=Bacillus subtilis (strain 168) GN=ydbD PE=1 SV=1
Uncharacterized protein YvyF OS=Bacillus subtilis (strain 168) GN=yvyF PE=4 SV=1
Holliday junction ATP-dependent DNA helicase RuvB OS=Bacillus subtilis (strain 168) GN=ruvB PE=1 SV=2
Flagellar motor switch protein FliM OS=Bacillus subtilis (strain 168) GN=fliM PE=1 SV=1
General stress protein 69 OS=Bacillus subtilis (strain 168) GN=yhdN PE=1 SV=2
Transcriptional regulatory protein YvrH OS=Bacillus subtilis (strain 168) GN=yvrH PE=3 SV=4
Pyrophosphatase PpaX OS=Bacillus subtilis (strain 168) GN=ppaX PE=1 SV=1
Phage-like element PBSX protein XkdA OS=Bacillus subtilis (strain 168) GN=xkdA PE=4 SV=4
Prolipoprotein diacylglyceryl transferase OS=Bacillus subtilis (strain 168) GN=lgt PE=1 SV=1
Probable polyketide biosynthesis zinc-dependent hydrolase PksB OS=Bacillus subtilis (strain 168) GN=pksB PE=1 SV=1
Probable flavodoxin 2 OS=Bacillus subtilis (strain 168) GN=ykuP PE=3 SV=2
Chemotaxis protein CheV OS=Bacillus subtilis (strain 168) GN=cheV PE=1 SV=1
Aliphatic sulfonates import ATP-binding protein SsuB OS=Bacillus subtilis (strain 168) GN=ssuB PE=1 SV=4
Uncharacterized protein YlzI OS=Bacillus subtilis (strain 168) GN=ylzI PE=4 SV=1
Heme-degrading monooxygenase HmoB OS=Bacillus subtilis (strain 168) GN=hmoB PE=1 SV=1
UPF0374 protein YgaC OS=Bacillus subtilis (strain 168) GN=ygaC PE=3 SV=2
Molybdenum cofactor biosynthesis protein B OS=Bacillus subtilis (strain 168) GN=moaB PE=3 SV=1
Putative aldehyde dehydrogenase YfmT OS=Bacillus subtilis (strain 168) GN=yfmT PE=2 SV=1
GTP cyclohydrolase 1 type 2 homolog OS=Bacillus subtilis (strain 168) GN=yqfO PE=3 SV=2
Sensory transduction protein LytT OS=Bacillus subtilis (strain 168) GN=lytT PE=3 SV=1
Uncharacterized protein ymdB OS=Bacillus subtilis (strain 168) GN=ymdB PE=1 SV=2

Peptidyl-tRNA hydrolase OS=Bacillus subtilis (strain 168) GN=spoVC PE=3 SV=1
Ribosomal RNA large subunit methyltransferase H OS=Bacillus subtilis (strain 168) GN=rlmH PE=1 SV=1
Catalase-2 OS=Bacillus subtilis (strain 168) GN=katE PE=3 SV=2
DNA polymerase III PolC-type OS=Bacillus subtilis (strain 168) GN=polC PE=1 SV=2
Uncharacterized N-acetyltransferase YesJ OS=Bacillus subtilis (strain 168) GN=yesJ PE=3 SV=1
Methyl-accepting chemotaxis protein McpB OS=Bacillus subtilis (strain 168) GN=mcpB PE=1 SV=2
Methyl-accepting chemotaxis protein McpA OS=Bacillus subtilis (strain 168) GN=mcpA PE=1 SV=2
Uncharacterized protein YtwF OS=Bacillus subtilis (strain 168) GN=ytwF PE=4 SV=2
FMN-dependent NADH-azoreductase 1 OS=Bacillus subtilis (strain 168) GN=azoR1 PE=2 SV=1
L-aspartate oxidase OS=Bacillus subtilis (strain 168) GN=nadB PE=3 SV=1
2-oxoisovalerate dehydrogenase subunit alpha OS=Bacillus subtilis (strain 168) GN=bfmBAA PE=1 SV=1
Uncharacterized HTH-type transcriptional regulator YobS OS=Bacillus subtilis (strain 168) GN=yobS PE=4 SV=1
Uncharacterized oxidoreductase YjdA OS=Bacillus subtilis (strain 168) GN=yjdA PE=3 SV=1
Thioredoxin reductase OS=Bacillus subtilis (strain 168) GN=trxB PE=1 SV=3
General stress protein 16O OS=Bacillus subtilis (strain 168) GN=yocK PE=1 SV=3
UPF0111 protein YkaA OS=Bacillus subtilis (strain 168) GN=ykaA PE=3 SV=1
Ribosome biogenesis GTPase A OS=Bacillus subtilis (strain 168) GN=rbgA PE=1 SV=1
Putative glycosyltransferase CsbB OS=Bacillus subtilis (strain 168) GN=csbB PE=2 SV=1
Uncharacterized protein YhjD OS=Bacillus subtilis (strain 168) GN=yhjD PE=4 SV=1
Minor teichoic acid biosynthesis protein GgaB OS=Bacillus subtilis (strain 168) GN=ggaB PE=3 SV=1
Putative ribonuclease YeeF OS=Bacillus subtilis (strain 168) GN=yeeF PE=1 SV=2
Phosphate acetyltransferase OS=Bacillus subtilis (strain 168) GN=pta PE=1 SV=3
Pantothenate synthetase OS=Bacillus subtilis (strain 168) GN=panC PE=3 SV=1
Chemotaxis protein CheA OS=Bacillus subtilis (strain 168) GN=cheA PE=1 SV=2
UDP-N-acetylmuramoyl-L-alanyl-D-glutamate--2,6-diaminopimelate ligase OS=Bacillus subtilis (strain 168) GN=murE PE=3 SV=1
3-methyl-2-oxobutanoate hydroxymethyltransferase OS=Bacillus subtilis (strain 168) GN=panB PE=3 SV=1
Dephospho-CoA kinase OS=Bacillus subtilis (strain 168) GN=coaE PE=3 SV=1
Uncharacterized protein YtxK OS=Bacillus subtilis (strain 168) GN=ytxK PE=4 SV=2
HTH-type transcriptional regulator NsrR OS=Bacillus subtilis (strain 168) GN=nsrR PE=4 SV=1
Response regulator aspartate phosphatase B OS=Bacillus subtilis (strain 168) GN=rapB PE=3 SV=1
Methyl-accepting chemotaxis protein McpC OS=Bacillus subtilis (strain 168) GN=mcpC PE=1 SV=2
Uncharacterized ATP-dependent helicase YprA OS=Bacillus subtilis (strain 168) GN=yprA PE=3 SV=1
Transcriptional regulatory protein CssR OS=Bacillus subtilis (strain 168) GN=cssR PE=1 SV=1
Branched-chain-amino-acid aminotransferase 2 OS=Bacillus subtilis (strain 168) GN=ilvK PE=1 SV=5
Recombination protein RecR OS=Bacillus subtilis (strain 168) GN=recR PE=3 SV=2
Uncharacterized protein YpjQ OS=Bacillus subtilis (strain 168) GN=ypjQ PE=1 SV=1
Uncharacterized protein YwnB OS=Bacillus subtilis (strain 168) GN=ywnB PE=4 SV=1
Dihydroxy-acid dehydratase OS=Bacillus subtilis (strain 168) GN=ilvD PE=1 SV=4
Cystathionine beta-lyase MetC OS=Bacillus subtilis (strain 168) GN=metC PE=1 SV=1
UPF0403 protein YphP OS=Bacillus subtilis (strain 168) GN=yphP PE=1 SV=1
DNA polymerase III subunit alpha OS=Bacillus subtilis (strain 168) GN=dnaE PE=3 SV=1
33 kDa chaperonin OS=Bacillus subtilis (strain 168) GN=hslO PE=1 SV=1

RNA polymerase sigma factor SigA OS=Bacillus subtilis (strain 168) GN=sigA PE=1 SV=2
Carbamoyl-phosphate synthase pyrimidine-specific large chain OS=Bacillus subtilis (strain 168) GN=pyrAB PE=3 SV=1
ATP-dependent helicase/deoxyribonuclease subunit B OS=Bacillus subtilis (strain 168) GN=addB PE=1 SV=2
Methionine--tRNA ligase OS=Bacillus subtilis (strain 168) GN=metG PE=3 SV=1
Ferrochelatase OS=Bacillus subtilis (strain 168) GN=hemH PE=1 SV=1
Glycine--tRNA ligase beta subunit OS=Bacillus subtilis (strain 168) GN=glyS PE=3 SV=2
Holliday junction ATP-dependent DNA helicase RuvA OS=Bacillus subtilis (strain 168) GN=ruvA PE=3 SV=2
Putative uncharacterized hydrolase YsaA OS=Bacillus subtilis (strain 168) GN=ysaA PE=3 SV=2
Phosphoglycerate kinase OS=Bacillus subtilis (strain 168) GN=pgk PE=1 SV=3
Dihydroorotase OS=Bacillus subtilis (strain 168) GN=pyrC PE=3 SV=2
Pyruvate carboxylase OS=Bacillus subtilis (strain 168) GN=pyc PE=3 SV=1
2,3-dihydroxybenzoate-AMP ligase OS=Bacillus subtilis (strain 168) GN=dhbE PE=1 SV=2
Transaldolase OS=Bacillus subtilis (strain 168) GN=tal PE=1 SV=4
Swarming motility protein SwrC OS=Bacillus subtilis (strain 168) GN=swrC PE=1 SV=2
Uncharacterized membrane protein YhaH OS=Bacillus subtilis (strain 168) GN=yhaH PE=4 SV=1
Nuclease SbcCD subunit C OS=Bacillus subtilis (strain 168) GN=sbcC PE=3 SV=3
Glyceraldehyde-3-phosphate dehydrogenase 1 OS=Bacillus subtilis (strain 168) GN=gapA PE=1 SV=2
Hypoxanthine-guanine phosphoribosyltransferase OS=Bacillus subtilis (strain 168) GN=hprT PE=3 SV=1
Uncharacterized protein YxjG OS=Bacillus subtilis (strain 168) GN=yxjG PE=4 SV=3
DNA gyrase subunit B OS=Bacillus subtilis (strain 168) GN=gyrB PE=3 SV=1
Carbamoyl-phosphate synthase pyrimidine-specific small chain OS=Bacillus subtilis (strain 168) GN=pyrAA PE=3 SV=1
3-dehydroquinate dehydratase OS=Bacillus subtilis (strain 168) GN=yqhS PE=1 SV=1
Uncharacterized protein YqhY OS=Bacillus subtilis (strain 168) GN=yqhY PE=3 SV=2
50S ribosomal protein L23 OS=Bacillus subtilis (strain 168) GN=rplW PE=1 SV=2
Transcriptional regulatory protein DegU OS=Bacillus subtilis (strain 168) GN=degU PE=1 SV=2
Sporulation initiation inhibitor protein Soj OS=Bacillus subtilis (strain 168) GN=soj PE=1 SV=1
Uncharacterized oxidoreductase YcsN OS=Bacillus subtilis (strain 168) GN=ycsN PE=3 SV=1
Heme-degrading monooxygenase HmoA OS=Bacillus subtilis (strain 168) GN=hmoA PE=1 SV=2
Putative aldehyde dehydrogenase DhaS OS=Bacillus subtilis (strain 168) GN=dhaS PE=3 SV=1
Immunity protein WapI OS=Bacillus subtilis (strain 168) GN=wapI PE=1 SV=1
Putative esterase YitV OS=Bacillus subtilis (strain 168) GN=yitV PE=4 SV=2
Citrate synthase 2 OS=Bacillus subtilis (strain 168) GN=citZ PE=1 SV=2
Guanylate kinase OS=Bacillus subtilis (strain 168) GN=gmk PE=3 SV=2
3-oxoacyl-[acyl-carrier-protein] reductase FabG OS=Bacillus subtilis (strain 168) GN=fabG PE=3 SV=3
Uncharacterized protein YkvS OS=Bacillus subtilis (strain 168) GN=ykvS PE=4 SV=2
Uncharacterized protein YxaI OS=Bacillus subtilis (strain 168) GN=yxaI PE=4 SV=1
10 kDa chaperonin OS=Bacillus subtilis (strain 168) GN=groS PE=1 SV=2
Probable phosphate butyryltransferase OS=Bacillus subtilis (strain 168) GN=yqiS PE=3 SV=2
Uncharacterized protein YvfG OS=Bacillus subtilis (strain 168) GN=yvfG PE=1 SV=1
Glutamyl-tRNA(Gln) amidotransferase subunit C OS=Bacillus subtilis (strain 168) GN=gatC PE=3 SV=3
Uncharacterized protein YwfO OS=Bacillus subtilis (strain 168) GN=ywfO PE=4 SV=2
Uncharacterized protein YdjO OS=Bacillus subtilis (strain 168) GN=ydjO PE=4 SV=1

Carbon storage regulator homolog OS=Bacillus subtilis (strain 168) GN=csrA PE=1 SV=1
Uncharacterized lipoprotein YjhA OS=Bacillus subtilis (strain 168) GN=yjhA PE=1 SV=1
Putative amidohydrolase YhaA OS=Bacillus subtilis (strain 168) GN=yhaA PE=3 SV=3
UPF0291 protein YnzC OS=Bacillus subtilis (strain 168) GN=ynzC PE=1 SV=1
Cell wall-binding protein YqgA OS=Bacillus subtilis (strain 168) GN=yqgA PE=1 SV=2
PTS system fructose-specific EIIB component OS=Bacillus subtilis (strain 168) GN=levE PE=1 SV=1
Uncharacterized peptidase YuxL OS=Bacillus subtilis (strain 168) GN=yuxL PE=3 SV=3
Uncharacterized protein YdhI OS=Bacillus subtilis (strain 168) GN=ydhI PE=4 SV=1
Uncharacterized protein YkuJ OS=Bacillus subtilis (strain 168) GN=ykuJ PE=1 SV=1
Uncharacterized protein YkzF OS=Bacillus subtilis (strain 168) GN=ykzF PE=1 SV=1
Surfactin synthase subunit 2 OS=Bacillus subtilis (strain 168) GN=srfAB PE=1 SV=3
Sec-independent protein translocase protein TatAc OS=Bacillus subtilis (strain 168) GN=tatAc PE=3 SV=1
Uncharacterized protein YwqB OS=Bacillus subtilis (strain 168) GN=ywqB PE=4 SV=2
DNA-entry nuclease OS=Bacillus subtilis (strain 168) GN=nucA PE=4 SV=2
Spore coat-associated protein N OS=Bacillus subtilis (strain 168) GN=tasA PE=1 SV=1
Sec-independent protein translocase protein TatAy OS=Bacillus subtilis (strain 168) GN=tatAy PE=1 SV=1
Stage V sporulation protein S OS=Bacillus subtilis (strain 168) GN=spoVS PE=1 SV=1
Transcriptional repressor SdpR OS=Bacillus subtilis (strain 168) GN=sdpR PE=2 SV=1
Surfactin synthase subunit 3 OS=Bacillus subtilis (strain 168) GN=srfAC PE=1 SV=2
Sporulation delaying protein C OS=Bacillus subtilis (strain 168) GN=sdpC PE=1 SV=1
Signal peptidase I W OS=Bacillus subtilis (strain 168) GN=sipW PE=1 SV=1
Uncharacterized protein YwqH OS=Bacillus subtilis (strain 168) GN=ywqH PE=4 SV=1
Asparagine synthetase [glutamine-hydrolyzing] 2 OS=Bacillus subtilis (strain 168) GN=asnH PE=1 SV=2
Uncharacterized lipoprotein YcdA OS=Bacillus subtilis (strain 168) GN=ycdA PE=1 SV=1
Uncharacterized protein YwoF OS=Bacillus subtilis (strain 168) GN=ywoF PE=3 SV=1
Surfactin synthase subunit 1 OS=Bacillus subtilis (strain 168) GN=srfAA PE=1 SV=4
Response regulator aspartate phosphatase F OS=Bacillus subtilis (strain 168) GN=rapF PE=1 SV=2
Uncharacterized protein YsxB OS=Bacillus subtilis (strain 168) GN=ysxB PE=4 SV=2
Trifunctional nucleotide phosphoesterase protein YfkN OS=Bacillus subtilis (strain 168) GN=yfkN PE=1 SV=1
Uncharacterized protein YfmG OS=Bacillus subtilis (strain 168) GN=yfmG PE=4 SV=1
Uncharacterized protein YxbA OS=Bacillus subtilis (strain 168) GN=yxbA PE=4 SV=1
D-gamma-glutamyl-meso-diaminopimelic acid endopeptidase CwlS OS=Bacillus subtilis (strain 168) GN=cwlS PE=1 SV=1
Flagellin OS=Bacillus subtilis (strain 168) GN=hag PE=1 SV=2
Uncharacterized protein YxbC OS=Bacillus subtilis (strain 168) GN=yxbC PE=1 SV=1
Protein LiaH OS=Bacillus subtilis (strain 168) GN=liaH PE=2 SV=1
Single-stranded DNA-binding protein B OS=Bacillus subtilis (strain 168) GN=ssbB PE=1 SV=1
Response regulator aspartate phosphatase A OS=Bacillus subtilis (strain 168) GN=rapA PE=2 SV=2
Thioredoxin-like protein SkfH OS=Bacillus subtilis (strain 168) GN=skfH PE=1 SV=2
NTD biosynthesis operon regulator NtdR OS=Bacillus subtilis (strain 168) GN=ntdR PE=4 SV=1
Uncharacterized protein YpbG OS=Bacillus subtilis (strain 168) GN=ypbG PE=2 SV=1
Response regulator aspartate phosphatase C OS=Bacillus subtilis (strain 168) GN=rapC PE=3 SV=1
Putative phage-related protein YobO OS=Bacillus subtilis (strain 168) GN=yobO PE=4 SV=1

Uncharacterized protein YtfP OS=Bacillus subtilis (strain 168) GN=ytfP PE=4 SV=2
Uncharacterized protein YxnB OS=Bacillus subtilis (strain 168) GN=yxnB PE=4 SV=1
N-acetylmuramoyl-L-alanine amidase XlyA OS=Bacillus subtilis (strain 168) GN=xlyA PE=1 SV=1
ComG operon protein 1 OS=Bacillus subtilis (strain 168) GN=comGA PE=1 SV=2
Uncharacterized protein YebG OS=Bacillus subtilis (strain 168) GN=yebG PE=4 SV=1
SkfA peptide export ATP-binding protein SkfE OS=Bacillus subtilis (strain 168) GN=skfE PE=1 SV=1
Uncharacterized protein YlbL OS=Bacillus subtilis (strain 168) GN=ylbL PE=1 SV=2
Uncharacterized protein YpmA OS=Bacillus subtilis (strain 168) GN=ypmA PE=4 SV=1
Uncharacterized protein YxbB OS=Bacillus subtilis (strain 168) GN=yxbB PE=3 SV=1
Carboxy-terminal processing protease CtpA OS=Bacillus subtilis (strain 168) GN=ctpA PE=2 SV=1
Sporulation inhibitor sda OS=Bacillus subtilis (strain 168) GN=sda PE=1 SV=1
Uncharacterized protein XkzA OS=Bacillus subtilis (strain 168) GN=xkzA PE=4 SV=1
Putative peptide biosynthesis protein YydG OS=Bacillus subtilis (strain 168) GN=yydG PE=4 SV=1
Endonuclease V OS=Bacillus subtilis (strain 168) GN=nfi PE=1 SV=2
HTH-type transcriptional regulator GanR OS=Bacillus subtilis (strain 168) GN=ganR PE=4 SV=1
Uncharacterized protein YjcM OS=Bacillus subtilis (strain 168) GN=yjcM PE=3 SV=1

Accession Number	Molecular weight kDa	SpC 27255	SpC 27256	SpC 27257	SpC 27258	SpC 27259	SpC 27260
sp|P49937|FHUG_BACSU	36	0	0	0	2	2	2
sp|O34437|YFKH_BACSU	30	0	0	0	3	2	2
sp|Q797B3|LTAS1_BACSU	73	0	0	0	9	16	15
sp|O34497|YKGA_BACSU	32	0	0	0	2	2	2
sp|P42093|CGEE_BACSU	30	0	0	0	3	3	2
sp|C0SPC1|YTMP_BACSU	24	0	0	0	2	2	3
sp|Q45056|YNEA_BACSU	12	0	0	0	5	10	7
sp|P94560|YSNF_BACSU	31	0	2	0	3	7	9
sp|O32083|LYTG_BACSU	32	0	0	2	4	6	6
sp|P42101|GS30_BACSU	40	0	2	0	4	4	4
sp|Q45500|YKTD_BACSU	35	0	0	2	4	2	4
sp|P40398|YHXD_BACSU	32	3	4	2	6	11	12
sp|P54488|YQGFA_BACSU	80	5	6	0	10	9	13
sp|O31714|K1PF_BACSU	33	4	0	4	7	6	7
sp|P39737|YVYC_BACSU	13	6	3	4	10	9	13
sp|Q45612|YYCI_BACSU	33	3	2	2	6	4	5
sp|O31626|YJCD_BACSU	87	2	4	2	5	7	5
sp|P80873|GS39_BACSU	31	4	3	3	8	5	8
sp|P50734|MECA2_BACSU	22	3	2	2	4	4	6
sp|Q45588|RSIW_BACSU	23	12	14	16	29	23	25
sp|P80878|MCAT_BACSU	30	5	4	5	9	8	8
sp|P39807|YVYF_BACSU	16	7	6	5	8	12	11

sp|O32055|RUVB_BACSU	37	3	5	7	9	8	9
sp|P23453|FLIM_BACSU	38	7	7	9	12	12	15
sp|P80874|GS69_BACSU	37	4	5	7	8	9	10
sp|P94504|YVRH_BACSU	27	7	8	8	13	11	14
sp|Q9JMQ2|PPAX_BACSU	24	8	9	8	16	10	15
sp|P39780|XKDA_BACSU	24	7	11	10	14	15	16
sp|O34752|LGT_BACSU	31	12	10	10	17	15	18
sp|O34769|PKSB_BACSU	26	8	7	7	12	10	12
sp|O34589|FLAW_BACSU	17	26	22	18	37	31	34
sp|P37599|CHEV_BACSU	35	27	22	28	45	34	40
sp|P97027|SSUB_BACSU	29	7	5	6	8	9	10
sp|C0H412|YLZI_BACSU	8	4	3	5	6	6	6
sp|P38049|HMOB_BACSU	19	7	7	6	11	8	11
sp|Q796Z1|YGAC_BACSU	21	14	11	12	20	15	20
sp|O34457|MOAB_BACSU	18	11	10	10	16	17	13
sp|O06478|ALDH5_BACSU	53	42	52	55	80	78	62
sp|P54472|GCH1L_BACSU	41	18	12	15	21	24	21
sp|P94514|LYTT_BACSU	28	5	4	4	7	6	6
sp|O31775|YMDB_BACSU	29	18	13	18	24	22	25
sp|P37470|PTH_BACSU	21	21	16	16	27	24	25
sp|Q45601|RLMH_BACSU	18	20	18	17	27	26	25
sp|P42234|CATE_BACSU	77	33	34	39	48	53	49
sp|P13267|DPO3_BACSU	163	104	99	91	147	134	135
sp|O31513|YESJ_BACSU	20	13	9	12	17	16	15
sp|P39215|MCPB_BACSU	72	79	73	70	102	92	118
sp|P39214|MCPA_BACSU	72	37	50	43	61	57	64
sp|O32072|YTWF_BACSU	12	15	15	17	22	20	23
sp|O35022|AZOR1_BACSU	23	66	47	51	81	76	67
sp|P38032|NADB_BACSU	58	54	68	54	79	75	86
sp|P37940|ODBA_BACSU	36	15	19	16	21	23	24
sp|O34892|YOBS_BACSU	21	10	8	10	13	11	14
sp|O31642|YJDA_BACSU	27	12	12	11	17	17	13
sp|P80880|TRXB_BACSU	35	26	28	26	37	33	37
sp|P80872|G16O_BACSU	19	9	8	10	11	13	12
sp|O34454|YKAA_BACSU	24	68	49	54	80	74	74
sp|O31743|RBGA_BACSU	32	25	29	29	40	34	37
sp|Q45539|CSBB_BACSU	38	7	7	7	10	9	9
sp|O07558|YHJD_BACSU	14	8	10	9	13	12	11
sp|P46918|GGAB_BACSU	107	93	93	81	131	103	119
sp|O31506|YEEF_BACSU	74	9	8	8	13	10	10
sp|P39646|PTAS_BACSU	35	82	74	69	100	102	94
sp|P52998|PANC_BACSU	32	26	26	27	40	31	33
sp|P29072|CHEA_BACSU	75	70	68	57	89	77	90

sp|Q03523|MURE_BACSU	54	25	28	24	33	34	34
sp|P52996|PANB_BACSU	30	27	29	31	42	33	39
sp|O34932|COAE_BACSU	22	13	13	13	18	17	16
sp|P37876|YTXK_BACSU	37	19	21	20	26	27	25
sp|O07573|NSRR_BACSU	17	8	8	8	10	11	10
sp|P70962|RAPB_BACSU	45	20	16	17	22	21	25
sp|P54576|MCPC_BACSU	72	49	52	57	68	63	72
sp|P50830|YPRA_BACSU	85	24	19	21	30	24	28
sp|O32192|CSSR_BACSU	26	13	14	12	17	17	16
sp|P39576|ILVE2_BACSU	40	93	102	92	128	119	119
sp|P24277|RECR_BACSU	22	8	7	7	10	9	9
sp|P54173|YPJQ_BACSU	20	14	15	16	18	18	21
sp|P71037|YWNB_BACSU	23	13	13	12	15	16	17
sp|P51785|ILVD_BACSU	60	126	122	108	150	156	142
sp|O31632|METC_BACSU	42	61	61	52	73	72	73
sp|P54170|YPHP_BACSU	16	50	48	41	59	57	58
sp|O34623|DPO3A_BACSU	125	66	74	76	88	84	96
sp|P37565|HSLO_BACSU	32	39	40	35	50	47	44
sp|P06224|SIGA_BACSU	43	52	47	49	68	57	57
sp|P25994|CARB_BACSU	118	412	358	419	497	492	455
sp|P23477|ADDB_BACSU	135	47	52	49	64	54	61
sp|P37465|SYM_BACSU	76	95	100	100	113	122	121
sp|P32396|HEMH_BACSU	35	10	10	11	13	12	12
sp|P54381|SYGB_BACSU	76	79	86	80	94	98	99
sp|O05392|RUVA_BACSU	23	15	16	17	19	18	20
sp|P94512|YSAA_BACSU	30	35	30	36	39	41	39
sp|P40924|PGK_BACSU	42	153	151	179	193	189	186
sp|P25995|PYRC_BACSU	47	99	102	92	113	110	121
sp|Q9KWU4|PYC_BACSU	128	642	587	656	791	692	693
sp|P40871|DHBE_BACSU	60	233	242	240	299	267	259
sp|P19669|TAL_BACSU	23	221	192	220	250	248	228
sp|O31501|SWRC_BACSU	114	249	242	257	290	272	295
sp|O07516|YHAH_BACSU	13	43	43	45	54	50	46
sp|O06714|SBCC_BACSU	129	114	107	115	140	126	118
sp|P09124|G3P1_BACSU	36	431	416	432	504	478	476
sp|P37472|HPRT_BACSU	20	49	49	49	58	56	53
sp|P42318|YXJG_BACSU	43	182	166	192	206	199	207
sp|P05652|GYRB_BACSU	72	78	74	79	89	86	85
sp|P25993|CARA_BACSU	40	81	81	81	92	90	90
sp|P54517|AROQ_BACSU	16	16	15	16	15	15	15
sp|P54519|YQHY_BACSU	15	46	43	42	40	39	41
sp|P42924|RL23_BACSU	11	171	158	173	159	157	138
sp|P13800|DEGU_BACSU	26	104	99	112	100	91	91

sp|P37522|SOJ_BACSU	28	25	26	25	25	21	22
sp|P42972|YCSN_BACSU	34	11	12	11	10	10	10
sp|O31534|HMOA_BACSU	13	78	71	72	65	67	62
sp|O34660|ALDH4_BACSU	54	37	39	37	35	31	30
sp|Q07836|WAPI_BACSU	16	83	81	92	74	70	72
sp|P70948|YITV_BACSU	29	25	25	24	19	23	19
sp|P39120|CISY2_BACSU	42	53	53	51	44	40	45
sp|O34328|KGUA_BACSU	23	17	19	17	15	14	14
sp|P51831|FABG_BACSU	26	90	76	78	67	63	66
sp|O31684|YKVS_BACSU	7	5	5	5	4	4	4
sp|P42108|YXAI_BACSU	17	19	17	18	15	13	15
sp|P28599|CH10_BACSU	10	95	81	92	79	76	58
sp|P54530|PTB_BACSU	32	15	17	17	15	12	12
sp|P71066|YVFG_BACSU	8	24	21	22	17	20	15
sp|O06492|GATC_BACSU	11	44	49	45	32	39	36
sp|P39651|YWFO_BACSU	51	16	16	20	14	14	12
sp|O34759|YDJO_BACSU	8	25	23	20	18	17	16
sp|P33911|CSRA_BACSU	8	17	15	14	11	12	11
sp|O34725|YJHA_BACSU	24	18	21	17	16	13	12
sp|O07598|YHAA_BACSU	43	44	53	44	31	39	32
sp|O31818|YNZC_BACSU	9	17	16	21	12	14	10
sp|P54484|YQGA_BACSU	15	42	40	41	24	24	32
sp|P26380|PTFB_BACSU	18	20	21	29	17	13	15
sp|P39839|YUXL_BACSU	74	11	11	8	7	7	5
sp|O05501|YDHI_BACSU	18	4	4	5	2	3	3
sp|O34588|YKUJ_BACSU	9	31	29	39	23	21	17
sp|O31697|YKZF_BACSU	8	8	8	9	6	4	5
sp|Q04747|SRFAB_BACSU	401	2687	2358	2041	1478	1329	1422
sp|O31804|TATAC_BACSU	7	13	12	14	8	9	6
sp|P96714|YWQB_BACSU	63	5	7	5	3	3	4
sp|P12667|NUCA_BACSU	16	15	15	11	9	7	8
sp|P54507|COTN_BACSU	28	75	62	60	45	37	32
sp|O05522|TATAY_BACSU	6	10	9	11	7	6	4
sp|P45693|SP5S_BACSU	9	14	14	20	9	10	8
sp|O32242|SDPR_BACSU	10	22	16	16	12	10	7
sp|Q08787|SRFAC_BACSU	144	508	455	398	262	213	253
sp|O34344|SDPC_BACSU	22	18	17	16	7	7	13
sp|P54506|LEPW_BACSU	21	6	7	6	4	4	2
sp|P96720|YWQH_BACSU	16	10	10	13	3	7	7
sp|P42113|ASNH_BACSU	86	17	20	13	10	7	9
sp|O34538|YCDA_BACSU	39	20	23	16	11	9	10
sp|P94576|YWOF_BACSU	51	5	7	6	3	2	4
sp|P27206|SRFAA_BACSU	402	2032	1788	1563	891	874	878

sp|P71002|RAPF_BACSU	46	39	38	42	9	26	22
sp|P26942|YSXB_BACSU	12	5	9	7	3	4	3
sp|O34313|NTPES_BACSU	160	13	12	13	5	6	7
sp|O34722|YFMG_BACSU	57	47	55	46	21	25	22
sp|P46325|YXBA_BACSU	10	17	15	12	5	8	5
sp|O31852|CWLS_BACSU	44	9	10	11	3	4	5
sp|P02968|FLA_BACSU	33	78	71	73	35	24	30
sp|P46327|YXBC_BACSU	37	21	23	24	8	8	9
sp|O32201|LIAH_BACSU	26	29	24	22	12	5	10
sp|C0SPB6|SSBB_BACSU	13	36	29	22	9	5	15
sp|Q00828|RAPA_BACSU	45	12	15	14	3	3	6
sp|O31430|SKFH_BACSU	16	8	9	7	3	0	4
sp|O07567|NTDR_BACSU	38	7	6	5	0	3	2
sp|P50733|YPBG_BACSU	29	4	2	3	2	0	0
sp|P94415|RAPC_BACSU	46	12	13	22	0	4	6
sp|O34433|YOBO_BACSU	88	3	3	5	2	0	0
sp|Q795R8|YTFP_BACSU	46	9	8	7	0	0	4
sp|O34704|YXNB_BACSU	19	8	4	7	0	3	0
sp|P39800|XLYA_BACSU	32	6	7	6	0	3	0
sp|P25953|COMGA_BACSU	40	6	5	3	2	0	0
sp|O34700|YEBG_BACSU	8	6	4	5	0	2	0
sp|O31427|SKFE_BACSU	27	2	3	2	0	0	0
sp|O34470|YLBL_BACSU	38	2	3	2	0	0	0
sp|P54395|YPMA_BACSU	7	2	2	2	0	0	0
sp|P46326|YXBB_BACSU	28	11	8	10	0	0	0
sp|O34666|CTPA_BACSU	51	19	22	15	0	0	0
sp|Q7WY62|SDA_BACSU	6	3	3	2	0	0	0
sp|C0H3Z9|XKZA_BACSU	10	2	2	3	0	0	0
sp|Q45595|YYDG_BACSU	37	5	3	5	0	0	0
sp|P96724|NFI_BACSU	27	4	2	3	0	0	0
sp|O07008|GANR_BACSU	37	2	4	2	0	0	0
sp|O31635|YJCM_BACSU	47	2	7	8	0	0	0

NSAF 27255	NSAF 27256	NSAF 27257	NSAF 27258	NSAF 27259	NSAF 27260
0.00E+00	0.00E+00	0.00E+00	2.02E-05	2.11E-05	2.12E-05
0.00E+00	0.00E+00	0.00E+00	3.64E-05	2.53E-05	2.54E-05
0.00E+00	0.00E+00	0.00E+00	4.49E-05	8.33E-05	7.84E-05
0.00E+00	0.00E+00	0.00E+00	2.28E-05	2.38E-05	2.39E-05
0.00E+00	0.00E+00	0.00E+00	3.64E-05	3.80E-05	2.54E-05
0.00E+00	0.00E+00	0.00E+00	3.03E-05	3.17E-05	4.77E-05

0.00E+00	0.00E+00	0.00E+00	1.52E-04	3.17E-04	2.23E-04
0.00E+00	2.50E-05	0.00E+00	3.52E-05	8.59E-05	1.11E-04
0.00E+00	0.00E+00	2.38E-05	4.55E-05	7.13E-05	7.16E-05
0.00E+00	1.94E-05	0.00E+00	3.64E-05	3.80E-05	3.82E-05
0.00E+00	0.00E+00	2.17E-05	4.16E-05	2.17E-05	4.36E-05
3.51E-05	4.85E-05	2.38E-05	6.83E-05	1.31E-04	1.43E-04
2.34E-05	2.91E-05	0.00E+00	4.55E-05	4.28E-05	6.20E-05
4.53E-05	0.00E+00	4.61E-05	7.72E-05	6.91E-05	8.10E-05
1.73E-04	8.95E-05	1.17E-04	2.80E-04	2.63E-04	3.82E-04
3.40E-05	2.35E-05	2.31E-05	6.62E-05	4.61E-05	5.78E-05
8.60E-06	1.78E-05	8.75E-06	2.09E-05	3.06E-05	2.19E-05
4.82E-05	3.75E-05	3.68E-05	9.40E-05	6.13E-05	9.85E-05
5.10E-05	3.52E-05	3.46E-05	6.62E-05	6.91E-05	1.04E-04
1.95E-04	2.36E-04	2.65E-04	4.59E-04	3.80E-04	4.15E-04
6.23E-05	5.17E-05	6.34E-05	1.09E-04	1.01E-04	1.02E-04
1.64E-04	1.45E-04	1.19E-04	1.82E-04	2.85E-04	2.62E-04
3.03E-05	5.24E-05	7.20E-05	8.86E-05	8.22E-05	9.28E-05
6.89E-05	7.14E-05	9.01E-05	1.15E-04	1.20E-04	1.51E-04
4.04E-05	5.24E-05	7.20E-05	7.87E-05	9.25E-05	1.03E-04
9.69E-05	1.15E-04	1.13E-04	1.75E-04	1.55E-04	1.98E-04
1.25E-04	1.45E-04	1.27E-04	2.43E-04	1.58E-04	2.39E-04
1.09E-04	1.78E-04	1.59E-04	2.12E-04	2.38E-04	2.54E-04
1.45E-04	1.25E-04	1.23E-04	2.00E-04	1.84E-04	2.22E-04
1.15E-04	1.04E-04	1.02E-04	1.68E-04	1.46E-04	1.76E-04
5.72E-04	5.02E-04	4.03E-04	7.92E-04	6.93E-04	7.63E-04
2.88E-04	2.44E-04	3.04E-04	4.68E-04	3.69E-04	4.36E-04
9.02E-05	6.68E-05	7.87E-05	1.00E-04	1.18E-04	1.32E-04
1.87E-04	1.45E-04	2.38E-04	2.73E-04	2.85E-04	2.86E-04
1.38E-04	1.43E-04	1.20E-04	2.11E-04	1.60E-04	2.21E-04
2.49E-04	2.03E-04	2.17E-04	3.47E-04	2.72E-04	3.64E-04
2.28E-04	2.15E-04	2.11E-04	3.24E-04	3.59E-04	2.76E-04
2.96E-04	3.80E-04	3.95E-04	5.50E-04	5.60E-04	4.47E-04
1.64E-04	1.13E-04	1.39E-04	1.86E-04	2.23E-04	1.96E-04
6.68E-05	5.54E-05	5.43E-05	9.10E-05	8.15E-05	8.18E-05
2.32E-04	1.74E-04	2.36E-04	3.01E-04	2.88E-04	3.29E-04
3.74E-04	2.95E-04	2.90E-04	4.68E-04	4.35E-04	4.54E-04
4.15E-04	3.88E-04	3.59E-04	5.46E-04	5.49E-04	5.30E-04
1.60E-04	1.71E-04	1.93E-04	2.27E-04	2.62E-04	2.43E-04
2.39E-04	2.35E-04	2.12E-04	3.28E-04	3.13E-04	3.16E-04
2.43E-04	1.74E-04	2.28E-04	3.09E-04	3.04E-04	2.86E-04
4.10E-04	3.93E-04	3.70E-04	5.16E-04	4.86E-04	6.26E-04
1.92E-04	2.69E-04	2.27E-04	3.08E-04	3.01E-04	3.39E-04
4.67E-04	4.85E-04	5.39E-04	6.68E-04	6.34E-04	7.32E-04

1.07E-03	7.92E-04	8.44E-04	1.28E-03	1.26E-03	1.11E-03
3.48E-04	4.54E-04	3.54E-04	4.96E-04	4.92E-04	5.66E-04
1.56E-04	2.05E-04	1.69E-04	2.12E-04	2.43E-04	2.54E-04
1.78E-04	1.48E-04	1.81E-04	2.25E-04	1.99E-04	2.54E-04
1.66E-04	1.72E-04	1.55E-04	2.29E-04	2.39E-04	1.84E-04
2.78E-04	3.10E-04	2.83E-04	3.85E-04	3.59E-04	4.04E-04
1.77E-04	1.63E-04	2.00E-04	2.11E-04	2.60E-04	2.41E-04
1.06E-03	7.91E-04	8.56E-04	1.21E-03	1.17E-03	1.18E-03
2.92E-04	3.51E-04	3.45E-04	4.55E-04	4.04E-04	4.41E-04
6.89E-05	7.14E-05	7.01E-05	9.58E-05	9.01E-05	9.04E-05
2.14E-04	2.77E-04	2.45E-04	3.38E-04	3.26E-04	3.00E-04
3.25E-04	3.37E-04	2.88E-04	4.46E-04	3.66E-04	4.25E-04
4.55E-05	4.19E-05	4.11E-05	6.40E-05	5.14E-05	5.16E-05
8.76E-04	8.20E-04	7.50E-04	1.04E-03	1.11E-03	1.03E-03
3.04E-04	3.15E-04	3.21E-04	4.55E-04	3.68E-04	3.94E-04
3.49E-04	3.51E-04	2.89E-04	4.32E-04	3.90E-04	4.58E-04
1.73E-04	2.01E-04	1.69E-04	2.23E-04	2.39E-04	2.40E-04
3.37E-04	3.75E-04	3.93E-04	5.10E-04	4.18E-04	4.96E-04
2.21E-04	2.29E-04	2.25E-04	2.98E-04	2.94E-04	2.78E-04
1.92E-04	2.20E-04	2.06E-04	2.56E-04	2.77E-04	2.58E-04
1.76E-04	1.82E-04	1.79E-04	2.14E-04	2.46E-04	2.25E-04
1.66E-04	1.38E-04	1.44E-04	1.78E-04	1.77E-04	2.12E-04
2.54E-04	2.80E-04	3.01E-04	3.44E-04	3.33E-04	3.82E-04
1.06E-04	8.67E-05	9.40E-05	1.29E-04	1.07E-04	1.26E-04
1.87E-04	2.09E-04	1.76E-04	2.38E-04	2.49E-04	2.35E-04
8.69E-04	9.88E-04	8.75E-04	1.17E-03	1.13E-03	1.14E-03
1.36E-04	1.23E-04	1.21E-04	1.66E-04	1.56E-04	1.56E-04
2.62E-04	2.91E-04	3.04E-04	3.28E-04	3.42E-04	4.01E-04
2.11E-04	2.19E-04	1.98E-04	2.37E-04	2.65E-04	2.82E-04
7.85E-04	7.88E-04	6.85E-04	9.10E-04	9.89E-04	9.03E-04
5.43E-04	5.63E-04	4.71E-04	6.33E-04	6.52E-04	6.63E-04
1.17E-03	1.16E-03	9.75E-04	1.34E-03	1.35E-03	1.38E-03
1.97E-04	2.29E-04	2.31E-04	2.56E-04	2.56E-04	2.93E-04
4.56E-04	4.85E-04	4.16E-04	5.69E-04	5.58E-04	5.25E-04
4.52E-04	4.24E-04	4.33E-04	5.76E-04	5.04E-04	5.06E-04
1.31E-03	1.18E-03	1.35E-03	1.53E-03	1.59E-03	1.47E-03
1.30E-04	1.49E-04	1.38E-04	1.73E-04	1.52E-04	1.72E-04
4.67E-04	5.10E-04	5.01E-04	5.41E-04	6.10E-04	6.08E-04
1.07E-04	1.11E-04	1.20E-04	1.35E-04	1.30E-04	1.31E-04
3.89E-04	4.39E-04	4.00E-04	4.50E-04	4.90E-04	4.97E-04
2.44E-04	2.70E-04	2.81E-04	3.01E-04	2.98E-04	3.32E-04
4.36E-04	3.88E-04	4.57E-04	4.73E-04	5.20E-04	4.96E-04
1.36E-03	1.39E-03	1.62E-03	1.67E-03	1.71E-03	1.69E-03

7.88E-04	8.41E-04	7.45E-04	8.75E-04	8.90E-04	9.83E-04
1.88E-03	1.78E-03	1.95E-03	2.25E-03	2.06E-03	2.07E-03
1.45E-03	1.56E-03	1.52E-03	1.81E-03	1.69E-03	1.65E-03
3.59E-03	3.24E-03	3.64E-03	3.96E-03	4.10E-03	3.78E-03
8.17E-04	8.23E-04	8.58E-04	9.26E-04	9.07E-04	9.88E-04
1.24E-03	1.28E-03	1.32E-03	1.51E-03	1.46E-03	1.35E-03
3.30E-04	3.22E-04	3.39E-04	3.95E-04	3.71E-04	3.49E-04
4.48E-03	4.48E-03	4.57E-03	5.10E-03	5.05E-03	5.05E-03
9.16E-04	9.50E-04	9.32E-04	1.06E-03	1.06E-03	1.01E-03
1.58E-03	1.50E-03	1.70E-03	1.74E-03	1.76E-03	1.84E-03
4.05E-04	3.98E-04	4.17E-04	4.50E-04	4.54E-04	4.51E-04
7.57E-04	7.85E-04	7.70E-04	8.37E-04	8.56E-04	8.59E-04
3.74E-04	3.63E-04	3.80E-04	3.41E-04	3.56E-04	3.58E-04
1.15E-03	1.11E-03	1.07E-03	9.71E-04	9.89E-04	1.04E-03
5.81E-03	5.57E-03	5.98E-03	5.26E-03	5.43E-03	4.79E-03
1.50E-03	1.48E-03	1.64E-03	1.40E-03	1.33E-03	1.34E-03
3.34E-04	3.60E-04	3.40E-04	3.25E-04	2.85E-04	3.00E-04
1.21E-04	1.37E-04	1.23E-04	1.07E-04	1.12E-04	1.12E-04
2.24E-03	2.12E-03	2.11E-03	1.82E-03	1.96E-03	1.82E-03
2.56E-04	2.80E-04	2.61E-04	2.36E-04	2.18E-04	2.12E-04
1.94E-03	1.96E-03	2.19E-03	1.68E-03	1.66E-03	1.72E-03
3.22E-04	3.34E-04	3.15E-04	2.39E-04	3.02E-04	2.50E-04
4.72E-04	4.89E-04	4.62E-04	3.81E-04	3.62E-04	4.09E-04
2.76E-04	3.20E-04	2.81E-04	2.37E-04	2.31E-04	2.32E-04
1.29E-03	1.13E-03	1.14E-03	9.38E-04	9.21E-04	9.69E-04
2.67E-04	2.77E-04	2.72E-04	2.08E-04	2.17E-04	2.18E-04
4.18E-04	3.88E-04	4.03E-04	3.21E-04	2.91E-04	3.37E-04
3.55E-03	3.14E-03	3.50E-03	2.88E-03	2.89E-03	2.21E-03
1.75E-04	2.06E-04	2.02E-04	1.71E-04	1.43E-04	1.43E-04
1.12E-03	1.02E-03	1.05E-03	7.74E-04	9.51E-04	7.16E-04
1.50E-03	1.73E-03	1.56E-03	1.06E-03	1.35E-03	1.25E-03
1.17E-04	1.22E-04	1.49E-04	1.00E-04	1.04E-04	8.98E-05
1.17E-03	1.11E-03	9.51E-04	8.19E-04	8.08E-04	7.63E-04
7.95E-04	7.27E-04	6.66E-04	5.01E-04	5.70E-04	5.25E-04
2.80E-04	3.39E-04	2.69E-04	2.43E-04	2.06E-04	1.91E-04
3.83E-04	4.78E-04	3.89E-04	2.63E-04	3.45E-04	2.84E-04
7.06E-04	6.89E-04	8.88E-04	4.85E-04	5.91E-04	4.24E-04
1.05E-03	1.03E-03	1.04E-03	5.83E-04	6.08E-04	8.14E-04
4.15E-04	4.52E-04	6.13E-04	3.44E-04	2.75E-04	3.18E-04
5.56E-05	5.76E-05	4.11E-05	3.44E-05	3.60E-05	2.58E-05
8.31E-05	8.61E-05	1.06E-04	4.05E-05	6.34E-05	6.36E-05
1.29E-03	1.25E-03	1.65E-03	9.31E-04	8.87E-04	7.21E-04
3.74E-04	3.88E-04	4.28E-04	2.73E-04	1.90E-04	2.39E-04

2.51E-03	2.28E-03	1.94E-03	1.34E-03	1.26E-03	1.35E-03
6.94E-04	6.65E-04	7.61E-04	4.16E-04	4.89E-04	3.27E-04
2.97E-05	4.31E-05	3.02E-05	1.73E-05	1.81E-05	2.42E-05
3.51E-04	3.63E-04	2.62E-04	2.05E-04	1.66E-04	1.91E-04
1.00E-03	8.58E-04	8.15E-04	5.85E-04	5.02E-04	4.36E-04
6.23E-04	5.81E-04	6.97E-04	4.25E-04	3.80E-04	2.54E-04
5.82E-04	6.03E-04	8.45E-04	3.64E-04	4.22E-04	3.39E-04
8.23E-04	6.20E-04	6.09E-04	4.37E-04	3.80E-04	2.67E-04
1.32E-03	1.22E-03	1.05E-03	6.62E-04	5.62E-04	6.71E-04
3.06E-04	3.00E-04	2.77E-04	1.16E-04	1.21E-04	2.26E-04
1.07E-04	1.29E-04	1.09E-04	6.94E-05	7.24E-05	3.64E-05
2.34E-04	2.42E-04	3.09E-04	6.83E-05	1.66E-04	1.67E-04
7.39E-05	9.02E-05	5.75E-05	4.23E-05	3.09E-05	3.99E-05
1.92E-04	2.29E-04	1.56E-04	1.03E-04	8.77E-05	9.79E-05
3.67E-05	5.32E-05	4.48E-05	2.14E-05	1.49E-05	2.99E-05
1.89E-03	1.72E-03	1.48E-03	8.07E-04	8.27E-04	8.34E-04
3.17E-04	3.20E-04	3.47E-04	7.12E-05	2.15E-04	1.83E-04
1.56E-04	2.91E-04	2.22E-04	9.10E-05	1.27E-04	9.54E-05
3.04E-05	2.91E-05	3.09E-05	1.14E-05	1.43E-05	1.67E-05
3.08E-04	3.74E-04	3.07E-04	1.34E-04	1.67E-04	1.47E-04
6.36E-04	5.81E-04	4.57E-04	1.82E-04	3.04E-04	1.91E-04
7.65E-05	8.81E-05	9.51E-05	2.48E-05	3.46E-05	4.34E-05
8.84E-04	8.34E-04	8.42E-04	3.86E-04	2.77E-04	3.47E-04
2.12E-04	2.41E-04	2.47E-04	7.87E-05	8.22E-05	9.28E-05
4.17E-04	3.58E-04	3.22E-04	1.68E-04	7.31E-05	1.47E-04
1.04E-03	8.65E-04	6.44E-04	2.52E-04	1.46E-04	4.40E-04
9.97E-05	1.29E-04	1.18E-04	2.43E-05	2.53E-05	5.09E-05
1.87E-04	2.18E-04	1.66E-04	6.83E-05	0.00E+00	9.54E-05
6.89E-05	6.12E-05	5.01E-05	0.00E+00	3.00E-05	2.01E-05
5.16E-05	2.67E-05	3.94E-05	2.51E-05	0.00E+00	0.00E+00
9.75E-05	1.10E-04	1.82E-04	0.00E+00	3.31E-05	4.98E-05
1.27E-05	1.32E-05	2.16E-05	8.28E-06	0.00E+00	0.00E+00
7.32E-05	6.74E-05	5.79E-05	0.00E+00	0.00E+00	3.32E-05
1.57E-04	8.16E-05	1.40E-04	0.00E+00	6.00E-05	0.00E+00
7.01E-05	8.48E-05	7.13E-05	0.00E+00	3.56E-05	0.00E+00
5.61E-05	4.85E-05	2.85E-05	1.82E-05	0.00E+00	0.00E+00
2.80E-04	1.94E-04	2.38E-04	0.00E+00	9.51E-05	0.00E+00
2.77E-05	4.31E-05	2.82E-05	0.00E+00	0.00E+00	0.00E+00
1.97E-05	3.06E-05	2.00E-05	0.00E+00	0.00E+00	0.00E+00
1.07E-04	1.11E-04	1.09E-04	0.00E+00	0.00E+00	0.00E+00
1.47E-04	1.11E-04	1.36E-04	0.00E+00	0.00E+00	0.00E+00
1.39E-04	1.67E-04	1.12E-04	0.00E+00	0.00E+00	0.00E+00
1.87E-04	1.94E-04	1.27E-04	0.00E+00	0.00E+00	0.00E+00

7.48E-05	7.75E-05	1.14E-04	0.00E+00	0.00E+00	0.00E+00
5.05E-05	3.14E-05	5.14E-05	0.00E+00	0.00E+00	0.00E+00
5.54E-05	2.87E-05	4.23E-05	0.00E+00	0.00E+00	0.00E+00
2.02E-05	4.19E-05	2.06E-05	0.00E+00	0.00E+00	0.00E+00
1.59E-05	5.77E-05	6.48E-05	0.00E+00	0.00E+00	0.00E+00

Average NSAF WT	Average NSAF Mutant	Fold Change Average NSAF WT / Average NSAF Mutant	T-Test	Estimated Fold change (Mut/WT)
0.00E+00	2.09E-05	#DIV/0!	3.0E-07	6.02
0.00E+00	2.91E-05	#DIV/0!	1.4E-03	7.00
0.00E+00	6.89E-05	#DIV/0!	4.7E-03	40.35
0.00E+00	2.35E-05	#DIV/0!	3.0E-07	6.02
0.00E+00	3.33E-05	#DIV/0!	1.1E-03	8.01
0.00E+00	3.66E-05	#DIV/0!	2.8E-03	7.04
0.00E+00	2.30E-04	#DIV/0!	8.5E-03	22.19
8.34E-06	7.73E-05	9.27	4.4E-02	
7.93E-06	6.28E-05	7.92	9.4E-03	
6.46E-06	3.75E-05	5.81	8.7E-03	
7.25E-06	3.57E-05	4.92	4.8E-02	
3.58E-05	1.14E-04	3.19	3.2E-02	
1.75E-05	5.01E-05	2.87	3.8E-02	
3.05E-05	7.58E-05	2.49	4.4E-02	
1.26E-04	3.08E-04	2.44	1.5E-02	
2.68E-05	5.67E-05	2.11	1.2E-02	
1.17E-05	2.45E-05	2.09	4.2E-02	
4.09E-05	8.46E-05	2.07	2.4E-02	
4.03E-05	7.98E-05	1.98	4.1E-02	
2.32E-04	4.18E-04	1.80	3.6E-03	
5.91E-05	1.04E-04	1.76	5.7E-04	
1.43E-04	2.43E-04	1.71	4.1E-02	
5.16E-05	8.79E-05	1.70	4.3E-02	
7.68E-05	1.29E-04	1.67	1.6E-02	
5.49E-05	9.15E-05	1.67	3.5E-02	
1.08E-04	1.76E-04	1.63	7.6E-03	
1.32E-04	2.13E-04	1.61	4.5E-02	
1.48E-04	2.35E-04	1.58	2.2E-02	
1.31E-04	2.02E-04	1.54	5.4E-03	
1.07E-04	1.63E-04	1.52	4.5E-03	
4.92E-04	7.50E-04	1.52	1.1E-02	
2.79E-04	4.25E-04	1.52	1.3E-02	
7.86E-05	1.17E-04	1.48	2.8E-02	

1.90E-04	2.82E-04	1.48	2.8E-02
1.34E-04	1.97E-04	1.48	3.4E-02
2.23E-04	3.27E-04	1.47	3.0E-02
2.18E-04	3.19E-04	1.46	1.5E-02
3.57E-04	5.19E-04	1.45	2.7E-02
1.39E-04	2.02E-04	1.45	2.6E-02
5.88E-05	8.48E-05	1.44	6.9E-03
2.14E-04	3.06E-04	1.43	1.7E-02
3.20E-04	4.52E-04	1.42	1.0E-02
3.87E-04	5.42E-04	1.40	8.6E-04
1.75E-04	2.44E-04	1.40	7.5E-03
2.29E-04	3.19E-04	1.39	7.0E-04
2.15E-04	3.00E-04	1.39	1.8E-02
3.91E-04	5.42E-04	1.39	2.6E-02
2.30E-04	3.16E-04	1.38	2.6E-02
4.97E-04	6.78E-04	1.36	7.3E-03
9.03E-04	1.22E-03	1.35	3.6E-02
3.86E-04	5.18E-04	1.34	3.5E-02
1.76E-04	2.37E-04	1.34	3.5E-02
1.69E-04	2.26E-04	1.34	4.0E-02
1.64E-04	2.17E-04	1.32	4.1E-02
2.90E-04	3.82E-04	1.32	5.0E-03
1.80E-04	2.37E-04	1.32	3.3E-02
9.02E-04	1.19E-03	1.32	2.5E-02
3.29E-04	4.33E-04	1.32	1.3E-02
7.01E-05	9.21E-05	1.31	3.9E-04
2.45E-04	3.21E-04	1.31	2.4E-02
3.17E-04	4.12E-04	1.30	2.7E-02
4.28E-05	5.56E-05	1.30	4.3E-02
8.15E-04	1.06E-03	1.30	5.5E-03
3.13E-04	4.06E-04	1.30	2.4E-02
3.30E-04	4.27E-04	1.29	2.7E-02
1.81E-04	2.34E-04	1.29	1.0E-02
3.68E-04	4.75E-04	1.29	3.2E-02
2.25E-04	2.90E-04	1.29	6.1E-04
2.06E-04	2.64E-04	1.28	5.5E-03
1.79E-04	2.28E-04	1.27	6.8E-03
1.49E-04	1.89E-04	1.27	5.0E-02
2.79E-04	3.53E-04	1.27	2.1E-02
9.54E-05	1.21E-04	1.26	4.3E-02
1.90E-04	2.41E-04	1.26	9.0E-03
9.11E-04	1.14E-03	1.26	4.4E-03
1.27E-04	1.59E-04	1.25	4.6E-03

2.86E-04	3.57E-04	1.25	5.0E-02
2.10E-04	2.61E-04	1.25	2.2E-02
7.53E-04	9.34E-04	1.24	1.4E-02
5.26E-04	6.49E-04	1.24	1.4E-02
1.10E-03	1.36E-03	1.23	1.6E-02
2.19E-04	2.68E-04	1.22	4.2E-02
4.52E-04	5.51E-04	1.22	1.5E-02
4.36E-04	5.29E-04	1.21	2.1E-02
1.28E-03	1.53E-03	1.20	1.5E-02
1.39E-04	1.66E-04	1.19	3.9E-02
4.93E-04	5.86E-04	1.19	2.3E-02
1.12E-04	1.32E-04	1.18	8.3E-03
4.09E-04	4.79E-04	1.17	2.9E-02
2.65E-04	3.10E-04	1.17	4.4E-02
4.27E-04	4.96E-04	1.16	4.6E-02
1.46E-03	1.69E-03	1.16	4.8E-02
7.91E-04	9.16E-04	1.16	4.6E-02
1.87E-03	2.12E-03	1.14	3.3E-02
1.51E-03	1.72E-03	1.14	2.6E-02
3.49E-03	3.95E-03	1.13	4.3E-02
8.32E-04	9.40E-04	1.13	1.7E-02
1.28E-03	1.44E-03	1.13	3.7E-02
3.30E-04	3.72E-04	1.13	4.3E-02
4.51E-03	5.06E-03	1.12	7.6E-05
9.33E-04	1.04E-03	1.12	4.3E-03
1.59E-03	1.78E-03	1.12	4.5E-02
4.07E-04	4.52E-04	1.11	1.4E-03
7.71E-04	8.51E-04	1.10	1.6E-03
3.73E-04	3.52E-04	0.94	4.6E-02
1.11E-03	1.00E-03	0.90	2.9E-02
5.79E-03	5.16E-03	0.89	5.0E-02
1.54E-03	1.36E-03	0.88	3.2E-02
3.44E-04	3.03E-04	0.88	4.3E-02
1.27E-04	1.10E-04	0.87	3.4E-02
2.16E-03	1.87E-03	0.87	1.1E-02
2.66E-04	2.22E-04	0.84	1.3E-02
2.03E-03	1.69E-03	0.83	1.3E-02
3.24E-04	2.63E-04	0.81	4.0E-02
4.74E-04	3.84E-04	0.81	4.6E-03
2.93E-04	2.34E-04	0.80	1.4E-02
1.19E-03	9.43E-04	0.79	1.0E-02
2.72E-04	2.14E-04	0.79	1.8E-04
4.03E-04	3.16E-04	0.79	5.8E-03

3.40E-03	2.66E-03	0.78	4.6E-02
1.94E-04	1.52E-04	0.78	3.4E-02
1.06E-03	8.13E-04	0.77	3.2E-02
1.59E-03	1.22E-03	0.77	2.7E-02
1.29E-04	9.80E-05	0.76	4.5E-02
1.08E-03	7.97E-04	0.74	1.4E-02
7.29E-04	5.32E-04	0.73	9.7E-03
2.96E-04	2.13E-04	0.72	3.5E-02
4.17E-04	2.97E-04	0.71	3.9E-02
7.61E-04	5.00E-04	0.66	3.1E-02
1.04E-03	6.68E-04	0.64	7.2E-03
4.94E-04	3.12E-04	0.63	4.7E-02
5.14E-05	3.21E-05	0.62	3.3E-02
9.16E-05	5.58E-05	0.61	2.7E-02
1.40E-03	8.46E-04	0.61	1.8E-02
3.97E-04	2.34E-04	0.59	5.0E-03
2.24E-03	1.32E-03	0.59	5.4E-03
7.07E-04	4.11E-04	0.58	5.7E-03
3.43E-05	1.99E-05	0.58	4.2E-02
3.25E-04	1.87E-04	0.58	1.5E-02
8.92E-04	5.08E-04	0.57	5.6E-03
6.34E-04	3.53E-04	0.56	1.0E-02
6.77E-04	3.75E-04	0.55	2.7E-02
6.84E-04	3.61E-04	0.53	2.0E-02
1.20E-03	6.32E-04	0.53	2.7E-03
2.94E-04	1.54E-04	0.52	1.9E-02
1.15E-04	5.94E-05	0.52	1.5E-02
2.62E-04	1.34E-04	0.51	3.4E-02
7.39E-05	3.77E-05	0.51	2.3E-02
1.92E-04	9.61E-05	0.50	1.1E-02
4.49E-05	2.21E-05	0.49	2.4E-02
1.70E-03	8.22E-04	0.48	1.9E-03
3.28E-04	1.56E-04	0.48	1.8E-02
2.23E-04	1.04E-04	0.47	4.3E-02
3.01E-05	1.41E-05	0.47	6.1E-04
3.30E-04	1.49E-04	0.45	1.7E-03
5.58E-04	2.26E-04	0.40	7.3E-03
8.66E-05	3.43E-05	0.40	2.4E-03
8.53E-04	3.37E-04	0.39	1.3E-04
2.33E-04	8.46E-05	0.36	2.1E-04
3.66E-04	1.29E-04	0.35	4.1E-03
8.48E-04	2.80E-04	0.33	1.6E-02
1.16E-04	3.35E-05	0.29	2.6E-03

1.90E-04	5.46E-05	0.29	1.3E-02
6.00E-05	1.67E-05	0.28	1.4E-02
3.92E-05	8.37E-06	0.21	4.9E-02
1.30E-04	2.76E-05	0.21	2.8E-02
1.59E-05	2.76E-06	0.17	3.0E-02
6.62E-05	1.11E-05	0.17	9.9E-03
1.26E-04	2.00E-05	0.16	2.5E-02
7.54E-05	1.19E-05	0.16	7.6E-03
4.44E-05	6.07E-06	0.14	2.0E-02
2.37E-04	3.17E-05	0.13	7.0E-03
3.30E-05	0.00E+00	0.00	2.8E-03
2.34E-05	0.00E+00	0.00	2.8E-03
1.09E-04	0.00E+00	0.00	7.1E-08
1.31E-04	0.00E+00	0.00	2.5E-04
1.39E-04	0.00E+00	0.00	9.5E-04
1.69E-04	0.00E+00	0.00	1.4E-03
8.88E-05	0.00E+00	0.00	2.2E-03
4.45E-05	0.00E+00	0.00	2.4E-03
4.21E-05	0.00E+00	0.00	5.4E-03
2.76E-05	0.00E+00	0.00	1.8E-02
4.61E-05	0.00E+00	0.00	3.9E-02

Table 2.5 Proteomics data set. The proteomics data for the 183 proteins identified as having significantly different levels (p-value < 0.05) in the protease double mutant relative to the control are presented.

Strain	Genotype	Reference/Source
PY79	*B. subtilis* PY79	Youngman et al., 1984
BTH101	E. coli BTH101	Euromedex (EUB001)
PEB66	*E. coli* Top10	ThermoFisher (C404010)
PEB67	*E. coli* BL21 DE3	Lab stock
PEB69	*E. coli* NiCo21 DE3	New England Biolabs (C2529H)
PEB75	*B. subtilis 168 ΔrecN::erm (used to generate other strains only)*	Bacillus Genetic Stock Center (BKE24240)
PEB85	*B. subtilis ΔrecN*	This study
PEB111	*E. coli* BL21 DE3 pLysY/lacIq	New England Biolabs (C3013)
PEB233	*E. coli* XL1-Blue pCJ41	Bacillus Genetic Stock Center (ECE310)
PEB234	*E. coli* (TB1) pMalC9	Bacillus Genetic Stock Center

		(ECE309)
PEB235	*B. subtilis* Δ*recR*	This study
PEB278	*B. subtilis* Δ*rnhC*	JWS224
PEB307	*B. subtilis* Δ*uvrA*	This study
PEB308	*B. subtilis* Δ*uvrB*	This study
PEB310	*B. subtilis* Δ*uvrC*	This study
PEB316	*B. subtilis* Δ*yprA*	This study
PEB318	*B. subtilis* Δ*yprB*	This study
PEB322	*B. subtilis* Δ*ylbK*	This study
PEB324	*B. subtilis* Δ*ylbL*	This study
PEB334	*B. subtilis* Δ*sodA*	This study
PEB336	*E. coli* MC1061	Lab stock
PEB346	*B. subtilis amyE::Pxyl-ylbL-S234A* (used to generate other strains only)	This study
PEB349	*B. subtilis ΔylbL, amyE::Pxyl-ylbL* (used to generate other strains only)	This study
PEB350	*B.subtilis amyE::Pxyl-ylbK* (used to generate other strains only)	This study
PEB353	*B. subtilis* Δ*queA*	This study
PEB355	*B. subtilis* Δ*ctpA*	This study
PEB357	*B. subtilis* Δ*ysoA*	This study
PEB373	*B. subtilis* Δ*ylbK*, *amyE::Pxyl-ylbK*	This study
PEB375	*B. subtilis* Δ*ylbL*, *amyE::Pxyl-ylbL*	This study
PEB377	*B. subtilis* Δ*ylbL*, *amyE::Pxyl-ylbL-S243A*	This study
PEB382	*B. subtilis* Δ*ylmE*	This study
PEB384	*B. subtilis* Δ*sepF*	This study
PEB386	*B. subtilis* Δ*ylmG*	This study
PEB390	*B. subtilis* Δ*ylbK*, *amyE::Pxyl-ylbL*	This study
PEB392	*B. subtilis* Δ*ylbK*, *amyE::Pxyl-ylbL-S243A*	This study
PEB418	*B. subtilis* Δ*ytmP*	This study
PEB420	*B. subtilis ΔbcrC*	This study
PEB422	*B. subtilis ΔecsA*	This study
PEB424	*B. subtilis ΔecsB*	This study
PEB427	*B. subtilis* Δ*ylbK-2*	This study
PEB432	*B. subtilis 168* Δ*yneA::erm* (used to generate other strains only)	Bacillus Genetic Stock Center (BKE17860)
PEB433	*B. subtilis* Δ*yneA::erm*	This study
PEB436	*B. subtilis* Δ*ylbL*, Δ*yneA::erm*	This study
PEB439	*B. subtilis* Δ*yneA::loxp*	This study
PEB441	*B. subtilis* Δ*ylbL*, Δ*yneA::loxp*	This study
PEB449	*B. subtilis 168* Δ*crh::erm* (used to generate other strains only)	Bacillus Genetic Stock Center (BKE34740)
PEB450	*B. subtilis 168* Δ*lgt::erm* (used to generate other strains only)	Bacillus Genetic Stock Center (BKE34990)

PEB452	*B. subtilis 168* Δ*sdaAB::erm* (used to generate other strains only)	Bacillus Genetic Stock Center (BKE15850)
PEB453	*B. subtilis 168* Δ*ydzU::erm* (used to generate other strains only)	Bacillus Genetic Stock Center (BKE06048)
PEB454	*B. subtilis 168* Δ*radA::erm* (used to generate other strains only)	Bacillus Genetic Stock Center (BKE00870)
PEB455	*B. subtilis 168* Δ*cymR::erm* (used to generate other strains only)	Bacillus Genetic Stock Center (BKE27520)
PEB456	*B. subtilis 168* Δ*ywrC::erm* (used to generate other strains only)	Bacillus Genetic Stock Center (BKE36110)
PEB461	*B. subtilis* Δ*crh::erm*	This study
PEB463	*B. subtilis* Δ*lgt::erm*	This study
PEB467	*B. subtilis* Δ*sdaAB::erm*	This study
PEB469	*B. subtilis* Δ*ydzU::erm*	This study
PEB471	*B. subtilis* Δ*radA::erm*	This study
PEB473	*B. subtilis* Δ*cymR::erm*	This study
PEB475	*B. subtilis* Δ*ywrC::erm*	This study
PEB477	*B. subtilis 168* Δ*recG::erm* (used to generate other strains only)	Bacillus Genetic Stock Center (BKE15870)
PEB478	*B. subtilis* Δ*recG::erm*	This study
PEB482	*B. subtilis Δ walH*	This study
PEB485	*B. subtilis Δ yycI*	This study
PEB488	*B. subtilis Δ walJ*	This study
PEB491	*B. subtilis Δ ruvB*	This study
PEB493	*B. subtilis Δ ripX*	This study
PEB533	*B. subtilis* Δ*ylbL*, *amyE::Pxyl-ylbL-K279A*	This study
PEB535	*B. subtilis 168* Δ*ponA::erm* (used to generate other strains only)	Bacillus Genetic Stock Center (BKE22320)
PEB551	*B. subtilis* Δ*ponA::erm*	This study
PEB555	B. subtilis ΔylbL, ΔctpA	This study
PEB557	B. subtilis ΔylbL, amyE::Pxyl-ylbL, ΔctpA	This study
PEB559	B. subtilis ΔyneA::loxp, ΔctpA	This study
PEB561	B. subtilis ΔylbL, ΔyneA::loxp, ΔctpA	This study
PEB585	B. subtilis ΔuvrA, ΔyneA::loxp	This study
PEB595	B. subtilis ΔylbL, amyE::Pxyl-ctpA	This study
PEB597	B. subtilis ΔylbL, amyE::Pxyl-ctpA-S297A	This study
PEB599	B. subtilis ΔctpA, amyE::Pxyl-ctpA	This study
PEB601	B. subtilis ΔctpA, amyE::Pxyl-ctpA-S297A	This study
PEB603	B. subtilis ΔctpA, amyE::Pxyl-ctpA-K322A	This study
PEB605	B. subtilis ΔctpA, amyE::Pxyl-ylbL	This study
PEB607	B. subtilis ΔctpA, amyE::Pxyl-ylbL-S234A	This study
PEB619	B. subtilis ΔylbL, ΔctpA, amyE::Pxyl-ctpA	This study
PEB621	B. subtilis ΔylbL, ΔctpA, amyE::Pxyl-ctpA-S297A	This study
PEB623	B. subtilis ΔylbL, ΔctpA, amyE::Pxyl-ylbL-S234A	This study
PEB677	B. subtilis amyE::Phyp-yneA	This study

PEB681	B. subtilis ΔylbL, amyE::Phyp-yneA	This study
PEB685	B. subtilis ΔctpA, amyE::Phyp-yneA	This study
PEB689	B. subtilis ΔylbL, ΔctpA, amyE::Phyp-yneA	This study
PEB778	B. subtilis ΔfhuG	This study
PEB780	B. subtilis ΔylbL, ΔctpA, ΔfhuG	This study
PEB782	B. subtilis ΔyfkH	This study
PEB784	B. subtilis ΔylbL, ΔctpA, ΔyfkH	This study
PEB786	B. subtilis ΔltaSA	This study
PEB788	B. subtilis ΔylbL, ΔctpA, ΔltaSA	This study
PEB790	B. subtilis ΔykgA	This study
PEB792	B. subtilis ΔylbL, ΔctpA, ΔykgA	This study
PEB794	B. subtilis ΔcgeE	This study
PEB796	B. subtilis ΔylbL, ΔctpA, ΔcgeE	This study
PEB798	B. subtilis ΔysnF	This study
PEB800	B. subtilis ΔylbL, ΔctpA, ΔysnF	This study
PEB802	B. subtilis ΔlytG	This study
PEB804	B. subtilis ΔylbL, ΔctpA, ΔlytG	This study
PEB806	B. subtilis ΔyxaB	This study
PEB808	B. subtilis ΔylbL, ΔctpA, ΔyxaB	This study
PEB810	B. subtilis ΔylbL, ΔctpA, ΔytmP	This study

Table 2.6 Strains used in this study.

Plasmid number	Plasmid name	Reference/Source
pDR244	pDR244	Bacillus Genetic Stock Center (ECE274)
pDR110	pDR110	A gift from David Rudner
pBR322	pBR322	New England Biolabs (N3033S)
pKT25	pKT25	Euromedex (EUP-25C)
pUT18C	pUT18C	Euromedex (EUP-18C)
pPB12	pET28b-10xHis-Smt3	A gift from Jayakrishnan Nandakumar
pPB13	pET28b-6xHis-Ulp1-403-621	A gift from Jayakrishnan Nandakumar
pPB41	pPB41	Burby and Simmons, 2017a, b
pPB44	pPB41-CRISPR::recR	This study
pPB46	pPB44-recR recombination template	This study
pPB47	pPB47	This study
pPB72	pPB41-CRISPR::uvrA	This study
pPB73	pPB41-CRISPR::uvrB	This study
pPB74	pPB41-CRISPR::uvrC	This study

pPB75	pPB41-CRISPR::yprA	This study
pPB76	pPB41-CRISPR::yprB	This study
pPB77	pPB41-CRISPR::ylbK	This study
pPB78	pPB41-CRISPR::ylbL	This study
pPB81	pPB41-CRISPR::sodA	This study
pPB82	pPB72-ΔuvrA recombination template	This study
pPB83	pPB73-ΔuvrB recombination template	This study
pPB85	pPB74-ΔuvrC recombination template	This study
pPB86	pPB75-ΔyprA recombination template	This study
pPB87	pPB76-ΔyprB recombination template	This study
pPB98	pPB77-ΔylbK recombination template	This study
pPB99	pPB78-ΔylbL recombination template	This study
pPB103	pPB81-ΔsodA recombination template	This study
pPB107	pPB47-amyE::Pxyl-ylbK-camR	This study
pPB108	pPB47-amyE::Pxyl-ylbL-camR	This study
pPB111	pPB47-amyE::Pxyl-ylbL-S234A-camR	This study
pPB113	pPB41-CRISPR::queA	This study
pPB114	pPB41-CRISPR::ctpA	This study
pPB115	pPB41-CRISPR::ysoA	This study
pPB116	pPB41-CRISPR::ylmE	This study
pPB117	pPB41-CRISPR::sepF	This study
pPB118	pPB41-CRISPR::ylmG	This study
pPB120	pPB113-ΔqueA recombination template	This study
pPB121	pPB114-ΔctpA recombination template	This study
pPB122	pPB115-ΔysoA recombination template	This study
pPB123	pPB116-ΔylmE recombination template	This study
pPB124	pPB117-ΔsepF recombination template	This study
pPB125	pPB118-ΔylmG recombination template	This study
pPB130	pPB41-CRISPR::ytmP	This study
pPB131	pPB41-CRISPR::bcrC	This study
pPB132	pPB41-CRISPR::ecsA	This study
pPB133	pPB41-CRISPR::ecsB	This study
pPB140	pPB130-ΔytmP recombination template	This study
pPB141	pPB131-ΔbcrC recombination template	This study
pPB142	pPB132-ΔecsA recombination template	This study
pPB143	pPB133-ΔecsB recombination template	This study
pPB149	pPB77-ΔylbK recombination template-2	This study
pPB154	pPB41-CRISPR::walH	This study
pPB155	pPB41-CRISPR::yycI	This study
pPB156	pPB41-CRISPR::yycJ	This study
pPB157	pPB12-ylbL-36-341	This study
pPB173	pPB47-amyE::Pxyl-ylbL-K279A-camR	This study
pPB174	pPB154-ΔwalH recombination template	This study

pPB175	pPB155-ΔyycI recombination template	This study
pPB176	pPB156-ΔyycJ recombination template	This study
pPB177	pPB41-CRISPR::ruvB	This study
pPB178	pPB41-CRISPR::ripX	This study
pPB179	pPB177-ΔruvB recombination template	This study
pPB180	pPB178-ΔripX recombination template	This study
pPB181	pPB12-ylbL-36-341-S234A	This study
pPB184	pPB47-amyE::Pxyl-ctpA-camR	This study
pPB185	pPB47-amyE::Pxyl-ctpA-S297A-camR	This study
pPB186	pPB47-amyE::Pxyl-ctpA-K322A-camR	This study
pPB194	pDR110-Phyp-yneA	This study
pPB200	pET28b-MBP-6xHis-Ulp1-403-621	This study
pPB203	pET28b-MBP-Smt3-ctpA-38-466	This study
pPB204	pPB12-yneA-28-103	This study
pPB214	pET28b-MBP-Smt3-ctpA-38-466-S297A	This study
pPB227	pPB41-CRISPR::fhuG	This study
pPB228	pPB41-CRISPR::yfkH	This study
pPB229	pPB41-CRISPR::ltaSA	This study
pPB230	pPB41-CRISPR::ykgA	This study
pPB231	pPB41-CRISPR::cgeE	This study
pPB232	pPB41-CRISPR::ysnF	This study
pPB233	pPB41-CRISPR::lytG	This study
pPB234	pPB41-CRISPR::yxaB	This study
pPB237	pPB227-fhuG	This study
pPB238	pPB228-yfkH	This study
pPB239	pPB229-ltaSA	This study
pPB240	pPB230-ykgA	This study
pPB241	pPB231-cgeE	This study
pPB242	pPB232-ysnF	This study
pPB243	pPB233-lytG	This study
pPB244	pPB234-yxaB	This study
pPB267	pU-T18-YneA	This study
pPB268	pU-T18-YneAΔN	This study
pPB270	pK-T25-YlbL-S234A	This study
pPB271	pK-T25-CtpA-S297A	This study

Table 2.7 Plasmids used in this study.

Primer	Sequence
oPEB3F	GCTAGCCGCATGCAAGCTAATTCG
oPEB54	ggcattgatggacgcatttgtg

oPEB55	gtttcaatcgcttgtgtttgggtttc
oPEB56	ACCTCCAATCTGTTCGCGGTG
oPEB57	taaTCGAGCACCACCACCACCAC
oPEB58	GCTAGTTATTGCTCAGCGG
oPEB116	ctctcgtttcatcggtatcattac
oPEB117	cgcttcgttaatacagatgtaggt
oPEB217	GAACCTCATTACGAATTCAGCATGC
oPEB218	GAATGGCGATTTTCGTTCGTGAATAC
oPEB227	CCGTCAATTGTCTGATTCGTTA
oPEB232	GCTGTAGGCATAGGCTTGGTTATG
oPEB234	GTATTCACGAACGAAAATCGCCATTCCTAGCAGCACGCCATAGTGACTG
oPEB241	aaacGCGCTATTTCTCCAATGGACGGCATCGGACg
oPEB242	aaaacGTCCGATGCCGTCCATTGGAGAAATAGCGC
oPEB243	GCATGCTGAATTCGTAATGAGGTTCcttttaattacgggtgctgtttct
oPEB244	cccatggatcgctttttcctccgttcttttatccccctagaataaacctggcatg
oPEB245	tattctagggggataaaagaacggaggaaaaagcgatccatgggt
oPEB246	GCATAACCAAGCCTATGCCTACAGCactctcctcttctgcactcaagtt
oPEB253	GAAGGGTAGTCCAGAAGATAACGA
oPEB259	ATGTATACCTCCTTAGTCGACTAAGCTTAATTGTTATCCGCTCACAATTACACACATTAT GCCACACCTTGTAGATA
oPEB267	TACGTTATTAGTTATAGTTActaacggattcaccactccaag
oPEB268	AACCCTTGCATAGGGGGATCgcctcgtgatacgcctatttttat
oPEB269	TAACTATAACTAATAACGTAACGTGACTGGCAAG
oPEB270	GATCCCCCTATGCAAGGGTTTATTGT
oPEB286	GCATGCTGAATTCGTAATGAGGTTCaagcacaatggggtaaaataagag
oPEB287	GCATAACCAAGCCTATGCCTACAGCggtattcctaaaattccgctgata
oPEB312	ACTCTTTCCCTACACGACGCTCTTCCGATCTNN
oPEB313	AGATCGGAAGAGCGTCGTGTAGGGAAAGAGTGTAGAT
oPEB314	AATGATACGGCGACCACCGAGATCTACACTCTTTCCCTACACGACGCTCTTC
oPEB315	CAAGCAGAAGACGGCATACGAGATATCACGGTGACTGGAGTTCAGACGTGTGCTCTTCCG ATCAGACCGGGGACTTATCATCCAACCTGT
oPEB316	CAAGCAGAAGACGGCATACGAGATCGATGTGTGACTGGAGTTCAGACGTGTGCTCTTCCG ATCAGACCGGGGACTTATCATCCAACCTGT
oPEB317	CAAGCAGAAGACGGCATACGAGATTTAGGCGTGACTGGAGTTCAGACGTGTGCTCTTCCG ATCAGACCGGGGACTTATCATCCAACCTGT
oPEB318	CAAGCAGAAGACGGCATACGAGATTGACCAGTGACTGGAGTTCAGACGTGTGCTCTTCCG ATCAGACCGGGGACTTATCATCCAACCTGT
oPEB319	CAAGCAGAAGACGGCATACGAGATACAGTGGTGACTGGAGTTCAGACGTGTGCTCTTCCG ATCAGACCGGGGACTTATCATCCAACCTGT
oPEB320	CAAGCAGAAGACGGCATACGAGATGCCAATGTGACTGGAGTTCAGACGTGTGCTCTTCCG ATCAGACCGGGGACTTATCATCCAACCTGT
oPEB321	CAAGCAGAAGACGGCATACGAGATCAGATCGTGACTGGAGTTCAGACGTGTGCTCTTCCG ATCAGACCGGGGACTTATCATCCAACCTGT

oPEB322	CAAGCAGAAGACGGCATACGAGATACTTGAGTGACTGGAGTTCAGACGTGTGCTCTTCCG ATCAGACCGGGGACTTATCATCCAACCTGT
oPEB323	CAAGCAGAAGACGGCATACGAGATGATCAGGTGACTGGAGTTCAGACGTGTGCTCTTCCG ATCAGACCGGGGACTTATCATCCAACCTGT
oPEB324	CAAGCAGAAGACGGCATACGAGATTAGCTTGTGACTGGAGTTCAGACGTGTGCTCTTCCG ATCAGACCGGGGACTTATCATCCAACCTGT
oPEB325	CAAGCAGAAGACGGCATACGAGATGGCTAGGTGACTGGAGTTCAGACGTGTGCTCTTCCG ATCAGACCGGGGACTTATCATCCAACCTGT
oPEB326	CAAGCAGAAGACGGCATACGAGATCTTGTAGTGACTGGAGTTCAGACGTGTGCTCTTCCG ATCAGACCGGGGACTTATCATCCAACCTGT
oPEB345	actcctttgtttatccaccgaac
oPEB348	TTATTTTTGACACCAGACCAACTG
oPEB368	CGACGGCCAGTGAATTGTAATACG
oPEB369	CAGGAAACAGCTATGACCATG
oPEB370	cacctacatctgtattaacgaagcgTCAATGGGGAAGAGAACCGCTTAAG
oPEB377	ggtaatgataccgatgaaacgagagAACAAAATTCTCCAGTCTTCACATCG
oPEB383	atgtatacctccttaggatcccatttcc
oPEB417	aaacGCTATGGATCGGATAGAGGTGAAGGGAGCCg
oPEB418	aaaacGGCTCCCTTCACCTCTATCCGATCCATAGC
oPEB419	GCATGCTGAATTCGTAATGAGGTTCCTTCTTGATTATTTCCCAGACGAT
oPEB420	taacagagggttttgttcaTCATCCTTCCGCTTTTAG
oPEB421	CTAAAAGCGGAAGGATGAtgaacaaaaccctctgttaagaggggacagcttgtcggcaag tccatccttgggcttagcaggcaagctttttctttac
oPEB422	GCATAACCAAGCCTATGCCTACAGCgaagactttgtaattgcggaaaac
oPEB423	ATATGATCTTGAAATGATGCGTGA
oPEB424	agaatgaatcgtgaaatgatcacc
oPEB425	CGCCGATAAAATAACGAAGTCTAT
oPEB426	aaacGCTTTGAGTTAGTCTCGAAATATCAGCCCCg
oPEB427	aaaacGGGGCTGATATTTCGAGACTAACTCAAAGC
oPEB428	GCATGCTGAATTCGTAATGAGGTTCtagtctcttgaagctggttgtcct
oPEB429	ATCCGATCCATAGCCATttgttcaaaaaataagcctccgtttctttaacg
oPEB430	ttaaagaaacggaggcttatttttgaacaaATGGCTATGGATCGGAT
oPEB431	GCATAACCAAGCCTATGCCTACAGCGCATTCTCCTTCAATGACAAATCT
oPEB432	acggatcgatatgattctctaagc
oPEB433	TACAGCACTTTATCCAGTTGATGC
oPEB434	ctgaggagggtttttgttgattac
oPEB437	aaacAGAAAAACTCGCCCTCCTTCCTGATCAACCg
oPEB438	aaaacGGTTGATCAGGAAGGAGGGCGAGTTTTTCT
oPEB439	GCATGCTGAATTCGTAATGAGGTTCcaatgtcagtcgtcttacttacgc
oPEB440	cagatcttatttaaaaggacaacaatgttacccttccttatgtttaatcct
oPEB441	attaaacataaggaagggtaacattgttgtccttttaaataagatctgataaaatg
oPEB442	GCATAACCAAGCCTATGCCTACAGCtgtcgtaatttcacaatcctctgt
oPEB443	aaaccggaatccttcagacaatac

oPEB444	cttctaacggcacttggtaatttt
oPEB445	gtaaaatgattgcacctgttcttg
oPEB446	aaacATCACTGACTGAACTCATTTCTGATTTAAAg
oPEB447	aaaacTTTAAATCAGAAATGAGTTCAGTCAGTGAT
oPEB448	GCATGCTGAATTCGTAATGAGGTTCcgagttgattaggttctgaaatcc
oPEB449	TAATGACATatccggcctccctcctctttacacctctttgtcaagtac
oPEB450	gtacttgacaaagaggtgtaaagaggagggaggccggatATGTCATTA
oPEB451	GCATAACCAAGCCTATGCCTACAGCCATTATGATGCAGGACACCTTTTA
oPEB452	tcttgtcatgcttgtaaaggtagc
oPEB453	CTGGTCCTCAAACGATTTTTCTAT
oPEB454	agaaaatgatgggagaaggaatag
oPEB455	aaacAAGGGAAACTCCAACGGATGAAAAAGCACAg
oPEB456	aaaacTGTGCTTTTTCATCCGTTGGAGTTTCCCTT
oPEB457	GCATGCTGAATTCGTAATGAGGTTCTCCCAGGAAAATGTCGTTATAGTT
oPEB458	gggaatatatccggcctccctccTTACGACA
oPEB459	AATGTCGTAAggagggaggccggatatattccccgggaaagcgcaaaagacgacttgtttcgccatgaatttt
oPEB460	GCATAACCAAGCCTATGCCTACAGCatggtgtgatgacagctaccttta
oPEB461	AGCCATGGAAGTCAGTGATATTCT
oPEB462	tctttattcggttctttccagttc
oPEB463	GTACGTCATTGCACTACGGAGAC
oPEB466	aaacCGGGTTAGCGTTAGGATCGGGAGGGGCCAGg
oPEB467	aaaacCTGGCCCCTCCCGATCCTAACGCTAACCCG
oPEB468	GCATGCTGAATTCGTAATGAGGTTCcataagaagcgtttgaacagaaga
oPEB469	CTAAAATGTTTTTTACGTAGCAAaagcgttaacctcctgcctgaatt
oPEB470	gaattcaggcaggaggttaacgcttTTGCTACGTAAAAAACATTTTAGCTGGAT
oPEB471	GCATAACCAAGCCTATGCCTACAGCAATATCGTAGCCTTTTGTTTCGTC
oPEB472	aaaacagacaaaacatcagtcagc
oPEB473	ACTGCGTTCTTATAATCGGAATTG
oPEB474	gcataaaaggctcaagcaaaac
oPEB475	aaacCATAAtTTGCTACGTAAAAAACATTTTAGCg
oPEB476	aaaacGCTAAAATGTTTTTTACGTAGCAAaTTATG
oPEB477	GCATGCTGAATTCGTAATGAGGTTCagcagtacctgtcctcttgattct
oPEB478	aatgtatagaaaaagcacctgagaaaTTATGAGCCCTCCCAATTCTCTAT
oPEB479	ATAGAGAATTGGGAGGGCTCATAAtttctcaggtgctttttctatacattt
oPEB480	GCATAACCAAGCCTATGCCTACAGCccagtatgtgacctcgattctaac
oPEB481	TACATAAGCACCAAATTGAAGTGG
oPEB482	agaaacagcacagcttattgatga
oPEB483	GAGAAAAGATTGTGTTCCGAAAAG
oPEB492	tgatgttctttttcctcctattcg
oPEB493	acgatattgccgtattcctcttat
oPEB504	aaacCGTACGATGCTTTAGAACCGCATATCGACAg
oPEB505	aaaacTGTCGATATGCGGTTCTAAAGCATCGTACG

oPEB506	GCATGCTGAATTCGTAATGAGGTTCaacaggacagagagcaaaaataca
oPEB507	ataatgaggaccttgtttgtgccagataattcctccttagtatatatgtac
oPEB508	catatatactaaggaggaattatctggcacaaacaaggtcctcattat
oPEB509	GCATAACCAAGCCTATGCCTACAGCagctcgctgtttgtctcaataaat
oPEB510	attgattttacggtccctgtactt
oPEB511	gcaaagtagtaggcaaagaaggaa
oPEB512	gtttattaatcgggccttttgtc
oPEB527	TAAAAGACAGGGTAAGGAAATGGA
oPEB557	taaCGGTTTCCATATGGGGATTGGTG
oPEB558	aatgggatcctaaggaggtatacatTTGGCCAAACCTAAAATCGGGTTAG
oPEB559	ACCAATCCCCATATGGAAACCGttaTTATGAGCCCTCCCAATTCTCTATT
oPEB560	aatgggatcctaaggaggtatacatTTGCTACGTAAAAAACATTTTAGCTG
oPEB561	ACCAATCCCCATATGGAAACCGttaTCAGGTGCTTTTCGCTTTCAGCTT
oPEB566	AATCGAAAATATTGGCGGCCCGGCTGCAGGGTTAATGATGTCCCTTGA
oPEB567	CAAGGGACATCATTAACCCTGCAGCCGGGCCGCCAATATTTTCGA
oPEB574	cattcttccgacataaattgtgag
oPEB575	attagtggtggctgttgctttatc
oPEB577	aaacTACCAGAACGTTTAATTGCACAAGTACCGTg
oPEB578	aaaacACGGTACTTGTGCAATTAAACGTTCTGGTA
oPEB579	GCATGCTGAATTCGTAATGAGGTTCgattgttgctaatgaaatgggagt
oPEB580	ttgatgaggcctcctgttctcaaagatgatttcacctttattctagtctt
oPEB581	gactagaataaaggtgaaatcatctttgagaacaggaggcctcatc
oPEB582	GCATAACCAAGCCTATGCCTACAGCgcatttttcatattgagtcgtcct
oPEB583	gtatatcgggcagcataaggtaaa
oPEB584	actcttctctgaaatcacccagac
oPEB585	cccgatatgactgaatttcctaa
oPEB586	aaacACGGAGCAATTAAAGGAATGATTCAATCACg
oPEB587	aaaacGTGATTGAATCATTCCTTTAATTGCTCCGT
oPEB588	GCATGCTGAATTCGTAATGAGGTTCcccctcctatcctgactttctatc
oPEB589	cgcggcagccgcgtatggtttttttaaacaccacctttttcttcttac
oPEB590	aagaagaaaaaggtggtgtttaaaaaaaaccatacgcggctgccgc
oPEB591	GCATAACCAAGCCTATGCCTACAGCtatgggtcattatgctgtttatgg
oPEB592	acgactttaccttgatggtttttg
oPEB593	gttgctctttacacattcttcagc
oPEB594	ggatacagcaaatgtcctaaataagc
oPEB595	aaacATGATACTGAATCCGATCTTCACTTAGGGAg
oPEB596	aaaacTCCCTAAGTGAAGATCGGATTCAGTATCAT
oPEB597	GCATGCTGAATTCGTAATGAGGTTCacatgatcaaagggaagaaggtag
oPEB598	gcgctttcaactatatggcgcgatacctatattcctttcaggcatttatt
oPEB599	taaatgcctgaaaggaatataggtatcgcgccatatagttgaaagc
oPEB600	GCATAACCAAGCCTATGCCTACAGCagttaattcagcaagtgtttccac
oPEB601	cgtgcttatgaatatatgggattg
oPEB602	aacaagctcttcacgcaatttag

oPEB603	cattcgctgatattttccatca
oPEB604	aaacTCACAAAATATGTATCACCTGAAAGAGCACg
oPEB605	aaaacGTGCTCTTTCAGGTGATACATATTTTGTGA
oPEB606	GCATGCTGAATTCGTAATGAGGTTCtaagtgaaccacatgcataaacct
oPEB607	TTTCAGTTTATTTTTCATACTCATgatcttttatgcctccttcattcc
oPEB608	ggaatgaaggaggcataaaagatcATGAGTATGAAAAATAAACTGAAAAACTTT
oPEB609	GCATAACCAAGCCTATGCCTACAGCccacctccatttttacatttcagt
oPEB610	aggtaaaggatgtcgtcaatgtct
oPEB611	cgtaatcttttctgacttgggcta
oPEB612	cctcagatatttacgctgttattgg
oPEB613	aaacAATATATTGAGACAGAGCGGGAATCTCATGg
oPEB614	aaaacCATGAGATTCCCGCTCTGTCTCAATATATT
oPEB615	CGAAAAAACTTGATAAAGGATCATTGCTGTACACCCCCTGTTTCAT
oPEB616	AAATGAAACAGGGGGTGTACAGCAATGATCCTTTATCAAGTTTTTTCGGT
oPEB617	GAAGTCATTCCATTCATACAGGAG
oPEB618	aaacTTTGCCCTGATCATATATATTTTTATGTCAg
oPEB619	aaaacTGACATAAAAATATATATGATCAGGGCAAA
oPEB620	ccaagcccctatcaaactgtcacactcgctTTACCACCTCTGATGTTC
oPEB621	GAACATCAGAGGTGGTAAagcgagtgtgacagtttgataggggcttg
oPEB622	TCCTCTAAAGTGGTGTTGAGTGAG
oPEB623	tctaaaaagtcggtcagcttcatc
oPEB624	GCATAACCAAGCCTATGCCTACAGCccaaaacctctgatagacagca
oPEB638	aaacTTGGGAGATCTTCCCCGCCGGAGGAGCTACg
oPEB639	aaaacGTAGCTCCTCCGGCGGGGAAGATCTCCCAA
oPEB640	GCATGCTGAATTCGTAATGAGGTTCcaagccagtccatcaattatgtc
oPEB641	aaggctaatcgtttctagtctatccagcgaatg
oPEB642	aaaggcattcgctggatagactagaaacgattagccttaattctaaaatattttaagaaa tgatgggtcaggaatacgaatccatttgct
oPEB643	GCATAACCAAGCCTATGCCTACAGCaaaagttcaagtagacccgtttca
oPEB644	gatatgtttcgtgacgctgtaaaa
oPEB645	tactcaaataaacctcggttgtcc
oPEB646	agacccaacagaaatcaagaaaac
oPEB647	aaacCTCATCACAATTCAGTTCTCGATTCCATTAg
oPEB648	aaaacTAATGGAATCGAGAACTGAATTGTGATGAG
oPEB649	GCATGCTGAATTCGTAATGAGGTTCctcgcttaaaaagaaattcggatac
oPEB650	ttcagacgccggcttttgtctttcataatcacctttacatttttatatttagtag
oPEB651	tataaaaatgtaaaaggtgattatgaaagacaaaagccggcgtctgaa
oPEB652	GCATAACCAAGCCTATGCCTACAGCcgtagagcaaggtgacaaagtaaa
oPEB653	cttccattattatcggcatcatc
oPEB654	tcgactgtgtatcaatctctttcc
oPEB655	aaatagaaattgtggtcagcaagg
oPEB656	aaacTCGGTAAAAGACTTGACCGGCGGATATACAg
oPEB657	aaaacTGTATATCCGCCGGTCAAGTCTTTTACCGA

oPEB658	GCATGCTGAATTCGTAATGAGGTTCgttttgcgatagaggaagagatgt
oPEB659	CAAATATCAAGCATATTATTCATaagtttctccccttatagtgtttttc
oPEB660	aaaaacactataaggggagaaacttATGAATAATATGCTTGATATTTGGCAG
oPEB661	GCATAACCAAGCCTATGCCTACAGCCTGACAAGAATGCCCAAATAATC
oPEB662	attatgatctctccctgttttcca
oPEB663	GTAATGAAAATGGCAAACACAGTC
oPEB664	acttgtttaatgcctaacgattcc
oPEB665	aaacATATGCTTGATATTTGGCAGTCGCGGCTGCg
oPEB666	aaaacGCAGCCGCGACTGCCAAATATCAAGCATAT
oPEB667	GCATGCTGAATTCGTAATGAGGTTCggccttgtttttggtactatgaag
oPEB668	gtcatttgattacctcttttcagtaTTATTCATGGCCAGCGTCTTCCTT
oPEB669	AGGAAGACGCTGGCCATGAATAAtactgaaaagaggtaatcaaatgacag
oPEB670	GCATAACCAAGCCTATGCCTACAGCgaacagccagagcgagtctatt
oPEB671	atgtccagaaccctgtctctttat
oPEB672	ggcgaggattttgcttattactta
oPEB673	TGAAGCAGAAGGTTATGATTATGTG
oPEB677	TGGTGGTGGTGGTGGTGCTCGAttaTCAGGTGCTTTTCGCTTTCAGCT
oPEB709	TATTTCTTTTCTTATCTTGCTGATTTTGGCCAAagcgttaacctcct
oPEB710	caggaggttaacgctTTGGCCAAAATCAGCAAGATAAGAAAAGAAATAGAGAA
oPEB738	aaacACCCAAAAGCTGTCTGAAACGGTAAGGCCAg
oPEB739	aaaacTGGCCTTACCGTTTCAGACAGCTTTTGGGT
oPEB740	GCATGCTGAATTCGTAATGAGGTTCttagtggaacagcaggattctatg
oPEB741	CTTCCTCAATAAATCCTTTGTAATTTCACGCTTCATcccaatcatcct
oPEB742	gaggatgattgggATGAAGCGTGAAATTACAAAGGATTTATTGAGGAAGGAGG
oPEB743	GCATAACCAAGCCTATGCCTACAGCtactcgaccgtaattctccatacc
oPEB744	cttagaaatgccgattacgagttt
oPEB745	tctaaaatcgtactctccaaagca
oPEB746	tctatatcagcgtgaaggatgaag
oPEB747	aaacGTATGAAGGCTTGAATAAGGAAGCAACAGAg
oPEB748	aaaacTCTGTTGCTTCCTTATTCAAGCCTTCATAC
oPEB749	GCATGCTGAATTCGTAATGAGGTTCaatcagcaaactaccggaacatta
oPEB750	tcatgtttgtctcactccattatttTCACTTATTCCACTCCACtgttagc
oPEB751	ggggctaacaGTGGAGTGGAATAAGTGAaaataatggagtgagacaaacatga
oPEB752	GCATAACCAAGCCTATGCCTACAGCggatcggtgtcgtataagtcaaat
oPEB753	agtcgtttgaatacagttcgtttg
oPEB754	taatccaccatattccatcctttc
oPEB755	ccgattaaaacaagtgaaacagag
oPEB756	aaacGGACGCCGGTTTGAGCGGAAAAGCCATGGAg
oPEB757	aaaacTCCATGGCTTTTCCGCTCAAACCGGCGTCC
oPEB758	GCATGCTGAATTCGTAATGAGGTTCtcgttgccttcctcattttagata
oPEB759	aatagtcatgatttacatagaaaaagtttgtctcactccattattttcattg
oPEB760	atgaaaataatggagtgagacaaacttttttctatgtaaatcatgactattctagg
oPEB761	GCATAACCAAGCCTATGCCTACAGCcaatgaccttcccatccatattta

oPEB762	ccgattacaaaggatttattgagg
oPEB763	cctttccgtatctctctaaatcctc
oPEB764	aattacggtcgagtacgagaaaaa
oPEB771	CCCGATCGGCGGCATTGATCAAGCTGTCGTCGCCGCAGACAAAGCC
oPEB772	CGGCTTTGTCTGCGGCGACGACAGCTTGATCAATGCCGCCGATCGG
oPEB773	GGCTCACCGCGAACAGATTGGAGGTACAGAGCTTGCTTCATTGATAAAAG
oPEB780	gaaagagctaggggaaatggtag
oPEB781	gccatagctcttcttttgtgatct
oPEB782	aaatcttgcagtcatcatcgaagt
oPEB783	gattcagcatatttcccagtacaa
oPEB786	gtattccatgtgatgaggttatcg
oPEB787	cttcatctgtaataaaggggttg
oPEB788	gtacgaggagattgaggttgagat
oPEB789	tcgaatataggcctgcaatttaac
oPEB790	taaaggacaacaacactggtgaaa
oPEB791	ttccttctcaactagcccattatc
oPEB792	aggacagcatattgttcttgatgt
oPEB793	cgtccaccacttcttttacttttatc
oPEB794	aatggcttcatctatcatctctcc
oPEB795	tctctgccaaatgaatgaatactg
oPEB796	ggagcctgatttttcacatctact
oPEB797	atttctccgaattcatcatcgt
oPEB798	aaacTAGATGCGGCGAAAATGAGACAGGAGACGCg
oPEB799	aaaacGCGTCTCCTGTCTCATTTTCGCCGCATCTA
oPEB800	GCATGCTGAATTCGTAATGAGGTTCattgatttagaaaggctggaaagc
oPEB801	taatgatcttaggaaatTCAGTCATgaacatcaccTTACTTTAATAGTTTTTG
oPEB802	AAACTATTAAAGTAAggtgatgttcATGACTGAatttcctaagatcattatg
oPEB803	GCATAACCAAGCCTATGCCTACAGCatattatgctcttccacttcatcg
oPEB804	aggtcaacgggtatatcggtgtat
oPEB805	ccgccattttctcttactttgtt
oPEB806	AGAAAGGCTTGAAAAGCAAACA
oPEB807	aaacTACATATTATCCAATACTTAAAGCATTTGAg
oPEB808	aaaacTCAAATGCTTTAAGTATTGGATAATATGTA
oPEB809	GCATGCTGAATTCGTAATGAGGTTCaactgcactcatccagctataaac
oPEB810	ttggaaataatgagaaacttcaatattttctgtcgctctaaacaaaaaagccgcagccac ctgcggtcttgatctactccccgttttggt
oPEB811	gagcgacagaaaatattgaagtttc
oPEB812	GCATAACCAAGCCTATGCCTACAGCccttctccgtcgtaaatatcagag
oPEB813	ttagcgctgatttcatctctcttt
oPEB814	aagctcagacccgtaaaatcttct
oPEB815	tataactggaaccatagggaaagg
oPEB817	aatgggatcctaaggaggtatacatTTGAAACGGCAATTAAAACTGTTTTTTATTG
oPEB818	ACCAATCCCCATATGGAAACCGttaTTACATTTCTTTTTTCAGTGTTTCAATTGC

oPEB819	AATGACGGTACAGCAGCTGCAGCCGAAATTATGGCCGCTGCCCTTCATGAATCGTCAAAC
oPEB820	CAGCGGCCATAATTTCGGCTGCAGCTGCTGTACCGTCATTTACTAAAACG
oPEB821	GTTAATCGGCGAGACGACATTCGGCGCTGGTACAGTACAAACGGCAAAAGAATATG
oPEB822	ATATTCTTTTGCCGTTTGTACTGTACCAGCGCCGAATGTCGTCTCGCCGATTAA
oPEB831	AGGCTCACCGCGAACAGATTGGAGGTAGCACAGGAGACAGCAAGTTCGAC
oPEB832	GTGGTGGTGGTGGTGGTGCTCGAttaTTACATTTCTTTTTTCAGTGTTTCAATTGC
oPEB833	GGTAAATGGAAAAAGCGTAAAAGG
oPEB835	ACCCATGGTATATCTCCTTCTTAAA
oPEB836	AAGAAGGAGATATACCATGGGTgaagaaggtaaactggtaatctggattaacggcgataa aggctataacggtctcgctgaagtcggtaagaaattcgagaaagataccggaattaaagt caccgttgagcatccggataaactggaagagaaattcccacaggttgcggcaactggcga tggccctgacattatcttctgggcacacgaccgctttggtggctacgctcaatctggcct gttggctgaaatcaccccggacaaagcgttccaggacaagctgtatccgtttacctggga tgccgtacgttacaacggcaagctgattgcttacccgatcgctgttgaagcgttatcgct gatttataacaaagatctgctgccgaacccgccaaaaacctgggaagagatcccggcgct ggataaagaactgaaagcgaaaggtaagagcgcgctgatgttcaacctgcaagaaccgta cttcacctggccgctgattgctgctgacgggggttatgcgttcaagtatgaaaacggcaa gtacgacattaaagacgtgggcgtggataacgctggcgcgaaagcgggtctgaccttcct ggttgacctgattaaaaacaaacacatgaatgcagacaccgattactccatcgcagaagc tgcctttaataaaggcgaaacagcgatgaccatcaacggcccgtgggcatggtccaacat cgacaccagcaaagtgaattatggtgtaacggtactgccgaccttcaagggtcaaccatc caaaccgttcgttggcgtgctgagcgcaggtattaacgccgccagtccgaacaaagagct ggcaaaagagttcctcgaaaactatctgctgactgatgaaggtctggaagcggttaataa agacaaaccgctgggtgccgtagcgctgaagtcttacgaggaagagttggcgaaagatcc acgtattgccgccactatggaaaacgcccagaaaggtgaaatcatgccgaacatcccgca gatgtccgctttctggtatgccgtgcgtactgcggtgatcaacgccgccagcggtcgtca gactgtcgatgaagccctgaaagacgcgcagactaattcgagctcgGGTGGTGGTGGTTC TGGTGGTGGTGGTTCTGGGTCCCTGCAGGACTCAGAAGTCAATCAAGAAGCTAAGCCAGA GGTCAAGCCAGAAGTCAAGCCTGAGACTCACATCAATTTAAAGGTGTCCGATGGATCTTC AGAGATCTTCTTCAAGATCAAAAAGACCACTCCTTTAAGAAGGCTGATGGAAGCGTTCGC TAAAAGACAGGGTAAGGAAATGGACTCCTTAAGATTCTTGTACGACGGTATTAGAATTCA AGCTGATCAGGCCCCTGAAGATTTGGACATGGAGGATAACGATATTATTGAGGCTCACCG CGAACAGATTGGAGGT
oPEB837	aagtatgaaaacggcaagtacga
oPEB838	TTTAAGAAGGAGATATACCATGGGTgaagaaggtaaactggtaatctgga
oPEB839	cgagctcgaattagtctgcgcgtc
oPEB840	gaaagacgcgcagactaattcgagctcgGGTGGTGGTGGTTCTGGTGGTGGTGGTTCTat gcggggttctcatcatcatc
oPEB841	TGGTGGTGGTGGTGGTGCTCGAttattattttaaagcgtcggttaaaatcaaatg
oPEB842	AGGCTCACCGCGAACAGATTGGAGGTAGCGGCCAAGAGCTTAATCAGTAT
oPEB843	TGGTGGTGGTGGTGGTGCTCGAttaCTATCTTACAGTTGCTAATTCATATG
oPEB856	CTTAGTCGACTAAGGAGGTATACATATGAGTAAAGAATCTATTATTTTTGTCGGT
oPEB857	GAATTAGCTTGCATGCGGCTAGCttaCTATCTTACAGTTGCTAATTCATATG
oPEB866	TTTATGCAGCAATGGCAAGAAC
oPEB867	GCCGACTCAAACATCAAATCTTAC
oPEB912	aaacAAGCGTGTCTCAAAATGAACTTGCCGAGCCg
oPEB913	aaaacGGCTCGGCAAGTTCATTTTGAGACACGCTT

oPEB914	GCATGCTGAATTCGTAATGAGGTTCcaaattatacatgatcttcggcttc
oPEB915	aatgaattcatattcggccccctccttacagccctctcctttcacgacgt
oPEB916	gcacgtcgtgaaaggagagggctgtaaggaggggggccgaatatgaattca
oPEB917	GCATAACCAAGCCTATGCCTACAGCcaagtcatatgtcaagcatacagg
oPEB918	atatacggactgcatcagaagaaa
oPEB919	tttcttcttggacacaacgatct
oPEB920	actggttggcatgcttattgtagt
oPEB921	aaacTCTGCGTCTAATGGAATGAATGCGATCGTCg
oPEB922	aaaacGACGATCGCATTCATTCCATTAGACGCAGA
oPEB923	GCATGCTGAATTCGTAATGAGGTTCagagaaataggggcaaagaatagg
oPEB924	tgaaccgaagttcgtttatagggtgcggtcgtctcacctcgcatgtttga
oPEB925	tgatcaaacatgcgaggtgagacgaccgcaccctataaacgaacttcggt
oPEB926	GCATAACCAAGCCTATGCCTACAGCcgtggctttttgttttctttctac
oPEB927	tccatcctttctatgcgcaatata
oPEB928	acctgtctatttatgggctttcct
oPEB929	tcactgtacaaaagcaacccagag
oPEB930	aaacCATTCTCAAGCGCCGTCTTCTTTTTAGGACg
oPEB931	aaaacGTCCTAAAAAGAAGACGGCGCTTGAGAATG
oPEB932	GCATGCTGAATTCGTAATGAGGTTCgtgatgatgtcgtgatgtttatcc
oPEB933	atgcgcccgctcaaggctctttttcatcatttacctgctctttatatcctg
oPEB934	aggcaggatataaagagcaggtaaatgatgaaaaagagccttgagcgg
oPEB935	GCATAACCAAGCCTATGCCTACAGCcatacttgttgtccttgattccac
oPEB936	tactattcgatttcaagctctcca
oPEB937	caccaaatagcttcctaaaagacc
oPEB938	aaggcacacatgacaaaagaaatc
oPEB939	aaacCGTTGAGGTCGTCCTTTTGCCCGTTCGCGAg
oPEB940	aaaacTCGCGAACGGGCAAAAGGACGACCTCAACG
oPEB941	GCATGCTGAATTCGTAATGAGGTTCcaatacgggtacagtgcttttaat
oPEB942	aaaacatgaaaaaggggaagattctttgtttttcctcctaaagtgtgaag
oPEB943	cttcacactttaggaggaaaaacaaagaatcttccccttttcatgttttg
oPEB944	GCATAACCAAGCCTATGCCTACAGCcctggctgttatctgtaaaatcatc
oPEB945	gtttcctaattggtcaatgtttgc
oPEB946	ttccttctgtcgacactctttctac
oPEB947	gtattatggttgttcgtgtcaagc
oPEB948	aaacGTTCAGCTCCATGATACGTTTCCATTGGAGg
oPEB949	aaaacCTCCAATGGAAACGTATCATGGAGCTGAAC
oPEB950	GCATGCTGAATTCGTAATGAGGTTCgccgttcgttacttaatctcattc
oPEB951	ccaaatggtttgtgcaaacgcctattgaacgtctccttttttatgacctat
oPEB952	gtataggtcataaaaaggagacgttcaataggcgtttgcacaaaccatttg
oPEB953	GCATAACCAAGCCTATGCCTACAGCtttaatcatggtgtccagttcatc
oPEB954	caagagttttcacataagcctgaa
oPEB955	cacttcatctgcaataaaaagcac
oPEB956	gattacgtggaaacgatctgaa

oPEB957	aaacCAGAAGTCAATCAAGCTATCGATGCACATCg
oPEB958	aaaacGATGTGCATCGATAGCTTGATTGACTTCTG
oPEB959	GCATGCTGAATTCGTAATGAGGTTCactccctctggaatgtactcctc
oPEB960	aggttttttgttgtcggtctatgatttatcaatctcctcctttatgaatttgca
oPEB961	tgcaaattcataaaggaggagattgataaatcatagaccgacaacaaaaaacct
oPEB962	GCATAACCAAGCCTATGCCTACAGCtgttgaagggtatattgctgaaga
oPEB963	caactttccgcagcagtactatc
oPEB964	gagctgaaaggtatcgaaaaagaa
oPEB965	gaagaaattgtgagacggctttat
oPEB966	aaacGCATCACAATTGCTCAGGCCATTCTCGAATg
oPEB967	aaaacATTCGAGAATGGCCTGAGCAATTGTGATGC
oPEB968	GCATGCTGAATTCGTAATGAGGTTCgtttgctcattggtctattgattg
oPEB969	gaattaaaaataccagtaaaaagggcgaaaaccttccttcgaattaaaagat
oPEB970	atcttttaattcgaaggaaggttttcgccctttttactggtatttttaattc
oPEB971	GCATAACCAAGCCTATGCCTACAGCctagattttggaagcatgagagaa
oPEB972	atttctcaggagcatctcattctt
oPEB973	cgctatgcttacggtctttatttt
oPEB974	cgaaggcaactgtcaaatcata
oPEB975	aaacATGAATACATTGAGATTATGGATTATGCGAg
oPEB976	aaaacTCGCATAATCCATAATCTCAATGTATTCAT
oPEB977	GCATGCTGAATTCGTAATGAGGTTCctcatcactacaacaaggggaac
oPEB978	ccccgggggagggcagtctttttcgtatctgcgtcctccttctgggat
oPEB979	aattcatcccagaaggaggacgcagatacgaaaaagactgccctcccccg
oPEB980	GCATAACCAAGCCTATGCCTACAGCgcagggtttttattatccttcctt
oPEB981	gatcatagagcaagttgtcacagg
oPEB982	ccattcagcatctgtttcatttac
oPEB983	ggatcaatttcccgagacagta
oPEB1014	TTGGCCTTGTCCTTGACCTTCACCGGGATCCTCTAGAGTCGACCCTG
oPEB1015	TAActaagaattcggccgtcgttt
oPEB1017	TTGGCCTTGTCCTTGACCTTCACCCTCTAGAGTCGACCTGCAGTGG
oPEB1018	TAActaagtaatatggtgcactctcagt
oPEB1021	ATTATGCCGCATCTGTCCAACT
oPEB1022	gcaaggcgattaagttgggtaa
oPEB1024	TTCTCGCCGGATGTACTGGAAAC
oPEB1025	tggcttaactatgcggcatcaga
oPEB1034	CTAGAGGGTGAAGGTCAAGGACAAGGCCAAATGAGTAAAGAATCTATTATTTTTGTCGGT

oPEB1035	gtactgagagtgcaccatattacttagTTACTATCTTACAGTTGCTAATTCATATGCA
oPEB1036	TAGAGGGTGAAGGTCAAGGACAAGGCCAAATGAGTAGCGGCCAAGAGCTTAATCAGT
oPEB1039	GGATCCCGGTGAAGGTCAAGGACAAGGCCAATTGCTACGTAAAAAACATTTTAGCTGGA
oPEB1040	acgttgtaaaacgacggccgaattcttagTTATCAGGTGCTTTTCGCTTTCAGCTT
oPEB1041	ATCCCGGTGAAGGTCAAGGACAAGGCCAATTGAAACGGCAATTAAAACTGTTTTTTATTG
oPEB1042	gttgtaaaacgacggccgaattcttagTTATTACATTTCTTTTTTCAGTGTTTCAATTGC

Table 2.8 Oligonucleotides used in this study.

Supplemental text

Supplemental Results

ylbK disruption results in a polar effect on *ylbL*

We noticed that *ylbK*, the gene upstream of *ylbL*, had a phenotype similar to *ylbL* in the Tn-seq experiments **(Tables 2.2, 2.3, & 2.4)**. Therefore, we tested whether *ylbKL* functioned together in the DNA damage response. Deletion of *ylbK* resulted in sensitivity to MMC **(Fig 2.14A)**. Ectopic expression of *ylbK* failed to complement the Δ*ylbK* phenotype **(Fig 2.14A)**. Given that *ylbK* is upstream of *ylbL* we attempted to complement the Δ*ylbK* phenotype using *ylbL* and found that sensitivity to MMC was rescued **(Fig 2.14A)**. Closer examination of the *ylbKL* locus revealed that a putative ribosome binding site (RBS) for *ylbL* translation was present within the 3′ end of *ylbK* **(Fig 2.14B)**. Thus, a second deletion of *ylbK* was made (Δ*ylbK-2*) which included deletion of the codons for all but the first 3 and the last 14 amino acids, leaving the RBS for *ylbL* intact **(Fig 2.14B)**. This deletion was not sensitive to MMC **(Fig 2.14A)**. Western blotting revealed that the initial Δ*ylbK* strain did not express YlbL, whereas Δ*ylbK-2* did **(Fig 2.14C)**. We conclude that disruption of *ylbK* results in a polar effect on *ylbL*, indicating that YlbL functions independently of YlbK.

In order to better understand the prevalence of false positives in Tn-seq experiments we attempted to validate the MMC phenotypes of the forty genes with the lowest relative fitness

values in the second growth period of the experiment. Intriguingly, we found that seven additional genes, *queA*, *ylmG*, *lgt*, *ylmE*, *sdaAB*, *cymR*, and *ywrC*, resulted in no sensitivity to MMC when deleted **(Table 2.3)**. We also found that the genomic loci of *queA*, *cymR*, *ylmG*, *ylmE*, and *sdaAB*, were proximal to genes with validated phenotypes **(Table 2.3)**. The other two genes, *ywrC* and *lgt* have less obvious explanations. For *lgt* it is possible that the polar effect is on the upstream gene *hprK*, which codes for the kinase HprK that phosphorylates Crh (71). Deletion of *crh* resulted in sensitivity to MMC **(Table 2.3)**, but we did not detect *hprK* in our Tn-seq experiments. Finally, *ywrC* does not have a clear explanation. We could not identify validated mutant phenotypes or essential genes proximal to *ywrC*. It is possible that the transposon resulted in increased expression of neighboring genes that resulted in sensitivity to MMC, and that increased expression is not duplicated in the deletion mutant, though other explanations exist. Taken together, our results underscore the importance of validating results from forward genetic screens.

Cell wall metabolism genes are sensitive to DNA damage

Our forward genetic screens identified several cell wall metabolism genes as being sensitive to DNA damaging agents, including *walH*, *yycI*, *walJ*, *ponA*, and *brcC* **(Tables 2.2 & 2.3)**. We validated that deletion mutants were indeed sensitive to MMC **(Table 2.3)**. These genes have not previously been implicated in the DNA damage response, though it is possible that they function in regulating cell division. Specifically, the genes *walH* and *yycI* are negative regulators of the essential two-component system WalRK (72-75). A recent publication provided evidence that the WalRK system interacts with components of the divisome (76). Further, a study of *walJ* found that WalJ likely coordinates cell division with DNA replication (77). As a result, it is tempting to speculate that WalRK and the associated WalHIJ represent one of the connections between DNA replication, the DNA damage response, cell wall metabolism, and cell division.

Supplemental Materials and Methods

Transposon insertion mutant library construction

Extraction of PY79 chromosomal DNA

Cell pellets (10 mL OD_{600} = 1 equivalent) from stationary phase cultures were re-suspended in lysis buffer (50 mM Tris, pH 8.0, 10 mM EDTA, pH 8.0, 1% (v/v) Triton X-100, 0.5 mg/mL RNase A, 1 mg/mL lysozyme) and incubated at 37°C for 30 minutes. Proteins were digested by addition of 40 µL 10 mg/mL proteinase K (dissolved in TE buffer plus 10% glycerol) and 30 µL of 10% SDS and incubated at 55°C for 30 minutes. 600 µL of PB buffer (5 M guanidine-HCl, and 30% (v/v) isopropanol) were added, mixed well by pipetting and added directly to a silica spin column (Epoch life sciences) and centrifuged at 12,000 *g* for 1 minute at room temperature. The column was washed with 500 µL PB buffer, then 750 µL PE buffer (10 mM Tris, pH 7.5, and 80% (v/v) ethanol), centrifuging as above to remove buffer. The column was dried by centrifugation as above. Chromosomal DNA was eluted by adding 100 µL ultra-pure water and centrifugation as above.

Purification of Himar1-C9 transposase

Himar1-C9 was purified as described previously (78). *E. coli* TB1 cells with plasmid pMalC9 (Strain PEB234) were struck out on LB + 100 µg/mL ampicillin and incubated at 37°C overnight. An overnight starter culture was grown in LB + 100 µg/mL ampicillin at 37°C. The starter culture was diluted 1:100 and incubated at 37°C until OD_{600} = 0.5 and Himar1-C9 was induced by addition of IPTG to a final concentration of 0.3 mM. The culture was incubated for 2 hours at 37°C. Cells were collected via centrifugation: 5,000 *g* for 20 minutes at 4°C. Cell pellets were re-suspended in 20 mL ice-cold column buffer (CB; 20 mM Tris, pH 7.5, 200 mM NaCl, 1 mM EDTA, and 1x Roche protease inhibitors). Cells were lysed via French press, and the lysate was clarified via centrifugation: 18,000 rpm (Sorvall SS-34 rotor) for 30 minutes at 4°C. The lysate was loaded onto 1 mL amylose resin (NEB) pre-equilibrated with CB, and placed on a rotator at 4°C for 1 hour. Resin was collected via centrifugation: 3,000 *g* for 10 minutes at 4°C. The supernatant was removed and the resin was washed with 4 volumes wash buffer (20 mM Tris, pH 7.5, 200 mM NaCl, 1 mM EDTA, 2 mM DTT, and 10% (v/v) glycerol) five times by re-suspending the resin, then collecting via centrifugation and aspirating the wash buffer. The column was eluted by adding 0.8 volume of elution buffer (20 mM Tris-HCl, pH 7.5, 200 mM

NaCl, 1 mM EDTA, 2 mM DTT, 10% (v/v) glycerol, and 10 mM maltose) and incubating on ice for 5 minutes and agitating frequently. The protein was analyzed via SDS-PAGE and concentration was determined using a Bradford assay. The protein was aliquoted, frozen in liquid nitrogen and stored at -80°C.

Transposition reaction

A transposon insertion library was constructed *in vitro* as described with minor modifications (61). A 50 µL transposition was prepared: 3 µg chromosomal DNA, 1 µg PCR product mariner transposon (The mariner transposon was PCR amplified from pCJ41 using primers oPEB368/369 and Q5 DNA polymerase (NEB)), 10 µL 5x Buffer A (102.5 mM HEPES pH 7.9, 47.5% glycerol, 467.5 mM NaCl, 47.5 mM $MgCl_2$, 1.19 mg/mL BSA, 9.5 mM DTT), 100 nM Himar1-C9. Reactions were incubated at 30 °C for 16 hours. DNA was precipitated via addition of 0.1 volume sodium acetate, pH 5.2 and 2.5 volume 100% ice-cold ethanol. DNA was collected via centrifugation: 16,000g for 20 minutes at 4°C. DNA pellet was washed with 5 volumes (relative to reaction volume) ice-cold 70% ethanol and pelleted again via centrifugation: 16,000g for 10 minutes at 4°C. The ethanol wash was aspirated and the DNA pellet was dried at room temperature. The transposon junctions were repaired by re-suspending the DNA pellet in the following 50 µL reaction: 1x T_4 DNA ligase buffer (Lucigen), 1 mg/mL BSA (NEB), 0.5 mM dNTPs, 1 mM ATP, 50 mM NaCl, 6 units T_4 DNA polymerase exo- (Lucigen), and 480 units T_4 DNA ligase (Lucigen), and incubating at room temperature for 2 hours. The reactions were mixed by pipetting every 30 minutes over the 2 hour incubation. The reactions were moved to 16°C for 16 hours, and then stored at 4°C until used to transform PY79.

Transformation of PY79

PY79 was struck out on LB agar and incubated at 37°C overnight. A single colony was used to inoculate a 2 mL LM culture (LB + 3 mM $MgSO_4$) in a 14 mL round bottom culture tube. The culture was incubated at 37°C on a rolling rack until OD_{600} of about 1.5. Then, 40 µL of the LM culture was transferred to 1.2 mL pre-warmed MD media (1x PC buffer (107 g/L K_2HPO4, 60 g/L KH_2PO_4, 11.8 g/L trisodium citrate dihydrate), 2% glucose, 50 µg/mL phenylalanine, 50 µg/mL tryptophan, 11 µg/mL ferric ammonium citrate, 2.5 mg/mL potassium aspartate, 3 mM $MgSO_4$) and incubated on a rolling rack at 37°C for 6 hours. To each 1.2 mL

competent cell culture, 15 µL of the transposase reaction were added, and the cultures were incubated on a rolling rack at 37°C for an additional 1.5 hours. Transformations were plated on LB agar + 100 µg/mL spectinomycin (200 µL per 100 cm plate, and 124 plates in total), and incubated at 37°C overnight. The Library consisted of approximately 900,000 transformants, which were pooled in 1x $S7_{50}$ salts + 15% glycerol with a resulting OD_{600} of approximately 37.0. The library was distributed into 1 mL aliquots, frozen in liquid nitrogen, and stored at -80°C.

Tn-seq experimental details

Tn-seq experiments were designed with multiple growth periods similar to a prior description (28). The experiment was performed using triplicate samples for each condition, which originated from three aliquots of the transposon insertion library. The experiment was initiated by thawing three aliquots of the transposon insertion library in a beaker of water at 37°C. Each aliquot of the thawed library was used to inoculate 50 mL starter cultures in 500 mL beakers. For the MMC experiment 270 µL were used to inoculate, and 500 µL were used for the MMS and phleomycin experiment. The three starter cultures were incubated with shaking (200 rpm) at 30°C until OD_{600} of about 0.8. Starter cultures were used to inoculate paired 25 mL cultures in 250 mL flasks at an OD_{600} = 0.05 for control or treatment. For the MMC experiment, MMC was added to a final concentration of 15 ng/mL and an equal volume of the vehicle in which MMC was dissolved (25% v/v DMSO) was added to the control flasks. For MMS, a final concentration of 50 µg/mL was used, and a final concentration of 25 ng/mL was used for phleomycin. An equal volume of water was used for the vehicle control in the MMS and phleomycin experiment. The paired cultures were incubated with shaking (200 rpm) at 30°C until OD_{600} of about 1.5 (growth period 1). Then the cultures were back diluted into fresh control or treatment media at an OD_{600} = 0.05, and incubated with shaking (200 rpm) at 30°C until OD_{600} of about 1.5 (growth period 2). The cultures were back diluted as above one more time and grown as above (growth period 3). At all steps of the experiment three samples of OD_{600} = 10 were saved as cell pellets, and each sample was serially diluted and plated for viable cells in triplicate to estimate the number of cells at the start and end of the growth periods **(Table 2.1)**, which were used in the fitness calculations.

Tn-seq sequencing library construction

Sequencing libraries were prepared similar to previous reports (35, 61), with some modifications in adaptor sequences to increase compatibility with standard Hi-seq reagents. Genomic DNA was extracted from each sample as described in "Extraction of PY79 genomic DNA." A 200 µL restriction digest using MmeI was assembled for each sample as follows: 6 µg gDNA, 1x Cutsmart buffer (NEB), 64 µM SAM (NEB), 12 units MmeI (NEB). Reactions were incubated at 37°C for 4 hours. CIP (20 units) was added and the reactions were incubated at 37°C for 1 hour. MmeI was heat inactivated by incubating at 65°C for 30 minutes, and the digested genomic DNA was extracted by addition of 600 µL of PB buffer and binding to a silica spin-column. The column was washed with 500 µL PB, then 750 µL PE buffer, and then eluted with 65 µL ultra-pure water. Adaptors (oPEB312/313) were annealed in 1x annealing buffer (10 mM Tris, pH 8.0, 100 mM NaCl, 10 µM EDTA) at a concentration of 25 mM each, by boiling at 100°C for 5 minutes, followed by transferring to a beaker of 100°C water which was allowed to cool slowly to room temperature. The adaptors were ligated to the digested genomic DNA in two 40 µL reactions, each containing 30 µL of the eluate from above, 1x T_4 DNA ligase buffer (NEB), 2.5 µM annealed adaptors, and 800 units T_4 DNA ligase (NEB). Reactions were left at room temperature for 30 minutes, and then transferred to 16°C for 16 hours. The resulting reactions were pooled for each sample, and the DNA was extracted via spin-column as above, but the PB wash was excluded, and the sample was eluted with 100 µL ultra-pure water. Transposon/genomic DNA junctions were PCR amplified in two 50 µL reactions each containing 4 µL of eluate from the previous step, 1x Q5 DNA polymerase buffer (NEB), 200 µM dNTPs, 400 nM forward primer (oPEB314), 400 nM reverse primer with multiplexing barcode (one of oPEB315-326), and 1 unit of Q5 DNA polymerase (NEB). The reactions were cycled as follows: 1) 98°C for 3 minutes; 2) 98°C for 30 seconds; 3) 55°C for 30 seconds; 4) 72°C for 30 seconds; 5) repeat steps 2-4 for 18 cycles; 6) 72°C for 2 minutes; 7) hold at 4°C. The reactions were separated on a 2.5% agarose gel and the reaction product at approximately 160 bp was excised. The DNA was extracted by dissolving the gel slice in 400 µL QG buffer (5.5 M guanidine thiocyanate and 20 mM Tris, pH 6.6) by heating at 65°C, and then 250 µL of isopropanol were added and the mixture was added to a silica spin-column. The column was washed with PB and PE buffer as above, and eluted with 120 µL ultra-pure water. The eluate was submitted for

sequencing using a Hi-seq 2500 instrument on high output mode with v3 (MMC experiment) or v4 reagents (MMS and phleomycin experiment).

Tn-seq data analysis

The 50 bp sequencing reads were trimmed to 43 bp using Fastx Trimmer, because the sequencing reaction went outside of the inverted repeat, and those seven base pairs could not be aligned to our reference database. The trimmed reads were aligned to a reference database in which every TA site found in the PY79 genome was placed adjacent to the transposon sequence (reference database fasta file and sequencing data accession number GSE109366) using bwa (79). The reads were imported into the R statistical software package RStudio (RStudio 80) for further analysis. Each transposon insertion site was provided a coverage value where each read was equal to a coverage of one. Each transposon insertion site was indexed to its position in the genome and the gene or intergenic region in which it resides. Fitness was calculated for each insertion for the control and the treatment using the equation:

$$W = \frac{\ln \frac{(N_f \cdot F_f)}{N_0 \cdot F_0}}{\ln \frac{N_f(1 - F_f)}{N_0(1 - F_0)}}$$

where N_0 and N_f are the number of bacteria at the start and end of the growth period, respectively, and F_0 and F_f are the transposon frequency in the population as measured by Illumina sequencing (insertion coverage divided by total reads in the sample), respectively (35) **(also see Fig 2.1C)**. The ratio of treatment to control was calculated and defined as the relative fitness **(see Fig 2.1C)**. For each gene (or intergenic region), the insertions containing less than 10 reads were removed and any gene without at least 12 insertions from the combined triplicate data were also removed, thus requiring that each gene have at least 4 insertions in each replicate to be included in the analysis. Each gene's average relative fitness was then calculated by determining the mean relative fitness of all insertion sites within each gene. We trimmed insertions in our fitness calculation that were in the upper or lower five percent of the data for that gene, reasoning that not all insertions will be a true representation of a null allele. A t-test was used to determine if the gene relative fitness differed significantly from one. P-values were adjusted for multiple comparisons using the method of Benjamini and Hochberg (37).

Proteomics experimental details

Ms Bioworks processed samples as described below. Submitted samples were washed three times with PBS. The washed pellets were suspended in modified RIPA buffer (2% SDS, 150 mM NaCl, 50 mM Tris HCl pH 8) and lysed using mechanical disruption in a Next Advance Bullet Blender using 1.0mm silica beads, setting 8 for 3 minutes. The lysate was centrifuged at 10,000 g for 10 minutes. Protein concentrations were determined by Qubit fluorometry. 20 µg of each sample was processed by SDS-PAGE using a 10% Bis-Tris NuPAGE gel (Invitrogen) with the MES buffer system; the gel was electrophoresed approximately 5 cm. The mobility region was excised into 20 equal sized segments for further processing by in-gel digestion. In-gel digestion was performed on each submitted sample using a robot (ProGest, DigiLab) with the following protocol: 1) Washed with 25mM ammonium bicarbonate followed by acetonitrile. 2) Reduced with 10mM dithiothreitol at 60°C followed by alkylation with 50mM iodoacetamide at room temperature. 3) Digested with trypsin (Promega) at 37°C for 4h. 4) Quenched with formic acid and the supernatant was analyzed directly without further processing.

Each gel digest was analyzed by nano LC-MS/MS with a Waters NanoAcquity HPLC system interfaced to a ThermoFisher Q Exactive. Peptides were loaded on a trapping column and eluted over a 75µm analytical column at 350 nL/min; both columns were packed with Luna C18 resin (Phenomenex). The mass spectrometer was operated in data-dependent mode, with the Orbitrap operating at 60,000 FWHM and 17,500 FWHM for MS and MS/MS, respectively. The fifteen most abundant ions were selected for MS/MS.

Proteomics data analysis

Data were processed as described by MS Bioworks. Data were searched using a local copy of Mascot with the following parameters: Enzyme: Trypsin/P; Database: UniProt *Bacillus subtilis* (concatenated forward and reverse plus common potential contaminants); Fixed modification: Carbamidomethyl (C); Variable modifications: Oxidation (M), Acetyl (N-term), Pyro-Glu (N-term Q), Deamidation (N/Q); Mass values: Monoisotopic; Peptide Mass Tolerance: 10 ppm; Fragment Mass Tolerance: 0.02Da; Max Missed Cleavages: 2. Mascot DAT files were parsed into Scaffold (Proteome Sciences) for validation, filtering and to create a non-redundant list per sample. Data were filtered using at 1% protein and peptide FDR and requiring at least

two unique peptides per protein. A student's t-test was performed to determine if wild-type and the double mutant levels were significantly different ($\alpha = 0.05$).

Protein purification

YlbL

YlbL for antibody production was purified as follows. 10xHis-Smt3-YlbL (a.a 36-341) was expressed from plasmid pPB157 in *E. coli* NiCo21 cells (NEBC2529H). One liter LB + 50 µg/mL kanamycin cultures were inoculated with an overnight culture (1:100) and grown at 37°C with shaking (200 rpm) until OD_{600} of about 0.5. Cultures were iced briefly and IPTG was added to 0.5 mM and incubated at 20°C with shaking overnight. Cells were harvested via centrifugation: 4,000 *g* for 20 minutes at 4°C. Cell pellets were re-suspended in lysis buffer (50 mM potassium phosphate pH 8.0, 300 mM NaCl, 5% (v/v) glycerol, and 20 mM imidazole). Cells were lysed via sonication and lysates were cleared via centrifugation: 18,000 rpm (Sorvall SS-34 rotor) for 45 minutes at 4°C. The supernatant was removed and incubated with Ni^{2+}-NTA-agarose (Qiagen) for 1 hour at 4°C. The lysate/bead slurry was loaded onto a gravity flow column and the beads were allowed to settle for 5-10 minutes. The lysate was collected as the flow-through. The column was washed with 50 column volumes wash buffer (50 mM potassium phosphate pH 8.0, 300 mM NaCl, 5% (v/v) glycerol, and 30 mM imidazole). YlbL was eluted from the column via digestion with 6xHis-Ulp1 in digestion buffer (50 mM potassium phosphate pH 8.0, 150 mM NaCl, 5% (v/v) glycerol, 1 mM DTT, and 10 mM imidazole) on a rotator at room temperature for 2 hours, yielding untagged YlbL (a.a. 36-341). The digestion buffer was collected as the flow-through and concentrated to approximately 5 mL using a 10 kDa Amicon centrifugal filter. YlbL was then loaded onto a HiLoad superdex 200-PG 16/60 column pre-equilibrated with SEC buffer (50 mM potassium phosphate pH 8.0, 150 mM NaCl, and 5% (v/v) glycerol) and the column was washed using SEC buffer at a flow rate of 1 mL/min. The peak fractions were pooled, glycerol was added to a final concentration of 20%, and concentrated using a 10 kDa Amicon centrifugal filter. Aliquots were frozen in liquid nitrogen, and stored at 80°C.

YlbL and YlbL-S234A were purified for *in vitro* assays as follows. 10xHis-Smt3-YlbL (a.a 36-341) and 10His-Smt3-YlbL-S234A (a.a. 36-341) were expressed from plasmids pPB157

and pPB181, respectively, as described above for antibody production. Cell pellets from a one liter culture were re-suspended in 30 mL lysis buffer (50 mM Tris pH 7.5, 250 mM NaCl, 10% sucrose, and 20 mM imidazole) and lysed via sonication. Cell lysates were clarified via centrifugation: 18,000 rpm (Sorvall SS-34 rotor) for 30 minutes at 4°C. Clarified lysates were applied to Ni^{2+}-NTA-agarose pre-equilibrated with lysis buffer. The column was washed with 20 column volumes wash buffer (25 mM Tris pH 8.0, 100 mM NaCl, 30 mM imidazole, and 5% glycerol). The Ni^{2+} column was eluted in four fractions of 1.2 column volumes using elution buffer (25 mM Tris pH 8.0, 100 mM NaCl, 10% glycerol, and 250 mM imidazole). Fractions 1-3 were pooled, DTT was added to 2.5 mM and 0.3 mg of Ulp1 was added. The elution was digested at 4°C overnight yielding untagged YlbL (a.a. 36-341) or untagged YlbL-S234A (a.a 36-341). The digest was desalted using a Zeba spin column into equilibration buffer (25 mM Tris pH 8.0, 50 mM NaCl, 5% glycerol, and 10 mM imidazole). The desalted digest was applied to a second column of Ni^{2+}-NTA-agarose and the flow-through was collected. The column was washed with one column volume of equilibration buffer. The flow-through and wash fractions were pooled and concentrated using a 10 kDa Amicon centrifugal filter. The concentrated protein was loaded onto a Sephacryl S-200 size exclusion column pre-equilibrated with SEC buffer (25 mM Tris pH 7.5, 5% glycerol, and 25 mM NaCl) and eluted over 1 column volume with SEC buffer at a flow rate of 1 ml/min. Peak fractions were pooled, glycerol was added to 20% and the final protein was concentrated using a 10 kDa Amicon centrifugal filter. The concentrated protein was aliquoted, frozen in liquid nitrogen, and stored at -80°C.

YneA

10xHis-Smt3-YneA (a.a. 28-103) was expressed from pPB204 and harvested as described for YlbL above. Cell pellets were re-suspended in lysis buffer (50 mM Tris pH 7.5, 250 mM NaCl, 10% (w/v) sucrose, 20 mM imidazole). Cells were lysed via sonication and the lysate was clarified as described for YlbL above. The clarified lysate was incubated with Ni^{2+}-NTA-agarose beads, pre-equilibrated with lysis buffer, and incubated on rotator at 4°C for 1 hour. The lysate/bead slurry was loaded into a gravity flow column and the beads were allowed to settle for 5-10 minutes. The lysate was collected as the flow-through. The column was washed with 30 column volumes wash buffer (25 mM Tris pH 7.5, 150 mM NaCl, 5% (v/v) glycerol, and 20 mM imidazole). The column was eluted in 6 fractions of 1 column volume each of elution

buffer (25 mM Tris pH 7.5, 150 mM NaCl, 10% (v/v) glycerol, 250 mM imidazole). The fractions with the highest protein concentration were pooled, DTT was added to 1 mM and digested with MBP-Ulp1 overnight at 4°C. The resulting digest, yielding untagged YneA (a.a. 28-103), was loaded onto a sephacryl S200 26/60 column pre-equilibrated with SEC buffer (25 mM Tris pH 8.0, 100 mM NaCl, and 5% (v/v) glycerol) and washed at a flow rate of 2 mL/min. The peak fractions were pooled, and glycerol was added to 20%. The protein was loaded onto a HiTrap Q column (GE life sciences), pre-equilibrated with 7.5% Q-finish buffer (25 mM Tris pH 8.0, 5% (v/v) glycerol, and 1 M NaCl) and 92.5% Q-start buffer (25 mM Tris pH 8.0, and 5% (v/v) glycerol). The column was washed with 5 column volumes 7.5% Q-finish buffer. The column was eluted with 30 column volumes over a linear gradient from 7.5% to 50% Q-finish buffer at a flow rate of 2 mL/min. Peak fractions were pooled, glycerol was added to a final concentration of 20%, and the protein was concentrated using a 3 kDa Amicon centrifugal filter. Aliquots were frozen in liquid nitrogen and stored at -80°C.

CtpA and CtpA-S297A

Expression conditions for CtpA fusions were similar to previous reports for CtpB (81). MBP-Smt3-CtpA and MBP-Smt3-CtpA-S297A were expressed in BL21 pLysY/LacIq (NEBC3013) cells from pPB203 and pPB214, respectively. A starter culture of LB + 50 μg/mL kanamycin was inoculated using several colonies from a fresh transformation and incubated at 37°C with shaking (200 rpm) until an OD_{600} = 0.5. One liter LB + 50 μg/mL kanamycin cultures were inoculated by diluting the starter culture 1:50 and incubated at 37°C until an OD_{600} of about 0.7. Glucose was added to 0.2% and expression was induced by addition of IPTG to 1 mM and incubating at 37°C for 45 minutes. Cells were harvested via centrifugation: 4,000 *g* for 20 minutes at 4°C. Cell pellets were re-suspended in 30 mL lysis buffer (50 mM Tris pH 7.5, 250 mM NaCl, 10% (w/v) sucrose) per one liter of culture and lysed via sonication. Lysates were clarified via centrifugation: 12,500 rpm (Sorvall SS-34 rotor) for 45 minutes at 4°C. Clarified lysates were mixed with pre-equilibrated 2.5 mL amylose resin (NEB) on a rotator at 4°C. The lysate/resin mixture was loaded into a gravity flow column and the resin was allowed to settle for 5-10 minutes. The lysate was allowed to flow over the packed resin. The column was washed with 20 column volumes of wash buffer (25 mM Tris pH 8.0, 100 mM NaCl, 10%(v/v) glycerol). The column was eluted with 4 fractions of 3 mL each in elution buffer (25 mM Tris pH 8.0, 100

mM NaCl, 10%(v/v) glycerol, and 50 mM maltose). Fractions 1-3 were pooled, DTT was added to 2 mM, and digested with MBP-Ulp1 overnight at 4°C. The resulting digest, yielding untagged CtpA (or CtpA-S297A), was diluted two-fold with Q-start buffer (25 mM Tris, pH 8.0, 5% glycerol) to bring the NaCl concentration to 50 mM, and loaded onto a HiTrap Q-column pre-equilibrated with 5% Q-finish buffer (25 mM Tris, pH 8.0, 1 M NaCl, 5% glycerol). The column was washed with 5 column volumes 5% Q-finish buffer. The column was eluted with 25 column volumes over a linear gradient from 5 to 50% Q finish buffer. The peak fractions were pooled, concentrated using a 30 kDa Amicon centrifugal filter, and loaded onto a sephacryl 16/60 S-200 column pre-equilibrated with SEC buffer (25 mM Tris pH 7.5, 25 mM NaCl, 5% glycerol). The column was washed with SEC buffer at a flow rate of 1 mL/min. Peak fractions were pooled, glycerol was added to 20%, and concentrated using a 30 kDa Amicon centrifugal filter. Aliquots were frozen in liquid nitrogen, and stored at -80°C.

6xHis-Ulp1

6xHis-Ulp1 was expressed from plasmid pPB13 in *E. coli* NiCo21 cells (NEBC2529H). One liter cultures of LB + 50 μg/mL kanamycin were inoculated with an overnight culture at 1:100 and grown at 37°C until OD_{600} of about 0.7. Cultures were induced with 0.5 mM IPTG and incubated at 37°C for 3 hours. Cells were pelleted via centrifugation: 4,000 *g* for 20 minutes at 4°C. Cells were re-suspended in lysis buffer (50 mM Tris pH 7.5, 300 mM NaCl, 5% (w/v) sucrose, and 20 mM imidazole) and lysed via sonication. Lysates were clarified via centrifugation: 18,000 rpm (Sorvall SS-34 rotor) for 45 minutes at 4°C. Clarified lysates were loaded onto Ni^{2+}-NTA-agarose beads pre-equilibrated with lysis buffer and incubated at 4°C for 1 hour on a rotator. The lysate was collected as the flow through and the column was washed with 25 column volumes wash buffer (25 mM Tris pH 7.5, 300 mM NaCl, and 20 mM imidazole). The column was eluted in elution buffer (25 mM Tris pH 7.5, 300 mM NaCl, and 250 mM imidazole). The most concentrated fractions were pooled; aliquots were frozen in liquid nitrogen, and stored at -80°C.

MBP-Ulp1

MBP-Ulp1 was expressed from pPB200 in *E. coli* BL21 DE3 cells. One liter LB + 50 μg/mL kanamycin cultures were inoculated with an overnight culture at 1:100. Cultures were

grown at 37°C until OD_{600} of about 0.5, glucose was added to 0.2%, and then protein expression was induced by addition of 0.25 mM IPTG. Cultures were incubated at 20°C overnight. Cells were pelleted via centrifugation: 4,000 *g* for 20 minutes at 4°C. Cell pellets were re-suspended in lysis buffer (50 mM Tris pH 7.5, 250 mM NaCl, 10% (w/v) sucrose, and 1 mM DTT), and lysed via sonication. Lysates were cleared via centrifugation and MBP-Ulp1 was purified on an amylose column as described for CtpA above. Peak fractions from the amylose column were loaded onto a sephacryl S200 26/60 column, pre-equilibrated with SEC buffer (25 mM Tris pH 7.5, 200 mM NaCl, 2% glycerol). The column was washed with SEC buffer at a flow rate of 2 mL/min. Peak fractions were pooled, glycerol was added to 20%, and DTT was added to 1 mM. MBP-Ulp1 was concentrated to about 1.7 mg/mL, aliquots were frozen in liquid nitrogen and stored at -80°C.

Strain construction

General strain construction methods

Generation of competent *B. subtilis* cultures for generating new genotypes was performed as described below in "Transposon insertion mutant library construction," or as previously reported (62).

Genome editing using CRISPR/Cas9 was performed as described previously (62, 82). *B. subtilis* strains were transformed with the indicated plasmid (prepared from *E. coli* MC1061), plated on LB agar + 100 μg/mL spectinomycin and incubated at 30°C overnight. Isolates were colony purified by restreaking on LB agar + 100 μg/mL spectinomycin and incubating at 30°C overnight. The editing plasmid was evicted by restreaking isolates on LB agar and incubating at 45°C for 8-12 hours or overnight. Loss of the editing plasmid was verified by restreaking LB agar + 100 μg/mL spectinomycin and on LB agar. Isolates that were unable to grow in the presence of spectinomycin were used for PCR genotyping.

Gene deletions using the *B. subtilis* knockout library were performed as described (83). Chromosomal DNA, extracted as described below (see extraction of PY79 chromosomal DNA), was used to transform PY79 or the indicated strain. Incorporation of the *erm* cassette at the appropriate locus was verified via PCR genotyping. Removal of the *erm* cassette was performed following transformation with pDR244, which contains *cre* recombinase. Eviction of pDR244

was performed as described for a CRISPR/Cas9 genome editing plasmid. Loss of the *erm* cassette was verified by sensitivity to erythromycin and PCR genotyping.

Integration of inducible constructs at the *amyE* locus was achieved via double crossover recombination. For constructs containing a xylose inducible promoter (P_{xyl}), strains were transformed with plasmids that had been digested with two unique restriction enzymes (KpnI-HF and ScaI-HF) or with genomic DNA of a strain already generated (see detailed strain construction) and transformants were selected using LB agar + 5 µg/mL chloramphenicol. Isolates were colony purified by restreaking on LB agar + 5 µg/mL chloramphenicol. Incorporation via double cross-over at *amyE* was determined by screening for an inability to utilize starch and by testing for the absence of a spectinomycin resistance cassette that is present on part of the plasmid that is not integrated. For constructs containing an IPTG inducible promoter (P_{hyp}), strains were transformed with plasmids that had been digested with two unique restriction enzymes (SpeI and SacI-HF) and transformants were selected using LB agar + 100 µg/mL spectinomycin. Isolates were colony purified by restreaking on LB agar + 100 µg/mL spectinomycin. Incorporation via double cross-over at *amyE* was determined by screening for an inability to utilize starch.

Individual strain construction

PEB85 (Δ*recN::erm*): PY79 was transformed with genomic DNA isolated from PEB75. Replacement of *recN* with the *erm* cassette was verified via PCR genotyping using oPEB54/55.

PEB235 (Δ*recR*): PY79 was edited using CRISPR/Cas9 genome editing with plasmid pPB46. Deletion of recR was verified via PCR genotyping using oPEB243/246.

PEB278 (Δ*rnhC*): PEB278 is a clonal isolate of JWS224, which was generated by deletion of *rnhC* from PY79 using the pMiniMAD method as described previously (62).

PEB307 (Δ*uvrA*): PY79 was edited using CRISPR/Cas9 genome editing with plasmid pPB82. Deletion of *uvrA* was verified via PCR genotyping using oPEB423/424.

PEB308 (Δ*uvrB*): PY79 was edited using CRISPR/Cas9 genome editing with plasmid pPB83. Deletion of *uvrB* was verified via PCR genotyping using oPEB432/433.

PEB310 (Δ*uvrC*): PY79 was edited using CRISPR/Cas9 genome editing with plasmid pPB85. Deletion of *uvrC* was verified via PCR genotyping using oPEB443/444.

PEB316 (Δ*yprA*): PY79 was edited using CRISPR/Cas9 genome editing with plasmid pPB86. Deletion of *yprA* was verified via PCR genotyping using oPEB452/453.

PEB318 (Δ*yprB*): PY79 was edited using CRISPR/Cas9 genome editing with plasmid pPB87. Deletion of *yprB* was verified via PCR genotyping using oPEB461/462.

PEB322 (Δ*ylbK*): PY79 was edited using CRISPR/Cas9 genome editing with plasmid pPB98. Deletion of *ylbK* was verified via PCR genotyping using oPEB472/473.

PEB324 (Δ*ylbL*): PY79 was edited using CRISPR/Cas9 genome editing with plasmid pPB99. Deletion of *ylbL* was verified via PCR genotyping using oPEB481/482.

PEB334 (Δ*sodA*): PY79 was edited using CRISPR/Cas9 genome editing with plasmid pPB103. Deletion of *sodA* was verified via PCR genotyping using oPEB510/511.

PEB346: PY79 was transformed with plasmid pPB111. This strain was only used to generate other strains using extracted genomic DNA.

PEB349: PEB324 was transformed with plasmid pPB108. This strain was only used to generate other strains using extracted genomic DNA.

PEB350: PY79 was transformed with plasmid pPB107. This strain was only used to generate other strains using extracted genomic DNA.

PEB353 (Δ*queA*): PY79 was edited using CRISPR/Cas9 genome editing with plasmid pPB120. Deletion of *queA* was verified via PCR genotyping using oPEB583/584.

PEB355 (Δ*ctpA*): PY79 was edited using CRISPR/Cas9 genome editing with plasmid pPB121. Deletion of *ctpA* was verified via PCR genotyping using oPEB592/593.

PEB357 (Δ*ysoA*): PY79 was edited using CRISPR/Cas9 genome editing with plasmid pPB122. Deletion of *ysoA* was verified via PCR genotyping using oPEB601/602.

PEB373 (Δ*ylbK, amyE::Pxyl-ylbK*): PEB322 was transformed with genomic DNA from PEB350. Retention of the Δ*ylbK* allele was verified via PCR genotyping oPEB472/473.

PEB375 (Δ*ylbL, amyE::Pxyl-ylbL*): PEB324 was transformed with genomic DNA from PEB349.

PEB377 (Δ*ylbL, amyE::Pxyl-ylbL-S243A*): PEB324 was transformed with genomic DNA from PEB346. Retention of the Δ*ylbL* allele was verified via PCR genotyping using oPEB481/482.

PEB382 (Δ*ylmE*): PY79 was edited using CRISPR/Cas9 genome editing with plasmid pPB123 as a Gibson assembly reaction because the plasmid was not able to be isolated from *E. coli*. Deletion of *ylmE* was verified via PCR genotyping using oPEB610/611.

PEB384 (Δ*sepF*): PY79 was edited using CRISPR/Cas9 genome editing with plasmid pPB124 as a Gibson assembly reaction because the plasmid was not able to be isolated from *E. coli*. Deletion of *sepF* was verified via PCR genotyping using oPEB612/623.

PEB386 (Δ*ylmG*): PY79 was edited using CRISPR/Cas9 genome editing with plasmid pPB125 as a Gibson assembly reaction because the plasmid was not able to be isolated from *E. coli*. Deletion of *ylmG* was verified via PCR genotyping using oPEB612/623.

PEB390 (Δ*ylbK, amyE::*P_{xyl}*-ylbL*): PEB322 was transformed with genomic DNA from PEB349. Retention of the Δ*ylbK* allele was verified via PCR genotyping using oPEB472/473. A wild-type *ylbL* locus was verified via PCR genotyping using oPEB481/482.

PEB392 (Δ*ylbK, amyE::*P_{xyl}*-ylbL-S243A*): PEB322 was transformed with genomic DNA from PEB346. Retention of the Δ*ylbK* allele was verified via PCR genotyping using oPEB472/473.

PEB418 (Δ*ytmP*): PY79 was edited using CRISPR/Cas9 genome editing with plasmid pPB140. Deletion of *ytmP* was verified via PCR genotyping using oPEB644/645.

PEB420 (Δ*bcrC*): PY79 was edited using CRISPR/Cas9 genome editing with plasmid pPB141. Deletion of *bcrC* was verified via PCR genotyping using oPEB653/654.

PEB422 (Δ*ecsA*): PY79 was edited using CRISPR/Cas9 genome editing with plasmid pPB142. Deletion of *ecsA* was verified via PCR genotyping using oPEB662/663.

PEB424 (Δ*ecsB*): PY79 was edited using CRISPR/Cas9 genome editing with plasmid pPB143. Deletion of *ecsB* was verified via PCR genotyping using oPEB671/672.

PEB427 (Δ*ylbK-2*): PY79 was edited using CRISPR/Cas9 genome editing with plasmid pPB149. Deletion of *ylbK-2* (deletion of amino acids 4-246; leaving amino acids 1-3 and 247-260) was verified via PCR genotyping using oPEB472/473.

PEB433 (Δ*yneA::erm*): PY79 was transformed using genomic DNA from PEB 432. Replacement of *yneA* with the *erm* cassette was verified via PCR genotyping using oPEB492/493.

PEB436 (Δ*ylbL,* Δ*yneA::erm*): PEB433 was edited using CRISPR/Cas9 genome editing with plasmid pPB99. Deletion of *ylbL* was verified via PCR genotyping using oPEB481/482.

PEB439 (Δ*yneA::loxP*): PEB433 was transformed with pDR244, which was then evicted.

PEB441 (Δ*ylbL,* Δ*yneA::loxP*): PEB436 was transformed with pDR244, which was then evicted.

PEB461 (Δ*crh::erm*): PY79 was transformed using genomic DNA from PEB 449. Replacement of *crh* with the *erm* cassette was verified via PCR genotyping using oPEB780/781.

PEB463 (Δ*lgt::erm*): PY79 was transformed using genomic DNA from PEB 450. Replacement of *lgt* with the *erm* cassette was verified via PCR genotyping using oPEB780/781.

PEB465 (Δ*crh::erm*): PY79 was transformed using genomic DNA from PEB 449. Replacement of *crh* with the *erm* cassette was verified via PCR genotyping using oPEB782/783.

PEB467 (Δ*sdaAB::erm*): PY79 was transformed using genomic DNA from PEB 452. Replacement of *sdaAB* with the *erm* cassette was verified via PCR genotyping using oPEB788/789.

PEB469 (Δ*ydzU::erm*): PY79 was transformed using genomic DNA from PEB 453. Replacement of *ydzU* with the *erm* cassette was verified via PCR genotyping using oPEB790/791.

PEB471 (Δ*radA::erm*): PY79 was transformed using genomic DNA from PEB 454. Replacement of *radA* with the *erm* cassette was verified via PCR genotyping using oPEB792/793.

PEB473 (Δ*cymR::erm*): PY79 was transformed using genomic DNA from PEB 455. Replacement of *cymR* with the *erm* cassette was verified via PCR genotyping using oPEB794/795.

PEB475 (Δ*ywrC::erm*): PY79 was transformed using genomic DNA from PEB 456. Replacement of *ywrC* with the *erm* cassette was verified via PCR genotyping using oPEB796/797.

PEB478 (Δ*recG::erm*): PY79 was transformed using genomic DNA from PEB 477. Replacement of *recG* with the *erm* cassette was verified via PCR genotyping using oPEB786/787.

PEB482 (Δ*walH*): PY79 was edited using CRISPR/Cas9 genome editing with plasmid pPB174. Deletion of *walH* was verified via PCR genotyping using oPEB744/745.

PEB485 (Δ*yycI*): PY79 was edited using CRISPR/Cas9 genome editing with plasmid pPB175. Deletion of *yycI* was verified via PCR genotyping using oPEB753/754.

PEB488 (Δ*walJ*): PY79 was edited using CRISPR/Cas9 genome editing with plasmid pPB176. Deletion of *walJ* was verified via PCR genotyping using oPEB762/763.

PEB491 (Δ*ruvB*): PY79 was edited using CRISPR/Cas9 genome editing with plasmid pPB179. Deletion of *ruvB* was verified via PCR genotyping using oPEB804/805.

PEB493 (Δ*ripX*): PY79 was edited using CRISPR/Cas9 genome editing with plasmid pPB180. Deletion of *ripX* was verified via PCR genotyping using oPEB813/814.

PEB533 (Δ*ylbL, amyE::*P_{xyl}*-ylbL-K279A*): PEB324 was transformed with plasmid pPB173.

PEB551 (Δ*ponA*): PY79 was transformed using genomic DNA from PEB 535. Replacement of *ponA* with the *erm* cassette was verified via PCR genotyping using oPEB574/575.

PEB555 (Δ*ylbL,* Δ*ctpA*): PEB324 was edited using CRISPR/Cas9 genome editing with plasmid pPB121. Deletion of *ctpA* was verified via PCR genotyping using oPEB592/593.

PEB557 (Δ*ylbL,* Δ*ctpA, amyE::*P_{xyl}*-ylbL*): PEB375 was edited using CRISPR/Cas9 genome editing with plasmid pPB121. Deletion of *ctpA* was verified via PCR genotyping using oPEB592/593.

PEB559 (Δ*yneA::loxP,* Δ*ctpA*): PEB439 was edited using CRISPR/Cas9 genome editing with plasmid pPB121. Deletion of *ctpA* was verified via PCR genotyping using oPEB592/593.

PEB561 (Δ*ylbL,* Δ*ctpA*, Δ*yneA::loxP*): PEB441 was edited using CRISPR/Cas9 genome editing with plasmid pPB121. Deletion of *ctpA* was verified via PCR genotyping using oPEB592/593.

PEB585 (Δ*uvrA,* Δ*yneA::loxP*): PEB439 was edited using CRISPR/Cas9 genome editing with plasmid pPB82. Deletion of *uvrA* was verified via PCR genotyping using oPEB423/424.

PEB595 (Δ*ylbL, amyE::*P_{xyl}*-ctpA*): PEB324 was transformed with plasmid pPB184.

PEB597 (Δ*ylbL, amyE::*P_{xyl}*-ctpA-S297A*): PEB324 was transformed with plasmid pPB185.

PEB599 (Δ*ctpA, amyE::*P_{xyl}*-ctpA*): PEB355 was transformed with plasmid pPB184.

PEB601 (Δ*ctpA, amyE::*P_{xyl}*-ctpA-S297A*): PEB355 was transformed with plasmid pPB185.

PEB603 (Δ*ctpA, amyE::*P_{xyl}*-ctpA-K322A*): PEB355 was transformed with plasmid pPB186.

PEB605 (Δ*ctpA, amyE::*P_{xyl}*-ylbL*): PEB355 was transformed with plasmid pPB108.

PEB607 (Δ*ctpA, amyE::*P_{xyl}*-ylbL-S234A*): PEB355 was transformed with plasmid pPB111.

PEB619 (Δ*ylbL,* Δ*ctpA, amyE::*P_{xyl}*-ctpA*): PEB555 was transformed with plasmid pPB184.

PEB621 (Δ*ylbL,* Δ*ctpA, amyE::*P_{xyl}*-ctpA-S297A*): PEB555 was transformed with plasmid pPB185.

PEB623 (Δ*ylbL,* Δ*ctpA, amyE::*P_{xyl}*-ylbL-S234A*): PEB555 was transformed with plasmid pPB111.

PEB677 (*amyE::*P_{hyp}*-yneA*): PY79 was transformed with plasmid pPB194.

PEB681 (Δ*ylbL, amyE::P_{hyp}-yneA*): PEB324 was transformed with plasmid pPB194.

PEB685 (Δ*ctpA, amyE::P_{hyp}-yneA*): PEB355 was transformed with plasmid pPB194.

PEB689 (Δ*ylbL,* Δ*ctpA, amyE::P_{hyp}-yneA*): PEB555 was transformed with plasmid pPB194.

PEB778 (Δ*fhuG*): PY79 was edited using CRISPR/Cas9 genome editing with plasmid pPB237. Deletion of *fhuG* was verified via PCR genotyping using oPEB918/919.

PEB780 (Δ*ylbL,* Δ*ctpA,* Δ*fhuG*): PEB555 was edited using CRISPR/Cas9 genome editing with plasmid pPB237. Deletion of *fhuG* was verified via PCR genotyping using oPEB918/919.

PEB782 (Δ*yfkH*): PY79 was edited using CRISPR/Cas9 genome editing with plasmid pPB238. Deletion of *yfkH* was verified via PCR genotyping using oPEB927/928.

PEB784 (Δ*ylbL,* Δ*ctpA,* Δ*yfkH*): PEB555 was edited using CRISPR/Cas9 genome editing with plasmid pPB238. Deletion of *yfkH* was verified via PCR genotyping using oPEB927/928.

PEB786 (Δ*ltaSA*): PY79 was edited using CRISPR/Cas9 genome editing with plasmid pPB239. Deletion of *ltaSA* was verified via PCR genotyping using oPEB936/937.

PEB788 (Δ*ylbL,* Δ*ctpA,* Δ*ltaSA*): PEB555 was edited using CRISPR/Cas9 genome editing with plasmid pPB239. Deletion of *ltaSA* was verified via PCR genotyping using oPEB936/937.

PEB790 (Δ*ykgA*): PY79 was edited using CRISPR/Cas9 genome editing with plasmid pPB240. Deletion of *ykgA* was verified via PCR genotyping using oPEB945/946.

PEB792 (Δ*ylbL,* Δ*ctpA,* Δ*ykgA*): PEB555 was edited using CRISPR/Cas9 genome editing with plasmid pPB240. Deletion of *ykgA* was verified via PCR genotyping using oPEB945/946.

PEB794 (Δ*cgeE*): PY79 was edited using CRISPR/Cas9 genome editing with plasmid pPB241. Deletion of *cgeE* was verified via PCR genotyping using oPEB954/955.

PEB796 (Δ*ylbL,* Δ*ctpA,* Δ*cgeE*): PEB555 was edited using CRISPR/Cas9 genome editing with plasmid pPB241. Deletion of *cgeE* was verified via PCR genotyping using oPEB954/955.

PEB798 (Δ*ysnF*): PY79 was edited using CRISPR/Cas9 genome editing with plasmid pPB242. Deletion of *ysnF* was verified via PCR genotyping using oPEB963/964.

PEB800 (Δ*ylbL,* Δ*ctpA,* Δ*ysnF*): PEB555 was edited using CRISPR/Cas9 genome editing with plasmid pPB242. Deletion of *ysnF* was verified via PCR genotyping using oPEB963/964.

PEB802 (Δ*lytG*): PY79 was edited using CRISPR/Cas9 genome editing with plasmid pPB243. Deletion of *lytG* was verified via PCR genotyping using oPEB972/973.

PEB804 (Δ*ylbL,* Δ*ctpA,* Δ*lytG*): PEB555 was edited using CRISPR/Cas9 genome editing with plasmid pPB243. Deletion of *lytG* was verified via PCR genotyping using oPEB972/973.

PEB806 (Δ*yxaB*): PY79 was edited using CRISPR/Cas9 genome editing with plasmid pPB244. Deletion of *yxaB* was verified via PCR genotyping using oPEB981/982.

PEB808 (Δ*ylbL,* Δ*ctpA,* Δ*yxaB*): PEB555 was edited using CRISPR/Cas9 genome editing with plasmid pPB244. Deletion of *yxaB* was verified via PCR genotyping using oPEB981/982.

PEB810 (Δ*ylbL,* Δ*ctpA,* Δ*ytmP*): PEB555 was edited using CRISPR/Cas9 genome editing with plasmid pPB140. Deletion of *ytmP* was verified via PCR genotyping using oPEB644/645.

Plasmid construction

General cloning techniques

Plasmids were assembled using Gibson assembly (84). Gibson assembly reactions were 10 or 12 µL consisting of 1x Gibson assembly master mix (0.1 M Tris pH 8.0, 5% PEG-8000, 10 mM $MgCl_2$, 10 mM DTT, 0.2 mM dNTPs, 1 mM NAD^+, 4 units/mL T_5 exonuclease, 25 units/mL Phusion DNA polymerase, 4,000 units/mL Taq DNA ligase) and 40-100 ng of each PCR product and incubated at 50°C for 60 minutes or 90 minutes for CRISPR/Cas9 editing plasmids. All PCR products were isolated via gel extraction from an agarose gel. Gibson assembly reactions were used to transform Top10 or MC1061 *E. coli*.

Plasmids that were intermediate products of editing plasmids containing only the targeting spacer were generated by ligation of the proto-spacer into pPB41 as described previously (62, 82). Briefly, pPB41 was digested with BsaI-HF (NEB), and then treated with CIP (NEB). The digestion product was purified by gel extraction from an agarose gel. Proto-spacers were annealed in 1x annealing buffer (10 mM Tris, pH 8.0, 100 mM NaCl, 10 µM EDTA) at a concentration of 10 µM each by incubation in a 100°C heat block for 5 minutes, followed by

transferring to a beaker of water pre-heated to 100°C. The annealing reactions were allowed to cool slowly to room temperature in the beaker of water. The annealed proto-spacers were phosphorylated using T_4 PNK (NEB). The phosphorylated proto-spacers were ligated to digested pPB41 using T_4 DNA ligase (NEB). The resulting ligations were used to transform Top10 or MC1061 *E. coli*. Plasmids sequences were verified by Sanger sequencing using oPEB253.

Individual plasmid construction

pPB44: A proto-spacer targeting *recR* (oPEB241/242) was ligated to pPB41.

pPB46: The upstream and downstream portions of the Δ*recR* editing template were PCR amplified using oPEB286/244 and oPEB245/287, respectively. CRISPR/Cas9 was PCR amplified using oPEB232/234 and pPB46 as the template. The pPB41 vector was PCR amplified using oPEB217/218. These four PCR products were used in a Gibson assembly reaction to generate a Δ*recR* editing plasmid. Clones were verified by Sanger sequencing with oPEB227 and oPEB253.

pPB47: pBR322 was PCR amplified using oPEB267/268, and the spectinomycin resistance cassette was PCR amplified from pDR110 using oPEB269/270. The resulting PCR products were used in a Gibson assembly reaction generating a plasmid in which the tetracycline resistance cassette of pBR322 had been replaced with the spectinomycin resistance cassette of pDR110.

pPB72: A proto-spacer targeting *uvrA* (oPEB417/418) was ligated to pPB41.

pPB73: A proto-spacer targeting *uvrB* (oPEB426/427) was ligated to pPB41.

pPB74: A proto-spacer targeting *uvrC* (oPEB437/438) was ligated to pPB41.

pPB75: A proto-spacer targeting *yprA* (oPEB446/447) was ligated to pPB41.

pPB76: A proto-spacer targeting *yprB* (oPEB455/456) was ligated to pPB41.

pPB77: A proto-spacer targeting *ylbK* (oPEB466/467) was ligated to pPB41.

pPB78: A proto-spacer targeting *ylbL* (oPEB475/476) was ligated to pPB41.

pPB81: A proto-spacer targeting *sodA* (oPEB504/505) was ligated to pPB41.

pPB82: The upstream and downstream portions of the Δ*uvrA* editing template were PCR amplified using oPEB419/420 and oPEB421/422, respectively. CRISPR/Cas9 was PCR amplified using oPEB232/234 and pPB72 as the template. The pPB41 vector was PCR amplified using oPEB217/218. These four PCR products were used in a Gibson assembly reaction to generate a Δ*uvrA* editing plasmid. Clones were verified by Sanger sequencing with oPEB227, oPEB253, and oPEB425.

pPB83: The upstream and downstream portions of the Δ*uvrB* editing template were PCR amplified using oPEB428/429 and oPEB430/431, respectively. CRISPR/Cas9 was PCR amplified using oPEB232/234 and pPB73 as the template. The pPB41 vector was PCR amplified using oPEB217/218. These four PCR products were used in a Gibson assembly reaction to generate a Δ*uvrB* editing plasmid. Clones were verified by Sanger sequencing with oPEB227, oPEB253, and oPEB434.

pPB85: The upstream and downstream portions of the Δ*uvrC* editing template were PCR amplified using oPEB439/440 and oPEB441/442, respectively. CRISPR/Cas9 was PCR amplified using oPEB232/234 and pPB74 as the template. The pPB41 vector was PCR amplified using oPEB217/218. These four PCR products were used in a Gibson assembly reaction to generate a Δ*uvrC* editing plasmid. Clones were verified by Sanger sequencing with oPEB227, oPEB253, and oPEB445.

pPB86: The upstream and downstream portions of the Δ*yprA* editing template were PCR amplified using oPEB448/449 and oPEB450/451, respectively. CRISPR/Cas9 was PCR amplified using oPEB232/234 and pPB75 as the template. The pPB41 vector was PCR amplified using oPEB217/218. These four PCR products were used in a Gibson assembly reaction to generate a Δ*yprA* editing plasmid. Clones were verified by Sanger sequencing with oPEB227, oPEB253, and oPEB454.

pPB87: The upstream and downstream portions of the Δ*yprB* editing template were PCR amplified using oPEB457/458 and oPEB459/460, respectively. CRISPR/Cas9 was PCR amplified using oPEB232/234 and pPB76 as the template. The pPB41 vector was PCR amplified using oPEB217/218. These four PCR products were used in a Gibson assembly reaction to

generate a Δ*yprB* editing plasmid. Clones were verified by Sanger sequencing with oPEB227, oPEB253, and oPEB463.

pPB98: The upstream and downstream portions of the Δ*ylbK* editing template were PCR amplified using oPEB468/469 and oPEB470/471, respectively. CRISPR/Cas9 was PCR amplified using oPEB232/234 and pPB77 as the template. The pPB41 vector was PCR amplified using oPEB217/218. These four PCR products were used in a Gibson assembly reaction to generate a Δ*ylbK* editing plasmid. Clones were verified by Sanger sequencing with oPEB227, oPEB253, and oPEB474.

pPB99: The upstream and downstream portions of the Δ*ylbL* editing template were PCR amplified using oPEB477/478 and oPEB479/480, respectively. CRISPR/Cas9 was PCR amplified using oPEB232/234 and pPB78 as the template. The pPB41 vector was PCR amplified using oPEB217/218. These four PCR products were used in a Gibson assembly reaction to generate a Δ*ylbL* editing plasmid. Clones were verified by Sanger sequencing with oPEB227, oPEB253, and oPEB483.

pPB103: The upstream and downstream portions of the Δ*sodA* editing template were PCR amplified using oPEB506/507 and oPEB508/509, respectively. CRISPR/Cas9 was PCR amplified using oPEB232/234 and pPB81 as the template. The pPB41 vector was PCR amplified using oPEB217/218. These four PCR products were used in a Gibson assembly reaction to generate a Δ*sodA* editing plasmid. Clones were verified by Sanger sequencing with oPEB227, oPEB253, and oPEB512.

pPB107: The upstream portion of *amyE* and the P_{xyl} promoter were PCR amplified using oPEB370/383. The chloramphenicol resistance cassette and the downstream portion of *amyE* were amplified using oPEB557/377. pPB47 was PCR amplified using oPEB116/117. The open reading frame (ORF) of *ylbK* was PCR amplified using oPEB558/559. These four PCR products were used in a Gibson assembly reaction to generate a plasmid to integrate *ylbK* under the control of P_{xyl} at the *amyE* locus. Clones were verified by Sanger sequencing with oPEB345 and oPEB348.

pPB108: The upstream portion of *amyE* and the P_{xyl} promoter were PCR amplified using oPEB370/383. The chloramphenicol resistance cassette and the downstream portion of *amyE*

were amplified using oPEB557/377. pPB47 was PCR amplified using oPEB116/117. The ORF of *ylbL* was PCR amplified using oPEB560/561. These four PCR products were used in a Gibson assembly reaction to generate a plasmid to integrate *ylbL* under the control of P_{xyl} at the *amyE* locus. Clones were verified by Sanger sequencing with oPEB345 and oPEB348.

pPB111: The upstream portion of *amyE* and the P_{xyl} promoter were PCR amplified using oPEB370/383. The chloramphenicol resistance cassette and the downstream portion of *amyE* were amplified using oPEB557/377. Plasmid pPB47 was PCR amplified using oPEB116/117. The upstream portion of the *ylbL* ORF containing the *S234A* mutation was PCR amplified using oPEB560/567. The downstream portion of the *ylbL* ORF containing the *S234A* mutation was PCR amplified using oPEB566/561. These five PCR products were used in a Gibson assembly reaction to generate a plasmid to integrate *ylbL-S234A* under the control of P_{xyl} at the *amyE* locus. Clones were verified by Sanger sequencing with oPEB345 and oPEB348.

pPB113: A proto-spacer targeting *queA* (oPEB577/578) was ligated to pPB41.

pPB114: A proto-spacer targeting *ctpA* (oPEB586/587) was ligated to pPB41.

pPB115: A proto-spacer targeting *ysoA* (oPEB595/596) was ligated to pPB41.

pPB116: A proto-spacer targeting *ylmE* (oPEB604/605) was ligated to pPB41.

pPB117: A proto-spacer targeting *sepF* (oPEB613/614) was ligated to pPB41.

pPB118: A proto-spacer targeting *ylmG* (oPEB618/619) was ligated to pPB41.

pPB120: The upstream and downstream portions of the Δ*queA* editing template were PCR amplified using oPEB579/580 and oPEB581/582, respectively. CRISPR/Cas9 was PCR amplified using oPEB232/234 and pPB113 as the template. The pPB41 vector was PCR amplified using oPEB217/218. These four PCR products were used in a Gibson assembly reaction to generate a Δ*queA* editing plasmid. Clones were verified by Sanger sequencing with oPEB227, oPEB253, and oPEB585.

pPB121: The upstream and downstream portions of the Δ*ctpA* editing template were PCR amplified using oPEB588/589 and oPEB590/591, respectively. CRISPR/Cas9 was PCR amplified using oPEB232/234 and pPB114 as the template. The pPB41 vector was PCR

amplified using oPEB217/218. These four PCR products were used in a Gibson assembly reaction to generate a Δ*ctpA* editing plasmid. Clones were verified by Sanger sequencing with oPEB227, oPEB253, and oPEB594.

pPB122: The upstream and downstream portions of the Δ*ysoA* editing template were PCR amplified using oPEB597/598 and oPEB599/600, respectively. CRISPR/Cas9 was PCR amplified using oPEB232/234 and pPB115 as the template. The pPB41 vector was PCR amplified using oPEB217/218. These four PCR products were used in a Gibson assembly reaction to generate a Δ*ysoA* editing plasmid. Clones were verified by Sanger sequencing with oPEB227, oPEB253, and oPEB603.

pPB123: The upstream and downstream portions of the Δ*ylmE* editing template were PCR amplified using oPEB606/607 and oPEB608/609, respectively. CRISPR/Cas9 was PCR amplified using oPEB232/234 and pPB116 as the template. The pPB41 vector was PCR amplified using oPEB217/218. These four PCR products were used in a Gibson assembly reaction to generate a Δ*ylmE* editing plasmid. The Gibson assembly reaction was used to transform PY79.

pPB124: The upstream and downstream portions of the Δ*sepF* editing template were PCR amplified using oPEB606/615 and oPEB616/609, respectively. CRISPR/Cas9 was PCR amplified using oPEB232/234 and pPB117 as the template. The pPB41 vector was PCR amplified using oPEB217/218. These four PCR products were used in a Gibson assembly reaction to generate a Δ*sepF* editing plasmid. The Gibson assembly reaction was used to transform PY79.

pPB125: The upstream and downstream portions of the Δ*ylmG* editing template were PCR amplified using oPEB606/620 and oPEB621/609, respectively. CRISPR/Cas9 was PCR amplified using oPEB232/234 and pPB118 as the template. The pPB41 vector was PCR amplified using oPEB217/218. These four PCR products were used in a Gibson assembly reaction to generate a Δ*ylmG* editing plasmid. The Gibson assembly reaction was used to transform PY79.

pPB130: A proto-spacer targeting *ytmP* (oPEB638/639) was ligated to pPB41.

pPB131: A proto-spacer targeting *bcrC* (oPEB647/648) was ligated to pPB41.

pPB132: A proto-spacer targeting *ecsA* (oPEB656/657) was ligated to pPB41.

pPB133: A proto-spacer targeting *ecsB* (oPEB665/666) was ligated to pPB41.

pPB140: The upstream and downstream portions of the Δ*ytmP* editing template were PCR amplified using oPEB640/641 and oPEB642/643, respectively. CRISPR/Cas9 was PCR amplified using oPEB232/234 and pPB130 as the template. The pPB41 vector was PCR amplified using oPEB217/218. These four PCR products were used in a Gibson assembly reaction to generate a Δ*ytmP* editing plasmid. Clones were verified by Sanger sequencing with oPEB227, oPEB253, and oPEB646.

pPB141: The upstream and downstream portions of the Δ*bcrC* editing template were PCR amplified using oPEB649/650 and oPEB651/652, respectively. CRISPR/Cas9 was PCR amplified using oPEB232/234 and pPB131 as the template. The pPB41 vector was PCR amplified using oPEB217/218. These four PCR products were used in a Gibson assembly reaction to generate a Δ*bcrC* editing plasmid. Clones were verified by Sanger sequencing with oPEB227, oPEB253, and oPEB655.

pPB142: The upstream and downstream portions of the Δ*ecsA* editing template were PCR amplified using oPEB658/659 and oPEB660/661, respectively. CRISPR/Cas9 was PCR amplified using oPEB232/234 and pPB132 as the template. The pPB41 vector was PCR amplified using oPEB217/218. These four PCR products were used in a Gibson assembly reaction to generate a Δ*ecsA* editing plasmid. Clones were verified by Sanger sequencing with oPEB227, oPEB253, and oPEB664.

pPB143: The upstream and downstream portions of the Δ*ecsB* editing template were PCR amplified using oPEB667/668 and oPEB669/670, respectively. CRISPR/Cas9 was PCR amplified using oPEB232/234 and pPB133 as the template. The pPB41 vector was PCR amplified using oPEB217/218. These four PCR products were used in a Gibson assembly reaction to generate a Δ*ecsB* editing plasmid. Clones were verified by Sanger sequencing with oPEB227, oPEB253, and oPEB673.

pPB149: The upstream and downstream portions of the Δ*ylbK-2* (deletion of all but the codons for the first 3 and the last 14 amino acids) editing template were PCR amplified using oPEB468/709 and oPEB710/471, respectively. CRISPR/Cas9 was PCR amplified using oPEB232/234 and pPB77 as the template. The pPB41 vector was PCR amplified using oPEB217/218. These four PCR products were used in a Gibson assembly reaction to generate a Δ*ylbK-2* editing plasmid. Clones were verified by Sanger sequencing with oPEB227, oPEB253, and oPEB474.

pPB154: A proto-spacer targeting *walH* (oPEB738/739) was ligated to pPB41.

pPB155: A proto-spacer targeting *yycI* (oPEB747/748) was ligated to pPB41.

pPB156: A proto-spacer targeting *walJ* (oPEB756/757) was ligated to pPB41.

pPB157: The ORF coding for a.a. 36-341 of YlbL was PCR amplified using oPEB773/677. The plasmid pPB12 was PCR amplified using oPEB56/57. These two PCR products were used in a Gibson assembly to generate a plasmid for overexpression of a 10xHis-Smt3-YlbL(36-341) fusion protein in *E. coli*. Clones were verified via Sanger sequencing using oPEB527 and oPEB58.

pPB173: The upstream portion of *amyE* and the P_{xyl} promoter were PCR amplified using oPEB370/383. The chloramphenicol resistance cassette and the downstream portion of *amyE* were amplified using oPEB557/377. pPB47 was PCR amplified using oPEB116/117. The upstream portion of the *ylbL* ORF containing the *K279A* mutation was PCR amplified using oPEB560/772. The downstream portion of the *ylbL* ORF containing the *K279A* mutation was PCR amplified using oPEB771/561. These five PCR products were used in a Gibson assembly reaction to generate a plasmid to integrate *ylbL-K279A* under the control of P_{xyl} at the *amyE* locus. Clones were verified by Sanger sequencing with oPEB345 and oPEB348.

pPB174: The upstream and downstream portions of the Δ*walH* editing template were PCR amplified using oPEB740/741 and oPEB742/743, respectively. CRISPR/Cas9 was PCR amplified using oPEB232/234 and pPB154 as the template. The pPB41 vector was PCR amplified using oPEB217/218. These four PCR products were used in a Gibson assembly

reaction to generate a Δ*walH* editing plasmid. Clones were verified by Sanger sequencing with oPEB227, oPEB253, and oPEB746.

pPB175: The upstream and downstream portions of the Δ*yycI* editing template were PCR amplified using oPEB749/750 and oPEB751/752, respectively. CRISPR/Cas9 was PCR amplified using oPEB232/234 and pPB155 as the template. The pPB41 vector was PCR amplified using oPEB217/218. These four PCR products were used in a Gibson assembly reaction to generate a Δ*yycI* editing plasmid. Clones were verified by Sanger sequencing with oPEB227, oPEB253, and oPEB755.

pPB176: The upstream and downstream portions of the Δ*walJ* editing template were PCR amplified using oPEB758/759 and oPEB760/761, respectively. CRISPR/Cas9 was PCR amplified using oPEB232/234 and pPB156 as the template. The pPB41 vector was PCR amplified using oPEB217/218. These four PCR products were used in a Gibson assembly reaction to generate a Δ*walJ* editing plasmid. Clones were verified by Sanger sequencing with oPEB227, oPEB253, and oPEB764.

pPB177: A proto-spacer targeting *ruvB* (oPEB798/799) was ligated to pPB41.

pPB178: A proto-spacer targeting *ripX* (oPEB807/808) was ligated to pPB41.

pPB179: The upstream and downstream portions of the Δ*ruvB* editing template were PCR amplified using oPEB800/801 and oPEB802/803, respectively. CRISPR/Cas9 was PCR amplified using oPEB232/234 and pPB177 as the template. The pPB41 vector was PCR amplified using oPEB217/218. These four PCR products were used in a Gibson assembly reaction to generate a Δ*ruvB* editing plasmid. Clones were verified by Sanger sequencing with oPEB227, oPEB253, and oPEB806.

pPB180: The upstream and downstream portions of the Δ*ripX* editing template were PCR amplified using oPEB809/810 and oPEB811/812, respectively. CRISPR/Cas9 was PCR amplified using oPEB232/234 and pPB178 as the template. The pPB41 vector was PCR amplified using oPEB217/218. These four PCR products were used in a Gibson assembly reaction to generate a Δ*ripX* editing plasmid. Clones were verified by Sanger sequencing with oPEB227, oPEB253, and oPEB815.

pPB181: The ORF coding for a.a. 36-341 of YlbL was PCR amplified with primers oPEB773/677 using pPB111 as a template to incorporate the S234A mutation. The plasmid pPB12 was PCR amplified using oPEB56/57. These two PCR products were used in a Gibson assembly to generate a plasmid for overexpression of a 10xHis-Smt3-YlbL-S234A-(36-341) fusion protein in *E. coli*. Clones were verified via Sanger sequencing using oPEB527 and oPEB58.

pPB184: The upstream portion of *amyE* and the P_{xyl} promoter were PCR amplified using oPEB370/383. The chloramphenicol resistance cassette and the downstream portion of *amyE* were amplified using oPEB557/377. pPB47 was PCR amplified using oPEB116/117. The ORF of *ctpA* was PCR amplified using oPEB817/818. These four PCR products were used in a Gibson assembly reaction to generate a plasmid to integrate *ctpA* under the control of P_{xyl} at the *amyE* locus. Clones were verified by Sanger sequencing with oPEB345 and oPEB348.

pPB185: The upstream portion of *amyE* and the P_{xyl} promoter were PCR amplified using oPEB370/383. The chloramphenicol resistance cassette and the downstream portion of *amyE* were amplified using oPEB557/377. pPB47 was PCR amplified using oPEB116/117. The upstream portion of the *ctpA* ORF containing the *S297A* mutation was PCR amplified using oPEB817/820. The downstream portion of the *ctpA* ORF containing the *S297A* mutation was PCR amplified using oPEB819/818. These five PCR products were used in a Gibson assembly reaction to generate a plasmid to integrate *ctpA-S297A* under the control of P_{xyl} at the *amyE* locus. Clones were verified by Sanger sequencing with oPEB345 and oPEB348.

pPB186: The upstream portion of *amyE* and the P_{xyl} promoter were PCR amplified using oPEB370/383. The chloramphenicol resistance cassette and the downstream portion of *amyE* were amplified using oPEB557/377. pPB47 was PCR amplified using oPEB116/117. The upstream portion of the *ctpA* ORF containing the *K322A* mutation was PCR amplified using oPEB817/822. The downstream portion of the *ctpA* ORF containing the *K322A* mutation was PCR amplified using oPEB821/818. These five PCR products were used in a Gibson assembly reaction to generate a plasmid to integrate *ctpA-K322A* under the control of P_{xyl} at the *amyE* locus. Clones were verified by Sanger sequencing with oPEB345 and oPEB348.

pPB194: pDR110 was amplified using primers oPEB3F/259, resulting in the conversion of promoter P_{spac} to P_{hyp}. The *yneA* ORF was amplified using oPEB856/857. These two PCR products were used in a Gibson assembly reaction to generate a plasmid to integrate *yneA* under the control of P_{hyp} at the *amyE* locus. Clones were verified by Sanger sequencing using oPEB866 and oPEB867.

pPB200: The pET28b vector was PCR amplified using oPEB835/57. The ORF of MBP was PCR amplified using oPEB838/839 with the IDT gBlock oPEB836 as a template. The Ulp1 ORF (a.a. 403-621) was PCR amplified using oPEB840/841 with plasmid pPB13 as a template. These three PCR products were used in a Gibson assembly reaction to generate a plasmid for overexpression of the fusion protein MBP-Ulp1(403-621) in *E. coli*. Clones were verified by Sanger sequencing using oPEB527, oPEB58, and oPEB837.

pPB203: The pET28b vector was PCR amplified using oPEB835/57. The CtpA ORF (coding for a.a. 38-466) was PCR amplified using oPEB831/832. These two PCR products and the IDT gBlock oPEB836 were used in a Gibson assembly reaction to generate a plasmid for overexpression of the fusion protein MBP-Smt3-CtpA(38-466) in *E. coli*. Clones were verified by Sanger sequencing using oPEB527, oPEB58, oPEB833, and oPEB837.

pPB204: The ORF coding for a.a. 28-103 of YneA was PCR amplified using oPEB842/843. The plasmid pPB12 was PCR amplified using oPEB56/57. These two PCR products were used in a Gibson assembly to generate a plasmid for overexpression of a 10xHis-Smt3-YneA(28-103) fusion protein in *E. coli*. Clones were verified via Sanger sequencing using oPEB527 and oPEB58.

pPB214: The pET28b-MBP-Smt3 vector was PCR amplified using oPEB56/57 using pPB203 as a template. The *ctpA-S297A* ORF (coding for a.a. 38-466) was PCR amplified using oPEB831/832 using pPB185 as a template. These two PCR products were used in a Gibson assembly reaction to generate a plasmid for overexpression of the fusion protein MBP-Smt3-CtpA-S297A (38-466) in *E. coli*. Clones were verified by Sanger sequencing using oPEB527, oPEB58, and oPEB833.

pPB227: A proto-spacer targeting *fhuG* (oPEB912/913) was ligated to pPB41.

pPB228: A proto-spacer targeting *yfkH* (oPEB921/922) was ligated to pPB41.

pPB229: A proto-spacer targeting *ltaSA* (oPEB930/931) was ligated to pPB41.

pPB230: A proto-spacer targeting *ykgA* (oPEB939/940) was ligated to pPB41.

pPB231: A proto-spacer targeting *cgeE* (oPEB948/949) was ligated to pPB41.

pPB232: A proto-spacer targeting *ysnF* (oPEB957/958) was ligated to pPB41.

pPB233: A proto-spacer targeting *lytG* (oPEB966/967) was ligated to pPB41.

pPB234: A proto-spacer targeting *yxaB* (oPEB975/976) was ligated to pPB41.

pPB237: The upstream and downstream portions of the Δ*fhuG* editing template were PCR amplified using oPEB914/915 and oPEB916/917, respectively. CRISPR/Cas9 was PCR amplified using oPEB232/234 and pPB227 as the template. The pPB41 vector was PCR amplified using oPEB217/218. These four PCR products were used in a Gibson assembly reaction to generate a Δ*fhuG* editing plasmid. Clones were verified by Sanger sequencing with oPEB227, oPEB253, and oPEB920.

pPB238: The upstream and downstream portions of the Δ*yfkH* editing template were PCR amplified using oPEB923/924 and oPEB925/926, respectively. CRISPR/Cas9 was PCR amplified using oPEB232/234 and pPB228 as the template. The pPB41 vector was PCR amplified using oPEB217/218. These four PCR products were used in a Gibson assembly reaction to generate a Δ*yfkH* editing plasmid. Clones were verified by Sanger sequencing with oPEB227, oPEB253, and oPEB929.

pPB239: The upstream and downstream portions of the Δ*ltaSA* editing template were PCR amplified using oPEB932/933 and oPEB934/935, respectively. CRISPR/Cas9 was PCR amplified using oPEB232/234 and pPB229 as the template. The pPB41 vector was PCR amplified using oPEB217/218. These four PCR products were used in a Gibson assembly reaction to generate a Δ*ltaSA* editing plasmid. Clones were verified by Sanger sequencing with oPEB227, oPEB253, and oPEB938.

pPB240: The upstream and downstream portions of the Δ*ykgA* editing template were PCR amplified using oPEB941/942 and oPEB943/944, respectively. CRISPR/Cas9 was PCR amplified using oPEB232/234 and pPB230 as the template. The pPB41 vector was PCR amplified using oPEB217/218. These four PCR products were used in a Gibson assembly reaction to generate a Δ*ykgA* editing plasmid. Clones were verified by Sanger sequencing with oPEB227, oPEB253, and oPEB947.

pPB241: The upstream and downstream portions of the Δ*cgeE* editing template were PCR amplified using oPEB950/951 and oPEB952/953, respectively. CRISPR/Cas9 was PCR amplified using oPEB232/234 and pPB231 as the template. The pPB41 vector was PCR amplified using oPEB217/218. These four PCR products were used in a Gibson assembly reaction to generate a Δ*cgeE* editing plasmid. Clones were verified by Sanger sequencing with oPEB227, oPEB253, and oPEB956.

pPB242: The upstream and downstream portions of the Δ*ysnF* editing template were PCR amplified using oPEB959/960 and oPEB961/962, respectively. CRISPR/Cas9 was PCR amplified using oPEB232/234 and pPB232 as the template. The pPB41 vector was PCR amplified using oPEB217/218. These four PCR products were used in a Gibson assembly reaction to generate a Δ*ysnF* editing plasmid. Clones were verified by Sanger sequencing with oPEB227, oPEB253, and oPEB965.

pPB243: The upstream and downstream portions of the Δ*lytG* editing template were PCR amplified using oPEB968/969 and oPEB970/972, respectively. CRISPR/Cas9 was PCR amplified using oPEB232/234 and pPB233 as the template. The pPB41 vector was PCR amplified using oPEB217/218. These four PCR products were used in a Gibson assembly reaction to generate a Δ*lytG* editing plasmid. Clones were verified by Sanger sequencing with oPEB227, oPEB253, and oPEB974.

pPB244: The upstream and downstream portions of the Δ*yxaB* editing template were PCR amplified using oPEB977/978 and oPEB979/980, respectively. CRISPR/Cas9 was PCR amplified using oPEB232/234 and pPB234 as the template. The pPB41 vector was PCR amplified using oPEB217/218. These four PCR products were used in a Gibson assembly

reaction to generate a Δ*yxaB* editing plasmid. Clones were verified by Sanger sequencing with oPEB227, oPEB253, and oPEB983.

pPB267: YneA was amplified with primers oPEB1034/1035 and the plasmid pUT18C was amplified using primers oPEB1017/1018. These two PCR products were used in a Gibson assembly reaction to generate a T18-YneA fusion for expression in BTH101 cells in a bacterial two-hybrid assay. Clones were selected on LB agar containing 100 μg/mL ampicillin and 0.2% glucose. Clones were verified via Sanger sequencing using oPEB1024 and 1025.

pPB268: YneAΔN (a.a 28-103) was amplified with primers oPEB1036/1035 and the plasmid pUT18C was amplified using primers oPEB1017/1018. These two PCR products were used in a Gibson assembly reaction to generate a T18-YneAΔN (a.a 28-103) fusion for expression in BTH101 cells in a bacterial two-hybrid assay. Clones were selected on LB agar containing 100 μg/mL ampicillin and 0.2% glucose. Clones were verified via Sanger sequencing using oPEB1024 and 1025.

pPB270: YlbL-S234A was amplified with primers oPEB1039/1040 and using pPB111 as a template. The plasmid pKT25 was amplified with primers oPEB1014/1015. These two PCR products were used in a Gibson assembly reaction to generate a T25-YlbL-S234A fusion for expression in BTH101 cells in a bacterial two-hybrid assay. Clones were selected on LB agar containing 50 μg/mL kanamycin and 0.2% glucose. Clones were verified via Sanger sequencing using oPEB1021 and 1022.

pPB271: CtpA-S297A was amplified with primers oPEB1041/1042 and using pPB185 as a template. The plasmid pKT25 was amplified with primers oPEB1014/1015. These two PCR products were used in a Gibson assembly reaction to generate a T25-CtpA-S297A fusion for expression in BTH101 cells in a bacterial two-hybrid assay. Clones were selected on LB agar containing 50 μg/mL kanamycin and 0.2% glucose. Clones were verified via Sanger sequencing using oPEB833, 1021, and 1022.

References

1. **Jackson SP, Bartek J.** 2009. The DNA-damage response in human biology and disease. Nature **461:**1071-1078.
2. **Blanpain C, Mohrin M, Sotiropoulou PA, Passegue E.** 2011. DNA-damage response in tissue-specific and cancer stem cells. Cell Stem Cell **8:**16-29.

3. **Kreuzer KN.** 2013. DNA damage responses in prokaryotes: regulating gene expression, modulating growth patterns, and manipulating replication forks. Cold Spring Harb Perspect Biol **5:**a012674.
4. **Michel B.** 2005. After 30 years of study, the bacterial SOS response still surprises us. PLoS Biol **3:**e255.
5. **Baharoglu Z, Mazel D.** 2014. SOS, the formidable strategy of bacteria against aggressions. FEMS Microbiol Rev **38:**1126-1145.
6. **Friedberg EC, Walker GC, Siede W, Wood RD, Schultz RA, Ellenberger T.** 2006. DNA Repair and Mutagenesis, 2nd ed. ASM Press, Washington, D.C.
7. **Sancar A, Lindsey-Boltz LA, Unsal-Kacmaz K, Linn S.** 2004. Molecular mechanisms of mammalian DNA repair and the DNA damage checkpoints. Annu Rev Biochem **73:**39-85.
8. **Ciccia A, Elledge SJ.** 2010. The DNA damage response: making it safe to play with knives. Mol Cell **40:**179-204.
9. **Simmons LA, Foti JJ, Cohen SE, Walker GC.** 2008. The SOS Regulatory Network. EcoSal Plus **2008**.
10. **Huisman O, D'Ari R.** 1981. An inducible DNA replication-cell division coupling mechanism in E. coli. Nature **290:**797-799.
11. **Huisman O, D'Ari R, Gottesman S.** 1984. Cell-division control in Escherichia coli: specific induction of the SOS function SfiA protein is sufficient to block septation. Proc Natl Acad Sci U S A **81:**4490-4494.
12. **Bi E, Lutkenhaus J.** 1993. Cell division inhibitors SulA and MinCD prevent formation of the FtsZ ring. J Bacteriol **175:**1118-1125.
13. **Huang J, Cao C, Lutkenhaus J.** 1996. Interaction between FtsZ and inhibitors of cell division. J Bacteriol **178:**5080-5085.
14. **Mukherjee A, Cao C, Lutkenhaus J.** 1998. Inhibition of FtsZ polymerization by SulA, an inhibitor of septation in Escherichia coli. Proc Natl Acad Sci U S A **95:**2885-2890.
15. **Trusca D, Scott S, Thompson C, Bramhill D.** 1998. Bacterial SOS checkpoint protein SulA inhibits polymerization of purified FtsZ cell division protein. J Bacteriol **180:**3946-3953.
16. **Mizusawa S, Gottesman S.** 1983. Protein degradation in Escherichia coli: the lon gene controls the stability of sulA protein. Proc Natl Acad Sci U S A **80:**358-362.
17. **Sonezaki S, Ishii Y, Okita K, Sugino T, Kondo A, Kato Y.** 1995. Overproduction and purification of SulA fusion protein in Escherichia coli and its degradation by Lon protease in vitro. Appl Microbiol Biotechnol **43:**304-309.
18. **Canceill D, Dervyn E, Huisman O.** 1990. Proteolysis and modulation of the activity of the cell division inhibitor SulA in Escherichia coli lon mutants. J Bacteriol **172:**7297-7300.
19. **Wu WF, Zhou Y, Gottesman S.** 1999. Redundant in vivo proteolytic activities of Escherichia coli Lon and the ClpYQ (HslUV) protease. J Bacteriol **181:**3681-3687.
20. **Seong IS, Oh JY, Yoo SJ, Seol JH, Chung CH.** 1999. ATP-dependent degradation of SulA, a cell division inhibitor, by the HslVU protease in Escherichia coli. FEBS Lett **456:**211-214.
21. **Kanemori M, Yanagi H, Yura T.** 1999. The ATP-dependent HslVU/ClpQY protease participates in turnover of cell division inhibitor SulA in Escherichia coli. J Bacteriol **181:**3674-3680.

22. **Modell JW, Hopkins AC, Laub MT.** 2011. A DNA damage checkpoint in Caulobacter crescentus inhibits cell division through a direct interaction with FtsW. Genes Dev **25:**1328-1343.
23. **Kawai Y, Moriya S, Ogasawara N.** 2003. Identification of a protein, YneA, responsible for cell division suppression during the SOS response in Bacillus subtilis. Mol Microbiol **47:**1113-1122.
24. **Ogino H, Teramoto H, Inui M, Yukawa H.** 2008. DivS, a novel SOS-inducible cell-division suppressor in Corynebacterium glutamicum. Mol Microbiol **67:**597-608.
25. **Chauhan A, Lofton H, Maloney E, Moore J, Fol M, Madiraju MV, Rajagopalan M.** 2006. Interference of Mycobacterium tuberculosis cell division by Rv2719c, a cell wall hydrolase. Mol Microbiol **62:**132-147.
26. **Modell JW, Kambara TK, Perchuk BS, Laub MT.** 2014. A DNA damage-induced, SOS-independent checkpoint regulates cell division in Caulobacter crescentus. PLoS Biol **12:**e1001977.
27. **Mo AH, Burkholder WF.** 2010. YneA, an SOS-induced inhibitor of cell division in Bacillus subtilis, is regulated posttranslationally and requires the transmembrane region for activity. J Bacteriol **192:**3159-3173.
28. **Byrne RT, Chen SH, Wood EA, Cabot EL, Cox MM.** 2014. Escherichia coli genes and pathways involved in surviving extreme exposure to ionizing radiation. J Bacteriol **196:**3534-3545.
29. **Iyer VN, Szybalski W.** 1963. A molecular mechanism of mitomycin action: Linking of complementary DNA strands. Proc Natl Acad Sci U S A **50:**355-362.
30. **Noll DM, Mason TM, Miller PS.** 2006. Formation and repair of interstrand cross-links in DNA. Chem Rev **106:**277-301.
31. **Sedgwick B.** 2004. Repairing DNA-methylation damage. Nat Rev Mol Cell Biol **5:**148-157.
32. **Reiter H, Milewskiy M, Kelley P.** 1972. Mode of action of phleomycin on Bacillus subtilis. J Bacteriol **111:**586-592.
33. **Kross J, Henner WD, Hecht SM, Haseltine WA.** 1982. Specificity of deoxyribonucleic acid cleavage by bleomycin, phleomycin, and tallysomycin. Biochemistry **21:**4310-4318.
34. **Robinson DG, Chen W, Storey JD, Gresham D.** 2014. Design and analysis of Bar-seq experiments. G3 (Bethesda) **4:**11-18.
35. **van Opijnen T, Bodi KL, Camilli A.** 2009. Tn-seq: high-throughput parallel sequencing for fitness and genetic interaction studies in microorganisms. Nat Methods **6:**767-772.
36. **van Opijnen T, Camilli A.** 2013. Transposon insertion sequencing: a new tool for systems-level analysis of microorganisms. Nat Rev Microbiol **11:**435-442.
37. **Benjamini Y, Hochberg Y.** 1995. Controlling the false discovery rate: a practical and powerful approach to multiple testing. Journal of the Royal Statistical Society Series B-Methodological **57:**289-300.
38. **Lenhart JS, Schroeder JW, Walsh BW, Simmons LA.** 2012. DNA repair and genome maintenance in Bacillus subtilis. Microbiol Mol Biol Rev **76:**530-564.
39. **Sancar A.** 1996. DNA excision repair. Annu Rev Biochem **65:**43-81.
40. **Friedman BM, Yasbin RE.** 1983. The genetics and specificity of the constitutive excision repair system of Bacillus subtilis. Mol Gen Genet **190:**481-486.

41. **Walsh BW, Bolz SA, Wessel SR, Schroeder JW, Keck JL, Simmons LA.** 2014. RecD2 helicase limits replication fork stress in Bacillus subtilis. J Bacteriol **196:**1359-1368.
42. **Au N, Kuester-Schoeck E, Mandava V, Bothwell LE, Canny SP, Chachu K, Colavito SA, Fuller SN, Groban ES, Hensley LA, O'Brien TC, Shah A, Tierney JT, Tomm LL, O'Gara TM, Goranov AI, Grossman AD, Lovett CM.** 2005. Genetic composition of the Bacillus subtilis SOS system. Journal of Bacteriology **187:**7655-7666.
43. **Goranov AI, Kuester-Schoeck E, Wang JD, Grossman AD.** 2006. Characterization of the global transcriptional responses to different types of DNA damage and disruption of replication in Bacillus subtilis. Journal of Bacteriology **188:**5595-5605.
44. **Wu LJ, Errington J.** 2004. Coordination of cell division and chromosome segregation by a nucleoid occlusion protein in Bacillus subtilis. Cell **117:**915-925.
45. **Goranov AI, Katz L, Breier AM, Burge CB, Grossman AD.** 2005. A transcriptional response to replication status mediated by the conserved bacterial replication protein DnaA. Proc Natl Acad Sci U S A **102:**12932-12937.
46. **Bramkamp M, Weston L, Daniel RA, Errington J.** 2006. Regulated intramembrane proteolysis of FtsL protein and the control of cell division in Bacillus subtilis. Mol Microbiol **62:**580-591.
47. **Karimova G, Pidoux J, Ullmann A, Ladant D.** 1998. A bacterial two-hybrid system based on a reconstituted signal transduction pathway. Proc Natl Acad Sci U S A **95:**5752-5756.
48. **Karimova G, Gauliard E, Davi M, Ouellette SP, Ladant D.** 2017. Protein-Protein Interaction: Bacterial Two-Hybrid. Methods Mol Biol **1615:**159-176.
49. **Karimova G, Dautin N, Ladant D.** 2005. Interaction network among Escherichia coli membrane proteins involved in cell division as revealed by bacterial two-hybrid analysis. J Bacteriol **187:**2233-2243.
50. **Beebe KD, Shin J, Peng J, Chaudhury C, Khera J, Pei D.** 2000. Substrate recognition through a PDZ domain in tail-specific protease. Biochemistry **39:**3149-3155.
51. **Silber KR, Keiler KC, Sauer RT.** 1992. Tsp: a tail-specific protease that selectively degrades proteins with nonpolar C termini. Proc Natl Acad Sci U S A **89:**295-299.
52. **Walsh NP, Alba BM, Bose B, Gross CA, Sauer RT.** 2003. OMP peptide signals initiate the envelope-stress response by activating DegS protease via relief of inhibition mediated by its PDZ domain. Cell **113:**61-71.
53. **Sohn J, Grant RA, Sauer RT.** 2007. Allosteric activation of DegS, a stress sensor PDZ protease. Cell **131:**572-583.
54. **Sohn J, Sauer RT.** 2009. OMP peptides modulate the activity of DegS protease by differential binding to active and inactive conformations. Mol Cell **33:**64-74.
55. **Shaltiel IA, Krenning L, Bruinsma W, Medema RH.** 2015. The same, only different - DNA damage checkpoints and their reversal throughout the cell cycle. J Cell Sci **128:**607-620.
56. **Wang H, Zhang X, Teng L, Legerski RJ.** 2015. DNA damage checkpoint recovery and cancer development. Exp Cell Res **334:**350-358.
57. **Bernard R, Marquis KA, Rudner DZ.** 2010. Nucleoid occlusion prevents cell division during replication fork arrest in Bacillus subtilis. Mol Microbiol **78:**866-882.

58. **Daniel RA, Harry EJ, Katis VL, Wake RG, Errington J.** 1998. Characterization of the essential cell division gene ftsL(yIID) of Bacillus subtilis and its role in the assembly of the division apparatus. Mol Microbiol **29:**593-604.
59. **Buchholz M, Nahrstedt H, Pillukat MH, Deppe V, Meinhardt F.** 2013. yneA mRNA instability is involved in temporary inhibition of cell division during the SOS response of Bacillus megaterium. Microbiology **159:**1564-1574.
60. **Youngman P, Perkins JB, Losick R.** 1984. Construction of a cloning site near one end of TN917 into which foreign DNA may be inserted without affecting transposition in Bacillus subtilis or expression of the transposon-bourne ERM gene. Plasmid **12:**1-9.
61. **Johnson CM, Grossman AD.** 2014. Identification of host genes that affect acquisition of an integrative and conjugative element in Bacillus subtilis. Mol Microbiol **93:**1284-1301.
62. **Burby PE, Simmons LA.** 2017. MutS2 Promotes Homologous Recombination in Bacillus subtilis. J Bacteriol **199**.
63. **Matthews LA, Simmons LA.** 2018. Cryptic adaptor protein interactions regulate DNA replication initiation. bioRxiv doi:10.1101/313882.
64. **Kidane D, Sanchez H, Alonso JC, Graumann PL.** 2004. Visualization of DNA double-strand break repair in live bacteria reveals dynamic recruitment of Bacillus subtilis RecF, RecO and RecN proteins to distinct sites on the nucleoids. Mol Microbiol **52:**1627-1639.
65. **Sanchez H, Kidane D, Castillo Cozar M, Graumann PL, Alonso JC.** 2006. Recruitment of Bacillus subtilis RecN to DNA double-strand breaks in the absence of DNA end processing. J Bacteriol **188:**353-360.
66. **Sanchez H, Kidane D, Reed P, Curtis FA, Cozar MC, Graumann PL, Sharples GJ, Alonso JC.** 2005. The RuvAB branch migration translocase and RecU Holliday junction resolvase are required for double-stranded DNA break repair in Bacillus subtilis. Genetics **171:**873-883.
67. **Alonso JC, Luder G, Tailor RH.** 1991. Characterization of Bacillus subtilis recombinational pathways. J Bacteriol **173:**3977-3980.
68. **Mascarenhas J, Sanchez H, Tadesse S, Kidane D, Krisnamurthy M, Alonso JC, Graumann PL.** 2006. Bacillus subtilis SbcC protein plays an important role in DNA inter-strand cross-link repair. Bmc Molecular Biology **7:**15.
69. **Sanchez H, Carrasco B, Cozar MC, Alonso JC.** 2007. Bacillus subtilis RecG branch migration translocase is required for DNA repair and chromosomal segregation. Mol Microbiol **65:**920-935.
70. **Cardenas PP, Carrasco B, Defeu Soufo C, Cesar CE, Herr K, Kaufenstein M, Graumann PL, Alonso JC.** 2012. RecX facilitates homologous recombination by modulating RecA activities. PLoS Genet **8:**e1003126.
71. **Galinier A, Haiech J, Kilhoffer MC, Jaquinod M, Stulke J, Deutscher J, Martin-Verstraete I.** 1997. The Bacillus subtilis crh gene encodes a HPr-like protein involved in carbon catabolite repression. Proc Natl Acad Sci U S A **94:**8439-8444.
72. **Fabret C, Hoch JA.** 1998. A two-component signal transduction system essential for growth of Bacillus subtilis: implications for anti-infective therapy. J Bacteriol **180:**6375-6383.
73. **Szurmant H, Nelson K, Kim EJ, Perego M, Hoch JA.** 2005. YycH regulates the activity of the essential YycFG two-component system in Bacillus subtilis. J Bacteriol **187:**5419-5426.

74. **Szurmant H, Mohan MA, Imus PM, Hoch JA.** 2007. YycH and YycI interact to regulate the essential YycFG two-component system in Bacillus subtilis. J Bacteriol **189:**3280-3289.
75. **Szurmant H, Bu L, Brooks CL, 3rd, Hoch JA.** 2008. An essential sensor histidine kinase controlled by transmembrane helix interactions with its auxiliary proteins. Proc Natl Acad Sci U S A **105:**5891-5896.
76. **Fukushima T, Furihata I, Emmins R, Daniel RA, Hoch JA, Szurmant H.** 2011. A role for the essential YycG sensor histidine kinase in sensing cell division. Mol Microbiol **79:**503-522.
77. **Biller SJ, Wayne KJ, Winkler ME, Burkholder WF.** 2011. The putative hydrolase YycJ (WalJ) affects the coordination of cell division with DNA replication in Bacillus subtilis and may play a conserved role in cell wall metabolism. J Bacteriol **193:**896-908.
78. **Akerley BJ, Lampe DJ.** 2002. Analysis of gene function in bacterial pathogens by GAMBIT. Methods Enzymol **358:**100-108.
79. **Li H, Durbin R.** 2009. Fast and accurate short read alignment with Burrows-Wheeler transform. Bioinformatics **25:**1754-1760.
80. **Team R.** 2016. RStudio: Integrated Development Environment for R, *on* RStudio, Inc. http://www.rstudio.com/. Accessed
81. **Campo N, Rudner DZ.** 2006. A branched pathway governing the activation of a developmental transcription factor by regulated intramembrane proteolysis. Mol Cell **23:**25-35.
82. **Burby PE, Simmons LA.** 2017. CRISPR/Cas9 Editing of the Bacillus subtilis Genome. Bio Protoc **7**.
83. **Koo BM, Kritikos G, Farelli JD, Todor H, Tong K, Kimsey H, Wapinski I, Galardini M, Cabal A, Peters JM, Hachmann AB, Rudner DZ, Allen KN, Typas A, Gross CA.** 2017. Construction and Analysis of Two Genome-Scale Deletion Libraries for Bacillus subtilis. Cell Syst **4:**291-305.e297.
84. **Gibson DG.** 2011. Enzymatic assembly of overlapping DNA fragments, p 349-361. *In* Voigt C (ed), Synthetic Biology, Pt B: Computer Aided Design and DNA Assembly, vol 498. Elsevier Academic Press Inc, San Diego.

CHAPTER III

DdcA antagonizes a bacterial DNA damage checkpoint

Abstract

Bacteria coordinate DNA replication and cell division, ensuring a complete set of genetic material is passed onto the next generation. When bacteria encounter DNA damage, a cell cycle checkpoint is activated by expressing a cell division inhibitor. The prevailing model is that activation of the DNA damage response and protease mediated degradation of the inhibitor is sufficient to regulate the checkpoint process. Our recent genome-wide screens identified the gene *ddcA* as critical for surviving exposure to DNA damage. Similar to the checkpoint recovery proteases, the DNA damage sensitivity resulting from *ddcA* deletion depends on the checkpoint enforcement protein YneA. Using several genetic approaches, we show that DdcA function is distinct from the checkpoint recovery process. Deletion of *ddcA* resulted in sensitivity to *yneA* overexpression independent of YneA protein levels and stability, further supporting the conclusion that DdcA regulates YneA independent of proteolysis. Using a functional GFP-YneA fusion we found that DdcA prevents YneA-dependent cell elongation independent of YneA localization. Together, our results suggest that DdcA acts by helping to set a threshold of YneA required to establish the cell cycle checkpoint, uncovering a new regulatory step controlling activation of the DNA damage checkpoint in *Bacillus subtilis*.

Introduction

The logistics of the cell cycle are of fundamental importance in biology. All organisms need to control cell growth, DNA replication, and the process of cell division. In bacteria the

---

The contents of this chapter were published in *Molecular Microbiology* by Peter E. Burby, Zackary W. Simmons, and Lyle A. Simmons. ZWS helped with spot titer assays in figures 3.1, 3.2, 3.3, 3.5. I designed experiments and collected data. LAS and I analyzed data and wrote the manuscript.

initiation of DNA replication is coupled to growth rate and the cell cycle (1-4). Bacteria also regulate cell division in response to DNA replication status through the use of DNA damage checkpoints (5, 6). The models for the DNA damage response (SOS) were developed based on studies of *Escherichia coli* and subsequently extended to other bacteria. In these models, DNA damage results in perturbations to DNA replication and the accumulation of ssDNA (7). RecA is loaded onto ssDNA (8-12), and the resulting RecA/ssDNA nucleoprotein filament induces the SOS response by activating auto-cleavage of the transcriptional repressor LexA (13). LexA inactivation results in increased transcription of genes involved in DNA repair and the DNA damage checkpoint (14-18). The DNA damage checkpoint is established by relieving the LexA-dependent repression of a cell division inhibitor that enforces the checkpoint by blocking cell division (19-22). Once the checkpoint is established, the delay in cytokinesis provides the cell with enough time to repair and complete DNA replication, thereby ensuring a complete and accurate copy of the chromosome is segregated to both daughter cells. Over several decades of study, this overarching model has been consistently demonstrated among bacteria that contain a RecA and LexA-dependent DNA damage checkpoint mechanism (5, 23).

Where the DNA damage response varies between bacteria is in the process that enforces and alleviates the checkpoint. In *E. coli* and closely related Gram-negative bacteria, the checkpoint is enforced by SulA, which is a cytoplasmic protein that acts by directly inhibiting formation of the FtsZ proto-filament blocking cell division (20, 24-27). In many other bacteria the checkpoint is enforced by a small membrane binding protein (21, 28-31). In *Caulobacter crescentus*, the small membrane proteins SidA and DidA inhibit cell division through direct interactions with components of the essential cell division complex known as the divisome (30, 31). In other bacteria the exact mechanism of checkpoint enforcement remains unclear. In the Gram-positive bacterium *Bacillus subtilis*, the checkpoint enforcement protein YneA inhibits cell division in response to DNA damage (21). YneA is a small protein containing a transmembrane domain as well as a LysM domain (22). A previous study found that several amino acids on one side of the transmembrane alpha helix are important for function, which led the authors to speculate that YneA may also interact with a component of the divisome (22). The same study also suggested full length YneA is the active form, and that the transmembrane domain alone is not sufficient for activity (22). Although YneA is clearly involved in cell division inhibition, the role of this checkpoint in ensuring that daughter cells each receive an intact copy of the genome

has not yet been firmly established, and the mechanism by which YneA enforces the checkpoint is still unknown.

The mechanism of relieving the DNA damage checkpoint has only been identified in two bacterial species, *E. coli* and *B. subtilis*. Despite the checkpoint mechanisms functioning in different cellular compartments, the strategy for checkpoint recovery is remarkably similar between these two organisms. In *E. coli,* Lon protease is the major protease responsible for degrading SulA (32-34), and the protease ClpYQ appears to play a secondary role (35-37). In *B. subtilis*, there are two proteases YlbL, which we rename here to DdcP (DNA damage checkpoint recovery protease) and CtpA that degrade YneA (38). In the case of DdcP and CtpA, the former seems to be the primary protease in minimal media; however, during chronic exposure to DNA damage in rich media both proteases are important and they can functionally replace each other when overexpressed (38). DdcP and CtpA are not regulated by DNA damage (38), suggesting that the proteases act as a buffer to YneA accumulation helping to set the threshold for checkpoint activation. Thus, in order for the checkpoint to be enforced both proteases must be saturated. Following repair of damaged DNA, LexA represses expression of YneA, and the remaining YneA is cleared by DdcP and CtpA, allowing cell division to proceed (38).

Although the DNA damage checkpoint in bacteria is well understood, it is becoming increasingly clear that establishing the checkpoint is more complex than what earlier models suggest. Work from Goranov and co-workers demonstrated that the initiation protein and transcription factor DnaA regulates *ftsL* levels in response to DNA replication perturbations, which contributes to cell filamentation (39). Further, our recent report identified several genes not previously implicated in genome maintenance or cell cycle control that are critical for surviving chronic exposure to a broad spectrum of DNA damage (38). We identified genes involved in cell division and cell wall synthesis as well as genes of unknown function that rendered the deletion mutants sensitive to DNA damage (38). To understand how the DNA damage response in bacteria is regulated, we investigated the contribution of one of the unstudied genes *ddcA* (formerly *ysoA*, see below) in the DNA damage response. We report here that DdcA antagonizes YneA action, functioning to help set a threshold of DNA damage required for checkpoint activation.

Results

Deletion of *ddcA* (*ysoA*) results in sensitivity to DNA damage

We recently published a set of genome wide screens using three distinct classes of DNA damaging agents, uncovering many genes that have not been previously implicated in the DNA damage response or DNA repair (38). One gene that conferred a sensitive phenotype to all three types of DNA damage tested was *ysoA*, which we rename here to DNA damage checkpoint antagonist (*ddcA*). DdcA is a protein that is predicted to have three tetratrichopeptide repeats **(Fig 3.1A)**, which are often involved in protein-protein interactions, protein complex formation, and virulence mechanisms in bacteria (40). In order to better understand the mechanism of the DNA damage response in *B. subtilis*, we investigated the contribution of DdcA. To begin, we tested the sensitivity of the *ddcA* deletion to DNA damage. Deletion of *ddcA* resulted in sensitivity to mitomycin C (MMC), an agent that causes DNA crosslinks and bulky adducts (41, 42), and phleomycin a peptide that forms double and single strand DNA breaks (43, 44). We found that expression of P_{xyl}-*ddcA* from an ectopic locus (*amyE)* was sufficient to complement deletion of *ddcA* with or without inducing expression using xylose **(Fig 3.1B)**. We conclude that deletion of *ddcA* results in a *bona-fide* sensitivity to DNA damage.

DNA damage sensitivity of *ddcA* deletion is dependent on *yneA*.

We asked how DdcA functions in the DNA damage response. Our observation that a *ddcA* deletion allele results in sensitivity to several DNA damaging agents is similar to the result of deleting the checkpoint recovery proteases (38). Our prior study (38) showed that DNA damage phenotypes in checkpoint recovery protease mutants depend on the checkpoint enforcement protein, YneA, which is likely the result of aberrant activation of the checkpoint in the absence of YneA degradation. We asked whether deletion of *yneA* could rescue DNA damage sensitivity resulting from *ddcA* deletion. Indeed, deletion of *yneA* in the *ddcA* deletion background rescued sensitivity to MMC **(Fig 3.2)**.

We also tested for a genetic interaction with nucleotide excision repair, reasoning that the absence of nucleotide excision repair would result in increased *yneA* expression and increased sensitivity in the *ddcA* deletion. Indeed, deletion of *uvrAB*, genes coding for components of nucleotide excision repair (45), resulted in hypersensitivity to MMC **(Fig 3.2)**. These data,

together with the initial observation of general DNA damage sensitivity and suppression of the sensitivity with loss of *yneA* function suggests that DdcA participates in regulating the DNA damage checkpoint protein YneA.

DdcA functions independent of DNA damage checkpoint recovery proteases

Based on the observation that sensitivity to DNA damage in a Δ*ddcA* mutant was rescued by deletion of *yneA*, similar to our observations with the checkpoint recovery proteases (38), we hypothesized that DdcA could function within the checkpoint recovery process. For example, DdcA could affect CtpA and/or DdcP activity. To test this idea, we generated double mutant strains of Δ*ddcA* with Δ*ctpA* or Δ*ddcP*. If DdcA functions together with CtpA or DdcP we would expect that the double mutant would have the same phenotype as the single mutant. In contrast, we observed that deletion of *ddcA* in a *ctpA* or *ddcP* mutant resulted in increased sensitivity to MMC **(Fig 3.3A)**. These results support the hypothesis that DdcA does not function with the proteases in checkpoint recovery. To test this idea further, we determined the effect of deletion of *ddcA* in a Δ*ddcP*, Δ*ctpA* double mutant on MMC sensitivity. We found that deletion of *ddcA* resulted in increased MMC sensitivity relative to the double protease mutants **(Fig 3.3B)**, suggesting that DdcA functions independently of both DdcP and CtpA. We then asked if *yneA* was responsible for the phenotype of Δ*ddcA* in the absence of the checkpoint recovery proteases. Strikingly, we found that the sensitivity of the triple mutant was mostly dependent on *yneA*, but at elevated concentrations of MMC, there was a slight but reproducible difference when *ddcA* was deleted in the Δ*ddcP*, Δ*ctpA*, Δ*yneA::loxP* mutant background **(Fig 3.3B)**. Taken together, these data suggest that DdcA regulation of the checkpoint is independent of the recovery proteases. Further, because the *ddcA* phenotype is dependent on *yneA* we suggest that DdcA negatively regulates the checkpoint enforcement protein YneA.

In our previous study we found that the checkpoint recovery proteases could substitute for each other (38). Therefore to more firmly establish when DdcA regulates the checkpoint we asked if DdcA could replace the checkpoint recovery proteases or if the proteases could function in place of DdcA. To test this idea, we overexpressed *ddcP* and *ctpA* in a Δ*ddcA* mutant and found that neither protease could rescue a *ddcA* deletion phenotype **(Fig 3.4A)**. We also found that expression of *ddcA* in the double protease mutant could not rescue the MMC sensitive phenotype **(Fig 3.4B)**. Further, expression of *ddcP* or *ctpA* were each able to partially

complement the phenotype of the triple mutant, but expression of *ddcA* had no effect at higher concentrations of MMC **(Fig 3.4B)**. As a control, we verified that overexpression of *ddcA* using high levels of xylose (0.5% xylose) could complement a Δ*ddcA* mutant **(Fig 3.5)**. We also found that at lower concentrations of MMC, expression of *ddcA* could rescue the *ddcA* deficiency of the triple mutant resulting in a phenotype indistinguishable from the double protease mutant **(Fig 3.4C)**. Given that DdcA cannot substitute for DdcP and CtpA, we hypothesized that DdcA would not affect YneA protein levels following DNA damage. We tested this by monitoring YneA protein levels following MMC treatment and after recovering from MMC treatment for two hours. Deletion of *ddcA* alone did not result in a detectable difference in YneA protein levels compared to WT **(Fig 3.6)**. Further, deletion of *ddcA* in the double protease mutant also did not result in an increase in YneA protein levels relative to the double protease mutant with *ddcA* intact **(Fig 3.6)**. With these data we conclude that DdcA does not regulate YneA protein abundance.

ddcA deletion results in sensitivity to *yneA* overexpression independent of YneA stability

Prior work established that overexpression of *yneA* resulted in growth inhibition (21, 22). Previously, we demonstrated that the double checkpoint recovery protease mutant was considerably more sensitive than the WT strain or the single checkpoint protease mutants to *yneA* overexpression (38). Given that treatment with DNA damage has cellular consequences in addition to expression of *yneA*, we wanted to test whether overexpression of *yneA* was sufficient for enhanced growth inhibition in the absence of *ddcA*. Indeed, we found that the Δ*ddcA* mutant was more sensitive to *yneA* overexpression than WT **(Fig 3.7A)**, and that deletion of *ddcA* in the double protease mutant background resulted in even greater sensitivity to *yneA* overexpression than the double mutant or each single mutant **(Fig 3.7A)** (38). Therefore, we asked whether YneA protein levels changed under these conditions, and again there was no detectable difference when *ddcA* was deleted alone or in combination with the double protease mutant **(Fig 3.7B)**. We also considered the possibility that DdcA could affect the stability of YneA rather than the overall amount. To test this idea, we performed a translation shut-off experiment and monitored YneA stability over time. We induced expression of *yneA* in the double protease mutant with and without *ddcA* and blocked translation. We found that YneA protein abundance

decreased at a similar rate regardless of whether *ddcA* was present **(Fig 3.7C)**. We conclude that DdcA negatively regulates YneA independent of protein stability.

DdcA is an intracellular protein and DdcP and CtpA are membrane anchored with extracellular protease domains

The observation that DdcA and the checkpoint recovery proteases have distinct functions led us to ask where these proteins are located within the cell to determine if there are spatial constraints on their regulation of the DNA damage checkpoint. YneA is a membrane protein with the majority of the protein located extracellularly (22). We hypothesized that proteases DdcP and CtpA should be similarly localized since YneA is a direct substrate (38). We used the transmembrane prediction software TMHMM (46) and found that both DdcP and CtpA were predicted to have an N-terminal transmembrane domain, as reported previously (47). We tested this prediction directly using a subcellular fractionation assay (48). We found that DdcP and CtpA were present predominantly in the membrane fraction **(Fig 3.8A)**. DdcP is predicted to have a signal peptide cleavage site (47), however, we did not detect DdcP in the media **(Fig 3.8A)**, suggesting that DdcP is membrane anchored and not secreted. The membrane topology of DdcP and CtpA could put the protease domains inside or outside of the cell **(Fig 3.8B)**. To determine their location we used a protease sensitivity assay **(Fig 3.8B)** (49). Cells were treated with lysozyme, followed by incubation with proteinase K. We found that DdcP and CtpA were digested by proteinase K, but that the intracellular protein DnaN was not **(Fig 3.8C)**. In control reactions we added Triton X-100 to disrupt the plasma membrane, which rendered all three proteins susceptible to proteinase K **(Fig 3.8C)**. To verify that the N-terminal transmembrane domain is required for DdcP and CtpA to be extracellular we created N-terminal truncations **(Fig 3.8D)** and repeated the proteinase K sensitivity assay. With these variants, DdcP and CtpA should be locked inside the cell, and indeed, both N-terminal truncations were now resistant to proteinase K similar to DnaN **(Fig 3.8E)**. We conclude that DdcP and CtpA are tethered to the plasma membrane through N-terminal transmembrane domains and their protease domains are extracellular **(Fig 3.8B, left panel)**.

YneA has a transmembrane domain and has previously been shown to be localized to the plasma membrane (22), and we now show that DdcP and CtpA are membrane anchored as well. To better understand how DdcA limits YneA activity, we asked where DdcA is located. We were

unable to find DdcA detected in any previous proteomic experiments that interrogated cytosolic or extracellular proteins (50-52). Also, the secretome of *B. subtilis* was analyzed using bioinformatics and did not report DdcA as a secreted protein (47). Therefore, we used several programs to predict the subcellular location of DdcA (46, 53-55), all of which suggested that DdcA is cytosolic.

In order to experimentally determine the location of DdcA, we generated GFP fusions to the N- and C-termini of DdcA. We tested whether GFP-DdcA and DdcA-GFP were functional by assaying for the ability to complement a *ddcA* deletion. We found that GFP-DdcA was able to complement a *ddcA* deletion in the presence or absence of xylose for induced expression **(Fig 3.9A)**, similar to that observed with untagged DdcA **(Fig 3.1)**. In contrast, DdcA-GFP was partially functional, because complete complementation was only observed when expression of *ddcA-gfp* was induced using xylose, but not in the absence of xylose **(Fig 3.9A)**. As a control we asked if we could detect free GFP via Western blotting using GFP specific antiserum. We did not detect the fusion proteins in lysates if expression was not induced using xylose. We found that both DdcA fusions were detectable at their approximate molecular weight of 67.6 kDa when induced with 0.05% xylose **(Fig 3.9B)**, though we did see that the C-terminal fusion had a slight increase in mobility **(Figure 3.9B, arrowhead)**. Importantly, we did not detect a significant band near 25 kDa, the approximate size of GFP **(Fig 3.9B)**, suggesting that GFP is not cleaved from DdcA. We did detect a very faint proteolytic fragment **(Fig 3.9B, arrow)** that seemed to occur during the lysis procedure. After establishing the functionality and integrity of the GFP-DdcA fusion we chose to visualize DdcA localization via fluorescence microscopy.

To compare the background fluorescence of *B. subtilis* cells, we imaged WT (PY79) cells under the same conditions as the GFP-DdcA fusion strain. We found a low level of background fluorescence in WT cells, and when a line scan of fluorescence intensity through a cell was plotted there was a very slight increase in signal intensity in the span between the fluorescent membrane peaks **(Fig 3.9C)**. The GFP-DdcA fusion was detectable throughout the cell at very low levels in the absence of xylose induction, with the intensity being slightly greater than WT cells **(Fig 3.9C)**. We then imaged cells under conditions in which *gfp-ddcA* expression was induced with 0.05% xylose. This experiment shows that GFP-DdcA was found throughout the cytosol, and the scan of fluorescence intensity was significantly greater than WT **(Fig 3.9C)**. We

observed that the partially functional DdcA-GFP fusion was also present diffusely throughout the cytosol **(Fig 3.6A)**. Finally, we tested DdcA localization using subcellular fractionation. We found that GFP-DdcA was detectable in the membrane and cytosolic fractions **(Fig 3.9D)**, and similar results were obtained with DdcA-GFP **(Fig 3.10B)**. As controls, we found that DdcP was found in the membrane fraction and not the cytosolic fraction **(Fig 3.9D)**, and a cross-reacting protein detected by our GFP antiserum was found in the cytosol and not the membrane fractions **(Fig 3.9D)**. Taken together, DdcA appears to be an intracellular protein that is primarily located in the cytosol with some molecules localized to the membrane. Importantly we now show that DdcA and the checkpoint recovery proteases are separated in space by the plasma membrane, demonstrating that YneA regulators are present in the cytosol (DdcA) and in the extracellular space (DdcP and CtpA). Further, the demonstration of DdcA occupying a different subcellular location from DdcP and CtpA explains their distinct roles in regulating YneA.

YneA-dependent cell elongation is enhanced in cells lacking DdcA and the recovery proteases.

DdcA appears to regulate YneA activity independently of protein abundance and stability. We initially hypothesized that DdcA could interact directly with YneA to inhibit its activity. To test this hypothesis, we assayed for a protein-protein interaction using a bacterial two-hybrid, but did not detect an interaction **(Fig 3.11)**. We then asked whether DdcA affected the localization of YneA, hypothesizing that DdcA could prevent YneA from reaching the plasma membrane. To address this question, we built a strain in which GFP was fused to the N-terminus of YneA, and placed *gfp-yneA* under the control of the xylose-inducible promoter P_{xyl}. We expressed both YneA and GFP-YneA in strains lacking *ddcA*, the checkpoint recovery proteases, or the triple mutant and found that GFP-YneA is able to inhibit growth to a similar extent as YneA **(Fig 3.12A)**, suggesting that the GFP fusion is functional. We visualized GFP-YneA following induction with 0.1% xylose for 30 minutes. We found that GFP-YneA localized to the mid-cell, while also demonstrating diffuse intracellular fluorescence **(Fig 3.12B)**, which we suggest is free GFP generated by the checkpoint recovery proteases after YneA cleavage. Deletion of *ddcA* alone did not affect GFP-YneA localization, with both WT and Δ*ddcA* strains having similar mid-cell localization frequencies **(Fig 3.12B)**. The absence of both checkpoint recovery proteases resulted in puncta throughout the plasma membrane **(Fig 3.12B)**.

Intriguingly, deletion of *ddcA* in addition to the checkpoint recovery proteases resulted in severe cell elongation, however, GFP-YneA localization was not affected **(Fig 3.12B)**. The difference in cell length was quantified by measuring the cell length of at least 600 cells following growth in the presence of 0.1% xylose for 30 minutes. The cell length distributions of strains lacking *ddcA* or *ddcP* and *ctpA* were similar to the WT control **(Fig 3.12C)**. The distribution for the strain lacking *ddcA*, *ddcP*, and *ctpA* had a significant skew to the right indicating greater cell lengths **(Fig 3.12C)**. The percentage of cells greater than 5 μm in length was approximately 22% for the triple mutant and significantly greater than the other three strains in which approximately 1% of cells were greater than 5 μm **(Table 3.1)**. As a control, we determined the cell length distributions prior to xylose addition and found all four strains to have similar cell length distributions in the absence of xylose **(Fig 3.12C)**. With these data, we conclude that DdcA prevents YneA from inhibiting cell division.

Discussion

A model for DNA damage checkpoint activation and recovery

The DNA damage checkpoint in bacteria was discovered through seminal work using *E. coli* as a model organism (7). An underlying assumption in the models is that the input signal of RecA coated ssDNA and the affinity of LexA for its binding site is sufficient to control the rate of cell division in response to DNA damage. A finding that the initiator protein, DnaA, controls the transcription of *ftsL*, and as a result the rate of cell division, in response to replication stress, gave a hint that coordination of cell division and DNA replication may be more complex (39). Here, we elaborate on the complexity of regulating cell division in response to DNA damage by uncovering a DNA damage checkpoint antagonist, DdcA **(Fig 3.13)**. In response to DNA damage, the repressor LexA is inactivated, which results in expression of *yneA*. Accumulation of YneA must saturate two proteases, DdcP and CtpA, and overcome DdcA-dependent inhibition in order to block cell division. We previously reported that DdcP and CtpA are not induced by DNA damage (38), and a previous study reported that transcripts of *ddcA*, *ddcP*, and *ctpA* are not induced by DNA damage or inhibition of DNA replication (18). Thus, we model all three proteins functioning to set a threshold of YneA required for checkpoint activation with DdcA located in the cytosol and DdcP and CtpA protease domains located extracellularly. These

regulators require that YneA expression overcomes a cytosolic regulator and then two extracellular regulators before the checkpoint can be activated. After the checkpoint is established, DNA repair occurs and the integrity of the DNA is restored, the SOS response is turned off, LexA represses *yneA* expression, and the checkpoint recovery proteases degrade the remaining YneA. The genetic experiments attempting to substitute the checkpoint proteases for DdcA and vice versa strongly suggest that DdcA does not function in the checkpoint recovery process **(Fig 3.4)**. Together, our results uncover a unique strategy in regulating a bacterial DNA damage checkpoint by identifying a proteolysis independent mechanism of setting a threshold for DNA damage checkpoint activation.

How does DdcA inhibit YneA?

Our results are most supportive of DdcA acting as an antagonist to YneA, rather than functioning in checkpoint recovery. Two lines of evidence support this model. First, DdcA does not affect YneA protein levels, stability, or localization **(Fig 3.6 & 3.7)**. Second, if DdcA was involved in checkpoint recovery, we would predict that expression of one of the checkpoint proteases would be able to compensate for deletion of *ddcA*. Instead, we found that the checkpoint recovery proteases and DdcA cannot replace each other **(Fig 3.4)**. As a result, we hypothesized that DdcA acts by preventing YneA from accessing its target. We tested for an interaction between YneA and DdcA using a bacterial two-hybrid assay and we were unable to identify an interaction with full length or a cytoplasmic "locked" YneA mutant lacking its transmembrane domain **(Fig 3.11)**. We also ruled out the hypothesis that DdcA affects the subcellular localization of YneA using a GFP-YneA fusion, which had similar localization patterns with and without *ddcA* **(Fig 3.12B)**. Taken together, all these results support a model where DdcA prevents YneA from inhibiting cell division, which could occur through preventing access to the target of YneA or through an indirect mechanism.

The YneA target that results in the inhibition of cell division is unknown. YneA is a membrane bound cell division inhibitor. This class of inhibitor in bacteria is typified as being a small protein that contains an N-terminal transmembrane domain, and they have been identified in several species (21, 28-31, 56). In *Caulobacter crescentus*, the cell division inhibitors SidA and DidA inhibit the activity of FtsW/N, which are components of the divisome. A recent study in *Staphylococcus aureus* identified a small membrane division inhibitor, SosA, and its target

appears to be PBP1 (56), which is involved in peptidoglycan synthesis at the septum (57, 58). It is tempting to speculate that YneA could target an essential component of the cell division machinery, in particular because previous work found a conserved face of the transmembrane domain that was required for activity (22). Prior studies of *C. crescentus* and *S. aureus* were able to detect interactions between the cell division inhibitors and their targets using the bacterial two-hybrid assay (30, 31, 56). We reasoned that we might be able to identify an interacting partner of YneA or DdcA using this approach. We used DdcA and YneA in a bacterial two-hybrid assay using several proteins involved in cell division and cell wall synthesis, many of which had phenotypes in our previous Tn-seq genetic screens (38), but we were unable to identify a positive interaction (data not shown). Still, there are fundamental differences between YneA and other membrane bound cell division inhibitors. YneA has two major predicted features: an N-terminal transmembrane domain and a C-terminal LysM domain, and both have been found to be required for full activity (22). The other cell division inhibitors SidA, DidA, and SosA do not have a LysM domain (30, 31, 56). LysM domains bind to peptidoglycan (PG) and many proteins containing LysM domains have cell wall hydrolase activity (59). Thus, another possibility is that YneA acts directly on the cell wall to inhibit cell division instead of or in addition to targeting a membrane protein.

Intriguingly, the cell division inhibitor of *Mycobacterium tuberculosis*, Rv2719c, also contains a LysM domain and was shown to have cell wall hydrolase activity *in vitro* (28). The localization of GFP-YneA is also similar to previous reports of fluorescent vancomycin labeling of nascent peptidoglycan synthesis **(Fig 3.12B)** (60, 61). The difficulty with the model of targeting cell wall synthesis directly is that it is not clear how DdcA would prevent YneA activity given that these proteins are separated by the plasma membrane. One explanation is that DdcA directly or indirectly affects the folding of YneA as it is transported across the membrane, resulting in a form of YneA that is not competent for PG binding. DdcA contains a TPR domain and proteins containing TPR domains have been found to have chaperone activity and act as co-chaperones (62). It is intriguing that *ddcA* is just upstream of the chaperone trigger factor (*tig*) in the *B. subtilis* genome, and this organization is conserved in some bacterial species.

Negative regulation of YneA occurs through three distinct mechanisms

The checkpoint recovery proteases and DdcA utilize multiple strategies to inhibit YneA. Although both DdcP and CtpA degrade YneA, they are very different proteases. DdcP has a Lon peptidase domain and a PDZ domain, whereas CtpA has an S41 peptidase domain and a PDZ domain. The PDZ domains of DdcP and CtpA have different functions *in vivo* and show homology to different classes of PDZ domains found in proteases in *E. coli* **(Fig 3.14, see supplemental results)**. Thus, it appears that the proteases utilize different strategies to degrade YneA. DdcA is unique, because it acts as an antagonist without affecting protein abundance, stability, or localization. Also, DdcA appears to function prior to checkpoint establishment and not in recovery, whereas the proteases perform both functions. Together, DdcA, DdcP, and CtpA provide a buffer to expression of YneA, thereby setting a threshold of YneA for checkpoint enforcement.

The discovery of a specific DNA damage checkpoint antagonist brings the total known proteins to negatively regulate YneA to three, which begs the question: why isn't a single protein sufficient? One explanation is that the process can be fine-tuned. By utilizing several proteins, the process has more nodes for regulation, which is advantageous at least for *B. subtilis*. A second explanation is that this strategy evolved in response to more efficient DNA repair. The SOS-regulon is highly conserved in bacteria and yet the checkpoint strategies vary significantly (23). If an organism evolves a more efficient DNA repair system in which DNA repair could be completed faster, the same level of checkpoint protein will no longer be required, because the checkpoint would delay cell division longer than necessary to complete DNA repair. This could be the explanation for the highly divergent nature of cell division inhibitors in bacteria as well as the explanation for the complex control over YneA found in *B. subtilis*.

Materials and Methods

Bacteriological and molecular methods

All *B. subtilis* strains are derivatives of PY79 (63), and are listed in **Table 3.2**. Construction of individual strains is detailed in the supporting methods using double cross-over recombination or CRISPR/Cas9 genome editing as previously described (38, 64). *B. subtilis*

strains were grown in LB (10 g/L NaCl, 10 g/L tryptone, 5 g/L yeast extract) or $S7_{50}$ media [1x $S7_{50}$ salts (diluted from 10x $S7_{50}$ salts: 104.7g/L MOPS, 13.2 g/L, ammonium sulfate, 6.8 g/L monobasic potassium phosphate, pH 7.0 adjusted with potassium hydroxide), 1x metals (diluted from 100x metals: 0.2 M $MgCl_2$, 70 mM $CaCl_2$, 5 mM $MnCl_2$, 0.1 mM $ZnCl_2$, 100 µg/mL thiamine-HCl, 2 mM HCl, 0.5 mM $FeCl_3$), 0.1% potassium glutamate, 40 µg/mL phenylalanine, 40 µg/mL tryptophan] containing either 2% glucose or 1% arabinose as indicated in each method. Plasmids used in this study are listed in **Table 3.3**. Individual plasmids were constructed using Gibson assembly as described previously (38, 65). The details of plasmid construction are described in the supporting methods. Oligonucleotides used in this study are listed in **Table 3.4** and were obtained from Integrated DNA technologies (IDT). Antibiotics for selection in *B. subtilis* were used at the following concentrations: 100 µg/mL spectinomycin, 5 µg/mL chloramphenicol, and 0.5 µg/mL erythromycin. Antibiotics used for selection in *Escherichia coli* were used at the following concentrations: 100 µg/mL spectinomycin, 100 µg/mL ampicillin, and 50 µg/mL kanamycin. Mitomycin C (Fisher bioreagents) and phleomycin (Sigma) were used at the concentrations indicated in the figures and legends.

Spot titer assays

Spot titer assays were performed as previously described (38). Briefly, *B. subtilis* strains were grown on an LB agar plate at 30°C overnight and a single colony was used to inoculate a liquid LB culture. The cultures were grown at 37°C to an OD_{600} between 0.5 and 1. Cultures were normalized to an OD_{600} = 0.5, and serial dilutions were spotted on to LB agar media containing the drugs as indicated in the figures. Plates were grown at 30°C overnight (16-20 hours). All spot titer assays were performed at least twice.

Western blotting

Western blotting experiments for YneA were performed essentially as described (38). Briefly, for the MMC recovery assay, samples of an OD_{600} = 10 were harvested via centrifugation and washed twice with 1x PBS pH 7.4 and re-suspended in 400 µL of sonication buffer (50 mM Tris, pH 8.0, 10 mM EDTA, 20% glycerol, 2x Roche protease inhibitors, and 5 mM PMSF) and lysed via sonication. SDS sample buffer was added to 2x and samples (10 µL) were incubated at 100°C and separated using 10% SDS-PAGE (DnaN) or 16.5% Tris-Tricine

SDS-PAGE (YneA). Proteins were transferred to a nitrocellulose membrane using the BioRad transblot-turbo following the manufacturer's instructions. Membranes were blocked in 5% milk in TBST for 1 hour at room temperature. Membranes were incubated with YneA antiserum at a 1:3000 dilution in 2% milk in TBST for two hours at room temperature or at 4°C overnight. Membranes were washed three times with TBST for five minutes each and secondary antibodies (LiCor goat anti-Rabbit-680LT; 1:15000) were added and incubated for one hour at room temperature. Membranes were washed three times with TBST for five minutes each. Images of membranes were captured using the LiCor Odyssey.

For overexpression of YneA, cultures of LB were inoculated at an OD_{600} = 0.05 and incubated at 30°C until an OD_{600} of about 0.2 (about 90 minutes). Xylose was added to 0.1% and cultures were incubated at 30°C for 2 hours. Samples of an OD_{600} = 25 were harvested and re-suspended in 500 µL sonication buffer as above. All subsequent steps were performed as described above.

For GFP-DdcA and DdcA-GFP, samples of an OD_{600} = 1 were harvested from LB + 0.05% xylose cultures via centrifugation and washed twice with 1x PBS pH 7.4. Samples were re-suspended in 100 µL 1x SMM buffer (0.5 M sucrose, 0.02 M maleic acid, 0.02 M $MgCl_2$, adjusted to pH 6.5) containing 1 mg/mL lysozyme and 2x Roche protease inhibitors. Samples were incubated at room temperature for one hour and SDS sample buffer was added to 1x and incubated at 100°C for 7 minutes. Samples (10 µL) were separated via 10% or 4-20% SDS-PAGE. All subsequent steps were as described above, except GFP antisera (lot 1360-ex) was used at a 1:5000 dilution at 4°C overnight.

YneA stability assay

Cultures of LB were inoculated at an OD_{600} = 0.05 and incubated at 30°C until an OD_{600} of about 0.2 (about 90 minutes). Xylose was added to 0.1% and cultures were incubated at 30°C for 2 hours. To stop translation, erythromycin was added to 50 µg/mL and samples (OD_{600} = 10) were taken at 0, 60, 120, and 180 minutes (the strains for this experiment contain the chloramphenicol resistant gene, *cat*, which prevents chloramphenicol from being used). Western blotting was performed as described above.

Subcellular fractionation

Fractionation experiments were performed as described previously (48). A cell pellet equivalent to 1 mL OD_{600} = 1 was harvested via centrifugation (10,000 *g* for 5 minutes at room temperature), and washed with 250 µL 1x PBS. Protoplasts were generated by resuspension in 100 µL 1x SMM buffer (0.5 M sucrose, 0.02 M maleic acid, 0.02 M $MgCl_2$, adjusted to pH 6.5) containing 1 mg/mL lysozyme and 1x Roche protease inhibitors at room temperature for 2 hours. Protoplasts were pelleted via centrifugation: 5,000 *g* for 6 minutes at room temperature. Protoplasts were re-suspended in 100 µL TM buffer (20 mM Tris, pH 8.0, 5 mM $MgCl_2$, 40 units/mL DNase I (NEB), 200 µg/mL RNase A (Sigma), 0.5 mM $CaCl_2$, and 1x Roche protease inhibitors) and left at room temperature for 30 minutes. The membrane fraction was pelleted via centrifugation: 20,800 *g* for 30 minutes at 4°C. The cytosolic fraction (supernatant) was transferred to a new tube and placed on ice, and the pellet was washed with 100 µL of TM buffer and pelleted via centrifugation as above. The supernatant was discarded and the pellet was re-suspended in 120 µL of 1x SDS dye. SDS loading dye was added to 1x to the cytosolic fraction and 12 µL of each fraction were used for Western blot analysis.

Culture supernatant protein precipitation

Culture supernatants were concentrated by TCA precipitation as described previously with minor modifications (66). A culture was grown at 30°C until OD_{600} about 1, and the cells were pelleted via centrifugation: 7,000 *g* for 10 minutes at room temperature. The culture supernatant (30 mL) was filtered using a 0.22 µm filter and placed on ice. Proteins were precipitated by addition of 6 mL ice-cold 100% TCA (6.1N), and left on ice for 30 minutes. Precipitated proteins were pelleted via centrifugation: 18,000 rpm (Sorvall SS-34 rotor) for 30 minutes at 4°C. Pellets were washed with 1 mL ice-cold acetone and pelleted again via centrifugation: 20,000 *g* for 15 minutes at 4°C. The supernatant was discarded, and the residual acetone was evaporated by placing tubes in 100°C heat block for 1-2 minutes. Protein pellets were re-suspended in 120 µL 6x SDS-loading dye and 12 µL were used in Western blot analysis.

Proteinase K sensitivity assay

Proteinase K sensitivity assays were performed similar to previous reports (49, 67). A cell pellet from 0.5 mL OD_{600} = 1 equivalent was harvested and washed as in "subcellular

fractionation." Protoplasts were generated by resuspension in 36 µL 1x SMM buffer (0.5 M sucrose, 0.02 M maleic acid, 0.02 M $MgCl_2$, adjusted to pH 6.5) containing 1 mg/mL lysozyme at room temperature for 1 hour. Either 9 µL of 1x SMM buffer or 0.5 mg/mL proteinase K (dissolved in 1x SMM buffer) was added (final proteinase K concentration of 100 µg/mL) and incubated at 37°C for the time indicated in the figures. Reactions were stopped by the addition of 5 µL 50 mM PMSF (final concentration of 5 mM) and 25 µL 6x SDS-dye (final concentration of 2x). For Western blot analysis, 12 µL were used.

Microscopy

Strains were grown on LB agar plates containing 5 µg/mL chloramphenicol at 30°C overnight. For GFP-DdcA and DdcA-GFP, LB agar plates were washed with $S7_{50}$ media containing 1% arabinose and cultures of $S7_{50}$ media containing 1% arabinose and 0.05% xylose were inoculated at an OD_{600} = 0.1 and incubated at 30°C until an OD_{600} of about 0.4. Samples were taken and incubated with 2 µg/mL FM4-64 for 5 minutes and transferred to pads of 1x Spizizen salts and 1% agarose. Images were captured with an Olympus BX61 microscope using 250 ms and 1000 ms exposure times for FM4-64 (membranes) and GFP, respectively. The brightness and contrast were adjusted for FM4-64 images with adjustments applied to the entire image. Strains with GFP-YneA were grown on LB agar plates containing 5 µg/mL chloramphenicol overnight at 30°C. Plates were washed with $S7_{50}$ minimal media containing 1% arabinose and cultures started at an OD_{600} = 0.1. Cultures were grown at 30°C until an OD_{600} of about 0.3 and xylose was added to 0.1%. Cultures were grown for 30 minutes at 30°C and imaged as for GFP-DdcA with exposure times of 300 ms for FM4-64 and 500 ms for GFP.

Figures and Tables

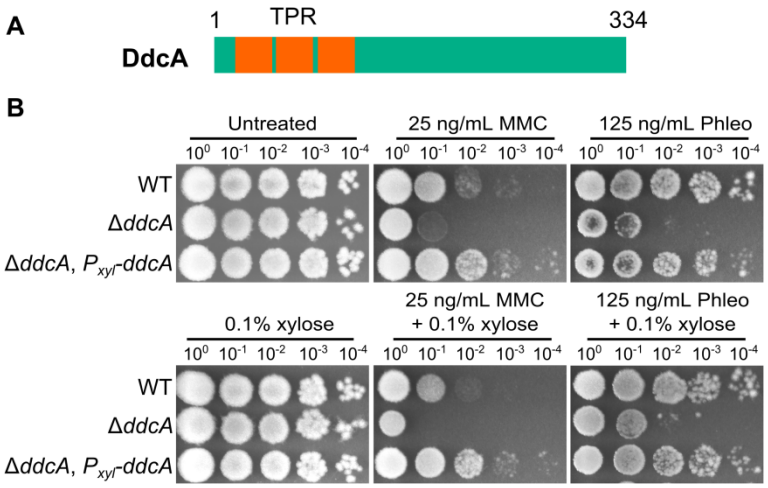

Figure 3.1 Deletion of *ddcA* (*ysoA*) results in sensitivity to DNA damage. (A) A schematic of the DdcA protein. DdcA is predicted to have 334 amino acids and 3 tetratrichopeptide repeats at its N-terminus. **(B)** A spot titer assay in which exponentially growing cultures of *B. subtilis* strains WT (PY79), Δ*ddcA* (PEB357), and Δ*ddcA*, *amyE::P*$_{xyl}$*-ddcA* (PEB503) were spotted on the indicated media and incubated at 30°C overnight.

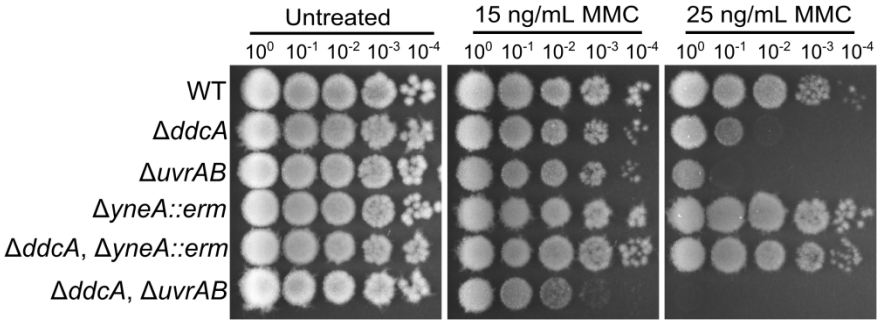

Figure 3.2 DNA damage sensitivity of *ddcA* deletion is dependent on DNA damage checkpoint protein YneA and independent of nucleotide excision repair. A spot titer assay using *B. subtilis* strains WT (PY79), Δ*ddcA* (PEB357), Δ*uvrAB* (PEB309), Δ*yneA::erm* (PEB433), Δ*ddcA* Δ*yneA::erm* (PEB495), and Δ*ddcA* Δ*uvrAB* (PEB497) spotted on the indicated media.

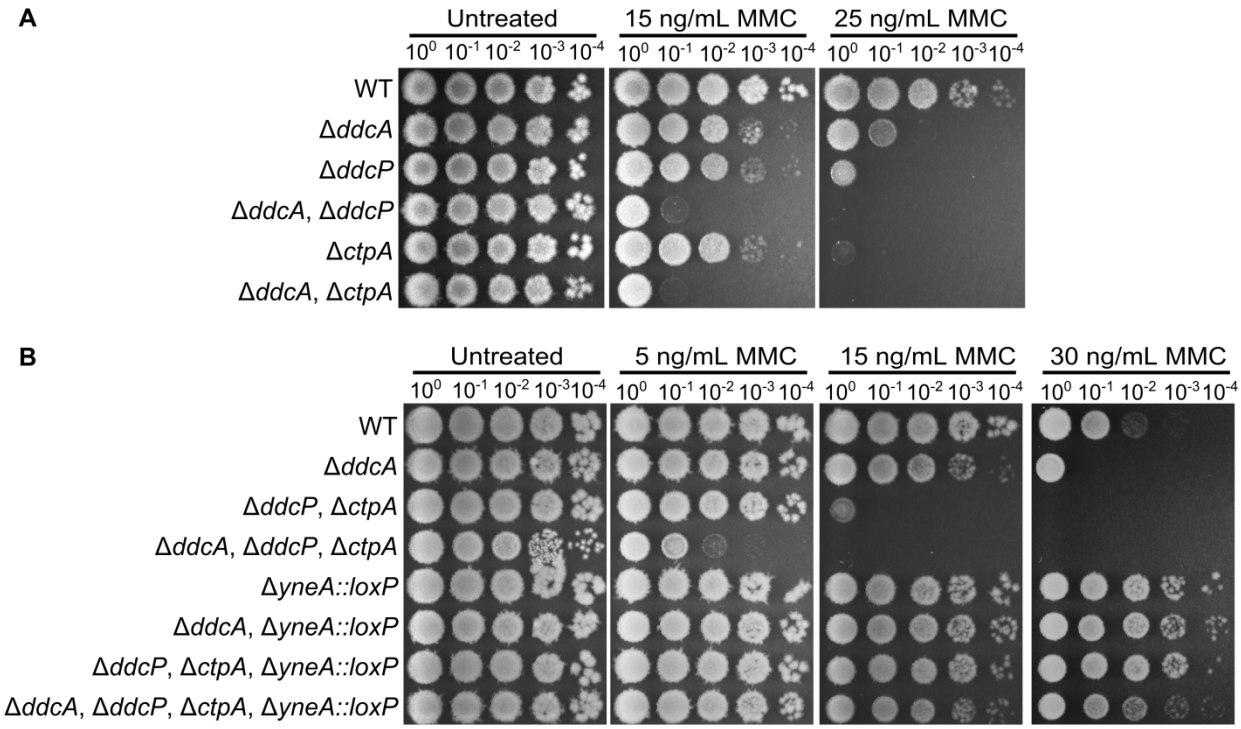

Figure 3.3 DdcA functions independent of the checkpoint recovery proteases. (A) Spot titer assay using *B. subtilis* strains WT (PY79), Δ*ddcA* (PEB357), Δ*ddcP* (PEB324), Δ*ddcA* Δ*ddcP* (PEB499), Δ*ctpA* (PEB355), and Δ*ddcA* Δ*ctpA* (PEB579) spotted on the indicated media. **(B)** Spot titer assay using *B. subtilis* strains WT (PY79), Δ*ddcA* (PEB357), Δ*ddcP* Δ*ctpA* (PEB555), Δ*ddcA* Δ*ddcP* Δ*ctpA* (PEB639), Δ*yneA::loxP* (PEB439), Δ*ddcA* Δ*yneA::loxP* (PEB587), Δ*ddcP* Δ*ctpA* Δ*yneA::loxP* (PEB561), and Δ*ddcA* Δ*ddcP* Δ*ctpA* Δ*yneA::loxP* (PEB643) spotted on the indicated media.

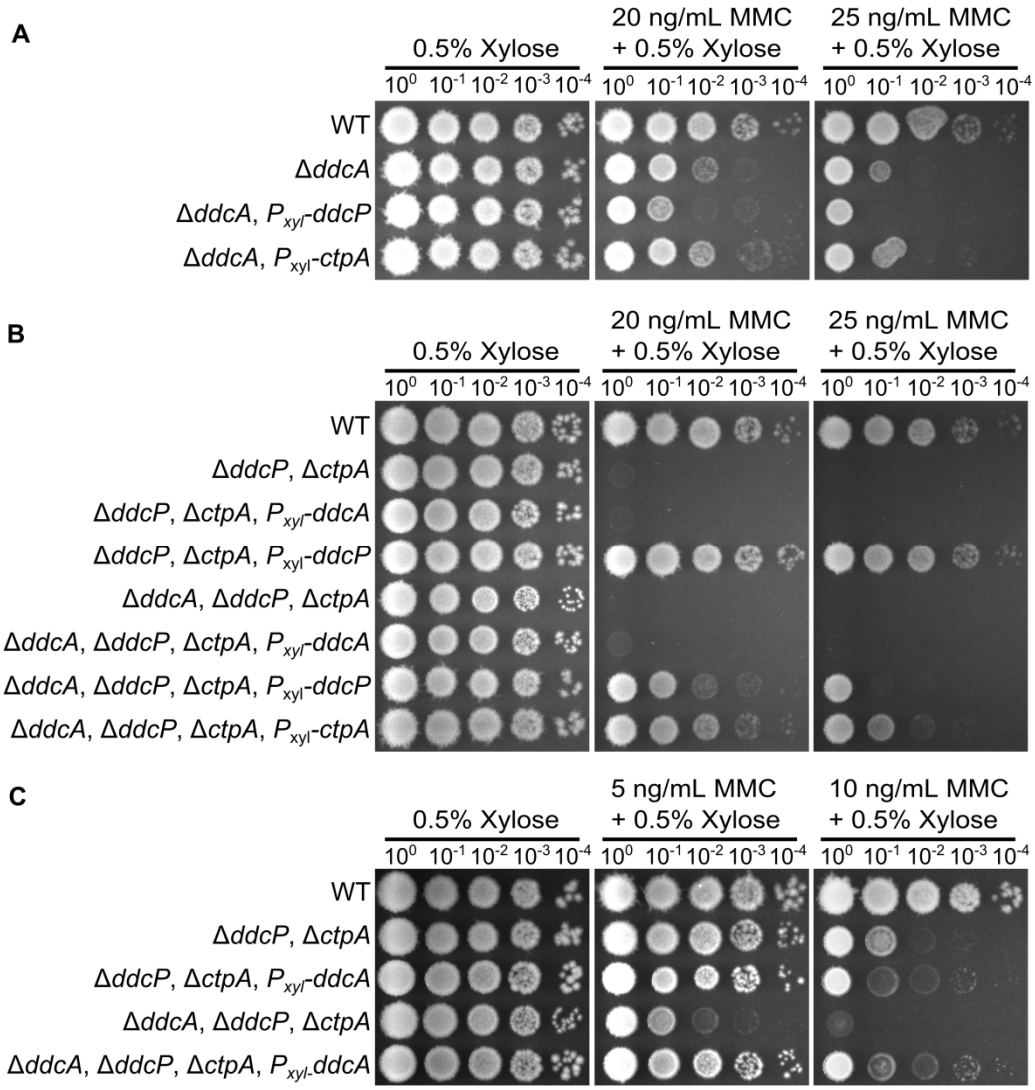

Figure 3.4 DdcA cannot complement loss of checkpoint recovery proteases. (A) Spot titer assay using *B. subtilis* strains WT (PY79), Δ*ddcA* (PEB357), Δ*ddcA amyE::*P_{xyl}*-ddcP* (PEB836), and Δ*ddcA amyE::*P_{xyl}*-ctpA* (PEB837) spotted on the indicated media. **(B)** Spot titer assay using *B. subtilis* strains WT (PY79), Δ*ddcP* Δ*ctpA* (PEB555), Δ*ddcP,* Δ*ctpA*, *amyE::*P_{xyl}*-ddcA* (PEB838), Δ*ddcP,* Δ*ctpA*, *amyE::*P_{xyl}*-ddcP* (PEB557), Δ*ddcA* Δ*ddcP* Δ*ctpA* (PEB639), Δ*ddcP,* Δ*ctpA*, Δ*ddcA*, *amyE::*P_{xyl}*-ddcA* (PEB840), Δ*ddcP,* Δ*ctpA*, Δ*ddcA*, *amyE::*P_{xyl}*-ddcP* (PEB839), and Δ*ddcP,* Δ*ctpA*, Δ*ddcA*, *amyE::*P_{xyl}*-ctpA* (PEB841) spotted on the indicated media. **(C)** Spot titer assay using *B. subtilis* strains WT (PY79), Δ*ddcP* Δ*ctpA* (PEB555), Δ*ddcP,* Δ*ctpA*, *amyE::*P_{xyl}*-ddcA* (PEB838), Δ*ddcA* Δ*ddcP* Δ*ctpA* (PEB639), Δ*ddcP,* Δ*ctpA*, and Δ*ddcA*, *amyE::*P_{xyl}*-ddcA* (PEB840) spotted on the indicated media.

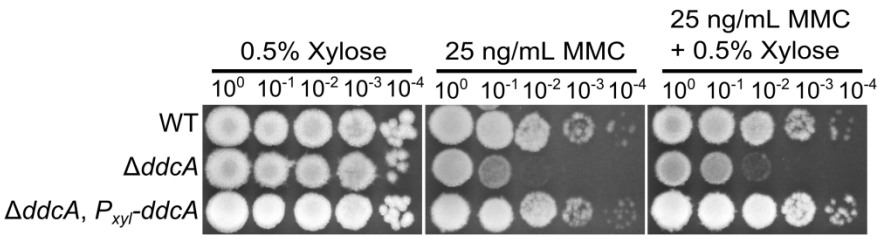

Figure 3.5 Deletion of *ddcA* can be complemented by ectopic expression using high levels of xylose. A Spot titer assay using WT (PY79), Δ*ddcA* (PEB357), and Δ*ddcA amyE::P*$_{xyl}$*-ddcA* (PEB503) spotted on the indicated media and incubated at 30°C overnight.

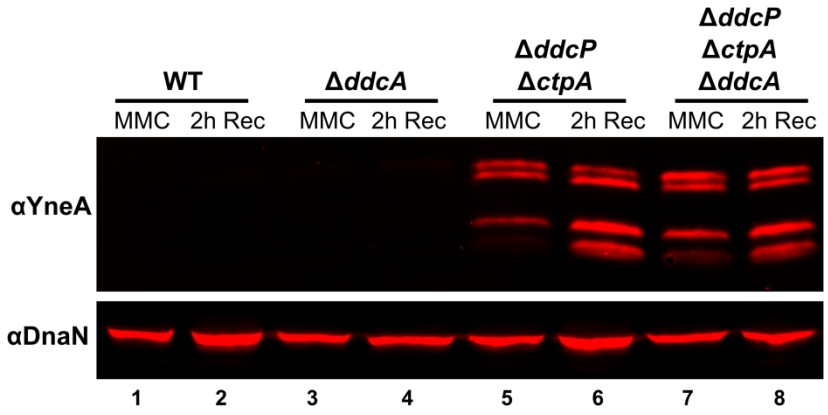

Figure 3.6 Deletion of *ddcA* does not increase YneA protein levels following MMC treatment and recovery. Western blotting using antisera against YneA (top panel) or DnaN (bottom panel) using whole cell extracts from WT (PY79), Δ*ddcA* (PEB357), Δ*ddcP* Δ*ctpA* (PEB555), Δ*ddcA* Δ*ddcP* Δ*ctpA* (PEB639) after a two hour treatment with 100 ng/mL MMC (lanes labeled "MMC") or after recovering for two hours from MMC treatment (lanes labeled "2h Rec").

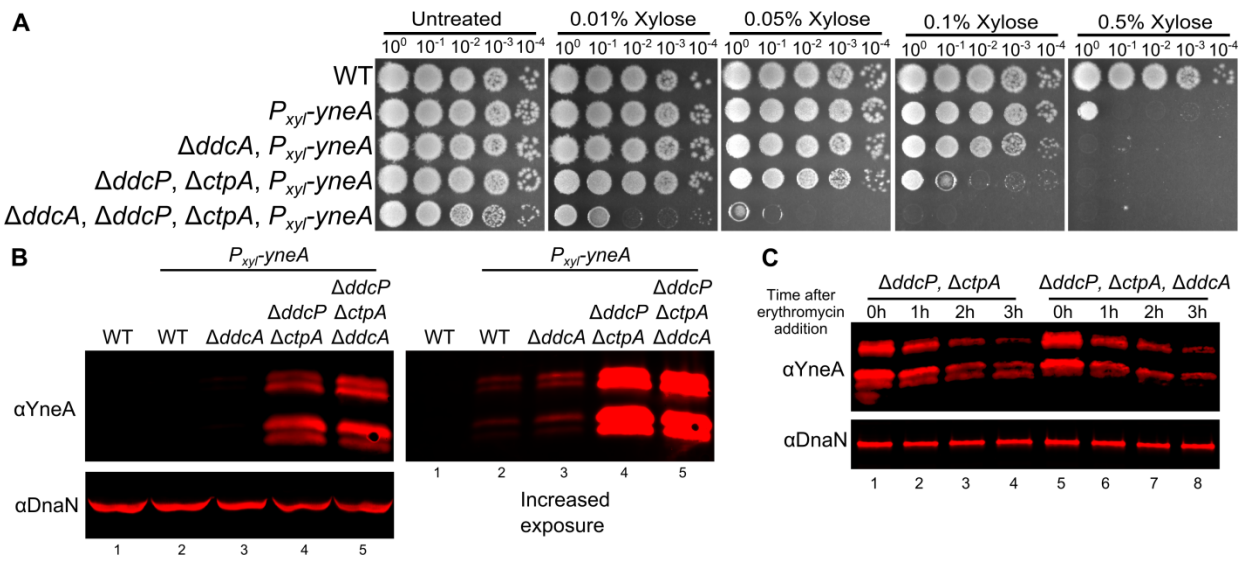

Figure 3.7 Deletion of *ddcA* results in sensitivity to *yneA* overexpression independent of YneA stability. (A) Spot titer testing the effect of *yneA* overexpression. *B. subtilis* strains WT (PY79), *amyE::P*$_{xyl}$*-yneA* (PEB846), Δ*ddcA amyE::P*$_{xyl}$*-yneA* (PEB848), Δ*ddcP,* Δ*ctpA*, *amyE::P*$_{xyl}$*-yneA* (PEB850), and Δ*ddcA* Δ*ddcP* Δ*ctpA, amyE::P*$_{xyl}$*-yneA* (PEB852) were spotted on LB agar media containing increasing concentrations of xylose to induce *yneA* expression. **(B)** A Western blot using antisera against YneA (Upper panels), or DnaN lower panel using *B. subtilis* strains WT (PY79), *amyE::P*$_{xyl}$*-yneA* (PEB846), Δ*ddcA amyE::P*$_{xyl}$*-yneA* (PEB848), Δ*ddcP,* Δ*ctpA*, *amyE::P*$_{xyl}$*-yneA* (PEB850), and Δ*ddcA* Δ*ddcP* Δ*ctpA, amyE::P*$_{xyl}$*-yneA* (PEB852) after growing in the presence of 0.1% xylose for two hours. The panel on the right is an increased exposure to show the faint bands of WT and Δ*ddcA*. **(C)** A Western blot using antisera against YneA (upper panel) or DnaN (lower panel). Cultures of Δ*ddcP,* Δ*ctpA*, *amyE::P*$_{xyl}$*-yneA* (PEB850) and Δ*ddcA* Δ*ddcP* Δ*ctpA, amyE::P*$_{xyl}$*-yneA* (PEB852) were grown as in panel B, except at 0 hours erythromycin was added and samples were harvest every hour for three hours.

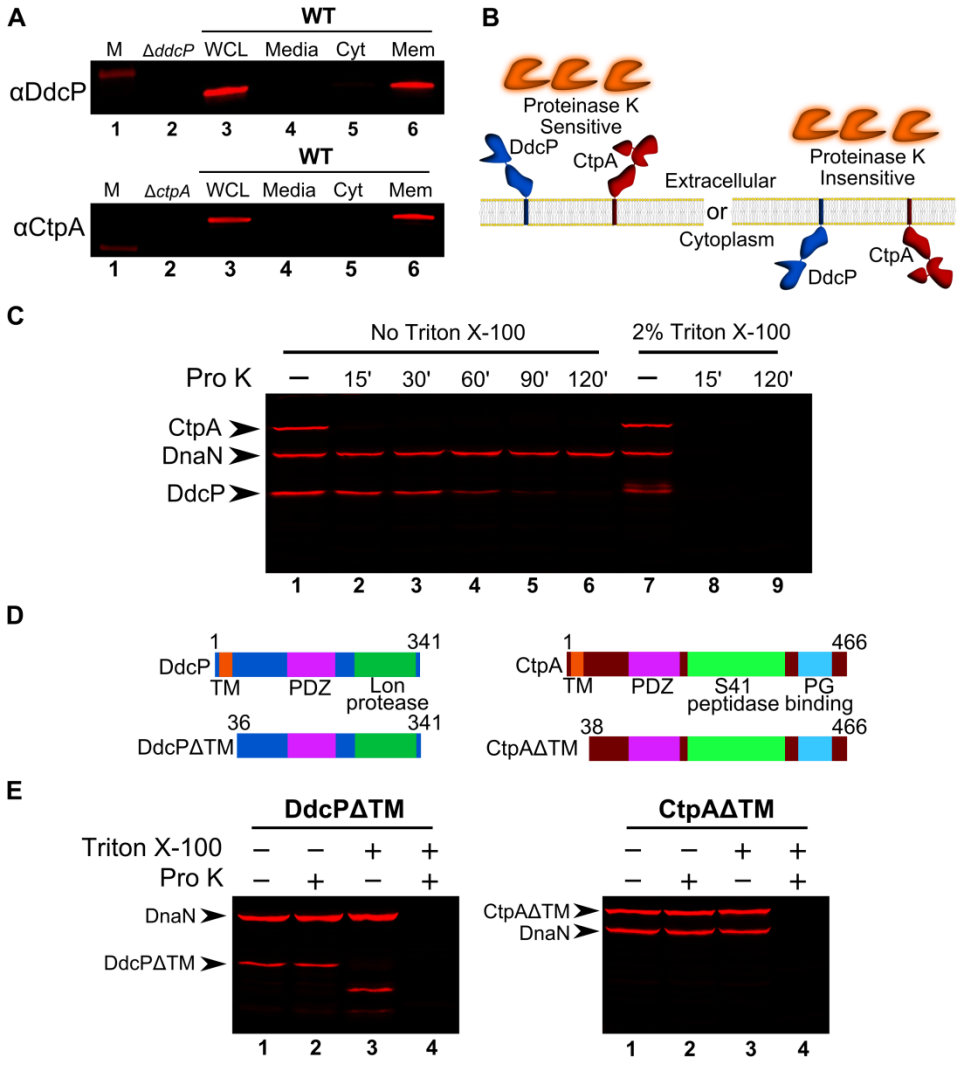

Figure 3.8 DdcP and CtpA are membrane anchored with extracellular protease domains. **(A)** Subcellular fractionation followed by Western blot analysis of WT (PY79) lysates using DdcP and CtpA antisera (M, molecular weight standard, WCL, whole cell lysates; Media, precipitated media proteins; Cyt, cytosolic fraction; Mem, membrane fraction). **(B)** Competing models for membrane topology of DdcP and CtpA tested using a proteinase K sensitivity assay. **(C)** Proteinase K sensitivity assay followed by Western blot detection of DdcP, CtpA, and DnaN with antiserum. Samples were treated with lysozyme to generate protoplasts and incubated with proteinase K for the indicated time (lanes 1-6), or the samples were incubated with lysozyme and Triton X-100 to disrupt the plasma membrane and incubated with proteinase K for the indicated time (lanes 7-9). **(D)** Schematics depicting the DdcPΔTM (left) and CtpAΔTM (right) in which the transmembrane domain was deleted. **(E)** Proteinase K sensitivity assay followed by Western blot analysis of strains expressing DdcPΔTM (left, PEB719) or CtpAΔTM (right, PEB772) performed as in panel C using a 2 hour incubation with proteinase K.

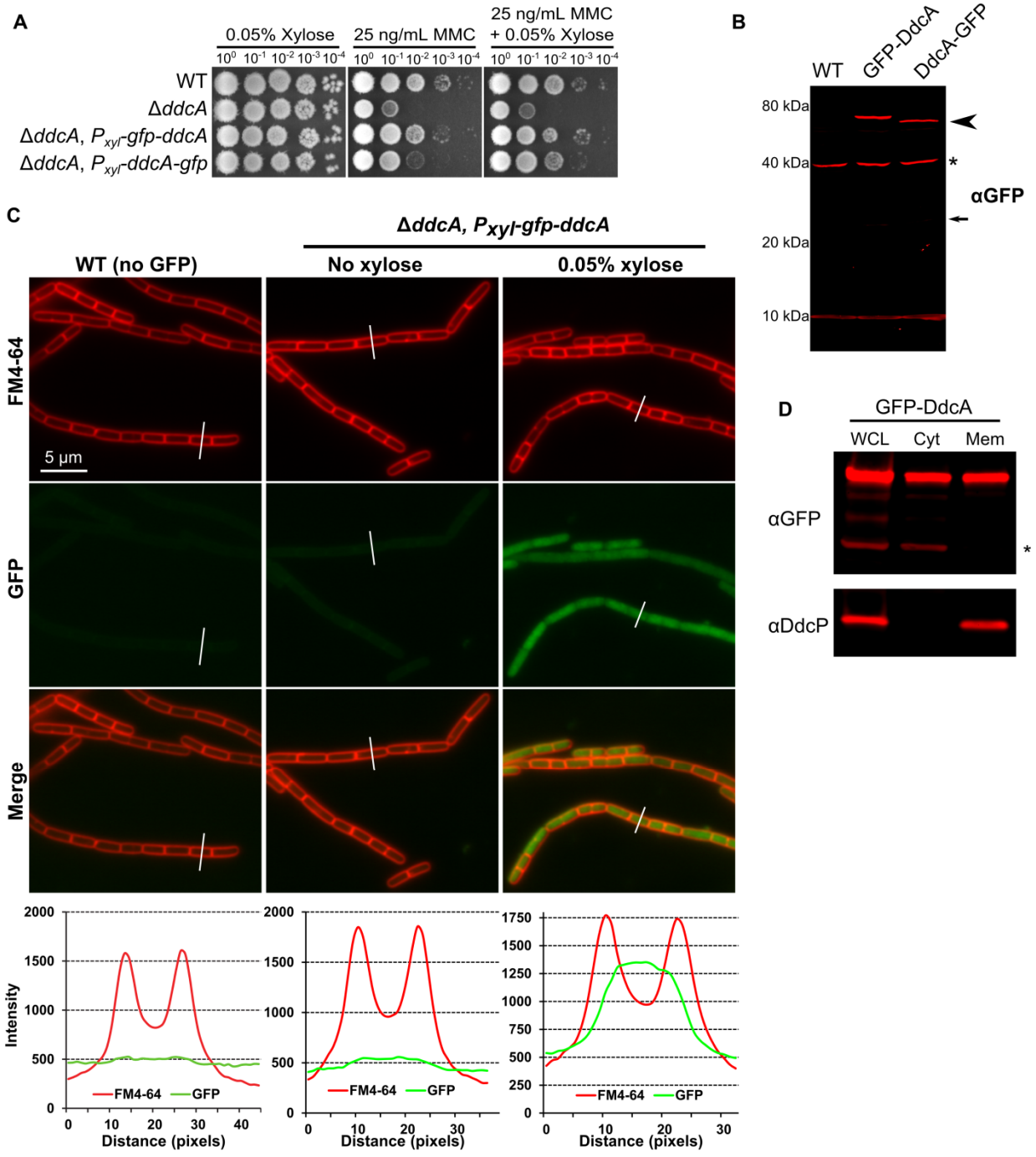

Figure 3.9 GFP-DdcA is an intracellular protein and is present in the cytosolic and membrane fractions. (A) Spot titer assay using *B. subtilis* strains WT (PY79), Δ*ddcA* (PEB357), Δ*ddcA amyE::P*$_{xyl}$*-gfp-ddcA* (PEB854), and Δ*ddcA amyE::P*$_{xyl}$*-ddcA-gfp* (PEB856) spotted on the indicated media. **(B)** Western blot of cell extracts from *B. subtilis* strains WT (PY79), Δ*ddcA amyE::P*$_{xyl}$*-gfp-ddcA* (PEB854), and Δ*ddcA amyE::P*$_{xyl}$*-ddcA-gfp* (PEB856) using antiserum against GFP. The arrowhead highlights the slightly increased mobility of DdcA-GFP, and the asterisk denotes a cross-reacting species detected by the GFP antiserum. The smaller arrow indicates the expected migration of free GFP. **(C)** Micrographs from WT (PY79) and

Δ*ddcA amyE::P*$_{xyl}$*-gfp-ddcA* (PEB854) cultures grown in S7$_{50}$ minimal media containing 1% arabinose with (far left and right panels) or without (middle panels) 0.05% xylose. Images in red are the membrane stain FM4-64, green are GFP fluorescence and the bottom images are a merge of FM4-64 and GFP fluorescence. The white lines through cells in the images are a representation of the line scans of fluorescence intensity generated in ImageJ and plotted below the micrographs. Scale bar is 5 µm. **(D)** Western blot of whole cell lysate (WCL), cytosolic fraction (Cyt), and membrane fraction (Mem) from Δ*ddcA amyE::P*$_{xyl}$*-gfp-ddcA* (PEB854) cell extracts using antisera against GFP (upper panel) or DdcP (lower panel). The asterisk denotes a cross-reacting species detected by the GFP antiserum.

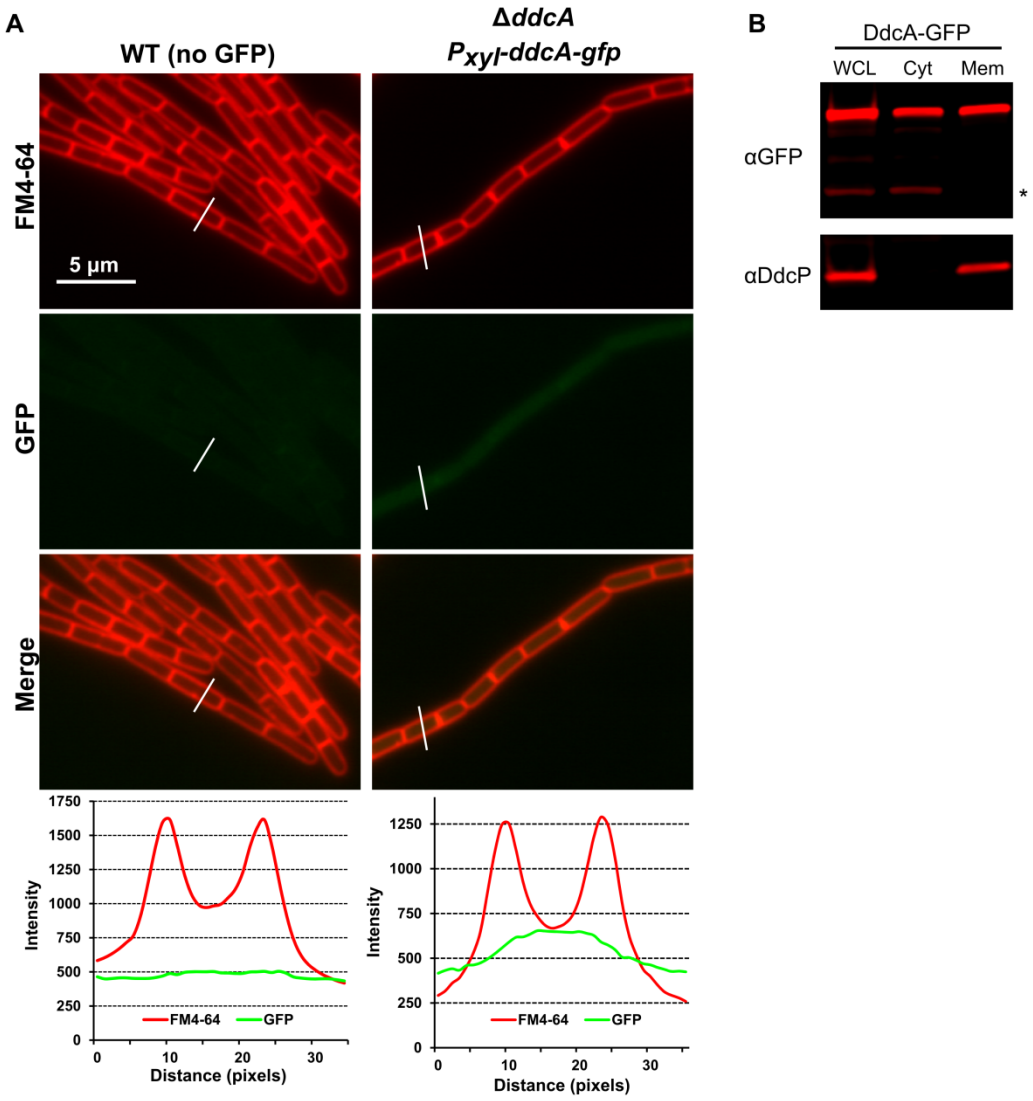

Figure 3.10 DdcA-GFP is intracellular and found in the cytosolic and membrane fractions. **(A)** Micrographs from WT (PY79) and Δ*ddcA amyE::P*$_{xyl}$*-ddcA-gfp* (PEB856) cultures grown in S7$_{50}$ minimal media containing 1% arabinose and 0.05% xylose. Images in red are the membrane stain FM4-64, green are GFP fluorescence and the bottom images are a merge of FM4-64 and GFP fluorescence. The white lines through cells in the images are a representation of the line scans of fluorescence intensity generated in ImageJ and plotted below the micrographs. Scale bar

is 5 µm. **(B)** Western blot of the whole cell lysate (WCL), cytosolic fraction (Cyt), and membrane fraction (Mem) from Δ*ddcA amyE::P*$_{xyl}$*-ddcA-gfp* (PEB856) cell extracts using antisera against GFP (upper panel) or DdcP (lower panel). The asterisk denotes a cross-reacting species detected by the GFP antiserum.

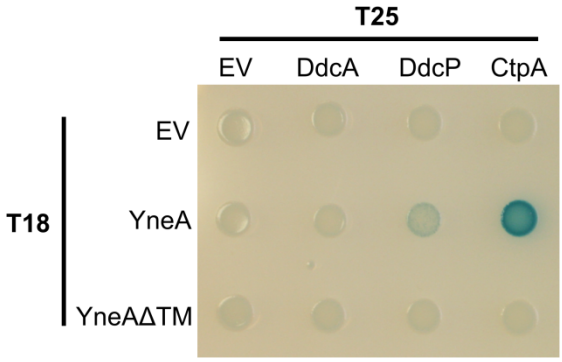

Figure 3.11 DdcA and YneA do not interact in bacterial two hybrid assay. Plasmids containing the indicated T18 (rows) and T25 (columns) fusions were used to co-transform *E. coli* BTH101 cells, which were spotted onto LB containing X-gal and IPTG.

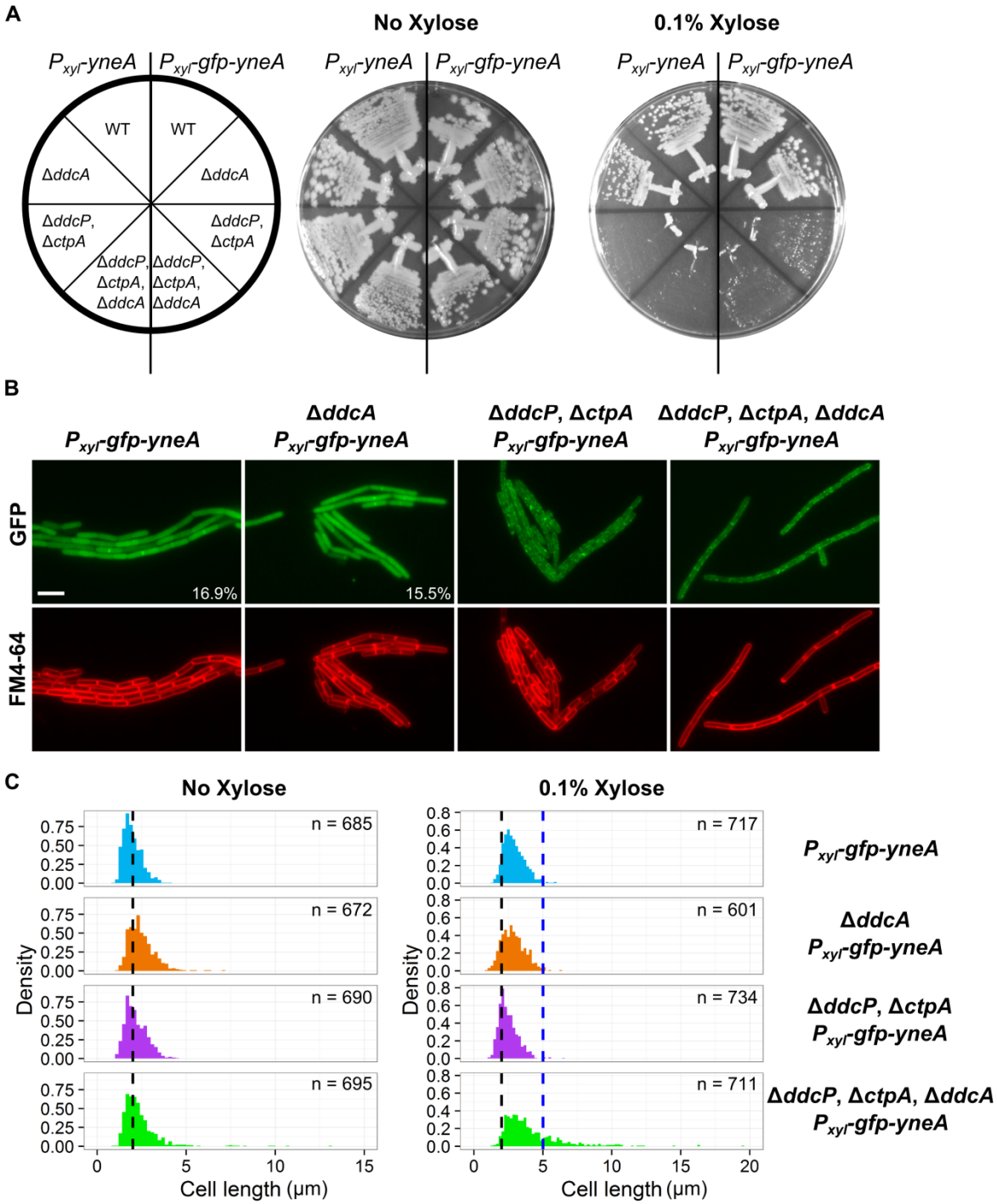

Figure 3.12 DdcA inhibits YneA. (A) *B. subtilis* strains *amyE::*P_{xyl}*-yneA* (PEB846), Δ*ddcA amyE::*P_{xyl}*-yneA* (PEB848), Δ*ddcP,* Δ*ctpA*, *amyE::*P_{xyl}*-yneA* (PEB850), and Δ*ddcA* Δ*ddcP* Δ*ctpA, amyE::*P_{xyl}*-yneA* (PEB852), *amyE::*P_{xyl}*-gfp-yneA* (PEB876), Δ*ddcA amyE::*P_{xyl}*-gfp-yneA* (PEB882), Δ*ddcP,* Δ*ctpA*, *amyE::*P_{xyl}*-gfp-yneA* (PEB888), and Δ*ddcA* Δ*ddcP* Δ*ctpA, amyE::*P_{xyl}*-gfp-yneA* (PEB894) were struck onto LB or LB + 0.1% xylose and incubated at 30°C overnight. **(B)** Micrographs from the indicated strains from Panel A, grown in minimal media and treated with 0.1% xylose for 30 minutes. Green images are GFP fluorescence and red images are FM4-

64 membrane stain. The percentage of septal localization is shown for PEB876 (n=591) and PEB882 (n=542). The p-value of a two-tailed z-test was 0.516. Scale bar is 5 μm. **(C)** Cell length distributions of strains grown with (right) or without (left) 0.1% xylose. The number of cells measured (n) for each condition is indicated. The black vertical dashed line is at 2 μm and the blue vertical dashed line is at 5μm.

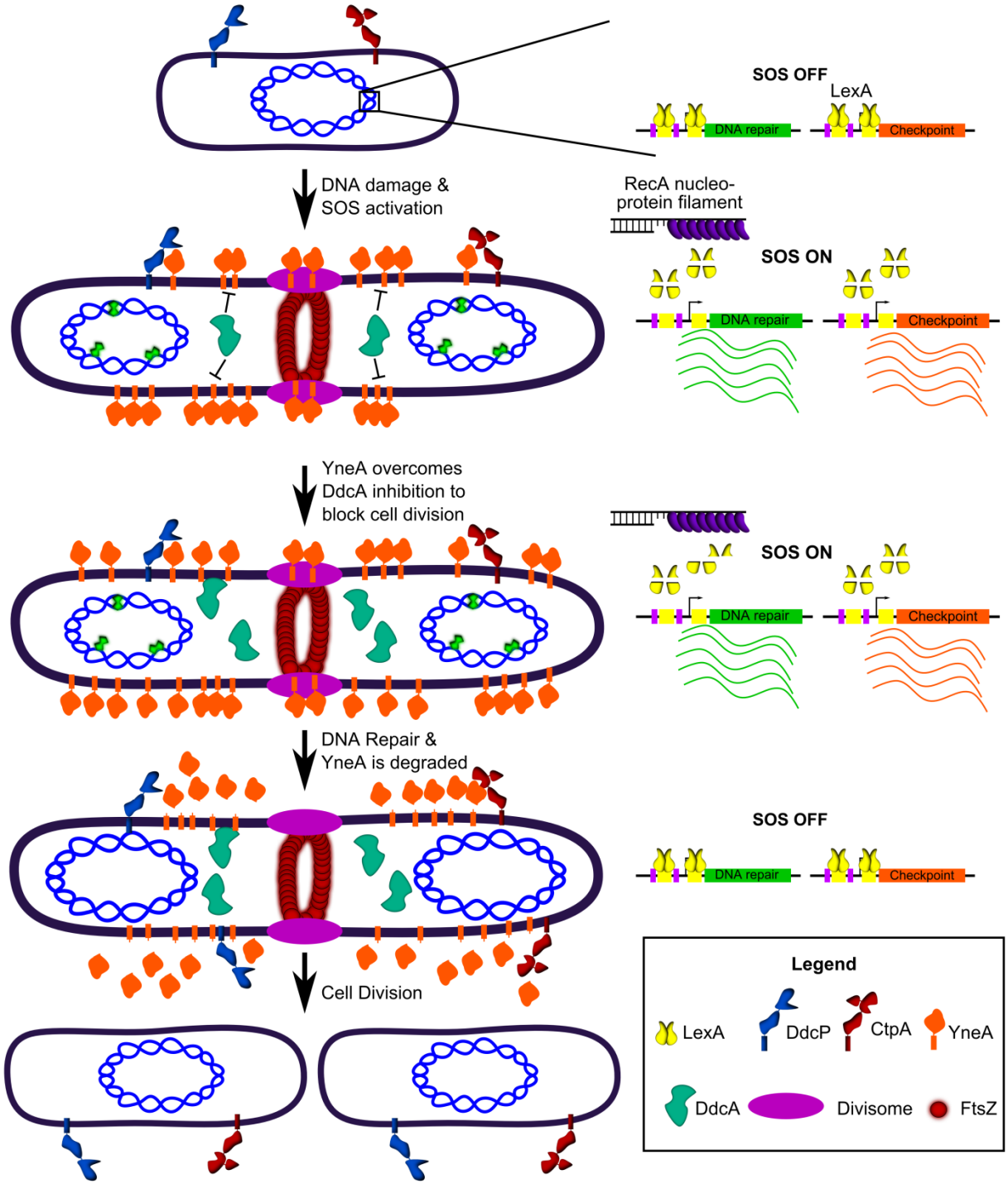

Figure 3.13 DdcA inhibits enforcement of the DNA damage checkpoint. A working model for how DdcA inhibits YneA. DdcA prevents access to the target of YneA, however, when the SOS response has been activated for a prolonged period of time, YneA is able to overcome DdcA dependent inhibition to prevent cell division. Following DNA repair and completion of DNA replication the SOS response is turned off and the checkpoint recovery proteases degrade YneA allowing cell division to resume.

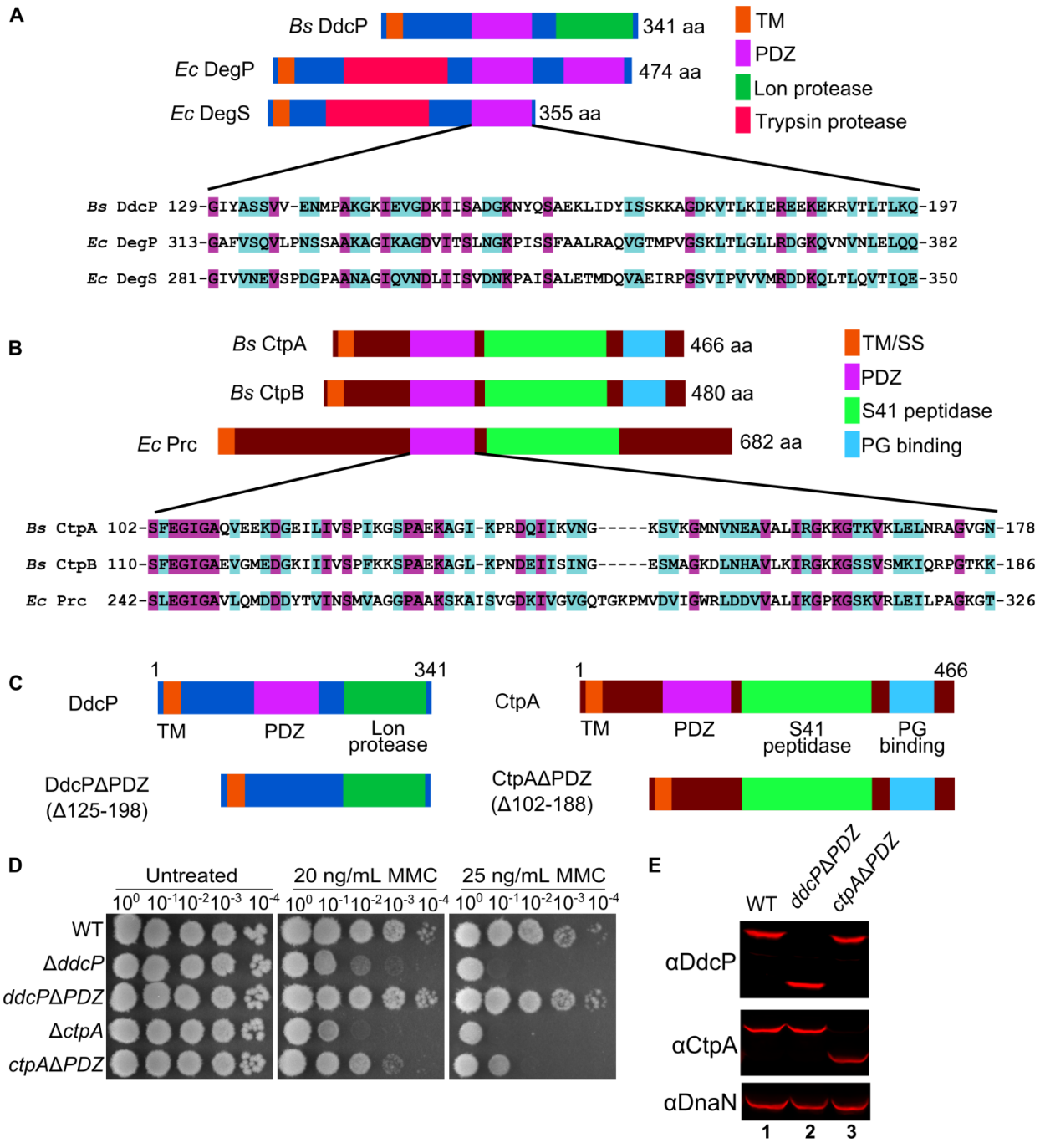

Figure 3.14 DdcP and CtpA PDZ domains have different functions *in vivo*. (A) Alignment of the PDZ domain of DdcP to the PDZ domains of DegP and DegS from *E. coli*. **(B)** Alignment of

the PDZ domain of CtpA to the PDZ domains of CtpB from *B. subtilis* and Prc from *E. coli*. **(C)** Schematics of ΔPDZ constructs used in panels B and C. **(D)** Spot titer assay using *B. subtilis* strains WT (PY79), Δ*ddcP* (PEB324), *ddcP*Δ*PDZ* (PEB774), Δ*ctpA* (PEB355), and *ctpA*Δ*PDZ* (PEB776) media. **(E)** Western blot analysis of WT (PY79), *ddcP*Δ*PDZ* (PEB774), and *ctpA*Δ*PDZ* (PEB776) cell lysates using DdcP, CtpA, and DnaN antiserum.

		No Xylose	0.1% Xylose		
Strain	**Genotype**	**Cell length (mean ± sd)**	**Cell length (mean ± sd)**	**% ≥ 5 µm**	**p-value**
PEB876	*amyE::P$_{xyl}$-gfp-yneA*	1.98 ± 0.51 (n = 685)	2.91 ± 0.75	0.84% (6/717)	N/A
PEB882	Δ*ddcA*, *amyE::P$_{xyl}$-gfp-yneA*	2.48 ± 0.73 (n = 672)	2.86 ± 0.85	1.16% (7/601)	0.55
PEB888	Δ*ddcP,* Δ*ctpA*, *amyE::P$_{xyl}$-gfp-yneA*	2.18 ± 0.60 (n = 690)	2.49 ± 0.70	0.68% (5/734)	0.73
PEB894	Δ*ddcP,* Δ*ctpA*, Δ*ddcA*, *amyE::P$_{xyl}$-gfp-yneA*	2.39 ± 1.10 (n = 695)	4.09 ± 2.09	22.4% (159/711)	<0.00001

Table 3.1 Over-expression of GFP-YneA results in a significant increase in cells greater than 5 µm in cells lacking *ddcP*, *ctpA*, and *ddcA*. Data are from expression of GFP-YneA using 0.1% xylose for 30 minutes. The mean cell length ± the standard deviation is listed. The percent of cells greater than 5 µm (number/total cells scored) and the p-value from a two-tailed z-test are listed.

Strain	Genotype	Reference
PY79	PY79	(63)
PEB309	Δ*uvrAB*	This study
PEB324	Δ*ddcP* (*ylbL*)	(38)
PEB355	Δ*ctpA*	(38)
PEB357	Δ*ddcA* (*ysoA*)	(38)
PEB433	Δ*yneA::erm*	(38)
PEB439	Δ*yneA::loxP*	(38)
PEB495	Δ*ddcA,* Δ*yneA::erm*	This study
PEB497	Δ*uvrAB,* Δ*ddcA*	This study
PEB499	Δ*ddcP,* Δ*ddcA*	This study
PEB503	Δ*ddcA*, *amyE::P$_{xyl}$-ddcA*	This study
PEB555	Δ*ddcP,* Δ*ctpA*	(38)
PEB557	Δ*ddcP,* Δ*ctpA*, *amyE::P$_{xyl}$-ddcP*	(38)
PEB561	Δ*ddcP,* Δ*ctpA*, Δ*yneA::loxP*	(38)
PEB579	Δ*ctpA,* Δ*ddcA*	This study
PEB587	Δ*ddcA,* Δ*yneA::loxP*	This study
PEB619	Δ*ddcP,* Δ*ctpA*, *amyE::P$_{xyl}$-ctpA*	(38)
PEB639	Δ*ddcP,* Δ*ctpA*, Δ*ddcA*	This study
PEB643	Δ*ddcP,* Δ*ctpA*, Δ*ddcA*, Δ*yneA::loxP*	This study
PEB719	Δ*ddcP, amyE::P$_{xyl}$-ddcP*Δ*TM*	This study
PEB772	Δ*ctpA, amyE::P$_{xyl}$-ctpA*Δ*TM*	This study
PEB774	*ddcP*Δ*PDZ*	This study
PEB776	*ctpA*Δ*PDZ*	This study
PEB836	Δ*ddcA*, *amyE::P$_{xyl}$-ddcP*	This study
PEB837	Δ*ddcA*, *amyE::P$_{xyl}$-ctpA*	This study
PEB838	Δ*ddcP,* Δ*ctpA*, *amyE::P$_{xyl}$-ddcA*	This study
PEB839	Δ*ddcP,* Δ*ctpA*, Δ*ddcA*, *amyE::P$_{xyl}$-ddcP*	This study
PEB840	Δ*ddcP,* Δ*ctpA*, Δ*ddcA*, *amyE::P$_{xyl}$-ddcA*	This study
PEB841	Δ*ddcP,* Δ*ctpA*, Δ*ddcA*, *amyE::P$_{xyl}$-ctpA*	This study
PEB846	*amyE::P$_{xyl}$-yneA*	This study
PEB848	Δ*ddcA*, *amyE::P$_{xyl}$-yneA*	This study
PEB850	Δ*ddcP,* Δ*ctpA*, *amyE::P$_{xyl}$-yneA*	This study
PEB852	Δ*ddcP,* Δ*ctpA*, Δ*ddcA*, *amyE::P$_{xyl}$-yneA*	This study
PEB854	Δ*ddcA*, *amyE::P$_{xyl}$-gfp-ddcA*	This study
PEB856	Δ*ddcA*, *amyE::P$_{xyl}$-ddcA-gfp*	This study
PEB876	*amyE::P$_{xyl}$-gfp-yneA*	This study
PEB882	Δ*ddcA*, *amyE::P$_{xyl}$-gfp-yneA*	This study
PEB888	Δ*ddcP,* Δ*ctpA*, *amyE::P$_{xyl}$-gfp-yneA*	This study
PEB894	Δ*ddcP,* Δ*ctpA*, Δ*ddcA*, *amyE::P$_{xyl}$-gfp-yneA*	This study

Table 3.2 Strains used in this study.

Plasmid number	Plasmid name	Reference/Source
pKT25	pKT25	Euromedex (EUP-25C)
pUT18C	pUT18C	Euromedex (EUP-18C)
pDR244	pDR244	*Bacillus* Genetic Stock Center
pPB41	pPB41	(64, 68)
pPB47	pPB47	(38)
pPB73	pPB41-CRISPR::*uvrB*	(38)
pPB84	pPB73-Δ*uvrAB* editing template	This Study
pPB108	pPB47-*amyE::*P_{xyl}*-ddcP-cam*^{R}	(38)
pPB122	pPB115-Δ*ddcA* editing template	(38)
pPB147	pPB47-*amyE::*P_{xyl}*-ddcA-cam*^{R}	This study
pPB184	pPB47-*amyE::*P_{xyl}*-ctpA-cam*^{R}	(38)
pPB192	pPB47-*amyE::*P_{xyl}*-yneA-cam*^{R}	This study
pPB216	pPB47--*amyE::*P_{xyl}*-ddcPΔTM-cam*^{R}	This study
pPB235	pPB41-CRISPR::*ddcP-PDZ*	This study
pPB236	pPB41-CRISPR::*ctpA-PDZ*	This study
pPB245	pPB235-*ddcP*Δ*PDZ* editing template	This study
pPB246	pPB236-*ctpA*Δ*PDZ* editing template	This study
pPB254	pPB47-*amyE::*P_{xyl}*-gfp-ddcA-cam*^{R}	This study
pPB255	pPB47-*amyE::*P_{xyl}*-ddcA-gfp-cam*^{R}	This study
pPB257	pPB47-*amyE::*P_{xyl}*-gfp-yneA-cam*^{R}	This study
pPB267	pUT18-YneA	(38)
pPB268	pUT18-YneAΔN	(38)
pPB269	PKT25-DdcA	This study
pPB270	pKT25-DdcP-S234A	(38)
pPB271	pKT25-CtpA-S297A	(38)

Table 3.3 Plasmids used in this study.

Primer name	Sequence
oPEB116	Ctctcgtttcatcggtatcattac
oPEB117	Cgcttcgttaatacagatgtaggt
oPEB217	GAACCTCATTACGAATTCAGCATGC
oPEB218	GAATGGCGATTTTCGTTCGTGAATAC
oPEB227	CCGTCAATTGTCTGATTCGTTA
oPEB232	GCTGTAGGCATAGGCTTGGTTATG
oPEB234	GTATTCACGAACGAAAATCGCCATTCCTAGCAGCACGCCATAGTGACTG
oPEB253	GAAGGGTAGTCCAGAAGATAACGA
oPEB345	Actcctttgtttatccaccgaac
oPEB348	TTATTTTTGACACCAGACCAACTG
oPEB370	cacctacatctgtattaacgaagcgTCAATGGGGAAGAGAACCGCTTAAG
oPEB377	ggtaatgataccgatgaaacgagagAACAAAATTCTCCAGTCTTCACATCG
oPEB383	Atgtatacctccttaggatcccatttcc
oPEB422	GCATAACCAAGCCTATGCCTACAGCgaagactttgtaattgcggaaaac
oPEB424	Agaatgaatcgtgaaatgatcacc
oPEB428	GCATGCTGAATTCGTAATGAGGTTCtagtctcttgaagctggttgtcct
oPEB432	Acggatcgatatgattctctaagc
oPEB434	Ctgaggagggtttttgttgattac
oPEB435	Taacagagggttaaaaataagcctccgtttctttaacg
oPEB436	Ttcgttaaagaaacggaggcttatttttaaccctctgttaagaggggacagcttgt cggcaagtccatccttgggcttagcaggcaagcttttttctttac
oPEB477	GCATGCTGAATTCGTAATGAGGTTCagcagtacctgtcctcttgattct
oPEB480	GCATAACCAAGCCTATGCCTACAGCccagtatgtgacctcgattctaac
oPEB481	TACATAAGCACCAAATTGAAGTGG
oPEB482	Agaaacagcacagcttattgatga
oPEB483	GAGAAAAGATTGTGTTCCGAAAAG
oPEB492	Tgatgttctttttcctcctattcg
oPEB493	Acgatattgccgtattcctcttat
oPEB557	taaCGGTTTCCATATGGGGATTGGTG
oPEB561	ACCAATCCCCATATGGAAACCGttaTCAGGTGCTTTTCGCTTTCAGCTT
oPEB588	GCATGCTGAATTCGTAATGAGGTTCcccctcctatcctgactttctatc
oPEB591	GCATAACCAAGCCTATGCCTACAGCtatgggtcattatgctgtttatgg
oPEB592	Acgactttaccttgatggtttttg
oPEB593	Gttgctctttacacattcttcagc
oPEB594	Ggatacagcaaatgtcctaaataagc
oPEB601	Cgtgcttatgaatatatgggattg
oPEB602	Aacaagctcttcacgcaatttag
oPEB706	aaatgggatcctaaggaggtatacatATGACGCATGACAAGAAAAACGCA
oPEB707	CACCAATCCCCATATGGAAACCGttaTTACAAATAAGAAATTTCTTCAATATCTTT TAAC
oPEB708	AGAAGTCAAAAGCACCATTGAAG

oPEB818	ACCAATCCCCATATGGAAACCGttaTTACATTTCTTTTTTCAGTGTTTCAATTGC
oPEB854	aatgggatcctaaggaggtatacatATGAGTAAAGAATCTATTATTTTTGTCGGT
oPEB855	CACCAATCCCCATATGGAAACCGttaCTATCTTACAGTTGCTAATTCATATG
oPEB887	aatgggatcctaaggaggtatacatTTGACAGAGCTTGCTTCATTGATAA
oPEB911	gaaatgggatcctaaggaggtatacatTTGAGCACAGGAGACAGCAAGTTCGAC
oPEB984	aaacAGAAGTCGGTGATAAAATCATCAGCGCAGAg
oPEB985	aaaacTCTGCGCTGATGATTTTATCACCGACTTCT
oPEB986	TTCCTGCCCGATCCGGCTCATCAGGGCTGACTTTTTTTCCTGCCTTTTGA
oPEB987	ATCAAAAGGCAGGAAAAAAAGTCAGCCCTGATGAGCCGGATCGGGCAG
oPEB988	aaacGAATGTAAATGAAGCCGTCGCTTTAATCCGg
oPEB989	aaaacCGGATTAAAGCGACGGCTTCATTTACATTC
oPEB990	CATCTCTGAATAGACAGTCTCTACAGGTGCTGAAATCGTCTCGTCGAATG
oPEB991	AATCATTCGACGAGACGATTTCAGCACCTGTAGAGACTGTCTATTCAGAG
oPEB998	aaatgggatcctaaggaggtatacatATGAGTAAAGGAGAAGAACTTTTCAC
oPEB999	TTTTGCGTTTTTCTTGTCATGCGTCATGAGCTCAGAGCGGTAAGCGTAA
oPEB1000	GTGGTTACGCTTACCGCTCTGAGCTCATGACGCATGACAAGAAAAACGCA
oPEB1001	AAAGATATTGAAGAAATTTCTTATTTGGGTGAAGGTCAAGGACAAGGCCA
oPEB1002	CCACCAATCCCCATATGGAAACCGttaTTATTTGTATAGTTCATCCATGCCATGTG
oPEB1003	TCCTTGGCCTTGTCCTTGACCTTCACCCAAATAAGAAATTTCTTCAATATCTTTTA AC
oPEB1005	GAGCTCAGAGCGGTAAGCGTAAC
oPEB1006	GGACGTGGTTACGCTTACCGCTCTGAGCTCATGAGTAAAGAATCTATTATTTTTGT CGGT
oPEB1014	TTGGCCTTGTCCTTGACCTTCACCGGGATCCTCTAGAGTCGACCCTG
oPEB1015	TAActaagaattcggccgtcgttt
oPEB1021	ATTATGCCGCATCTGTCCAACT
oPEB1022	Gcaaggcgattaagttgggtaa
oPEB1037	AGGATCCCGGTGAAGGTCAAGGACAAGGCCAAATGACGCATGACAAGAAAAACGCA
oPEB1038	taaaacgacggccgaattcttagTTATTACAAATAAGAAATTTCTTCAATATCTTT TAAC

Table 3.4 Oligonucleotides used in this study.

Supplemental text

Supplemental Results

The PDZ domains of DdcP and CtpA have different functions *in vivo*

The influence of a PDZ domain on protease activity has been found to be both positive and negative (69). Both DdcP and CtpA have PDZ domains, but the function of the PDZ domains in YneA degradation is unknown. We performed a PSI-BLAST search using the PDZ domain of DdcP against the *E. coli* protein database. We found that the PDZ domain of DdcP was most similar to the PDZ domain of DegS and PDZ1 from DegP **(Fig 3.14A)**, both of which have been reported to inhibit protease activity (70-73). We asked if CtpA would yield the same PSI-BLAST result, so we repeated our search using the PDZ domain of CtpA. CtpA was most similar to the PDZ domain of the C-terminal processing protease Prc (also known as Tsp; **Fig 3.14B**), which was expected because CtpA and its homolog CtpB return Prc in a standard BLAST search (data not shown). Intriguingly, the PDZ domains of CtpB and Prc have been reported to function in substrate recognition (74, 75). Together, our homology searches predict that the PDZ domains of DdcP and CtpA may have different functions.

To test our hypothesis that DdcP and CtpA have PDZ domains with different functions, we constructed ΔPDZ constructs for both DdcP and CtpA **(Fig 3.14C)** at the native locus of each gene. We tested for MMC sensitivity using a spot titer assay. Deletion of the PDZ domain of DdcP had no effect on MMC sensitivity **(Fig 3.14D)**, suggesting that this PDZ domain is inhibitory similar to the PDZ domain of DegS. Deletion of the PDZ domain of CtpA resulted in a mutant that was sensitive to MMC, but not to the same extent as deletion of *ctpA* **(Fig 3.14D)**, suggesting that the PDZ domain of CtpA functions in substrate recognition similar to Prc and CtpB. As a control, we verified that the ΔPDZ variants were stably expressed *in vivo* **(Fig 3.14E)**. Taken together, our results support the bioinformatics predictions, and we conclude that the PDZ domains of DdcP and CtpA have different functions in regulating protease activity.

Supporting Materials and Methods

Bacterial two-hybrid assays

Bacterial two-hybrid assays were performed as previously described (38, 76, 77).

Strain construction

Individual strains were generated using CRISPR/Cas9 genome editing or double cross-over recombination as previously described (38). Strains using P_{xyl} at the *amyE* locus have a chloramphenicol resistance cassette and were selected for using LB agar + 5 μg/mL chloramphenicol.

PEB309 (Δ*uvrAB*): PY79 was transformed with editing plasmid pPB84 to delete *uvrAB*. Deletion of *uvrAB* was verified via PCR genotyping using oPEB424/432.

PEB495 (Δ*ddcA,* Δ*yneA::erm*): PEB357 (Δ*ddcA*) was transformed with chromosomal DNA purified from PEB432 (Δ*yneA::erm*, BKE17860 from *Bacillus* Genetic Stock Center). Replacement of *yneA* with the *erm* cassette was verified via PCR genotyping using oPEB492/493.

PEB497 (Δ*uvrAB,* Δ*ddcA*): PEB309 was transformed with editing plasmid pPB122 to delete *ddcA*. Deletion of *ddcA* was verified via PCR genotyping using oPEB601/602.

PEB499 (Δ*ddcP,* Δ*ddcA*): PEB324 was transformed with editing plasmid pPB122 to delete *ddcA*. Deletion of *ddcA* was verified via PCR genotyping using oPEB601/602.

PEB503 (Δ*ddcA*, *amyE::*P_{xyl}*-ddcA*): PEB357 was transformed with pPB147 digested with two restriction enzymes (KpnI-HF and ScaI-HF). Replacement of *amyE* via double crossover recombination was verified by testing for an inability to utilize starch and for the absence of a spectinomycin resistance cassette present on the portion of the plasmid that is not incorporated.

PEB579 (Δ*ctpA,* Δ*ddcA*): PEB355 was transformed with editing plasmid pPB122 to delete *ddcA*. Deletion of *ddcA* was verified via PCR genotyping using oPEB601/602.

PEB587 (Δ*ddcA,* Δ*yneA::loxP*): The *erm* cassette at the *yneA* locus was removed via Cre recombinase by transforming PEB495 with pDR244, which was subsequently evicted. The

absence of the *erm* cassette was verified by testing for sensitivity to erythromycin and by PCR genotyping using oPEB492/493.

PEB639 (Δ*ddcP,* Δ*ctpA*, Δ*ddcA*): PEB555 was transformed with editing plasmid pPB122 to delete *ddcA*. Deletion of *ddcA* was verified via PCR genotyping using oPEB601/602.

PEB643 (Δ*ddcP,* Δ*ctpA*, Δ*ddcA*, Δ*yneA::loxP*): PEB561 was transformed with editing plasmid pPB122 to delete *ddcA*. Deletion of *ddcA* was verified via PCR genotyping using oPEB601/602.

PEB719 (Δ*ddcP, amyE::*P_{xyl}*-ddcP*Δ*TM*): PEB324 was transformed with plasmid pPB216.

PEB772 (Δ*ctpA, amyE::*P_{xyl}*-ctpA*Δ*TM*): PEB355 was transformed with a PCR product containing the portion of *amyE::*P_{xyl}*-ctpA*Δ*TM* using oPEB370/377, as the plasmid could not be isolated from *E. coli*. Briefly, *ctpA*Δ*TM* was amplified using oPEB911/818, the upstream portion of *amyE* and the P_{xyl} promoter were amplified using oPEB370/383, and the chloramphenicol resistance cassette and the downstream portion of *amyE* were amplified using oPEB557/377. The final PCR product used for transformation of PEB355 was generated using the three preceding PCR products as a template and oPEB370/377.

PEB774 (*ddcP*Δ*PDZ*): PY79 was edited using CRISPR/Cas9 genome editing with plasmid pPB245. Deletion of the sequence encoding the PDZ domain of DdcP was verified via PCR genotyping using oPEB481/482.

PEB776 (*ctpA*Δ*PDZ*): PY79 was edited using CRISPR/Cas9 genome editing with plasmid pPB246. Deletion of the sequence encoding the PDZ domain of CtpA was verified via PCR genotyping using oPEB592/593.

PEB836 (Δ*ddcA*, *amyE::*P_{xyl}*-ddcP*): PEB357 was transformed with pPB108 digested with two restriction enzymes (KpnI-HF and ScaI-HF). Replacement of *amyE* via double crossover recombination was verified by testing for an inability to utilize starch and for the absence of a spectinomycin resistance cassette present on the portion of the plasmid that is not incorporated.

PEB837 (Δ*ddcA*, *amyE::*P_{xyl}*-ctpA*): PEB357 was transformed with pPB184 digested with two restriction enzymes (KpnI-HF and ScaI-HF). Replacement of *amyE* via double crossover

recombination was verified by testing for an inability to utilize starch and for the absence of a spectinomycin resistance cassette present on the portion of the plasmid that is not incorporated.

PEB838 (Δ*ddcP,* Δ*ctpA*, *amyE::P$_{xyl}$-ddcA*): PEB555 was transformed with pPB147 digested with two restriction enzymes (KpnI-HF and ScaI-HF). Replacement of *amyE* via double crossover recombination was verified by testing for an inability to utilize starch and for the absence of a spectinomycin resistance cassette present on the portion of the plasmid that is not incorporated.

PEB839 (Δ*ddcP,* Δ*ctpA*, Δ*ddcA*, *amyE::P$_{xyl}$-ddcP*): PEB639 was transformed with pPB108 digested with two restriction enzymes (KpnI-HF and ScaI-HF). Replacement of *amyE* via double crossover recombination was verified by testing for an inability to utilize starch and for the absence of a spectinomycin resistance cassette present on the portion of the plasmid that is not incorporated.

PEB840 (Δ*ddcP,* Δ*ctpA*, Δ*ddcA*, *amyE::P$_{xyl}$-ddcA*): PEB639 was transformed with pPB147 digested with two restriction enzymes (KpnI-HF and ScaI-HF). Replacement of *amyE* via double crossover recombination was verified by testing for an inability to utilize starch and for the absence of a spectinomycin resistance cassette present on the portion of the plasmid that is not incorporated.

PEB841 (Δ*ddcP,* Δ*ctpA*, Δ*ddcA*, *amyE::P$_{xyl}$-ctpA*): PEB639 was transformed with pPB184 digested with two restriction enzymes (KpnI-HF and ScaI-HF). Replacement of *amyE* via double crossover recombination was verified by testing for an inability to utilize starch and for the absence of a spectinomycin resistance cassette present on the portion of the plasmid that is not incorporated.

PEB846 (*amyE::P$_{xyl}$-yneA*): PY79 was transformed with pPB192 digested with two restriction enzymes (KpnI-HF and ScaI-HF). Replacement of *amyE* via double crossover recombination was verified by testing for an inability to utilize starch and for the absence of a spectinomycin resistance cassette present on the portion of the plasmid that is not incorporated.

PEB848 (Δ*ddcA*, *amyE::P$_{xyl}$-yneA*): PEB357 was transformed with pPB192 digested with two restriction enzymes (KpnI-HF and ScaI-HF). Replacement of *amyE* via double crossover

recombination was verified by testing for an inability to utilize starch and for the absence of a spectinomycin resistance cassette present on the portion of the plasmid that is not incorporated.

PEB850 (Δ*ddcP,* Δ*ctpA*, *amyE::P$_{xyl}$-yneA*): PEB555 was transformed with pPB192 digested with two restriction enzymes (KpnI-HF and ScaI-HF). Replacement of *amyE* via double crossover recombination was verified by testing for an inability to utilize starch and for the absence of a spectinomycin resistance cassette present on the portion of the plasmid that is not incorporated.

PEB852 (Δ*ddcP,* Δ*ctpA*, Δ*ddcA*, *amyE::P$_{xyl}$-yneA*): PEB639 was transformed with pPB192 digested with two restriction enzymes (KpnI-HF and ScaI-HF). Replacement of *amyE* via double crossover recombination was verified by testing for an inability to utilize starch and for the absence of a spectinomycin resistance cassette present on the portion of the plasmid that is not incorporated.

PEB854 (Δ*ddcA*, *amyE::P$_{xyl}$-gfp-ddcA*): PEB357 was transformed with pPB254 digested with two restriction enzymes (KpnI-HF and ScaI-HF). Replacement of *amyE* via double crossover recombination was verified by testing for an inability to utilize starch and for the absence of a spectinomycin resistance cassette present on the portion of the plasmid that is not incorporated.

PEB856 (Δ*ddcA*, *amyE::P$_{xyl}$-ddcA-gfp*): PEB357 was transformed with pPB255 digested with two restriction enzymes (KpnI-HF and ScaI-HF). Replacement of *amyE* via double crossover recombination was verified by testing for an inability to utilize starch and for the absence of a spectinomycin resistance cassette present on the portion of the plasmid that is not incorporated.

PEB876 (*amyE::P$_{xyl}$-gfp-yneA*): PY79 was transformed with pPB257 digested with two restriction enzymes (KpnI-HF and ScaI-HF). Replacement of *amyE* via double crossover recombination was verified by testing for an inability to utilize starch and for the absence of a spectinomycin resistance cassette present on the portion of the plasmid that is not incorporated.

PEB882 (Δ*ddcA*, *amyE::P$_{xyl}$-gfp-yneA*): PEB357 was transformed with pPB257 digested with two restriction enzymes (KpnI-HF and ScaI-HF). Replacement of *amyE* via double crossover recombination was verified by testing for an inability to utilize starch and for the absence of a spectinomycin resistance cassette present on the portion of the plasmid that is not incorporated.

PEB888 (Δ*ddcP,* Δ*ctpA*, *amyE::P$_{xyl}$-gfp-yneA*): PEB555 was transformed with pPB257 digested with two restriction enzymes (KpnI-HF and ScaI-HF). Replacement of *amyE* via double crossover recombination was verified by testing for an inability to utilize starch and for the absence of a spectinomycin resistance cassette present on the portion of the plasmid that is not incorporated.

PEB894 (Δ*ddcP,* Δ*ctpA*, Δ*ddcA*, *amyE::P$_{xyl}$-gfp-yneA*): PEB639 was transformed with pPB257 digested with two restriction enzymes (KpnI-HF and ScaI-HF). Replacement of *amyE* via double crossover recombination was verified by testing for an inability to utilize starch and for the absence of a spectinomycin resistance cassette present on the portion of the plasmid that is not incorporated.

Plasmid construction

Plasmids were constructed via Gibson assembly (65) using the PCR amplicons listed below as previously described (38).

pPB84: Plasmid pPB84 was constructed via Gibson assembly using four PCR products: 1) the vector pPB41 was amplified using oPEB217/218; 2) Cas9/CRISPR::*uvrB* was amplified using pPB73 as a template with oPEB232/234; 3) the sequence upstream of *uvrAB* for the editing template was amplified using oPEB428/435; and 4) the sequence downstream of *uvrAB* for the editing template was amplified using oPEB436/422. Clones were verified via Sanger sequencing using oPEB227, oPEB253, and oPEB434.

pPB147: Plasmid pPB147 was constructed via Gibson assembly using four PCR products: 1) pPB47 was amplified using oPEB116/117; 2) the upstream portion of *amyE* and the P_{xyl} promoter was amplified using oPEB370/383; 3) the chloramphenicol resistance cassette and the downstream portion of *amyE* were amplified using oPEB557/377; 4) the *ddcA* ORF was amplified using oPEB706/707. Clones were verified via Sanger sequencing using oPEB345, oPEB348, and oPEB708.

pPB192: Plasmid pPB192 was constructed via Gibson assembly using four PCR products: 1) pPB47 was amplified using oPEB116/117; 2) the upstream portion of *amyE* and the P_{xyl} promoter was amplified using oPEB370/383; 3) the chloramphenicol resistance cassette and the

downstream portion of *amyE* were amplified using oPEB557/377; 4) the *yneA* ORF was amplified using oPEB854/855. Clones were verified via Sanger sequencing using oPEB345 and oPEB348.

pPB216: The upstream portion of *amyE* and the P_{xyl} promoter were PCR amplified using oPEB370/383. The chloramphenicol resistance cassette and the downstream portion of *amyE* were amplified using oPEB557/377. Plasmid pPB47 was PCR amplified using oPEB116/117. The ORF of *ddcP* (coding for a.a. 36-341) was PCR amplified using oPEB887/561. These four PCR products were used in a Gibson assembly reaction to generate a plasmid to integrate *ddcP*ΔTM under the control of P_{xyl} at the *amyE* locus. Clones were verified by Sanger sequencing with oPEB345 and oPEB348.

pPB235: A proto-spacer targeting *ddcP* in the sequence coding for the PDZ domain (oPEB984/985) was ligated to pPB41.

pPB236: A proto-spacer targeting *ctpA* in the sequence coding for the PDZ domain (oPEB988/989) was ligated to pPB41.

pPB245: The upstream and downstream portions of the *ddcP*Δ*PDZ* editing template were PCR amplified using oPEB477/986 and oPEB987/480, respectively. CRISPR/Cas9 was PCR amplified using oPEB232/234 and pPB235 as the template. The pPB41 vector was PCR amplified using oPEB217/218. These four PCR products were used in a Gibson assembly reaction to generate a *ddcP*Δ*PDZ* editing plasmid. Clones were verified by Sanger sequencing with oPEB227, oPEB253, and oPEB483.

pPB246: The upstream and downstream portions of the *ctpA*Δ*PDZ* editing template were PCR amplified using oPEB588/990 and oPEB991/591, respectively. CRISPR/Cas9 was PCR amplified using oPEB232/234 and pPB236 as the template. The pPB41 vector was PCR amplified using oPEB217/218. These four PCR products were used in a Gibson assembly reaction to generate a *ctpA*Δ*PDZ* editing plasmid. Clones were verified by Sanger sequencing with oPEB227, oPEB253, and oPEB594.

pPB254: Plasmid pPB254 was constructed via Gibson assembly using five PCR products: 1) pPB47 was amplified using oPEB116/117; 2) the upstream portion of *amyE* and the P_{xyl}

promoter was amplified using oPEB370/383; 3) the chloramphenicol resistance cassette and the downstream portion of *amyE* were amplified using oPEB557/377; 4) *gfp* with a linker was amplified using oPEB998/999; 5) the *ddcA* ORF was amplified using oPEB1000/707. Clones were verified via Sanger sequencing using oPEB345, oPEB348, and oPEB708.

pPB255: Plasmid pPB255 was constructed via Gibson assembly using five PCR products: 1) pPB47 was amplified using oPEB116/117; 2) the upstream portion of *amyE* and the P_{xyl} promoter was amplified using oPEB370/383; 3) the chloramphenicol resistance cassette and the downstream portion of *amyE* were amplified using oPEB557/377; 4) the *ddcA* ORF was amplified using oPEB706/1003; 5) *gfp* with a linker was amplified using oPEB1001/1002. Clones were verified via Sanger sequencing using oPEB345, oPEB348, and oPEB708.

pPB257: Plasmid pPB257 was constructed via Gibson assembly using five PCR products: 1) pPB47 was amplified using oPEB116/117; 2) the upstream portion of *amyE* and the P_{xyl} promoter was amplified using oPEB370/383; 3) the chloramphenicol resistance cassette and the downstream portion of *amyE* were amplified using oPEB557/377; 4) *gfp* with a linker was amplified using oPEB998/1005; 5) the *yneA* ORF was amplified using oPEB1006/855. Clones were verified via Sanger sequencing using oPEB345 and oPEB348.

pPB269: DdcA was amplified with primers oPEB1037/1038. The plasmid pKT25 was amplified with primers oPEB1014/1015. These two PCR products were used in a Gibson assembly reaction to generate a T25-DdcA fusion for expression in BTH101 cells in a bacterial two-hybrid assay. Clones were selected on LB agar containing 50 μg/mL kanamycin and 0.2% glucose. Clones were verified via Sanger sequencing using oPEB708, 1021 and 1022.

References

1. **Westfall CS, Levin PA.** 2017. Bacterial Cell Size: Multifactorial and Multifaceted. Annu Rev Microbiol **71:**499-517.
2. **Wang JD, Levin PA.** 2009. Metabolism, cell growth and the bacterial cell cycle. Nat Rev Microbiol **7:**822-827.
3. **Donachie WD, Blakely GW.** 2003. Coupling the initiation of chromosome replication to cell size in Escherichia coli. Curr Opin Microbiol **6:**146-150.
4. **Hill NS, Kadoya R, Chattoraj DK, Levin PA.** 2012. Cell size and the initiation of DNA replication in bacteria. PLoS Genet **8:**e1002549.

5. **Kreuzer KN.** 2013. DNA damage responses in prokaryotes: regulating gene expression, modulating growth patterns, and manipulating replication forks. Cold Spring Harb Perspect Biol **5:**a012674.
6. **Lenhart JS, Schroeder JW, Walsh BW, Simmons LA.** 2012. DNA repair and genome maintenance in Bacillus subtilis. Microbiol Mol Biol Rev **76:**530-564.
7. **Friedberg EC, Walker GC, Siede W, Wood RD, Schultz RA, Ellenberger T.** 2006. DNA Repair and Mutagenesis, 2nd ed. ASM Press, Washington, D.C.
8. **Ivancic-Bace I, Vlasic I, Salaj-Smic E, Brcic-Kostic K.** 2006. Genetic evidence for the requirement of RecA loading activity in SOS induction after UV irradiation in Escherichia coli. J Bacteriol **188:**5024-5032.
9. **Anderson DG, Kowalczykowski SC.** 1997. The translocating RecBCD enzyme stimulates recombination by directing RecA protein onto ssDNA in a chi-regulated manner. Cell **90:**77-86.
10. **Churchill JJ, Anderson DG, Kowalczykowski SC.** 1999. The RecBC enzyme loads RecA protein onto ssDNA asymmetrically and independently of chi, resulting in constitutive recombination activation. Genes Dev **13:**901-911.
11. **Morimatsu K, Kowalczykowski SC.** 2003. RecFOR proteins load RecA protein onto gapped DNA to accelerate DNA strand exchange: a universal step of recombinational repair. Mol Cell **11:**1337-1347.
12. **Ivancic-Bace I, Peharec P, Moslavac S, Skrobot N, Salaj-Smic E, Brcic-Kostic K.** 2003. RecFOR function is required for DNA repair and recombination in a RecA loading-deficient recB mutant of Escherichia coli. Genetics **163:**485-494.
13. **Slilaty SN, Little JW.** 1987. Lysine-156 and serine-119 are required for LexA repressor cleavage: a possible mechanism. Proc Natl Acad Sci U S A **84:**3987-3991.
14. **Little JW, Mount DW, Yanisch-Perron CR.** 1981. Purified lexA protein is a repressor of the recA and lexA genes. Proc Natl Acad Sci U S A **78:**4199-4203.
15. **Lewis LK, Harlow GR, Gregg-Jolly LA, Mount DW.** 1994. Identification of high affinity binding sites for LexA which define new DNA damage-inducible genes in Escherichia coli. J Mol Biol **241:**507-523.
16. **Little JW, Mount DW.** 1982. The SOS regulatory system of Escherichia coli. Cell **29:**11-22.
17. **Au N, Kuester-Schoeck E, Mandava V, Bothwell LE, Canny SP, Chachu K, Colavito SA, Fuller SN, Groban ES, Hensley LA, O'Brien TC, Shah A, Tierney JT, Tomm LL, O'Gara TM, Goranov AI, Grossman AD, Lovett CM.** 2005. Genetic composition of the Bacillus subtilis SOS system. Journal of Bacteriology **187:**7655-7666.
18. **Goranov AI, Kuester-Schoeck E, Wang JD, Grossman AD.** 2006. Characterization of the global transcriptional responses to different types of DNA damage and disruption of replication in Bacillus subtilis. Journal of Bacteriology **188:**5595-5605.
19. **Huisman O, D'Ari R.** 1981. An inducible DNA replication-cell division coupling mechanism in E. coli. Nature **290:**797-799.
20. **Huisman O, D'Ari R, Gottesman S.** 1984. Cell-division control in Escherichia coli: specific induction of the SOS function SfiA protein is sufficient to block septation. Proc Natl Acad Sci U S A **81:**4490-4494.
21. **Kawai Y, Moriya S, Ogasawara N.** 2003. Identification of a protein, YneA, responsible for cell division suppression during the SOS response in Bacillus subtilis. Mol Microbiol **47:**1113-1122.

22. **Mo AH, Burkholder WF.** 2010. YneA, an SOS-induced inhibitor of cell division in Bacillus subtilis, is regulated posttranslationally and requires the transmembrane region for activity. J Bacteriol **192:**3159-3173.
23. **Erill I, Campoy S, Barbe J.** 2007. Aeons of distress: an evolutionary perspective on the bacterial SOS response. FEMS Microbiol Rev **31:**637-656.
24. **Bi E, Lutkenhaus J.** 1993. Cell division inhibitors SulA and MinCD prevent formation of the FtsZ ring. J Bacteriol **175:**1118-1125.
25. **Huang J, Cao C, Lutkenhaus J.** 1996. Interaction between FtsZ and inhibitors of cell division. J Bacteriol **178:**5080-5085.
26. **Mukherjee A, Cao C, Lutkenhaus J.** 1998. Inhibition of FtsZ polymerization by SulA, an inhibitor of septation in Escherichia coli. Proc Natl Acad Sci U S A **95:**2885-2890.
27. **Trusca D, Scott S, Thompson C, Bramhill D.** 1998. Bacterial SOS checkpoint protein SulA inhibits polymerization of purified FtsZ cell division protein. J Bacteriol **180:**3946-3953.
28. **Chauhan A, Lofton H, Maloney E, Moore J, Fol M, Madiraju MV, Rajagopalan M.** 2006. Interference of Mycobacterium tuberculosis cell division by Rv2719c, a cell wall hydrolase. Mol Microbiol **62:**132-147.
29. **Ogino H, Teramoto H, Inui M, Yukawa H.** 2008. DivS, a novel SOS-inducible cell-division suppressor in Corynebacterium glutamicum. Mol Microbiol **67:**597-608.
30. **Modell JW, Hopkins AC, Laub MT.** 2011. A DNA damage checkpoint in Caulobacter crescentus inhibits cell division through a direct interaction with FtsW. Genes Dev **25:**1328-1343.
31. **Modell JW, Kambara TK, Perchuk BS, Laub MT.** 2014. A DNA damage-induced, SOS-independent checkpoint regulates cell division in Caulobacter crescentus. PLoS Biol **12:**e1001977.
32. **Canceill D, Dervyn E, Huisman O.** 1990. Proteolysis and modulation of the activity of the cell division inhibitor SulA in Escherichia coli lon mutants. J Bacteriol **172:**7297-7300.
33. **Mizusawa S, Gottesman S.** 1983. Protein degradation in Escherichia coli: the lon gene controls the stability of sulA protein. Proc Natl Acad Sci U S A **80:**358-362.
34. **Sonezaki S, Ishii Y, Okita K, Sugino T, Kondo A, Kato Y.** 1995. Overproduction and purification of SulA fusion protein in Escherichia coli and its degradation by Lon protease in vitro. Appl Microbiol Biotechnol **43:**304-309.
35. **Wu WF, Zhou Y, Gottesman S.** 1999. Redundant in vivo proteolytic activities of Escherichia coli Lon and the ClpYQ (HslUV) protease. J Bacteriol **181:**3681-3687.
36. **Seong IS, Oh JY, Yoo SJ, Seol JH, Chung CH.** 1999. ATP-dependent degradation of SulA, a cell division inhibitor, by the HslVU protease in Escherichia coli. FEBS Lett **456:**211-214.
37. **Kanemori M, Yanagi H, Yura T.** 1999. The ATP-dependent HslVU/ClpQY protease participates in turnover of cell division inhibitor SulA in Escherichia coli. J Bacteriol **181:**3674-3680.
38. **Burby PE, Simmons ZW, Schroeder JW, Simmons LA.** 2018. Discovery of a dual protease mechanism that promotes DNA damage checkpoint recovery. PLoS Genet **14:**e1007512.

39. **Goranov AI, Katz L, Breier AM, Burge CB, Grossman AD.** 2005. A transcriptional response to replication status mediated by the conserved bacterial replication protein DnaA. Proc Natl Acad Sci U S A **102:**12932-12937.
40. **Cerveny L, Straskova A, Dankova V, Hartlova A, Ceckova M, Staud F, Stulik J.** 2013. Tetratricopeptide repeat motifs in the world of bacterial pathogens: role in virulence mechanisms. Infect Immun **81:**629-635.
41. **Noll DM, Mason TM, Miller PS.** 2006. Formation and repair of interstrand cross-links in DNA. Chem Rev **106:**277-301.
42. **Iyer VN, Szybalski W.** 1963. A molecular mechanism of mitomycin action: Linking of complementary DNA strands. Proc Natl Acad Sci U S A **50:**355-362.
43. **Reiter H, Milewskiy M, Kelley P.** 1972. Mode of action of phleomycin on Bacillus subtilis. J Bacteriol **111:**586-592.
44. **Kross J, Henner WD, Hecht SM, Haseltine WA.** 1982. Specificity of deoxyribonucleic acid cleavage by bleomycin, phleomycin, and tallysomycin. Biochemistry **21:**4310-4318.
45. **Sancar A.** 1996. DNA excision repair. Annu Rev Biochem **65:**43-81.
46. **Krogh A, Larsson B, von Heijne G, Sonnhammer EL.** 2001. Predicting transmembrane protein topology with a hidden Markov model: application to complete genomes. J Mol Biol **305:**567-580.
47. **Tjalsma H, Bolhuis A, Jongbloed JD, Bron S, van Dijl JM.** 2000. Signal peptide-dependent protein transport in Bacillus subtilis: a genome-based survey of the secretome. Microbiol Mol Biol Rev **64:**515-547.
48. **Wu LJ, Errington J.** 1997. Septal localization of the SpoIIIE chromosome partitioning protein in Bacillus subtilis. Embo j **16:**2161-2169.
49. **Wilson MJ, Carlson PE, Janes BK, Hanna PC.** 2012. Membrane topology of the Bacillus anthracis GerH germinant receptor proteins. J Bacteriol **194:**1369-1377.
50. **Buttner K, Bernhardt J, Scharf C, Schmid R, Mader U, Eymann C, Antelmann H, Volker A, Volker U, Hecker M.** 2001. A comprehensive two-dimensional map of cytosolic proteins of Bacillus subtilis. Electrophoresis **22:**2908-2935.
51. **Eymann C, Dreisbach A, Albrecht D, Bernhardt J, Becher D, Gentner S, Tam le T, Buttner K, Buurman G, Scharf C, Venz S, Volker U, Hecker M.** 2004. A comprehensive proteome map of growing Bacillus subtilis cells. Proteomics **4:**2849-2876.
52. **Hirose I, Sano K, Shioda I, Kumano M, Nakamura K, Yamane K.** 2000. Proteome analysis of Bacillus subtilis extracellular proteins: a two-dimensional protein electrophoretic study. Microbiology **146 (Pt 1):**65-75.
53. **Hofmann K, Stoffel, W.** 1993. TMBASE - A database of membrane spanning protein segments, Biol. Chem. Hoppe-Seyler 374,166.
54. **Bendtsen JD, Kiemer L, Fausboll A, Brunak S.** 2005. Non-classical protein secretion in bacteria. BMC Microbiol **5:**58.
55. **Yu NY, Wagner JR, Laird MR, Melli G, Rey S, Lo R, Dao P, Sahinalp SC, Ester M, Foster LJ, Brinkman FS.** 2010. PSORTb 3.0: improved protein subcellular localization prediction with refined localization subcategories and predictive capabilities for all prokaryotes. Bioinformatics **26:**1608-1615.
56. **Bojer MS, Wacnik K, Kjelgaard P, Gallay C, Bottomley AL, Cohn MT, Lindahl G, Frees D, Veening J-W, Foster SJ, Ingmer H.** 2018. SosA inhibits cell division in Staphylococcus aureus in response to DNA damage. bioRxiv doi:10.1101/364299.

57. **Scheffers DJ, Errington J.** 2004. PBP1 is a component of the Bacillus subtilis cell division machinery. J Bacteriol **186:**5153-5156.
58. **Claessen D, Emmins R, Hamoen LW, Daniel RA, Errington J, Edwards DH.** 2008. Control of the cell elongation-division cycle by shuttling of PBP1 protein in Bacillus subtilis. Mol Microbiol **68:**1029-1046.
59. **Buist G, Steen A, Kok J, Kuipers OP.** 2008. LysM, a widely distributed protein motif for binding to (peptido)glycans. Mol Microbiol **68:**838-847.
60. **Daniel RA, Errington J.** 2003. Control of cell morphogenesis in bacteria: two distinct ways to make a rod-shaped cell. Cell **113:**767-776.
61. **Tiyanont K, Doan T, Lazarus MB, Fang X, Rudner DZ, Walker S.** 2006. Imaging peptidoglycan biosynthesis in Bacillus subtilis with fluorescent antibiotics. Proc Natl Acad Sci U S A **103:**11033-11038.
62. **Smith DF.** 2004. Tetratricopeptide repeat cochaperones in steroid receptor complexes. Cell Stress Chaperones **9:**109-121.
63. **Youngman P, Perkins JB, Losick R.** 1984. Construction of a cloning site near one end of TN917 into which foreign DNA may be inserted without affecting transposition in Bacillus subtilis or expression of the transposon-bourne ERM gene. Plasmid **12:**1-9.
64. **Burby PE, Simmons LA.** 2017. MutS2 Promotes Homologous Recombination in Bacillus subtilis. J Bacteriol **199**.
65. **Gibson DG.** 2011. Enzymatic assembly of overlapping DNA fragments, p 349-361. *In* Voigt C (ed), Synthetic Biology, Pt B: Computer Aided Design and DNA Assembly, vol 498. Elsevier Academic Press Inc, San Diego.
66. **Link AJ, LaBaer J.** 2011. Trichloroacetic acid (TCA) precipitation of proteins. Cold Spring Harb Protoc **2011:**993-994.
67. **Navarre WW, Schneewind O.** 1994. Proteolytic cleavage and cell wall anchoring at the LPXTG motif of surface proteins in gram-positive bacteria. Mol Microbiol **14:**115-121.
68. **Burby PE, Simmons LA.** 2017. CRISPR/Cas9 Editing of the Bacillus subtilis Genome. Bio Protoc **7**.
69. **Clausen T, Kaiser M, Huber R, Ehrmann M.** 2011. HTRA proteases: regulated proteolysis in protein quality control. Nat Rev Mol Cell Biol **12:**152-162.
70. **Walsh NP, Alba BM, Bose B, Gross CA, Sauer RT.** 2003. OMP peptide signals initiate the envelope-stress response by activating DegS protease via relief of inhibition mediated by its PDZ domain. Cell **113:**61-71.
71. **Sohn J, Grant RA, Sauer RT.** 2007. Allosteric activation of DegS, a stress sensor PDZ protease. Cell **131:**572-583.
72. **Spiess C, Beil A, Ehrmann M.** 1999. A temperature-dependent switch from chaperone to protease in a widely conserved heat shock protein. Cell **97:**339-347.
73. **Krojer T, Sawa J, Huber R, Clausen T.** 2010. HtrA proteases have a conserved activation mechanism that can be triggered by distinct molecular cues. Nat Struct Mol Biol **17:**844-852.
74. **Beebe KD, Shin J, Peng J, Chaudhury C, Khera J, Pei D.** 2000. Substrate recognition through a PDZ domain in tail-specific protease. Biochemistry **39:**3149-3155.
75. **Mastny M, Heuck A, Kurzbauer R, Heiduk A, Boisguerin P, Volkmer R, Ehrmann M, Rodrigues CD, Rudner DZ, Clausen T.** 2013. CtpB assembles a gated protease tunnel regulating cell-cell signaling during spore formation in Bacillus subtilis. Cell **155:**647-658.

76. **Karimova G, Pidoux J, Ullmann A, Ladant D.** 1998. A bacterial two-hybrid system based on a reconstituted signal transduction pathway. Proc Natl Acad Sci U S A **95:**5752-5756.
77. **Karimova G, Dautin N, Ladant D.** 2005. Interaction network among Escherichia coli membrane proteins involved in cell division as revealed by bacterial two-hybrid analysis. J Bacteriol **187:**2233-2243.

CHAPTER IV

A bacterial DNA repair pathway specific to a natural antibiotic

Abstract

All organisms possess DNA repair pathways that are used to maintain the integrity of their genetic material. Although many DNA repair pathways are well understood, new pathways continue to be discovered. Here, we report an antibiotic specific DNA repair pathway in *Bacillus subtilis* that is composed of a previously uncharacterized helicase (*mrfA*) and exonuclease (*mrfB*). Deletion of *mrfA* and *mrfB* results in sensitivity to the DNA damaging agent mitomycin C, but not to any other type of DNA damage tested. We show that MrfAB function independent of canonical nucleotide excision repair, forming a novel excision repair pathway. We demonstrate that MrfB is a metal-dependent exonuclease and that the N-terminus of MrfB is required for interaction with MrfA. We determined that MrfAB failed to unhook inter-strand crosslinks *in vivo*, suggesting that MrfAB are specific to the monoadduct or the intra-strand crosslink. A phylogenetic analysis uncovered MrfAB homologs in diverse bacterial phyla, and cross-complementation indicates that MrfAB function is conserved in closely related species. *B. subtilis* is a soil dwelling organism and mitomycin C is a natural antibiotic produced by the soil bacterium *Streptomyces lavendulae*. The specificity of MrfAB suggests that these proteins are an adaptation to environments with mitomycin producing bacteria.

Introduction

A defining feature of biology is the ability to reproduce, which requires replication of the genetic material. High fidelity DNA replication depends on the integrity of the template DNA which can be damaged by UV light, ionizing radiation, and numerous chemicals (1). Many DNA

The contents of this chapter were published in *Molecular Microbiology* by Peter E. Burby and Lyle A. Simmons. I designed experiments and collected data. LAS and I analyzed data and wrote the manuscript.

damaging agents have been used as chemotherapeutics and are also produced from natural sources such as bacteria, fungi, or plants (2). One such naturally produced antibiotic is mitomycin C (MMC), originally isolated from *Streptomyces lavendulae* (3). MMC is produced as an inactive metabolite that must be activated by enzymatic or chemical reduction to react with DNA (4). MMC reacts specifically with guanine residues in DNA and results in three principle modifications (5). MMC forms a mono-adduct by reacting with a single guanine, however, MMC has two reactive centers, which can result in intra-strand crosslinks on adjacent guanines on the same strand, or in inter-strand crosslinks wherein the two guanines on opposite strands of CpG sequences are covalently linked (6-12). The toxicity of these different adducts is a result of preventing DNA synthesis (5).

In bacteria, MMC adducts and intra-strand crosslinks are repaired by nucleotide excision repair and inter-strand crosslinks are repaired by a combination of nucleotide excision repair and homologous recombination (13-15). Both mono-adducts and crosslinks are recognized in genomic DNA by UvrA to initiate repair (16-19). In some nucleotide excision repair models UvrB functions in complex with UvrA (17, 20, 21), while *in vitro* studies and a recent *in vivo* study using single molecule microscopy suggests that UvrB is recruited by UvrA (19, 22). In any event, once UvrA and UvrB are present at the lesion, the subsequent step is the disassociation of UvrA and the recruitment of UvrC which incises the DNA on either side of the lesion (22).

In *E. coli* there is a second UvrC-like protein called Cho that can also perform the incision function (23, 24). Mono-adducts and intra-strand crosslinks are removed from the DNA via UvrD helicase in *E. coli* after UvrC excision. The resulting single-stranded gap is resynthesized by DNA polymerase with DNA ligase sealing the remaining nick, completing the repair process (17, 25). For an inter-strand crosslink, the process requires another step because the lesion containing DNA remains covalently bonded to the opposite strand. Most current models propose that homologous recombination acts subsequently to pair the lesion containing strand with a second copy of the chromosome if present and then an additional round of nucleotide excision repair can remove the crosslink followed by DNA polymerase and DNA ligase to complete the repair process (13, 14). Importantly, homologous recombination and UvrABC-dependent nucleotide excision repair are general DNA repair pathways that participate in the repair of many different types of DNA lesions including MMC adducted DNA.

Although the pathways discussed above are known to function in the repair of MMC damaged DNA, it is unclear if other pathways exist in bacteria that also repair MMC lesions. We recently reported a forward genetic screen in *B. subtilis* where we identified two genes, *mrfA* and *mrfB* (formerly *yprA* and *yprB*, respectively) that when deleted resulted in sensitivity to MMC (26). Here, we report that MrfAB are part of a MMC specific DNA repair pathway in *B. subtilis*. Deletion of the *mrfAB* (formerly *yprAB*) operon renders *B. subtilis* sensitive to MMC, but not to other DNA damaging agents known to be repaired by the canonical nucleotide excision repair pathway. MrfAB are a putative helicase and exonuclease, respectively, and we demonstrate that conserved residues required for their activities are important for function *in vivo*. We show that MrfAB operate independent of UvrABC. We monitored DNA repair status over time using RecA-GFP as a reporter, and we show that deletion of *mrfAB* and *uvrABC* results in a synergistic decrease in RecA-GFP foci, suggesting that MrfAB are part of a novel nucleotide excision repair pathway in bacteria. We also found that MrfAB do not contribute to inter-strand crosslink repair, suggesting that MrfAB are specific to MMC mono-adducts or intra-strand crosslinks. A phylogenetic analysis shows that MrfAB homologs are present in many bacterial species and that the function of MrfAB is conserved in closely related species. Together, our study identifies a novel strategy used by bacteria to counteract the natural antibiotic MMC.

Results

DNA damage sensitivity of Δ*mrfAB* is specific to mitomycin C

Our recent study using a forward genetic screen identified genes important for surviving exposure to several DNA damaging agents, uncovering many genes that had not previously been implicated in DNA repair or regulation of the SOS-response (26). As part of this screen, we identified a gene pair, *yprAB*, in which disruption by a transposon resulted in sensitivity to MMC but not phleomycin or methyl methanesulfonate **(Fig 4.1A)** (26). Because the phenotypes appeared specific to MMC (see below), we rename *yprAB* to mitomycin repair factors A and B (*mrfAB*). To follow up on the phenotype of the transposon insertions we tested clean deletion strains of *mrfA* and *mrfB* and found that deletion of either gene resulted in sensitivity to MMC **(Fig 4.1B)**. Further, we ectopically expressed each gene in its respective deletion background and were able to complement the MMC sensitive phenotype **(Fig 4.1B)**.

The absence of phenotypes with phleomycin and methyl methanesulfonate, is similar to the phenotypic profile of nucleotide excision repair (NER) mutants **(Fig 4.1A)** (26). Therefore, we asked if deletion of *mrfA* would result in sensitivity to other agents known to be repaired by NER. We tested for sensitivity to three other agents that cause DNA lesions that are repaired by NER: UV light, 4-NQO, and the DNA crosslinking agent psoralen (trioxsalen) (25). Interestingly, we found that deletion of *mrfA* did not cause sensitivity to any of these agents **(Fig 4.1C)**. We also tested whether the presence of *uvrAB* was masking the effect, but no additional sensitivity was observed when *mrfA* was deleted in the Δ*uvrAB* background **(Fig 4.1C)**. Given the absence of phenotypes to other DNA damaging agents, MrfAB do not function as a general nucleotide excision repair pathway. In addition, *mrfAB* deletion did not result in sensitivity to another crosslinking agent, psoralen, indicating that MrfAB are not part of a general crosslink repair mechanism. We conclude that MrfAB are important for mitigating the toxicity of MMC-generated DNA lesions.

MrfA and MrfB function in the same pathway

The phenotypes of *mrfA* and *mrfB* mutants were identical **(Fig 4.1A & B)**, and the two genes are predicted to be an operon. Therefore, we hypothesized that MrfA and MrfB function together. We tested this hypothesis by combining the deletion mutants. We found that deletion of both genes gave the same sensitivity to MMC as each single mutant **(Fig 4.2A)**, indicating that they function in the same pathway. If MrfAB function in the same pathway, it is possible that each protein acts successively, MrfA and MrfB interact forming a complex, or one protein serves to recruit the other in a stepwise fashion.

To provide insight into these possible mechanisms we tested for a protein-protein interaction between MrfA and MrfB using a bacterial two-hybrid assay (27, 28). We found that MrfA and MrfB formed a robust interaction, indicated by the formation of blue colonies **(Fig 4.2B)**. Next, we wanted to understand how these proteins interacted and whether we could localize the interaction to a particular domain. We performed a deletion analysis with MrfA and found that deletion of either the N-terminus or the C-terminus was sufficient to abolish the interaction with MrfB **(Fig 4.2C)**, and the N-terminus of MrfA was not sufficient for MrfB interaction **(Fig 4.2C)**. Thus, it appears that the portion of MrfA that is required for the interaction is not limited to a single domain. We tested whether the N-terminus or C-terminus of

MrfB was required for MrfA interaction. We found that the C-terminus of MrfB was not required, though the signal was reduced, whereas deletion of the N-terminus of MrfB abolished the interaction with MrfA **(Fig 4.2D)**. Therefore, the N-terminus of MrfB is required for interaction with MrfA. We conclude that MrfAB interaction is specific and that these proteins function as a complex or one protein subsequently recruits the other.

MrfA helicase motifs and C-terminus is required for function *in vivo*

MrfA is a predicted DEXH box helicase containing a C-terminal domain of unknown function **(Fig 4.3 & 4.4A)**. The C-terminal domain of unknown function contains four conserved cysteines that are thought to function in coordinating a metal ion (29, 30). We initially searched for a similar helicase in other well studied organisms. We were unable to identify a homolog of MrfA containing both the ATPase domain and the C-terminal domain in *E. coli*, however, Hrq1 from *Saccharomyces cerevisiae* shares the same domain structure with 32% identity and 55% positives. Hrq1 has been shown to be a RecQ family helicase with 3′→ 5′ helicase activity and has been observed to exist as a heptamer (31, 32). We performed an alignment with Hrq1 and identified helicase motifs typical of super family 2 helicases **(Fig 4.3)**. A homolog of MrfA from *Mycobacterium smegmatis* has also been shown to be a 3′→ 5′ helicase, however, unlike Hrq1, SftH exists as a monomer in solution (29).

To address whether residues predicted to be important for MrfA helicase activity are required for function, we used a complementation assay using variants containing alanine substitutions in several conserved helicase motifs. Mutations in helicase motif I (K82A), motif II (DE185-186AA), and motif III (S222A) all failed to complement a *mrfA* deficiency **(Fig 4.4B)**. Intriguingly, when motif Ib (T134V) was mutated *mrfA* MMC sensitivity could still be complemented, and this residue, although conserved in Hrq1, it is not conserved in SftH **(Fig 4.4B)**. We asked whether the C-terminal domain of unknown function and the conserved cysteines were required for function. Deletion of the entire C-terminal domain, mutation of the first two cysteines, or mutation of all four cysteines all resulted in a failure to complement MMC sensitivity in a Δ*mrfA* strain **(Fig 4.4B)**. Together, we suggest that both the putative helicase domain and the C-terminal domain of unknown function are required for MrfA *in vivo*.

MrfB is a metal-dependent exonuclease

MrfB is predicted to be a DnaQ-like exonuclease and to have three tetratrichopeptide repeats at the C-terminus **(Fig 4.5A)**. To search for putative catalytic residues in MrfB, we aligned MrfB to ExoI, ExoX, and DnaQ from *E. coli* **(Fig 4.6A)**. MrfB has the four acidic residues typical of DnaQ-like exonucleases **(Fig 4.6A)**. This type of nuclease also has a histidine located proximal to the last aspartate (33), and we identified two histidine residues, one of which was conserved **(Fig 4.6A,** conserved histidine highlighted in red and the other in green**)**. DnaQ exonucleases coordinate a metal ion that is used in catalysis (33). We hypothesized that MrfB catalytic residues would cluster together in the tertiary structure. We modelled MrfB using Phyre2.0 (34), which used DNA polymerase epsilon catalytic subunit A (DnaQ) [pdb structure c5okiA (35)], and show that the conserved aspartate and glutamate residues are indeed clustered together in the model **(Fig 4.6B)**.

Interestingly, we found that the histidine conserved in the *E. coli* exonucleases was facing the opposite direction, whereas the non-conserved histidine was facing the putative catalytic residues in the MrfB model **(Fig 4.6C)**. An alignment of MrfB homologs demonstrates that the histidine (labeled in green) facing the other putative catalytic residues is conserved in MrfB homologs, whereas the other is not (see supplemental text). To test whether these residues were important for function, we used variants with alanine substitutions at each putative catalytic residue in a complementation assay. We found that all five mutants could not complement the Δ*mrfB* mutant phenotype **(Fig 4.5B)**.

With these results we wanted to test whether MrfB had exonuclease activity *in vitro*. We overexpressed and purified MrfB to homogeneity as determined by SDS-PAGE **(Fig 4.5C)**. We tested for exonuclease activity using a plasmid linearized by restriction digest. We found that MrfB could degrade linear dsDNA in the presence of Mg^{2+}, demonstrating that MrfB is a metal-dependent exonuclease **(Fig 4.5D)**. With exonuclease activity established we tested the substrate preference of MrfB using a covalently closed circular plasmid (CCC), a nicked plasmid or a linear plasmid using T_5 and λ exonucleases as controls. T_5 exonuclease is able to degrade both nicked and linear substrates but T_5 cannot degrade a CCC plasmid (36, 37). In contrast, λ exonuclease can only degrade a linear substrate (38). The T_5 and λ exonuclease controls performed as predicted, and MrfB demonstrated activity on a linear substrate and lower activity

using a nicked substrate **(Fig 4.5E)**. We conclude that MrfB is a metal-dependent exonuclease with a preference for linear DNA.

MrfAB function independent of UvrABC dependent nucleotide excision repair

Given that DNA damage sensitivity in *mrfAB* mutants was restricted to MMC and that both proteins have nucleic acid processing activities, we hypothesized that MrfAB were part of a nucleotide excision repair pathway. We tested whether MrfAB were within the canonical, UvrABC-dependent nucleotide excision repair pathway using an epistasis analysis. We found that deletion of *mrfA* or *mrfB* rendered *B. subtilis* hypersensitive to MMC in the absence of *uvrAB* **(Fig 4.7A)**, *uvrC*, or *uvrABC* **(Fig 4.7B)**. We also show that *uvrABC* function as a single pathway showing that deletion of each gene resulted in the same phenotype as the triple deletion **(Fig 4.8)**. It is important to note that *B. subtilis uvrABC* functioning as a single pathway differs from *E. coli* (23, 39).

To test whether deletion of *mrfAB* have an effect on acute treatment with MMC, we performed an epistasis analysis using a MMC survival assay. We tested mutants in *mrfAB*, *uvrABC*, and the double pathway mutant. We found that deletion of *mrfAB* had a limited, yet statistically significant (Mann-Whitney U-test; p-value < 0.05) effect on acute sensitivity to MMC at the 150 and 200 ng/mL treatments. Deletion of *uvrABC* had a significant and more pronounced decrease in survival following MMC treatment **(Fig 4.7C)**. Deletion of both pathways resulted in hypersensitivity to acute MMC exposure, suggesting that MrfAB are part of a second nucleotide excision repair pathway. The difference in phenotypes between the individual pathway mutants suggests that the roles of each pathway may be specific for different MMC induced lesions. Given that the inter-strand crosslink is the more toxic lesion, our data suggest that UvrABC could be more efficient for repair of crosslinks and MrfAB could be more specific to the mono-adducted lesions (see below). We conclude that MrfAB and UvrABC are part of two distinct pathways for MMC repair.

MrfAB are not required for unhooking inter-strand DNA crosslinks

As stated previously, MMC results in several DNA lesions, one of which is the inter-strand crosslink. Our results from treating acutely with MMC suggested that MrfAB may not function in repair of the inter-strand crosslink. Therefore, we asked whether one or both

pathways contribute to unhooking DNA crosslinks *in vivo*. Crosslinked DNA can be detected by heat denaturing and snap cooling due to the fact that crosslinked DNA will renature during the rapid cooling process and DNA that is not crosslinked will remain denatured when cooled rapidly (7). Therefore, we hypothesized that if both pathways contributed to unhooking a crosslink, we would observe stable DNA crosslinks only in the double pathway mutant. If only a single pathway was required, we would observe stable DNA crosslinks in one mutant and the double pathway mutant background. To test these ideas, we treated *B. subtilis* strains with MMC to crosslink genomic DNA, and then allowed the cells to recover for 45 or 90 minutes. We monitored DNA crosslinks by denaturing and snap cooling the DNA followed by analysis on an agarose gel. We found that in WT and Δ*mrfAB* cells we could detect some crosslinked DNA that decreased slightly over time **(Fig 4.9A)**. Additionally, at the 90 minute recovery time point we observed a smaller DNA fragment in WT and Δ*mrfAB* samples, which we suggest is a result of a repair intermediate generated by UvrABC-dependent incision because formation of the intermediate requires UvrABC **(Fig 4.9A)**. In the absence of *uvrABC* there was a significant stabilization of crosslinked DNA that did not decrease over time and deleting *mrfAB* had no effect in the *uvrABC* mutant strain on crosslink stabilization **(Fig 4.9A)**. We quantified the crosslinked species and found that the inter-strand crosslink was stabilized in the absence of *uvrABC* and in the double pathway mutant **(Fig 4.9B)**. We conclude that UvrABC are the primary proteins responsible for repair of inter-strand crosslinks and MrfAB likely repair the more abundant mono-adducts (40) and potentially intra-strand crosslinks that form, though we cannot formerly exclude the possibility that MrfAB act on an intermediate of a crosslink repair pathway that is specific to MMC.

MrfAB and UvrABC are required for efficient RecA-GFP focus formation

The synergistic sensitivity to MMC observed in the double pathway mutant suggests that MrfAB are part of a novel nucleotide excision repair pathway that does not function in inter-strand crosslink repair. Thus, we sought to determine if DNA repair is altered following MMC treatment in the absence of *mrfAB*. Previous studies have demonstrated that RecA-GFP forms foci in response to DNA damage such as treatment with MMC (41-43). Additionally, the activation of the SOS response following treatment with MMC in bacteria requires the generation of a RecA/ssDNA nucleoprotein filament (44), which was also found to depend on

nucleotide excision repair (45). Therefore, to test whether the response of RecA was affected by the absence of *mrfAB*, *uvrABC*, or both pathways, we used a RecA-GFP fusion as a reporter to monitor RecA status over time **(Fig 4.10A & 4.11)**. We quantified the percentage of cells containing a focus or foci of RecA-GFP, and found an increase in RecA-GFP focus formation over time **(Fig 4.10B)**. In all three mutant strains there was a significant increase in RecA-GFP foci prior to MMC addition **(Fig 4.10B)**. We found that deletion of *mrfAB* did not have a significant impact on RecA-GFP focus formation **(Fig 4.10B)**. Deletion of *uvrABC* led to a slight decrease in RecA-GFP focus formation **(Fig 4.10B & 4.11)**. The double pathway mutant had a significant decrease in RecA-GFP foci relative to WT **(Fig 4.10B)**. With these results we suggest that the RecA response is substantially decreased in cells that lack the excision activity of *uvrABC* and *mrfAB*. These results further support the conclusion that MrfAB participate in the repair of MMC damaged DNA.

MrfAB are conserved in diverse bacterial phyla

Given the specificity of MrfAB for MMC, we became interested in understanding how conserved *mrfA* and *mrfB* are across different bacterial phyla. We performed a PSI-BLAST search using MrfA or MrfB against the proteomes of bacterial organisms from several phyla **(Fig 4.12A)**. We found that MrfA and MrfB are both present in organisms from 5 different phyla, though MrfA is more broadly conserved in bacteria **(Fig 4.12A)**. To test if MrfA and MrfB function is conserved, we attempted to complement the MMC sensitive phenotype using codon-optimized versions of the homologs from three organisms, *Bacillus cereus*, *Streptococcus pneumoniae*, and *Pseudomonas aeruginosa*. We found that expression of *Bc-mrfA* and *Bc-mrfB* were capable of complementing their respective deletions **(Fig 4.12B)**. Interestingly, *Sp-mrfB* complemented, but *Sp-mrfA* did not **(Fig 4.12B)**. The more distantly related homologs from *P. aeruginosa* were not able to complement the corresponding deletion alleles **(Fig 4.12B)**. We conclude that MrfA and MrfB function is conserved in closely related species, and that they likely have been adapted to other uses in more distantly related bacteria.

Discussion

MrfAB are founding members of a novel bacterial nucleotide excision repair pathway. The observation that RecA-GFP foci changes in a synergistic manner with deletion of both

uvrABC and *mrfAB* suggests that MrfAB are acting as a second excision repair pathway. Indeed, a study of SOS activation in *E. coli* found that deletion of *uvrA* results in decreased SOS response activation when treated with MMC (45). The activation of the SOS response requires the formation of the RecA/ssDNA nucleoprotein filament that can be observed *in vivo* using a RecA-GFP fusion (42, 43, 46-48). Thus, our data are supportive of the excision repair model. We cannot formerly exclude the possibility that MrfAB act on a DNA repair intermediate, however, given that the *mrfAB* deletion did not render cells sensitive to other DNA damaging agents, this intermediate would have to be specific to the repair of MMC generated lesions.

Our current model is that a MMC mono-adduct or intra-strand crosslink is recognized by MrfA or an unknown factor **(Fig 4.13)**. After the lesion is recognized it is possible that incisions occur on either side of the lesion or a single incision is used. It is also possible that no incision is required and that MrfAB make use of transient nicks in the chromosome that would be present during synthesis of the lagging strand, though this model would limit the lesions that MrfAB could repair. Once a nick is present, we hypothesize that MrfA acts as helicase to separate the DNA, exposing the MMC lesion. If a nick is generated 3′ to the lesion, MrfA could access the DNA at the nick and use its putative 3′→5′ helicase activity to separate the lesion containing strand for degradation by MrfB **(Fig 4.13)**. If MrfA made use of transient nicks in the chromosome generated during lagging strand synthesis, then it is possible that MrfA could recognize or be recruited to the MMC lesion and use its 3′→5′ helicase activity on the strand opposite the lesion thereby exposing the lesion containing strand which could be stabilized by SSB, and upon reaching the nick in the DNA strand containing the lesion, MrfB could access the 3′ end to degrade the lesion containing strand. Our data cannot distinguish between these models, however, Hrq1 and SftH have been observed to require a 3′ tail for helicase activity (29, 31, 49, 50). Therefore, we hypothesize that a 3′ tail is necessary after lesion recognition, to allow for MrfA to separate the lesion containing strand.

The specificity of the Δ*mrfAB* phenotype suggests that lesion recognition depends on MMC adduct structure. Our reported screen did not identify other candidates for this pathway (26) , though it remains possible that an essential protein or a protein that functions in homologous recombination, which would have a more severe phenotype than *mrfAB*, also acts as a lesion recognition factor. Nonetheless, we hypothesize that lesion recognition is a function

accomplished by either MrfA, MrfB, or by both proteins in complex. MrfA is a putative helicase with a C-terminal domain of unknown function containing four well conserved cysteine residues. A high throughput X-ray absorption spectroscopy study of over 3000 proteins including MrfA reported finding that MrfA binds zinc (30). Intriguingly, UvrA, the recognition factor of canonical nucleotide excision repair, also contains a zinc finger which is required for regulating recognition of damaged DNA (51). Indeed, three of the four recognition factors in eukaryotic nucleotide excision repair, XPA, RPA, and TFIIH also each contain a zinc finger component (25). Therefore, it is tempting to speculate that MrfA functions as the lesion recognition factor through its putative C-terminal zinc finger domain.

The initial finding that sensitivity to DNA damage in *mrfAB* mutants is specific to MMC suggested an antibiotic specific repair pathway. The major source of toxicity from MMC has long been thought to be the inter-strand crosslink (5). We found that MrfAB do not contribute to unhooking an inter-strand crosslink *in vivo* and yet deletion of *mrfAB* in the *uvrABC* mutant resulted in a significant decrease in survival following MMC treatment. These observations strongly suggest that the mono-adducts and/or the intra-strand crosslink make a significant contribution to the overall toxicity of MMC. Therefore, through identifying a new repair pathway in bacteria, we are able to provide new insight into the toxicity profile of a well-studied, natural antibiotic.

MrfAB homologs have likely evolved to perform different functions depending on the environments of their respective bacterial species, despite significant sequence similarity. We speculate that MrfAB specificity for MMC is a reflection of habitat overlap between *B. subtilis* and mitomycin producing bacteria such as *S. lavendulae*. Thus, MrfAB are an adaptation that allows *B. subtilis* to effectively compete in habitats where MMC is produced. Given that only closely related species could substitute for MrfA and MrfB in *B. subtilis*, we hypothesize that the MMC specific repair activity is restricted to those species. In fact, the homologs present in *P. aeruginosa* have diverged significantly. The N-terminus of *Pa*-MrfA is quite different from that of *Bs*-MrfA, and the C-terminal TPR domain of MrfB is completely absent in *Pa*-MrfB (see supplemental alignments), consistent with the notion that MrfAB function has diverged in more distantly related bacteria. Additionally, our results with MrfAB from *S. pneumoniae* are supportive of our hypothesis that MrfAB function in MMC repair is restricted to closely related

organisms. We speculate the interaction between *Sp*-MrfA and *Sp*-MrfB is conserved such that *Sp*-MrfB can still be recruited by *Bs*-MrfA and MrfB retains exonuclease activity, while the function of *Sp*-MrfA has diverged and the lesion recognition or recruitment activity is no longer present.

We recently investigated the mismatch repair homolog MutS2 and arrived at a similar conclusion—MutS2 has been adapted to the specific DNA repair needs of different organisms. MutS2 in *B. subtilis* promotes homologous recombination (52), whereas MutS2 in several other organisms inhibits homologous recombination (53-56). The reality that distantly related organisms have adapted their genetic repertoire inherited from the most recent common ancestor would seem obvious. Still, a major thrust of biological exploration is often to examine processes that are highly conserved. While well conserved processes are often critical for more organisms, it is the divergent functions that make each organism unique, which is a property of inherent value found throughout nature.

Materials and Methods

Bacteriological methods

All *B. subtilis* strains used in this study are isogenic derivatives of PY79 (57), and listed in **Table 4.1**. Detailed construction of strains, plasmids and a description of oligonucleotides used in this study are provided in the supplemental text. Plasmids and oligonucleotides are listed in **Tables 4.2 and 4.3**, respectively. Media used to culture *B. subtilis* include LB (10 g/L NaCl, 10 g/L tryptone, and 5 g/L yeast extract) and $S7_{50}$ minimal media with 2% glucose (1x $S7_{50}$ salts (diluted from 10x $S7_{50}$ salts: 104.7g/L MOPS, 13.2 g/L, ammonium sulfate, 6.8 g/L monobasic potassium phosphate, pH 7.0 adjusted with potassium hydroxide), 1x metals (diluted from 100x metals: 0.2 M $MgCl_2$, 70 mM $CaCl_2$, 5 mM $MnCl_2$, 0.1 mM $ZnCl_2$, 100 µg/mL thiamine-HCl, 2 mM HCl, 0.5 mM $FeCl_3$), 0.1% potassium glutamate, 2% glucose, 40 µg/mL phenylalanine, 40 µg/mL tryptophan). Selection of *B. subtilis* strains was done using spectinomycin (100 µg/mL) or chloramphenicol (5 µg/mL).

Spot titer and survival assays

Spot titer assays were performed as described previously (26). Survival assays were performed as previously described (26), except cells were treated at a density of OD_{600} = 1 instead of 0.5.

Microscopy

Strains containing RecA-GFP were grown on LB agar with 100 μg/mL spectinomycin at 30°C overnight. Plates were washed with $S7_{50}$ minimal media with 2% glucose. Cultures of $S7_{50}$ minimal media with 2% glucose and 100 μg/mL spectinomycin were inoculated at an OD_{600} = 0.1 and incubated at 30°C protected from light until an OD_{600} of about 0.3 (about 3.5 hours). Cultures were treated with 5 ng/mL MMC and samples were taken for imaging prior to MMC addition, 45 minutes, 90 minutes, and 180 minutes after MMC addition. The vital membrane stain FM4-64 was added to 2 μg/mL and left at room temperature for five minutes. Samples were transferred to 1% agarose pads containing 1x Spizizen salts as previously described (26). Images were captured using an Olympus BX61 microscope using 250 ms exposure times for both FM4-64 (membranes) and GFP. RecA-GFP foci were determined by using the find maxima function in ImageJ with the threshold set to the background of the image by comparing a line trace of an area without cells. The number of cells with foci was determined by taking the total number of foci and subtracting the foci greater than one in cells having multiple foci (*i.e.*, if a cell had two foci, one would be subtracted and if a cell had 3 foci two would be subtracted and so on). The percentage was determined by dividing the number of cells with a focus or foci by the total number of cells observed.

DNA crosslinking assay

Strains of *B. subtilis* were struck out on LB agar and incubated at 30°C overnight. Plates were washed with LB and samples of 0.5 mL OD_{600} = 3 were aliquoted. One sample was untreated and three samples were treated with 1 μg/mL MMC. Samples were incubated at 37°C for 1 hour. For the untreated and MMC treatment samples, one volume (0.5 mL) of methanol was added and samples were mixed by inversion. Samples were harvested via centrifugation (12,000 *g* for 5 minutes, washed twice with 0.5 mL 1x PBS pH 7.4 and stored at -20°C overnight). For recovery samples, cells from the remaining two treated samples were pelleted via

centrifugation (10,000 *g* for 5 minutes) washed twice with 1 mL LB media and then re-suspended in 0.6 mL LB media. Samples were then transferred to 14 mL round bottom culture tubes and incubated at 37°C on a rolling rack for 45 or 90 minutes. An equal volume (0.6 mL) of methanol was added and samples were mixed by inversion. Samples were harvested as stated above and stored at -20°C overnight. Chromosomal DNA was extracted using a silica spin-column as previously described (26). Samples were normalized by A_{260} to 15 ng/μL. Samples were heat denatured by incubating at 100°C for 6 minutes followed by placing directly into an ice-water bath for 5 minutes. For native samples and heat denatured samples, 300 ng and 600 ng, respectively, were loaded onto a 0.8% agarose gel with ethidium bromide and electrophoresed at 90 volts for approximately one hour. The crosslinked species was quantified in gels from two independent experiments in ImageJ. The intensity of the crosslinked band was determined using the Gel Analyzer tool, and the background from the region above the crosslinked band was subtracted and the difference was normalized to the intensity of the native chromosomal DNA band **(Fig 4.9A, lower panel)**. The average of two independent experiments is shown, with error bars representing the range of the two measurements.

Bacterial two-hybrid assays

Bacterial two-hybrid assays were performed as described (26, 27).

MrfB protein purification

MrfB was purified from *E. coli* cells as follows. 10xHis-Smt3-MrfB was expressed from plasmid pPB97 in *E. coli* NiCo21 cells (NEB) at 37°C. Cells were pelleted and resuspended in lysis buffer (50 mM Tris pH7.5, 300 mM NaCl, 5% sucrose, 25 mM imidazole, 1x Roche protease inhibitor cocktail). Cells were lysed via sonication and lysates were clarified via centrifugation: 18,000 rpm (Sorvall SS-34 rotor) for 45 minutes at 4°C. Clarified lysates were loaded onto Ni^{2+}-NTA-agarose pre-equilibrated in lysis buffer in a gravity column. The column was washed with 25 column volumes wash buffer (50 mM Tris pH 7.5, 500 mM NaCl, 10% (v/v) glycerol, 40 mM imidazole). MrfB was eluted from the column by cleavage of the 10xHis-Smt3 tag using 6xHis-Ulp1 in 10 column volumes of digestion buffer (50 mM Tris pH 7.5, 150 mM NaCl, 10% glycerol, 10 mM imidazole, 1 mM DTT, and 20 μg/mL 6xHis-Ulp1) at room temperature for 150 minutes. The eluate containing untagged MrfB was collected as the flow

through. MrfB was concentrated using a 10 kDa Amicon centrifugal filter. MrfB was loaded onto a HiLoad superdex 200-PG 16/60 column pre-equilibrated with gel filtration buffer (50 mM Tris pH 7.5, 250 mM NaCl, and 5% (v/v) glycerol). The column was eluted with gel filtration buffer at a flow rate of 1 mL/min. Peak fractions were pooled, glycerol was added to a final concentration of 20%, and concentrated using a 10 kDa Amicon centrifugal filter. MrfB aliquots were frozen at a final concentration of 2.6 μM in liquid nitrogen, and stored at 80°C.

Exonuclease assays

Exonuclease reactions (20 μL) were performed in 25 mM Tris pH 7.5, 20 mM KCl, and 5 mM $MgCl_2$ as indicated in the figure legends. The plasmid pUC19 was used as a substrate at a concentration of 13.5 ng/μL. To generate linear or nicked substrate, pUC19 was first incubated with BamHI-HF (NEB) or Nt.BSPQ1 (NEB), respectively, for 30 minutes at 37°C. To test metal dependency of MrfB, the linearized pUC19 was purified using a silica spin-column. Reactions were initiated by adding MrfB to 130 nM, 10 units of T_5 exonuclease (NEB), or 5 units of λ exonuclease (NEB) and incubating at 37°C as indicated in the figure legends. Reactions were terminated by the addition of 8 μL of nuclease stop buffer (50% glycerol and 100 mM EDTA) followed by resolving reaction products by agarose gel electrophoresis.

Phylogenetic analysis

The protein sequences of MrfA (AHA78094.1) and MrfB (AHA78093.1) were used in a PSI-BLAST search in several organisms **(Fig 4.12A)**. If a putative homolog was detected, the coverage and percent identity were both recorded. For MrfA, the protein was considered a homolog if the DEXH helicase domain, the C-terminal domain, and the four conserved cysteines were all present. For MrfB, the protein was considered a homolog if the putative catalytic residues were conserved.

Figures and Tables

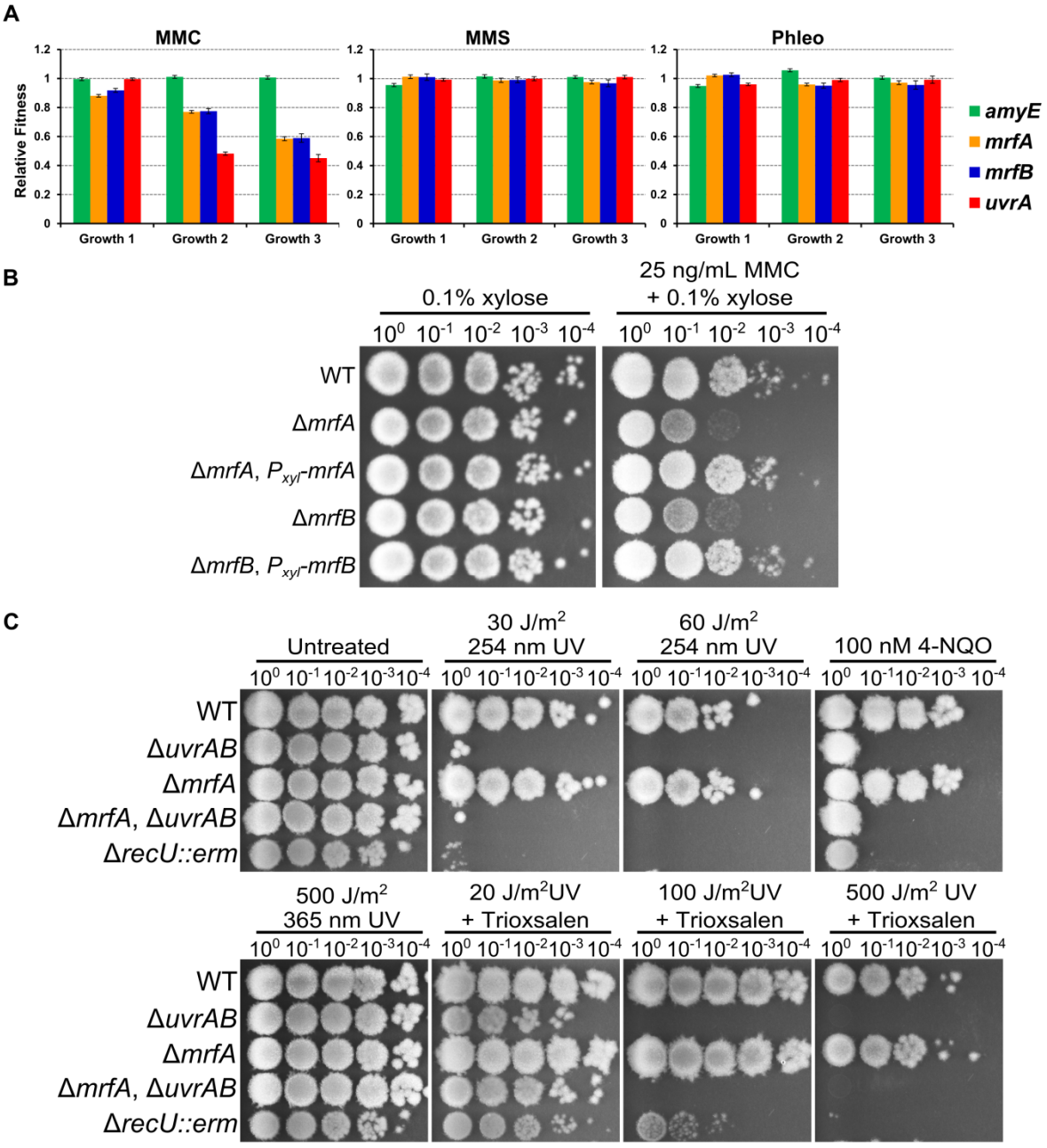

Figure 4.1 DNA damage sensitivity of Δ*mrfAB* is specific to mitomycin C. (A) Relative fitness plots for the indicated gene disruptions from Tn-seq experiments previously reported (26). The mean fitness is plotted as a bar graph and the error bars represent the 95% confidence interval. **(B)** Spot titer assay using strains with the indicated genotypes grown on LB with the indicated supplements. **(C)** Spot titer assay using strains with the indicated genotypes grown on LB media with the indicated treatments. For UV irradiation, cells were exposed to the indicated dose after serial dilutions were spotted on plates. For trioxsalen plates, 1 µg/mL was used and the UV wavelength for irradiation was 365 nm.

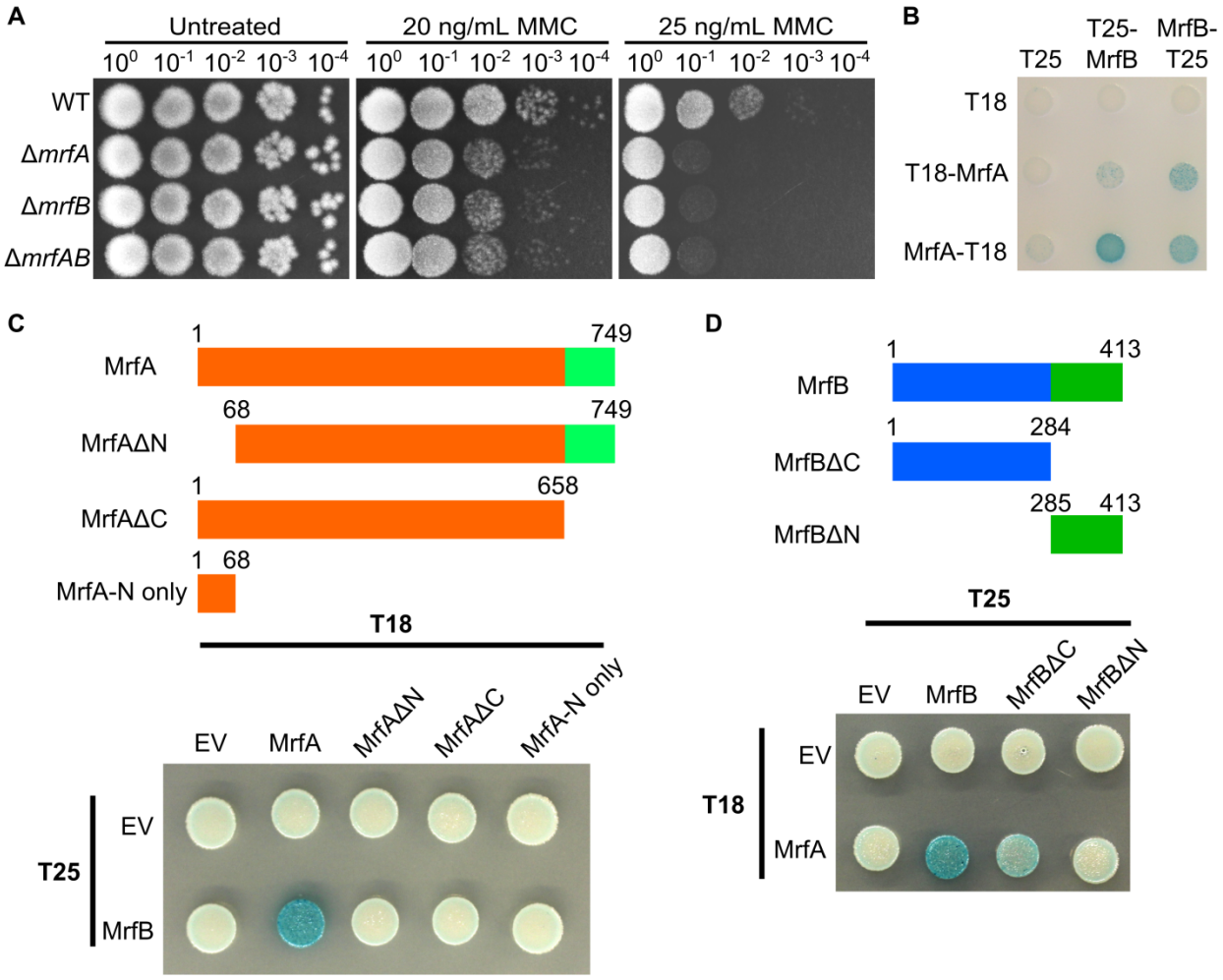

Figure 4.2 MrfA and MrfB function in the same pathway. (A) Spot titer assay using strains with the indicated genotypes grown on the indicated media. **(B)** Bacterial two-hybrid assay using the indicated T18 and T25 fusions. **(C)** MrfA constructs used in deletion analysis of MrfA-MrfB interaction (upper) and a bacterial two-hybrid assay using T25-MrfB and the indicated MrfA-T18 fusions (lower). **(D)** MrfB constructs used in deletion analysis of MrfA-MrfB interaction (upper) and a bacterial two-hybrid assay using MrfA-T18 and the indicated T25-MrfB fusions (lower).

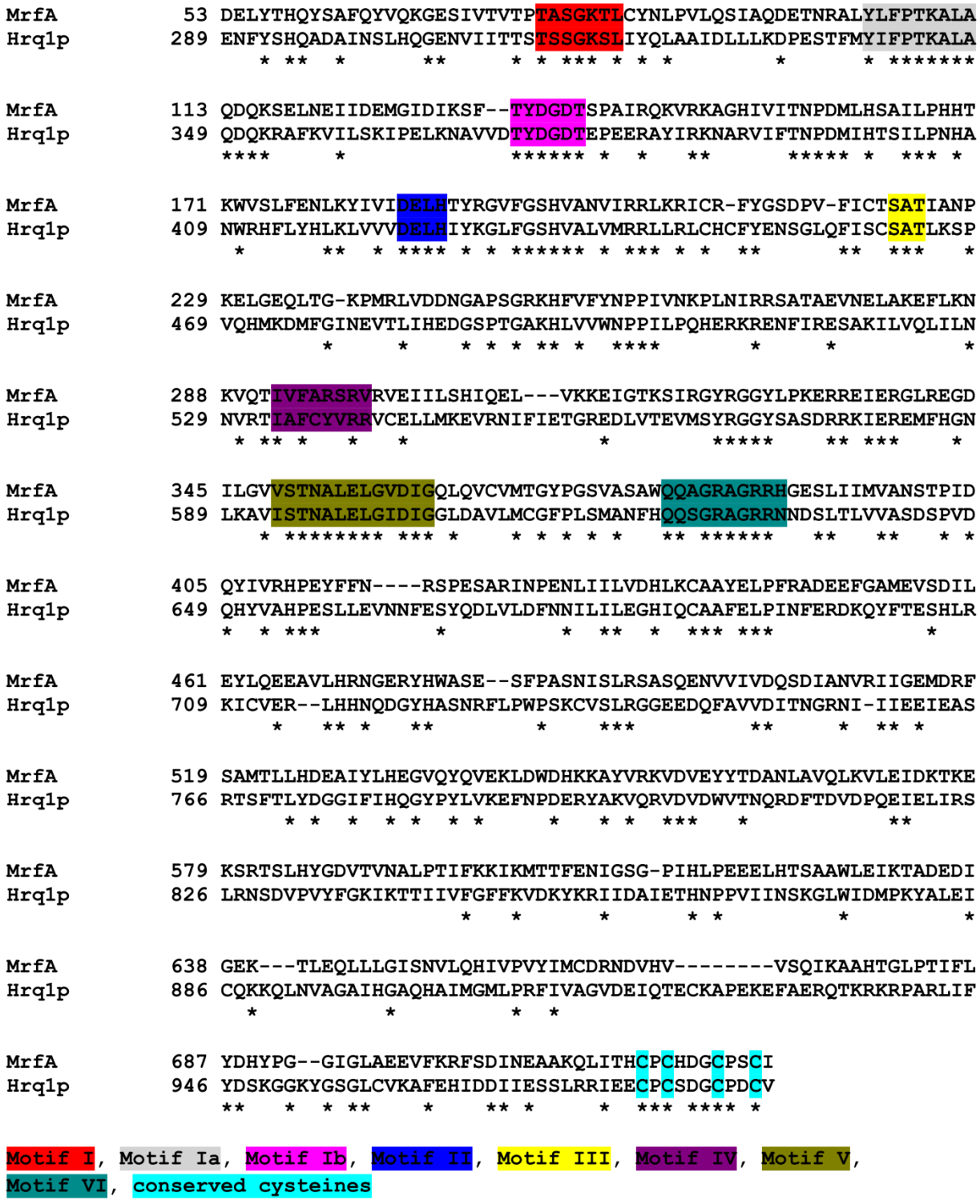

Figure 4.3 Helicase motifs of MrfA. An alignment of MrfA to Hrq1 from *S. cerevisiae*. Helicase motifs are highlighted as shown. The alignment was constructed using SIM (58).

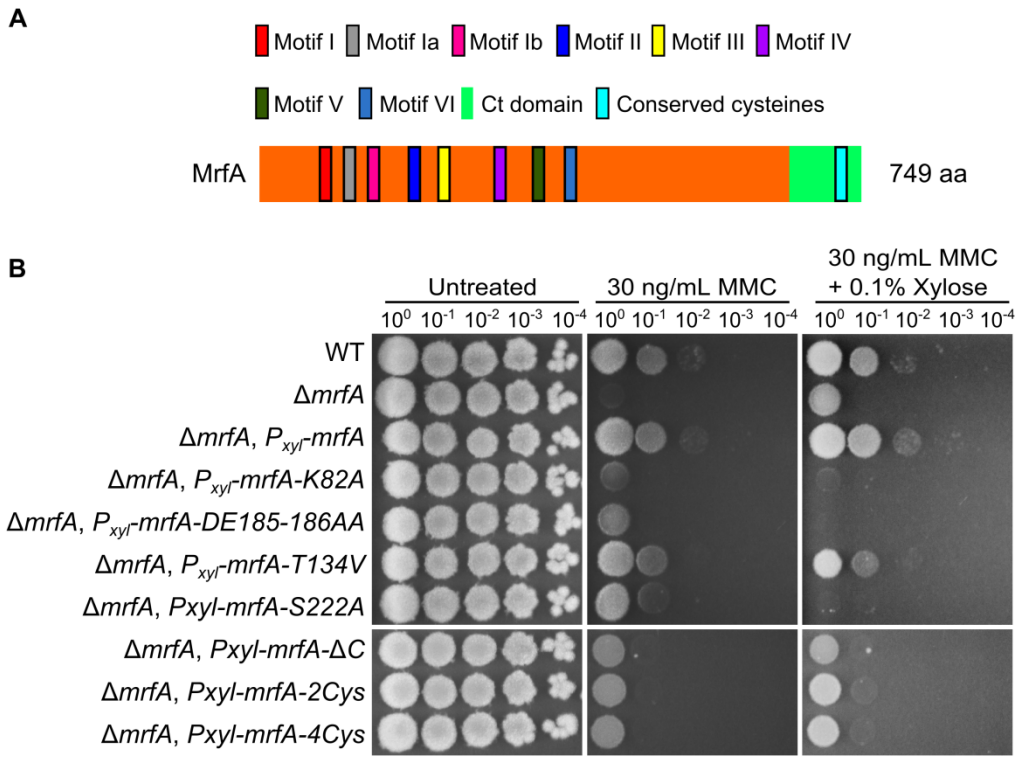

Figure 4.4 MrfA helicase motifs and conserved cysteines are required for function. (A) A schematic of MrfA depicting putative helicase motifs, C-terminal (Ct) domain, and conserved cysteines. **(B)** Spot titer assay using strains with the indicated genotypes spotted on the indicated media.

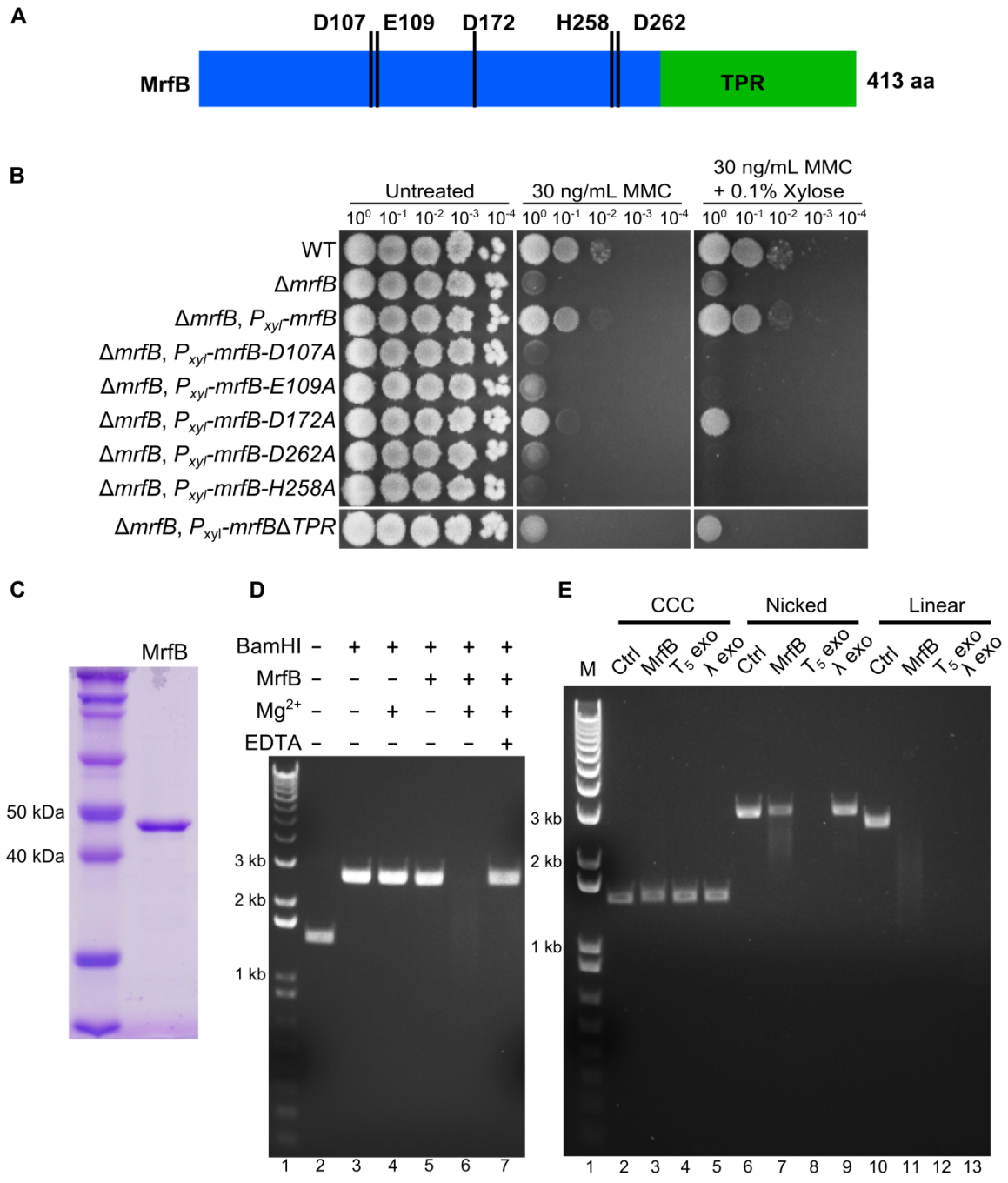

Figure 4.5 MrfB is a metal-dependent exonuclease. (A) A schematic of MrfB depicting putative catalytic residues and C-terminal tetratrichopeptide repeat (TPR) domain. **(B)** Spot titer assay using strains with the indicated genotypes spotted on the indicated media. **(C)** 1 µg of purified MrfB stained with Coomassie brilliant blue. **(D)** Exonuclease assay using pUC19 linearized with BamHI (lanes 3-7). Reactions were incubated at 37°C for 15 minutes with or without MrfB, $MgCl_2$, or EDTA as indicated, and separated on an agarose gel stained with ethidium bromide. Lane 1 is a 1 kb plus molecular weight marker and lane 2 is undigested pUC19 plasmid. **(E)** Exonuclease assay testing substrate preference. The indicated exonucleases

were incubated with a covalently closed circular plasmid (CCC), a nicked plasmid (Nicked) or a linear plasmid (Linear) in the presence of Mg^{2+} at 37°C for 10 minutes. Reaction products were separated on an agarose gel stained with ethidium bromide. Lane 1 is a 1 kb plus molecular weight marker (M).

A

```
MrfB      VEYPLSHRHGLYSFSELEEVITLWNQSGLSHTLSAKGYNKNNLFFFDTETTGLGGGA---      117
ExoI      ---------------------------------MMNDGKQQSTFLFHDYETFGTHPA----      24
DnaQ      ---------------------------------MST--AITRQIVLDTETTGMNQIGAHY      25
ExoX      ----------------------------------------MLRIIDTETCGLQ------      13
                                                    . * ** *

MrfB      -GNTIFLLGHAR-VYEDRVT-------------------------VKQHLLPKPGNEVA      149
ExoI      -LDRPAQFAAIRTDSEFNVIGEPEVFYCKPADDYLPQPGAVLITGITPQEARAKGENEAA      83
DnaQ      EGHKIIEIGAVE-VVNRRLTGNNFHVYLKPDRLV--DPEAFGVHGIADEFLLDKP----T      78
ExoX      --GGIVEIASVD-VIDGKIV-NPMSHLVRPDRPI--SPQAMAIHRITEAMVADKP----W      63
                 :.      : .:                          .      *

MrfB      LYQSFLS--EVDITSLVTYNGKAFD------------------WPQVKTRHTLIRDRLP      188
ExoI      FAARIHSLFTVPKTCILGYNNVRFDDEVTRNIFYRNFYDPYAWSWQHDNSRW-----DLL      138
DnaQ      FAEVADEFMDYIRGAELVIHNAAFDIG----------FMDYEFSLLKR---------DIP      119
ExoX      IEDVIPHY---YGSEWYVAHNASFDRR----------VLPE-----------------MP      93
          :                   :.  **                                 :

MrfB      KLPEFG-HFDLLHGARRLWKHKMDRVSLGTVEKEELGIRRLEDTPGYLAPMLYFHFIKAQ      247
ExoI      DVMRACY---ALRPEGINWPENDDGLPSFRL----------------------EHLTKAN      173
DnaQ      KTNTFCKVTDSLAVARKMFPGKRNSLDALCA----------------------RYEIDNS      157
ExoX      G-EWIC----TMKLARRLWPGIKYSNMALYK----------------------TRKLNVQ      126
                    :      :                                    . .

MrfB      EPDLLKGVLHHNEMDVLSLISLYIHMSKKILSESHA-------------------P----      284
ExoI      GIE--HSNAHDAMADVYATIAMAK---------------------------------      195
DnaQ      -----KRTLHGALLDAQILAEVYLAM--------------TGGQTSMAFAMEGETQQQQG      198
ExoX      TPP--GLHHHRALYDCYITAALLIDIMNTSGWTAEQMADITGRPSLMTTFTFGK---YRG      181
                   *    *      :

MrfB      ----KEHSEAYAMAKWFMAH-----------------------------------------      300
ExoI      ----LVKTRQPRLFDYLFTHRNKHKLMALIDVPQMKPLVHVSGMFGAWRGNTSWVAPLAW      251
DnaQ      EATIQRIVRQASKLRVVFATDEEIAA-----HEARLDLVQKKGGSCLWRA----------      243
ExoX      KAVSDVAERDPGYLRWLFNNLDSMS------PELRLTLKHYLENT---------------      220
                   .       .:
```

Putative catalytic residues, Putative catalytic residue from structural model

B

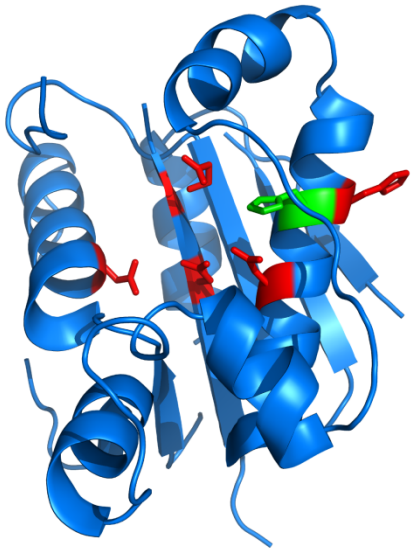

C

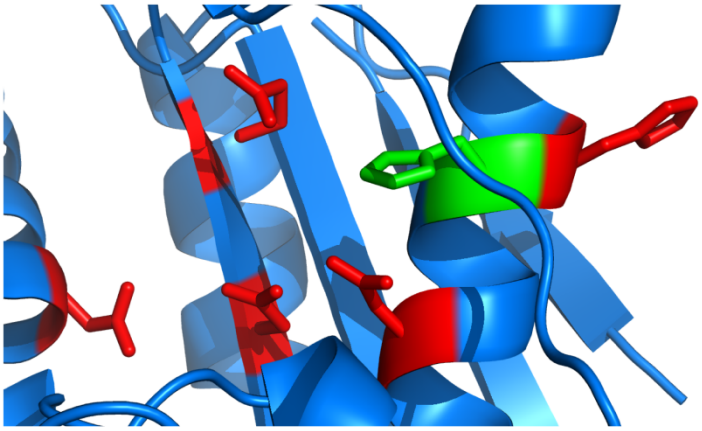

Figure 4.6 Putative catalytic residues of MrfB. (A) Alignment of the exonuclease domain of MrfB to ExoI (SbcD), DnaQ, and ExoX from *E. coli* using Clustal Omega (59). Putative catalytic residues are highlighted in red, and a putative non-conserved catalytic residue is highlighted in green. **(B)** A structural model of MrfB, modelled on DNA polymerase epsilon catalytic subunit A (pdb structure c5okiA (35)), was generated using Phyre2 (34). The model depicting amino acids 100-270 of MrfB is shown as a cartoon in blue, and the putative catalytic residues are colored as in A. **(C)** A close up view of the putative catalytic residues from the model shown in B.

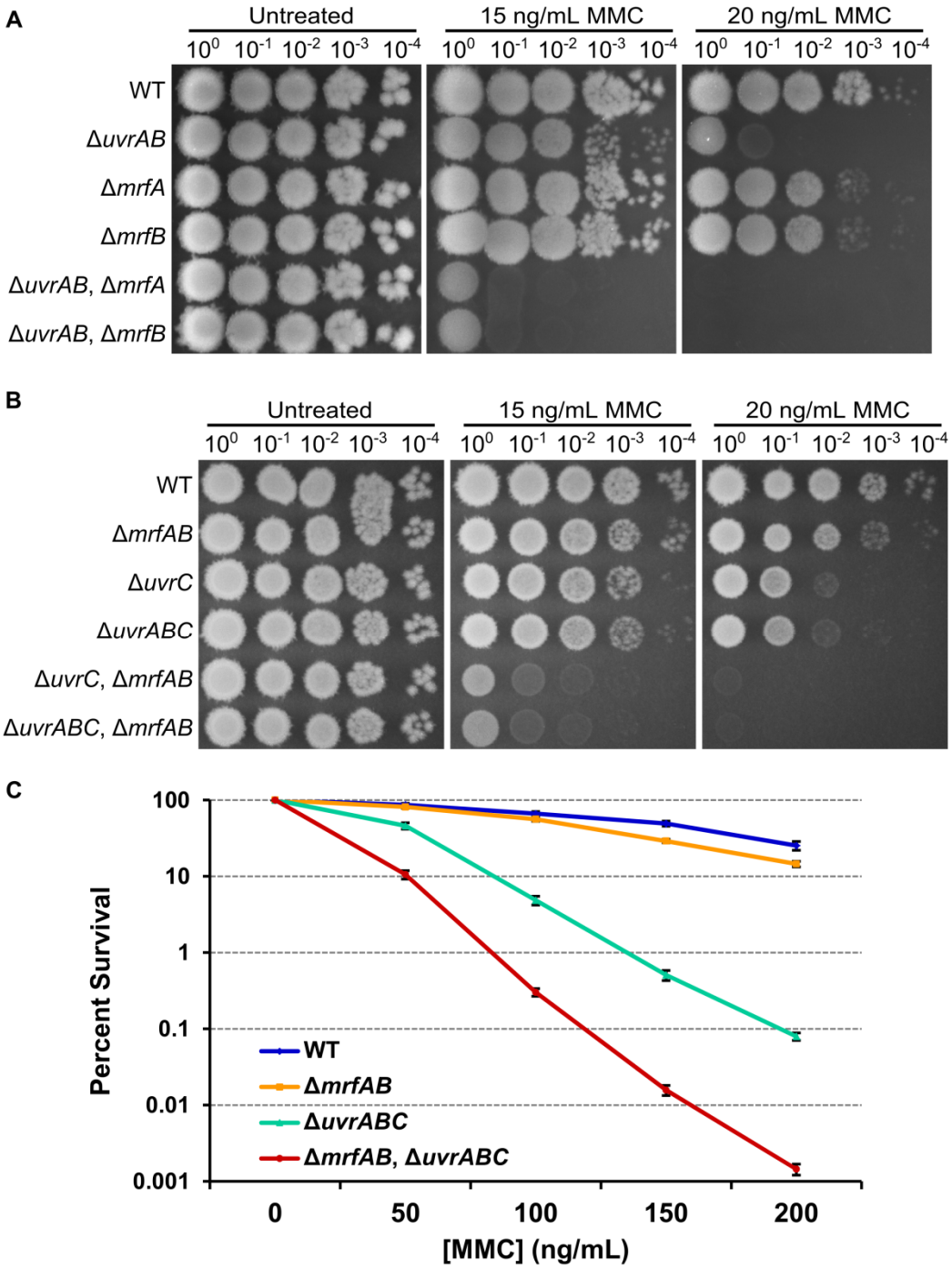

Figure 4.7 MrfAB function independent of UvrABC dependent nucleotide excision repair. **(A & B)** Spot titer assays using strains with the indicated genotypes grown on the indicated media. **(C)** Survival assay using strains with the indicated genotypes. The y-axis is the percent survival relative to the untreated (0 ng/mL) condition. The x-axis indicates the concentration of MMC used for a 30 minute acute exposure. The data points represent the mean of three independent experiments performed in triplicate (n=9) ± SEM.

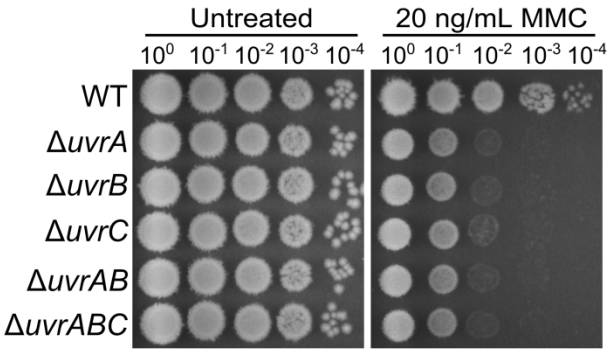

Figure 4.8 UvrABC function in the same pathway. Spot titer assay using the indicated *uvr* deletion strains grown on the indicated media.

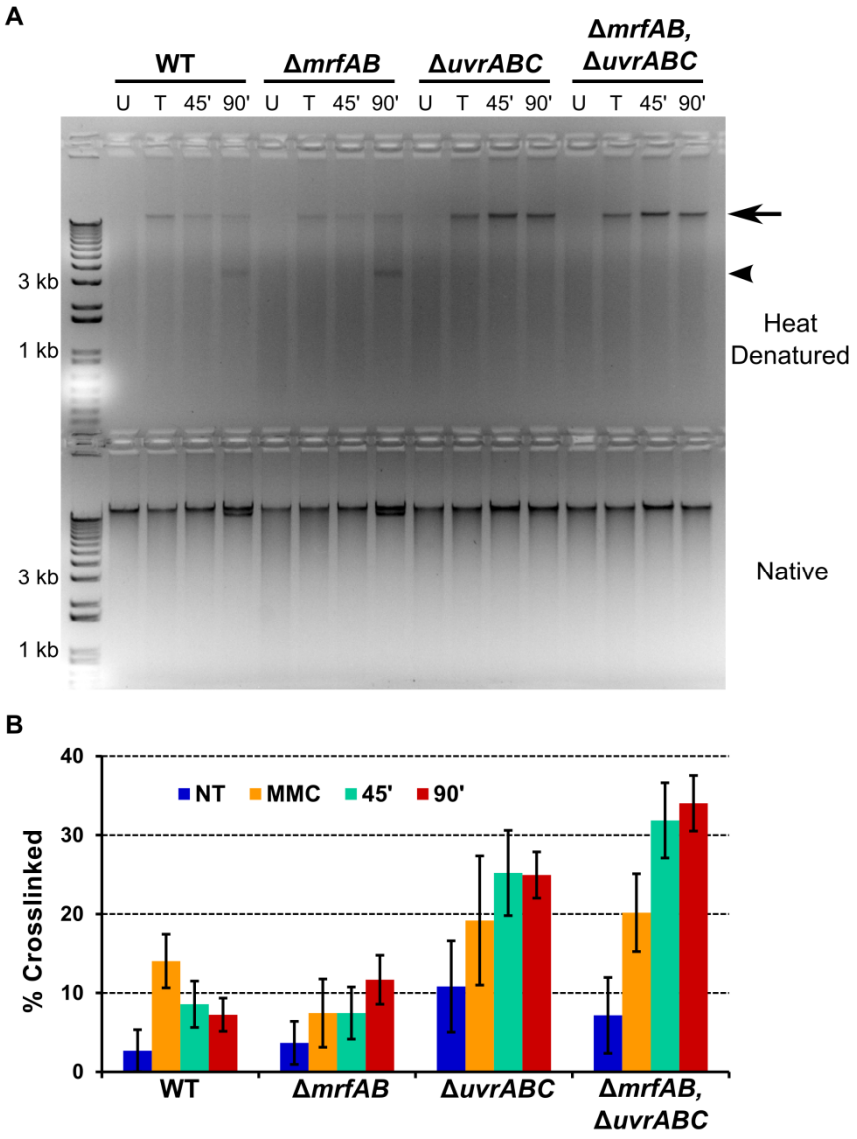

Figure 4.9 MrfAB are not required for unhooking inter-strand DNA crosslinks. (A) DNA crosslinking repair assay. Chromosomal DNA from untreated samples (U), 1 µg/mL MMC treated samples (T), and recovery samples (45' and 90') were heat denatured and snap cooled (upper) or native chromosomal DNA (lower) was separated on an agarose gel stained with ethidium bromide. A 1 kb plus molecular weight marker is shown in the first lane. **(B)** A bar graph showing the mean percent of crosslinked DNA (see methods) from two independent experiments, and error bars represent the range of the two measurements.

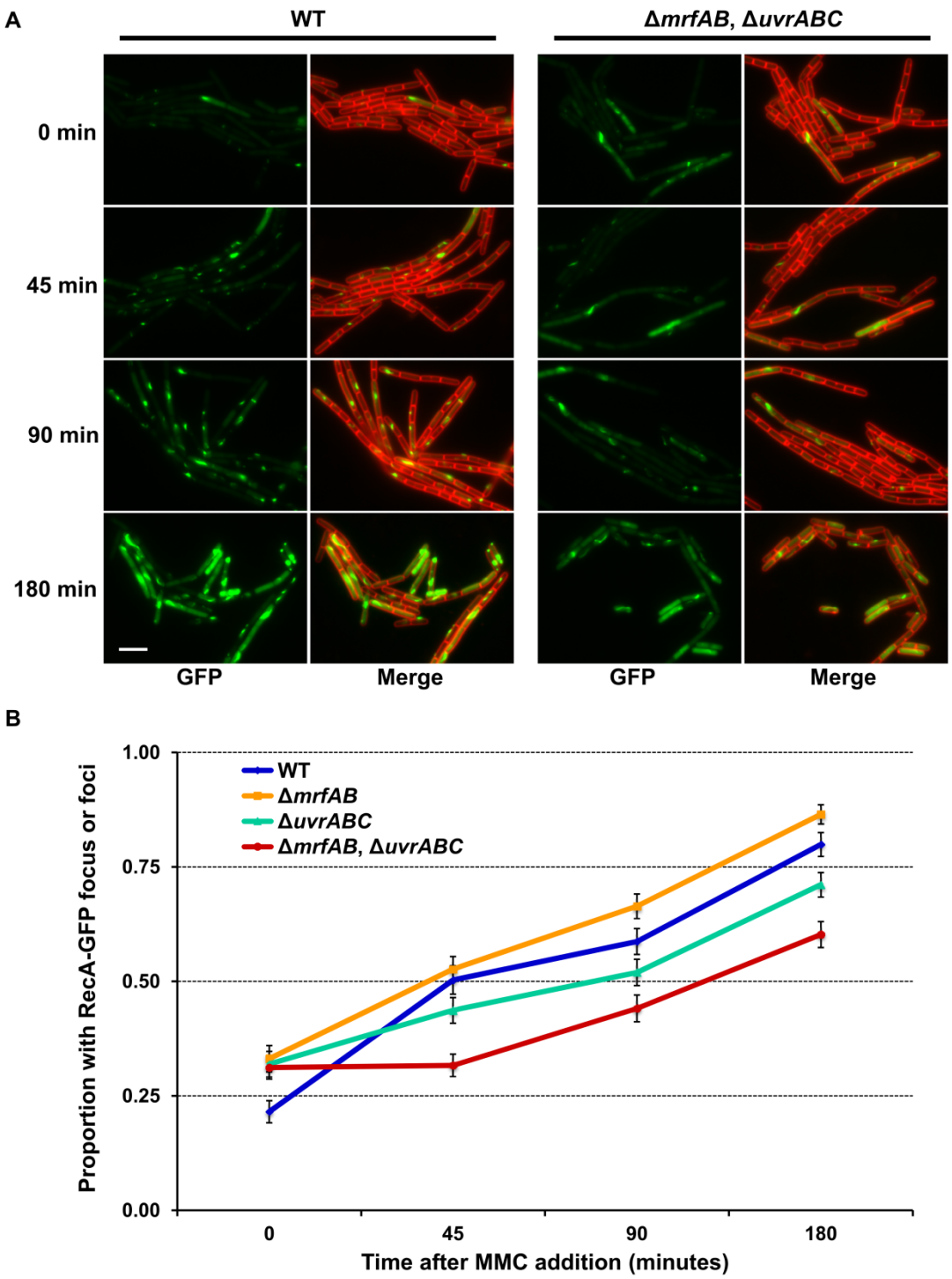

Figure 4.10 MrfAB and UvrABC are required for efficient RecA-GFP focus formation. (A) Representative micrographs of strains containing RecA-GFP expressed from the native locus in addition to the indicated genotypes. Images were captured at the indicated times following MMC addition (5 ng/mL). RecA-GFP is shown in green and the merged images show RecA-GFP (green) and membranes stained with FM4-64 (red). The white bar indicates 5 µm **(B)** Percentage

of cells with a RecA-GFP focus or foci over the indicated time course of MMC treatment (5 ng/mL). The error bars represent the 95% confidence interval.

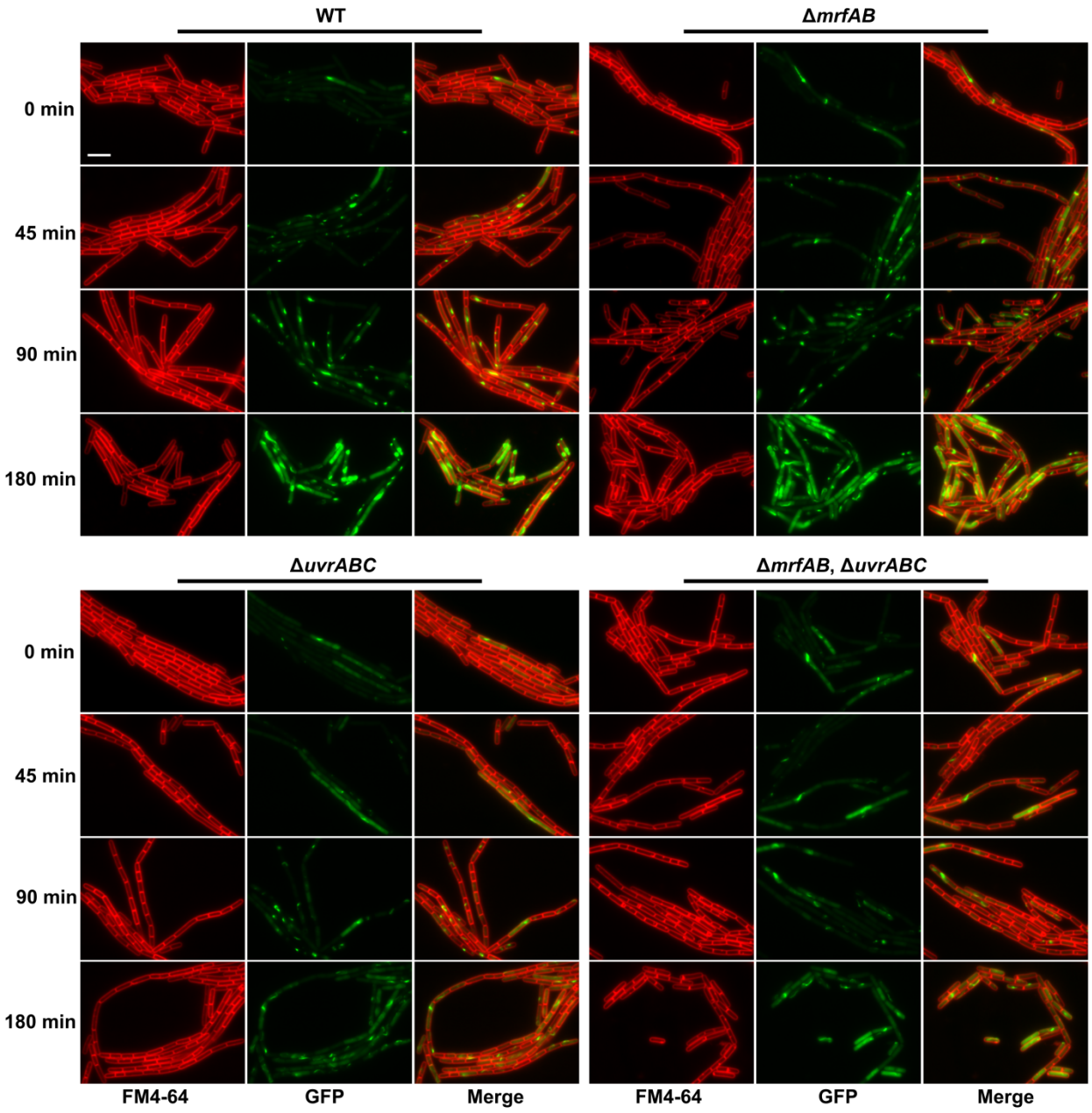

Figure 4.11 MrfAB are not required for unhooking inter-strand DNA crosslinks. Representative micrographs of cells from the indicated genotypes that also contain RecA-GFP expressed from the native locus. Time of imaging post MMC treatment (5 ng/mL) is indicated (rows). Membranes, stained with FM4-64 are shown in red, RecA-GFP is shown in green, and both are shown in the merged images. The white scale bar indicates 5 μm. The images for WT and Δ*mrfAB*, Δ*uvrABC* are also in Figure 4.10 and are shown here for comparison.

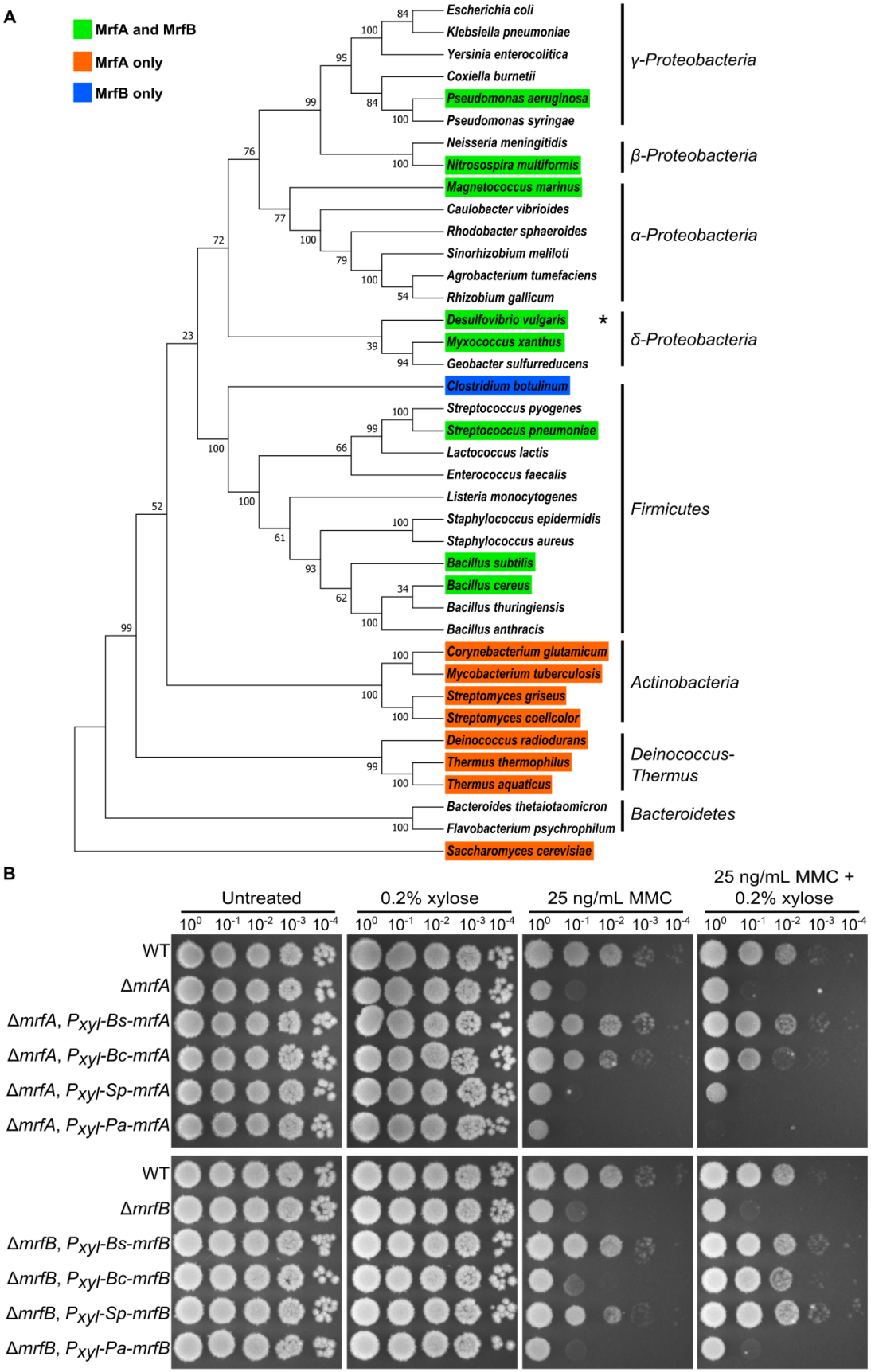
A
MrfA and MrfB
MrfA only
MrfB only
Escherichia coli
Klebsiella pneumoniae
Yersinia enterocolitica
Coxiella burnetii
Pseudomonas aeruginosa
Pseudomonas syringae
Neisseria meningitidis
Nitrosospira multiformis
Magnetococcus marinus
Caulobacter vibrioides
Rhodobacter sphaeroides
Sinorhizobium meliloti
Agrobacterium tumefaciens
Rhizobium gallicum
Desulfovibrio vulgaris
Myxococcus xanthus
Geobacter sulfurreducens
Clostridium botulinum
Streptococcus pyogenes
Streptococcus pneumoniae
Lactococcus lactis
Enterococcus faecalis
Listeria monocytogenes
Staphylococcus epidermidis
Staphylococcus aureus
Bacillus subtilis
Bacillus cereus
Bacillus thuringiensis
Bacillus anthracis
Corynebacterium glutamicum
Mycobacterium tuberculosis
Streptomyces griseus
Streptomyces coelicolor
Deinococcus radiodurans
Thermus thermophilus
Thermus aquaticus
Bacteroides thetaiotaomicron
Flavobacterium psychrophilum
Saccharomyces cerevisiae
γ-Proteobacteria
β-Proteobacteria
α-Proteobacteria
δ-Proteobacteria
Firmicutes
Actinobacteria
Deinococcus-Thermus
Bacteroidetes
B
Untreated
0.2% xylose
25 ng/mL MMC
25 ng/mL MMC + 0.2% xylose
WT
ΔmrfA
ΔmrfA, Pxyl-Bs-mrfA
ΔmrfA, Pxyl-Bc-mrfA
ΔmrfA, Pxyl-Sp-mrfA
ΔmrfA, Pxyl-Pa-mrfA
WT
ΔmrfB
ΔmrfB, Pxyl-Bs-mrfB
ΔmrfB, Pxyl-Bc-mrfB
ΔmrfB, Pxyl-Sp-mrfB
ΔmrfB, Pxyl-Pa-mrfB

Figure 4.12 MrfAB are conserved in diverse bacterial *phyla*. (A) A rooted phylogenetic tree constructed using 16s rRNA sequences (18s rRNA for *S. cerevisiae*), aligned with muscle (60), using the neighbor joining method (61), and the evolutionary distances were calculated using the p-distance method (62). The percentage of replicate trees that resulted in the associated species clustering together in a bootstrap test (500 replicates) is indicated next to the branches (63). Evolutionary analysis was performed in MEGA (64). *In this organism MrfA and MrfB homologs are fused into a single protein. **(B)** Spot titer assay using codon optimized versions of MrfA and MrfB from the indicated species to complement Δ*mrfA* (upper) or Δ*mrfB* (lower).

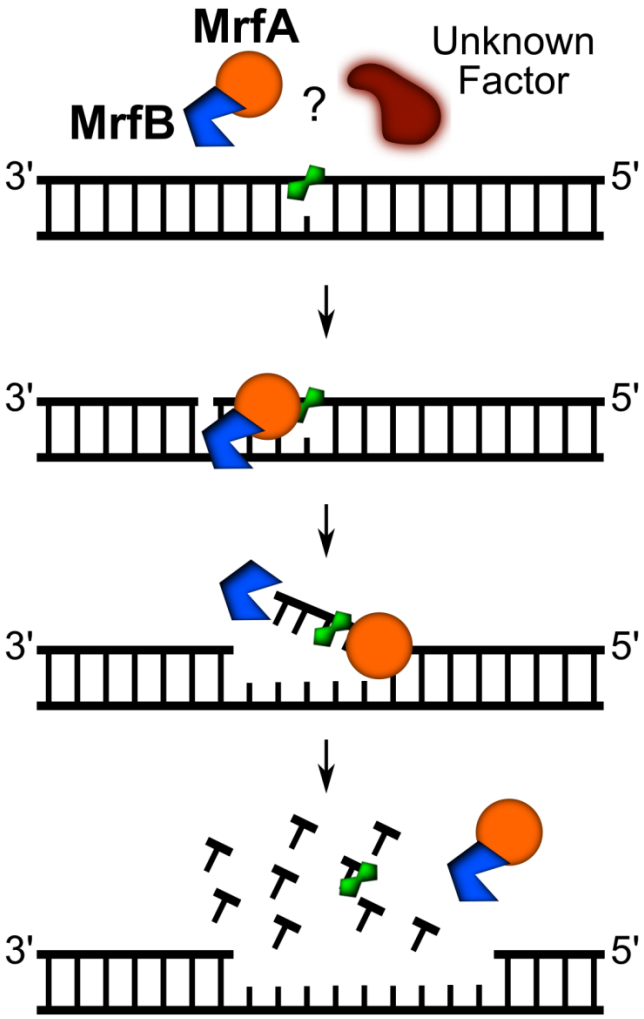

Figure 4.13 A model for MrfAB mediated nucleotide excision repair. We propose that either an unknown factor or MrfA recognizes an MMC adduct. MrfB is then recruited, and MrfA uses its helicase activity to separate the strand containing the MMC adduct, facilitating MrfB-dependent degradation of the adduct containing DNA. The source of the nick used to direct excision is unknown.

Strain	Genotype	Reference
PY79	PY79	(57)
LAS40	*recA::recA-gfp*	(43)
PEB125	Δ*recU::erm*	(52)
PEB307	Δ*uvrA*	(26)
PEB308	Δ*uvrB*	(26)
PEB309	Δ*uvrAB*	(65)
PEB310	Δ*uvrC*	(26)
PEB316	Δ*mrfA* (*yprA*)	(26)
PEB318	Δ*mrfB* (*yprB*)	(26)
PEB320	Δ*mrfAB*	This study
PEB337	Δ*mrfA*, Δ*uvrAB*	This study
PEB339	Δ*mrfB*, Δ*uvrAB*	This study
PEB369	Δ*mrfA*, *amyE::P_{xyl}-mrfA*	This study
PEB371	Δ*mrfB*, *amyE::P_{xyl}-mrfB*	This study
PEB505	Δ*mrfA*, *amyE::P_{xyl}-mrfA-K82A*	This study
PEB507	Δ*mrfA*, *amyE::Pxyl-mrfA-DE185-186AA*	This study
PEB509	Δ*mrfA*, *amyE::Pxyl-mrfA-T134V*	This study
PEB511	Δ*mrfA*, *amyE::Pxyl-mrfA-S222A*	This study
PEB513	Δ*mrfA*, *amyE::Pxyl-mrfA-ΔC*	This study
PEB515	Δ*mrfA*, *amyE::Pxyl-mrfA-C718A & C720A*	This study
PEB517	Δ*mrfA*, *amyE::Pxyl-mrfA-C718A, C720A, C724C, & C727A*	This study
PEB519	Δ*mrfB*, *amyE::Pxyl-mrfB-D107A*	This study
PEB521	Δ*mrfB*, *amyE::Pxyl-mrfB-E109A*	This study
PEB523	Δ*mrfB*, *amyE::Pxyl-mrfB-D172A*	This study
PEB525	Δ*mrfB*, *amyE::Pxyl-mrfB-D262A*	This study
PEB527	Δ*mrfB*, *amyE::Pxyl-mrfB-H258A*	This study
PEB529	Δ*mrfB*, *amyE::Pxyl-mrfB-ΔC*	This study
PEB812	Δ*mrfAB*, Δ*uvrAB*	This study
PEB822	Δ*uvrABC*	This study
PEB824	Δ*mrfAB*, Δ*uvrC*	This study
PEB826	Δ*mrfAB*, Δ*uvrABC*	This study
PEB828	*recA::recA-gfp*	This study
PEB830	Δ*mrfAB*, *recA::recA-gfp*	This study
PEB832	Δ*uvrABC*, *recA::recA-gfp*	This study
PEB834	Δ*mrfAB*, Δ*uvrABC*, *recA::recA-gfp*	This study
PEB866	Δ*mrfA*, *amyE::P_{xyl}-Bc-mrfA*	This study
PEB870	Δ*mrfB*, *amyE::P_{xyl}-Bc-mrfB*	This study
PEB872	Δ*mrfB*, *amyE::P_{xyl}-Pa-mrfB*	This study
PEB898	Δ*mrfA*, *amyE::P_{xyl}-Sp-mrfA*	This study
PEB900	Δ*mrfB*, *amyE::P_{xyl}-Sp-mrfB*	This study
PEB902	Δ*mrfA*, *amyE::P_{xyl}-Pa-mrfA*	This study

Table 4.1 Strains used in this study.

Plasmid number	Plasmid name	Reference/Source
pUC19	pUC19	NEB (3041S)
pKT25	pKT25	Euromedex (EUP-25C)
pKNT25	pKNT25	Euromedex (EUP-25N)
pUT18	pUT18	Euromedex (EUP-18N)
pUT18C	pUT18C	Euromedex (EUP-18C
pPB41	pPB41	(52, 66)
pPB47	pPB47	(26)
pPB73	pPB41-CRISPR::*uvrB*	(26)
pPB74	pPB41-CRISPR::*uvrC*	(26)
pPB75	pPB41-CRISPR::*mrfA*	(26)
pPB84	pPB73-Δ*uvrAB* editing template	(65)
pPB85	pPB74-Δ*uvrC* editing template	(26)
pPB88	pPB75-Δ*mrfAB* editing template	This study
pPB97	pET-28b-10xHis-Smt3-MrfB	This study
pPB109	pPB47-*amyE::Pxyl-mrfA-camR*	This study
pPB110	pPB47-*amyE::Pxyl-mrfB-camR*	This study
pPB159	pPB47-*amyE::Pxyl-mrfA-K82A-camR*	This study
pPB160	pPB47-*amyE::Pxyl-mrfA-DE185-186AA-camR*	This study
pPB161	pPB47-*amyE::Pxyl-mrfA-T134V-camR*	This study
pPB162	pPB47-*amyE::Pxyl-mrfA-S222A-camR*	This study
pPB163	pPB47-*amyE::Pxyl-mrfA-ΔC-camR*	This study
pPB164	pPB47-*amyE::Pxyl-mrfA-C718A & C720A-camR*	This study
pPB165	pPB47-*amyE::Pxyl-mrfA-C718A, C720A, C724A, & C727A-camR*	This study
pPB166	pPB47-*amyE::Pxyl-mrfB-D107A-camR*	This study
pPB167	pPB47-*amyE::Pxyl-mrfB-E109A-camR*	This study
pPB168	pPB47-*amyE::Pxyl-mrfB-D172A-camR*	This study
pPB169	pPB47-*amyE::Pxyl-mrfB-D262A-camR*	This study
pPB170	pPB47-*amyE::Pxyl-mrfB-H258A-camR*	This study
pPB171	pPB47-*amyE::Pxyl-mrfB-ΔC-camR*	This study
pPB263	pU-T18-MrfA	This study
pPB264	pU-MrfA-T18	This study
pPB265	pK-T25-MrfB	This study
pPB266	pK-MrfB-T25	This study
pPB273	pK-T25-MrfBΔC	This study
pPB274	pK-T25-MrfBΔN	This study
pPB283	pU-MrfAΔN-T18	This study
pPB284	pU-MrfAΔC-T18	This study
pPB285	pU-MrfA-N-T18	This study

Table 4.2 Plasmids used in this study.

Primer name	Sequence
oPEB56	ACCTCCAATCTGTTCGCGGTG
oPEB57	taaTCGAGCACCACCACCACCAC
oPEB58	GCTAGTTATTGCTCAGCGG
oPEB116	ctctcgtttcatcggtatcattac
oPEB117	cgcttcgttaatacagatgtaggt
oPEB217	GAACCTCATTACGAATTCAGCATGC
oPEB218	GAATGGCGATTTTCGTTCGTGAATAC
oPEB227	CCGTCAATTGTCTGATTCGTTA
oPEB232	GCTGTAGGCATAGGCTTGGTTATG
oPEB234	GTATTCACGAACGAAAATCGCCATTCCTAGCAGCACGCCATAGTGACTG
oPEB253	GAAGGGTAGTCCAGAAGATAACGA
oPEB345	actcctttgtttatccaccgaac
oPEB348	TTATTTTTGACACCAGACCAACTG
oPEB370	cacctacatctgtattaacgaagcgTCAATGGGGAAGAGAACCGCTTAAG
oPEB377	ggtaatgataccgatgaaacgagagAACAAAATTCTCCAGTCTTCACATCG
oPEB383	atgtatacctccttaggatcccatttcc
oPEB424	agaatgaatcgtgaaatgatcacc
oPEB432	acggatcgatatgattctctaagc
oPEB443	aaaccggaatccttcagacaatac
oPEB444	cttctaacggcacttggtaatttt
oPEB448	GCATGCTGAATTCGTAATGAGGTTCcgagttgattaggttctgaaatcc
oPEB452	tcttgtcatgcttgtaaaggtagc
oPEB454	agaaaatgatgggagaaggaatag
oPEB460	GCATAACCAAGCCTATGCCTACAGCatggtgtgatgacagctaccttta
oPEB461	AGCCATGGAAGTCAGTGATATTCT
oPEB462	tctttattcggttctttccagttc
oPEB464	gggaatattctttacacctctttgtcaagtac
oPEB465	tgtacttgacaaagaggtgtaaagaatattccccgggaaagcgcaaaagacgacttgtttcg ccatgaatttt
oPEB527	TAAAAGACAGGGTAAGGAAATGGA
oPEB543	CAATCAGACAAAAGGTGAGAAAAG
oPEB544	AGAAATCGAAAGAGGACTGAGAGA
oPEB545	GCTCACCGCGAACAGATTGGAGGTATGTCATTAAAAGGGAAACTCCAAC
oPEB546	CTCAGTGGTGGTGGTGGTGGTGCTCGAttaTTAAGAGGAATATTTCCTCTTTAGCCGGGCAA TTCTCACATGCAGTT
oPEB547	TAAGCGAGGTTGACATTACATCAC
oPEB557	taaCGGTTTCCATATGGGGATTGGTG
oPEB562	aatgggatcctaaggaggtatacatATGAAAAAGAAATCACTGACTGAACT
oPEB563	ACCAATCCCCATATGGAAACCGttaTTACGACATTTGATCCAACAGCTG
oPEB564	aatgggatcctaaggaggtatacatATGTCATTAAAAGGGAAACTCCAAC
oPEB565	ACCAATCCCCATATGGAAACCGttaTTAAGAGGAATATTTCCTCTTTAGCCGGGCAATTCTC

	ACATGCAGTT
oPEB720	GTAACGCCAACAGCATCAGGAGCTACGTTATGCTACAACCTCCCAGTC
oPEB721	TGGGAGGTTGTAGCATAACGTAGCTCCTGATGCTGTTGGCGTTACGGT
oPEB722	ACCTTAAGTATATCGTCATCGCTGCACTTCATACGTATCGAGGTGTGTTC
oPEB723	ACACCTCGATACGTATGAAGTGCAGCGATGACGATATACTTAAGGTTTTCAAAC
oPEB724	GGGCATTGATATTAAAAGCTTTGTATATGACGGGGATACGTCTCCGGCA
oPEB725	CCGGAGACGTATCCCCGTCATATACAAAGCTTTTAATATCAATGCCCATTTCATC
oPEB726	GTGATCCAGTTTTTATTTGTACTGCTGCAACGATTGCCAACCCAAAGGAA
oPEB727	CCTTTGGGTTGGCAATCGTTGCAGCAGTACAAATAAAAACTGGATCACTTCCA
oPEB728	CAATCCCCATATGGAAACCGttaTTAAGGGACAATATGCTGCAGCACA
oPEB729	TCGCCACCAATCCCCATATGGAAACCGttaTTACGACATTTGATCCAACAGCTGCAAAATTC TTTCCTTTGCTTTTATCCCTTCTATTTCCGTACCTATACAAGACGGACAGCCGTCATGAGCA GGAGCATGTGTAATCAGTTGTTTCGCCGCTT
oPEB730	TCGCCACCAATCCCCATATGGAAACCGttaTTACGACATTTGATCCAACAGCTGCAAAATTC TTTCCTTTGCTTTTATCCCTTCTATTTCCGTACCTATAGCAGACGGAGCGCCGTCATGAGCA GGAGCATGTGTAATCAGTTGTTTCGCCGCTT
oPEB731	ACAAAAACAACCTCTTTTTCTTTGCTACAGAAACAACCGGTCTTGGGGGT
oPEB732	CCCCAAGACCGGTTGTTTCTGTAGCAAAGAAAAAGAGGTTGTTTTTGTTATACCCT
oPEB733	CAACCTCTTTTTCTTTGATACAGCTACAACCGGTCTTGGGGGTGGA
oPEB734	CTCCACCCCCAAGACCGGTTGTAGCTGTATCAAAGAAAAAGAGGTTGTTTTTGTT
oPEB735	GACCTACAACGGCAAAGCCTTTGCTTGGCCGCAGGTGAAAACAAGGCA
oPEB736	GCCTTGTTTTCACCTGCGGCCAAGCAAAGGCTTTGCCGTTGTAGGTCAC
oPEB737	CAATCCCCATATGGAAACCGttaTTATGGCGCATGTGATTCTGAAAGGAT
oPEB765	TGTCCTGCATCATAATGAAATGGCTGTGTTATCACTCATTTCATTGTACATC
oPEB766	ACAATGAAATGAGTGATAACACAGCCATTTCATTATGATGCAGGACACCT
oPEB767	TCTTTTAAAAGGTGTCCTGCATGCTAATGAAATGGATGTGTTATCACTCATTTC
oPEB768	GTGATAACACATCCATTTCATTAGCATGCAGGACACCTTTTAAAAGATCC
oPEB1012	CATagctgtttcctgtgtgaaattg
oPEB1013	GGTGAAGGTCAAGGACAAGGCCAAGCCTGCAGGTCGACTCTAGAGGA
oPEB1014	TTGGCCTTGTCCTTGACCTTCACCGGGATCCTCTAGAGTCGACCCTG
oPEB1015	TAActaagaattcggccgtcgttt
oPEB1016	GGTGAAGGTCAAGGACAAGGCCAACCGAGCTCGAATTCAGCCGCCA
oPEB1017	TTGGCCTTGTCCTTGACCTTCACCCTCTAGAGTCGACCTGCAGTGG
oPEB1018	TAActaagtaatatggtgcactctcagt
oPEB1019	caggctttacactttatgcttcc
oPEB1020	GTAACCAGCCTGATGCGATT
oPEB1021	ATTATGCCGCATCTGTCCAACT
oPEB1022	gcaaggcgattaagttgggtaa
oPEB1023	GATTTTCCACAACAAGTCGATG
oPEB1024	TTCTCGCCGGATGTACTGGAAAC
oPEB1025	tggcttaactatgcggcatcaga
oPEB1026	GGTGAAGGTCAAGGACAAGGCCAAATGAAAAAGAAATCACTGACTGAACT

oPEB1027	actgagagtgcaccatattacttagTTATTACGACATTTGATCCAACAGCTG
oPEB1028	acaatttcacacaggaaacagctATGAAAAAGAAATCACTGACTGAACT
oPEB1029	CTCGGTTGGCCTTGTCCTTGACCTTCACCCGACATTTGATCCAACAGCTGCA
oPEB1030	CCCGGTGAAGGTCAAGGACAAGGCCAAATGTCATTAAAAGGGAAACTCCAAC
oPEB1031	aaaacgacggccgaattcttagTTATTAAGAGGAATATTTCCTCTTTAGCCGGGCAATTC
oPEB1032	gataacaatttcacacaggaaacagctATGTCATTAAAAGGGAAACTCCAAC
oPEB1033	AGGCTTGGCCTTGTCCTTGACCTTCACCAGAGGAATATTTCCTCTTTAGCCGGGCAATTC
oPEB1053	cggataacaatttcacacaggaaacagctATGAAAGGAGAGAGCATCGTTACCGTAA
oPEB1054	GAGCTCGGTTGGCCTTGTCCTTGACCTTCACCAGGGACAATATGCTGCAGCACATTC
oPEB1055	CGAGCTCGGTTGGCCTTGTCCTTGACCTTCACCTTTTTGCACATATTGAAAAGCGGAA
oPEB1056	ttgtaaaacgacggccgaattcttagTTATGGCGCATGTGATTCTGAAAGGAT
oPEB1057	GGATCCCGGTGAAGGTCAAGGACAAGGCCAAATGAAAGAACACAGTGAAGCCTATG

Table 4.3 Oligonucleotides used in this study.

Supplemental text

Supplemental Methods

Strain construction

Strains were constructed using CRISPR/Cas9 genome editing (52, 66) or double crossover recombination(26).

PEB320 (Δ*mrfAB*): PY79 was transformed with pPB88 to delete *mrfAB* using CRISPR/Cas9 genome editing. Deletion of *mrfAB* was verified by PCR genotyping using oPEB452/462.

PEB337 (Δ*mrfA*, Δ*uvrAB*): PEB316 was transformed with pPB84 to delete *uvrAB* using CRISPR/Cas9 genome editing. Deletion of *uvrAB* was verified by PCR genotyping using oPEB424/432.

PEB339 (Δ*mrfB*, Δ*uvrAB*): PEB316 was transformed with pPB84 to delete *uvrAB* using CRISPR/Cas9 genome editing. Deletion of *uvrAB* was verified by PCR genotyping using oPEB424/432.

PEB369 (Δ*mrfA*, *amyE::*P_{xyl}*-mrfA*): PEB316 was transformed with pPB109. Replacement of *amyE* with P_{xyl}*-mrfA* by double crossover recombination was verified by testing for an inability to utilize starch and for the absence of a spectinomycin resistance marker found on the plasmid,

but not on the integrated construct. Genomic DNA from the resulting strain, PEB347, was used to transform PEB316, and replacement of *amyE* was verified by an inability to utilize starch.

PEB371 (Δ*mrfB*, *amyE::*P_{xyl}*-mrfB*): PY79 was transformed with pPB110. Replacement of *amyE* with P_{xyl}*-mrfB* by double crossover recombination was verified by testing for an inability to utilize starch and for the absence of a spectinomycin resistance marker found on the plasmid, but not on the integrated construct. Genomic DNA from the resulting strain, PEB345, was used to transform PEB318, and replacement of *amyE* was verified by an inability to utilize starch. Retention of the *mrfB* deletion allele was verified by PCR genotyping using oPEB461/462.

PEB505 (Δ*mrfA*, *amyE::*P_{xyl}*-mrfA-K82A*): PEB316 was transformed with pPB159 digested with the restriction enzymes ScaI and BsaI. Replacement of *amyE* with P_{xyl}*-mrfA-K82A* by double crossover recombination was verified by testing for an inability to utilize starch and for the absence of a spectinomycin resistance marker found on the plasmid, but not on the integrated construct.

PEB507 (Δ*mrfA*, *amyE::Pxyl-mrfA-DE185-186AA*): PEB316 was transformed with pPB160 digested with the restriction enzymes ScaI and BsaI. Replacement of *amyE* with P_{xyl}*-mrfA-DE185-186AA* by double crossover recombination was verified by testing for an inability to utilize starch and for the absence of a spectinomycin resistance marker found on the plasmid, but not on the integrated construct.

PEB509 (Δ*mrfA*, *amyE::Pxyl-mrfA-T134V*): PEB316 was transformed with pPB161 digested with the restriction enzymes ScaI and BsaI. Replacement of *amyE* with P_{xyl}*-mrfA-T134V* by double crossover recombination was verified by testing for an inability to utilize starch and for the absence of a spectinomycin resistance marker found on the plasmid, but not on the integrated construct.

PEB511 (Δ*mrfA*, *amyE::Pxyl-mrfA-S222A*): PEB316 was transformed with pPB162 digested with the restriction enzymes ScaI and BsaI. Replacement of *amyE* with P_{xyl}*-mrfA-S222A* by double crossover recombination was verified by testing for an inability to utilize starch and for the absence of a spectinomycin resistance marker found on the plasmid, but not on the integrated construct.

PEB513 (Δ*mrfA*, *amyE::Pxyl-mrfA-ΔC*): PEB316 was transformed with pPB163 digested with the restriction enzymes ScaI and BsaI. Replacement of *amyE* with P_{xyl}-*mrfAΔC* by double crossover recombination was verified by testing for an inability to utilize starch and for the absence of a spectinomycin resistance marker found on the plasmid, but not on the integrated construct.

PEB515 (Δ*mrfA*, *amyE::Pxyl-mrfA-C718A & C720A*): PEB316 was transformed with pPB164 digested with the restriction enzymes ScaI and BsaI. Replacement of *amyE* with P_{xyl}-*mrfA-C718A & C720A* by double crossover recombination was verified by testing for an inability to utilize starch and for the absence of a spectinomycin resistance marker found on the plasmid, but not on the integrated construct.

PEB517 (Δ*mrfA*, *amyE::Pxyl-mrfA-C718A, C720A, C724C, & C727A*):): PEB316 was transformed with pPB165 digested with the restriction enzymes ScaI and BsaI. Replacement of *amyE* with P_{xyl}- *mrfA-C718A, C720A, C724C, & C727A* by double crossover recombination was verified by testing for an inability to utilize starch and for the absence of a spectinomycin resistance marker found on the plasmid, but not on the integrated construct.

PEB519 (Δ*mrfB*, *amyE::Pxyl-mrfB-D107A*): PEB318 was transformed with pPB166 digested with the restriction enzymes ScaI and KpnI. Replacement of *amyE* with P_{xyl}-*mrfB-D107A* by double crossover recombination was verified by testing for an inability to utilize starch and for the absence of a spectinomycin resistance marker found on the plasmid, but not on the integrated construct.

PEB521 (Δ*mrfB*, *amyE::Pxyl-mrfB-E109A*): PEB318 was transformed with pPB167 digested with the restriction enzymes ScaI and KpnI. Replacement of *amyE* with P_{xyl}-*mrfB-E109A* by double crossover recombination was verified by testing for an inability to utilize starch and for the absence of a spectinomycin resistance marker found on the plasmid, but not on the integrated construct.

PEB523 (Δ*mrfB*, *amyE::Pxyl-mrfB-D172A*): PEB318 was transformed with pPB168 digested with the restriction enzymes ScaI and KpnI. Replacement of *amyE* with P_{xyl}-*mrfB-D172A* by double crossover recombination was verified by testing for an inability to utilize starch and for

the absence of a spectinomycin resistance marker found on the plasmid, but not on the integrated construct.

PEB525 (Δ*mrfB*, *amyE::Pxyl-mrfB-D262A*): PEB318 was transformed with pPB169 digested with the restriction enzymes ScaI and KpnI. Replacement of *amyE* with P_{xyl}-*mrfB-D262A* by double crossover recombination was verified by testing for an inability to utilize starch and for the absence of a spectinomycin resistance marker found on the plasmid, but not on the integrated construct.

PEB527 (Δ*mrfB*, *amyE::Pxyl-mrfB-H258A*): PEB318 was transformed with pPB170 digested with the restriction enzymes ScaI and KpnI. Replacement of *amyE* with P_{xyl}-*mrfB-H258A* by double crossover recombination was verified by testing for an inability to utilize starch and for the absence of a spectinomycin resistance marker found on the plasmid, but not on the integrated construct.

PEB529 (Δ*mrfB*, *amyE::Pxyl-mrfB*-Δ*C*): PEB318 was transformed with pPB171 digested with the restriction enzymes ScaI and KpnI. Replacement of *amyE* with P_{xyl}- *mrfB*-Δ*C* by double crossover recombination was verified by testing for an inability to utilize starch and for the absence of a spectinomycin resistance marker found on the plasmid, but not on the integrated construct.

PEB812 (Δ*mrfAB*, Δ*uvrAB*): PEB320 was transformed with pPB84 to delete *uvrAB* using CRISPR/Cas9 genome editing. Deletion of *uvrAB* was verified by PCR genotyping using oPEB424/432.

PEB822 (Δ*uvrABC*): PEB309 was transformed with pPB85 to delete *uvrC* using CRISPR/Cas9 genome editing. Deletion of *uvrC* was confirmed by PCR genotyping using oPEB443/444.

PEB824 (Δ*mrfAB*, Δ*uvrC*): PEB320 was transformed with pPB85 to delete *uvrC* using CRISPR/Cas9 genome editing. Deletion of *uvrC* was confirmed by PCR genotyping using oPEB443/444.

PEB826 (Δ*mrfAB*, Δ*uvrABC*): PEB812 was transformed with pPB85 to delete *uvrC* using CRISPR/Cas9 genome editing. Deletion of *uvrC* was confirmed by PCR genotyping using oPEB443/444.

PEB828 (*recA::recA-gfp*): PY79 was transformed with chromosomal DNA from LAS40.

PEB830 (Δ*mrfAB*, *recA::recA-gfp*): PEB320 was transformed with chromosomal DNA from LAS40. Retention of the Δ*mrfAB* allele was verified by PCR genotyping using oPEB452/462.

PEB832 (Δ*uvrABC*, *recA::recA-gfp*): PEB822 was transformed with chromosomal DNA from LAS40. Retention of the Δ*uvrAB* allele was verified by PCR genotyping using oPEB424/432, and retention of the Δ*uvrC* allele was verified by PCR genotyping using oPEB443/444.

PEB834 (Δ*mrfAB*, Δ*uvrABC*, *recA::recA-gfp*): PEB826 was transformed with chromosomal DNA from LAS40. Retention of the Δ*mrfAB* allele was verified by PCR genotyping using oPEB452/462. Retention of the Δ*uvrAB* allele was verified by PCR genotyping using oPEB424/432, and retention of the Δ*uvrC* allele was verified by PCR genotyping using oPEB443/444.

PEB866 (Δ*mrfA*, *amyE::P_{xyl}-Bc-mrfA*): The *mrfA* homolog from *Bacillus cereus* (CUB17870.1) was codon optimized and used to generate a gBlock (IDT). The gBlock oPEB1044 was used in an overlap PCR reaction with two other PCR amplicons (*amyE* upstream and P_{xyl} generated using oPEB370/383 and a chloramphenicol resistance cassette and *amyE* downstream generated with oPEB557/377) using oPEB370/377. The resulting PCR product containing *amyE-up-P_{xyl}-Bc-mrfA-camR-amyE-down* was gel extracted and used to transform PEB316. Replacement of *amyE* with *P_{xyl}-Bc-mrfA-camR* was verified by testing for an inability to utilize starch.

PEB870 (Δ*mrfB*, *amyE::P_{xyl}-Bc-mrfB*): The *mrfB* homolog from *Bacillus cereus* (CUB17873.1) was codon optimized and used to generate a gBlock (IDT). The gBlock oPEB1046 was used in an overlap PCR reaction with two other PCR amplicons (*amyE* upstream and P_{xyl} generated using oPEB370/383 and a chloramphenicol resistance cassette and *amyE* downstream generated with oPEB557/377) using oPEB370/377. The resulting PCR product containing *amyE-up-P_{xyl}-Bc-mrfB-camR-amyE-down* was gel extracted and used to transform PEB318. Replacement of *amyE* with *P_{xyl}-Bc-mrfB-camR* was verified by testing for an inability to utilize starch.

PEB872 (Δ*mrfB*, *amyE::P_{xyl}-Pa-mrfB*): The *mrfB* homolog from *Pseudomonas aeruginosa* (CRP88025.1) was codon optimized and used to generate a gBlock (IDT). The gBlock oPEB1045 was used in an overlap PCR reaction with two other PCR amplicons (*amyE* upstream

and P_{xyl} generated using oPEB370/383 and a chloramphenicol resistance cassette and *amyE* downstream generated with oPEB557/377) using oPEB370/377. The resulting PCR product containing *amyE-up-*P_{xyl}*-Pa-mrfB-camR-amyE-down* was gel extracted and used to transform PEB318. Replacement of *amyE* with P_{xyl}*-Pa-mrfB-camR* was verified by testing for an inability to utilize starch.

PEB898 (Δ*mrfA*, *amyE::*P_{xyl}*-Sp-mrfA*): The *mrfA* homolog from *Streptococcus pneumoniae* (COD01438.1) was codon optimized and used to generate a gBlock (IDT). The gBlock oPEB1047 was used in an overlap PCR reaction with two other PCR amplicons (*amyE* upstream and P_{xyl} generated using oPEB370/383 and a chloramphenicol resistance cassette and *amyE* downstream generated with oPEB557/377) using oPEB370/377. The resulting PCR product containing *amyE-up-*P_{xyl}*-Sp-mrfA-camR-amyE-down* was gel extracted and used to transform PEB318. Replacement of *amyE* with P_{xyl}*-Sp-mrfA-camR* was verified by testing for an inability to utilize starch.

PEB900 (Δ*mrfB*, *amyE::*P_{xyl}*-Sp-mrfB*): The *mrfB* homolog from *Streptococcus pneumoniae* (COD01468.1) was codon optimized and used to generate a gBlock (IDT). The gBlock oPEB1048 was used in an overlap PCR reaction with two other PCR amplicons (*amyE* upstream and P_{xyl} generated using oPEB370/383 and a chloramphenicol resistance cassette and *amyE* downstream generated with oPEB557/377) using oPEB370/377. The resulting PCR product containing *amyE-up-*P_{xyl}*-Sp-mrfB-camR-amyE-down* was gel extracted and used to transform PEB318. Replacement of *amyE* with P_{xyl}*-Sp-mrfB-camR* was verified by testing for an inability to utilize starch.

PEB902 (Δ*mrfA*, *amyE::*P_{xyl}*-Pa-mrfA*): The *mrfA* homolog from *Pseudomonas aeruginosa* (CRP88044.1) was codon optimized and used to generate a gBlock (IDT). The gBlock oPEB1043 was used in an overlap PCR reaction with two other PCR amplicons (*amyE* upstream and P_{xyl} generated using oPEB370/383 and a chloramphenicol resistance cassette and *amyE* downstream generated with oPEB557/377) using oPEB370/377. The resulting PCR product containing *amyE-up-*P_{xyl}*-Pa-mrfA-camR-amyE-down* was gel extracted and used to transform PEB318. Replacement of *amyE* with P_{xyl}*-Pa-mrfA-camR* was verified by testing for an inability to utilize starch.

Plasmid construction

Plasmids were constructed via Gibson assembly as described (26, 67). Plasmids for the bacterial two-hybrid assays were constructed using 0.2% glucose in the media for selection of clones and cultures grown for plasmid isolation.

pPB88: Plasmid pPB88 was constructed using four PCR products: 1) the vector pPB41 was amplified using oPEB217/218; 2) Cas9/CRISPR::*mrfA* was amplified using pPB75 as a template with oPEB232/234; 3) the sequence upstream of *mrfA* for the editing template was amplified using oPEB448/464; and 4) the sequence downstream of *mrfB* for the editing template was amplified using oPEB465/460. Clones were verified via Sanger sequencing using oPEB227, oPEB253, and oPEB454.

pPB97: Plasmid pPB97 was constructed using two PCR products: 1) the vector pET28b-10xHis-Smt3 was amplified using oPEB56/57; and 2) the MrfB ORF was amplified using oPEB545/546. Clones were verified via Sanger sequencing using oPEB58, oPEB527, and oPEB547.

pPB109: Plasmid oPEB109 was constructed using four PCR products: 1) the vector pPB47 was amplified using oPEB116/117; 2) the upstream portion of *amyE* and the P_{xyl} promoter were amplified using oPEB370/383; 3) the chloramphenicol resistance cassette and the downstream portion of *amyE* was amplified using oPEB557/377; and 4) the *mrfA* ORF was amplified using oPEB562/563. Clones were verified via Sanger sequencing using oPEB345, oPEB348, oPEB543, and oPEB544.

pPB110: Plasmid oPEB110 was constructed using four PCR products: 1) the vector pPB47 was amplified using oPEB116/117; 2) the upstream portion of *amyE* and the P_{xyl} promoter were amplified using oPEB370/383; 3) the chloramphenicol resistance cassette and the downstream portion of *amyE* was amplified using oPEB557/377; and 4) the *mrfB* ORF was amplified using oPEB564/565. Clones were verified via Sanger sequencing using oPEB345, oPEB348, and oPEB547.

pPB159: Plasmid oPEB159 was constructed using five PCR products: 1) the vector pPB47 was amplified using oPEB116/117; 2) the upstream portion of *amyE* and the P_{xyl} promoter were

amplified using oPEB370/383; 3) the chloramphenicol resistance cassette and the downstream portion of *amyE* was amplified using oPEB557/377; 4) the 5′ portion of the *mrfA-K82A* ORF was amplified using oPEB562/721; and 5) the 3′ portion of the *mrfA-K82A* ORF was amplified using oPEB720/563. Clones were verified via Sanger sequencing using oPEB345, oPEB348, oPEB543, and oPEB544.

pPB160: Plasmid oPEB160 was constructed using five PCR products: 1) the vector pPB47 was amplified using oPEB116/117; 2) the upstream portion of *amyE* and the P_{xyl} promoter were amplified using oPEB370/383; 3) the chloramphenicol resistance cassette and the downstream portion of *amyE* was amplified using oPEB557/377; 4) the 5′ portion of the *mrfA-DE185-186AA* ORF was amplified using oPEB562/723; and 5) the 3′ portion of the *mrfAK-DE185-186AA* ORF was amplified using oPEB722/563. Clones were verified via Sanger sequencing using oPEB345, oPEB348, oPEB543, and oPEB544.

pPB161: Plasmid oPEB161 was constructed using five PCR products: 1) the vector pPB47 was amplified using oPEB116/117; 2) the upstream portion of *amyE* and the P_{xyl} promoter were amplified using oPEB370/383; 3) the chloramphenicol resistance cassette and the downstream portion of *amyE* was amplified using oPEB557/377; 4) the 5′ portion of the *mrfA-T134V* ORF was amplified using oPEB562/725; and 5) the 3′ portion of the *mrfA-T134V* ORF was amplified using oPEB724/563. Clones were verified via Sanger sequencing using oPEB345, oPEB348, oPEB543, and oPEB544.

pPB162: Plasmid oPEB162 was constructed using five PCR products: 1) the vector pPB47 was amplified using oPEB116/117; 2) the upstream portion of *amyE* and the P_{xyl} promoter were amplified using oPEB370/383; 3) the chloramphenicol resistance cassette and the downstream portion of *amyE* was amplified using oPEB557/377; 4) the 5′ portion of the *mrfA-S222A* ORF was amplified using oPEB562/727; and 5) the 3′ portion of the *mrfA-S222A* ORF was amplified using oPEB726/563. Clones were verified via Sanger sequencing using oPEB345, oPEB348, oPEB543, and oPEB544.

pPB163: Plasmid oPEB163 was constructed using four PCR products: 1) the vector pPB47 was amplified using oPEB116/117; 2) the upstream portion of *amyE* and the P_{xyl} promoter were amplified using oPEB370/383; 3) the chloramphenicol resistance cassette and the downstream

portion of *amyE* was amplified using oPEB557/377; and 4) the *mrfA*ΔC ORF was amplified using oPEB562/728. Clones were verified via Sanger sequencing using oPEB345, oPEB348, oPEB543, and oPEB544.

pPB164: Plasmid oPEB164 was constructed using four PCR products: 1) the vector pPB47 was amplified using oPEB116/117; 2) the upstream portion of *amyE* and the P_{xyl} promoter were amplified using oPEB370/383; 3) the chloramphenicol resistance cassette and the downstream portion of *amyE* was amplified using oPEB557/377; and 4) the *mrfA-C718A & C720A* ORF was amplified using oPEB562/729. Clones were verified via Sanger sequencing using oPEB345, oPEB348, oPEB543, and oPEB544.

pPB165: Plasmid oPEB165 was constructed using four PCR products: 1) the vector pPB47 was amplified using oPEB116/117; 2) the upstream portion of *amyE* and the P_{xyl} promoter were amplified using oPEB370/383; 3) the chloramphenicol resistance cassette and the downstream portion of *amyE* was amplified using oPEB557/377; and 4) the *mrfA-C718A, C720A, C724A, & C727A* ORF was amplified using oPEB562/730. Clones were verified via Sanger sequencing using oPEB345, oPEB348, oPEB543, and oPEB544.

pPB166: Plasmid oPEB166 was constructed using five PCR products: 1) the vector pPB47 was amplified using oPEB116/117; 2) the upstream portion of *amyE* and the P_{xyl} promoter were amplified using oPEB370/383; 3) the chloramphenicol resistance cassette and the downstream portion of *amyE* was amplified using oPEB557/377; 4) the 5′ portion of the *mrfB-D107A* ORF was amplified using oPEB564/732; and 5) the 3′ portion of the *mrfB-D107A* ORF was amplified using oPEB731/565. Clones were verified via Sanger sequencing using oPEB345, oPEB348, and oPEB547.

pPB167: Plasmid oPEB167 was constructed using five PCR products: 1) the vector pPB47 was amplified using oPEB116/117; 2) the upstream portion of *amyE* and the P_{xyl} promoter were amplified using oPEB370/383; 3) the chloramphenicol resistance cassette and the downstream portion of *amyE* was amplified using oPEB557/377; 4) the 5′ portion of the *mrfB-E109A* ORF was amplified using oPEB564/734; and 5) the 3′ portion of the *mrfB-E109A* ORF was amplified using oPEB733/565. Clones were verified via Sanger sequencing using oPEB345, oPEB348, and oPEB547.

pPB168: Plasmid oPEB168 was constructed using five PCR products: 1) the vector pPB47 was amplified using oPEB116/117; 2) the upstream portion of *amyE* and the P_{xyl} promoter were amplified using oPEB370/383; 3) the chloramphenicol resistance cassette and the downstream portion of *amyE* was amplified using oPEB557/377; 4) the 5′ portion of the *mrfB-D172A* ORF was amplified using oPEB564/736; and 5) the 3′ portion of the *mrfB-D172A* ORF was amplified using oPEB735/565. Clones were verified via Sanger sequencing using oPEB345, oPEB348, and oPEB547.

pPB169: Plasmid oPEB169 was constructed using five PCR products: 1) the vector pPB47 was amplified using oPEB116/117; 2) the upstream portion of *amyE* and the P_{xyl} promoter were amplified using oPEB370/383; 3) the chloramphenicol resistance cassette and the downstream portion of *amyE* was amplified using oPEB557/377; 4) the 5′ portion of the *mrfB-D262A* ORF was amplified using oPEB564/766; and 5) the 3′ portion of the *mrfB-D262A* ORF was amplified using oPEB765/565. Clones were verified via Sanger sequencing using oPEB345, oPEB348, and oPEB547.

pPB170: Plasmid oPEB170 was constructed using five PCR products: 1) the vector pPB47 was amplified using oPEB116/117; 2) the upstream portion of *amyE* and the P_{xyl} promoter were amplified using oPEB370/383; 3) the chloramphenicol resistance cassette and the downstream portion of *amyE* was amplified using oPEB557/377; 4) the 5′ portion of the *mrfB-H258A* ORF was amplified using oPEB564/768; and 5) the 3′ portion of the *mrfB-H258A* ORF was amplified using oPEB767/565. Clones were verified via Sanger sequencing using oPEB345, oPEB348, and oPEB547.

pPB171: Plasmid oPEB171 was constructed using four PCR products: 1) the vector pPB47 was amplified using oPEB116/117; 2) the upstream portion of *amyE* and the P_{xyl} promoter were amplified using oPEB370/383; 3) the chloramphenicol resistance cassette and the downstream portion of *amyE* was amplified using oPEB557/377; and 4) the *mrfB*ΔC ORF was amplified using oPEB564/737. Clones were verified via Sanger sequencing using oPEB345, oPEB348, and oPEB547.

pPB263: Plasmid pPB263 was constructed using two PCR products: 1) the vector pUT18C was amplified using oPEB1017/1018; and 2) the *mrfA* ORF was amplified using oPEB1026/1027.

Clones were verified via Sanger sequencing using oPEB543, oPEB544, oPEB1024, and oPEB1025.

pPB264: Plasmid pPB264 was constructed using two PCR products: 1) the vector pUT18 was amplified using oPEB1016/1012; and 2) the *mrfA* ORF was amplified using oPEB1028/1029. Clones were verified by Sanger sequencing using oPEB543, oPEB544, oPEB1019, and oPEB1023.

pPB265: Plasmid pPB265 was constructed using two PCR products: 1) the vector pKT25 was amplified using oPEB1014/1015; and 2) the *mrfB* ORF was amplified using oPEB1030/1031. Clones were verified by Sanger sequencing using oPEB547, oPEB1021, and oPEB1022.

pPB266: Plasmid pPB266 was constructed using two PCR products: 1) the vector pKNT25 was amplified using oPEB1012/1013; and 2) the *mrfB* ORF was amplified using oPEB1032/1033. Clones were verified by Sanger sequencing using oPEB547, oPEB1019, and oPEB1020.

pPB273: Plasmid pPB273 was constructed using two PCR products: 1) the vector pKT25 was amplified using oPEB1014/1015; and 2) the *mrfB*ΔC ORF was amplified using oPEB1030/1056. Clones were verified by Sanger sequencing using oPEB1021 and oPEB1022.

pPB274: Plasmid pPB274 was constructed using two PCR products: 1) the vector pKT25 was amplified using oPEB1014/1015; and 2) the *mrfB*ΔN ORF was amplified using oPEB1057/1031. Clones were verified by Sanger sequencing using oPEB1021 and oPEB1022.

pPB283: Plasmid pPB283 was constructed using two PCR products: 1) the vector pUT18 was amplified using oPEB1016/1012; and 2) the *mrfA*ΔN ORF was amplified using oPEB1053/1029. Clones were verified by Sanger sequencing using oPEB543, oPEB544, oPEB1019, and oPEB1023.

pPB284: Plasmid pPB284 was constructed using two PCR products: 1) the vector pUT18 was amplified using oPEB1016/1012; and 2) the *mrfA*ΔC ORF was amplified using oPEB1028/1054. Clones were verified by Sanger sequencing using oPEB543, oPEB544, oPEB1019, and oPEB1023.

pPB285: Plasmid pPB285 was constructed using two PCR products: 1) the vector pUT18 was amplified using oPEB1016/1012; and 2) the *mrfA-N* ORF was amplified using oPEB1028/1055. Clones were verified by Sanger sequencing using oPEB1019 and oPEB1023.

gBlocks used in this study

oPEB1043:

caaaggggaaatgggatcctaaggaggtatacatATGGCGTACGAACTGGCGAAACGGACTGCGGACGCTGAACAG
AAGCTCGCTACTCGCGACGGACTTCCTGCCCGGGACGGGGCCCTGTTATCTGCTCGCCTTCAGAGAAGATATCAAGA
CCGTATTACGGGAAGCTTTGCGATCCCTGGACGTGAGGGCCGTTACGCTCCAATACCTGACTCTGTTCCACCTGCCC
TGGCAGCAGCCTTAAAGGCGCGTGGTATTGAACAGCTTTACAGCCATCAAGCTGAGGCCTGGGAGGCCTCTCAACGC
GGAGAGCACGTCGCGATCGTAACGCCGACAGCATCCGGCAAGAGCCTGTGCTATACCTTGCCTGTTGTTTCTGCAGC
TATGCAGGATAAGGCGAAGGCGCTCTACCTCTTCCCTACTAAGGCACTGGCTCAAGACCAGGTCGCCGAGCTCCTGG
AGTTGAACAGAGCAGGAGATCTGGGTGTCAAAGCATTCACTTTCGATGGCGATACGCCGGGGGATGCACGTCAAGCT
ATTCGCTTACATGGCGATATTGTCGTGAGTAACCCAGATATGTTACATCAAGCGATACTCCCACATCATACCAAATG
GGCACAGTTTTTTGAGAATTTGCGTTATATAGTGATCGATGAAGTTCATACGTACCGCGGAGTATTCGGGTCCCATG
TGACTAACGTATTGAGACGGCTCAAAAGAATCTGCGCGTTTTACGGCGTACAACCTCAGTTCATTCTCTGTTCTGCA
ACCATTGGCAATCCTCAGGCGCATGCAGAAGCACTCATCGAGGCTCCTGTAACTGCTGTTACTGAATCTGGCGCACC
TACAGGGCCGAAGCAAGTACTTTTGTGGAACCCACCGGTGATAAACCCGGATTTAGGGCTCCGTGCTAGCGCGAGAA
GTCAAAGCAATCGCATAGCCAGAATAGCTATCAAGTCTGGCCTTAAAACTTTAGTATTCGCCCAAACTCGCCTCATG
GTAGAAGTTTTGACGAAGTACTTAAAAGACATTTTCGATCACGACCCGCGTAAACCGCCGCGTATCCGCGCGTACAG
AGGAGGTTATTTACCGACTGAACGGCGGGAAACTGAAAGAGCCATGCGGGCCGGTAATATCGACGGGATAGTATCTA
CTAGCGCTTTGGAACTGGGTGTAGATATCGGAAGCTTGGACGTCGTCATTCTGAATGGCTATCCGGGAAGCGTAGCG
GCCACATGGCAGCGCTTCGGAAGAGCGGGACGTCGCCAACAACCTGCGTTGGGAGTCATGGTCGCCTCAAGCCAACC
ATTAGACCAATACGTTGTGCGGCATCCGGACTTCTTCGCCGAGGCCTCTCCTGAGCACGCCCGGATTGCTCCGGATC
AGCCACTGATTCTCTTCGATCATATAAGATGTGCCGCTTTTGAATTACCGTTTCGGGTGGGCGACGGTTTCGGGCCT
ATTGATCCTGAGGTCTTTCTCGAAGCATTGGCTGAGACAGAGGTGATTCATCGGGAAGGTGAGCGTTGGGAATGGAT
AGCCGACTCATATCCGGCGAATGCTGTGTCCTTGCGGGCTGTGGCAGATGGCAATTTCGTCGTTGTTGACCGGTCTG
ACGGTAGACAACAGATAATCGCGGAGGTTGATTATAGTGCTGCAGCTTTGACACTGTACGAAGGCGCGATCCACATG
GTGCAATCAACTCCATACCAAGTAGAAACTCTTGATTGGGAGGGACGTAAGGCTTACGTGACACGTACTCACGTCGA
CTACTATACGGACTCAATCGACTTTACAAAACTGAAGGTCCTTGATAGATTTGATGGAGGAGTCGCAGGACGTGGCG
ACTCCCATCATGGGGAGGTCCATGTAGTACGTCGCGTCGCTGGTTACAAAAAGATTCGCTATTATACCCATGAGAAT
ATCGGATACGGACCTGTTAACTTGCCGGACCAAGAACTTCACACCACCGCTGTCTGGTGGCAATTGCCACAGGCATT
ACTGCTGAGAGCCTTTGCCAGCCGGCAAGATCCTTTAGATGGTTTCTTGGGAGCTGCATATGCGTTGCACATCGTGG
CAACTGTCGCAGTAATGGCCGATGCAAGAGACTTGCAAAAGTCTGTAGGAAACGGAGATGGCTCATGGTTCGCAATT
GCAGACCAGTCAGGACGCGGTCAACTCCGGGGGAGTGAAGGTGACCCGGGCGGTGTTGAACTCTTGCAGGAATTTGT
TCCGACGGTGTATCTCTATGACAACTTTCCGGGAGGCGTGGGACTGAGCGAACCTCTCTGGCAACGGCAGGCAGAGC
TTGTGCAAAGAGCGAGAGAGCTCGTCCAAAGATGTGACTGCAAGGCCGGTTGCCCTGCTTGCGTAGGGCCGGTGTTG
GCAGCGCAAGAGGAAGACGAAACATCCCCTCGGGCGCTGGCACTCAGAGTCCTTGACTTGTTTGACGCGGAGGCCTG
TAGACATGTACCGGACGTAGTGGTGACTACACGCGACCCTATGGAATTACTTGCCCCGTAAtaaCGGTTTCCATATG
GGGATTGGTGGCGACGACT

oPEB1044:

caaaggggaaatgggatcctaaggaggtatacatATGAAAAAAAAAAGTTTAACCGAGTTGATAAGTGAACTCAAA
GGTAACGAAAACATAGTTAACTGGCACGAAATAGAACCGAGAGAAGCTAGAACGCGGCCTATGCCTGAAAGTATCGA
TGAGAGAATAAAGGCCGCCTTGAGCAAAAGAGGTATCGACGAATTATATACGCACCAATTCTCAGCTTTCCAATACG
TGCAAAAAGGGGAAAGTATTGTTACTGTCACCCCGACTGCTTCAGGAAAGACACTCAGTTACAATTTGCCAGTTCTG
CAAAGTATAGCCCAAGATGAGACGAATCGCGCACTTTACCTTTTCCCGACTAAGGCCCTGGCTCAAGATCAAAAATC

TGAGCTGAACGAAATAATAGACGAAATGGGAATCGATATTAAAAGCTTTACGTACGATGGTGATACCAGCCCTGCTA
TACGGCAGAAAGTACGGAAAGCCGGTCATATCGTCATTACCAATCCTGACATGCTTCACAGTGCCATATTGCCGCAC
CATACAAAGTGGGTCAGTTTATTTGAAAACCTGAAGTACATCGTAATTGATGAGCTCCATACATATCGGGGCGTCTT
CGGCTCCCACGTAGCAAATGTTATACGTCGCCTGAAAAGAATATGTCGTTTTTACGGATCAGACCCAGTATTCATCT
GTACTTCAGCCACTATTGCTAATCCTAAGGAGTTGGGCGAGCAGTTGACTGGCAAGCCGATGCGTCTGGTCGATGAC
AATGGTGCGCCTTCTGGTAGAAAGCATTTTGTATTTTACAATCCTCCGATAGTTAACAAGCCGCTCAATATTCGTAA
GAGCGCGACAGCGGAGGTAAATGAACTGGCCAAGGAATTTCTTAAGAACAAGGTACAGACTATCGTCTTTGCACGGT
CACGCGTCCGTGTTGAAATTATATTGAGCCACATCCAGGAACTTGTAAAAAAGGAGATTGGTACTAAGAGCATCCGC
GGTTACCGGGGCGGGTACCTCCCGAAGGAAAGACGCGAGATAGAGCGCGGACTCCGGGAAGGTGAAATCCTGGGGGT
GGTAAGTACGAATGCTCTGGAACTCGGAGTGGACATCGGACAGTTACAGGTGTGTGTGATGACAGGCTATCCGGGAA
GTGTCGCGTCCGCATGGCAGCAAGCGGGCCGGGCCGGACGGAGACATGGCGAAAGCTTAATAATCATGGTAGCCAAC
TCCACGCCGATCGACCAGTATATAGTACGTCACCCGGAATACTTTTTTAACCGCTCTCCTGAAAGTGCTCGCATTAA
CCCGGAGAATCTTATTATCTTGGTCGATCACCTTAAGTGCGCGGCCTATGAATTACCATTCAGAGCTGATGAGGAGT
TCGGCCCTATGGACGTGTCTGATATTCTTGAATATTTACAAGAAGAAGCCGTCTTACATCGGAATGGCGAGCGTTAC
CATTGGGCATCCGAGAGCTTCCCTGCTAGCAATATCAGCCTCCGTTCTGCGTCACAGGAAAACGTTGTGATAGTTGA
TCAGTCTGACATAGCCAACGTTAGAATTATAGGAGAAATGGACCGTTTCTCCGCCATGACCCTTTTACATGATGAGG
CAATATACCTGCATGAAGGAGTGCAATATCAAGTTGAGAAACTCGATTGGGACCACAAAAAAGCGTACGTCCGGAAA
GTGGACGTGGAGTATTATACAGATGCCAACTTAGCCGTCCAGCTGAAGGTTTTAGAAATAGACAAGACTAAAGAAAA
GTCTAGAACGTCCCTCCATTATGGTGATGTCACAGTCAACGCGCTCCCAACGATTTTCAAAAAAATTAAAATGACAA
CCTTTGAGAACATTGGGAGCGGGCCTATCCACTTGCCGGAGGAAGAGTTGCATACCTCTGCCGCTTGGCTCGAAATT
AAGACGGCCGATGAAGATATAGGAGAAAAGACGCTCGAACAGCTCTTACTTGGTATATCAAATGTTTTACAGCACAT
AGTGCCGGTCTATATCATGTGCGACCGGAACGATGTTCATGTAATATCCCAGATCAAAGCTGCCCATACCGGACTTC
CGACAATTTTCTTGTATGATCACTATCCTGGGGGCATTGGCCTTGCTGAAGAGGTTTTTAAACGCTTCAGCGATATA
AACGAAGCAGCCAAACAGCTGATAAAGCAATGCCCATGCCACGACGGTTGTCCTTCATGTATTGGAACTGAAATCGA
GGGTATAAAAGCTAAAGAGCGTATACTGCAGTTGTTAGTTCAAATGGCGTAAtaaCGGTTTCCATATGGGGATTGGT
GGCGACGACT

oPEB1045:

caaaggggaaatgggatcctaaggaggtatacatATGTCATTAAGTTTGGATAAGCTTCGCCTGCTTCGGCGGCAA
GCCGGAGACCCAAAAGCAAGCACTCCTGCAGTCCCAGATGTACCGCCGGCCCCACCTGCCCCAGTTGCTGCTAACGA
CGCCCGCCAGCCACCTGCAGAGCGTAGTGTATTCGCCTGGGTGGAGCAAGAGATCCGCCACAAGCCAACAGGCGCGG
CTGCGCCAACCCCTGCTTCAGCACCTCTGCGGCGGCCAGAGGTTGGGTCCCTGCATAGACTCTTGGGGCTGCGCACC
AGAAGCGGGGCCACTCCTGCTCGCGCCAGTGCACAGGATCGCCAGTTGCCTGGAGAGGAAATAGCACCGGGCCTGTT
CCTCATTGAATCCCTTCAGCCGCAGGCTATACCGGCTCAACCTCTTAGCTTAGATTTCGCTCGGCGGGATGGCGAAC
ACGTTGCCGCTAGAGATTTGTTGTTTTTTGACACAGAAACCACGGGTCTTGCTGGCGGAACTGGCACGCGCGCTTTT
ATGATCGGAGCAGCCGACTGGCATGTATGCCCTCAACGTGGGGAGGGCCTGAGAATCAGACAACTCCTTATGGCTAC
GATGGCTGCTGAAGACGCTATGTTAGCAACGTTTGCAGGTTGGTTGCAGCCAAGTACGGTATTTTGCAGTTACAATG
GCCGTAGCTATGACGCCCCTTTATTGAAAGCTCGGTATCGTTTGGCAAGACAGCGCGACCCAATCAGTGCGTTAGAT
CACGTGGACCTGCTCTACCCAACACGTAGACGTTATCGCGGAACCTGGGAGAATTGCAAGCTTAGCACCATAGAACG
TCAGCTCCTTCGTGTAGTACGTGAGGATGACCTCCCTGGTAGTGAAGCGCCAGGTGCTTGGCTTCGGTTTCTGCGGG
GAGGAGACGCCGTTAACTTGAGACGCGTTGCAGACCATAATCACCAGGATGTAGTAACCCTTGCCCTGCTCCTGCAA
AGACTTGTCCGCGAGGAGCAACGTGAACGCGAGACACTTGCCCTTGTCGGACAGTAAtaaCGGTTTCCATATGGGGA
TTGGTGGCGACGACT

oPEB1046:

caaaggggaaatgggatcctaaggaggtatacatATGTCTTTGAAGGGAAAGTTACAACGTATGAAGAAACACATG
GTCCTTGACGAAGGAGAGCACAAAATAGAGGCGGGTCAGCGCGAGAACAATTTTGCAGAAATCCCATTTTTAGAGGA
ATGGGAGGCTTTTGGCATGAAGCCTTTCTTTTTTGAAGACGAATATTGTTTGATCCGTGAGGTAGAATATCCATTAT
CCCACCGCCATGGACTTTATCGGTTCAGTGAGTTAGATGAGGTCATAACATTGTGGAACCAAAGCAGTCTCAGTCAT

ACGCTCAGTGCTAAGGGTTACAACAAAAATAGCCTTTTTTTTTTTGATACTGAAACCACAGGATTGGGAGGGGGGGC
TGGGAATACGATTTTTTTATTAGGACACGCACGGGTCTATGAAGACCGCGTGACAGTCAAGCAACATCTTCTCCCTA
AACCTGGTAACGAGGTGGCCTTGTATCAGTCCTTCCTGAGTGAGGTGGACATTACAAGCCTTGTTACATATAATGGC
AAAGCGTTCGATTGGCCACAGGTAAAGACTCGGCACACATTAATACGTGATCGTCTGCCAAAACTTCCTGAATTTGG
CCATTTCGATCTTCTTCATGGTGCTCGTCGCTTGTGGAAACACAAGATGGATCGGGTAAGCCTGGGAACGGTGGAAA
AGGAAGAATTGGGTATTCACCGGCAGGAGGACACCCCTGGGTACCTCGCTCCAATGCTCTATTTTCATTTCATTAAA
GCGCAAGAACCAGACCTTCTTAAAGGTGTACTTCACCACAATGAGATGGACGTTCTGTCTTTGATTTCTTTATATAT
CCACATGTCAAAAAAAATCTTATCCGCTAGTTACGCTAGTAAGGAACATATTGAGCACTCCGAAGCATATGCCATGG
CGAAGTGGTTTATGGCTCACAAAGAAACCGACCAAGCGGTGAAGCAACTTGAGCGGTTAAAGGAAAAATCATTCGAG
GACCAGGACCGTGCTCGGCTTGATCTCTCCCTCCTTTATAAAAAACAAAACAGACTCGAAGAGGCAGTACCTTTGTG
GGAAAAACTGAGCCGCTCTCAGAATCAGAAGTGTCGTTACACTGCCGTTATAGAGTTAGCCAAGTACTTTGAGCATA
AAAAAAAGGAATTCGGCAAAGCCTTATACATAGCGGAGCAACTTTTGAGTGATGCGGCGTTTCTGTCAGAAAAGGAA
AGTGAGAAGTTACAAGTACGCATAGCAAGACTTAAAAGAAAGTATTCCAGCTAAtaaCGGTTTCCATATGGGGATTG
GTGGCGACGACT

oPEB1047:

caaaggggaaatgggatcctaaggaggtatacatATGAAAAAGAAGAGCCTCTCAGAGCTTATTCAAGAGTTAAAG
AATCATGAGAATATAGTGCATTGGCATGAGGAGGAGCCGCGGGAAGCCAAAACTATGCCAATGCCGGAACAAGTTGA
CCCTAATATACGTGCAGCGCTGGAAAAGCGTGGAATTGAGCGGTTATTTACTCACCAGTACTCCGCGTTCCAAACTG
TCCAGAACGGTGAGAGTATTGTTGCAGTCACGCCGACCGCCTCTGGAAAGACTTTATGTTATAATCTTCCTGTATTA
CAGAGCATCGCCGAAGACGCGAGTTCCCGGGCTTTGTACTTGTTCCCAACCAAGGCGCTCGCACAGGACCAAAAGAG
CGAGCTCAACGAAATTATTGACGAGACAGGCATGGATATTAAGAGTTTCACATATGACGGCGATACTTCTCCGGCGA
TAAGACAGAAAGTACGTAAAGCCGGGCACATCGTTATCACTAACCCGGATATGCTCCATTCTGCGATCCTGCCTCAC
CATACCAAGTGGGTTAGCCTTTTCGAAAACTTGAAATATATCGTGATTGATGAACTTCATACCTACAGAGGCGTGTT
TGGTAGCCATGTCGCTAACGTGATTCGTCGTCTTATGCGCATTTGTGCCTTTTACGGATCAAAACCTTCTTTTATTT
GCACTTCAGCGACGATTGCTAATCCACGGGAATTGGCAGAACAGTTGACAGGGAAGTCAGTGCGTCTGATCGACGAT
AACGGGGCTCCAGCAGGGCGGAAACATTTTGCGTTCTATAATCCTCCGATAGTCAACAAACCGCTGCATATCCGCAA
GTCTGCAACGGTAGAGGTGAACGAATTAGCCAAGACTTTCCTTAAGAATAAAATACAAACGATCGTGTTTGCGCGGT
CCCGGGTGAGAGTGGAAATCATCCTTAGCCACATACAAGAGATAGTTAAGAAGGAGATCGGTGCTAAAAGCGTTCGT
GGTTATCGGGGCGGGTACCTCAGTAAGGAGAGAAGAGAGATCGAACGCGGACTCAGAGATGGAAGCATCCTTGGTGT
AGTCAGTACAAATGCTCTTGAGCTCGGTGTTGACATTGGACAGCTCCAAGTGTGCGTTATGACTGGTTATCCTGGAT
CTGTTGCAAGCGCTTGGCAGCAGGCAGGACGGGCCGGTAGACGGCAAGGCGAGGCATTGATTGTCATGGTTGCAAAC
TCAGATCCAATAGACCAGTACATAGTTAGACACCCTGATTACTTCTTCAAACGTAGTCCTGAAAGCGCACGCATAAA
CCCGGACAATCTGATTATACTTGTAGACCACTTAAAATGCGCAGCCTACGAGCTCCCTTTCCGTGCTGACGAGACAT
TCGGCGAGAACGACGCCCGTGATATTTTGGAATACCTCGAAGAAGAAGGCGTATTACATGAAAATCGGGAAAGATAT
CATTGGGCATCAGAATCATTTCCGGCGTCTAACATCAGTTTGCGGTCAGCATCTCAGGAGAACGTAGTCATTGTGGA
CCGCTCTGAGACGGCGGATGTCAAAATCATAGGGGAAATGGATCGCTTCTCTGCGATGACCCTCTTGCATGATGAAG
CGATCTATCTTCACGAAGGGGTGCAGTACCAGGTTGAAAAATTAGATTGGGATCATAAAAAGGCATACGTCAGAAAA
GTTGACGTAGAGTACTACACTGATGCAAACCTGGCAGTACAACTCAAGGTGCTTGACATAGATCGCACAGATAGCCG
TAAGAAAACAGCACTCCACTTTGGAGATGTTACCGTGAATGCGCTTCCGACTATATTTAAAAAAATTAAAATGACGA
CGTTCGAAAACATAGGTTCTGGTCCAATACACCTCCCGGAGGAAGAGTTGCACACTTCAGCAGCATGGTTGGAACTT
AAAGAAACTGATTCCGAGATAGGTGAAAAGACATTAGAGCAGCTGCTCCTTGGTATCGCACACGTTTTGCAGCACAT
TGTCCCTGTCTATGTCATGTGTGATCGTAATGACGTCCATGTAGTTCCTCAAATCAAGGCAGCACATACTGGCCTCC
CAACAATTTTTCTCTACGATCACTATCCTGGTGGCATTGGTTTAGCCGATGAAGTTTATAAGCGCTTCGATGAAATA
AATGAGGGAGCAGAACGCCTTATTCGTCAATGTCCATGTCAAGATGGATGTCCGTCTTGCATTGGGAGCGAAATAGA
AGGGATAGATGCGAAGAAGGCCATTCTTCGCTTACTGAATTATGTTTAAtaaCGGTTTCCATATGGGGATTGGTGGC
GACGACT

oPEB1048:

caaaggggaaatgggatcctaaggaggtatacatATGTCTCTTAAAAATAAATTAAAGCGTATGAAGAATCACTTA
AATGTGCCGGAGGCAGAGAAAAAGCCAGCAGCAAGTCAATTGTCTGTCCCGGATATTCAAGTACCGTTCCGGGAGGA
GTGGGAAGCTCTGGGAGTCAAGCCGTTTTTTTTTGAAGACGAATACTGTTTGATTAGAGAGACGGTATATCCGTTAT
CCCATCGCCATGGGAGATATAGTTTTAGTGAGCTCGACGACGTGATGGCCTTATGGAATAAGGGAGGGCTCACACAC
ACCTTGTCTGCGAAAGGGTATGAGAAGAGCCAACTCTTTTTTTTCGATACGGAAACCACAGGCTTAGGAGGAGGTGC
GGGCAATATGATCTTTTTGCTTGGACACGCTCGTGTTTACGAAGATCGGGTTGCGGTGAAGCAGCACTTATTGCCAA
AGCCGGGCAATGAAACGGCATTGTACAAGAGCTTTCTGAGCGAGGTGGATATAACATCCCTTGTGACCTACAATGGA
AAAGCCTTCGATTGGCCACAGGTGAAAACGCGCCACACGCTTTTACGCGATAGACTGCCAAAGCTGCCAGATTTCGG
GCATTTCGACCTGTTGCATGGCGCTAGACGCCTGTGGAAACACAAATTGGAGCGTGTCTCATTATCCGCGGTAGAAA
ATGAGGAGTTAGCATTCAAACGTGACGAAGATACTCCTGGTTACCTCGCTCCGATGCTTTACTTCCAATTCCTTAAA
GCGGAAGACCCTGCCTTACTCAAGGGAGTGTTAAGCCATAATGAGCAGGACGTCCTCTCCCTTATAGCGCTTTACAT
CCATATGTCCAAAAAAATATTTGCTTCCTCAGACCAAACGTCCGAACGGCAAGAAGCGTATGCCATGGCTAAATGGT
TCATAGCTCACAAAGAGACCGACCGCGCGGTCAGTCAACTTGAGGCATTACAGGGTAAGGATTTCGAAGACTCTGAC
AGAGCCCTTTTTGATCTCGCTATGCTTTATAAGAAGCAAAATCGCCGTCAAGATGCTGTACCGCTCTGGGAAAAACT
TACAGATAGTGATTTACACACGTGTCGTCACCATAGTGCGGTCGAACTCGCCATCTACTTCGAACATCACGCTAAGG
ATTATAAGAAGGCACTCCAAGCCGCCCAGCAGGCGGCGGAGGACGGAGAGATATCTGAAAAAGAGGCAGAGAAACTC
CATGTCCGTATAGCCCGTCTGAAAAGAAAGTACAGTAGCTAAtaaCGGTTTCCATATGGGGATTGGTGGCGACGACT

Supplemental alignments

MrfA alignment

```
Pa-MrfA      MAYELAKRTADAEQKLATRDGLPARDGALLSARLQRRYQDRITGSFAIPGREGRYAPIPD   60
Sp-MrfA      ----------------------MKKKSLSELIQELKNHENIVHWHEEEPREAKTMPMPE   37
Bs-MrfA      ----------------------MKKKSLTELISDLKGNENVVNWHEIEPREAKTRPMPE   37
Bc-MrfA      ----------------------MKKKSLTELISELKGNENIVNWHEIEPREARTRPMPE   37
                                   :. :* .   : : ::.:.  .    **.:  *:*:

Pa-MrfA      SVPPALAAALKARGIEQLYSHQAEAWEASQRGEHVAIVTPTASGKSLCYTLPVVSAAMQD   120
Sp-MrfA      QVDPNIRAALEKRGIERLFTHQYSAFQTVQNGESIVAVTPTASGKTLCYNLPVLQSIAED   97
Bs-MrfA      SIDERIKAALSKRGIDELYTHQYSAFQYVQKGESIVTVTPTASGKTLCYNLPVLQSIAQD   97
Bc-MrfA      SIDERIKAALSKRGIDELYTHQFSAFQYVQKGESIVTVTPTASGKTLSYNLPVLQSIAQD   97
             .:   : ***. ***:.*::** .*::  *.** :. ********:*.*.***:.:  :*

Pa-MrfA      -KAKALYLFPTKALAQDQVAELLELNRAGDLGVKAFTFDGDTPGDARQAIRLHGDIVVSN   179
Sp-MrfA      ASSRALYLFPTKALAQDQKSELNEIIDETGMDIKSFTYDGDTSPAIRQKVRKAGHIVITN   157
Bs-MrfA      ETNRALYLFPTKALAQDQKSELNEIIDEMGIDIKSFTYDGDTSPAIRQKVRKAGHIVITN   157
Bc-MrfA      ETNRALYLFPTKALAQDQKSELNEIIDEMGIDIKSFTYDGDTSPAIRQKVRKAGHIVITN   157
              . :************** :** *:    .:.:*:**:****    ** :*  *.**::*

Pa-MrfA      PDMLHQAILPHHTKWAQFFENLRYIVIDEVHTYRGVFGSHVTNVLRRLKRICAFYGVQPQ   239
Sp-MrfA      PDMLHSAILPHHTKWVSLFENLKYIVIDELHTYRGVFGSHVANVIRRLMRICAFYGSKPS   217
Bs-MrfA      PDMLHSAILPHHTKWVSLFENLKYIVIDELHTYRGVFGSHVANVIRRLKRICRFYGSDPV   217
Bc-MrfA      PDMLHSAILPHHTKWVSLFENLKYIVIDELHTYRGVFGSHVANVIRRLKRICRFYGSDPV   217
             *****.*********..:****:******:***********:**:*** *** *** .*

Pa-MrfA      FILCSATIGNPQAHAEALIEAPVTAVTESGAPTGPKQVLLWNPPVINPDLGLRASARSQS   299
Sp-MrfA      FICTSATIANPRELAEQLTGKSVRLIDDNGAPAGRKHFAFYNPPIVNKPLHIRKSATVEV   277
Bs-MrfA      FICTSATIANPKELGEQLTGKPMRLVDDNGAPSGRKHFVFYNPPIVNKPLNIRRSATAEV   277
Bc-MrfA      FICTSATIANPKELGEQLTGKPMRLVDDNGAPSGRKHFVFYNPPIVNKPLNIRKSATAEV   277
             **  ****.**:  .* *    :  : :.***:* *:. ::***::*  * :* **  :

Pa-MrfA      NRIARIAIKSGLKTLVFAQTRLMVEVLTKYLKDIFDHDPRKPPRIRAYRGGYLPTERRET   359
Sp-MrfA      NELAKTFLKNKIQTIVFARSRVRVEIILSHIQEIVKKE-IGAKSVRGYRGGYLSKERREI   336
Bs-MrfA      NELAKEFLKNKVQTIVFARSRVRVEIILSHIQELVKKE-IGTKSIRGYRGGYLPKERREI   336
Bc-MrfA      NELAKEFLKNKVQTIVFARSRVRVEIILSHIQELVKKE-IGTKSIRGYRGGYLPKERREI   336
```

```
            *.:*:  :*. ::*:***::*: **:: .::::::.::      :*.****** .****

Pa-MrfA     ERAMRAGNIDGIVSTSALELGVDIGSLDVVILNGYPGSVAATWQRFGRAGRRQQPALGVM   419
Sp-MrfA     ERGLRDGSILGVVSTNALELGVDIGQLQVCVMTGYPGSVASAWQQAGRAGRRQGEALIVM   396
Bs-MrfA     ERGLREGDILGVVSTNALELGVDIGQLQVCVMTGYPGSVASAWQQAGRAGRRHGESLIIM   396
Bc-MrfA     ERGLREGEILGVVSTNALELGVDIGQLQVCVMTGYPGSVASAWQQAGRAGRRHGESLIIM   396
            **.:* *.* *:***.*********.*:* ::.*******::**: ******:  :* :*

Pa-MrfA     VASSQPLDQYVVRHPDFFAEASPEHARIAPDQPLILFDHIRCAAFELPFRVGDGFGPIDP   479
Sp-MrfA     VANSDPIDQYIVRHPDYFFKRSPESARINPDNLIILVDHLKCAAYELPFRADETFGENDA   456
Bs-MrfA     VANSTPIDQYIVRHPEYFFNRSPESARINPENLIILVDHLKCAAYELPFRADEEFGAMEV   456
Bc-MrfA     VANSTPIDQYIVRHPEYFFNRSPESARINPENLIILVDHLKCAAYELPFRADEEFGPMDV   456
            **.* *:***:****::* : *** *** *:: :**.**::***:*****..: **  :

Pa-MrfA     EVFLEALAETEVIHREGERWEWIADSYPANAVSLRAVADGNFVVVDRSDGRQ-QIIAEVD   538
Sp-MrfA     RDILEYLEEEGVLHENRERYHWASESFPASNISLRSASQENVVIVDRSETADVKIIGEMD   516
Bs-MrfA     SDILEYLQEEAVLHRNGERYHWASESFPASNISLRSASQENVVIVDQSDIANVRIIGEMD   516
Bc-MrfA     SDILEYLQEEAVLHRNGERYHWASESFPASNISLRSASQENVVIVDQSDIANVRIIGEMD   516
              :** * *  *:*.: **:.* ::*:**. :***:.:: *.*:**:*:  : :**.*:*

Pa-MrfA     YSAAALTLYEGAIHMVQSTPYQVETLDWEGRKAYVTRTHVDYYTDSIDFTKLKVLDRFDG   598
Sp-MrfA     RFSAMTLLHDEAIYLHEGVQYQVEKLDWDHKKAYVRKVDVEYYTDANLAVQLKVLDIDRT   576
Bs-MrfA     RFSAMTLLHDEAIYLHEGVQYQVEKLDWDHKKAYVRKVDVEYYTDANLAVQLKVLEIDKT   576
Bc-MrfA     RFSAMTLLHDEAIYLHEGVQYQVEKLDWDHKKAYVRKVDVEYYTDANLAVQLKVLEIDKT   576
              :*   *:: **:: :.. ****.***: :**** :..*:****:   .:****:

Pa-MrfA     GVAGRGDSHHGEVHVVRRVAGYKKIRYYTHENIGYGPVNLPDQELHTTAVWWQLPQALLL   658
Sp-MrfA     DSRKKTALHFGDVTVNALPTIFKKIKMTTFENIGSGPIHLPEEELHTSAAWLELKETDSE   636
Bs-MrfA     KEKSRTSLHYGDVTVNALPTIFKKIKMTTFENIGSGPIHLPEEELHTSAAWLEIKTADED   636
Bc-MrfA     KEKSRTSLHYGDVTVNALPTIFKKIKMTTFENIGSGPIHLPEEELHTSAAWLEIKTADED   636
                :   *.*:* *    : :***:  *.**** **::**::****:*.* ::  :

Pa-MrfA     RAFASRQDPLDGFLGAAYALHIVATVAVMADARDLQKSVGNGDGSWFAIADQSGRGQLRG   718
Sp-MrfA     IGEKT---LEQLLLGIAHVLQHIVPVYVMCDRNDVHVV----------------------   671
Bs-MrfA     IGEKT---LEQLLLGISNVLQHIVPVYIMCDRNDVHVV----------------------   671
Bc-MrfA     IGEKT---LEQLLLGISNVLQHIVPVYIMCDRNDVHVI----------------------   671
             .  :     : :** : .*: :. * :*.* .*::

Pa-MrfA     SEGDPGGVELLQEFVPTVYLYDNFPGGVGLSEPLWQRQAELVQRARELVQRCDCKAGCPA   778
Sp-MrfA     -----PQIKAAHTGLPTIFLYDHYPGGIGLADEVYKRFDEINEGAERLIRQCPCQDGCPS   726
Bs-MrfA     -----SQIKAAHTGLPTIFLYDHYPGGIGLAEEVFKRFSDINEAAKQLITHCPCHDGCPS   726
Bc-MrfA     -----SQIKAAHTGLPTIFLYDHYPGGIGLAEEVFKRFSDINEAAKQLIKQCPCHDGCPS   726
                  ::  :  :**::***::***:**:: :::*  :: : *..*: :* *: ***:

Pa-MrfA     CVGPVLAAQEEDETSPRALALRVLDLFDAEACRHVPDVVVTTRDPMELLAP    829
Sp-MrfA     CIGSEIEGIDAKKAI-----LRLLNYV-----------------------    748
Bs-MrfA     CIGTEIEGIKAKERI-----LQLLDQMS----------------------    749
Bc-MrfA     CIGTEIEGIKAKERI-----LQLLVQMA----------------------    749
            *:*  : . . .:       *::*  .
```

MrfB alignment

```
Pa-MrfB     MSLSLDKLRLLRRQAGDPKASTPAVPDVPPAPPAPVAANDARQPPAERSVFAWVEQEIRH   60
Sp-MrfB     MSLKNKLKR-MKNHLN--------VP------------------------------EAEK   21
Bs-MrfB     MSLKGKLQR-MKKHMA--------LD------------------------------EGEQ   21
Bc-MrfB     MSLKGKLQR-MKKHMV--------LD------------------------------EGEH   21
            ***. .  * ::.:          :                                * .:

Pa-MrfB     KPTGAAAPTP-ASAPLRRPEVGSLHRLLGLRTRSGATPARASA-----QDRQLPGEEIAP   114
Sp-MrfB     KPAASQLSVPDIQVPFREE-----WEALGV------KPFFFEDEYCLIRETVYPL-SHRH   69
Bs-MrfB     KIEAGKQENHFDDIPFLEE-----WEAFGM------KPFIFEDEYCLIREVEYPL-SHRH   69
```

```
Bc-MrfB      KIEAGQRENNFAEIPFLEE-----WEAFGM------KPFFFEDEYCLIREVEYPL-SHRH   69
             *  ..       . *: .       . :*:      .*   .      ::   *  .

Pa-MrfB      GLFLIESLQPQAIPAQPLSLDFARRDGEHVAARDLLFFDTETTGLAGGTGTRAFMIGAAD  174
Sp-MrfB      GRYSFSELDDVMALWNKGGLT-HTLSAKGYEKSQLFFFDTETTGLGGGAGNMIFLLGHAR  128
Bs-MrfB      GLYSFSELEEVITLWNQSGLS-HTLSAKGYNKNNLFFFDTETTGLGGGAGNTIFLLGHAR  128
Bc-MrfB      GLYRFSELDEVITLWNQSSLS-HTLSAKGYNKNSLFFFDTETTGLGGGAGNTIFLLGHAR  128
             * : :..*:      :  .*     ..:     .*:*********.**:*.  *::* *

Pa-MrfB      WHVCPQRGEGLRIRQLLMATMAAEDAMLATFAGWLQPSTVFCSYNGRSYDAPLLKARYRL  234
Sp-MrfB      VYE-----DRVAVKQHLLPKPGNETALYKSFLSEV-DITSLVTYNGKAFDWPQVKTRHTL  182
Bs-MrfB      VYE-----DRVTVKQHLLPKPGNEVALYQSFLSEV-DITSLVTYNGKAFDWPQVKTRHTL  182
Bc-MrfB      VYE-----DRVTVKQHLLPKPGNEVALYQSFLSEV-DITSLVTYNGKAFDWPQVKTRHTL  182
              :      : : ::* *: . . * *:  :* . :   * : :***:::* * :*:*: *

Pa-MrfB      ARQRDP-ISALDHVDLLYPTRRRYRGTWENCKLSTIERQLLRVVREDDLPGSEAPGAWLR  293
Sp-MrfB      LRDRLPKLPDFGHFDLLHGARRLWKHKLERVSLSAVENEELAFKRDEDTPGYLAPMLYFQ  242
Bs-MrfB      IRDRLPKLPEFGHFDLLHGARRLWKHKMDRVSLGTVEKEELGIRRLEDTPGYLAPMLYFH  242
Bc-MrfB      IRDRLPKLPEFGHFDLLHGARRLWKHKMDRVSLGTVEKEELGIHRQEDTPGYLAPMLYFH  242
              *:* * :  :.*.***: :** :: . :. .*.::*.: * . * :* **  **  :::

Pa-MrfB      FLRGGDAVNLRRVADHNHQDVVTLALLLQRLVREEQR---------E-RETLALVGQ---  340
Sp-MrfB      FLKAEDPALLKGVLSHNEQDVLSLIALYIHMSKKIFASSDQT---SERQEAYAMAKWFIA  299
Bs-MrfB      FIKAQEPDLLKGVLHHNEMDVLSLISLYIHMSKKILSESHAPK---EHSEAYAMAKWFMA  299
Bc-MrfB      FIKAQEPDLLKGVLHHNEMDVLSLISLYIHMSKKILSASYASKEHIEHSEAYAMAKWFMA  302
             *::. :   *: *  **. **::*  *  :: ::            *  *: *:.

Pa-MrfB      ------------------------------------------------------------  340
Sp-MrfB      HKETDRAVSQLEALQGKDFEDSDRALFDLAMLYKKQNRRQDAVPLWEKLTDSDLHTCRHH  359
Bs-MrfB      HKETDQAIKQLERLIEKSFEDQDSARLDLSLLYKKQNRLEEAVPLWEKLSRSQNQKCRYA  359
Bc-MrfB      HKETDQAVKQLERLKEKSFEDQDRARLDLSLLYKKQNRLEEAVPLWEKLSRSQNQKCRYT  362


Pa-MrfB      ------------------------------------------------------- 340
Sp-MrfB      SAVELAIYFEHHAKDYKKALQAAQQAAED-GEISEKEAEKLHVRIARLKRKYSS 412
Bs-MrfB      AVIELAKYFEHKKKEFGKALQVAEQSLSDAACLSEKETEKLHVRIARLKRKYSS 413
Bc-MrfB      AVIELAKYFEHKKKEFGKALYIAEQLLSDAAFLSEKESEKLQVRIARLKRKYSS 416
```

References

1. **Friedberg EC, Walker GC, Siede W, Wood RD, Schultz RA, Ellenberger T.** 2006. DNA Repair and Mutagenesis, 2nd ed. ASM Press, Washington, D.C.
2. **Demain AL, Vaishnav P.** 2011. Natural products for cancer chemotherapy. Microb Biotechnol **4:**687-699.
3. **Hata T, Hoshi T, Kanamori K, Matsumae A, Sano Y, Shima T, Sugawara R.** 1956. Mitomycin, a new antibiotic from Streptomyces. I. J Antibiot (Tokyo) **9:**141-146.
4. **Tomasz M.** 1995. Mitomycin C: small, fast and deadly (but very selective). Chem Biol **2:**575-579.
5. **Bargonetti J, Champeil E, Tomasz M.** 2010. Differential toxicity of DNA adducts of mitomycin C. J Nucleic Acids **2010**.
6. **Tomasz M, Chowdary D, Lipman R, Shimotakahara S, Veiro D, Walker V, Verdine GL.** 1986. Reaction of DNA with chemically or enzymatically activated mitomycin-c - isolation and structure of the major covalent adduct. Proceedings of the National Academy of Sciences of the United States of America **83:**6702-6706.
7. **Iyer VN, Szybalski W.** 1963. A molecular mechanism of mitomycin action: Linking of complementary DNA strands. Proc Natl Acad Sci U S A **50:**355-362.

8. **Tomasz M, Lipman R, Chowdary D, Pawlak J, Verdine GL, Nakanishi K.** 1987. Isolation and structure of a covalent cross-link adduct between mitomycin C and DNA. Science **235:**1204-1208.
9. **Bizanek R, McGuinness BF, Nakanishi K, Tomasz M.** 1992. Isolation and structure of an intrastrand cross-link adduct of mitomycin-c and DNA. Biochemistry **31:**3084-3091.
10. **Borowyborowski H, Lipman R, Chowdary D, Tomasz M.** 1990. Duplex oligodeoxyribonucleotides cross-linked by mitomycin-c at a single site - synthesis, properties, and cross-link reversibility. Biochemistry **29:**2992-2999.
11. **Borowyborowski H, Lipman R, Tomasz M.** 1990. Recognition between mitomycin-c and specific DNA-sequences for cross-link formation. Biochemistry **29:**2999-3006.
12. **Kumar S, Lipman R, Tomasz M.** 1992. Recognition of specific DNA-sequences by mitomycin-c for alkylation. Biochemistry **31:**1399-1407.
13. **Noll DM, Mason TM, Miller PS.** 2006. Formation and repair of interstrand cross-links in DNA. Chem Rev **106:**277-301.
14. **Dronkert ML, Kanaar R.** 2001. Repair of DNA interstrand cross-links. Mutat Res **486:**217-247.
15. **Lenhart JS, Schroeder JW, Walsh BW, Simmons LA.** 2012. DNA repair and genome maintenance in Bacillus subtilis. Microbiol Mol Biol Rev **76:**530-564.
16. **Weng MW, Zheng Y, Jasti VP, Champeil E, Tomasz M, Wang YS, Basu AK, Tang MS.** 2010. Repair of mitomycin C mono- and interstrand cross-linked DNA adducts by UvrABC: a new model. Nucleic Acids Research **38:**6976-6984.
17. **Kisker C, Kuper J, Van Houten B.** 2013. Prokaryotic Nucleotide Excision Repair. Cold Spring Harbor Perspectives in Biology **5:**18.
18. **Jaciuk M, Nowak E, Skowronek K, Tanska A, Nowotny M.** 2011. Structure of UvrA nucleotide excision repair protein in complex with modified DNA. Nat Struct Mol Biol **18:**191-197.
19. **Stracy M, Jaciuk M, Uphoff S, Kapanidis AN, Nowotny M, Sherratt DJ, Zawadzki P.** 2016. Single-molecule imaging of UvrA and UvrB recruitment to DNA lesions in living Escherichia coli. Nat Commun **7:**12568.
20. **Truglio JJ, Croteau DL, Van Houten B, Kisker C.** 2006. Prokaryotic nucleotide excision repair: the UvrABC system. Chem Rev **106:**233-252.
21. **Van Houten B, Croteau DL, DellaVecchia MJ, Wang H, Kisker C.** 2005. 'Close-fitting sleeves': DNA damage recognition by the UvrABC nuclease system. Mutat Res **577:**92-117.
22. **Orren DK, Sancar A.** 1989. The (A)BC excinuclease of Escherichia coli has only the UvrB and UvrC subunits in the incision complex. Proc Natl Acad Sci U S A **86:**5237-5241.
23. **Perera AV, Mendenhall JB, Courcelle CT, Courcelle J.** 2016. Cho Endonuclease Functions during DNA Interstrand Cross-Link Repair in Escherichia coli. J Bacteriol **198:**3099-3108.
24. **Moolenaar GF, van Rossum-Fikkert S, van Kesteren M, Goosen N.** 2002. Cho, a second endonuclease involved in Escherichia coli nucleotide excision repair. Proc Natl Acad Sci U S A **99:**1467-1472.
25. **Petit C, Sancar A.** 1999. Nucleotide excision repair: from E. coli to man. Biochimie **81:**15-25.

26. **Burby PE, Simmons ZW, Schroeder JW, Simmons LA.** 2018. Discovery of a dual protease mechanism that promotes DNA damage checkpoint recovery. PLoS Genet **14:**e1007512.
27. **Karimova G, Gauliard E, Davi M, Ouellette SP, Ladant D.** 2017. Protein-Protein Interaction: Bacterial Two-Hybrid. Methods Mol Biol **1615:**159-176.
28. **Karimova G, Pidoux J, Ullmann A, Ladant D.** 1998. A bacterial two-hybrid system based on a reconstituted signal transduction pathway. Proc Natl Acad Sci U S A **95:**5752-5756.
29. **Yakovleva L, Shuman S.** 2012. Mycobacterium smegmatis SftH exemplifies a distinctive clade of superfamily II DNA-dependent ATPases with 3' to 5' translocase and helicase activities. Nucleic Acids Res **40:**7465-7475.
30. **Shi W, Punta M, Bohon J, Sauder JM, D'Mello R, Sullivan M, Toomey J, Abel D, Lippi M, Passerini A, Frasconi P, Burley SK, Rost B, Chance MR.** 2011. Characterization of metalloproteins by high-throughput X-ray absorption spectroscopy. Genome Res **21:**898-907.
31. **Bochman ML, Paeschke K, Chan A, Zakian VA.** 2014. Hrq1, a homolog of the human RecQ4 helicase, acts catalytically and structurally to promote genome integrity. Cell Rep **6:**346-356.
32. **Rogers CM, Wang JC, Noguchi H, Imasaki T, Takagi Y, Bochman ML.** 2017. Yeast Hrq1 shares structural and functional homology with the disease-linked human RecQ4 helicase. Nucleic Acids Res **45:**5217-5230.
33. **Yang W.** 2011. Nucleases: diversity of structure, function and mechanism. Q Rev Biophys **44:**1-93.
34. **Kelley LA, Mezulis S, Yates CM, Wass MN, Sternberg MJ.** 2015. The Phyre2 web portal for protein modeling, prediction and analysis. Nat Protoc **10:**845-858.
35. **Grabarczyk DB, Silkenat S, Kisker C.** 2018. Structural Basis for the Recruitment of Ctf18-RFC to the Replisome. Structure **26:**137-144.e133.
36. **Sayers JR, Eckstein F.** 1990. Properties of overexpressed phage T5 D15 exonuclease. Similarities with Escherichia coli DNA polymerase I 5'-3' exonuclease. J Biol Chem **265:**18311-18317.
37. **Sayers JR, Eckstein F.** 1991. A single-strand specific endonuclease activity copurifies with overexpressed T5 D15 exonuclease. Nucleic Acids Res **19:**4127-4132.
38. **Little JW.** 1981. Lambda exonuclease. Gene Amplif Anal **2:**135-145.
39. **Lage C, Goncalves SR, Souza LL, de Padula M, Leitao AC.** 2010. Differential survival of Escherichia coli uvrA, uvrB, and uvrC mutants to psoralen plus UV-A (PUVA): Evidence for uncoupled action of nucleotide excision repair to process DNA adducts. J Photochem Photobiol B **98:**40-47.
40. **Warren AJ, Maccubbin AE, Hamilton JW.** 1998. Detection of mitomycin C-DNA adducts in vivo by 32P-postlabeling: time course for formation and removal of adducts and biochemical modulation. Cancer Res **58:**453-461.
41. **Kidane D, Graumann PL.** 2005. Dynamic formation of RecA filaments at DNA double strand break repair centers in live cells. J Cell Biol **170:**357-366.
42. **Simmons LA, Goranov AI, Kobayashi H, Davies BW, Yuan DS, Grossman AD, Walker GC.** 2009. Comparison of responses to double-strand breaks between Escherichia coli and Bacillus subtilis reveals different requirements for SOS induction. J Bacteriol **191:**1152-1161.

43. **Simmons LA, Grossman AD, Walker GC.** 2007. Replication is required for the RecA localization response to DNA damage in Bacillus subtilis. Proc Natl Acad Sci U S A **104:**1360-1365.
44. **Kreuzer KN.** 2013. DNA damage responses in prokaryotes: regulating gene expression, modulating growth patterns, and manipulating replication forks. Cold Spring Harb Perspect Biol **5:**a012674.
45. **Sassanfar M, Roberts JW.** 1990. Nature of the SOS-inducing signal in Escherichia coli. The involvement of DNA replication. J Mol Biol **212:**79-96.
46. **Ivancic-Bace I, Vlasic I, Salaj-Smic E, Brcic-Kostic K.** 2006. Genetic evidence for the requirement of RecA loading activity in SOS induction after UV irradiation in Escherichia coli. J Bacteriol **188:**5024-5032.
47. **Lenhart JS, Brandes ER, Schroeder JW, Sorenson RJ, Showalter HD, Simmons LA.** 2014. RecO and RecR are necessary for RecA loading in response to DNA damage and replication fork stress. J Bacteriol **196:**2851-2860.
48. **Simmons LA, Foti JJ, Cohen SE, Walker GC.** 2008. The SOS Regulatory Network. EcoSal Plus **2008**.
49. **Kwon SH, Choi DH, Lee R, Bae SH.** 2012. Saccharomyces cerevisiae Hrq1 requires a long 3'-tailed DNA substrate for helicase activity. Biochem Biophys Res Commun **427:**623-628.
50. **Rogers CM, Bochman ML.** 2017. Saccharomyces cerevisiae Hrq1 helicase activity is affected by the sequence but not the length of single-stranded DNA. Biochem Biophys Res Commun **486:**1116-1121.
51. **Croteau DL, DellaVecchia MJ, Wang H, Bienstock RJ, Melton MA, Van Houten B.** 2006. The C-terminal zinc finger of UvrA does not bind DNA directly but regulates damage-specific DNA binding. J Biol Chem **281:**26370-26381.
52. **Burby PE, Simmons LA.** 2017. MutS2 Promotes Homologous Recombination in Bacillus subtilis. J Bacteriol **199**.
53. **Damke PP, Dhanaraju R, Marsin S, Radicella JP, Rao DN.** 2015. The nuclease activities of both the Smr domain and an additional LDLK motif are required for an efficient anti-recombination function of Helicobacter pylori MutS2. Mol Microbiol **96:**1240-1256.
54. **Fukui K, Nakagawa N, Kitamura Y, Nishida Y, Masui R, Kuramitsu S.** 2008. Crystal structure of MutS2 endonuclease domain and the mechanism of homologous recombination suppression. J Biol Chem **283:**33417-33427.
55. **Pinto AV, Mathieu A, Marsin S, Veaute X, Ielpi L, Labigne A, Radicella JP.** 2005. Suppression of homologous and homeologous recombination by the bacterial MutS2 protein. Mol Cell **17:**113-120.
56. **Wang G, Maier RJ.** 2017. Molecular basis for the functions of a bacterial MutS2 in DNA repair and recombination. DNA Repair (Amst) **57:**161-170.
57. **Youngman P, Perkins JB, Losick R.** 1984. Construction of a cloning site near one end of TN917 into which foreign DNA may be inserted without affecting transposition in Bacillus subtilis or expression of the transposon-bourne ERM gene. Plasmid **12:**1-9.
58. **Huang XQ, Miller W.** 1991. A TIME-EFFICIENT, LINEAR-SPACE LOCAL SIMILARITY ALGORITHM. Advances in Applied Mathematics **12:**337-357.
59. **Sievers F, Higgins DG.** 2014. Clustal Omega, accurate alignment of very large numbers of sequences. Methods Mol Biol **1079:**105-116.

60. **Edgar RC.** 2004. MUSCLE: multiple sequence alignment with high accuracy and high throughput. Nucleic Acids Res **32:**1792-1797.
61. **Saitou N, Nei M.** 1987. The neighbor-joining method: a new method for reconstructing phylogenetic trees. Mol Biol Evol **4:**406-425.
62. **Nei M, Kumar S.** 2000. Molecular Evolution and Phylogenetics. Oxford University Press, New York.
63. **Felsenstein J.** 1985. CONFIDENCE LIMITS ON PHYLOGENIES: AN APPROACH USING THE BOOTSTRAP. Evolution **39:**783-791.
64. **Kumar S, Stecher G, Tamura K.** 2016. MEGA7: Molecular Evolutionary Genetics Analysis Version 7.0 for Bigger Datasets. Mol Biol Evol **33:**1870-1874.
65. **Burby PE, Simmons ZW, Simmons LA.** 2018. DdcA antagonizes a bacterial DNA damage checkpoint. bioRxiv doi:10.1101/391730.
66. **Burby PE, Simmons LA.** 2017. CRISPR/Cas9 Editing of the Bacillus subtilis Genome. Bio Protoc **7**.
67. **Gibson DG.** 2011. Enzymatic assembly of overlapping DNA fragments, p 349-361. *In* Voigt C (ed), Synthetic Biology, Pt B: Computer Aided Design and DNA Assembly, vol 498. Elsevier Academic Press Inc, San Diego.

CHAPTER V

MutS2 promotes homologous recombination in Bacillus subtilis

Abstract

Bacterial MutS proteins are subdivided into two families, MutS1 and MutS2. MutS1 family members recognize DNA replication errors during their participation in the well-characterized mismatch repair pathway (MMR). In contrast, to the well-described function of MutS1, the function of MutS2 in bacteria has remained less clear. In *Helicobacter pylori* and *Thermus thermophilus*, MutS2 has been shown to suppress homologous recombination. The role of MutS2 is unknown in the Gram-positive bacterium *Bacillus subtilis*. In this work, we investigated the contribution of MutS2 to maintaining genome integrity in *B. subtilis*. We found that deletion of *mutS2* renders *B. subtilis* sensitive to the natural antibiotic mitomycin C (MMC), which requires homologous recombination for repair. We demonstrate that the C-terminal Smr domain is necessary but not sufficient for tolerance to MMC. Further, we developed a CRISPR/Cas9 genome editing system to test if the inducible prophage PBSX was the underlying cause of the observed MMC sensitivity. Genetic analysis revealed that MMC sensitivity was dependent on recombination and not on nucleotide excision repair or a symptom of prophage PBSX replication and cell lysis. We found that deletion of *mutS2* resulted in decreased transformation efficiency using both plasmid and chromosomal DNA. Further, deletion of *mutS2* in a strain lacking the Holliday junction endonuclease *recU* resulted in increased MMC sensitivity and decreased transformation efficiency, suggesting that MutS2 could function redundantly with RecU. Together, our results support a model where *B. subtilis* MutS2 helps to promote homologous recombination, demonstrating a new function for bacterial MutS2.

The contents of this chapter were published in the *Journal of Bacteriology* by Peter E. Burby and Lyle A. Simmons. I designed and performed the experiments, analyzed the data. LAS and I wrote the manuscript.

Importance

Cells contain pathways that promote or inhibit recombination. MutS2 homologs are Smr-endonuclease domain containing proteins that have been shown to function in anti-recombination in some bacteria. We present evidence that *B. subtilis* MutS2 promotes recombination providing a new function for MutS2. We found that cells lacking *mutS2* are sensitive to DNA damage that requires homologous recombination for repair, and have reduced transformation efficiency. Further analysis indicates that the C-terminal Smr domain requires the N-terminal portion of MutS2 for function *in vivo*. Moreover, we show that a *mutS2* deletion is additive with a r*ecU* deletion suggesting that these proteins may have a redundant function in homologous recombination. Together, our study shows that MutS2 proteins have adapted different functions that impact recombination.

Introduction

Many processes contribute to maintaining genetic information and generating genetic variation in bacterial cells. One process, critical for the repair of DNA breaks and horizontal gene transfer, is homologous recombination. Homologous recombination has been well-defined in organisms ranging from bacteria to mammals [for review (1)]. The Gram-positive soil bacterium *Bacillus subtilis* is a naturally competent organism that can uptake DNA from its surroundings and, if sufficient homology exists, incorporate the exogenous DNA into its chromosome [for review (2)]. In *B. subtilis* a number of proteins have been shown to function in promoting homologous recombination either by assaying for DNA uptake and integration or through the study of DNA damaging agents called clastogens that require homologous recombination for repair [for review (3, 4)]. These approaches have helped define the RecA-dependent homologous recombination and the RecA-independent non-homologous end joining (NHEJ) pathways in *B. subtilis* [(3, 5-7)].

In addition to promoting recombination many bacteria and eukaryotes contain anti-recombination pathways. In general terms, anti-recombination suppresses the formation of deleterious crossover species, which have the potential to decrease cell viability [for review (8-10). In eukaryotes, RecQ family helicases can unwind recombination intermediates thereby suppressing aberrant crossover formation (11). In *Escherichia coli*, deletion of the helicase *uvrD*

and the helicase *ruvA* from the RuvABC Holliday junction endonuclease causes the formation of toxic recombination intermediates referred to as bimolecular recombination intermediates (12). In addition to UvrD and RuvA, the MMR pathway has been shown to suppresses recombination between non-identical DNA sequences often referred to as homeologous recombination (13). Such an activity has been shown to provide a barrier to horizontal gene transfer by conjugation between *E. coli* and *Salmonella typhimurium* (14). Biochemical evidence shows that MutS interferes with RecA-mediated strand exchange inhibiting recombination intermediates between non-identical or methylated substrates (15, 16), and can recruit UvrD to unwind recombination intermediates (17). Therefore, in bacteria a number of different proteins have been shown to limit hyper-recombination between identical sequences or homeologous recombination between non-identical sequences.

Interestingly, some bacteria contain a MutS paralog, MutS2, which has been shown to possess anti-recombination activity (18-20). MutS2 is composed of an N-terminal region involved in DNA binding, followed by a central ABC ATPase domain, which also participates in dimerization (21, 22). The MutS2 C-terminal domain contains the small MutS related (Smr) region, harboring a DNase I-like endonuclease domain (22). MutS2 in *Helicobacter pylori* and *Thermus thermophilus* contributes to anti-recombination (19, 21). *H. pylori* and *T. thermophilus* strains lacking *mutS2* are more efficiently transformed with DNA and Δ*mutS2 T. thermophilus* is more resistant than wild type to mitomycin C (MMC), an antibiotic that damages DNA and requires homologous recombination for repair (19, 22). Biochemical studies have shown that *Hp*MutS2 and *Tt*MutS2 both have ATPase activity that is stimulated by recombination intermediates, and *Tt*MutS2 has endonuclease activity toward recombination intermediates including Holliday junctions (19, 22). These data support the hypothesis that MutS2 proteins suppress homologous recombination in bacteria. Therefore, although homologous recombination is critical for DNA repair and horizontal gene transfer, bacteria also contain pathways that suppress recombination because hyper-recombination can lead to genome instability and cell death. It is not clear, however, if the anti-recombination activity shown for *H. pylori* and *T. thermophilus* MutS2 are representative of how MutS2 functions in other bacteria.

The Gram-positive bacterium *B. subtilis* has a *mutS2* gene. (23). The function of *B. subtilis* MutS2 in genome maintenance is unknown. We initially hypothesized that *B. subtilis*

MutS2 participated in anti-recombination as demonstrated for *H. pylori* and *T. thermophilus* MutS2 (19, 22). Instead, here we report that MutS2 promotes homologous recombination in *B. subtilis*. We show that *B. subtilis* cells with *mutS2* deleted have a lower efficiency of plasmid and chromosomal DNA transformation. In addition, deletion of *mutS2* results in sensitivity to the DNA damaging agent MMC and we provide genetic evidence that MutS2 functions redundantly with the Holliday junction endonuclease RecU. Therefore, our results support a new function for the MutS2 endonuclease in bacteria where it functions as a Holliday junction endonuclease. In addition to our study of MutS2, we also describe a new, efficient single plasmid-based CRISPR/Cas9 genome editing system for use in *B. subtilis*. Our method allows for efficient removal of the plasmid after genome editing providing a significant advancement in marker-less genetic manipulation of *B. subtilis*.

Results

***Bacillus subtilis* MutS2 is a MutS paralog.** In *B. subtilis* MutS2 is encoded by the *yshC* (or *mutSB*) gene referred to herein as *mutS2* (23). MutS2 is a MutS paralog of 785 amino acids **(Fig 5.1A)** (18, 22, 24). Domain predictions suggest that the N-terminal region of MutS2 corresponds to DNA binding, followed by a central ABC ATPase domain. The MutS2 C-terminal domain harbors the Smr region containing endonuclease activity (18, 22, 24). Based on sequence alignment, *B. subtilis* MutS2 lacks the domain involved in mismatch recognition and the C-terminal unstructured region involved in β-clamp (DnaN) binding, two functions well characterized in *B. subtilis* MutS that are important for mismatch repair (MMR) **(Fig 5.1A)** (25-27).

Prior work initially characterizing *B. subtilis mutS2* showed that *mutS2* transcript abundance was constant during exponential phase and decreased towards stationary phase in rich medium, using a transcriptional fusion reporter (23). To begin, we monitored MutS2 protein abundance *in vivo* using antiserum raised against purified MutS2 ("Materials and Methods"). In rich media, MutS2 protein abundance was stable throughout exponential growth and to the onset of stationary phase **(Fig 5.1B)**. As a control, we show that the immune-reactive species is absent from a Δ*mutS2* bearing strain. Therefore, we find that MutS2 protein abundance remains constant throughout exponential phase and into stationary phase **(Fig 5.1B)**.

We mentioned above that MutS2 lacks a recognizable mismatch-binding domain and β-clamp interaction site (23) **(Fig 5.1A)**. Prior work showed that MutS2 has no impact on spontaneous mutagenesis using rifampin resistance as an indicator for mutation rate in the presence or absence of the MMR genes *mutS* and *mutL* (23). Interestingly, however this study also reported a modest increase in transversion mutations in a strain lacking *mutS2* after sequencing the reporter. Although it seems clear that MutS2 does not function in MMR, it could impact mutagenesis through a different pathway (23). Assessing spontaneous rifampin resistance only provides a limited sampling of mutations due to the restricted group of point mutations in the *rpoB* gene that are able to confer rifampin resistance (28-30). As a result, the number of measurable transversion mutations is limited. Additionally, MutS homologs in eukaryotes have been shown to have more specialized roles in recognizing insertions and deletions, two mutations that are not detected in rifampin resistance assays (31).

We chose to empirically test whether the absence of MutS2 could impact mutagenesis using an assay that can detect a broader range of mutations. We thus used an assay for spontaneous trimethoprim resistance, which samples a much wider range of base pair substitutions while also sampling insertion and deletion mutations that occur in the *thyA* gene (32). We found that the mutation rate of a Δ*mutS2* mutant strain was identical to wild type, and if we combined the Δ*mutS2* allele with a Δ*mutL* mutation, we found no difference relative to the Δ*mutL* strain alone **(Fig 5.1C)**. Similar results using a mutational reporter were observed in *H. pylori* (19). If loss of *mutS2* impacted the number of transversions, we should have observed some difference in the mutation rate using trimethoprim resistance as an indicator. With these data, we conclude *B. subtilis* MutS2 does not function in suppressing mutagenesis.

The C-terminal Smr domain is necessary but not sufficient for mitomycin C tolerance. Having excluded MutS2 from suppressing mutagenesis we screened Δ*mutS2* cells through several different DNA damaging agents to determine if MutS2 was important for survival or resistance to damage (data not shown). We found that Δ*mutS2* cells were reproducibly more sensitive to mitomycin C (MMC), a DNA cross-linking/alkylating agent (33-36), than the wild type control **(Fig 5.2A)**. An MMC titration revealed that Δ*mutS2* cells are approximately 10-fold more sensitive relative to wild type cells during a chronic exposure **(Fig 5.2A)**. To better understand whether the sensitivity is a result of growth inhibition or survival we

used quantitative plating efficiency and survival assays. We found that during chronic exposure to MMC the strain lacking *mutS2* was 10-fold more sensitive than wild-type **(Fig 5.2B)**, whereas there was no difference in survival following acute treatment **(Fig 5.2C)**. From these data, we conclude that the absence of *mutS2* results in a 10-fold sensitivity to MMC, which results from growth inhibition. To our knowledge, our observation of MMC sensitivity is the first phenotype shown for a Δ*mutS2* deletion in *B. subtilis*. A previous study of *Thermus thermophilus mutS2* found that deletion of *mutS2* resulted in resistance to MMC treatment relative to wild type, consistent with the inhibitory effect of TtMutS2 on recombination (22). Given that deletion of *B. subtilis mutS2* has the opposite effect compared with TtΔ*mutS2*, these results could suggest that *B. subtilis* MutS2 may promote homologous recombination, a novel result for a bacterial MutS2 protein.

We next asked whether sensitivity could be complemented via ectopic expression of *mutS2* from the chromosome. Indeed, expression of full-length MutS2 results in complementation of the MMC sensitivity observed with the deletion **(Fig 5.3B & C).** We took advantage of the Δ*mutS2* complementation assay to determine functional domains of MutS2 important for MMC tolerance **(Fig 5.3A)**. We found that ectopic expression of a MutS2 variant lacking the C-terminal Smr domain (*mutS2*Δ*C*) failed to complement the observed MMC sensitivity **(Fig 5.3B & C)**. A Western blot confirmed that MutS2ΔC was stably expressed **(Fig 5.3D)**. Conversely, expression of an N-terminal truncation (*mutS2*Δ*N*) leaving the Smr domain intact was able to partially complement the Δ*mutS2* MMC phenotype **(Fig 5.3B & C)**, and Western blot analysis confirmed stable expression of the MutS2ΔN variant **(Fig 5.3D)**. From these data we conclude that the Smr domain is necessary but not sufficient to allow for wild type growth in the presence of MMC, indicating that the Smr domain requires the N-terminal portion of MutS2 for full function *in vivo*.

Genetic analysis suggests MutS2 participates in homologous recombination. To begin to understand the contribution of MutS2 to tolerating MMC exposure we performed a genetic analysis of the Δ*mutS2* phenotype. *B. subtilis* contains a prophage PBSX that is induced following DNA damage (37, 38), and has the ability to cause cell lysis (39, 40). One potential explanation for the MMC sensitivity of the Δ*mutS2* strain is that in the absence of MutS2, SOS induction has increased and PBSX prophage induction results in cell lysis conferring the

observed sensitivity. To test this idea, we developed a CRISPR/Cas9 genome editing system to delete the PBSX lysis genes (Δ*xlyABxhlB*) (41) or the entire 30.5 kb PBSX prophage in an otherwise wild type strain or in a strain combined with Δ*mutS2* **(Fig 5.4-5.6)**. The spot plate analysis showed that in both the Δ*PBSX* and Δ*xlyABxhlB* deletion strains a Δ*mutS2* still conferred an ~10 fold sensitivity to MMC **(Fig 5.7)**. We conclude that the growth inhibition of Δ*mutS2* cells to DNA damage is independent of the PBSX prophage.

We asked whether MutS2 functioned in the pathways responsible for repair of MMC induced DNA damage. MMC adducts are repaired by the combined action of nucleotide excision repair (NER) and homologous recombination [for review (42, 43)]. We combined *ΔmutS2* with an *uvrA* deletion to determine if MutS2 contributed to the NER pathway. Because *uvrA* deficient strains are very sensitive to MMC we used a lower dose as compared to the experiment shown in Figure 3. If MutS2 functions in NER we would expect the sensitivity of a strain lacking *uvrA* (Δ*uvrA::spc*) to have the same sensitivity as a strain carrying both the Δ*uvrA::spc* (44) and Δ*mutS2* alleles. Instead, we found that strains with Δ*mutS2* and Δ*uvrA::spec* are more sensitive to MMC than the Δ*uvrA::spec* allele alone **(Fig 5.8A)**. These data support the hypothesis that the *ΔmutS2* sensitivity to MMC is independent of NER.

We then tested if Δ*mutS2* was epistatic or additive with a *recA* deletion (Δ*recA::loxP*). We found that the Δ*mutS2*, Δ*recA::loxP* double mutant was as sensitive to MMC as the Δ*recA::loxp* single mutant **(Fig 5.8B)**. In this experiment we used an even lower dose of MMC because *recA* deficient strains are exquisitely sensitive to MMC. Taken together, these results suggest that during repair of MMC adducts, MutS2 contributes to a step that is *recA*-dependent and that MutS2 does not participate in a step of MMC repair involving NER. Given that MutS2 proteins in other organisms have been shown to bind Holliday junctions (19, 22, 45), we chose to test whether there was a genetic interaction with the primary Holliday junction endonuclease *recU* (46). To this end, we tested a strain either lacking *recU* (Δ*recU::erm*) or lacking both *mutS2* and *recU* in the plating efficiency assay. In contrast to the experiment with *recA* we found that deletion of *mutS2* in a strain lacking *recU* resulted in an increased sensitivity to MMC **(Fig 5.8C)**. Taken together, our data suggest that MutS2 functions in a pathway dependent on RecA yet independent of RecU.

MutS2 is important for DNA transformation with plasmid and chromosomal DNA. To further test if MutS2 promotes homologous recombination, we employed a transformation efficiency assay. Transformation of naturally competent *B. subtilis* cells with plasmid or chromosomal DNA is dependent on the function of several homologous recombination proteins, although the requirements for chromosomal DNA integration relative to plasmid assembly and maintenance are not identical (47, 48). Thus, if MutS2 functions by promoting homologous recombination, as the MMC phenotype suggests, we would expect to observe decreased transformation efficiency using plasmid and/or chromosomal DNA. Indeed, we found that a strain lacking *mutS2* had decreased transformation efficiency with both plasmid **(Fig 5.9A)** and chromosomal DNA **(Fig 5.9B)**. In order to determine whether the transformation efficiency phenotype was specific to *mutS2* or both *mutS1* and *mutS2*, we tested transformation efficiency in a strain lacking *mutS1* (Δ*mutS*), and a strain lacking both *mutS* genes. We found that cells with Δ*mutS1* had decreased plasmid transformation efficiency that is independent of *mutS2* **(Fig 5.10)**. In contrast, we found that in the absence of *mutS1* there is no change in chromosomal DNA transformation efficiency and deletion of *mutS1* in a *mutS2* deletion strain resulted in a transformation efficiency indistinguishable from a *mutS2* single mutant. As a result, it appears that decreased chromosomal transformation efficiency is specific to *mutS2*.

To further examine the role of MutS2 in transformation, we tested chromosomal DNA transformation in a strain lacking the Holliday junction endonuclease *recU* and the *recU*, *mutS2* double mutant. Our hypothesis that MutS2 functions in a pathway independent of RecU predicts that these mutants should have an additive effect on transformation efficiency. Indeed, we found that deletion of *mutS2* or *recU* resulted in a 4.9-fold and 11.6-fold decrease in transformation efficiency, respectively **(Fig 5.9B)**. An additive effect predicts an approximate 57-fold decrease in transformation efficiency, and strikingly the double mutant had a 57-fold decrease in transformation efficiency **(Fig 5.9B)**. These data further support the hypothesis that MutS2 functions independently of *recU*, potentially as a Holliday junction endonuclease (see discussion).

As a control we examined whether the complementation analysis performed in Figure 3 would yield similar results in the chromosomal DNA transformation efficiency assay. Indeed, expression of full-length MutS2 resulted in a transformation efficiency that was not significantly

different from WT **(Fig 5.9C)**. We also found that expression of the variant lacking the C-terminus was not significantly different from the *mutS2* deletion strain **(Fig 5.9C)**. Further, expression of the C-terminal Smr domain alone resulted in a partial complementation similar to the results obtained in Figure 3 **(Fig 5.9C)**. Together, these results indicate that the C-terminal Smr domain requires the N-terminal ATPase domain to fully function *in vivo*.

MutS2-GFP is diffusely distributed *in vivo*. Our previous research investigating MutS1 has shown that *B. subtilis* MutS1-GFP forms foci that are recruited to the site of DNA synthesis (25-28, 49). Further, both homologous recombination proteins and nucleotide excision repair proteins have been shown to form foci or localize to the nucleoid, respectively, following MMC treatment (44, 50). We fused a monomeric version of GFP (*gfpmut3*) to *mutS2* resulting in a *gfp-mutS2* allele, which is functional in the spot-titer assay for MMC sensitivity **(Fig 5.11A),** expressed from the native locus as the only source of MutS2 *in vivo* **(Fig 5.11B)**. Fluorescence microscopy showed that MutS2-GFP was diffusely distributed in cells and did not show focus formation during normal growth or following growth in the presence of MMC **(Fig 5.11C)**. We conclude that MutS2 is diffusely distributed in *B. subtilis* cells, and that MutS2 is not specifically recruited to sites of DNA damage in quantities detectable using bulk fluorescence.

Discussion

Our investigation of *B. subtilis* MutS2 function led to the observation that cells lacking MutS2 are growth inhibited to the natural antibiotic mitomycin C (MMC). Although the sensitivity is a modest 10-fold during chronic exposure, it is highly reproducible, and can be complemented via ectopic *mutS2* expression, suggesting the sensitivity is indeed dependent on the absence of *mutS2*. This observation is a novel phenotype for a bacterial *mutS2* mutant and is the opposite of the phenotype observed in *T. thermophilus* (22), suggesting that MutS2 promotes recombination in *B. subtilis*.

Our finding that a Δ*mutS2* mutant is sensitive to MMC provided an assay to further characterize the genetic interactions of *mutS2*. Our initial genetic analysis resulted in the creation of a CRISPR/Cas9 genome editing system on a single, temperature sensitive plasmid that results in marker-less mutations that can be quickly introduced into many genetic

backgrounds. Although this is not the first report of CRISPR/Cas9 genome editing in *Bacillus subtilis* (51, 52), the system described here does not require an inducer for Cas9 expression and still allows for efficient removal of the plasmid editing system. We further demonstrated that the novel *mutS2* phenotype depends on *recA*, and does not depend on *uvrA* or *recU*. These results suggested that MutS2 functions in homologous recombination in a pathway independent of RecU.

To further test the hypothesis that MutS2 promotes homologous recombination, we assayed transformation efficiency with both plasmid and chromosomal DNA. Our hypothesis predicts a decrease in transformation, and indeed we observed decreased transformation efficiency with plasmid and chromosomal DNA. We further demonstrate that the Smr endonuclease domain is necessary, but not sufficient for chromosomal transformation and MMC tolerance. These results indicate that the C-terminal Smr domain requires the N-terminal portion of the protein for complete function *in vivo*. Additionally, we performed an epistasis analysis with *recU* using chromosomal DNA transformation. Similar to our results with MMC sensitivity, the double mutant had a more severe reduction in transformation efficiency than either single mutant. In fact, this assay revealed an additive effect of *recU* and *mutS2* deletions. With these results we suggest that MutS2 may function as a back-up Holliday junction endonuclease, though other mechanisms could also explain our results.

Previous studies of bacterial *mutS2* have observed a role in inhibiting recombination. Our findings suggest that different lineages of bacteria are capable of adapting specific proteins to their repair requirements. Interestingly, although a BLAST search finds 99% and 83% coverage when comparing *B. subtilis* MutS2 to *T. thermophilus* and *H. pylori*, respectively, the percent identity is only 35 and 28, respectively (data not shown).

Despite the sequence divergence, we speculate that MutS2 performs a similar function in these bacteria: a nuclease that is capable of processing recombination intermediates. *Hp*MutS2 has been shown to have ATPase activity that is stimulated by a four-way junction (Holliday junction) and by a fork or "Y" structure (19). A more recent study found that *Hp*MutS2 has nuclease activity toward both ssDNA and Holliday junctions that is dependent on two nuclease sites in the protein: the Smr domain and an N-terminal LDLK motif (45). Interestingly, the LDLK motif is not conserved in *B. subtilis* or *T. thermophilus*. Studies using *Tt*MutS2 have

found that MutS2 has an Smr domain dependent nuclease activity (53). Further analysis revealed that *Tt*MutS2 recognizes Holliday junctions and D-loops (22). Unfortunately, we were unable to obtain active preparations of *Bs*MutS2 to gain a more mechanistic understanding of its role in promoting recombination. Based on our genetic results we suggest that *Bs*MutS2 has activity toward Holliday junctions or D-loops, and MutS2 may function as a secondary Holliday junction endonuclease in addition to RecU.

Materials and methods

Bacteriological methods and chemicals

All *B. subtilis* strains used in this study are isogenic derivatives of PY79. All strains, plasmids, and primers used in this study are listed in the supplemental materials **(Tables 5.1-5.3)**. Construction of all strains and plasmids is detailed in the supplemental methods. For all experiments with *B. subtilis*, strains were struck out from frozen stocks on LB agar plates or LB agar plates containing the appropriate antibiotics and incubated at 30°C overnight. Antibiotics were used at the following concentrations: spectinomycin, 100 μg/mL; chloramphenicol, 5 μg/mL; erythromycin, 0.5 μg/mL. Mitomycin C was obtained from Fisher Scientific (Fisher BioReagents), and used at the final concentrations as indicated in the figures.

Trimethoprim resistance assay

Trimethoprim resistance assays were performed essentially as described (32). Briefly, an LB (10 g/L NaCl, 10 g/L Tryptone, 5 g/L yeast extract) culture for each strain was inoculated and grown at 37°C until an OD_{600} of about 1.0. Cultures were back diluted 1:500 into LB with 200 μM thymidine and grown for 4 hours at 37°C. Cultures were then serially diluted and plated on LB with 200 μM thymidine for viable cells, and minimal media plates containing trimethoprim (1x $S7_{50}$ salts (54, 55), 1% glucose, 0.1% glutamate, 0.1 μM tryptophan, 0.1 μM phenylalanine, 200 μM thymidine, 1x metals (54, 55), 0.2% casamino acids, 1.8% agar, and 34 μM trimethoprim) to select for *thyA* mutants. For viable cells, 100 μL of the 10^{-6} dilution were incubated on plates at 30°C overnight. For trimethoprim plates, 100 μL of the 10^{0} (PY79 and PEB11) or 10^{-1} (PEB112 and PEB118) dilutions were plated and incubated at 45°C overnight. A total of 17 independent cultures were used for each strain. Mutation rate was calculated via

fluctuation analysis using the online tool FALCOR at http://www.mitochondria.org/protocols/FALCOR.html as described (56, 57).

Western blotting

For Western blot analysis cultures were grown in LB at 37°C to an OD_{600} ~1-3 or as indicated for Figure 1B. Then 1 mL of an OD_{600} = 1 from each strain was pelleted via centrifugation (10,000*g* for 5 min at room temperature (RT)). Cell pellets were re-suspended in 50 µL RE buffer (50 mM Tris·Cl pH 7.5, 150 mM NaCl, 50 mM EDTA, 1x Roche Complete EDTA-free protease inhibitor cocktail (04693132001), and 10 mg/mL lysozyme) and incubated at 37°C for 20 minutes. The samples were then iced briefly (2-3 minutes) followed by the addition of SDS to a final concentration of 1% and SDS loading dye to 1x. Samples were incubated at 100°C for 10 minutes, followed by SDS-PAGE (8% for Figure 1B and S5B; 4-15% gradient gel for Figure 3C). Proteins were transferred to a nitrocellulose membrane using the Bio-Rad Trans-Blot Turbo apparatus using the manufacturer's kit and manufacturer's recommendations. Membranes were blocked using 5% milk in TBST overnight at 4°C or for 1 hour at RT. Primary antibodies were used at a 1:5,000 dilution (both MutS2 and DnaN) in 2% milk in TBST for 1 hour at RT. Secondary antibodies (LI-COR Goat anti-rabbit conjugated to an IR dye) were used at a 1:15,000 dilution in 2% milk in TBST for 1 hour at RT. The membranes were then visualized using the LI-COR Odyssey infra-red imaging system. For Figure 3, cells were lysed via sonication in RE buffer without lysozyme on ice. All Western blots were performed from two independent replicates.

Spot-titer assays

A single colony was used to inoculate an LB culture and grown to an $OD_{600} \approx 3$. Cultures were normalized via OD_{600}, serially diluted, and 5 µL of the 10^{-1} through 10^{-6} were spotted onto LB agar plates or plates with the indicated concentration of MMC. LB agar with a vehicle control was performed as well and showed identical results to the untreated control (data not shown). Dilutions were spotted using a BioTek precision XS pipetting robotics system. Plates were incubated at 30°C overnight (16-20 hours). All spot-titer assays were performed at least twice.

Plating efficiency assays

A single colony was used to inoculate an LB culture grown to an OD_{600} between 0.5 and 1. Cultures were normalized via OD_{600} and a scorable dilution resulting in approximately 30-300 colonies was plated on LB for viable cells, and on plates containing the concentration of MMC indicated in the figures. Plating efficiency was determined by dividing the number of colony forming units (CFUs) on MMC plates by the number of CFUs on LB plates and multiplying by 100 to obtain a percentage. All experiments were performed in biological triplicate and each triplicate was performed at least twice. The data plotted are the mean of the pooled data and the error bars represent standard errors of the mean.

Acute MMC survival assays

A single colony was used to inoculate an LB culture and grown to an OD_{600} between 0.5 and 1. An equivalent OD_{600} was taken and cells were washed in 0.85% NaCl. Cells were then resuspended in saline as a no treatment control or the concentration of MMC in figure 2C and treated at 37°C for 30 minutes. Cells were pelleted, the supernatant removed, and resuspended in saline. As above a scorable serial dilution was then plated on LB to determine the number of surviving CFUs. The percent survival is the number of CFUs from the indicated MMC treatment divided by the number of CFUs from the no treatment control multiplied by 100. Each experiment was performed in triplicate at least twice. The data plotted are the mean of the pooled data and the error bars represent the standard errors of the mean.

Transformation efficiency assays

Transformation efficiency assays were performed by transforming cultures grown to natural competence. Competent cell cultures were prepared by inoculating a 2 mL culture of LM media (LB with 3 mM $MgSO_4$) with a single colony and grown at 37°C to an OD_{600} between 1 and 1.5, then transferring 20 μL of the LM culture into 500 μL pre-warmed MD media (1x PC buffer (10x PC buffer is 107 g/L K_2HPO_4, 60 g/L KH_2PO_4, and 10 g/L trisodium citrate$\cdot (H_2O)_5$), 2% glucose, 50 μg/mL tryptophan, 50 μg/mL phenylalanine, 11 μg/mL ferric ammonium citrate, 2.5 mg/mL potassium aspartate, 3 mM $MgSO_4$) and incubated at 37°C for 4 hours. 10 ng of pPB153 plasmid DNA (purified from *E. coli* strain MC1061, which is *recA*+ resulting in oligomeric plasmid preparations, using the Qiagen plasmid hi-speed midi kit with DNA eluted in

ddH_2O) or 25 ng of chromosomal DNA (purified using a spin column method; see supplementary methods) from PEB43 were added to cultures followed by incubation at 37°C for 1.5 hours. The cultures were serially diluted and 100 µL of the 10^{-6} were plated for viable cells on LB agar, and for transformants 100 µL of a scorable serial dilution as described above were plated on LB with 100 µg/mL spectinomycin (plasmid transformations) or LB with 5 µg/mL chloramphenicol (chrDNA transformations) followed by incubation at 30°C overnight. Transformation experiments were performed in at least biological triplicate and each experiment was performed three times.

CRISPR/Cas9 editing plasmid construction

Construction of a CRISPR/Cas9 genome editing plasmid was done in two cloning steps (see Fig S1). First the spacer was incorporated into the CRISPR array via restriction digest and ligation cloning. The plasmid was digested with BsaI-HF (NEB) in CutSmart buffer at 37°C. Meanwhile, the spacer was prepared to ligate into the plasmid. First the oligonucleotides, ordered with the correct overhangs (58), were annealed by mixing the oligonucleotides at 10 µM each in 1x annealing buffer (10 mM Tris·Cl, pH 7.5, 100 mM NaCl, and 0.1 mM EDTA). Annealed oligonucleotides were phosphorylated using T_4 polynucleotide kinase (PNK; NEB): a 50 µL reaction was assembled with 1x T_4 DNA ligase buffer, and 1 µM annealed oligonucleotides and incubated at 37°C for 30 minutes. T_4 PNK was heat inactivated at 65°C for 20 minutes. A 20 µL ligation reaction was assembled using 1x T_4 DNA ligase buffer, 40-100 ng plasmid DNA, 25 nM phosphorylated and annealed oligonucleotides, and 400 units T_4 DNA ligase (NEB). The ligase reaction was performed at room temperature for 2-3 hours. The ligation was then used to transform chemically competent ($CaCl_2$ method) *E. coli* cells (Top10; Thermo Fisher Scientific): 10 µL of the ligation reaction was used to transform 60-100 µL competent cells. The plasmid was verified via Sanger Sequencing. The resulting plasmid (essentially a targeting plasmid) was then used to create the editing plasmid.

The editing plasmid was constructed using Gibson Assembly (59) of the following four (or more) PCR amplicons that were gel purified from an agarose gel: 1) the vector backbone of pPB41, amplified using oPEB217/oPEB218; 2) the Cas9/CRISPR array containing the spacer incorporated in the "targeting plasmid" was amplified using oPEB232/oPEB234; 3) the upstream portion of the editing template was amplified and contains overlaps for pPB41 at oPEB217 and

for the downstream portion of the editing template (see pPB50 and pPB51 for examples); 4) the downstream portion of the editing template was amplified and contains overlaps for the upstream portion of the editing template and for pPB41 at oPEB232 (see pPB50 and pPB51 for examples). A 10 µL Gibson Assembly reaction was assembled using 1x Gibson Assembly master mix, 40-100 ng of the vector backbone of pPB41, 40-100 ng of the Cas9/CRISPR array containing the spacer, and about 20-40 ng of each portion of the editing template. The Gibson reaction was performed at 50°C for 90 minutes. The reaction was then used to transform chemically competent MC1061 *E. coli* cells. Clones were verified using Sanger sequencing at the University of Michigan Core Facility. The result of this second step yields a complete editing plasmid that can be used to efficiently manipulate the *B. subtilis* genome.

CRISPR/Cas9 genome editing

After construction of the editing plasmid, fresh *B. subtilis* competent cells (500 µL; see transformation efficiency assays) were transformed with 200-600 ng of the editing plasmid that had been purified from a strain of *E. coli* that yields multimers (*e.g.*, MC1061). Transformations were plated on LB agar plates with spectinomycin and incubated at 30°C overnight. The next day 6-24 isolates were colony purified by re-streaking on LB agar plates with spectinomycin. The editing plasmid contains a temperature sensitive origin of replication (derived from pDR244). To evict the plasmid, isolates were re-struck on LB and incubated at 42-45°C for 10-16 hours. Isolates were then screened for loss of the plasmid by re-streaking on LB agar plates with and without spectinomycin and incubating at 42-45°C overnight. The isolates that were found to be spectinomycin sensitive were further screened via PCR to determine if the isolate had the expected deletion.

Live cell microscopy

For live imaging experiments, a plate grown overnight at 30°C was washed using $S7_{50}$ minimal media supplemented with 2% glucose essentially as described (60). The OD_{600} was measured and cells were diluted to an OD_{600} of 0.1. Cultures were incubated at 30°C for 2 hours (OD_{600} = 0.2). Cultures were treated with either a vehicle control or 100 µg/mL MMC, and incubated at 30°C for an additional 2 hours ($OD_{600} \approx 0.5$). An aliquot of cells were removed followed by incubation with the membrane stain FM4-64 at 1 µg/mL. Cells were then placed on

1% agarose pads made of 1x Spizizen's salts (26, 27, 54, 55). Cells were imaged using an Olympus BX61 microscope as described previously (26, 27, 60).

Figures and Tables

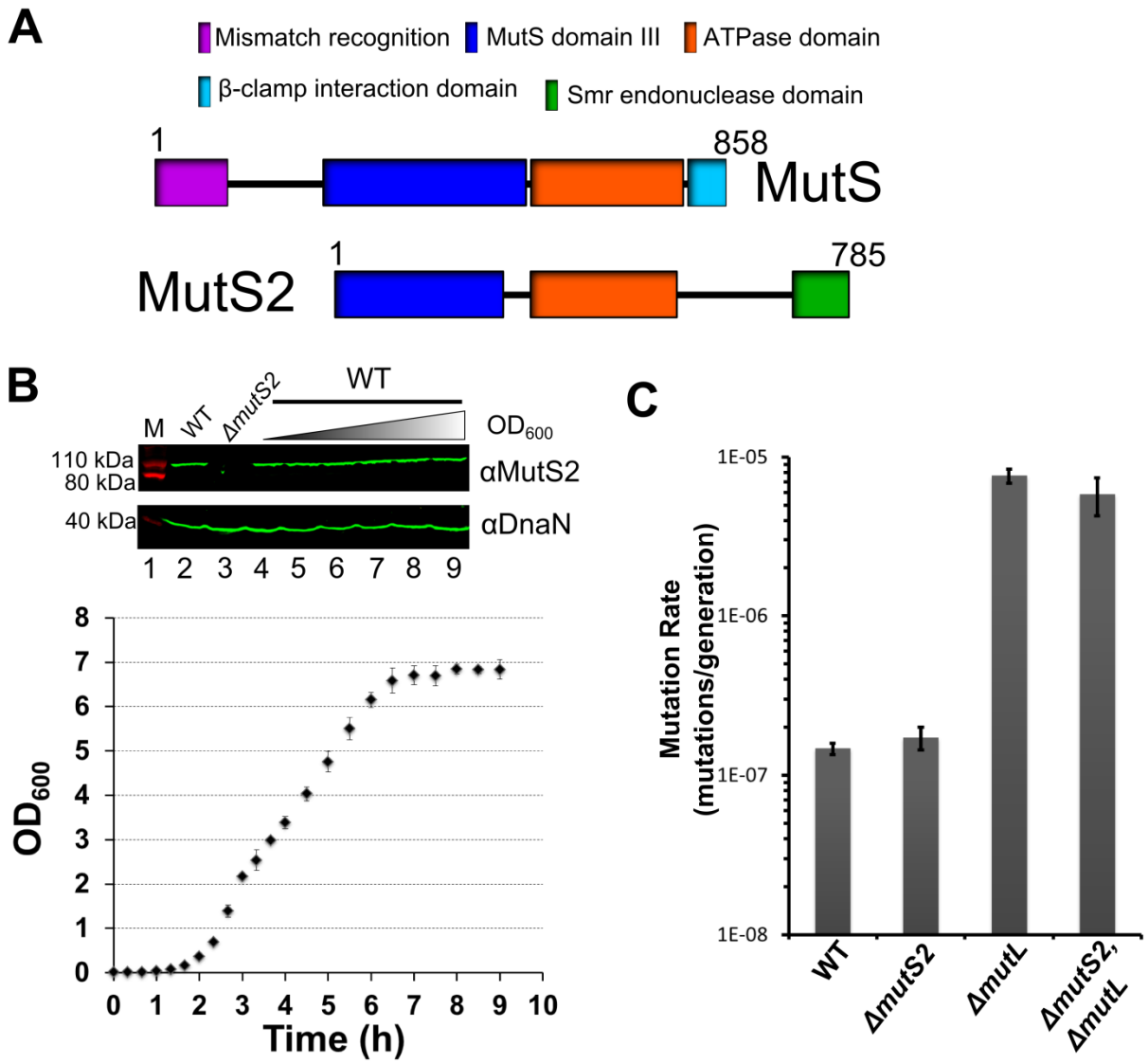

Figure 5.1 MutS2 is a MutS paralog expressed throughout exponential growth, and has no role in mutagenesis. (A) A predicted domain alignment of MutS and MutS2 proteins. **(B)** Western blot of MutS2 protein levels throughout exponential growth. Cultures were grown at 37°C and samples of equivalent OD_{600} were taken at increasing optical densities (OD_{600} from 0.8-5.9). Lane 1: molecular weight marker, 2: WT (OD_{600} = 5.9), 3: Δ*mutS2* control (OD_{600} = 5.6), 4-9: samples taken at increasing OD_{600} (from 0.8-3.8). An antibody for DnaN was used as a

loading control. The lower panel is a growth curve of *B. subtilis* at 37°C. Data are the mean of six independent replicates from two experiments and the error bars are the standard errors of the mean. **(C)** A trimethoprim resistance assay to measure mutagenesis. Data were plotted as the average of three independent experiments and error bars represent the standard error of the mean.

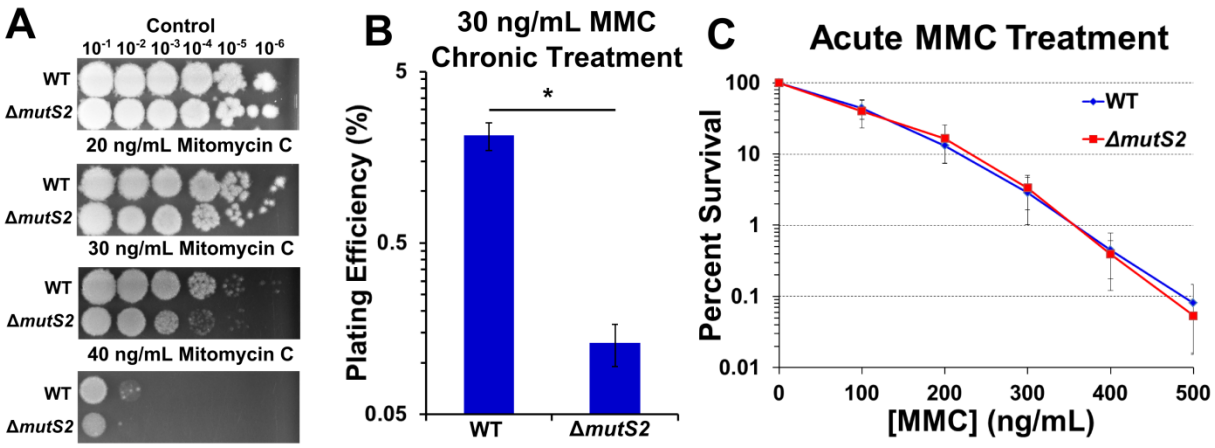

Figure 5.2 Δ*mutS2* cells are sensitive to mitomycin C chronic exposure. (A) Spot-titer assay of WT and Δ*mutS2* cells. Cultures were normalized via OD_{600}, serial diluted, and the indicated dilutions were spotted on an untreated control plate and the indicated concentrations of mitomycin C (MMC). **(B)** Plating efficiency assay. Cultures were normalized via OD_{600}, serial diluted, and plated on either LB or LB with 30 ng/mL MMC to determine colony forming units (CFUs). Plating efficiency is the percent CFUs on MMC relative to the LB control. A Mann-Whitney U-test was used to determine statistical significance. *: one-sided p-value < 0.05. **(C)** Survival assay. WT and Δ*mutS2* cultures were normalized via OD_{600}, and treated with the indicated concentration of MMC for 30 minutes in saline followed by plating for viable cells on LB. Percent survival is the percentage of CFUs from the treatment relative to the untreated control.

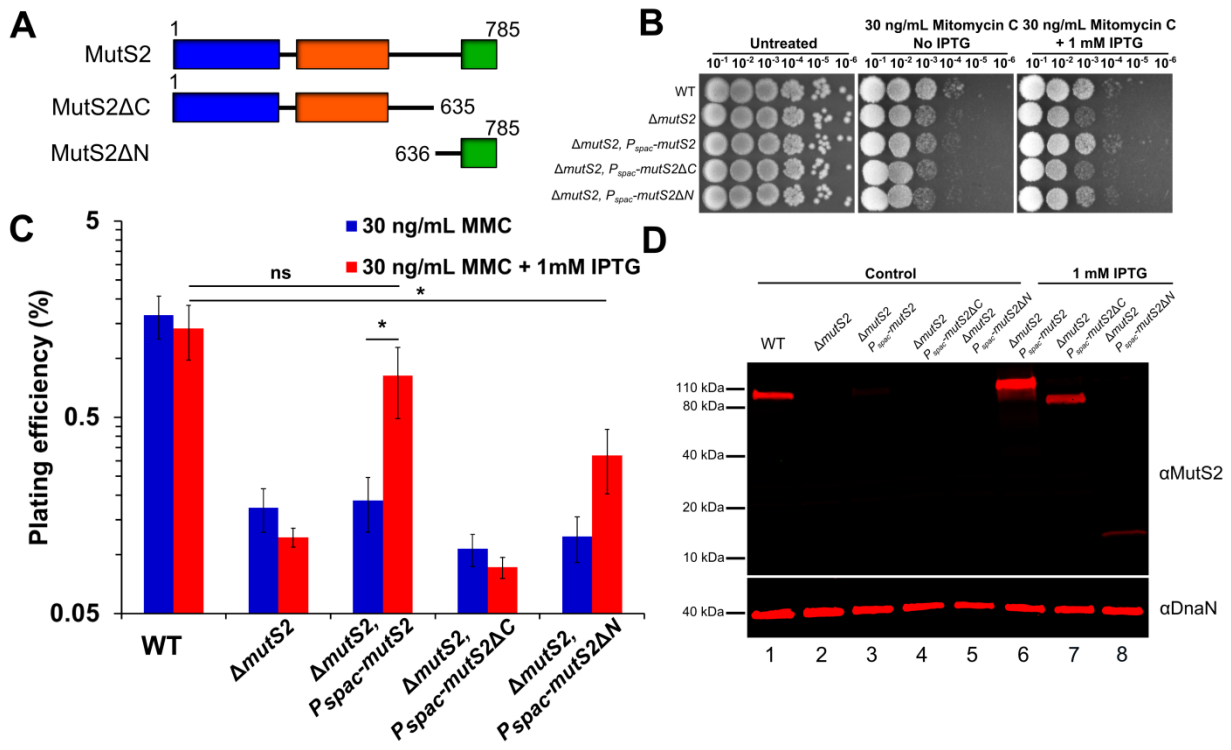

Figure 5.3 The C-terminal Smr domain is necessary but not sufficient for MMC tolerance. **(A)** MutS2 constructs used for complementation experiments in B, C, & D. **(B)** A spot-titer assay was done as in Figure 2. Complementation constructs were under the control of the IPTG inducible P_{spac} promoter. **(C)** Plating efficiency assay performed as in Figure 2 with 1 mM IPTG (red bars) or without IPTG (blue bars). The Mann-Whitney U-test was used to determine statistical significance. ns: not significant; *: one-sided p-value < 0.05. **(D)** Western blot using a MutS2 antibody and a DnaN antibody as a loading control. Cultures of the indicated genotypes were grown in the absence (lanes 1-5) or presence (lanes 6-8) of IPTG. The cultures were normalized via OD_{600} and analyzed via Western blotting.

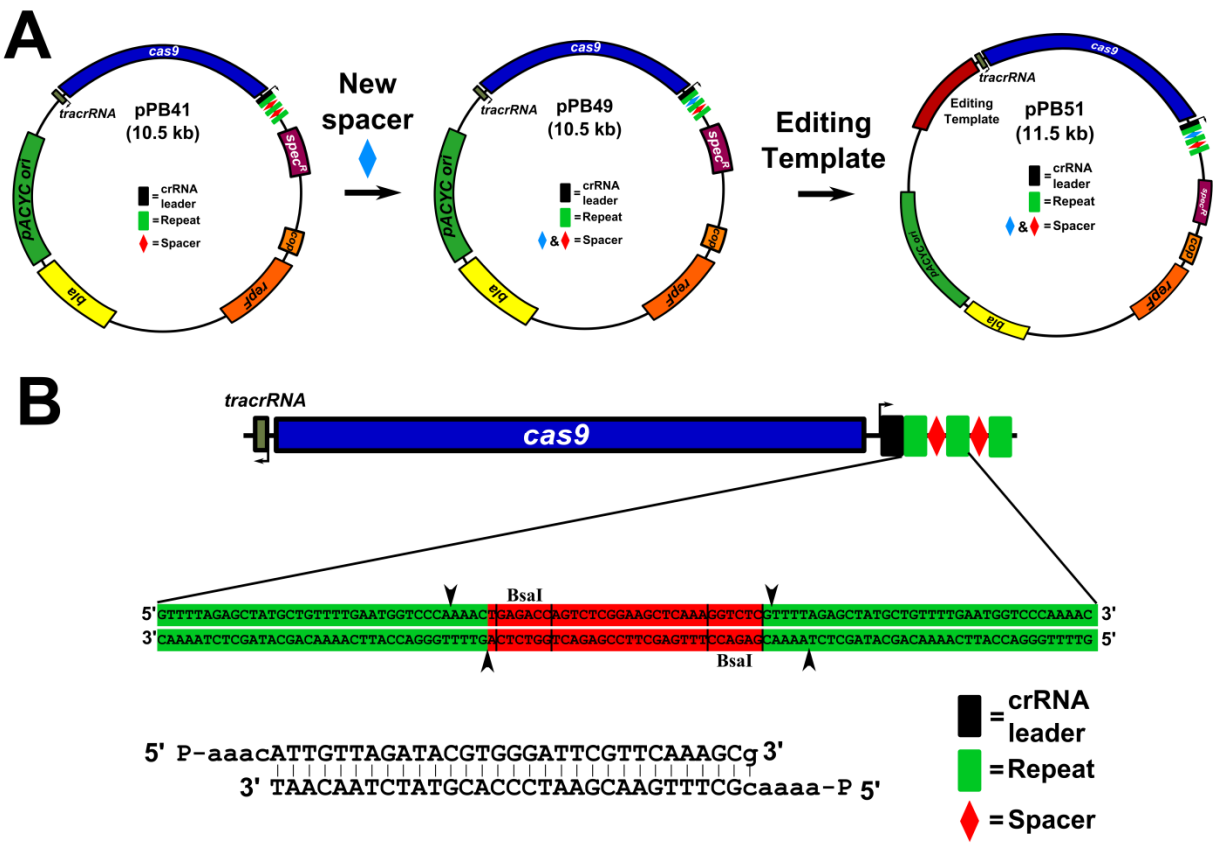

Figure 5.4 Overview of constructing a CRISPR/Cas9 editing plasmid. (A) The editing plasmid is created using two cloning stages. First the spacer is incorporated using the method previously described (58), wherein the BsaI digested plasmid is ligated to the spacer with the appropriate overhangs (see B). In the second stage Gibson Assembly is used to combine the temperature sensitive plasmid containing Cas9/CRISPR and the spacer of interest with the editing template. **(B)** A close up of the overhangs required to ligate a spacer inside of the CRISPR array as described (58). See "Materials and Methods" for a detailed protocol.

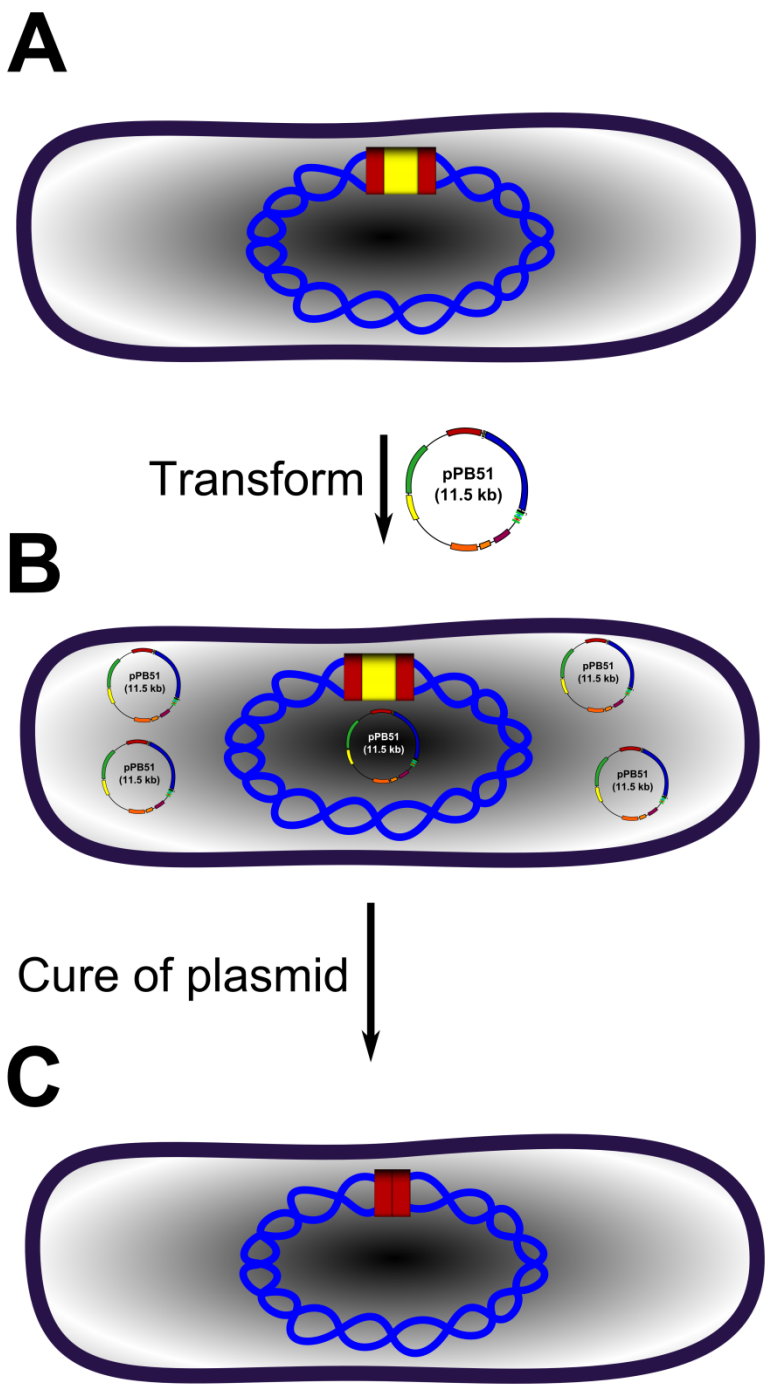

Figure 5.5 Overview of CRISPR/Cas9 genome editing in *Bacillus subtilis.* (A) The desired strain of *B. subtilis* is transformed with the editing plasmid containing Cas9, the CRISPR array with spacer, and the editing template and grown at the permissive temperature (30°C). **(B)** Upon transformation, Cas9 generates a double strand break, which the cell repairs utilizing the editing template on the plasmid containing the genetic change of interest. The cells are then cured of the

plasmid by growing at the non-permissive temperature (42-45°C). **(C)** Finally isolates are screened for loss of the plasmid and the genetic change.

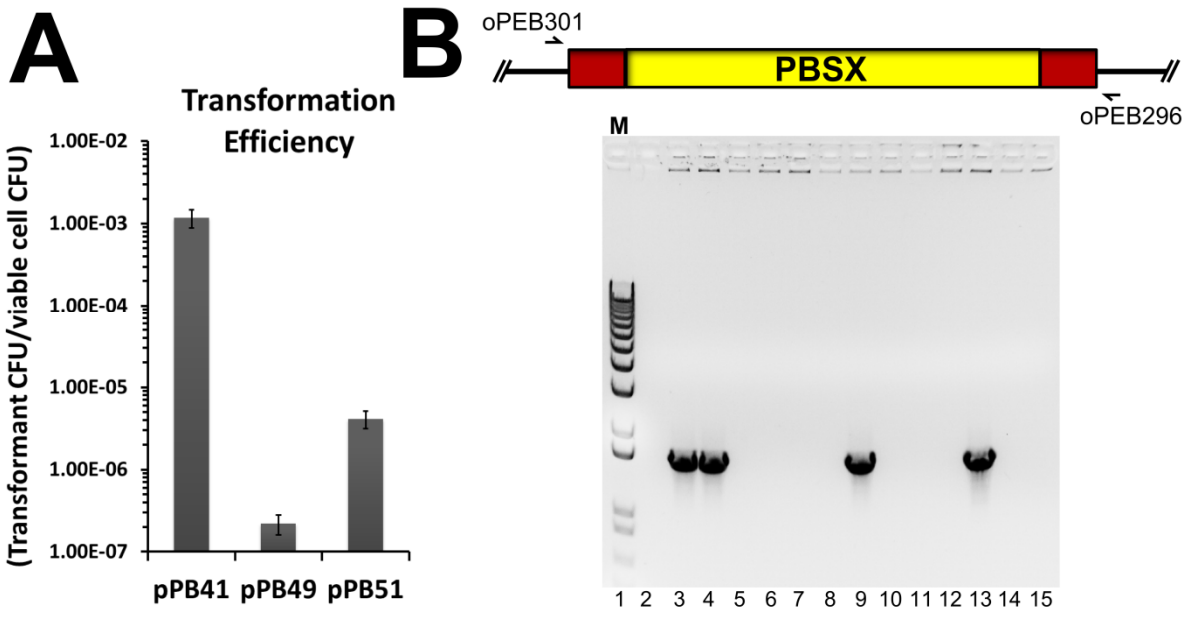

Figure 5.6 Deletion of prophage PBSX using CRISPR/Cas9 genome editing. (A) Transformation efficiency assay using a plasmid with no spacer (pPB41), a plasmid with a spacer targeting the genome inside PBSX (pPB49), and a plasmid containing the spacer and the editing template that would remove the entire 30.5 kb prophage from the *B. subtilis* genome. Data are plotted as the mean of two independent experiments performed in triplicate and the error bars represent the standard deviation of the pooled data set. **(B)** PBSX genomic locus and PCR primers, located outside the editing template sequence, used to verify deletion of the prophage. Of 24 isolates, 13 lost the antibiotic resistance of the plasmid. Those 13 were used in colony PCR genotyping reactions. Lane 1: Molecular weight standard, lane 2: PCR performed using WT genomic DNA (yielding no band), lanes 3-15: colony PCR reactions of 13 isolates that lost the plasmid. Four isolates (lanes 3, 4, 9, and 13) of 24 with the deletion were obtained using this method.

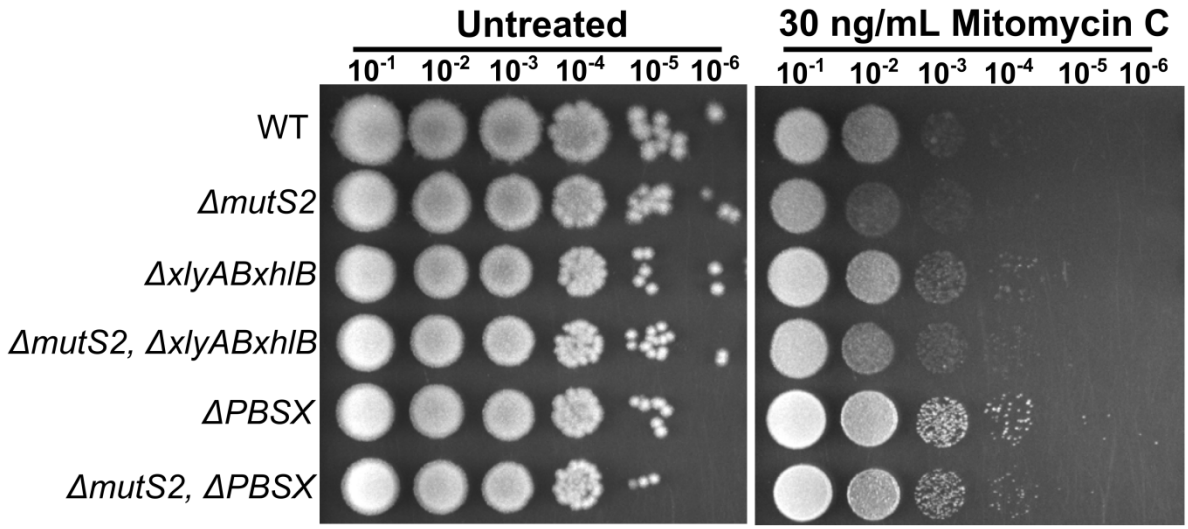

Figure 5.7 *ΔmutS2* MMC sensitivity is independent of the prophage PBSX. Spot-titer assay as done in Figure 2 using the indicated strains spotted on an untreated control plate and the indicated concentrations of MMC.

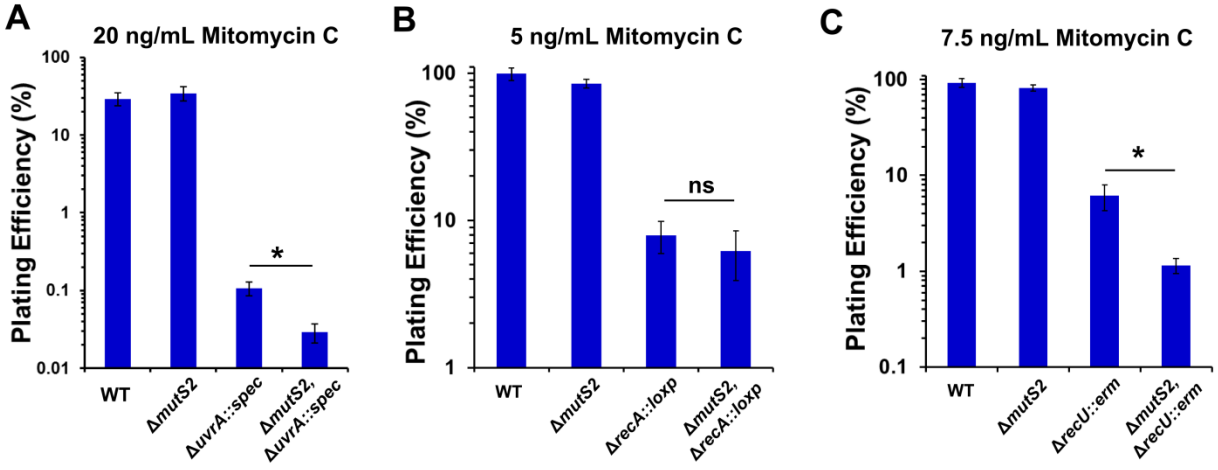

Figure 5.8 Δ*mutS2* sensitivity is independent of *uvrA* and *recU*, and shows no additive effects with *recA*. (A), (B), & (C) Plating efficiency assays performed as in Figure 2 with the indicated genotypes and the indicated concentrations of MMC. The Mann-Whitney U-test was used to determine statistical significance. ns: not significant; *: one-sided p-value < 0.05. Note that lower concentrations of MMC were used for this experiment and Δ*mutS2* cells do not show a phenotype.

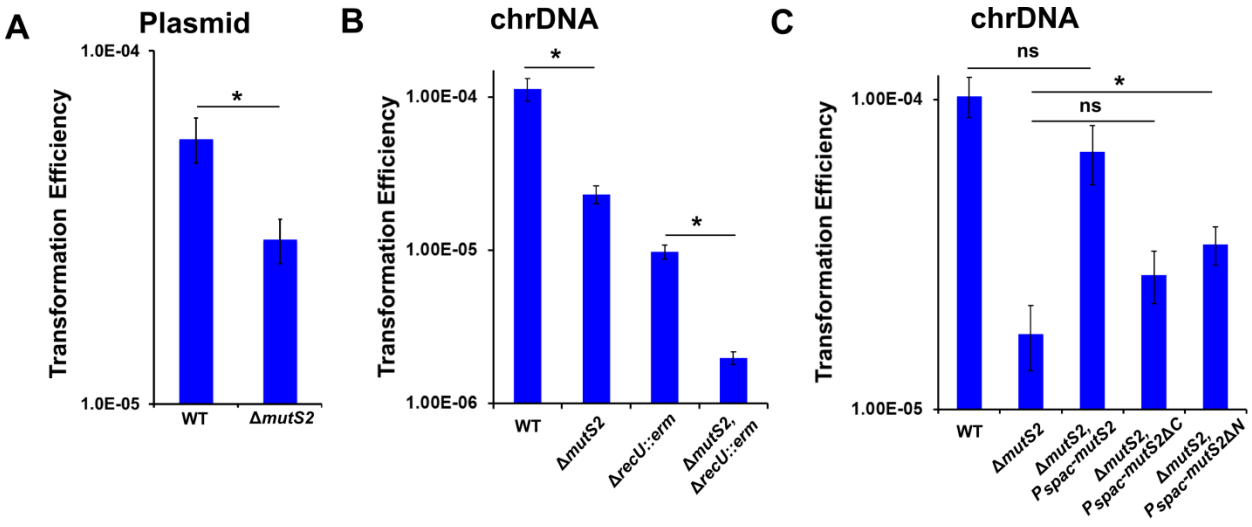

Figure 5.9 MutS2 is important for plasmid transformation, and *mutS2* deletion is additive with a *recU* deletion in chromosomal DNA transformation. (A) Transformation efficiency assay using plasmid DNA. **(B)** Transformation efficiency using chromosomal DNA. **(C)** Transformation efficiency assay using chromosomal DNA in the presence of 1 mM IPTG. Transformation efficiency is the ratio of transformants (CFUs) to viable cells (CFUs). The Mann-Whitney U-test was used to determine statistical significance. ns: not significant; *: two-sided p-value < 0.05.

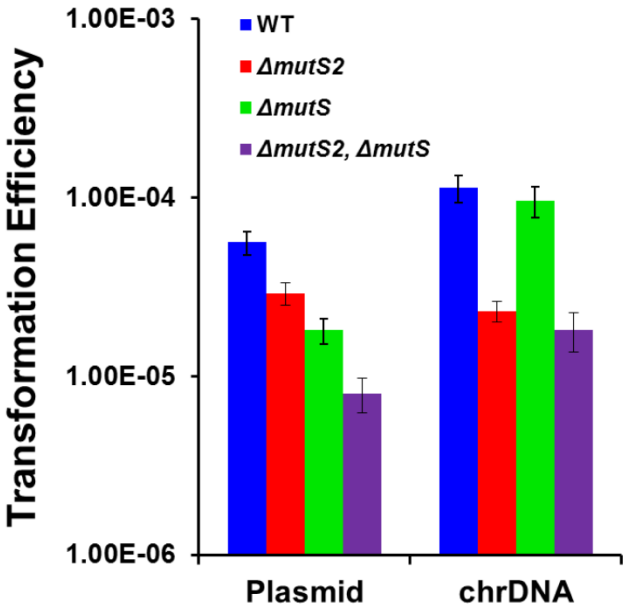

Figure 5.10 MutS and MutS2 have different roles in recombination. Transformation efficiency assays using chromosomal and plasmid DNA. Transformation efficiency is a ratio of

transformants (CFU) to viable cell (CFU). Transformation efficiencies for WT and Δ*mutS2* are the same as shown in Figure 5.

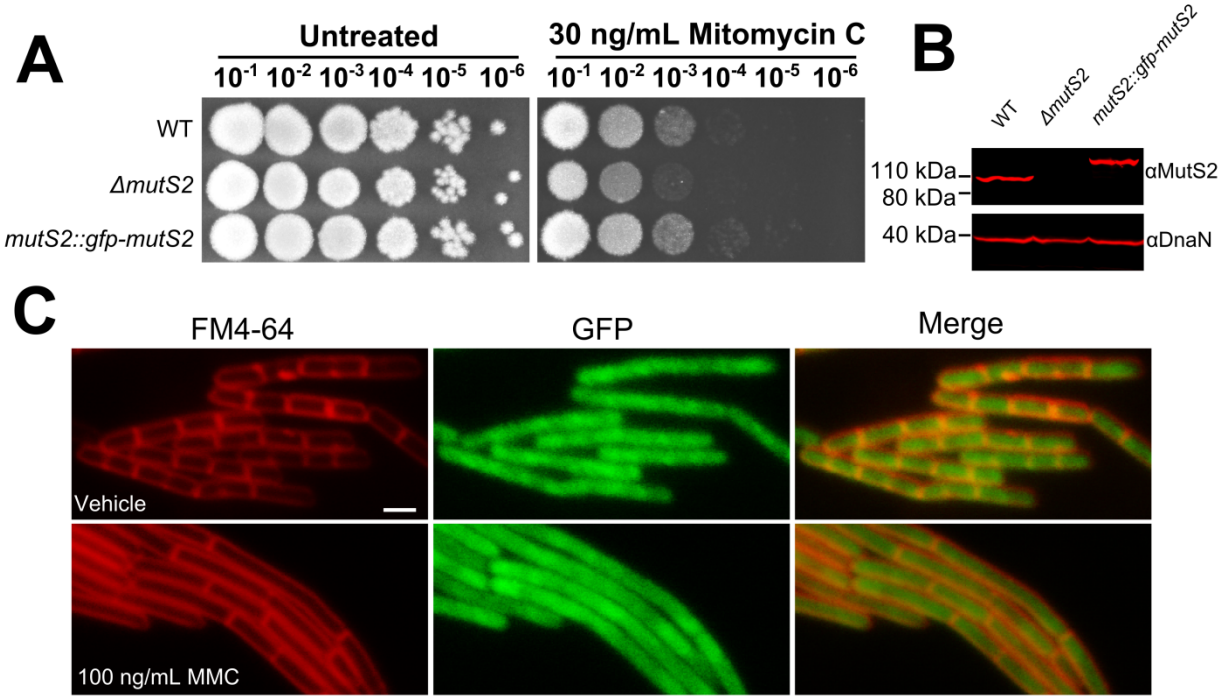

Figure 5.11 A functional GFP-MutS2 fusion has a diffuse cytosolic distribution. (A) A spot-titer assay showing that GFP fused to the N-terminus of MutS2 expressed from the native locus is functional. **(B)** Western blot using a MutS2 antibody shows that GFP-MutS2 is expressed and we do not detect degradative products indicating MutS2 is intact. **(C)** Fluorescence microscopy to visualize GFP-MutS2 under vehicle control, and 100 ng/mL Mitomycin C (MMC) treatment conditions (red: membranes stained with FM4-64; green: GFP-MutS2; scale bar is 2 μm).

Strain	Relevant genotype	Reference
PY79	WT	(62)
PEB11	*ΔmutSB*	This Work
PEB32	*mutSB::gfp-mutSB*	This Work
PEB43	*amyE::cat*	This Work
PEB112	*ΔmutL*	This Work
PEB118	*ΔmutSB, ΔmutL*	This Work
PEB125	*ΔrecU::erm*	This Work
PEB128	*ΔmutSB, ΔrecU::erm*	This Work
PEB204	*ΔrecA::erm*	This Work
PEB207	ΔmutSB, ΔrecA::erm	This Work
PEB214	*ΔrecA::loxP*	This Work
PEB215	*ΔmutSB, ΔrecA::loxP*	This Work
PEB218	*ΔmutS*	(27)
PEB247	*ΔxhlAB-xlyA*	This Work
PEB249	*ΔmutSB, ΔxhlAB-xlyA*	This Work
PEB251	*ΔxlyB-xlyA*	This Work
PEB254	*ΔmutSB, ΔxlyB-xlyA*	This Work
PEB295	*ΔuvrA::spec*	This Work
PEB298	*ΔmutSB, ΔuvrA::spec*	This Work
PEB410	*ΔmutSB, amyE::Pspac-mutSB*	This Work
PEB412	*ΔmutSB, amyE::Pspac-mutSB-ΔC*	This Work
PEB414	*ΔmutSB, amyE::Pspac-mutSB-ΔN*	This Work
PEB671	*ΔmutSB, ΔmutS*	This Work

Table 5.1 Strains used in this study.

Plasmid	Plasmid name	Reference
pDR244	pDR244	BGSC (ECE274)
pCas9	pCas9	(58); Addgene plasmid # 42876
pDR110	pDR110	A gift from David Rudner
pDR154	pDR154	A gift from David Rudner
pPB1	pMini-MAD-MutSB-up/down	This work
pPB3	pMini-MAD-GFP-MutS2	This work
pPB14	pET28b-10xHis-Smt3-MutS2	This work
pPB31	pMiniMad-mutL	This work
pPB41	pDR244-cas9	This work
pPB49	pPB41-CRISPR::PBSX	This work
pPB50	pPB49-PBSX-lysis recombination template	This work
pPB51	pPB49-PBSX-cure recombination template	This work

pPB105	pPB41-ΔspecR::camR	This work
pPB126	pDR110-MutS2	This work
pPB127	pDR110-MutS2-ΔC	This work
pPB128	pDR110-MutS2-ΔN	This work
pPB153	pDR244-Δcre	This work

Table 5.2 Plasmids used in this study.

Primer	Sequence
o3F	GCTAGCCGCATGCAAGCTAATTCG
o3R	ATGTATACCTCCTTAGTCGACTAAGCTTAATTGTTATC
oPEB5F	cccaggctttacactttatgcttccagatggatatcctgcctgacggtac
oPEB5R	aaatcactcatggccatactcccttgattgtgtgagcctccttacttaatcgtt g
oPEB6F	attaagtaaggaggctcacacaatcaagggagtatggccatgagtgatttttg
oPEB6R	cacagatgcgtaaggagaaaataccaacagatatataagaccaattaacaaaa agattcccgctg
oPEB7F	GGCTCACCGCGAACAGATTGGAGGTATGCAGCAAAAAGTATTATCAGCTCTTG AATTTC
oPEB7R	CAGTGGTGGTGGTGGTGGTGCTCGAttaTTATTTTAGTTCAACAACCGTAACG CCTGATC
oPEB16	TGAAAAGTTCTTCTCCTTTACTCATgattgtgtgagcctccttacttaatcgtt g
oPEB17	attaagtaaggaggctcacacaatcATGAGTAAAGGAGAAGAACTTTTCACTG GAG
oPEB18	CTTGGCCTTGTCCTTGACCTTCACCTTTGTATAGTTCATCCATGCCATGTGTA ATC
oPEB19	GGTGAAGGTCAAGGACAAGGCCAAGGACCAGGACGTGGTTACGCTTACCGCTC TGAGCTC
oPEB20	GAGCTCAGAGCGGTAAGCGTAACCACGTCCTGGTCCTTGGCCTTGTCCTTGAC CTTCACC
oPEB21	TGGTTACGCTTACCGCTCTGAGCTCGTGCAGCAAAAAGTATTATCAGCTCTTG
oPEB22	cacagatgcgtaaggagaaaataccGGATCTGTACTCCTGTTTGACCGG
oPEB56	ACCTCCAATCTGTTCGCGGTG
oPEB57	taaTCGAGCACCACCACCACCAC
oPEB65	CTGCATGTGTCAGAGGTTTTCAC
oPEB78	aatggatcaatgcctaccacccccgattcatcaccccgttttaatgtaatttc ttttg
oPEB79	attacattaaaacggggtgatgaatcgggggtggtaggcattgatc

oPEB114	ggtattttctccttacgcatctgtgc
oPEB115	ggaagcataaagtgtaaagcctggg
oPEB151	gctttacactttatgcttccaagcggtgctcccgattttcgat
oPEB152	atgcgtaaggagaaaatacctctccatacttggcatcacatacgcttc
oPEB174	ttcttccgacataaattgtgagac
oPEB175	atgtgaaagaagggagtttttgac
oPEB189	gagggaggaaaggcaggatacc
oPEB190	CGCCGTATCTGTGCTCTCTCTACC
oPEB201	acacctacatctgtattaacgaagcgactgttcttcgctttttcggtatc
oPEB202	GGTATCCTGCCTTTCCTCCCTCtctatttttttcctcctttatgttaccactaca
oPEB203	TAGAGAGAGCACAGATACGGCGaaataaaataagtttcaaatgatacaaaaggctgag
oPEB204	gtaatgataccgatgaaacgagagataaatatcacccgctccatacag
oPEB205	cttgtgttaaatgatgaggcattc
oPEB206	ggcgtaaacatcttttcatagctt
oPEB217	GAACCTCATTACGAATTCAGCATGC
oPEB218	GAATGGCGATTTTCGTTCGTGAATAC
oPEB229	agccggtgagcgtggTtcCcgcggtatcattgcagcactggg
oPEB230	tgcaatgataccgcgGgaAccacgctcaccggctccagattta
oPEB231	GAACCTCATTACGAATTCAGCATGCGCTATCTAGAGGGAAACCGTTGTGGGATCCCTATAGTGAGTCGTATTAATTTCGCGGGATCG
oPEB232	GCTGTAGGCATAGGCTTGGTTATG
oPEB233	GCATGCTGAATTCGTAATGAGGTTCGCTGTAGGCATAGGCTTGGTTATG
oPEB234	GTATTCACGAACGAAAATCGCCATTCCTAGCAGCACGCCATAGTGACTG
oPEB283	CGTGAGCTATTAAGCCGACCATTC
oPEB288	aaacATTGTTAGATACGTGGGATTCGTTCAAAGCg
oPEB289	aaaacGCTTTGAACGAATCCCACGTATCTAACAAT
oPEB290	GCATGCTGAATTCGTAATGAGGTTCcgacggactgggtatatctttcta
oPEB291	gctccgggatttttatggtctttgactctcactcctccttcacatgcag
oPEB292	ctgcatgtgaaggaggagtgagagtcaaagaccataaaaatcccggagc
oPEB293	GCATAACCAAGCCTATGCCTACAGCtattcgacacaggctgataaagac
oPEB294	agatcgtgaaggtacgctctttat
oPEB295	ctgctgaaaacctatgctgataaa
oPEB298	GCATGCTGAATTCGTAATGAGGTTCacacagaatcagtctcacacacct
oPEB299	ctccgggatttttatggtctttgactatcatctctccttttctttttttcataaataggtg
oPEB300	gaaaaaagaaaaggagagatgatagtcaaagaccataaaaatcccggagc
oPEB301	caagtcggaaaagttcgataatct

oPEB625	CTTAGTCGACTAAGGAGGTATACATgtgcagcaaaaagtattatcagctcttg aatttc
oPEB626	CCGAATTAGCTTGCATGCGGCTAGCttaTTATTTTAGTTCAACAACCGTAACG CCTGATC
oPEB627	CCGAATTAGCTTGCATGCGGCTAGCttaTTATTGCGTTTTCGGCTTTTCCGGT
oPEB628	CTTAGTCGACTAAGGAGGTATACATGTGAAACGCGACTTTAAGCCTGG
oPEB775	GCATGCTGAATTCGTAATGAGGTTCGAATGGCGATTTTCGTTCGTGAATAC

Table 5.3 Oligonucleotides used in this study.

Supplemental text

MutS2 purification and antibody production

10xHis-Smt3-MutS2 was expressed in NiCo 21 *E. coli* cells (NEB) from pPB14. Cultures (3, 1 L cultures) were grown shaking at 37°C to an $OD_{600} \approx 0.8$, and induced using 0.5 mM IPTG. Cultures were incubated at 37°C for another 3h after induction. Cells were pelleted via centrifugation at 8,000*g* for 25 minutes at 4°C. Cell pellets were re-suspended in 20 mL lysis buffer (50 mM Tris·HCl, pH 7.5, 300 mM NaCl, 5% (w/v) sucrose, 20 mM imidazole) per liter of culture. Cells were lysed via sonication on ice and lysates were clarified via centrifugation (Sorvall SS-34 rotor, 18,000 rpm for 45 minutes at 4°C). Lysate was loaded onto Ni^{2+}-NTA agarose (Qiagen), 1 mL bead volume per 1 L of culture after prewashing with 5 column volumes lysis buffer, and left on a rotator at 4°C for 1 hour. The column was then loaded and flow-through was collected. The column was washed 3 times with 8 column volumes of wash buffer (25 mM Tris·HCl, pH 7.5, 500 mM NaCl, 10% (v/v) glycerol, 30 mM imidazole). The column was then re-suspended in 15 mL digestion buffer (50 mM Tris·HCl, pH 7.5, 300 mM NaCl, 10% (v/v) glycerol, 1 mM DTT, 10 mM imidazole), and the 10xHis-Smt3 tag was removed using 6xHis-Ulp1-403-621, resulting in elution of untagged, full-length MutS2 from the column, which was collected as a flow-through fraction. The 15 mL sample was concentrated to 5 mL using a 50 kDa molecular weight cutoff concentrator (Millipore), and loaded onto a Hiload 16/60 superdex 200 prep grade gel filtration column (GE Healthcare) pre-equilibrated with GF buffer (50 mM Tris·HCl, pH 7.5, 150 mM NaCl), with a flow rate of 1 mL/min for 120 minutes. Peak fractions were pooled and diluted in HA dilution buffer resulting in a solution at the final

concentrations of 16.7 mM Tris·HCl, pH 7.5, 50 mM NaCl, 5 mM KPO_4, pH 7.4, 1 mM DTT, 10% (v/v) glycerol. The diluted sample was loaded onto a hydroxyapatite Bio-Scale Mini CHT Type 1 column (Bio-Rad) pre-equilibrated with HA start buffer (5 mM KPO_4, pH 7.4, 50 mM KCl, 1 mM DTT, 10% (v/v) glycerol). The column was washed with 10 column volumes HA start buffer. The column was then eluted using a linear phosphate gradient from 100% HA start buffer to 100% HA finish buffer (500 mM KPO_4, pH 7.4, 50 mM KCl, 1 mM DTT, 10 % (v/v) glycerol), over 20 column volumes. The peak fractions were pooled and desalted using a HiPrep 26/10 desalting column (GE Healthcare) pre-equilibrated with protein storage buffer (25 mM Tris·HCl, pH 7.5, 50 mM KCl, 10% (v/v) glycerol). Peak fractions were pooled, concentrated using a 50 kDa molecular weight cutoff concentrator (Millipore), frozen in liquid nitrogen, and stored at -80°C.

Purified MutS2 was sent to Covance for antibody production using the 77 day protocol using two different rabbits. The MutS2 antibody used throughout this study was from antiserum lot MI-1444-2.

Chromosomal DNA purification

Cell pellets (OD_{600} mL^{-1} ≈ 4-8) were re-suspended in 200 µL lysis buffer (50 mM Tris·HCl, pH 8.0, 10 mM EDTA, pH 8.0, 1% Triton X-100, 0.5 mg/mL RNase A, 20 mg/mL lysozyme) and incubated at 37 °C for 30 minutes. SDS and protease K were added to a final concentration of 1% and 1.3 mg/mL, respectively and samples were incubated at 55-65°C for 30 minutes. Then, 600 µL of PB buffer were added and the sample was added to a silica spin-column (Epoch Life Sciences) and centrifuged at 13,000*g* for 1 min. The column was washed with 500 µL PB buffer, then 750 µL PE buffer. Finally columns were eluted with 100 µL ddH_2O.

Plasmid construction

All plasmids were constructed via Gibson Assembly (59). All primer sequences used for plasmid construction are listed in Supplementary Table 3 (Table S3). All plasmid clones were sequenced at the University of Michigan Sequencing core facility to verify the sequence of the DNA insert(s).

pPB1 was constructed using Gibson Assembly of the following three DNA amplicons: 1) the pMini-MAD vector, amplified with primers oPEB114/oPEB115; 2) a 505 bp fragment upstream of *mutS2*, amplified using oPEB5F/oPEB5R; 3) a 505 bp fragment downstream of

mutS2 amplified using oPEB6F/oPEB6R. The resulting construct contained an in-frame deletion of the *mutS2* open reading frame (ORF) in the pMini-MAD vector.

pPB3 was constructed using Gibson Assembly of a 60 bp annealed dsDNA fragment, using oPEB19/oPEB20 and the following four PCR amplicons: 1) the pMini-MAD vector, amplified with primers oPEB114/oPEB115; 2) a 505 bp fragment upstream of *mutS2*, amplified with oPEB5F/oPEB16; 3) *gfp-mut3-A206K* ORF, amplified using oPEB17/oPEB18; 4) a 621 bp fragment of the *mutS2* N-terminal coding region, amplified using oPEB21/oPEB22. The resulting construct contained an in-frame insertion of *gfp-mut3-A206K* with a 20 amino acid flexible linker fused to the coding region of *mutS2* in the pMini-MAD vector (27).

pPB14 was constructed using Gibson Assembly of the following two PCR amplicons: 1) The pET28b-10xHis-Smt3 vector, amplified using oPEB56/oPEB57; 2) the MutS2 open reading frame with the GTG start codon replaced with ATG was amplified using oPEB7F/oPEB7R. The resulting vector contained a 10xHis-Smt3-MutS2 fusion protein that was under IPTG inducible expression.

pPB31 was constructed using Gibson Assembly of the following three PCR amplicons: 1) the pMini-MAD vector, amplified with primers oPEB114/oPEB115; 2) a 698 bp fragment upstream of *mutL*, amplified using oPEB151/oPEB78; 3) a 711 bp fragment downstream of *mutL*, amplified using oPEB79/oPEB152. The resulting construct contained an in-frame deletion of the *mutL* ORF in the pMini-MAD vector.

pPB41 was constructed by amplifying portions of pDR244 (obtained from the BGSC) and pCas9 (58) (purchased from Addgene). pPB41 was constructed using Gibson Assembly of the following three PCR amplicons: 1) a part of the pDR244 vector was amplified using oPEB229/oPEB231; 2) a second part of the pDR244 vector was amplified using oPEB218/oPEB230; 3) the Cas9/CRISPR array was amplified using oPEB233/oPEB234. The resulting construct consisted of pDR244 with its two BsaI sites mutated and the *cre* recombinase deleted, and in its place Cas9/CRISPR was inserted.

pPB49 was constructed via restriction digest and ligation. The vector pPB41 was digested with BsaI-HF (NEB) and CIP (NEB) treated with alkaline phosphatase. The proto-spacer was generated by annealing oligos oPEB288/oPEB289 in annealing buffer (see section on editing plasmid construction), and phosphorylated using T_4 polynucleotide kinase (NEB). The vector

and proto-spacer ligated together using T_4 DNA ligase. The resulting construct consisted of pPB41 with the BsaI sites removed and a spacer targeting PBSX inserted into the CRISPR array.

pPB50 was constructed using Gibson Assembly of the following four PCR amplicons: 1) the pPB41 vector was amplified using oPEB217/oPEB218; 2) the Cas9/CRISPR array containing the PBSX spacer was amplified from pPB49 using oPEB232/oPEB234; 3) a 570 bp fragment upstream of *xhlA* (the upstream portion of the editing template) was amplified using oPEB290/oPEB291; 4) a 690 bp fragment downstream of *xlyA* (the downstream portion of the editing template) was amplified using oPEB292/oPEB293. The resulting construct consists of pPB49 with the *ΔxhlABxlyA* editing template added next to Cas9 (see Fig S1).

pPB51 was constructed using Gibson Assembly of the following four PCR amplicons: 1) the pPB41 vector was amplified using oPEB217/oPEB218; 2) the Cas9/CRISPR array containing the PBSX spacer was amplified from pPB49 using oPEB232/oPEB234; 3) a 725 bp fragment upstream of *xlyBA* (the upstream portion of the editing template) was amplified using oPEB298/oPEB299; 4) a 690 bp fragment downstream of *xlyA* (the downstream portion of the editing template) was amplified using oPEB293/oPEB300. The resulting construct consists of pPB49 with the *ΔPBSX* (*xlyB* through *xylA*) editing template added next to Cas9 (see Fig S1).

pPB105, although not utilized in this study, was constructed to allow for use of the CRISPR/Cas9 genome editing system using a chloramphenicol resistance marker instead of the spectinomycin resistance marker. pPB105 was constructed using Gibson Assembly of the following two PCR amplicons: 1) the pPB41 vector without the spectinomycin resistance cassette was amplified using oPEB549/oPEB550; 2) the chloramphenicol resistance marker was amplified from pBGSC6 (*Bacillus* Stock Center) using oPEB65/oPEB283. The resulting vector consists of pPB41 with the spectinomycin resistance cassette replaced with a chloramphenicol resistance cassette.

pPB126 was constructed using Gibson Assembly of the following two PCR amplicons: 1) the pDR110 vector (61) was amplified using oPEB3F/oPEB3R; the *mutS2* ORF was amplified using oPEB625/oPEB626. The resulting construct consists of *mutS2* under the control of the P_{spac} promoter in pDR110.

pPB127 was constructed using Gibson Assembly of the following two PCR amplicons: 1) the pDR110 vector was amplified using oPEB3F/oPEB3R; the *mutS2ΔC* ORF (amino acids 1-

635) was amplified using oPEB625/oPEB627. The resulting construct consists of *mutS2ΔC* under the control of the P_{spac} promoter in pDR110.

pPB128 was constructed using Gibson Assembly of the following two PCR amplicons: 1) the pDR110 vector was amplified using oPEB3F/oPEB3R; the *mutS2ΔN* ORF (the start codon and amino acids 636-785) was amplified using oPEB626/oPEB628. The resulting construct consists of *mutS2ΔN* under the control of the P_{spac} promoter in pDR110.

pPB153 was constructed using Gibson Assembly of a single PCR amplicon: pDR244 was amplified using oPEB217/oPEB775. The resulting construct consists of pDR244 without *cre* recombinase.

Strain construction

All *B. subtilis* strains are isogenic derivatives of PY79 (62) and were generated by transforming cells with a PCR product, plasmid DNA, or genomic DNA via natural competence (55).

PEB11 was generated by transforming PY79 with pPB1 plating on LB agar plates containing erythromycin and incubating at 37°C overnight, as the plasmid contains a temperature sensitive origin that is inactive at 37°C, which forces single crossover integration of the plasmid with the chromosome. Isolates were colony purified by re-streaking on LB agar plates with erythromycin and incubating at 37°C overnight. Isolates were then grown in 2 mL liquid LB at the permissive temperature (room temperature) for 10-14 hours. Cultures were back-diluted 100 fold and grown at the permissive temperature for 10-14 hours four times. Cultures were then back-diluted 100 fold and grown at 37°C until an $OD_{600} \approx 1$. Cultures were serially diluted and 100 µL of the 10^{-5} dilution were plated on LB agar and incubated at 37°C overnight. Single colonies were then colony purified and tested for sensitivity to erythromycin to screen for plasmid loss by re-streaking on LB agar plates and LB agar plates containing erythromycin. Erythromycin sensitive clones were further screened for loss of the *mutS2* ORF using PCR with primers oPEB5F/oPEB6R.

PEB32 was constructed as PEB11 with the exception of using pPB3 as the plasmid, and using PCR primers oPEB5F/oPEB22 to screen for GFP insertion at the *mutS2* locus.

PEB43 was constructed by transforming PY79 with pDR154 via double-crossover recombination at the *amyE* locus. Double crossover recombination was verified by screening for an inability to utilize starch (55).

PEB112 was constructed as PEB11 with the exception of using pPB31 as the plasmid, and using PCR primers oPEB151/oPEB152 were used to screen for the loss of the *mutL* ORF.

PEB118 was constructed as PEB112 using PEB11 as the parent strain instead of PY79.

PEB125 was constructed by transforming PY79 using genomic DNA from the *B. subtilis* knockout library strain BKE22310. Clones were verified via PCR genotyping at the *recU* locus using primers oPEB174/oPEB175.

PEB128 was constructed as described for PEB125 using PEB11 as the parent strain.

PEB204 was constructed by transforming PY79 with a PCR product containing 871 bp upstream of *recA*, a erythromycin resistance cassette from the *Bacillus* knockout library, and 1052 bp downstream of *recA* via double-crossover recombination. This PCR product was generated via overlap PCR using oPEB201/oPEB204, and the following three PCR amplicons as templates: 1) 871 bp upstream of *recA* were amplified using oPEB201/oPEB202; 2) the erythromycin resistance cassette was amplified using oPEB189/oPEB190; 3) 1052 bp downstream of *recA* were amplified using oPEB203/oPEB204. Clones were genotyped for the allelic replacement at the *recA* locus using PCR primers oPEB205/206.

PEB207 was constructed as PEB204, except PEB11 was used as the parent strain.

PEB214 was constructed by transforming PEB204 with pDR244 and plating on LB agar plates containing spectinomycin and incubating at 30°C overnight (the permissive temperature for the temperature sensitive origin of replication). Transformants were then colony purified by re-streaking on LB agar containing spectinomycin and incubating at 30°C overnight. The plasmid was evicted by re-streaking on LB agar plates and incubating at 45°C overnight. Isolates were screened for loss of the plasmid and the erythromycin cassette by re-streaking on LB, LB containing spectinomycin, and LB containing erythromycin agar plates. Isolates were further genotyped at the *recA* locus using PCR primers oPEB205/oPEB206.

PEB215 was constructed as was PEB214, except PEB207 was used as the parent strain.

PEB218 was saved from JSL 281 (27).

PEB247 & PEB249 were constructed via CRISPR/Cas9 genome editing described herein, by transforming PY79 and PEB11, respectively, with pPB50. Clones were genotyped at the *xhlABxlyA* loci using PCR primers oPEB294/oPEB295.

PEB251 & PEB254 were constructed via CRISPR/Cas9 genome editing described herein, by transforming PY79 and PEB11, respectively, with pPB51. Clones were genotyped at the *PBSX* locus using PCR primers oPEB295/oPEB301.

PEB295 was constructed by transforming PY79 with genomic DNA from LAS409 (32, 44). Loss of *uvrA* was verified by testing for sensitivity to UV (265 nm) light.

PEB298 was constructed by transforming PEB11 with genomic DNA from LAS409. Loss of *uvrA* was verified by testing for sensitivity to UV (265 nm) light.

PEB410 was constructed by transforming PEB11 with pPB126 via double-crossover recombination at the *amyE* locus. Double crossover recombination was verified by screening for an inability to utilize starch.

PEB412 was constructed by transforming PEB11 with pPB127 via double-crossover recombination at the *amyE* locus. Double crossover recombination was verified by screening for an inability to utilize starch.

PEB414 was constructed by transforming PEB11 with pPB128 via double-crossover recombination at the *amyE* locus. Double crossover recombination was verified by screening for an inability to utilize starch.

PEB671 was constructed as described for PEB11 using PEB218 as the parent strain.

References

1. **Friedberg EC, Walker GC, Siede W, Wood RD, Schultz RA, Ellenberger T.** 2006. DNA Repair and Mutagenesis: Second Edition. American Society for Microbiology, Washington, DC.
2. **Chen I, Dubnau D.** 2004. DNA uptake during bacterial transformation. Nat Rev Microbiol **2:**241-249.
3. **Lenhart JS, Schroeder JW, Walsh BW, Simmons LA.** 2012. DNA Repair and Genome Maintenance in Bacillus subtilis. Microbiology and molecular biology reviews : MMBR **76:**530-564.
4. **Ayora S, Carrasco B, Cardenas PP, Cesar CE, Canas C, Yadav T, Marchisone C, Alonso JC.** 2011. Double-strand break repair in bacteria: a view from Bacillus subtilis. FEMS Microbiol Rev.
5. **Weller GR, Kysela B, Roy R, Tonkin LM, Scanlan E, Della M, Devine SK, Day JP, Wilkinson A, d'Adda di Fagagna F, Devine KM, Bowater RP, Jeggo PA, Jackson SP, Doherty AJ.** 2002. Identification of a DNA nonhomologous end-joining complex in bacteria. Science **297:**1686-1689.
6. **Pitcher RS, Brissett NC, Doherty AJ.** 2007. Nonhomologous end-joining in bacteria: a microbial perspective. Annu Rev Microbiol **61:**259-282.
7. **Matthews LA, Simmons LA.** 2014. Bacterial Non-Homologous End Joining Requires Teamwork. J Bacteriol doi:10.1128/JB.02042-14.
8. **Rothstein R, Gangloff S.** 1995. Hyper-recombination and Bloom's syndrome: microbes again provide clues about cancer. Genome Res **5:**421-426.
9. **Radman M.** 1989. Mismatch repair and the fidelity of genetic recombination. Genome **31:**68-73.
10. **Evans E, Alani E.** 2000. Roles for mismatch repair factors in regulating genetic recombination. Mol Cell Biol **20:**7839-7844.
11. **Myung K, Datta A, Chen C, Kolodner RD.** 2001. SGS1, the Saccharomyces cerevisiae homologue of BLM and WRN, suppresses genome instability and homeologous recombination. Nat Genet **27:**113-116.
12. **Magner DB, Blankschien MD, Lee JA, Pennington JM, Lupski JR, Rosenberg SM.** 2007. RecQ promotes toxic recombination in cells lacking recombination intermediate-removal proteins. Mol Cell **26:**273-286.
13. **Rayssiguier C, Dohet C, Radman M.** 1991. Interspecific recombination between Escherichia coli and Salmonella typhimurium occurs by the RecABCD pathway. Biochimie **73:**371-374.
14. **Rayssiguier C, Thaler DS, Radman M.** 1989. The barrier to recombination between *Escherichia coli* and *Salmonella typhimurium* is disrupted in mismatch-repair mutants. Nature **342:**396-401.
15. **Calmann MA, Evans JE, Marinus MG.** 2005. MutS inhibits RecA-mediated strand transfer with methylated DNA substrates. Nucleic Acids Research **33:**3591-3597.
16. **Worth L, Jr., Clark S, Radman M, Modrich P.** 1994. Mismatch repair proteins MutS and MutL inhibit RecA-catalyzed strand transfer between diverged DNAs. Proc Natl Acad Sci U S A **91:**3238-3241.
17. **Tham KC, Hermans N, Winterwerp HH, Cox MM, Wyman C, Kanaar R, Lebbink JH.** 2013. Mismatch repair inhibits homeologous recombination via coordinated directional unwinding of trapped DNA structures. Mol Cell **51:**326-337.

18. **Moreira D, Philippe H.** 1999. Smr: a bacterial and eukaryotic homologue of the C-terminal region of the MutS2 family. Trends Biochem Sci **24:**298-300.
19. **Pinto AV, Mathieu A, Marsin S, Veaute X, Ielpi L, Labigne A, Radicella JP.** 2005. Suppression of homologous and homeologous recombination by the bacterial MutS2 protein. Mol Cell **17:**113-120.
20. **Fukui K, Kosaka H, Kuramitsu S, Masui R.** 2007. Nuclease activity of the MutS homologue MutS2 from Thermus thermophilus is confined to the Smr domain. Nucleic Acids Res **35:**850-860.
21. **Fukui K, Masui R, Kuramitsu S.** 2004. Thermus thermophilus MutS2, a MutS paralogue, possesses an endonuclease activity promoted by MutL. J Biochem **135:**375-384.
22. **Fukui K, Nakagawa N, Kitamura Y, Nishida Y, Masui R, Kuramitsu S.** 2008. Crystal structure of MutS2 endonuclease domain and the mechanism of homologous recombination suppression. J Biol Chem **283:**33417-33427.
23. **Rossolillo P, Albertini AM.** 2001. Functional analysis of the Bacillus subtilis y shD gene, a mutS paralogue. Mol Gen Genet **264:**809-818.
24. **Kang J, Huang S, Blaser MJ.** 2005. Structural and functional divergence of MutS2 from bacterial MutS1 and eukaryotic MSH4-MSH5 homologs. J Bacteriol **187:**3528-3537.
25. **Simmons LA, Davies BW, Grossman AD, Walker GC.** 2008. Beta clamp directs localization of mismatch repair in Bacillus subtilis. Mol Cell **29:**291-301.
26. **Lenhart JS, Pillon MC, Guarne A, Simmons LA.** 2013. Trapping and visualizing intermediate steps in the mismatch repair pathway in vivo. Mol Microbiol **90:**680-698.
27. **Lenhart JS, Sharma A, Hingorani MM, Simmons LA.** 2013. DnaN clamp zones provide a platform for spatiotemporal coupling of mismatch detection to DNA replication. Mol Microbiol **87:**553-568.
28. **Dupes NM, Walsh BW, Klocko AD, Lenhart JS, Peterson HL, Gessert DA, Pavlick CE, Simmons LA.** 2010. Mutations in the Bacillus subtilis beta clamp that separate its roles in DNA replication from mismatch repair. J Bacteriol **192:**3452-3463.
29. **Moeller R, Setlow P, Horneck G, Berger T, Reitz G, Rettberg P, Doherty AJ, Okayasu R, Nicholson WL.** 2008. Roles of the major, small, acid-soluble spore proteins and spore-specific and universal DNA repair mechanisms in resistance of Bacillus subtilis spores to ionizing radiation from X rays and high-energy charged-particle bombardment. J Bacteriol **190:**1134-1140.
30. **Moeller R, Vlasic I, Reitz G, Nicholson WL.** 2012. Role of altered rpoB alleles in Bacillus subtilis sporulation and spore resistance to heat, hydrogen peroxide, formaldehyde, and glutaraldehyde. Archives of microbiology doi:10.1007/s00203-012-0811-4.
31. **Acharya S, Wilson T, Gradia S, Kane MF, Guerrette S, Marsischky GT, Kolodner R, Fishel R.** 1996. hMSH2 forms specific mispair-binding complexes with hMSH3 and hMSH6. Proc Natl Acad Sci U S A **93:**13629-13634.
32. **Walsh BW, Bolz SA, Wessel SR, Schroeder JW, Keck JL, Simmons LA.** 2014. RecD2 helicase limits replication fork stress in Bacillus subtilis. J Bacteriol **196:**1359-1368.
33. **Iyer VN, Szybalski W.** 1963. A molecular mechanism of mitomycin action: Linking of complementary DNA strands. Proc Natl Acad Sci U S A **50:**355-362.

34. **Borowyborowski H, Lipman R, Chowdary D, Tomasz M.** 1990. Duplex oligodeoxyribonucleotides cross-linked by mitomycin-c at a single site - synthesis, properties, and cross-link reversibility. Biochemistry **29:**2992-2999.
35. **Bizanek R, McGuinness BF, Nakanishi K, Tomasz M.** 1992. Isolation and structure of an intrastrand cross-link adduct of mitomycin-c and DNA. Biochemistry **31:**3084-3091.
36. **Tomasz M, Chowdary D, Lipman R, Shimotakahara S, Veiro D, Walker V, Verdine GL.** 1986. Reaction of DNA with chemically or enzymatically activated mitomycin-c - isolation and structure of the major covalent adduct. Proceedings of the National Academy of Sciences of the United States of America **83:**6702-6706.
37. **Au N, Kuester-Schoeck E, Mandava V, Bothwell LE, Canny SP, Chachu K, Colavito SA, Fuller SN, Groban ES, Hensley LA, O'Brien TC, Shah A, Tierney JT, Tomm LL, O'Gara TM, Goranov AI, Grossman AD, Lovett CM.** 2005. Genetic composition of the Bacillus subtilis SOS system. J Bacteriol **187:**7655-7666.
38. **Goranov AI, Kuester-Schoeck E, Wang JD, Grossman AD.** 2006. Characterization of the global transcriptional responses to different types of DNA damage and disruption of replication in Bacillus subtilis. J Bacteriol **188:**5595-5605.
39. **Okamoto K, Mudd JA, Marmur J.** 1968. Conversion of bacillius subtilis DNA to phage DNA following mitomycin c induction. Journal of Molecular Biology **34:**429-&.
40. **Okamoto K, Mudd JA, Mangan J, Huang WM, Subbaiah TV, Marmur J.** 1968. Properties of defective phage of bacillus subtilis. Journal of Molecular Biology **34:**413-&.
41. **Krogh S, Jorgensen ST, Devine KM.** 1998. Lysis genes of the Bacillus subtilis defective prophage PBSX. Journal of Bacteriology **180:**2110-2117.
42. **Dronkert ML, Kanaar R.** 2001. Repair of DNA interstrand cross-links. Mutat Res **486:**217-247.
43. **Noll DM, Mason TM, Miller PS.** 2006. Formation and repair of interstrand cross-links in DNA. Chem Rev **106:**277-301.
44. **Smith BT, Grossman AD, Walker GC.** 2002. Localization of UvrA and effect of DNA damage on the chromosome of Bacillus subtilis. Journal of Bacteriology **184:**488-493.
45. **Damke PP, Dhanaraju R, Marsin S, Radicella JP, Rao DN.** 2015. The nuclease activities of both the Smr domain and an additional LDLK motif are required for an efficient anti-recombination function of Helicobacter pylori MutS2. Mol Microbiol **96:**1240-1256.
46. **McGregor N, Ayora S, Sedelnikova S, Carrasco B, Alonso JC, Thaw P, Rafferty J.** 2005. The structure of Bacillus subtilis RecU Holliday junction resolvase and its role in substrate selection and sequence-specific cleavage. Structure **13:**1341-1351.
47. **Ayora S, Carrasco B, Cardenas PP, Cesar CE, Canas C, Yadav T, Marchisone C, Alonso JC.** 2011. Double-strand break repair in bacteria: a view from Bacillus subtilis. FEMS Microbiol Rev **35:**1055-1081.
48. **Kidane D, Ayora S, Sweasy JB, Graumann PL, Alonso JC.** 2012. The cell pole: the site of cross talk between the DNA uptake and genetic recombination machinery. Crit Rev Biochem Mol Biol **47:**531-555.
49. **Liao Y, Schroeder JW, Gao B, Simmons LA, Biteen JS.** 2015. Single-molecule motions and interactions in live cells reveal target search dynamics in mismatch repair. Proc Natl Acad Sci U S A doi:10.1073/pnas.1507386112.

50. **Kidane D, Sanchez H, Alonso JC, Graumann PL.** 2004. Visualization of DNA double-strand break repair in live bacteria reveals dynamic recruitment of Bacillus subtilis RecF, RecO and RecN proteins to distinct sites on the nucleoids. Mol Microbiol **52:**1627-1639.
51. **Altenbuchner J.** 2016. Editing of the Bacillus subtilis Genome by the CRISPR-Cas9 System. Appl Environ Microbiol **82:**5421-5427.
52. **Westbrook AW, Moo-Young M, Chou CP.** 2016. Development of a CRISPR-Cas9 Tool Kit for Comprehensive Engineering of Bacillus subtilis. Applied and Environmental Microbiology **82:**4876-4895.
53. **Fukui K, Takahata Y, Nakagawa N, Kuramitsu S, Masui R.** 2007. Analysis of a nuclease activity of catalytic domain of Thermus thermophilus MutS2 by high-accuracy mass spectrometry. Nucleic Acids Res **35:**e100.
54. **Klocko AD, Crafton KM, Walsh BW, Lenhart JS, Simmons LA.** 2010. Imaging mismatch repair and cellular responses to DNA damage in Bacillus subtilis. Journal of visualized experiments : JoVE doi:10.3791/1736.
55. **Harwood CR, Cutting SM.** 1990. Modern microbiological methods: Molecular biological methods for *Bacillus*.
56. **Hall BM, Ma CX, Liang P, Singh KK.** 2009. Fluctuation analysis CalculatOR: a web tool for the determination of mutation rate using Luria-Delbruck fluctuation analysis. Bioinformatics **25:**1564-1565.
57. **Bolz NJ, Lenhart JS, Weindorf SC, Simmons LA.** 2012. Residues in the N-terminal domain of MutL required for mismatch repair in Bacillus subtilis. Journal of Bacteriology **194:**5361-5367.
58. **Jiang WY, Bikard D, Cox D, Zhang F, Marraffini LA.** 2013. RNA-guided editing of bacterial genomes using CRISPR-Cas systems. Nature Biotechnology **31:**233-239.
59. **Gibson DG.** 2011. Enzymatic assembly of overlapping DNA fragments, p 349-361. *In* Voigt C (ed), Synthetic Biology, Pt B: Computer Aided Design and DNA Assembly, vol 498. Elsevier Academic Press Inc, San Diego.
60. **Klocko AD, Schroeder JW, Walsh BW, Lenhart JS, Evans ML, Simmons LA.** 2011. Mismatch repair causes the dynamic release of an essential DNA polymerase from the replication fork. Mol Microbiol **82:**648-663.
61. **Rokop ME, Auchtung JM, Grossman AD.** 2004. Control of DNA replication initiation by recruitment of an essential initiation protein to the membrane of Bacillus subtilis. Molecular Microbiology **52:**1757-1767.
62. **Youngman P, Perkins JB, Losick R.** 1984. Construction of a cloning site near one end of TN917 into which foreign DNA may be inserted without affecting transposition in Bacillus subtilis or expression of the transposon-bourne ERM gene. Plasmid **12:**1-9.

CHAPTER VI

Future research and concluding remarks

Introduction

The DNA damage response is a cellular solution to a fundamental problem in biology—reproduction requires DNA replication, which can be prevented by DNA modifications called DNA damage. A major facet of the DNA damage response is the coordination of DNA replication and cell division (1, 2). Regulation of cell division in response to DNA damage was initially identified in *Escherichia coli*, and subsequent studies described in molecular detail how the process occurs (2). The application of the models developed in *E. coli*, however, has proved difficult as studies in numerous bacterial species have demonstrated that the cell division checkpoint exists, yet the mechanisms are not conserved. Although cell division inhibitors have been identified in several bacteria (3-8), the rest of the pathway remains unclear in these organisms. In Chapter II, I used forward genetics to identify the proteases responsible for removing the cell division inhibitor in *Bacillus subtilis*. In Chapter III, I demonstrate that a gene of unknown function helps to establish a threshold of cell division inhibitor required for establishing the cell cycle checkpoint. In addition, in Chapters IV and V, I describe roles for three genes involved in DNA repair. Prior to my studies it was not clear how organisms that use membrane bound cell division inhibitors would control the cell cycle checkpoint. Further, by identifying multiple mechanisms for regulating establishment of the checkpoint, my work underscores the complexity of this process. As discussed in Chapter I, the DNA damage checkpoint will be a function of DNA damage and the rate of cell division. Given that these factors will be highly variable depending on the environment and the organism, it should be no surprise that the mechanisms of the DNA damage checkpoint would also vary considerably. Thus, my study of the DNA damage response in *B. subtilis* has provided important insight into

this complex process, while also providing the basis for several new areas of research that are discussed below.

Checkpoint recovery proteases

The identification of the *B. subtilis* DNA damage checkpoint recovery mechanism is an important step toward understanding the mechanisms by which cell division and DNA replication are coupled. My studies of the proteases DdcP (YlbL) and CtpA presented in Chapter II led to the discovery that these proteases relieve the DNA damage-dependent cell cycle checkpoint. Both proteases degrade the cell division inhibitor YneA, resulting in removal of the protein that enforces the checkpoint, and therefore allowing cell division to proceed. Still, exactly how DdcP and CtpA recognize their substrate, YneA, is still not clear and warrants further exploration.

Substrate recognition is a critical aspect of protease function (9, 10). DdcP and CtpA are excellent model proteases for understanding how proteases with PDZ domains recognize their substrates. CtpA is similar to Tail-specific protease (Tsp) in *E. coli* which recognizes the C-terminus of its substrate through the PDZ domain (11). Substrate binding through the PDZ domain is most likely how CtpA recognizes YneA. I showed in Chapter III that the PDZ domain of CtpA is important for function **(Fig 3.14)**. In addition, a previous study found that a D97A mutation in the C-terminus of YneA resulted in a stabilized variant of YneA (12). Interestingly, CtpA from *Staphylococcus aureus* (*Sa*-CtpA) was found to negatively regulate the SOS-dependent cell division inhibitor SosA (8). The authors found the connection between *Sa*-CtpA and SosA because deletion of ten amino acids at the C-terminus of SosA resulted in a hyperactive variant, leading to the suggestion that *Sa*-CtpA recognizes the C-terminus of SosA (8). The hypothesis that *B. subtilis* CtpA recognizes YneA at its C-terminus can be tested by assaying YneA stability using C-terminal truncations and the D97A variant in cells lacking *ddcP* and in the presence or absence of CtpA. The model could be tested *in vitro* as well by purifying YneA variants that were stabilized and testing for CtpA protease activity. The requirement of the PDZ domain of CtpA could also be tested *in vitro* by examining protease activity of CtpAΔPDZ. Together, these experiments would test the hypothesis that CtpA uses its PDZ domain to recognize the C-terminus of YneA.

Although there is a very clear direction for CtpA, there is no clear hypothesis for how DdcP recognizes YneA. The protease domain of DdcP is similar to that of Lon proteases. Lon proteases are energy-dependent proteases that utilize an ATPase domain to drive substrate unfolding and proteolysis (13). In Chapter III DdcP was shown to be membrane anchored with an extracellular protease domain. Given that ATP is exceedingly low or absent outside the cell, it is no surprise that DdcP does not have an ATPase domain, and instead has a PDZ domain. The PDZ domain of DdcP is not required for function in the DNA damage checkpoint, as deletion of the PDZ domain had no effect on DNA damage sensitivity **(Fig 3.14)**. Intriguingly, a BLAST search revealed that the PDZ domain of DdcP is most similar to the one found in DegS **(Fig 3.14)**. The PDZ domain of DegS acts as an allosteric inhibitor of protease activity and was also found to be dispensable for function *in vivo* (14-16). For DdcP it is not clear what function, if any, the PDZ domain serves. To better understand how DdcP recognizes YneA two general strategies should be employed. First, a purification scheme yielding active DdcP should be devised. Optimizing purification of full length DdcP from *B. subtilis* should be the starting point. With active DdcP purified, detailed hypotheses about substrate recognition could be examined *in vitro*. Second, the stability of several YneA truncation variants should be measured in the presence and absence of DdcP to determine the critical parts of the substrate. Together, these experiments have the potential to elucidate how a Lon protease is able to function without an ATPase domain to degrade protein substrates.

DNA damage checkpoint antagonist

The discovery of a DNA damage checkpoint antagonist marks an exciting advance in the bacterial DNA damage response field that simultaneously opens new avenues of research. DdcA along with the checkpoint recovery proteases, DdcP and CtpA, set the threshold of YneA required for establishing the cell cycle checkpoint. It is still unclear whether DdcA acts on YneA or another cellular target. To address the gap in our understanding of DdcA function, parallel approaches should be employed to test each hypothesis.

The observation that DdcA and the checkpoint recovery proteases have YneA-dependent phenotypes, yet they are not functionally interchangeable, may suggest that DdcA acts on a protein other than YneA. DdcA contains a tetratrichopeptide repeat (TPR) domain, which could

mediate protein-protein interactions (17). I attempted to find a binding partner of DdcA using a bacterial two-hybrid assay. I screened several candidate proteins that are known to be involved in cell division for interaction with DdcA without obtaining a positive result. To more rigorously test the hypothesis that DdcA interacts with another protein, two methods should be employed. First, a tandem-affinity purification tag should be fused to DdcA and a pull-down assay should be optimized. Second, full-length DdcA, DdcA containing only the TPR domain, and DdcA lacking the TPR domain should be used in a genome-wide bacterial two-hybrid assay. DdcA likely interacts with other cellular proteins, and dissecting the entire network of interactions could help elucidate the function of DdcA in the DNA damage checkpoint, but could also inform whether DdcA has other important cellular functions.

DdcA could inhibit YneA function directly. DdcA does not affect YneA protein levels, stability, or localization. DdcA also did not interact with YneA in a bacterial two-hybrid assay **(Fig 3.11)**, though this experiment had two confounding factors. DdcA and YneA were likely separated by the plasma membrane, and in order to keep YneA in the cytoplasm the N-terminus of YneA had to be deleted, which could be required for DdcA to interact with YneA. Thus, it remains possible that DdcA acts on YneA prior to or during secretion, resulting in a form of YneA that is incompetent for cell division inhibition. I observed that DdcA is primarily intracellular, however, a portion of DdcA localized to the membrane fraction **(Fig 3.9)**. It is possible that DdcA interferes with YneA secretion in a way that does not alter GFP-YneA localization. One possibility is that the topology of YneA is somehow reversed when DdcA is present. The result would be that the extracellular portion of YneA would be inside the cell, preventing YneA from inhibiting cell division. This hypothesis could be tested by placing the N-terminal secretion signal of YneA at its C-terminus. If YneA orientation is reversed when DdcA is present, then by moving the secretion signal to the other side of the LysM domain, the function of DdcA would also be reversed. Another possibility is that DdcA affects YneA prior to secretion. Proteins containing TPR domains have been found to act as chaperones (18). Therefore, DdcA could act as a chaperone promoting YneA to fold into an inactive form. If YneA has cell wall hydrolase activity similar to that of the *Mycobacterium tuberculosis* cell division inhibitor (7) (see next section), then the effect of DdcA on YneA activity could be tested *in vitro*. In addition, the secondary structure of YneA could be monitored via circular dichroism or sensitivity of YneA to trypsin digestion could be tested to discern whether DdcA could indeed

alter YneA structure. Together with the more comprehensive study of DdcA interacting partners described above, these experiments will provide a deeper understanding of how the threshold for DNA damage checkpoint activation is established in *B. subtilis*.

Checkpoint enforcement

Although not a focus of my research, the mechanism by which YneA inhibits cell division remains the major open question in the *B. subtilis* DNA damage response field. YneA was identified as the SOS-dependent cell division inhibitor in *B. subtilis* in the early 2000s (3). A subsequent study provided evidence that full length YneA was the active form, and that several amino acids in the transmembrane domain were important for function (12). There are two major questions about YneA function that remain: 1) how does YneA inhibit cell division? and 2) what is the biological function of the YneA-dependent checkpoint?

The data that YneA can inhibit cell division are clear (3, 12), yet how this occurs remains obscure. There are two primary hypotheses that should be tested: 1) YneA inhibits activity of an essential component of the cell division or cell wall synthesis machinery; and 2) YneA acts on the cell wall to prevent cell division. Of course, these hypotheses are not mutually exclusive and both could be part of the mechanism of cell division inhibition.

I attempted to identify potential interacting partners of YneA using a bacterial two hybrid assay by using a candidate approach to screen several cell division and cell wall synthesis proteins. The experiment did not generate a positive result. It remains possible that YneA interacts with a component of the cell division or cell wall synthesis machinery. It is possible that YneA interacts with a protein I did not test or that YneA forms a complex with multiple proteins. To circumvent these technical difficulties, a pull down assay followed by mass-spectrometry using full length YneA similar to a previous report should be adapted (19), and a genome wide bacterial two hybrid should be performed. A genetic approach using a suppressor screen could also be used. Suppressor screens performed thus far have failed to identify suppressor mutations in genes other than *yneA*, however, a more high throughput approach can be employed based on my findings in Chapter II and Chapter III. A strain lacking both checkpoint proteases and *ddcA* with *yneA* under the control of the P_{xyl} promoter integrated at the *amyE* locus in addition to the

native *yneA* locus (genotype: Δ*ddcA*, Δ*ddcP*, Δ*ctpA*, *amyE::P$_{xyl}$-yneA*) should be grown for many generations using multiple parallel liquid cultures. The cultures should be plated on media containing xylose periodically to identify strains that are no longer sensitive to over-expression of YneA. Any suppressors that are identified should subsequently be screened for sensitivity to MMC. Suppressor strains that are resistant to both xylose and MMC could result from mutations at both loci expressing *yneA* (*yneA* and *amyE::P$_{xyl}$-yneA*), which would be a low probability event because the same cell would require two mutations. Alternatively, if a mutation occurred in a gene that functions downstream of YneA, such as the target or binding partner of YneA, the resulting strain would also be resistant to xylose and MMC. These experiments utilizing multiple independent approaches could identify potential binding partners of YneA and genetic suppressors of YneA over-expression.

It remains possible that YneA function does not depend on protein-protein interactions. YneA has a LysM domain, and LysM domains typically bind to the peptidoglycan cell wall (20). The cell division inhibitor of *Mycobacterium tuberculosis* contains a LysM domain and also has cell wall hydrolase activity (7, 21). It is possible that YneA has hydrolase activity and prevents cell division by interfering directly with cell wall synthesis. This hypothesis should be tested using three independent approaches. First, if YneA inhibits cell wall synthesis, we might predict that over-expression of YneA would lead to a cell morphology phenotype similar to that observed for mutants that cannot properly synthesize the cell wall (22, 23). Although I did not observe differences in cell morphology, I only imaged strains overexpressing lower levels of YneA after thirty minutes. Moreover, the original reports of YneA overexpression wherein cells were visualized following YneA over-expression were done in strain backgrounds containing DdcA, DdcP, and CtpA, which would allow for removal and inhibition of YneA. Thus, the experiment should be repeated using high levels of YneA expression in a strain lacking *ddcA*, *ddcP*, and *ctpA*, and cell morphology should be monitored over a longer period of time, such as four to eight hours following YneA induction. Second, YneA could be tested for cell wall hydrolase activity using purified YneA similar to previously described (7). If YneA has hydrolase activity, the amino acids required for activity should be identified. The residues should be mutated, and the resulting YneA variant should be tested for hydrolase activity *in vitro* and its ability to inhibit cell division *in vivo*. Finally, given that GFP-YneA localization resembles the localization pattern of nascent peptidoglycan synthesis **(Fig 3.12)** (24, 25), the effect of YneA

over-expression on peptidoglycan synthesis should be tested. If YneA interferes with cell wall synthesis, it is possible that staining of nascent peptidoglycan using fluorescent vancomycin is altered upon over-expression of YneA. The experiments outlined above will help elucidate how YneA inhibits cell division and further our understanding of the DNA damage checkpoint in bacteria.

The rationale for having a cell division inhibitor is to slow cell division to allow DNA repair and replication to complete prior to division. If the cell cycle checkpoint is removed, one would imagine that cells would not survive treatment with drugs that damage DNA. Paradoxically, deletion of *yneA* results in resistance to MMC relative to the wild type strain **(Fig 2.11)**. Thus, the question arises, what is the purpose of the YneA checkpoint? In *Caulobacter crescentus* there are two cell division inhibitors and deletion of either one alone gives no phenotype; however, the double mutant is sensitive to DNA damage (6). Further, although YneA is required for a significant portion of cell division inhibition in response to DNA damage, cells still elongate when YneA is deleted. It follows that there must be other mechanisms of checkpoint enforcement. As mentioned previously in Chapters I, II, and III, regulation of *ftsL* transcripts is a second mechanism of controlling cell division in response to replication stress (26). Still, there are other candidates for additional DNA damage-dependent cell division inhibitors. First, there are proteins in the prophage PBSX that have LysM domains (20), which could be functional analogs of YneA. I showed in Chapter V that deletion of PBSX results in a slight resistance to MMC **(Fig 5.7)**, similar to deletion of *yneA*. If there is an additional cell division inhibitor that is part of the PBSX prophage, we would predict that deletion of both PBSX and *yneA* would result in sensitivity to MMC if the checkpoint is completely ablated. A second possibility is that the FtsZ inhibitor EzrA contributes to establishing the DNA damage checkpoint. In my genetic screens presented in Chapter II, transposon insertions in *ezrA* resulted in decreased relative fitness measurements in all three experiments, consistent with the hypothesis that EzrA is an important checkpoint regulator. How this occurs is not clear as *ezrA* was not found to be DNA damage-inducible (27). A genetic investigation of *ezrA* in the DNA damage response would be informative. Overall, a methodical dissection of YneA function will be required to understand how the DNA damage checkpoint is controlled in *B. subtilis*.

Mitomycin specific nucleotide excision repair

My discovery of a nucleotide excision repair pathway specific for MMC is a fascinating observation that illuminated several open questions for further study. As I demonstrated in Chapter IV, *mrfAB* are important for surviving treatment with MMC, but not other types of DNA damage. I also found that MrfAB were not important for repair of the interstrand cross-link. These data strongly suggest that MrfAB repair the intrastrand cross-link and/or the mono-adducts (hereafter, referred to collectively as adducts). It is not clear how MrfAB recognize DNA containing MMC adducts. Understanding how MrfAB recognize adducts will help explain the specificity of this DNA repair pathway.

Although MrfAB are important for repair of DNA containing MMC adducts, it is not clear how those adducts are recognized. The observation that MrfAB are specific to MMC adducts suggests that some aspect of adduct structure can be recognized by this pathway. An attractive explanation is that the C-terminal domain of MrfA recognizes MMC adducts in DNA. The C-terminus of MrfA contains four highly conserved cysteines that likely coordinate a zinc ion (28, 29). Zinc binding domains are prevalent in DNA binding proteins (30), and the recognition factors in bacterial and eukaryotic nucleotide excision repair also have zinc binding domains (31, 32). Although MrfA functioning as the recognition factor is an intuitive hypothesis, it is possible that MrfB or both MrfA and MrfB are required for MMC adduct recognition. Therefore, each protein individually and the MrfAB combination should be tested for a direct interaction with DNA containing an MMC adduct *in vitro*, similar to experiments performed with UvrABC (33). These experiments are straightforward in theory, but in practice MMC reacts with DNA forming several different adducts, so generating a single substrate is challenging (34). If MrfA is found to be the recognition factor, testing the requirement of the C-terminal binding domain may not be possible *in vitro*. A study of the MrfA homolog in *M. smegmatis* found that deletion of the C-terminal domain or mutation of the cysteines rendered the protein insoluble when produced in *E. coli* (29). To overcome this obstacle, MrfA could be tagged with GFP, and localization of MrfA in the presence and absence of MMC could be tested. It was previously shown that UvrA-GFP localizes to the nucleoid region following treatment with UV and MMC (35). Thus, it is possible that MrfA would localize to the nucleoid region following MMC treatment and that effect would depend on the C-terminus. Together, these experiments will

clarify how MrfAB recognize DNA containing MMC adducts and further our understanding of the specificity of this pathway.

Concluding remarks

Throughout this dissertation I have shown that the DNA damage response has multiple ways to accomplish one task. I showed in Chapter II that two proteases degrade the cell division inhibitor, and I described in Chapter III the identification of a third protein, DdcA, that acts to antagonize the same cell division inhibitor. In Chapter IV, I demonstrated that there are two pathways for repair of MMC adducts. Finally, in Chapter V I provided evidence that MutS2, a paralog of MutS, functions as a secondary Holliday junction endonuclease.

Why are there so many cases of genetic redundancy in the DNA damage response pathway? Genetic redundancy in eukaryotes has been studied in numerous important cellular and developmental processes (36). The use of genetic redundancy in development is important for two main reasons. First, it allows for proteins with similar function to be used in different cell types or at different times, thus allowing a greater versatility than a single protein would allow. Second, if two proteins are under selective pressure for the same function, but each has an additional function that is also under selective pressure, then genes coding for both proteins would be maintained. Another, perhaps not inconsequential, advantage is that having two proteins for a single function would increase the robustness of the overall process. If one protein fails in early development, having the second protein could allow development to progress, thereby increasing survival rates. Bacteria have considerably smaller genomes than those of eukaryotes, and therefore it has long been thought that selective pressure against redundancy must be great. Although this argument seems intuitive, the same logic for the existence of genetic redundancy in eukaryotes applies to prokaryotes. By using multiple proteins with overlapping functions, the robustness of the process increases (37). Thus, when stress is encountered and cellular processes begin to fail, organisms with multiple strategies of mitigating the stress will outcompete those reliant on a single strategy that can be overwhelmed. As a result, when considering genetic redundancy in bacteria, the underlying circumstances also need to be incorporated into the model. The DNA damage response pathway is a stress response system; therefore, in hindsight it should not be surprising that nature would select for a robust response.

As research into mechanisms of bacterial stress response pathways progresses, I expect that the principles of redundancy I have uncovered in *B. subtilis* will serve as a model, allowing researchers to elucidate complex regulatory strategies present in bacteria.

References

1. **Kreuzer KN.** 2013. DNA damage responses in prokaryotes: regulating gene expression, modulating growth patterns, and manipulating replication forks. Cold Spring Harb Perspect Biol **5:**a012674.
2. **Friedberg EC, Walker GC, Siede W, Wood RD, Schultz RA, Ellenberger T.** 2006. DNA Repair and Mutagenesis, 2nd ed. ASM Press, Washington, D.C.
3. **Kawai Y, Moriya S, Ogasawara N.** 2003. Identification of a protein, YneA, responsible for cell division suppression during the SOS response in Bacillus subtilis. Mol Microbiol **47:**1113-1122.
4. **Ogino H, Teramoto H, Inui M, Yukawa H.** 2008. DivS, a novel SOS-inducible cell-division suppressor in Corynebacterium glutamicum. Mol Microbiol **67:**597-608.
5. **Modell JW, Hopkins AC, Laub MT.** 2011. A DNA damage checkpoint in Caulobacter crescentus inhibits cell division through a direct interaction with FtsW. Genes Dev **25:**1328-1343.
6. **Modell JW, Kambara TK, Perchuk BS, Laub MT.** 2014. A DNA damage-induced, SOS-independent checkpoint regulates cell division in Caulobacter crescentus. PLoS Biol **12:**e1001977.
7. **Chauhan A, Lofton H, Maloney E, Moore J, Fol M, Madiraju MV, Rajagopalan M.** 2006. Interference of Mycobacterium tuberculosis cell division by Rv2719c, a cell wall hydrolase. Mol Microbiol **62:**132-147.
8. **Bojer MS, Wacnik K, Kjelgaard P, Gallay C, Bottomley AL, Cohn MT, Lindahl G, Frees D, Veening J-W, Foster SJ, Ingmer H.** 2018. SosA inhibits cell division in Staphylococcus aureus in response to DNA damage. bioRxiv doi:10.1101/364299.
9. **Joshi KK, Chien P.** 2016. Regulated Proteolysis in Bacteria: Caulobacter. Annu Rev Genet **50:**423-445.
10. **Clausen T, Kaiser M, Huber R, Ehrmann M.** 2011. HTRA proteases: regulated proteolysis in protein quality control. Nat Rev Mol Cell Biol **12:**152-162.
11. **Silber KR, Keiler KC, Sauer RT.** 1992. Tsp: a tail-specific protease that selectively degrades proteins with nonpolar C termini. Proc Natl Acad Sci U S A **89:**295-299.
12. **Mo AH, Burkholder WF.** 2010. YneA, an SOS-induced inhibitor of cell division in Bacillus subtilis, is regulated posttranslationally and requires the transmembrane region for activity. J Bacteriol **192:**3159-3173.
13. **Sauer RT, Baker TA.** 2011. AAA+ proteases: ATP-fueled machines of protein destruction. Annu Rev Biochem **80:**587-612.
14. **Walsh NP, Alba BM, Bose B, Gross CA, Sauer RT.** 2003. OMP peptide signals initiate the envelope-stress response by activating DegS protease via relief of inhibition mediated by its PDZ domain. Cell **113:**61-71.

15. **Sohn J, Grant RA, Sauer RT.** 2007. Allosteric activation of DegS, a stress sensor PDZ protease. Cell **131:**572-583.
16. **Sohn J, Sauer RT.** 2009. OMP peptides modulate the activity of DegS protease by differential binding to active and inactive conformations. Mol Cell **33:**64-74.
17. **Cerveny L, Straskova A, Dankova V, Hartlova A, Ceckova M, Staud F, Stulik J.** 2013. Tetratricopeptide repeat motifs in the world of bacterial pathogens: role in virulence mechanisms. Infect Immun **81:**629-635.
18. **Smith DF.** 2004. Tetratricopeptide repeat cochaperones in steroid receptor complexes. Cell Stress Chaperones **9:**109-121.
19. **Campo N, Rudner DZ.** 2006. A branched pathway governing the activation of a developmental transcription factor by regulated intramembrane proteolysis. Mol Cell **23:**25-35.
20. **Buist G, Steen A, Kok J, Kuipers OP.** 2008. LysM, a widely distributed protein motif for binding to (peptido)glycans. Mol Microbiol **68:**838-847.
21. **Vadrevu IS, Lofton H, Sarva K, Blasczyk E, Plocinska R, Chinnaswamy J, Madiraju M, Rajagopalan M.** 2011. ChiZ levels modulate cell division process in mycobacteria. Tuberculosis (Edinb) **91 Suppl 1:**S128-135.
22. **Murray T, Popham DL, Setlow P.** 1998. Bacillus subtilis cells lacking penicillin-binding protein 1 require increased levels of divalent cations for growth. J Bacteriol **180:**4555-4563.
23. **Popham DL, Setlow P.** 1996. Phenotypes of Bacillus subtilis mutants lacking multiple class A high-molecular-weight penicillin-binding proteins. J Bacteriol **178:**2079-2085.
24. **Daniel RA, Errington J.** 2003. Control of cell morphogenesis in bacteria: two distinct ways to make a rod-shaped cell. Cell **113:**767-776.
25. **Tiyanont K, Doan T, Lazarus MB, Fang X, Rudner DZ, Walker S.** 2006. Imaging peptidoglycan biosynthesis in Bacillus subtilis with fluorescent antibiotics. Proc Natl Acad Sci U S A **103:**11033-11038.
26. **Goranov AI, Katz L, Breier AM, Burge CB, Grossman AD.** 2005. A transcriptional response to replication status mediated by the conserved bacterial replication protein DnaA. Proc Natl Acad Sci U S A **102:**12932-12937.
27. **Goranov AI, Kuester-Schoeck E, Wang JD, Grossman AD.** 2006. Characterization of the global transcriptional responses to different types of DNA damage and disruption of replication in Bacillus subtilis. Journal of Bacteriology **188:**5595-5605.
28. **Shi W, Punta M, Bohon J, Sauder JM, D'Mello R, Sullivan M, Toomey J, Abel D, Lippi M, Passerini A, Frasconi P, Burley SK, Rost B, Chance MR.** 2011. Characterization of metalloproteins by high-throughput X-ray absorption spectroscopy. Genome Res **21:**898-907.
29. **Yakovleva L, Shuman S.** 2012. Mycobacterium smegmatis SftH exemplifies a distinctive clade of superfamily II DNA-dependent ATPases with 3' to 5' translocase and helicase activities. Nucleic Acids Res **40:**7465-7475.
30. **Vallee BL, Coleman JE, Auld DS.** 1991. Zinc fingers, zinc clusters, and zinc twists in DNA-binding protein domains. Proc Natl Acad Sci U S A **88:**999-1003.
31. **Croteau DL, DellaVecchia MJ, Wang H, Bienstock RJ, Melton MA, Van Houten B.** 2006. The C-terminal zinc finger of UvrA does not bind DNA directly but regulates damage-specific DNA binding. J Biol Chem **281:**26370-26381.

32. **Petit C, Sancar A.** 1999. Nucleotide excision repair: from E. coli to man. Biochimie **81:**15-25.
33. **Weng MW, Zheng Y, Jasti VP, Champeil E, Tomasz M, Wang YS, Basu AK, Tang MS.** 2010. Repair of mitomycin C mono- and interstrand cross-linked DNA adducts by UvrABC: a new model. Nucleic Acids Research **38:**6976-6984.
34. **Bargonetti J, Champeil E, Tomasz M.** 2010. Differential toxicity of DNA adducts of mitomycin C. J Nucleic Acids **2010**.
35. **Smith BT, Grossman AD, Walker GC.** 2002. Localization of UvrA and effect of DNA damage on the chromosome of Bacillus subtilis. Journal of Bacteriology **184:**488-493.
36. **Nowak MA, Boerlijst MC, Cooke J, Smith JM.** 1997. Evolution of genetic redundancy. Nature **388:**167-171.
37. **Ghosh S, O'Connor TJ.** 2017. Beyond Paralogs: The Multiple Layers of Redundancy in Bacterial Pathogenesis. Front Cell Infect Microbiol **7:**467.